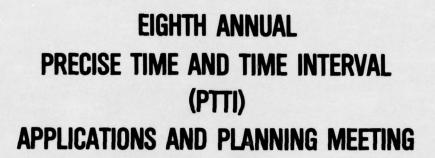
NATIONAL AERONAUTICS AND SPACE ADMINISTRATION GREENB--ETC F/6 14/2 PROCEEDINGS OF THE ANNUAL PRECISE TIME AND TIME INTERVAL (PTT1)--ETC(U) AD-A043 856 1977 UNCLASSIFIED NASA-6SFC-X-814-77-149 NL 1 OF 8 AD43856

X-814-77-149

PROCEEDINGS

OF THE



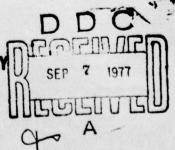
NOVEMBER 30 - DECEMBER 2, 1976





AD No. --

U. S. NAVAL RESEARCH LABORATORY WASHINGTON, D. C.



DISTRIBUTION STATEMENT A
Approved for public release;

Distribution Unlimited

For information concerning availability of this document contact:

Technical Information & Administrative Support Division
Code 250
Goddard Space Flight Center
Greenbelt, Maryland 20771

(Telephone 301-982-4488)

"This paper presents the views of the author(s), and does not necessarily reflect the views of the Goddard Space Flight Center, or NASA."

NASA-GSFC - X-814-77-149

I de checked

PROCEEDINGS

OF THE EIGHTH ANNUAL

PRECISE TIME AND TIME INTERVAL

(PTTI)

APPLICATIONS AND PLANNING MEETING

18th

Held at Naval Research Laboratory
November 30 - December 2, 1976

(2 763 P. 7

Sponsored by

Naval Electronic Systems Command NASA Goddard Space Flight Center Naval Research Laboratory Naval Observatory Defense Communications Agency

DDC DECEMBER SEP 7 1977 DISTOSSITISSI

Prepared by
GODDARD SPACE FLIGHT CENTER
Greenbelt, Maryland 20771

166 200 82

Approved for public release;
Distribution Unlimited

OFFICERS AND COMMITTEES

EXECUTIVE COMMITTEE

Ralph T. Allen Naval Electronic Systems Command

> John A. Bowman Naval Research Laboratory

James A. Cauffman Naval Electronic Systems Command

Andrew R. Chi Goddard Space Flight Center

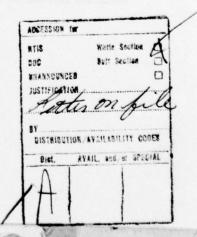
> Laura C. Fisher Naval Observatory

Andrew C. Johnson Naval Observatory

James A. Murray, Jr. Naval Research Laboratory

Dr. Harris A. Stover Defense Communications Agency

Schuyler C. Wardrip Goddard Space Flight Center



GENERAL CHAIRMAN

L. J. RUEGER Applied Physics Laboratory

TECHNICAL PROGRAM COMMITTEE

ANDREW R. CHI — CHAIRMAN NASA Goddard Space Flight Center

JAMES A. BUISSON Naval Research Laboratory

CAPTAIN WILLIAM L. PHILLIPS, USAF Space and Missile Systems Organization

LAURA C. FISHER U.S. Naval Observatory LAUREN J. RUEGER

APL, Johns Hopkins University

DR. HENRY FLIEGEL
Jet Propulsion Laboratory

DAVID SCULL Coast Guard

HUGH S. FOSQUE NASA Headquarters DR. HARRIS A. STOVER

Defense Communication Engineering

Smithsonian Astrophysical Observatory

Center

CHARLES FRIEND Wright Patterson AFB

DR. ROBERT F. C. VESSOT

RONALD HYATT Hewlett Packard Company

SCHUYLER C. WARDRIP

JAMES JESPERSEN
National Bureau of Standards

NASA Goddard Space Flight Center

EDITORIAL COMMITTEE

DR. ROBERT F. C. VESSOT — CHAIRMAN Smithsonian Astrophysical Observatory

DR. ROBERT J. COATES
NASA Goddard Space Flight Center

L. J. RUEGER
APL, Johns Hopkins University

DR. R. GLENN HALL Naval Observatory DR. GERNOT M. R. WINKLER Naval Observatory

DR. JAMES A. MULLEN Raytheon Company

ADVISOR TO THE EXECUTIVE COMMITTEE

THEODORE N. LIEBERMAN, RETIRED Naval Electronics Systems Command

SESSION CHAIRMEN

SESSION I Dr. Gernot M. R. Winkler U.S. Naval Observatory

SESSION II Dr. Jacques Bonanomi Director, Neuchatel Observatory, Switzerland

SESSION III
James Jespersen
U.S. National Bureau of Standards

SESSION IV Professor Norman F. Ramsey Harvard University

SESSION V Dr. Friedrich H. Reder U.S. Army Electronics Command

SESSION VI Dr. Leonard S. Cutler Hewlett-Packard Company

SESSION VII L. J. Rueger Applied Physics Laboratory

ARRANGEMENTS

John A. Bowman, NRL James A. Murray, Jr., NRL Herbert S. Poole, NRL

FINANCE COMMITTEE

Laura C. Fisher, USNO Schuyler C. Wardrip, GSFC

PUBLICATIONS

Virginia L. Walker, GSFC Schuyler C. Wardrip, GSFC

TECHNICAL ASSISTANCE

David Phillips, NRL Ruth Phillips, NRL William B. Berg, NRL Charles Mirachi, NRL William Beiles, NRL Joseph J. O'Neill, NRL Shirley Cornwell, NRL

RECEPTIONISTS

June Crass, NRL Edna Nacht, NRL Marie Nader, GSFC Dorothy Outlaw, USNO Eleanor Walker, NRL

ENTERTAINMENT

Roger Easton, NRL Dr. Gernot M. R. Winkler, USNO

BANQUET SPEAKER

Humphrey M. Smith, OBE Royal Greenwich Observatory Subject: The History of Time

CALL TO SESSION

L. J. Rueger, APL

WELCOME ADDRESS

Captain Lionel M. Noel Commanding Officer, Naval Research Laboratory

OPENING COMMENTS

Dr. Robert S. Cooper Director, NASA Goddard Space Flight Center

OPENING COMMENTS

Captain Joseph C. Smith Superintendent, U.S. Naval Observatory

CONTENTS

SESSION I	
NAVSTAR Global Position System (GPS) Capability and Plans for PTTI Applications, Cmdr. William G. Houston	1
The Hydrogen Maser Program for NAVSTAR GPS, Roger L. Easton	3
Operation Schedule and Plans of West Coast Loran C Chains Cyrus E. Potts and Paul E. Pakos	13
SESSION II	
ITU and United States Spectrum Management Structure S. E. Probst	15
The International Radio Consultative Committee (CCIR) Its Role, Function and Influence on the Distribution of Time and Frequency Information Hugh S. Fosque	17
The Bureau International de l'Heure Humphry M. Smith	29
Definition, Requirement, and the Determination of UT1 by the U.S. Naval Observatory (USNO) Dennis D. McCarthy	39
The Determination of UT1 by the Bureau International de l'Heure (BIH) Martine Feissel	47
SESSION III	
Precise Worldwide Station Synchronization via the NAVSTAR GPS, Navigation Technology Satellite (NTS-1) James Buisson, Thomas McCaskill, Humphrey Smith, Peter Morgan, and John Woodger	55

CONTENTS (Continued)

	Page
Navigation Technology Satellite (NTS) Low Cost Timing Receiver Development L. Raymond, J. Oaks, J. Osborne, G. Whitworth, J. Buisson, P. Landis, C. Wardrip, and J. Perry	85
A Time Code from NOAA's Geostationary Operational Environmental Satellites D. W. Hanson, J. V. Cateora, and D. D. Davis	105
Low Noise Multi Channel Space Communication Oscillators M. Bloch, M. Meirs, and M. Rosenfeld	125
A System for Near Real-Time Crustal Deformation Monitoring Peter F. MacDoran	127
Quartz Clocks Synchronized by LF Time Signals J. Bonanomi and P. Schumacher	135
Improved Time Reference Distribution for a Synchronous Digital Communications Network Harris A. Stover	147
A Microprocessor Data Logging System for Utilizing TV as a Time-Frequency Transfer Standard D. D. Davis	167
SESSION IV	
The Atomic Hydrogen Maser Norman F. Ramsey	183
Field Operable Hydrogen Maser Design Victor S. Reinhardt, Harry E. Peters, Lawrence A. Birnbaum	197
Hydrogen Maser Frequency Standards for the Deep Space Network Peter R. Dachel, Roger F. Meyer, Samuel M. Petty, and Richard L. Sydnor	213

CONTENTS (Continued)

	Page
Hydrogen Maser Design at the Laboratoire de l'Horloge Atomique Pierre Petit, Jacques Viennet, Roland Barillet, Michel Desaintfuscien, and Claude Audoin	229
A Hydrogen Maser Design for Ground Applications M. W. Levine, R. F. C. Vessot, E. M. Mattison, E. Blomberg, T. E. Hoffman, G. Nystrom, D. F. Graveline, R. L. Nicoli, C. Dovidio, and W. Brymer	249
Space-Borne Hydrogen Maser Design R. F. C. Vessot, M. W. Levine, E. M. Mattison, T. E. Hoffman, E. A. Imbier, M. Tetu, and G. Nystrom	277
Variable Volume Maser Techniques Victor S. Reinhardt	335
Problems in Hydrogen Maser Design and Suggested Improvements Stuart B. Crampton, Harry T. M. Wang, and John L. Barrett	351
New TE ₁₁₁ -Mode Hydrogen Maser Edward M. Mattison, Martin W. Levine, and Robert F. C. Vessot	355
Design and Results from a Prototype Passive Hydrogen Maser Frequency Standard F. L. Walls	369
Panel A Discussion	381
A Comparison of Various Hydrogen-Maser Frequency Standards A. E. E. Rogers, A. R. Whitney, and L. B. Hanson	399
Panel B Discussion	407
SESSION V	
Special Purpose Atomic (Molecular) Standard David J. Wineland, David A. Howe, and Helmut Hellwig	429

CONTENTS (Continued)

	Page
Calculation of OMEGA Propagation Group Delay and Application to Local Time Standard Monitoring R. Grover Brown, R. L. Van Allen, and Kim Strohbehn	449
OMEGA Synchronization: Current Operations and Future Plans Howard J. Santamore, Roger N. Schane, and Stephen F. Donnelly	467
SESSION VI	
A Brief Review of Frequency Stability Measures Gernot M. R. Winkler	489
First Results from a Satellite Data Link Radio Interferometer S. H. Knowles, W. B. Waltman, N. W. Broten, D. H. Fort, K. I. Kellermann, B. Rayhrer, J. L. Yen, and G. W. Swenson	529
Interpretation and Application of Oscillator Instability Measures Using Structure Functions W. C. Lindsey, C. M. Chie, and W. E. Leavitt	535
Identification of Noise Processes in Oscillators and Sample Data of Frequency Stability of Frequency Standards Robert F. C. Vessot	561
A Simple Technique for High Resolution Time Domain Phase Noise Measurement Victor S. Reinhardt and Theresa Donahoe	563
Frequency Stability Measurement Procedures Michael C. Fischer	575
Panel C Discussion	619

CONTENTS (Concluded)

	Page
SESSION VII	
NTS-2 Cesium Beam Frequency Standard for GPS J. White, F. Danzy, S. Falvey, A. Frank, and J. Marshall	637
A New Rugged Low Noise High Precision Oscillator D. A. Emmons	665
Performance of a Dual Beam High Performance Cesium Beam Tube Gary A. Seavey	681
Application of High Performance Cesium Beam Frequency Standards to VLBI W. J. Klepczynski	695
New Horologe for Air Force Metrology Laboratories Arnold Alpert and James F. Barnaba	706
Questions and Answers	715
8th PTTI Registration List	725

FOREWORD

The Proceedings contain the papers presented at the Eighth Annual Precise Time and Time Interval (PTTI) Applications and Planning Meeting. The edited record of the discussions following the papers and the panel discussions are also included.

This meeting provided a forum for the exchange of information on precise time and frequency technology among members of the scientific community and persons with program applications.

The 282 registered attendees came from various U. S. Government agencies, private industry, universities and a number of foreign countries were represented.

In this meeting, papers were presented that emphasized:

- a) definitions and international regulations of precise time sources and users,
- b) the scientific foundations of Hydrogen Maser standards, the current developments in this field and the application experience, and
- c) how to measure the stability performance properties of precise standards.

As in the previous meetings, update and new papers were presented on system applications with past, present and future requirements identified.

On behalf of the Executive Committee, I want to thank all those who contributed to the success of this year's meeting. Special credit should go to the Technical Program Chairman and his committee, the Editorial Chairman and his committee, the Session Chairmen, Speakers and Authors.

Lauren JV Rueger General Chairman

CALL TO SESSION

L. J. Rueger Applied Physics Laboratory

Good Morning. I am Lauren Rueger of the Johns Hopkins University Applied Physics Laboratory, and it is my pleasure to call to session, the 8th Annual Precise Time and Time Interval Applications and Planning Meeting.

A purpose of this meeting is the exchange of information that will enable us to make better use of existing and projected capabilities in the precision time and time interval technology.

I think that the technical program committee under Andy Chi has selected an excellent set of papers to initiate exchanges and information. We shall welcome participation from the attendees and the discussion periods that will be provided.

I must remind you that the sessions are being recorded for the purpose of preparing an accurate printing of the proceedings. You can help to keep the records correct by giving your name and affiliation, preceding any questions from the floor.

Last year, the attendees to this meeting were sent a questionnaire to help this year's committee being responsive to your interests. The results of this questionnaire indicate that you want predominantly short, technical papers. You want some flavor for the long-range needs and capabilities.

You want the discussions to be recorded in the proceedings. You want the meetings to continue on an annual basis, and you welcome the participation of the foreign countries and the United States industry to this meeting.

You will find the very gratifying response of papers has indeed required that the technical papers will be short. We hope the speakers will accordingly help us to keep the program on schedule.

The speakers are asked to see the session chairman prior to the scheduled sessions and to sit in seats reserved in the front rows here. There are a few late papers in the program that are listed on the last page. These will be given if time permits in the sessions that are indicated, but this will be at the discretion of the session chairman.

Again, this year we have a large foreign participation at this meeting. We apologize for any inconvenience to these people resulting from the security

regulations of the Naval Research Laboratory, but we are glad to have you here.

It is my pleasure to call upon representatives of the government sponsoring agencies for this meeting at this time. The first will be Captain Lionel Noel, the Commanding Officer of the Naval Research Laboratory.

WELCOME ADDRESS

Captain Lionel M. Noel Commanding Officer, Naval Research Laboratory

CAPT. NOEL: On behalf of the Naval Research Laboratory, I would like to welcome you to the 8th Annual Precise Time and Time Interval Application and Planning Meeting. It is a pleasure to host this meeting.

I have noted that the PTTI meeting has grown in prestige each year. For the past several years and this year also, we have included foreign visitors and speakers.

As you know, the Navy has always had a vital interest in time; its close cousin, frequency; and the many and varied uses to which they are put.

Recently called to my attention was an article on the Naval Observatory in an old report, the year, 1864, to be exact. And I quote.

"For the purpose of giving correct time to the city, the staff has been placed on the top of the dome, and a large but light ball is hoisted 10 minutes before 12:00 o'clock of each day except Sunday.

"The pulley is connected with an electro-magnetic battery after the ball is up and the circuit is broken by the assistant in the chronometer room at the instant of noon."

Also, you may be interested in the state of the art in timekeeping at the end of the Civil War. Again, this is from the same old reference document. Measuring the hundredth part of a second.

As a matter of popular information for the benefit of those who read and wonder at the accounts of astronomical observations which record the movements of the heavenly bodies to the hundredth part of a second of time, we extract from a pamphlet issued by one of our colleges the following description of the instrument and method by which that wonder is performed.

The elegant instrument of Professor W. C. Bond, known as the magnetic register, or spring governor, is one by and upon which through the influence of electromagnetism the instant of time at which an observation takes place can be precisely recorded by means of very delicate machinery regulated by the spring governor, a contrivance at once peculiar and beautiful, a horizontal cylinder 13 inches long and 6 in diameter is made to revolve with great uniformity precisely once per minute of sidereal time.

Around this cylinder is clamped a sheet of paper, and upon this rests a glass pen filled with ink which as the cylinder turns from under it marks a line from end to end of the sheet.

This line in length is the exact measure of the duration of one minute of time.

Upon the opposite end of a delicate level to which the glass pen is attached is a small vertical iron bar known as an armature, resting close in front of, but not in contact with the poles of a soft, iron horseshoe magnet. This magnet is coiled with wire, and is in the circuit of a galvanic battery, which circuit is also by an ingenious arrangement made to pass through a fine steel spring, dipping into a globule of quicksilver directly beneath the pendulum of the sidereal clock.

Attached to the lower extremity of the pendulum is a small, ivory index which at every vibration, drives the little spring out of the mercury, but instantly, on passing, allows it to return. In this manner, the circuit is almost instantaneously broken and closed.

At the termination of each second of time. And this break and make of circuit are at once answered by the pen in obedience to the action or rest of the magnet with which it is connected. Thus dotting upon the sheet as it revolves, a 60 seconds constituting the minute of its revolution.

The movement of the armature from the magnet during the instantaneous release of the latter from the influence of the galvanic circuit is effected by a little bow spring, and in order that the pen shall not return upon the lines already described, the whole magnet is moved forward on a miniature railway by means of a cord passing around the axle of one of the main wheels of the spring governor.

By means of this instrument and a break circuit, key always near his hand, the observer, by simply touching a delicate spring, is enabled to record with the utmost degree of precision in among the second marks of the clock, the time of any observation he may wish to obtain to the hundredth part of a second.

We at NRL are proud of the part we have played in time and frequency field since we opened our doors in 1923, having been in the forefront of most major developments from that day to this.

It is quite evident that requirements of frequency stability and time precision will continue to increase in the future as they have in the past.

It is therefore with great pleasure that I welcome you to this conference.

OPENING COMMENTS

Dr. Robert S. Cooper Director, Goddard Space Flight Center

DR. COOPER: Good morning, it is a pleasure for me to be here and to welcome you on behalf of all of the sponsors of this meeting, including the one I represent directly, the NASA Goddard Space Flight Center.

The sponsors intend these meetings to be a medium of exchange on PTTI activities and developments, laboratory progress and results and ideas for the future. When I learned how many of you had come from a great distance as Captain Noel pointed out, I was particularly impressed by the breadth and scope of the activities related to this conference and I was convinced that we are succeeding in both stimulating technical and programmatic exchanges in a meeting that meets a real need in the scientific world.

Those of you who come from Great Britain may know the tale about Lord Halifax who early in the 1900s once shared a railway compartment with two prim looking spinsters.

Just before reaching his destination, the train entered a tunnel. In the total darkness he kissed the back of his hand noisily a few times and moaned a little. When the train reached his station, he rose to leave, tipped his hat and said, "May I thank whichever one of you two ladies I am indebted to for the charming incident in the tunnel."

Like those good ladies, we all go through life partially in the dark about what the events actually were. Even in our chosen fields. And keeping abreast of all the important developments is getting more and more difficult every day.

The need to do this, the need to have this meeting has proven to be something that has been demonstrated by the growth and the breadth of the meeting itself.

The meeting started early in 1969, I understand, when about 60 local attendees got together and presented about a half dozen papers among one another. In the short seven years since that initial meeting, the PTTI meeting has achieved international scope and the attendance you will see here today is indicative of the importance that it now holds.

There are actually 40 papers on the schedule for this week, and having looked through the listing of papers I find that all of them are singularly interesting and I am sure will benefit all of you.

NASA is especially dependent on what you people are doing. Over the years, we have worked hard with many of you in the precise time and frequency generation and measurement. The Goddard Center along with the Bureau of Standards pioneered the development of dual frequency VLF transmissions for frequency and time synchronization.

With the Coast Guard, we developed the use of omega radio navigation system for precise timing and presently use LORAN sea navigation system to achieve about plus or minus 25 microseconds of global clock synchronization at our network of tracking sites which are located at various places around the world.

We have evaluated the use of various satellite time transfer techniques using the GEOS and ATS-1 and 3 satellites, and more recently, have had the support of NRL in the satellite technology, Roger Easton's NTS-1.

Time synchronization plays an important role in long-based line interferometry in which Goddard is vitally interested for astrophysical and geodetic purposes. We are now in cooperation with the Applied Physics Laboratory and the Naval Surface Weapons Center developing NTS timing receivers for use in NASA laser network for satellite tracking.

When fully operational, the laser network will require about a microsecond of time synchronization worldwide. One of the NTS receivers is on display here today, and several papers this afternoon will review the NTS time transfer technique and the receiver design, operation and performance. I am sure that you will all be interested in that development.

Goddard continues to evaluate time transfer techniques, recognizing that sub-microsecond timing will be required in the near future. We are looking at the possible use of our own tracking and data relay satellite system for timing which is being procured now for use during the early 1980s.

We are also studying the use of the Global Positioning System (GPS) for submicrosecond timing. This system will be well covered in papers presented today, and I believe is really one of the waves of the future.

I have a special interest in GPS because I was in the office of the Secretary of Defense in the Department of Defense before I came to Goddard, and was involved in getting the GPS system started and in working many of the problems associated with it.

GPS's unprecedented accuracy requirements will make it an excellent source of precise time and time interval information to any user with a simplified receiver anywhere on the surface of the earth.

Tomorrow, Goddard papers will discuss much of our activities in research on hydrogen maser frequency standards. I bring you some good news in this area. The design of our laboratory building at Goddard for frequency standards and measurements has been finalized and approved. Our primary hydrogen masers will be housed there. Construction is expected to start soon.

A low budget forced us to give up some of the conventional approaches for magnetically shielding the entire building. Also, we had to give up the idea of shielding the maser room alone. Instead, we will construct a shielded box which will drop down over each maser. This technique should achieve the same shielding factors, according to our tests, as the original goal.

Besides saving money, we will gain the freedom to move equipment and instruments around in the same room without affecting the masers. Even in adversity, ingenuity can sometimes cause benefits to be reaped. Be sure and keep that in mind when your next budget comes.

In our present hydrogen maser program, we are improving the shielding on our four field operable units so as to reduce the external magnetic sensitivity by a factor of five.

We are also developing new, second generation field operable masers based on the design of our NX series experimental masers.

Also, we are continuing our efforts on the development of variable volume masers with which we hope to achieve a part in 10 to the 14 accuracy. Using these variable volume masers as calibration standards, we should be able to determine the frequency stability and reproducibility of field masers at about 10 to the minus 14 level over long periods of time, perhaps as long as one to two years.

Further results on these developments will be given in NASA papers.

I am sure that you recognize that hydrogen masers are probably the clocks of the future. Our current time standards are based on cesium, largely, and the hydrogen masers are being brought along at a relatively rapid rate now due to expenditures that are being made by NASA and by the Air Force.

It is impressive that frequency standard technology has achieved parts in 10 to the 15 in frequency stability and parts in 10 to the 13 in accuracy, but future technology promises frequency standards with 10 to the minus 18 and 10 to the minus 16 in stability and accuracy respectively. This is something for all of you to work toward in your various laboratories.

There are many technologies that will benefit from these improved accuracies and stabilities. The technique of very long baseline interferometry will demand it.

Goddard, with collaborators at MIT Haystack Observatory and our friends at JPL, pioneered in applying hydrogen maser techniques to VLBI measurements in the geodetic and astro work.

Hydrogen masers are currently at use in tracking stations and radio astronomy stations in Massachusetts, California, West Virginia and Sweden, to study polar motion, the structure and kinematics of quasars and to develop VLBI techniques for subdecimeter accuracies necessary to measure continental drift.

The VLBI activity at Goddard is primarily a validation program to determine how well we can measure the long baseline distances between Haystack, Owens Valley National Radio Astronomy Observatory and JPL portable station sitting right on top of that fault up there in Pasadena.

We are striving to achieve a point to point accuracy of 5 to 10 centimeters between continents. We have demonstrated between Haystack and Owens Valley a transcontinental baseline capability between 5 and 10 centimeters accuracy.

In summary, the major PTTI thrusts at Goddard are precision frequency and timing support to our network tracking sites, first of all, hydrogen maser frequency standard development, time transfer or clock synchronization techniques and the VLBI validation program.

Goddard plans to press forward with its internal programs in these areas. In addition, we will continue to support and cooperate with the PTTI community nationally and internationally. The whole process of time and frequency measurement is one of the highest intellectual endeavors of mankind because it is our reach toward the reality, and it is clear that the technology is now moving very, very rapidly, and I expect that over the next 10 years, there will be some considerable breakthroughs in the measurement of frequency and time.

As I said before, the hydrogen masers are coming along and I believe that we have really not yet begun to think of the way of using the next generation, instead of a 1000 megahertz frequency oscillators, the terahertz frequency oscillators with high stability that will be coming available with the lasers of the future.

Laser stabilities in molecular lasers have achieved sub one hertz stabilities, and I believe that with the terahertz frequency capability, it will be possible to

make measurements of high accuracy and high precision in the future with these devices.

I thank you very much for the opportunity to greet you this morning, and I particularly thank Captain Noel and the director of the laboratory, Dr. Berman for hosting the 8th Annual PTTI Meeting.

I encourage all of you to continue with your needed and worthwhile research efforts and I look forward to greeting you next year when Goddard will have the pleasure of hosting your 9th meeting.

I wish you a very successful three days.

OPENING COMMENTS

Captain Joseph C. Smith Superintendent, U. S. Naval Observatory

CAPT. SMITH: Mr. Chairman, distinguished members and guests of the Eighth Annual Precise Time and Time Interval Applications and Planning Meeting, as one of the cosponsors representing the United States Naval Observatory, I am most honored to share this opportunity for reflective thinking with you.

Captain Noel mentioned how we used to drop the ball in time at the observatory. Dr. Strand, Dr. Winkler, the members of our time division, and I, hope we are still not doing that today.

The United States Naval Observatory since its inception has been deeply interested in and involved with time; for, as you are aware, time is integral to both fundamental and differential astronomy and, of course, in the precise location of any given point on this globe.

The United States Naval Observatory ties its Time Service Division, the Transit Circle Division, our Nautical Almanac Office, and our Exploratory Developmental staff closely together for exploitation of this basic truth.

Interaction between disciplines is always necessary if we are to progress in any given or collective field of endeavor. Specifically in the area of time, the mission of the United States Naval Observatory remains to derive, maintain and coordinate precise time and time interval, both astronomical and atomic, for the Department of Defense, and control distribution of and provide single management service and interservice support for precise time and time interval within the Department of Defense.

This mission area is supported by Navy and Department of Defense directives as well as deeply tied into public law. Our concern requires a time commitment improvement of our service. This requires feedback from users. We want to hear from you, and most specifically we want to hear from you about your timing problems.

We all know high-precision timing is expensive, and in today's climate this means that resources must be used optimally. This requires cooperation. The meeting today is a testimony that the timing community is interested and willing to cooperate, and this is very much appreciated by all of us at the observatory.

Our objective remains accomplishment of timing at minimum cost. We shall also take the necessary steps to assure worldwide continuity of precision. These goals would be incompatible without the support and cooperation which we receive from our friends throughout the services and other agencies, and overseas.

As I have examined the operations of the United States Naval Observatory during my short time on board, I am constantly reminded of the vastness of the unknown versus the known; of the continuing challenge to conquer, or at least reduce the size of this difference.

I am sure that the sessions and papers that will be presented here will be of significance in this endeavor. For "How much knowledge is enough?" The ancient sage told us, "Always just a little more."

I look forward to sharing this quest with you. Please continue to keep in contact with us on timing matters. We will make every effort to insure that the service we provide is as effective as we can make it.

My sincere thanks for joining us.

GUEST SPEAKER

THE HISTORY OF TIME

Humphry M. Smith, OBE Royal Greenwich Observatory, Sussex, England

Speech delivered at Banquet of Eighth Annual Precise Time and Time Interval (PTTI) Applications and Planning Meeting, Wednesday 1 December 1976. Naval Research Laboratory, Washington DC, USA.

Note

This was prepared for verbal presentation on a social occasion; hence the dilettante style and the omission of acknowledgements and references.

The subject suggested to me for my talk this evening is "The History of Time". The almost limitless scope of this topic makes me very conscious of my inadequacy to deal with it competently. Even the erudite and outstanding scientist Sir Isaac Newton once remarked, "I seem to have been only a boy playing on the seashore, and diverting myself in now and then finding a smoother pebble or a prettier shell than ordinary, whilst the great ocean of truth lay all undiscovered before me". For a lesser mortal like myself, my immediate reaction to the challenge you have put before me is to re-echo the classic comment of Sam Goldwyn, - "In two words: im-possible".

Clearly within the limitations imposed by my oratorical stamina and by your capacity for endurance, it is impracticable to attempt a comprehensive dissertation or a detailed review of all aspects of this fascinating theme. I could concentrate on the dramatic history of clocks through the ages, but even in this restricted sphere of horology I recall that the late Prof Torrens had accumulated a library of some 5000 books on mechanical time keepers alone. Alternatively we might trace the development of philosophical concepts of time over the centuries, but here we should be fishing in murky waters. Plato said that "the feeling of wonder is the genuine mark of the philosopher for philosophy has its origin in wonder". One is tempted to add that the reader may experience a similar sensation of wonder, not far short of bewilderment. (Theaetetus 155 CD). A cursory examination of the material soon reveals a whole gamut of opinions, some blatently ridiculous, many abstruse, others facile and trite. As Cicero remarked, "there is nothing so absurd but some philosopher has said it". (De Divinatione, ii.58). But serendipity comes to our aid, and among the plethora of verbiage we find occasional gems of sagacity and perceptive and stimulating aphorisms. Another fruitful field of study is those practical applications of timekeeping which directly affect humanity, since particularly in recent years much research has been carried out on the interaction between timekeeping and social trends. As we come to the scientific manifestations of time in the contemporary scene, developments in precise measurement have made it necessary to take into account hitherto insignificant or even unsuspected complications, and have opened up

entirely new fields of inter-disciplinary research.

In endeavouring to limit the scope of this review, and thus to avoid the Scylla of superficiality and the Charybdis of prolixity, I am encouraged by Derek de Solla Price to skip lightly over the superabundance of information so diligently compiled by assiduous but apparently gullible students of antiquarian horology, since he has concluded, and I quote "... from the history of astronomy and from the known development of sundials and other such devices that virtually all of the evidence for shadowand water-clocks being used as timekeepers before about the fourth century BC is fictional". He claims that "A great deal of damage and impediment to clear scholarship has been caused by the widespread and facile idea that man has always 'kept time' by primitive astronomical means". What then is his explanation of the well-established existence of such devices dating from the early days of civilisation? He proffers the speculation that there was a strong development of astronomy, long before time was used as a concept, in the context of special omen events which occurred in the heavens and which were reflected by happenings on Earth. He claims that Magalithic monuments like Stonehenge and other ancient stone circles, the water-clocks of ancient Egypt, all the early sundials and sand-clocks, were conceived primarily for the fixing of heliacal risings and settings, new moons, equinoxes and solstices. It was only much later, shortly before the time of Christ, that there was a new movement, almost synchronously in China and in Greece, which established a new trend leading to the modern practice. Man was able to use existing sophisticated techniques of technological brilliance to give him the possibility of doing something he had not wanted before it was readily available. This product, timekeeping, caught on, and by a process of evolution time became the matter of deep philosophical and scientific importance which it assumed in the classical and middle ages, and which it is today.

A significant contribution to our understanding of the concept of time was by the Athenian philosopher Plato (427-347 BC) who stands with Socrates and Aristotle as one of the founders of the intellectual ethos of Europe. Many of his ideas on time are contained in the "Timaeus", the sequel to his more familiar "Republic". He postulated a creator as a living being with the attribute of being eternal, and concluded that it was not possible for him to bestow this characteristic of immortality on the created universe. Plato explains:— "For before the heavens came into being, there were no days or nights or months or years... Time came into being with the heavens in order that, having come into being together, they would be dissolved together if ever they are dissolved. As a result of this plan and purpose of God for the birth of time, the Sun and Moon and five planets... came into being to define and preserve the measures of time".

Similar views have been reiterated in differing forms. A Buddhist priest, Nagasena, in the latter part of the second century BC, stated:-"For those who have entered nirvana, there is no time". In his Journal Intime, Amiel (1821-1881) says:- "Time is the supreme illusion. For the supreme intelligence there is no time; Time and space are fragments of the Infinite for the use of finite creatures". Such thinking is in general accord with the

mainstream of Christian doctrine: in Paul's first letter to Timothy he says of Christ "the only Sovereign, the King of kings and Lord of lords" that He "alone has immortality". The well-known theologian, I A Dorner, says:- "We must not make Kronos (time) and Uranos (space) earlier divinities before God." To round off these quotations, we add the apocryphal response popularly attributed to Augustine. While discussing concepts of temporal sequence, a persistent questioner asked what God was doing before He created the world, and allegedly received the response "He was making a hell for the persons who ask that kind of question". *

Although in many areas Aristotle was in substantial agreement with Plato, he is usually regarded as having been more confident in tone and more positive in character. As a result his authority became, throughout the middle ages, despotic and well-nigh sacrosanct. He regarded the Platonic unqualified identification of time with the cyclic movements of the heavenly bodies as untenable, but accepted the existence of an interrelation between them. "Not only do we measure the movement by the time, but also the time by the movement, because they define each other". Thus he rejected the possibility of continuous rectilinear motion, since this would imply motion in an infinite straight line, a concept which he found unacceptable. For Aristotle therefore time was a circle, measured by the cyclic movements in the heavens. We are reminded of the poetic insight of Henry Vaughan (1619-1645):-

"I saw Eternity the other night,
Like a great ring of pure and endless light,
And calm as it was bright; and round beneath it
Time in hours, days, years
Driven by the spheres,
Like a vast shadow moved, in which the world
And all her train were hurled".

Dissatisfied with Aristotle's close association of time and motion, Augustine adopted a more subjective attitude, and proclaimed:—"It is in thee, my mind, that I measure times". Unfortunately we cannot pursue the many ramifications of philosophical thought on this controversial question. So let us conclude by accepting a duality in time. At one extreme we have Newton who, at the beginning of his Principia makes a statement which has been one of the most criticized, and justly so, of all his postulates. "Hitherto I have laid down the definition of such words as are less known, and explained the sense in which I would have them understood in the following discourse. I do not define time, space, place and motion, as being well known to all. Only I must observe, that the vulgar conceive these quantities under no other notions but from the relation they bear

* In fact Augustine said: "My answer to those who ask 'what was God doing before he made heaven and earth?' is not 'He was preparing Hell for people who pry into mysteries'.... I shall refrain from giving this reply". (Confessions XI 12)

to sensible objects. And thence arise certain prejudices, for the removing of which it will be convenient to distinguish them into absolute and relative, true and apparent, mathematical and common.

Absolute, true and mathematical time, of itself, flows equably without regard to anything external, and by another name is called duration; relative, apparent, and common time is some sensible and external (whether accurate or unequable) measure of duration by the means of motion, which is commonly used instead of true time; such as an hour, a day, a month, a year." (Andrew Motte translation).

On the other hand, we cannot disregard the subjective consciousness of time. It is a common experience that, depending upon psychological factors, the passage of time can be fast or slow. When we talk of a long period of time having passed quickly or slowly, we speak not of the time but of our mode of remembering it. A person of rapid recapitulation always says the time has passed quickly, another of a contrary habit, the contrary; and this whether the rapidity is a consequence of quickness of ideas, or of having little to recall. The poet Henry Twells (1823-1900) wrote the following words which appear on a clock in Chester Cathedral:-

When I was a child I laughed and wept, Time crept When as a youth I waxed more bold, Time strolled When I became a full-grown man, Time ran When older still I daily grew, Time flew Soon I shall find, in passing on, Time gone O Christ! wilt Thou have saved me then? Amen.

No doubt we have all experienced the sensation epitomized in the succinct definition "Time is how long we have to wait". We can sympathize with the refugee, living under the borrowed name Schwartz, who in his agonizing experiences as recorded by Erich Maria Remarque in "The Night in Lisbon", said "Time - you know that - is diluted death, a poison administered slowly, in harmless doses". He looks back with nostalgia on happier interludes in Paris with his wife, Helen. "When your world is brimful of feeling, there's no room for time. You're on another shore, beyond time". As Oliver Herford said, 'There is no time like the pleasant'.

But let us leave the ruminations of the philosophers with an extract from the pen of Ralph Waldo Emerson. "Tobacco, coffee, alcohol, hashish, prussic acid, strychnine, are weak dilutions; the surest is time. This cup which nature puts to our lips, has a wonderful virtue, surpassing that of any other draught. It opens the senses, adds power, fills us with exalted dreams which we call hope, love, ambition, science; especially it creates a craving for larger draughts of itself"; and, in a more optimistic mood:— "God has infinite time to give us; but how did He give it? In one immense tract of lazy milleniums? No, He cut it up into a neat succession of new mornings".

This surely is the key to a full life, entering expectantly each new day

with all its potential for service, for challenge, for exercise of mind and body, for fellowship, for enjoyment, for achievement, and ultimately, for the contentment and rest which comes from a sense of fulfilment. Consider the cautionary tale of Methuselah. He lived for nine centuries, but according to the records, he never did, thought, or wrote anything to make such longevity worthwhile.

Aristotle said in his Metaphysics "But as more arts were invented, and some were directed to the necessities of life, others to recreation, the inventors of the latter were naturally always regarded as wiser than the inventors of the former, because their branches of knowledge did not aim at utility". Even in this present-day technological age, the theoretician and abstract intellectual whose lofty deliberations make no beneficial contributions to the creature comforts of the human race is accorded a higher status, and regards contemptuously, with a confident air of superiority, the most brilliant scientist and engineer who provides in greater abundance for his material needs and added luxuries. Nevertheless we must now turn our attention from the visionary speculations of the ideologue to the banausic level of the scientist, the engineer and the artificer.

Alexandria is a convenient place from which to commence our casual meander through the enthralling story of the development of timekeepers. The conquests of Alexander disseminated the Hellenistic civilisation, and created a new intellectual centre which soon also became established as the Western nucleus of technology. The early history of mechanical gearing is still enigmatic but a subject of avid investigation. It is known that Archimedes in about 250 BC used a gearwheel meshed with a worm, and a simple planetarium is also ascribed to him. Ctesibius of Alexandria, in the second century BC, constructed a striking water clock in which an anaphoric drive (so called because it displayed the successive rising, "anaphora", of constellations above the Eastern horizon during the night) was combined with gear wheels, mainly used for jack work. (Jack is the general term used for mechanically-activated figures, so named after Jaccomarchiadus, or Jacques Marck, a clock-and lock-maker of Lille, France).

Vetruvius also made an anaphoric clepsydra in about 30 BC. A float was attached to a cord wound round a drum and fastened to a counterweight. The drum was mounted on a horizontal axis which also carried a planispheric disc. Clocks of similar design were still in use as late as the end of the 17th century, but in later models the time dial was stationary and the pointer travelled over it. Historians distinguish three types of clepsydra. One as employed by Vetruvius, another using a tipping bucket or a syphon to give intermittent motion, and a third which achieved the same effect by using a continuous flow and a trip lever. Heron of Alexandria in 62 AD makes a reference in his Pneumatica to a device which may have been driven by pneumatic or hydraulic power.

Within the time at our disposal we cannot trace the history of the independent developments which took place in China. An acknowledged

authority on Chinese horology does however remark:- "There is no doubt that the Greeks were the more successful theorists, but equally none that the Chinese, on the whole, were the better practical instrument makers".

The Romans used three words to designate their timekeeping devices. Seneca in the first century AD used the Greek name "Clepsydra" for water clocks of varying degrees of complexity. The sundial was known as Solarium, and the same name was used for the smaller pocket sundials, such as the one only 3 cm in diameter, which was found in the Adriatic city of Aquileia. Another Graeco-Latin name frequently employed was horolgium, or "hourcounter". In fact the Romans were slow in acquiring their first timekeepers: the Sicilians in Syracuse had many and according to Pliny the Elder in his history of the first Punic War, the consul Marcus Valerius Messala brought a sundial back from Catana to Rome in 236 BC, where it was installed and continued to indicate the incorrect time for 99 years: no-one had realised that a sundial must be designed for the latitude in which it is to be used, and Rome was 4°23° north of Catana. Pliny lamented this deception of his unsuspecting fellow citizens, but the first sundial designed and constructed for the latitude of Rome was not installed until 164 BC. The number of dials increased rapidly. Cicero, who lived from 106 to 130 BC records that domestic clepsydra and sundials were common, and Juvenal, 60 to 130 BC, tells us that in empire days the upper classes not only possessed clocks but also had slaves who read the devices and announced the hours to their wealthy masters. Petronius, in "The Satiricon" tells of an invitation to dinner:- "Here, don't you know your host today? It's Trimalchio - he's terribly elegant... He has a clock in his dining room".

In general, however, the timekeepers, though much admired, were notoriously inaccurate. Lucius Seneca in his Apocolocyntosis (II, 2-3) confesses that although he can specify the date, he cannot give the time with any certainty, since it is easier to reach agreement between philosophers than between clocks, a truly devastating admission. (facilius inter philosophos quam inter horologia conveniet). A new class of technicians appeared during the reign of the Emperor Trajan 53-117 AD, and clocks became more attractive and more accurate. It is an interesting glimpse into Roman thinking that when Julius Caesar invaded the British Isles in 55 and 54 BC, he was very surprised to discover that the supposedly primitive Britons already had sundials.

One feature of Roman horologia still persists today in the use of Roman numerals to mark the hours. In order to achieve symmetry, it was customary to mark the four as IIII instead of the correct IV, since this balances the eight, VIII. A notable exception is the Westminster clock, with its famous "Big Ben" bell in the tower of the Palace of Westminster at the British Houses of Parliament.

Bells played a prominent part in the life of medieval towns, telling the hours, warning of impending dangers, summoning the populace for assemblies

and announcing good news. It is little wonder that skilled and enterprising craftsmen experimented with various mechanisms for controlling them and ringing them effectively. There was also a demand from astronomers and astrologers for instruments that would imitate the movements of the stars and planets. There is a continuity and gradualness in technological change, and the techniques being developed by craftsmen were moving towards the construction of mechanical clocks; but rarely there are radical advances by which progress takes a leap forward. Such an event was the invention, by an unidentified person, at a date that cannot be established with certainty, of the verge escapement. The general consensus of opinion tends to place the inception of the device in the second half of the thirteenth century, but the verge escapement with foliot introduced a new era in timekeepers, and the unknown inventor must have been a mechanical genius. The suggestion that this European development had its origins in a complicated Chinese mechanism built at the end of the eleventh century does not now appear tenable.

There are well-documented accounts of many mechanical clocks constructed and installed in Europe during the fourteenth century, but in many instances the indications of the hours were by the ringing of bells, and not by the movement of dials or hands. In fact the word "clock" derives from the medieval Latin "clocca", a bell.

I will depart for a moment from the chronological sequence to recount a brief story: It is the story of a factory owner who complained that his workers arrived back late after the dinner-break, which was scheduled to end at 1 o'clock. Their excuse was that they sometimes missed hearing the single stroke of the bell. He overcame the difficulty by arranging for the clock to strike thirteen. Which brings to mind another story told in Punch 60 years ago by A P Herbert, in which the Lord Chief Justice in the Court of Criminal Appeal felt unable to rely upon a statement that had been made. He said "it is like the 13th stroke of a crazy clock which not only is itself discredited but casts a shade of doubt over all previous assertions".

But to return to our narrative. An outstanding example of the complex astronomical clocks which characterized this stage of development was made in 1350 by Giovanni de Dondi, probably with the help of his father, Jacopo. It reproduced mechanically the movements of the Sun, Moon and five planets, and incorporated a perpetual calendar. After the death of its maker, no one could be found to take care of it, and it finally disintegrated. Accurate details were recorded, and we have complete infomation on the design.

In 1370 Charles V of France installed a clock that struck the hours on one of the towers of the royal palace. He was delighted and had two similar clocks erected in other parts of the town. Being concerned that the bells could not be heard by all the citizens, he ordered all the churches in Paris to ring their bells (par pointez à maniere d'orologe) when the royal clocks struck. Thus everyone should know the time "whether the Sun is shining or not" (luise le soleil ou non).

A big clock, especially a public clock, was very expensive in those days. It was expensive to build: the mechanism of a public clock at Montpellier constructed in 1410 weighed about 2 000 pounds, and the bell a like amount. In addition there was a striking figure and other paraphernalia. The estimated cost was 200 "escuts", an obsolete gold coin roughly equivalent to the more recent "ecu" which was replaced with the franc. Before the days of currency-juggling and devaluation, the "escut" might be thought of as a genuine original dollar. In addition, the supplier required "deux muids de vin" and "deux molons de ble"; say two barrels of wine and two heaps of grain. But apart from the capital cost, there was a commitment to the regular wage of a specially-appointed governor. This was no sinecure. Often the governor had to wind the clock twice a day, and he had therefore to climb twice a day to the top of the clock tower; he had very frequently to grease the machine and set or reset the hand because the clock lost or gained much time in the course of half a day. Despite the drain on local finances, civic pride, utilitarianism and mechanical interest fostered the installation of a growing number of clocks. Throughout the 14th and 15th centuries many complex and elaborate clocks embodied a strange combination of brilliance in conception with a deficient technique of construction. If and when they worked, they gained or lost much time in a day. Generally it was not considered necessary to provide a minute hand. Even the famous palace clock of Charles V was said by Parisians "to go as it pleased" (1'horloge du palais, elle vas comme il lui plait).

Until about the middle of the 15th century, there were only public clocks or those in the possession of the very wealthy. Moreover since weights provided the only motive power, clocks were not easily portable. It seems likely that the first spring-driven clocks were made in Italy about 1410, possibly by Filippo Brunelleschi. There is little doubt that portable spring-driven clocks were becoming more numerous by 1450, and that an ingenious device, the fusee, had been invented to minimise the deleterious effect of the slowly diminishing driving power of the spring. (An earlier mechanism, the stackfreed, had been designed for the same purpose, but although its use persisted until the beginning of the 17th century, its performance fell far short of that of the fusee). Pocket timekeepers made their appearance towards the end of the 15th century and at the beginning of the 16th. More craftsmen acquired the skills of the trade, and during the 16th and 17th centuries in Europe, there was a growing market among the middle classes, merchants, lawyers, doctors, and apothecaries, who could afford to buy better houses, good clothes, and such amenities of life as domestic clocks.

While the performance of clocks was irregular, a minute hand was superfluous. No exact date can be given for the introduction of this refinement, but in the Ilbert collection in the British Museum there is a two-handed clock made by Nicholas Vallin in 1598. The inner hand rotates once per hour, but the only markings are the quarters. The clock chimes on thirteen bells. It was only with the invention of the pendulum which significantly improved the timekeeping accuracy, that the general use of

a minute hand became justifiable. As is well-known, the isochronous property of the pendulum was discovered, or some authorities say "rediscovered" (see Note below) by the famous Italian astronomer, Galileo Galilei who also invented the thermometer, and the telescope, and was the founder of the science of dynamics. The application of the pendulum to a clock was due to Christiaan Huygens, the eminent Dutch astronomer and mathematician. In 1657 he assigned his invention to Saloman Coster, a master clockmaker at The Hague. On September 3, 1657, Coster made an agreement with John Fromanteel, a younger member of a family of clockmakers of Dutch descent living in London. Fromanteel agreed to pay Coster a royalty of 20 Carolus gulden for each clock he made, on condition he worked with his own steel and brass: if Coster supplied the material, he was to receive $18\frac{1}{2}$ gulden per clock. A pendulum clock made by Coster himself in 1657 had a chapter ring, outside the hour ring, to indicate the minutes.

As this is an informal social occasion, and not confined to serious scientific dissertations, may I depart from the strict limitations of my assignment and turn to one of the lighter aspects of time which may be culled from the pages of the famous book by Laurence Stern, "The Life and Opinions of Tristram Shandy"?

Tristram tells us that he was "begot in the night betwixt the first Sunday and the first Monday in the month of March, in the year of our Lord 1718. I am positive I was". He goes on to explain why he can be so certain. "My father was, I believe, one of the most regular men in everything he did, whether towas matter of business, or matter of amusement, that ever lived. As a small specimen of this extreme exactness of his, to which he was in truth a slave, - he had made it a rule for many years of his life, - on the first Sunday night of each month throughout the whole year, - as certain as ever the Sunday night came, - to wind up a large house-clock, which we had standing upon the backstairs head, with his own hands:- and being somewhere between fifty and sixty years of age, at the time I have been speaking of, - he had likewise gradually brought some other little family concernments to the same period, in order, as he would often say to my uncle Toby, to get them all out of the way at one time, and be no more plagued and pestered with them the rest of the month".

The euphemism, winding the clock, became quite common, and has even reappeared in the recent craze for resuscitating folk songs with a modern

Note: The dubious attribution to Leonardo da Vinci depends upon the exercise of unnecessary ingenuity by a translator: "fa che unora sia duj sa in 3 000 partj e cquesto faraj colloriolo allegeredo o agravado il cotrapeso" which, as pointed out in Baillie Clutton and Ilbert's revised Britten 'Old Clocks and Watches and Their Makers', is precisely the way of regulating a verge and foliot escapement.

musical setting. Those who are familiar with this trend may have come across the ditty with the chorus:-

Take your time, me lovely old lad There aint no reason to hurry, For so long as you're able to wind up me clock Then I'll have no need for to worry

At this point it is interesting to recount the increasing influence of the Livery Companies. In London it had been the custom for various trades or crafts to group themselves together in particular precincts of the City. Signs of supervision of the crafts and trades by their respective guilds appear as early as the twelfth century, regulating prices, instituting technical education through apprenticeship, inspection of products, and a form of quality control. Each guild limited the number of apprentices, and forbad the conduct of its trade to any other than those who had been admitted to its freedom. In the 17th century the Freemen Clockmakers had obtained the right to practice their craft through the Blacksmiths Company, and no doubt only the simplicity of the medieval iron clock allowed a specialist blacksmith to make one. (It must be made clear that the term "Blacksmith" implied an artist in iron; the role of shoeing horses was the province of the Farrier). After a number of attempts, which were opposed by the Blacksmiths, the Clockmakers eventually succeeded in obtaining their own Charter from King Charles I on 22 August 1631. The Worshipful Company of Clockmakers controlled the horological trade in the City of London and within ten miles thereof, and was governed by a Master, three Wardens, and a Court of Assistants. The executive officer is the Clerk, who is assisted on ceremonial occasions by his Beadle. I have the honour to be a liveryman of this distinguished Company which has numbered among its members many famous clockmakers, and which continues to cherish its traditions and to play an active role in contemporary horology.

But no history of timekeeping, however cursory, can fail to make some reference to the sociological changes which influenced, and were influenced by, the increasing infiltration of time in daily life. Jaques le Goff remarks:- "Perhaps the most important way the urban bourgeoisie spread its culture was the revolution it effected in the mental categories of medieval man. The most spectacular of these revolutions, without a doubt, was the one concerned with the concept and measurement of time". He examined in detail the gradual transition, in the middle ages of urban organization from Ecclesiastical to merchants' time. The practical time of the Church derived from antiquity, and the bells which announced the canonical hours, - Matins, Lauds, Prime, Terce, Sext, None and Vespers continued to regulate the religious life of the community. But often the church clocks were imprecise and variable, and shopkeepers and workmen required a more exact time-keeping geared to worldly and secular needs. Goff says (and I give a free translation) "The public clock is an instrument of economic, social and political domination, belonging to the tradesmen who rule the community: and for this purpose the necessity of strict

timekeeping becomes apparent, for in the textile industry it is advisable that the day-workers, the labourers of the industry, should come to and leave work at fixed times". It is evident that while cottage industry and agriculture were the backbone of rural life, even the church clock was almost superfluous; but as work became centered in the towns, and factories and mills were established, uniformity of time, within the locality, became of increasing importance. Thus to quote Goff again:"This is the great revolution of the community movement in time regulation; these clocks set up everywhere are in competition with the church bells".

It may be convenient here to depart again from our chronological sequence and follow the subsequent developments of unification in time keeping. The need for local time developed from the industrial revolution, but by the mid-17th century, facilities for travel, hitherto the privilege of the aristocracy and prosperous merchants, began to become available to an increasing number of the populace. The stage-coach service, established in England in 1784, led to the spread of London time, determined at Greenwich Observatory, throughout the length and breadth of the country. Early in the 19th century, the railway system began to extend its tracks from the capital to the provinces, and the network of telegraph cables enabled all the major towns to conform to a unified system. In 1851 the Great Exhibition in Hyde Park, London, resulted in travel on an unprecedented scale. In a paper presented at the symposium last year to celebrate the Tercentenary of the Royal Observatory, I quoted Aldous Huxley's comment: - "In inventing the locomotive, Watt and Stevenson were part inventors of time". When Greenwich Mean Time was adopted as the legal time for England, Scotland and Wales in 1880, the law was endorsing an already existing situation.

Another aspect of timekeeping which cannot be omitted on this occasion concerns navigation. Many of you will be familiar with the problem facing the maritime nations in finding a solution to the determination of longitude at sea. In A Short History of Navigation, Branch and Brook-Williams recount the difficulties encountered by Columbus, which it is surely appropriate to quote in the country he is generally credited or blamed for having discovered: - "Columbus in his voyages used a simple needle supporting a paper compass rose and pivoted on a steel point. His ships were wooden and non-magnetic, but they were also small with consequent large motions in a seaway. Steering by that compass and other similar types must have done a great deal to enrich our language!" But such calamities as the wreck of Vice-Admiral Sir Cloudesley Shovell's fleet off the Isles of Scilly in 1707 after a twelve-day voyage from Gibraltar under cloudy skies, with the loss of 2 000 seamen was an outstanding and tragic occurrence which emphasized the hazards of navigational uncertainty, and which led the British Government in 1714 to offer an award of £20 000 to any person who could devise a method of finding the longitude of a ship at sea within an accuracy of 1° (or 60 nautical miles) at the end of a voyage from Britain to the West Indies. The use of a timekeeper on a ship for this purpose had been proposed as long ago as 1530 by Gemma

Frisius, but the first attempt to make a sea-going clock by Huygens in 1659 was unsuccessful. The reward was eventually won by a Yorkshire carpenter, John Harrison. Tests at sea had to be postponed, as Britain was then at war with Spain, and it was feared that the instrument might be captured. Preliminary trials were conducted on a barge in the Humber. It was in 1761 that Harrison's fourth timekeeper was taken to Jamaica and back in HMS Deptford. It was supervised on the journey by Harrison's son, William. On arrival in Jamaica it was found to be in error by no more than five seconds. The long and frustrating story of Harrison's battle to receive his reward is well-documented; suffice to say, he was eighty years of age before payment was made in full.

The need now became apparent for an international agreement on a standard meridian from which time and longitude could be reckoned. Many pamphlets were written, proposing various solutions, but a conference in Rome in 1883 strongly advocated the adoption of a single reference meridian, that of Greenwich.

If we are to pick out one name as that of the man chiefly responsible for the system of time zones based on Greenwich, that man must surely be Charles F Dowd, Principal of Temple Grove Ladies Seminary at Saratoga Springs. He received strong support from W F Allen, Secretary of the U S General Railway Time Convention, and fellowcountrymen Cleveland Abbe and President Barnard of Columbia University. Independently, Sandford Fleming, the Scottish-Canadian Engineer-in-Chief of the Canadian Pacific Railway, wrote copiously in favour and enlisted the interest of the British Government, despite the unenthusiastic, and at times hostile, attitude of such personalities as the Astronomer Royal and the Superintendent of the U S Nautical Almanac Office. Sir George Airy said:- ".. as to the need of a prime meridian, no practical man ever wants such a thing" while Professor Simon Newcome roundly condemned the whole idea, saying:-"A capital plan for use during the millenium. Too perfect for the present state of humanity. See no more reason for considering Europe in the matter than for considering the inhabitants of the planet Mars. No: we don't care for other nations, can't help them, and they can't help us".

At the formal conference in Washington in 1884 the various arguments were restated until eventually there was an unexpected measure of agreement. The British repressed their congenital leaning towards tradition, and the French relaxed their characteristic preference for logic. Practical considerations carried the day. The system of time zones related to the Greenwich meridian, and the adoption of Greenwich Mean Time, were duly approved. Various points of detail remained. It was not until 1925 that the almanacs employed GMT reckoned from midnight. The designation Universal Time was introduced to replace GMT, but has only been implemented in astronomical and some related contexts. But in these matters it is the users and the general public who seem to prefer the more meaningful term GMT with its obvious link with longitudes. The Radio Regulations of the International Telecommunications Union still retain GMT in their documents

as the authorized designation of time in the radio and communications field, and the fourth annual Navigation symposium, meeting in Washington last year, unrepentantly demanded "that the terminology Greenwich Mean Time be continued in its present sense in the practice of navigation".

But let us return for a few moments to our consideration of clocks. Pendulum clocks were the subject of progressive improvement. Temperature compensated pendulums, dead-beat escapements, magnetic correction for variations in barometric pressure and in 1921, the free pendulum clock. W H Shortt, a railway engineer, was investigating the causes of excessive wear on the track, especially on curves, and came to the reluctant conclusion that perhaps some drivers were not adhering strictly to the permitted speed limits. He decided to carry out some tests, which involved checking the speed of trains over short distances, and thus demanded accurate timing. His interest having been aroused, he employed his engineering skills in the construction of a clock to his own original designs. The first Shortt free pendulum and slave were tested at the Royal Observatory, Edinburgh, in 1921-1924 by Prof Sampson. In collaboration with F Hope-Jones of the Synchronome Company, Shortt clocks were made and brought into service at many of the major timekeeping observatories throughout the world, and ushered in a new standard of accuracy.

Incidentally, I found very puzzling a letter to the Times of 15 November 1976 (from Nikolai Tolstoy) who claimed that 50 years ago the Soviet Government executed Nikolai von Meck of the Peoples Commissariat of Railways for the crime of causing the trains to attend with diobolical precision to their timetables: the prosecution was able to prove that his intention was to cause speeding trains to wear out their tracks, thus leaving the USSR helpless in the event of war.

It was during the first year of my service as Head of the Time Department at Greenwich that we installed our first quartz clock. Almost immediately we were committed to a programme of extensive replacement of all the ancillary equipment. The old radio receivers, with their externally-mounted variable-reaction coils ceded place to newer designs which incorporated multi-electrode valves. To the best of my knowledge, the Greenwich Time Department was the first to make all routine measures of clock comparisons with electronic counters.

Radio time signals were measured using a visual cathode ray tube display with phaseable clock markers. The 1939-1945 war initially delayed some plans, particularly as we had to set up two emergency stations, Abinger and Edinburgh, for the control of the Rugby radio time signals, together with the short-wave emissions which we had also inaugurated. On the other hand, we were presented with a requirement, arising from the rapid developments in radar, to achieve a ten-fold increase in the accuracy of the radio time signals. With the assistance and ready co-operation of colleagues, both within the observatory and in other establishments, the target was attained. A major contribution was the provision, by the Post Office, of daily information on the quartz clocks at Dollis Hill Radio

Research Laboratories, who later supplied us with a number of clocks for use at our two time service stations. At Abinger an electronics laboratory was set up, and proved of immense value.

Probably the most outstanding advance in recent years was the realisation of atomic standards for time and frequency. We enjoyed the cooperation of the National Physical Laboratory, when in 1955 data from the caesium beam frequency standard of Essen and Parry became available for the absolute calibration of our quartz clocks. This continued until we were able to acquire commercial atomic clocks and to maintain an independent atomic time scale, and thus to take our place as one of the seven establishments contributing to the formation of the BIH scale of atomic time. Nevertheless, not everyone is greatly impressed. H Notwotny writes: "Today, as befits an age dominated by scientific thinking, precision and unambiguity, we have agreed to the definition of a standard second in terms of a spectroscopic frequency. The impact of this uncritical quest for physical precision is evident in many facets of our daily lives". Notice the sly dig "this uncritical quest".

One of the major tasks of a timekeeping observatory is the determination of astronomical time. The Airy transit circle, which defines the zero meridian, was superseded for time observations by small reversible transit instruments in 1926, and various improvements in instrumentation and in procedures met with some success. Around 1940 the photographic zenith tube, which had been adapted for time and latitude work at the US Naval Observatory, began to engage our attention. By courtesy of the USNO, full working drawings were made available to us, but after careful consideration we decided to embark on a new design. A small instrumentation laboratory was formed, and D S Perfect, working closely with Grubb Parsons of Newcastle, designed the instrument which, with a number of later modifications, is still in use today, and giving results of the highest quality. The decision of the Canadian authorities to instal a PZT on the same latitude has proved outstandingly successful.

I must apologize for straying from my original brief, the History of Time, to reminiscences of events during my forty years at the Royal Observatory. May I draw this discursive narrative to a close by referring briefly to three examples of the close collaboration which has been built up between the Royal Greenwich Observatory and our colleagues here in the United States.

It may not be generally known that the present co-ordinated system for radio time signals came into being following the success of an experimental exercise initiated by the USA and UK. The preliminary informal agreement was reached at a meeting in the garden of my house in Bexhill on a sunny afternoon on 19th July 1959. For the record, those present were H Barrell of the NPL and Chairman of the International Committee of Weights and Measures, R L Corke of the British Post Office Radio Branch Laboratories, L Essen (NPL), W Markowitz, Director of the Time Service

at the USNO, and D H Sadler, C A Murray, N P J O'Hora and myself from the RGO. My wife provided tea. A more formal meeting at the USNO on 26 and 27 May 1960 endorsed the arrangements. Markowitz was in the Chair: other participants were Andrews, Hastings and McNish (USA), Corke, Essen and Smith (UK) and, as an observer, Kalra from Canada. The principles were unanimously agreed, but the details left fluid. Markowitz and I were to develop the scheme as circumstances required. Despite the fact that the method, as you all know, depends upon the introduction of time steps (now leap seconds), neither of us has so far experienced the fate of the legendary Chinese astronomers Hsi and Hso who in the reign of Chung Kang, 7th or 8th century BC, were guilty of transgressing the "inviolable laws" by which "astronomers who advance or set back the time shall implacably (or, without pardon) be punished with death".

The second example I choose is the close liaison which has been achieved in the use of Loran-C. In the early stages problems were legion, but together with the USNO and the US Coastguards, a firm and accurate link has been established.

My last example is still in the development stage. Using equipment loaned by the Naval Research Laboratory, we made a series of comparisons using the previous Timation satellite. We are now securing better data with the present NTS-1 satellite. There have been many interesting problems to solve, but useful experience is being built up. In this enterprise, as in the many others which have preceded it, an outstanding feature has been the happy and amicable spirit of co-operation which has developed spontaneously between the USA and UK partners in our technical and social contacts. I personally view the present satellite programme as one with a great future. Perhaps once again we are blazing a trail that others will follow. Another chapter in the History of Time is in the making.

NAVSTAR GLOBAL POSITION SYSTEM (GPS) CAPABILITY AND PLANS FOR PTTI APPLICATIONS*

Cmdr. William G. Houston

Space and Missile System Organization Los Angeles, California

ABSTRACT

The NAVSTAR Global Positioning System (GPS) consists of a network of satellites in 12 hour orbits. When fully operational, the primary function of the system will be to provide data for precision navigation. A user with a special GPS receiver will obtain transmission from four satellites, each including a satellite ephemeris. With this information the receiver can calculate its 3-dimensional position within approximately 10 meters. To provide the extremely accurate system time required for this positional precision, each satellite will carry an atomic (Cesium and/or Rubidium) frequency standard. As a result, in addition to its primary function of navigation, the NAVSTAR system will offer an excellent source of precision time, and time interval, information available to any user with a simplified receiver at any place on the earth's surface.

(Paper not Received)

^{*}Presented by Capt. David C. Holmes, U.S. Naval Research Laboratory

THE HYDROGEN MASER PROGRAM FOR NAVSTAR GPS

Roger L. Easton
U. S. Naval Research Laboratory, Washington, D. C.

ABSTRACT

The Department of Defense has assigned to the Navy the task of providing both ground and space maser for NAVSTAR GPS. Two ground masers are being built by the Smithsonian Astrophysical Observatory (SAO) and two contractors, RCA and Hughes, are building preliminary space models. SAO has also succeeded in having a ${\rm TE}_{111}$ cavity mase. The National Bureau of Standards (NBS) in Boulder is building a passive maser. Supplementary research for this program is being conducted at NRL.

INTRODUCTION

In 1974 the Office of the Director of Defense Research and Engineering of the Office of the Secretary of Defense assigned to the Navy the responsibility of providing hydrogen masers for NAVSTAR ground stations and a space qualified maser for NTS-3 and future satellites. This paper describes the NRL efforts being made to respond to the NAVELEX PME 106 assignment.

The reason for the DDR&E interest in masers is evident from figure 1. Here it is seen that the passive maser is 10 times more stable than the small cesium and the active maser has much better stability than the passive.

A word concerning the status of hydrogen masers. A rough count shows that perhaps 50 such masers have been built and of these about one half are in working conditions. Two fifths of the total number were built by Varian. After the Varian time and frequency functions were bought by Hewlett Packard the Hydrogen Maser portion was given to the Smithsonian Astrophysics Observatory (SAO) located at Harvard Observatory.

Ground Masers

SAO has built 9 ground masers and two space probes. Two of the 9 were delivered to NRL. The one with which I am familiar has worked reliably for more than one year. Initially, it had problems with the dissociator and with the isolation amplifier but since these were fixed, it has operated reliably and well.

SAO is building two improved models for the NAVSTAR GPS program. Initially these units will be used to check out the space masers; ultimately it is planned that they be used at the master control station.

Space Masers

Competitive contracts have been let to two firms, the Hughes Research Laboratory in Malibu, CA, and the RCA Sarnoff Laboratory in Princeton, N. J. These two firms are building advanced development models of the physics packages and experimental development models of the electronics packages. The winner of the competition will then be determined.

Cavities

One of the major problems in the space maser is that of making the unit small. The unit size is determined largely by the cavity size. For the ${\rm TE}_{011}$ type cavity, almost universally used, the size before loading is approximately 11" in diameter and 11" long. This size is increased substantially by the cavity shell, a pressure vessel, and numerous magnetic shields and heaters.

Another candidate cavity is the ${\rm TE}_{111}$ which recently has worked in an operating maser at SAO. This cavity is smaller in diameter by a factor of 2.1 than the ${\rm TE}_{011}$ type and hence less than 1/4 the volume. A paper on this cavity is scheduled for tomorrow's program.

The second method of making a smaller cavity is to load it with dielectric. Mattison of SAO and Folen, Schelling and Lynch of NRL have worked on this problem. Both the $\rm TE_{011}$ and $\rm TE_{111}$ cavities have been solved analytically for most purposes. The $\rm TE_{011}$ is the most interesting of the two. The size of a $\rm TE_{011}$ cavity loaded by a $\rm Al_2O_3$ is considerably smaller than the unloaded $\rm TE_{111}$ cavity. Figure 2 shows the relative sizes of these devices.

While the loaded TE_{011} is the smallest of the three it does not appear possible to have this cavity work with an active maser. The losses of known dielectrics are at the threshold of oscillation but not low enough to provide a reliable unit. These loaded cavities, then, are as of now suitable only for use in passive masers.

Passive Maser

The passive maser work being supported by this program is one proposed by the National Bureau of Standards at Boulder, Col. This type, of which more will be heard tomorrow, uses the cavity and the hydrogen line transition as a filter, somewhat like the cesium beam is used as a filter in a cesium standard.

The passive maser has an advantage in size in that its operation is not critically dependent on having a specific value of cavity Q. The passive maser can therefore use the dielectric loaded cavity and thereby be made smaller than the active type units.

Maser Problems

So far we have considered the problems of building masers and more especially, small ones. Other problems exist in masers. One is the problem of shielding the cavity from external magnetic fields. Another is related to the darkening of dissociator bulbs. A third concerns bulb coatings. All of these problems not being investigated elsewhere are being looked into at NRL.

In the area of magnetic shielding a shield obtained from SAO was measured for shielding at both high and low level fields. The results of this work by Wolf are shown in figure 3. With the shield used it is apparent that the high level magnetic field shielding is superior to that at low level. Further work, especially with multiple shields, will be performed.

The dissociator, shown in figure 4, has been a source of problems in the early masers. One of the problems has been a darkening of the bulb and a subsequent failure to produce atomic hydrogen. While these problems have been overcome by the use of larger bulbs and better cleaning techniques they are still of interest. Consequently a darkened bulb was obtained for analysis from NASA Goddard. Figure 3 shows the results obtained in Auger equipment by

Ritz, Bermudez and Folen. It is apparent that carbon is a probable villain. Figure 5 shows the atomic fraction of carbon obtained for two samples. An obvious solution, as brought out by JPL, is that a better cleaning method is indicated.

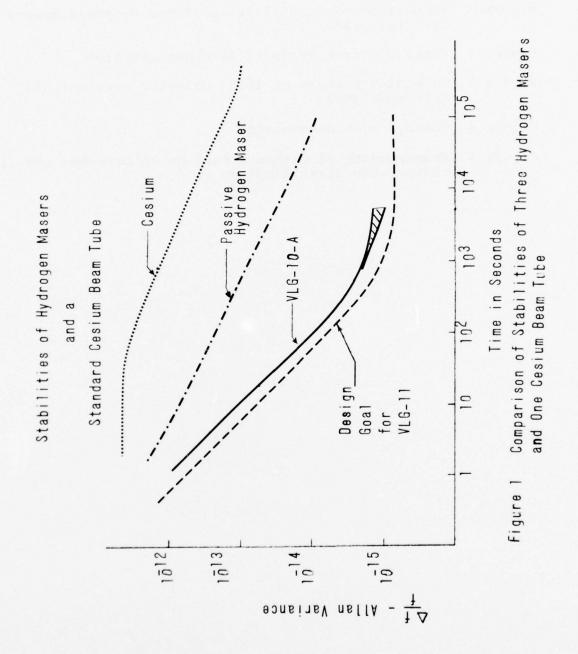
Another problem being supported by non GPS funds involves the bulb coatings. These coatings have been much maligned as possible weak points in maser design. While maligned, the measurements supporting any problem with bulb coating are scarce or non existant. This program is intended to determine if a problem exists in the coatings by measuring both old and new coatings by Auger and ESCA spectroscopy and Attenuated Total Reflection. In addition the use of highly florinated epoxy resins of the diclycidyl class will be evaluated.

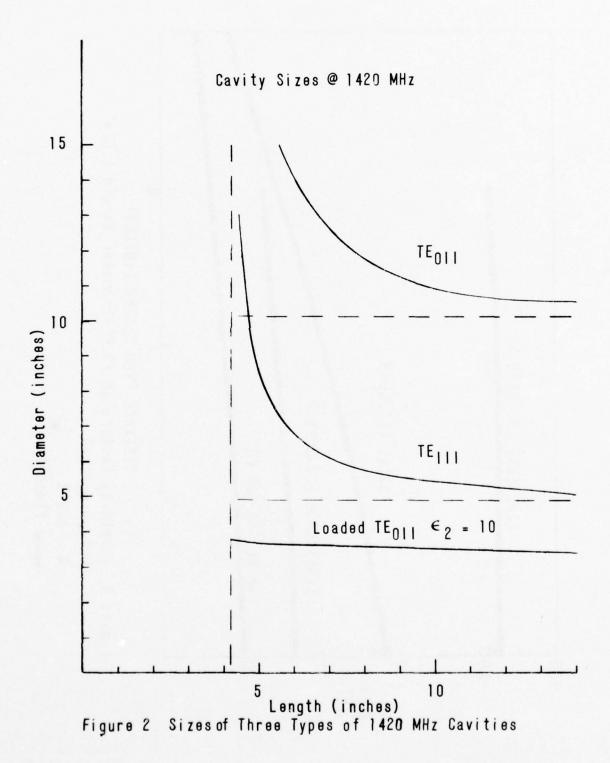
Summary

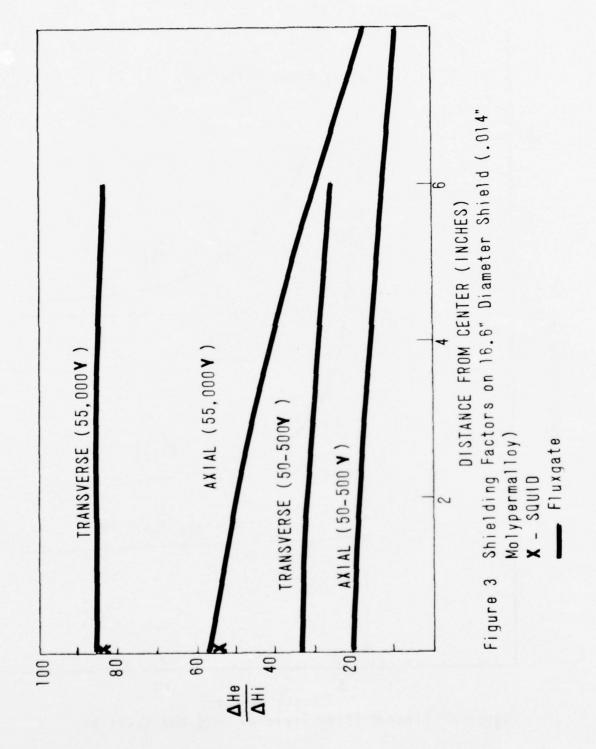
In summary it can be said that the hydrogen maser program for GPS is going well, especially well in the areas which make a small maser appear especially feasible. The TE_{111} cavity has been operated in an operating maser by SAO. The NBS work on the passive maser looks most encouraging, and the SAO-NRL work on dielectrically loaded cavities make a really small hydrogen maser conceptually possible.

Figures

- Figure 1 Comparison of Stabilities of Three Hydrogen Masers and One Cesium Beam Tube
- Figure 2 Sizes of Three Types of 1420 MHz Cavities
- Figure 3 Shielding Factors on 16.6" Diameter Shield (.014" Molypermalloy)
- Figure 4 The Hydrogen Dissociator
- Figure 5 Measurements of Carbon & Carbide on Darkened and Clear Dissociator Glass Samples







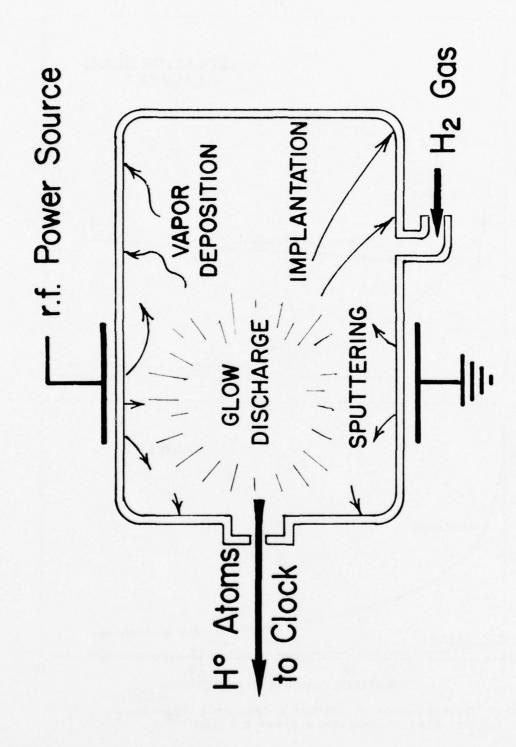


Figure 4 The Hydrogen Dissociator

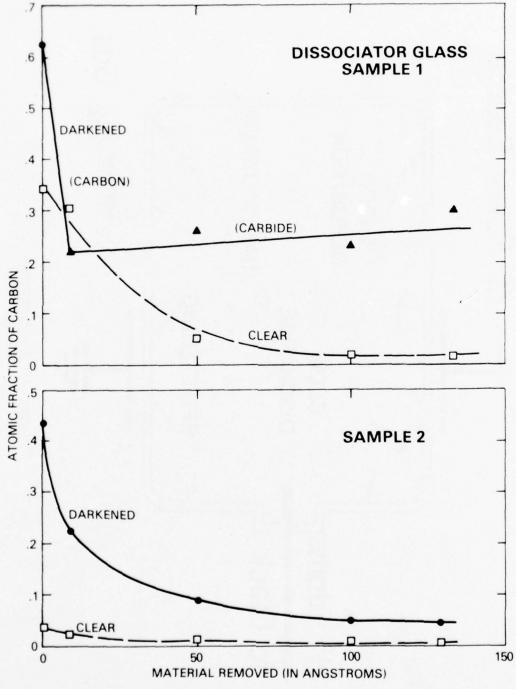


Figure 5 Measurements of Carbon & Carbide on Darkened and Clear Dissociator Glass Samples

OPERATION SCHEDULE AND PLANS OF WEST COAST LORAN C CHAINS

Cyrus E. Potts and Paul E. Pakos
U.S. Coast Guard

Washington, D.C.

ABSTRACT

The United States Coast Guard is in the process of expanding Loran-C radio-navigation coverage to include the entire Coastal Confluence Zone (CCZ) of the United States. This paper describes the status of that expansion program and reveals the plans for new Loran-C station locations and associated operational assignments. When completed, the Loran-C system will provide single station groundwave coverage over virtually the entire United States.

(Paper not Received)

ITU AND UNITED STATES SPECTRUM MANAGEMENT STRUCTURE

. 14

S. E. Probst

Assistant Director for Frequency Management
Office of Telecommunication Policy
Executive Office of the President
Washington, D. C.

ABSTRACT

Radio frequency management in the United States is derived from the Communications Act of 1934 and provides a system of dual management. This public law created the Federal Communications Commission (FCC), an independent Government agency directly responsible to the Congress, to be responsible for regulating non-federal government and international telecommunications. The FCC assigns radio frequencies to all public users including local governments and industry.

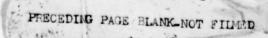
Under the same public law, the President has authority to assign frequencies to all Federal Government agencies. By Executive Order that authority is delegated to the Director of the Office of Telecommunications Policy, Executive Office of the President (OTP).

The Interdepartment Radio Advisory Committee (IRAC) with representatives of 18 Federal agencies advises the OTP on spectrum management matters. The FCC maintains a liaison contact with the IRAC.

The Spectrum Management Support Division of the Office of Telecommunications, Department of Commerce provides OTP and the IRAC with computer services and technical support.

In the United States frequency management policies are based on rules and regulations of the ITU. The Department of State is the link for international frequency coordination.

(Paper not Received)



THE INTERNATIONAL RADIO CONSULTATIVE COMMITTEE (CCIR)
ITS ROLE, FUNCTION AND INFLUENCE ON THE
DISTRIBUTION OF TIME AND FREQUENCY INFORMATION

Hugh S. Fosque
Chairman, U.S. CCIR Study Group 7
NASA Headquarters
Washington, D.C.

ABSTRACT

There are several organizations which play a role in the international coordination of frequency and time, and act to promote cooperation between nations in the standardization and regulation of frequency and time dissemination on a worldwide basis. Since dissemination methods depend predominantly on transmission of information by radio which does not recognize national boundaries, international organizations whose function is regulating the use of radio transmissions affect the way in which time and frequency information is promulgated between countries. The dominant international bodies dealing with radio transmission regulations are the International Telecommunications Union (ITU) and its advisory arm on technical matters, the International Radio Consultative Committee (CCIR). This paper will describe how the worldwide coordination of frequency and time is affected by the functions of the CCIR in its role of advising the ITU and the extent to which the workings of the CCIR influence frequency and time activities on a national and international basis.

INTRODUCTION

While not the only method, radio transmissions are the principal worldwide dissemination method used to coordinate time and frequency from one location to another. These transmissions transcend national borders and are regulated for the common good of all nations. The principal organizational body dealing with radio regulations is the International Telecommunications Union (ITU), which formulates and administers International Radio Regulations.

The ITU acts on technical matters principally on the advice of its technical advisor, the CCIR. Member nations provide information and advice directly to the ITU on non-technical matters and occasionally on technical issues when CCIR advice to the ITU is contrary to the national interest of a member country.

In order to understand the influence of the CCIR on these matters, it is necessary to review some of the history, background, and influence of its parent organization, the ITU.

THE ITU

The ITU was established in 1885 to provide coordination between countries for international telegraph communication. Today, the organization has about 153 member countries and concerns itself with radio as well as telegraph and telephone regulation. The ITU is affiliated with, but not a part of, the United Nations and maintains permanent offices and a staff of about 300 people in Geneva, Switzerland.

The ITU establishes agreements (regulations) at conferences participated in by its member countries. At about 20 year intervals, a "General World Administrative Radio Conference" (GWARC) is convened. At this meeting, all radio frequency allocation agreements between member nations are reviewed and updated. At more frequent intervals (5 years or so) limited "World Administrative Radio Conferences" (WARC's) are held which have authority only to suballocate the radio frequency spectrum already assigned at a GWARC to a particular service such as Space, Maritime Mobile, Aeronautical, or perhaps Space Broadcasting. The resulting allocation table from WARC meetings has treaty status between ITU member nations and in the U.S. must be ratified by the Senate and signed by the President prior to U.S. adherence to its provisions.

To perform its task of establishing worldwide standards and using these standards to effect regulation of the use of telecommunications between member nations, the ITU has three suborganizations to provide advice, new regulations, and information on current use of established telecommunication channels. These organizations are the International Telephone and Telegraph Consultative Committee (CCITT), the International Frequency Regulation Board (IFRB), and the International Radio Consultative Committee (CCIR). Figure 1 gives an organizational chart of the ITU

and indicates the general functions performed by each of these suborganizations.

THE CCIR

The CCIR provides the technical advice to the ITU on which the Radio Regulations are based. It has permanent offices and a small full-time staff located in Geneva. The CCIR accomplishes its work through international study groups whose meetings are usually held in Geneva. These study groups examine all technical aspects of radio frequency spectrum allocation and use; define technical problems which exist, or may arise, through the use of the radio frequency spectrum; and produce general technical recommendations to the ITU on how to allocate and regulate use of the radio frequency spectrum.

To accomplish CCIR work, international study group meetings are held. Attendees to these meetings are appointed by member countries. The chairmen of the various study groups for these meetings are internationally recognized experts and are elected to their offices at meetings of the CCIR, called Plenary Assemblies. At the Plenary meetings, the CCIR study groups sit as a body of the whole to ratify the work of the individual study groups prior to this advice being passed on to the ITU. The name and general scope of the activities of the CCIR study groups ege given in Figure 2.

To see how the CCIR works, refer to Figure 3. Member countries prepare and submit draft papers to the study group meetings, these national proposals are merged into studies and recommendations agreed upon by the international study group as a whole, then papers are circulated to the member nations for further consideration. After two such iterations, the papers are forwarded to the Plenary Assembly meeting of the CCIR. At the Plenary meetings all study groups are represented and each paper is examined. This allows review of the impact of the papers of one study group on another and avoids unexpected interaction between the recommendations of one study group on the work of another group. The coordinated recommendations from the Plenary meetings of the CCIR are then forwarded to the ITU.

UNITED STATES CCIR ACTIVITIES

In the U.S., the State Department serves as the U.S. focal point for policy formulation and dissemination of information relating to both CCIR and ITU and acts as the Head of the U.S. delegation at CCIR international meetings. The U.S. has established a U.S. study group organization which parallels the international study group structure (see Figure 2). The chairmen of the U.S. study groups are appointed by and serve at the pleasure of the State Department.

To accomplish the work of the CCIR in the U.S., an advisory committee has been formed called the National Committee of the CCIR. This committee is chaired by a State Department representative with membership consisting of U.S. CCIR study group chairmen, frequency managers for government departments and agencies, and interested private organizations. This advisory group reviews all U.S. CCIR documents prior to transmission to the CCIR for international consideration, and coordinates activity among U.S. CCIR groups. Figure 4 shows a working schedule of a typical U.S. study group in preparation for the various international CCIR meetings.

CCIR STUDY GROUP 7

The study group which influences frequency and time activities, both nationally and internationally, is Study Group 7. Figure 5 gives the terms of reference of Study Group 7 and the current international radio frequency allocations for frequency and time dissemination. The existing membership of U.S. Study Group 7 indicating the broad interest in its activities is given in Figure 6.

The activities of U.S. CCIR Study Group 7 at this time are in preparation for the next international meeting in January 1978. Work to prepare for this meeting falls into the following general areas:

1. In 1971, the International CCIR Study Group 7 recommended a new system of Coordinated Universal Time (UTC) be adopted and broadcasted by the time and frequency broadcast stations. This system went into effect on January 1, 1972. The new system makes possible the broadcast of the second as determined from atomic frequency standards and at the same time provides information on the earth's rotation rate, UT-1. There is continued work to eliminate problems related to the new UTC

System. Consideration will be given to change should serious problems arise.

- 2. To preclude misunderstandings due to the language used in CCIR recommendations, Study Group 7 currently has a significant effort underway to define certain important terms in an unambiguous manner.
- 3. There is mutual interference between standard frequency and time broadcast stations on the 2.5, 5, 10, and 15 MHz frequencies. This problem is accentuated in certain areas such as in Europe, and does cause problems for reception in other parts of the world. Study Group 7 has an interim working party looking into ways to reduce this serious problem.
- 4. In the last 5 to 10 years, considerable effort has been made to characterize frequency and phase noise of oscillators. This work has been largely successful and, to a very great extent, results of this work have been adopted by a broad spectrum of users including manufacturers of various types of oscillators. It is important for the future that an international standard for characterizing frequency and phase noise be available. In its current activity CCIR Study Group 7 is attempting to define such an international standard.
- 5. Study Group 7 has continuing effort to study and promote regional synchronization techniques such as the use of TV and other localized emissions.
- 6. There is a growing need for worldwide synchronization of time to less than 100 nanoseconds. The Study Group is engaged in defining the requirements for and practicality of providing operational systems capable of meeting these needs. For example: In the 1971 Space WARC, Study Group 7 proposed an allocation for two types of time synchronization service using earth orbiting satellites. These proposals were successful and resulted in a standard frequency and time service allocation at 400.1 MHz for one way broadcasts and allocation of 4202 and 6427 MHz for a two-way synchronization system. In view of the fact that the upcoming GWARC in 1979 may not be repeated for 20 years and in

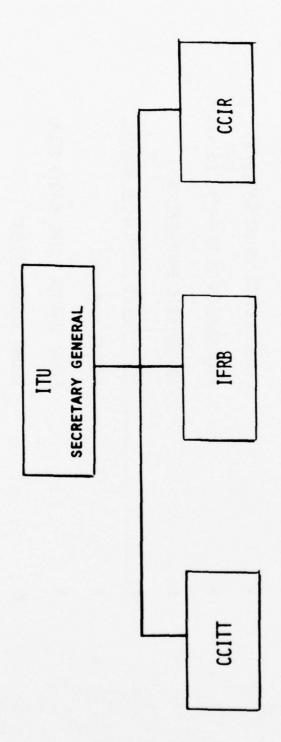
recognition of a need for future synchronization service to the 10 to 50 picosecond level, U.S. Study Group 7 is preparing a recommendation for a broadband frequency allocation in the 15-30 GHz band to allow for future satellite synchronization systems which can meet this need.

CONCLUSION

In summary, the current technology of time and frequency dissemination using radio has greatly improved our ability to transfer the information from place to place as required by most applications. Radio transfer methods have become so refined that it is now difficult to find a way to test the accuracy of radio dissemination. Methods which provided an alternate check means a few years ago, such as transportable atomic clocks, cannot today be depended upon to test satellite synchronization links to their full capability if the points to be synchronized are separated by 2000 miles or more, even when the clocks are carried from point to point by aircraft.

The future use of radio methods for time and frequency transfer will surely come into even greater use making the activities of the CCIR even more important to the interest of the time and frequency technologist and to the use of this technology for future system applications.

ITU ORGANIZATION



MAINTAINS FREQUENCY
 USAGE DATA

TELEPHONE & TELEGRAPH

STANDARDS

TARIFFS

ETC.

- MEDIATES INTERFERENCE PROBLEMS
- RADIO
- STANDARDS
 FREQUENCY SHARING
- INTERFERENCE
- ETC.

Figure 1

CCIR STUDY GROUPS

SCOPE	SPECTRUM UTILIZATION, MONITORING	SPACE RESEARCH AND RADIOASTRONOMY	FIXED SERVICE BELOW 30 MHz	FIXED SERVICE USING SATELLITES	PROPAGATION IN NON-IONIZED MEDIA	IONOSPHERIC PROPAGATION	STD-FREQUENCY AND TIME SERVICE	MOBILE SERVICES	FIXED SERVICE USING RADIO RELAY	SOUND BROADCASTING	TV BROADCASTING
STUDY GROUP		2	3	4	2	9	7	œ	6	0	=

HOW CCIR WORKS

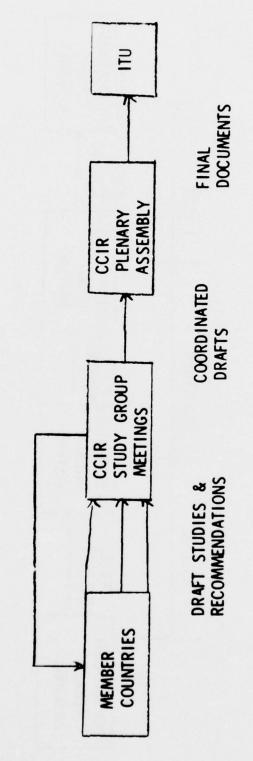


Figure 3

U. S. CCIR WORKING SCHEDULE

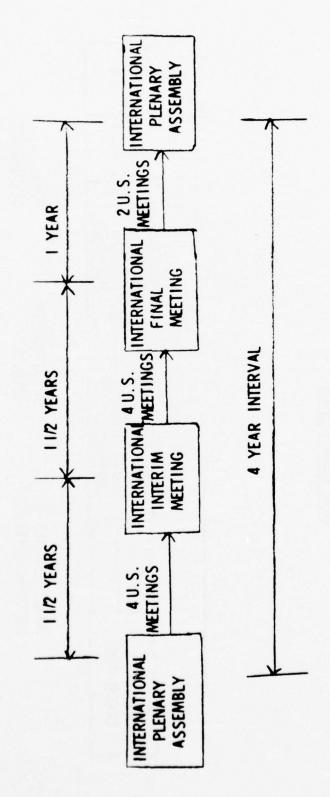


Figure 4

CCIR STUDY GROUP 7

TERMS OF REFERENCE

- COORDINATE WORLD-WIDE SERVICES OF STANDARD FRECUENCY & TIME SIGNAL EMISSION
- THE USE OF SATELLITE TECHNIQUES IN THESE SERVICES AND MEANS TO IMPROVE THE ACCURACY OF MEASUREMENT STUDY TECHNICAL ASPECTS OF EMISSION & RECEPTION INCLUDING

ALLOCATIONS FOR FREOUENCY & TIME

- 20.0 MHZ + 10 KHZ	- 25.0 MHZ ± 10 KHZ	- 400.1 MHZ + 25 KHZ (SPACE-TO-EARTH)	- 4202 MHZ + 2 MHZ (SPACE-TO-EARTH)	- 6427 MHZ + 2 MHZ (EARTH-TO-SPACE)
- 20 KHZ ± 0.05 KHZ	- 2.5 MHZ ± 5 KHZ	- 5.0 MHZ ± 5 KHZ	- 10.0 MHZ ± 5 KHZ	- 15.0 MHZ + 10 KHZ

MEMBERSHIP U.S. CCIR STUDY GROUP - 7

45 MEMBERS

• 60VI.

AIR FORCE

ARMY

COMMERCE DEPT.

DCA

DOT

NBS NELC NRL OTP

SAO

STATE DEPT.

USCG

FAA

USNO

PRIVATE CORP.

• NAVY

HUGHES

JAMES MILLEN

NATIONAL SCIENTIFIC LABS

UNIVERSITY

· MIT

. APL

INDIVIDUALS

Figure 6

THE BUREAU INTERNATIONAL DE L'HEURE

Humphry M. Smith, Chairman, Directing Board

Differences of longitude between observatories, hitherto restricted to rare exercises involving transport of chronometers, became practicable in the mid-1840's with the spread of the electric telegraph system, but a new era of international co-operation resulted from the successful pioneer experiments early in 1899 when radio signals from Dover. England, were received across the Channel at Boulogne, France. (1) It was soon realised that radio signals could be used, not only for the determination of longitude, but also for the dissemination of time. In September 1903 the U.S. Navy began short-range low-power transmissions from Navesink, New Jersey, (2) and in January 1905 inaugurated regular broadcasts at midday.(3) Experimental services commenced in Germany (Norddeich) in 1907 and in June 1910 details of a regular service were announced officially by the Reichs-Marine-Amts. In France the Bureau des Longitudes resolved in 1908 "that a service of time signals be installed as soon as possible at the Eiffel Tower as an experimental service for the determination of longitudes", and work started in January 1910. It was interrupted when some equipment was put out of action by the flooding of the Seine, and a regular service from the new installation commenced officially on 23 May 1910 "as much in respect of time as in the determination of longitudes". (4)

It is surely appropriate to commend the perspicacity of the Bureau des Longitudes in realizing that positive action should be taken to rationalize radio time signal emissions on a world-wide basis, and to acknowledge their initiative in arranging a conference in Paris in October 1912 "to study ways of effecting practical unification of time, and to prepare a plan for the organization of an international time service able to meet all needs". (5) Sixteen nations were represented, and following lengthy discussions, proposed the establishment of a "Commission International de l'Heure" to secure unification of radio time signals; to ensure the universal use of GMT; to create an executive organization, the Bureau International de l'Heure (BIH) in Paris, with the task of co-ordinating results from observatories and to deduce the most exact time. Discussion of the results was to be undertaken by the Association géodesique internationale at Potsdam.

At a further meeting held the following year, (6) formal statutes of the organization, renamed the Association International de l'Heure, were drawn up, (7) but were never ratified owing to the outbreak of war in Europe in 1914. Despite many difficulties, the BIH continued to operate, under the direction of B. Baillaud, with the invaluable support of General Ferrié. In 1918 the Royal Society in London called an Inter-Allies Conference of Scientific Academies for the reconstitution of the

international scientific organizations which had existed pre-war. It was proposed to form national committees which would be federated in an international council. At a further session, held in Paris later the same year, an executive committee was formed, and at a third session in Brussels in July 1919, formal statutes were adopted. One result was the creation of the International Astronomical Union (IAU), which included in its 32 commissions, number 31, the Commission de l'Heure. (8) The original statutes were taken as a model, and new regulations were drawn up to bring the Time Commission and the BIH under the auspices of the IAU. (9) It was pointed out, however, that the 1913 conference "included only 15 astronomers out of 54 delegates, the remainder being administrators, technicians and others. Consequently the authority of the Commission is more limited". Under the IAU, the field of activity was restricted to astronomical affairs, and ... "it is not in a position to give authoritative opinion upon matters of administrative convenience of different States, as to the needs of seafarers or on technical questions of electrical engineering ..." (10). It was probably a remanent effect of this attitude which subsequently led such organizations as the International Radio Scientific Union (URSI) and the International Radio Consultative Committee (CCIR) to take the initiative in questions involving radio time signal emissions.

When B. Baillaud became President of the Union, G. Bigourdan was appointed Director of the BIH (1 January 1920 until 31 December 1928). From 1929 to 1965, the Director of the Paris Observatory was "ex officio" Director of the BIH, and a "Chef des Services" was appointed.

		Director	Chef des Services
Jan.	1929 - Oct. 1929	H. Deslandres	A Lambert
Oct.	1929 - 1944	E Esclangon	" "
	1945 - Sept.1963	A Danjon	N Stoyko
Oct.	1963 - Sep. 1964	F Denisse	" "
Oct.	1964 - 1965		B Guinot

In addition to correlating data on astronomical observations of time, and on radio time signals, the BIH sponsored an international longitude operation in 1926, followed by a further programme seven years later. The results were published: (11) Some anomalous values were revised, and international co-operation was facilitated. In 1937 combined BIH data were employed in the determination of the seasonal fluctuation in the rotation of the Earth; (12) the amplitude obtained was less than had been deduced earlier, (13) although subsequent investigations gave an even smaller value. (14) Other research carried out at the BIH was concerned with geophysical phenomena.

At the International Telecommunication and Radio Conferences, Atlantic City, 1947 (15) a series of frequencies was allocated for standard

frequency services, and in Appendix B of the associated Radio Regulations the International Telecommunication Union (ITU) expressed the opinion that:- "The addition of time signals superimposed on these same broadcasts is also highly useful and should be included, if possible." (16) Among the proposals submitted to Study Group 3 (SG3) of the CCIR for consideration at the meeting in Stockholm in 1948 was a draft recommendation implementing the Atlantic City initiative, (17) and incorporating representations by the French administration that "The co-ordination of time signals falls within the competence of the International Committee for Time; The determination of Universal Time ... falls within the competence of the International Committee for Time... the organization in charge of international co-ordination of standard frequency transmissions can only be the CCIR or a special subcommittee constituted by the CCIR." (18) The adopted Recommendation No 18 specifically requires (para 12) "that Study Group No 7" (which took over these responsibilities from SG/3) "seek the co-operation of the International Committee of Time in the provision of the time service". (19)

At the Royal Greenwich Observatory, (RGC), the astronomical observations of time had been corrected for the effects of polar variation since 1948, and for the seasonal fluctuation since October 1949, thus providing a quasi-smooth time system "Provisional Uniform Time" (PUT). (20) By 1955 the BIH found that four independent systems of correction had come into use among participating observatories, and the resultant problems were discussed by the IAU in 1955, (21). Following subsequent correspondence, a report was prepared by N. Stoyko (Chef des Services, BIN), in October 1955 setting out the plans for the introduction of UTO, UT1 and UT2, and for the inauguration of the Service International Rapide des Latitudes (SIR) to compute current extrapolations of the polar motion to be used in the formation of UT1. Initially the SIR was located in Turin, but this led to some delays and the work was undertaken at the BIH. The number of stations furnishing data increased from 4 (1956) to 33 (1965). (22)

Another significant innovation took place in 1955. Following development work in the United States, where the National Bureau of Standards had built an ammonia molecular clock in 1948, (23) and caesium beam standards had been constructed, (24) - in one case running for six weeks in 1954 with an accuracy of +1 in 10°, L. Essen and J. Parry at the National Physical Laboratory (NPL) brought an atomic standard into regular use in 1955. The caesium transition frequency was determined as 9 192 631 830 + 10 in terms of PUT. (25) The atomic standard was then used for the calibration of quartz clocks employed in the formation of the Greenwich Atomic Time scale (GA). The data were also made available to the BIH where A and N Stoyko determined the progressive retardation in the rate of rotation of the Earth. (26) Measures made with the NPL standard were then compared with data from the US Naval Observatory over the period 1955 - 1958, and the caesium

frequency in terms of the second of ephemeris time furnished the now-familiar figure of 9 192 631 770. The BIH atomic time scale A3, with initial epoch 1955, based on the results from three independent standards, NPL (England); Neuchatel (Switzerland); NBS (USA) was formed from 1 January 1958 (20 h UT) using phase comparisons on VLF and LF. (28,29) This continued until near the end of 1968, when a few participating establishments started regular reception of the pulses of the Loran-C navigation system, and direct time comparisons became feasible.

A further significant advance arose from the pilot scheme for international co-operation which was inaugurated between the USA and UK on 1 January 1961. (30) In this scheme the radio time signals followed the uniform rate of Atomic Time, AT, but since the scale interval of AT had been chosen to conform to that of ET, it was necessary to apply an extrapolated frequency offset, reassessed annually to maintain approximate agreement with Earth rotational time, UT. If an excessive departure developed owing to an unforeseen change in the rate of rotation of the Earth, a step adjustment was applied to the radio signals. The principle of maintaining a constant rate, with step adjustments, had been in use in the UK since 1944, and had become more effective with the introduction of atomic standards. The USA/UK co-ordination operated through the informal mutual agreement of the observatories concerned, but other authorities found it advantageous to synchronize with the USA/UK system. Following discussions at the IAU in 1961 (31) the CCIR recommended in 1963 that all time signal emissions should conform to the co-ordinated system, (now designated UTC), and that the BIH should undertake the responsibility of promulgating the frequency offsets (in units of 50 parts in 1010) and the dates and times of step adjustments (in units of 0.1 s). (32) This action was confirmed by the IAU in 1964. (33).

It is perhaps fitting at this stage to pay tribute to the work of N. Stoyko, who joined the BIH 1 November 1924, and carried on the work after the arrest of A. Lambert 21 August 1943 (died in Germany 15 August 1944). Confirmation of his position as Chef des Services was granted in 1945, and he served with distinction in this capacity for nearly twenty years. It was with a real sense of personal loss that we heard of his death on 14 September 1976.

In 1965 the BIH was reorganized in order to conform with the statutes of the Federation of Astronomical and Geophysical Services. The Director of the Paris Observatory was no longer the ex-officio Director of the BIH, and B. Guinot became Director of the BIH. A Directing Board was formed, with two representatives of the IAU, one each from the IUGG and URSI, and an observer from CCIR: the Director BIH was also a member ex officio. (34) In the past, much of the work of the BIH had consisted of publishing extensive tables of times of reception of an ever-increasing number of radio time signals. Due to difficulties in ensuring prompt receipt of data from some observatories, the

definitive results only became available many months in arrear. With most authorities maintaining closer controls and conforming to the co-ordinated system, individual reception times were now of less interest. Other changes were seen to be advantageous, and the various publications were rationalized and a much accelerated publishing schedule was introduced. Operational procedures were modernised, and greater use made of computer techniques.

By 1968 considerable dissatisfaction was being expressed concerning the frequency offset, which caused the intervals between successive time signal pulses to depart from the second; moreover some world-wide radio navigation and communication systems experienced great practical difficulties in making simultaneous adjustments to the adopted frequency offset. The CCIR set up an International Working Party, IWP 7/1, to explore the possibility of eliminating the offset and making one-second step adjustments (the latter generally involved no physical readjustment, but could be applied arithmetically.) (35) In view of the wide repercussions of the proposed changes, efforts were made to publicise the conflicting requirements and to invite opinions on possible solutions (36).

In 1969 the Loran-C radio-navigation chains made practicable time comparisons between observatories on a regular basis to a higher accuracy than had been possible using VLF and LF phase measures. The former BIH scale of atomic time A3 was succeeded by TA (BIH), formed from the seven independent scales of the Physicalisch-Technische Bundesanstalt (PTB); US Naval Observatory (USNO); TA (F), a mean of the standards at three French establishments; Royal Greenwich Observatory (RGO); National Research Council (of Canada) (NRC); US National Bureau of Standards (NBS); Observatory of Neuchâtel (ON), all being linked through the Loran-C network. (37)

A recommendation of CCIR Study Group 7 in 1969, endorsed by the Plenary Assembly in 1970, (38) proposed the removal of the inconvenient offset from the co-ordinated radio time signals and, with the concurrence of the International Marine Consultative Organisation (IMCO) (38a), to substitute one-second step adjustments. Details were specified in Recommendation 517, (39) and the new UTC system was brought into operation by the BIH following an initial adjustment on 1 January 1972.

In the process of introducing new international units as the basis for measurements, the International Committee of Weights and Measures (CIPM) was concerned by the unsatisfactory situation in which one of the basic units, the second, was defined as a specified fraction of a time interval, the day, which was known to be variable in length. In 1956 there was little choice: atomic standards of frequency (and time interval) were rare and might still be regarded as unproven; the only alternative unit was the second of ephemeris time (ET) which, by

definition, is invariable. (40) It was soon realised that the choice was an unfortunate one, as ET can only be determined in arrear, and then only with insufficient accuracy for most modern needs. By 1964 it was realised that atomic standards could be used to make the ET second accessible. (41) Because of its convenience and superior accuracy, the atomic definition of the second was formally adopted in 1968. (42) The next task was to define and to maintain an international reference scale of time, so the CIPM recalled their consultative committee (CCDS) to examine the problems and make recommendations. The CCDS had little hesitation in proposing that the existscale of the BIH should be accorded formal recognition, (43) despite the fact that the BIH is a service of FAGS (and thus indirectly under the auspices of the International Council of Scientific Unions (ICSU) whereas the CIPM is an inter-Governmental organization. The 14th General Conference of Weights and Measures endorsed this arrangement; (44) a representative of the CIPM was invited to assist the Directing Board of the BIH, and a member of the staff of the International Bureau of Weights and Measures has been attached to the BIH to participate in the additional tasks involved. Discussions continue in the CCIR concerning the UTC system of radio time signals (particularly on time codes) (45) and in the CCDS (particularly on the national legal implications of the use of UTC). (46) In addition, these organizations, together with the IAU and other interested parties, are concerned with the manner in which the conflicting requirements of stability, and conformity of the scale unit with the consensus of primary laboratory standards, can be best resolved.

Among the important advances that have been made under the Direction of B. Guinot, the first concerns the international scale of atomic time, now designated by the language-independent acronym TAI. Because of (a) some doubt as to the strict independence of the seven constituent atomic scales, which vitiated statistical methods for the combination of data, and (b) the desire to include information from the maximum number of establishments possessing atomic clocks and adequate means for comparing them internationally, since August 1973 participants have communicated data from individual clocks. An algorithm (47) in which the clocks are objectively weighted according to their recent performance, has been devised, and is now being modified to take account of the measures made at the three standards laboratories: - PTB; NRC and NBS. A step adjustment in frequency (rate) is scheduled for 1 January 1977, and a modified algorithm will seek to achieve stability of rate while maintaining the time interval of TAI (and of UTC) in accord with the consensus of the determinations of the primary laboratory standards.

Another advance has been made in the formation of the BIH definitive scale of UT1. An improved impersonal method of weighting the astronomical observations was introduced in 1971 resulting in a significant enhancement of accuracy. (48). In order to meet the special needs of the space programme in the navigation of deep-space probes, a rapid service

was inaugurated: each collaborating observatory reduced the observations quickly and communicated the results to the BIH by radio or Telex. The data were correlated and communicated to the Jet Propulsion Laboratory with minimum delay. The success of the programme (which was carried out with financial assistance from NASA), permitted trajectory correction manoeuvres (reported by letter Fliegel, JPL, to Guinot, BIH, 9 April 1974) as follows:- "Mariner 10 encountered Mercury within 60 km of the predicted aiming point, with the most accurately determined orbit achieved so far Improvement in JPL operations since the inception of the BIH Rapid Service has been dramatic. Uncertainties in UT1 are no longer considered to be a dominant source of error in navigation ..."

A notable contribution to astronomical and geophysical research in recent years has been the availability in machine-readable form of the collated observational data received from all participating organizations. It is unfortunate that this facility is not widely known, and that some research has been carried out using unsuitable data. In all applications where errors associated with a particular station might be significant, the BIH data should be employed. It was with the aid of such material that it was demonstrated that tidal waves and the diurnal nutation significantly increased the scatter of astronomical observations of time: the appropriate corrections were tabulated in the BIH Annual Report for 1971. (49)

In 1972 the published values of the coordinates of the pole incorporated data supplied by the Dahlgren Polar Monitoring Service (DPMS) of the US Naval Weapons Laboratory and based on Doppler satellite observations. (50).

The many developments of the past 15 years, and particularly the added responsibilities of the BIH for the reference scale of atomic time, were considered by the IAU in 1976, and new terms of reference have been recommended. (See Appendix A).

It will be apparent that under a succession of devoted Directors the BIH has amply fulfilled the hopes of the farsighted scientists who were responsible for its foundation in 1912/1913. The emergence of newer techniques of radio astronomy, laser tracking, VLBI and Doppler ranging of artificial satellites confirm the belief that further progress may be anticipated with confidence, and that the Bureau is held in the highest esteem and merits continued support, both scientific and financial.

APPENDIX A

Revised terms of Reference of BIH Adopted by IAU General Assembly 2 September 1976

The functions of the BIH shall be

- (a) to establish the scale of the International Atomic Time TAI, in accordance with the decisions of the 14th Conférence Genérale des Poids et Mesures and in conjunction with the Bureau International des Poids et Measures;
- (b) to establish, from all relevant data, and to publish the current values of the Universal Time and of the angular velocity of the Earth's rotation and, in addition, the operational coordinates of the pole used for this purpose;
- (c) to implement the system of the Coordinated Universal Time UTC by the distribution of all necessary information for the coordination of time-signal emissions and the synchronization of clocks on the UTC scale;
- (d) to distribute information important for scientific users of time, and to supply on request the available data on the subject of time;
- (e) to perform scientific research as necessary for the improvement of the service.

References

- 1. Conference International de l'Heure (CIH 1912). Bureau des Longitudes p. 16, Gauthier-Villars, Paris 1912.
- 2. J.F. Hellweg, U.S. Navy Time Service. Pub. Astr. Soc. Pacific 52, 505, p.17, 1940.
- 3. CIH (1912) p. 84.
- 4. CIH (1912) p. 17.
- 5. CIH (1912) p. 1.
- 6. Conference International de l'Heure (CIH 1913), Gauthier-Villars, Paris, 1913.
- 7. Convention Internationale pour la création d'une Association Internationale de l'Heure, p. 73, CIH 1913.
- 8. G. Bigourdan, Bulletin Horaire Tome III, no. 46, p. 260, 1929.
- 9. IAU Trans. VIII, p. 223, 1922.
- 10. ibid, p. 110
- 11. N. Stoyko and Mme P. Dubois, La Deuxième operational Internationale des Longitudes. Resultats-Conclusions-Bureau Central de 1'AIG, Paris 1952.
- 12. N. Stoyko, Comptes Rendues, 205, p.79, 1937.
- 13. F. Pavel and W. Uhink, Astron. Nachr. 257, p. 365, 1935.
- 14. H.M. Smith, Proc. IEE, 99, Pt.IV, p.1. 1952.
- 15. Final Acts, Int. Tel. & Radio Conf., I.T.U. Atlantic City, 1947.
- 16. ibid. Radio Regulations, p.287.

- 17. Proposals Submitted to the CCIR; Stockholm, July 1948. ITU, Geneva, 1949.
- 18. Atlantic City Radio Conference. Document 456R, Appendix 7, pp. 19-21.
- 19. CCIR Recommendations; 5th Meeting Stockholm, p. 68, 1948.
- 20. H.M. Smith, Proc. IEE, <u>98</u>, II, p.1., 1951.
- 21. IAU Trans. IX. 1955.
- 22. N. Stoyko. Bulletin Horaire No. 9 (Série 6), p.229, 1964.
- 23. H. Lyons, Electronic Engrg. 68, p. 251, 1949.
- 24. J. Sherwood, H. Lyons, R. McCracken and P. Kusch, Bull. Am. Phys. Soc. 27, p. 43, 1952.
- 25. L. Essen and J. Parry. Nature, <u>176</u>, p.280, 1955.
- A. and N. Stoyko, Comptes Rendus, <u>246</u>, p.235, 1958.
 W. Markowitz, R. Hall, L. Essen and J. Parry, Phys. Rev. Lett, <u>1</u>, p.105, Aug. 1958.
- 28. Bulletin Horaire Série J. No. 1, p.3., 1964.
- 29. BIH Annual Report, pp. 14-16. 1968.
- 30. H.M. Smith, Proc IEEE, 60, p.479. May 1972.
- 31. IAU Proc. XI, 1961.
- 32. CCIR X Plen. Assembly, Geneva, 1963.
- 33. IAU Proc. XII. B., 1964.
- 34. IAU Info. Bull. No. 16, p.12, 1966.
- 35. CCIR Int. Mtg. SG VII, p.85. 1968.
- 36. H.M. Smith, Nature, 221, p. 221, 1969.
- 37. BIH Annual Report, 1969.
- 38. CCIR XII Plenary Assembly, Vol. III, p. 227, 1970.
- 38a. IMCO. 24th Session Maritime Safety Committee, London, September 1971.
- 39. ibid, p. 258a-d.
- 40. CIPM Procès-Verbaux, 2 Serie XXV, Paris, p. 77, 1957.
- 41. CR XII, CGPM, Paris, p.93, 1964.
- 42. CR XIII, CGPM, Paris, p.103, 1968.
- 43. CCDS 5 session (Rec. S2, p.22), BIPM, Paris, 1970.
- 44. CR XIV, CGPM, Paris, pp.77-78, 1971.
- 45. CCIR, Int. Meeting SG7, p. 117, 1976.
- 46. CCDS, p.11 (and Rec. S1, 1974, p.14) 7 session BIPM, 1974.
- 47. BIH Annual Report, p. A8, 1973.
- 48. BIH Annual Report; Table 2. (Explanation: Section E), 1971.
- 49. BIH Annual Report, p.A4, 1971.
- 50. BIH Annual Report, p.A2, 1972.

DEFINITION, REQUIREMENT, AND THE DETERMINATION OF UT1 BY THE U. S. NAVAL OBSERVATORY (USNO)

Dennis D. McCarthy
U. S. Naval Observatory
Washington, D. C.

Abstract

Universal Time (UT) is a form of mean solar time, the period of which is a fraction of the rotational period of the Earth measured with respect to a frame of reference fixed in space. The time scale determined from astronomical observations is designated as UTO. The UTl time-scale is obtained by correcting UTO for the changing orientation of the rotational pole with respect to the observer. The epoch of coordinated Universal Time (UTC) is adjusted occasionally so that UTC remains within ±0.9 second of UTl.

The UTl time scale is not only essential for timekeeping purposes but it is also necessary for geodesy; astronomical observations of all kinds; navigation on sea, air, and in space; and astronomical and geophysical research. The definition of UTl as well as the procedures for observing and determining this time scale will be outlined. It is important that we strive to obtain the most accurate determinations of UTl since many users have stringent requirements for precision, accuracy, and consistency.

Introduction.

Traditionally time has been based on the rotation of the Earth with respect to the Sun. The present realization of this time scale is called Universal Time. This is a form of mean solar time, the period of which is a fraction of the rotational period of the Earth with respect to a frame of reference fixed in space. Operationally, Universal Time is defined as "12 hours + Greenwich Hour Angle of a point on the equator whose right ascension is given by $R_{\rm u}=18h\ 38m\ 45.836+8640184.542T_{\rm u}+0.0929T_{\rm u}^2$ where $T_{\rm u}$ is the number of Julian centuries of 36525 days of Universal Time elapsed since the epoch of Greenwich mean noon (regarded as 12h UT) on 1900 Jan. 0." (Explanatory Supplement, p. 73).

Universal Time is by definition an observational time scale. The point, $R_{\rm u}$, referred to in the definition is not identified with any physically observable point. It is only a point used to define Universal Time. The Greenwich Hour

Angle of this point depends on the orientation of the Earth in the reference frame. Since it is known that the Earth experiences small, unpredictable changes in its rotational velocity the time scale is necessarily non-uniform. The time observed at observatory "i" is referred to as UTO(i). This quantity depends on the location of the observer on the surface of the Earth with respect to the instantaneous pole of rotation and its angular distance from Greenwich as well as the rotational speed of the Earth.

Since the rotational pole is moving with respect to the surface of the Earth its position with respect to the Conventional International Origin (CIO) is determined from observations in angular measures in two coordinates (x,y). The x-axis is directed along the meridian of Greenwich while the y-axis is directed along the meridian of 90° west longitude. The time scale UT1(i) is obtained from UTO(i) by correcting for the effect of polar motion using the expression

$$UTl(i) = UTO(i) + (x \sin \lambda(i) - y \cos \lambda(i))$$

$$\tan \phi(i)/15,$$
(1)

where $\lambda\left(i\right)$ and $\varphi\left(i\right)$ are the longitude and latitude of observatory i.

In addition, corrections for annual and semi-annual variations in the rotational speed of the Earth due to meteorological and tidal effects may be applied to obtain UT2(i). The empirically determined expression which has been in use as recommended by the Bureau International de 1'Heure (BIH) since March 1962 is

$$UT2(i) = UT1(i) + 0.022 \sin 2\pi T - 0.012 \cos 2\pi T$$

$$- 0.006 \sin 4\pi T + 0.007 \cos 4\pi T,$$
(2)

where T represents the fraction of the Besselian year of the observation.

Determination of Universal Time.

In practice UTO(i) is determined from the astronomical observations of the diurnal motion of stars through the intermediary of sidereal time. The sidereal time at any instant at any location is defined as the local hour angle of the equinox at that instant. Since the equinox is not an observable point, stars are observed whose positions with respect to the equinox are well known.

An observation of a star in this case usually is the determination of the time of transit of a star across the observer's meridian on some reference clock. This observation may be affected by accidental and systematic errors in the assumed position of the star, refraction in the atmosphere and by variations in the observer's apparent meridian caused by lunisolar lidal or other geophysical influences on the direction of the vertical.

Astronomical observations used in the determination of Universal Time are made by the U. S. Naval Observatory using photographic zenith tubes (PZT) located in Washington, DC, and Richmond, FL. This instrument has been described by Markowitz (1960). Essentially, it is used to determine the clock time of transit of selected stars across the instrumental meridian.

With the PZT the UTO time of transit of a star across the meridian of the instrument is computed using the expression

$$T_{C} = (\alpha + \lambda - ST - EQ)r, \qquad (3)$$

where

 α = apparent right ascension of the star,

 λ = astronomical longitude of the instrument,

ST = Greenwich mean sidereal time at Oh UT,

EQ = equation of the equinoxes, and

r = ratio of mean solar to mean sidereal interval

(0.997269566414 at epoch 12h UT January 0, 1900).

The apparent right ascension is computed using a standard method allowing for the effects of precession, nutation, stellar and diurnal aberration (Explanatory Supplement, p. 145; Woolard and Clemence, p. 299). The Greenwich mean sidereal time at 0h UT is computed from the expression

$$ST = 6h \ 38m \ 45.836 + 8640184.542 \ T_u + 0.0929 \ T_u^2$$
 (4)

(Explanatory Supplement, p. 75). The equation of the equinoxes is the difference between apparent and mean sidereal

time and is computed from the theory of nutation (Explanatory Supplement, p. 43).

The portion of (3) within the parentheses represents twelve hours of mean sidereal time + the interval in mean sidereal time between the passage of the star and the point $R_{\rm u}$ across the local meridian. This sidereal interval is then converted to a Universal Time interval using the ratio of mean solar to mean sidereal time interval.

Four exposures of the star are made with the PZT as the star crosses the instrumental meridian. The mean epoch in UTC of the four exposures can be denoted as $\rm T_{\rm O}$. The hour angle of the star at $\rm T_{\rm O}$ is found from the reduction of the measurements of the star's images on the photographic plate and is designated $\rm H_{\rm O}$. The difference $\rm T_{\rm C}$ - $(\rm T_{\rm O}$ - $\rm H_{\rm O})$ is then the quantity UTO-UTC as determined from the observation of that star.

Around 40 stars are observed on each clear night at each of the two sites at which the Naval Observatory has a PZT. The mean value of the individual determinations of UTO is accepted as the observed value of UTO(i) for that day. The value of UTI obtained using (1) and polar coordinates provided by the BIH are numerically smoothed and combined to obtain the final values of Naval Observatory UTI (McCarthy, 1976). Observations of UTO are also sent to the BIH where they are included in the international scale of UTI.

The internal mean error of one night's observation of UTO is approximately three to four milliseconds. There seems to be very little dependence of the internal mean error on the number of stars in one sight.

The external mean error of one night's PZT observation may be evaluated using the residuals from a smooth curve fitted to the observations. Analysis shows an external mean error of one sight to be about five to seven milliseconds. The difference between the internal and external errors of the PZT observations for one night lead to the conclusion that a systematic error of about six milliseconds may be present in each night's PZT observation (McCarthy, 1974).

The major sources of error are inaccuracies in the adopted positions and proper motions of the observed stars and refraction anomalies. The catalog positions and proper motions are determined from the observations with the PZT since no fundamental catalog positions and proper motions

of the required accuracy exist for the faint stars which are observed. The PZT star positions and proper motions are adjusted to minimize the star residuals. The resultant positions are then corrected by a constant amount determined from the systematic difference between the catalog positions and a catalog of PZT stars observed with a transit circle and referred to the FK4 system (McCarthy, 1973). The systematic errors resulting from the catalog are probably less than three milliseconds which would indicate that the systematic errors found in the PZT observations are largely due to refraction anomalies.

The anomalies in refraction which influence the PZT observations have characteristic periods of a minute and of a day. The short period anomalies affect the determination of time with a single star while the long period anomalies influence the night-to-night differences. Geophysical effects that influence the shape of the local geopotential surface may also provide a source of systematic error which, although probably very small, must be investigated. Instrumental errors can be kept minimal with proper maintenance.

Requirements for UT1.

The time scale UTl is required by all who need to know the orientation of the Earth with respect to some celestial object. In addition to astronomers and those engaged in geophysical research this includes the fields of surface and space navigation and geodesy. Requirements vary among users and to discuss these needs it must be clear what is meant by the terms precision, accuracy, and consistency in this context.

By precision we mean that the individual star observations made on one night agree internally with each other without regard to any external system. Precision may be estimated from the internal mean error of one night's determination of UTO. Accuracy refers to the day-to-day agreement of the observations with themselves in some defined system. This may be estimated by the goodness of the fit of the observations to some smooth curve. The defined coordinate system may be defined explicitly by the instrumental bias (if any), star catalogs, observational procedures and method of reduction. Consistency refers to the ability to maintain one system over an indefinite period of time. If changes are made in the system, consistency demands that they can be well documented and that new observations may be related to old ones in a known way. These

distinctions are important since some users may require extreme consistency but may not be concerned with the observational precision while others may be interested in high accuracy without much concern for the history of past observations and their consistency.

In general, precision is mostly of interest to those directly involved in determining UT1, where measures of precision are used to understand the reliability and workability of their instrumentation. Most actual users are concerned with accuracy and consistency of the data. It is difficult to state specific numbers for the accuracy and consistency required by the user since in most cases the error tolerance in UTl is part of an error budget which may contain many poorly defined errors. Thus some users may not have a specific numerical value for their tolerance levels. Apparently their needs are being met with currently available data since they have not shown a more specific requirement. Another problem incurred when requirements are assessed is that users will simply say that what is required is simply the best that can be provided. The most accurate and consistent data are, of course, desired by all and there are ongoing efforts to improve the quality of UTl data. Also, improvements in the quality of UT1 may lead to scientific and technological improvement by the user which in turn may produce more stringent requirements.

Classical celestial navigation on the surface or in the air demands a knowledge of UT1 with an accuracy of ± 0.5 5. Such an error could lead to a maximum uncertainty of 1/4 mile at the equator. This is well within the ± 2 mile uncertainty in a typical celestial fix (Dunlap & Shufeldt, p. 649). Navigation by artificial Earth satellites is presently used for navigation to a much higher accuracy and thus requires a more accurate UT1. The Global Positioning System which will be used in the future will have a ± 0.5007 requirement in accuracy for UT1. Navigation in space imposes a requirement of ± 0.5002 in accuracy. This is considered by Jet Propulsion Laboratory to be part of the error budget in the location of their monitoring stations.

Astro-geodetic work is an area in which accuracy is important, but consistency is of greater concern. Users in this field must be assured that astronomical longitude is referred to the same system for all of their observations which may extend for over 50 years. Accuracy of ±5 milliseconds may be tolerated in their error budget since the accuracy of a determination of longitude is typically on

the order of 15 milliseconds. However the consistency of the system must also be of the order of a few milliseconds so that systematic errors are not introduced in the network of observed astronomical longitudes.

Most astronomers can be satisfied with an accuracy of ± 0.51 . However, there are fields of astronomical research where the best possible accuracy and consistency is required. These include classical and radio astrometry, determination of astronomical constants, and research into the rotation of the Earth. The validity of the research in these areas depends directly on our ability to produce accurate and consistent UT1.

Conclusion.

The determination of UT1 tends to be overlooked in the era of nanosecond timing with clocks. However, it must be realized that there are many requirements for the use of UT1. The determination of UT1 is an area where extreme care must be used to insure that accuracy and consistency is not compromised but further improved for future needs.

References.

- 1. Dunlap, G. D. and Shufeldt, H. H., <u>Dutton's Navigation</u> and Piloting, 1972, Naval Institute Press, Annapolis.
- 2. Explanatory Supplement to the American Ephemeris and the American Ephemeris and Nautical Almanac, 1961, Her Majesty's Stationery Office, London.
- 3. Markowitz, Wm., 1960, "The Photographic Zenith Tube and the Dual-Rate Moon-Position Camera", in <u>Telescopes</u>, G. P. Kuiper and B. M. Middlehurst, editors, University of Chicago Press, Chicago.
- 4. McCarthy, D. D., 1973, Astron. J. 78, 642.
- 5. McCarthy, D. D., 1974, "The Determination of the Rotational Motion of the Earth with a Photographic Zenith Tube", Paper presented to AIAA Mechanics and Control of Flight Conference, (Available from AIAA Library, New York).
- 6. McCarthy, D. D., 1976, U. S. Naval Observatory Circular No. 154.

7. Woolard, E. W. and Clemence, G. M., 1966, Spherical Astronomy, Academic Press, New York.

THE DETERMINATION OF UT1 BY THE BUREAU INTERNATIONAL DE L'HEURE (BIH)

Martine FEISSEL

Bureau International de l'Heure Paris - France

ABSTRACT

The determination of UT1-UTC is obtained at the Bureau International de l'Heure from a world centralization of the astronomical measurements made in 60 stations.

The combination of the data, involving analysis and prediction of the individual behaviour of the stations, is described. The stability of the results made available to different kinds of users under various time delay/accuracy conditions is characterized.

INTRODUCTION

The rotation of the Earth is computed from ground optical measurements of star directions. An observation, at station i, gives a local value of the instantaneous angular position of the Earth: UTO(i) - UTC. UT1-UTC is obtained at the BIH by combining the local UTO(i) - UTC after they are corrected for the motion of the pole on the Earth. In 1976, 60 astronomical instruments are transmitting their observations of UTO to the BIH.

In the future, new methods are envisioned to measure the Earth rotation: Lunar Laser Ranging [1] (operation expected to start in 1977) and VLBI. These methods are expected to provide results with a greater precision and a better time-resolution than the classical astronomical method, but the latter is still improving, as shown by the following numbers for 1967 and 1975:

	1967	1975	ratio $\frac{1975}{1967}$
number of visual instruments	34	36	1.06
number of photographic instruments	16	24	1.50
number of observing nights per year	4 225	6 233	1.48
number of observed stars per year	93 882	187 831	2.00
Allan variance of the BIH 5-day raw values $\langle \sigma^2 (2, T = \tau = 5d) \rangle$	$(0,0022)^2$	(0°, 0011) ²	0.25

The above first four lines show the increasing effort of the observatories, which use photographic or photoelectric instruments rather than visual ones; moreover, the number of observing nights grows faster than the number of instruments, and the number of observed stars grows even faster. During the same time, our studies of the individual time series of UT1(i) - UTC led us to an improved prediction of their behaviour. These studies and their application to the current computations in order to get consistent values of UT1 will be outlined. Then the precision of the values of UT1-UTC as published by the BIH with time delays ranging from one week to one year will be estimated.

OPTIMAL FILTERING OF THE INDIVIDUAL TIME SERIES OF UT

The astronomical measurements of UT supply the instantaneous position of the Earth in its rotation by linking a network of stations which represent the Earth crust to a set of stars which provide an inertial reference system. These measurements may suffer from the influence of instrumental errors, tectonic motions, refraction irregularities, star catalog effects, etc. In addition, the time series of UT1(i), i.e., UT0(i) corrected for the longitude effect of polar motion, have a large individual annual component (see Figure 1). On the other hand, the BIH has to publish consistent values of UT1 with a time delay largely shorter than one year. We must then be able to predict the individual errors, according to an appropriate modeling of their statistical and deterministic features.

Determining the Power Density Spectrum of Errors

Assuming constancy of errors, we analysed the noise spectral density as a function of the frequency, $S(f) = h_{\alpha} f^{\alpha}$, for time intervals longer than one year. The Allan variance criterion $\sigma^2(n, T = \tau = 1y)$ [2] was used in order to determine α . The deterministic part of the errors is represented by a time independent term, an annual term and a semi annual term. The study of the yearly values (1962 to 1973) of these parameters indicate that in the mean the type of noise is significantly different for the three components:

- the time independent term shows a preponderant flicker noise (α = -1.0). This is the consequence of all the accidental local and instrumental changes.
- the amplitude of the semi annual term has white noise (α = -0.1): it suffers only from measurement errors.
- the amplitude of the annual term has an intermediate noise density spectrum ($\alpha = -0.6$): it is also affected by instrumental errors, but in a lesser proportion than the time independent term.

Predicting the Systematic Deviations

The monitoring of UT1 with a short time delay, providing homogeneous results in spite of the various sources, with irregular data acquisition rates, the starting and ending of operating stations, makes it necessary to predict the behaviour of each station. In the BIH computations, this prediction is repeated annually.

The optimum filter adapted to the types of noise of the three systematic components has been theoretically derived but its implementation is practically impossible on account of a poor knowledge of the noise levels of individual instruments and to the lack of constancy of their statistical properties. In practice, a white noise prediction, limiting the past to four years, which was adopted after a previous study [3], doesn't give rise to such difficulties and has shown to be satisfactory. The individual series of UT1(i) are corrected for their predicted time independent, annual and semi annual terms before being combined to give UT1.

CORRECTION OF SHORT TERM VARIATIONS AND SMOOTHING

Short-Term Variations

The astronomical measurements have short-term local variations due to diurnal nutation and earth tides: all known corrections are applied to the UT1(i) before combination. There are also some other variations in the Earth's rotation due to the zonal earth tides; they are not corrected. The components of period shorter than one month are thus present in the published raw values of UT1 (Table 6 of the BIH Annual Reports) but they vanish in the usual smoothing (circular D).

Smoothing

The raw values of UT1 in Table 6C of the BIH Annual Report are freed from all known or estimated systematic variations; they are the relevant data for studies of the Earth's rotation. As they indeed still have noise spectral density, an appropriate smoothing will provide the users of UT1 with better current values.

At the BIH, we use Vondrak's smoothing method [4], which is an extension of Whittaker-Robinson's one for the case of unequally spaced and weighted data. A parameter ϵ allows one to choose the roughness of the smoothed curve; the usual smoothing of the 5-day raw values of UT1 is made with $\epsilon=10^{-11}$, which attenuates the amplitude of waves of different frequencies according to Figure 2. This filtering is strong enough to remove the waves due to zonal tides (13.7 and 27.7 d) and weak enough to leave in the smoothing the semi annual variation which is also present in the Earth's rotation. The spectral analysis of the residuals of raw data with respect to this smoothing (Figure 2) shows the two zonal tide lines, noise outside the lines and a low frequency cutoff near 0.02 c/d: for time intervals longer than approximately 50 days, the time series of 5-day raw and smoothed values of UT1 are statistically equivalent.

PUBLICATION OF THE RESULTS - TIME DELAY AND PRECISION

The preceding sections dealt with the way in which the BIH insures the consistency and accuracy of its results: all the published values of UT1 are in the same system, which is linked to the conventional origin of longitudes. However, the various needs of the different users of its data lead the BIH to issue different publication series, with different time delays after the last observation date, which implies a varying precision according to the time delay of publication.

To characterize these precisions we shall take the usual Vondrak's smoothing ($\epsilon = 10^{-11}$) of raw values of Table 6C as a reference. The residuals of this smoothing since 1974 are shown on Figure 3. Over the time interval 1972.0 - 1976.5, their r.m.s. value is 05 0014, while their mean standard error is 05 0009. This indicates that some correlations still exist between the raw values independently computed. Astronomical time series are known to have sometimes transient systematic errors during intervals ranging from a few days to several months. These apparent steps can hardly be corrected and thus generate flicker noise in the global combination for UT1 [5], as shown by the Allan variance $\langle \sigma^2(2, T = \tau) \rangle$ of the residuals from a strong smoothing ($\epsilon = 10^{-15}$) for varying sampling intervals (Figure 4).

Publication Delay: One Week

Since April 1971, we have operated a Rapid Service, under a contract with the Jet Propulsion Laboratory. Our data are used for the navigation of deep space probes. The calculations for this weekly service are made with the astronomical data transmitted to us by teletype by 34 stations, three days after the last observation date; 16 soviet observatories recently joined this group. Every Thursday, 14 h UT, we are able to teletype smoothed daily values of UT1 and the pole coordinates for the preceding week. The r.m.s. deviation of these UT1 values (taken every 5 days) from the usual Vondrak's smoothing is 0.5 0021 (see Figure 3).

Publication Delay: One and a Half Months

The monthly Circular D is published at the beginning of month m; it provides the users with 5-day smoothed and raw values of UT1 and the pole coordinates for month m-2. The smoothed values are obtained by the usual Vondrak's smoothing, with only very few values available after the date of the last published point. This smoothing may then slightly differ from the final one. The measured r. m. s. deviation from Vondrak's usual smoothing is 0.50008 (see Figure 3).

Publication Delay: One Year - Definitive Values

The Annual Report of the BIH which is published every year in June gives definitive values for the preceding year. The values of UT1 in Table 6C are essentially the raw values of the monthly Circular D, with all improvements

made possible by the passing of time: individual weighting of the data according to the actual (and no longer predicted) dispersion, taking into account all known data amendments, and, more generally, the correction of any anomalies in the received data, which can only be detected after a while.

REFERENCES

- [1] STOLZ, P. L. et al. 1976. Earth Rotation measured by Lunar Laser Ranging, Science, 193, 997.
- [2] ALLAN, D. W., SHOAF, J. H., HALFORD, D. 1974. Statistics of time and frequency data analysis. NBS Monograph 140.
- [3] FEISSEL, M. 1972. Etude de la stabilité des instruments mesurant le Temps Universel ou la Latitude. Rapport Annuel du BIH pour 1971.
- [4] VONDRAK, J. 1969. A contribution to the problem of smoothing observational data, Bull. of the Astron. inst. of Czechoslovaquia, 20.
- [5] BARNES, J. A. 1969. The generation and recognition of flicker noise. Frequency and Time Stability seminar, NBS.

The description of the BIH methods for deriving UT1 and the pole coordinates is given in the Annual Report for 1969 (in French) and for 1970 (in English).

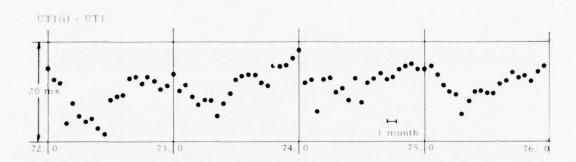


Fig. 1 A typical example of station residuals (means over $0.05\ y$).

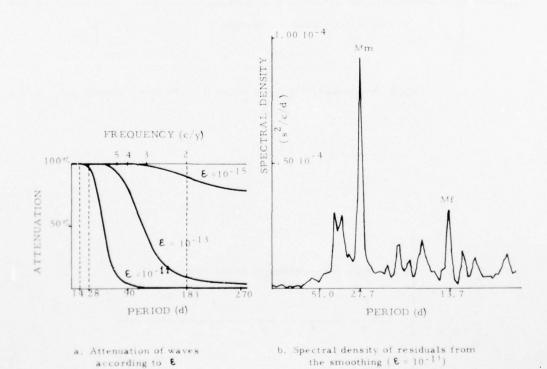


Fig. 2 Vondrak's smoothing of 5-day raw values of UT1-UTC.

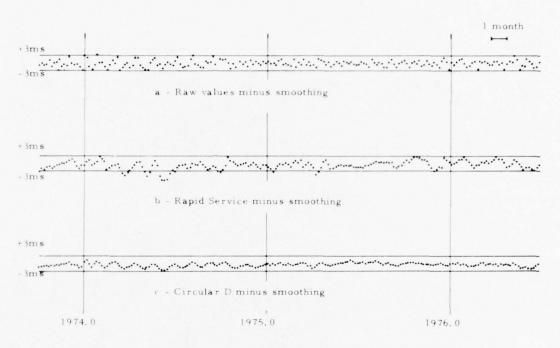


Fig. 3 Residuals of UT1 5-day values from Vondrak's smoothing ($\varepsilon = 10^{-11}$).

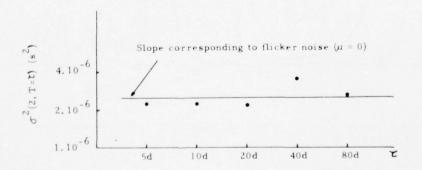


Fig. 4 Allan variance of "Tl as a function of measuring interval.

PRECISE WORLDWIDE STATION SYNCHRONIZATION VIA THE NAVSTAR GPS, NAVIGATION TECHNOLOGY SATELLITE (NTS-1)

James Buisson, Thomas McCaskill, U. S. Naval Research Laboratory, Washington, D. C., Humphry Smith, The Royal Greenwich Observatory, England, Peter Morgan, John Woodger, Department of National Mapping, Canberra, Australia

ABSTRACT

The NTS-1 satellite is currently being employed as a precursor to the phase I concept validation program of NAVSTAR GPS. The assigned tasks include measurement of components of the GPS error budget related to the performance of precise satellite clocks and orbital accuracy obtainable in an eight hour orbit.

Station Synchronization results are presented using stations located in the United States, England and Australia. Results show a time difference noise level of 3 ns. These single frequency measurements, collected over the past year, have been processed to produce station synchronization values between cesium clocks located at each station. A one month data span, using a zero satellite clock update time, produced a noise level of 43 ns, with a systematic bias of 9 ns. The synchronization noise level gradually increased as the satellite clock update time increased. The largest value measured is on the order of 250-500 ns, when comparing clocks located at the Australia station with clocks located at the central U.S.A. station. The method employed in precise station synchronization is sensitive to two components of satellite position error. The results show that long term predictions, on the order of 2-3 months, are possible with only a small increase in station synchronization error.

INTRODUCTION

The NAVSTAR Global Positioning System (GPS) is a DOD program (1) designed to provide precise navigation

to a wide variety of military and civil users via a constellation of 24 satellites deployed in sub-synchronous circular orbits of near 12 hr period (2). The Navigation Technology Segment (NTS) of GPS has been assigned the task of validating key concepts and hardware, with special emphasis on space-borne clocks and atomic frequency standards. Phase 1 of GPS employs time difference measurements between four of the spacecraft clocks and the user's clock (Fig. 1).

Navigation Technology Segment (NTS) Results

The NTS-1 satellite (Fig. 2), launched in 1974, has 11 on-board experiments. Results have been reported (3) on the frequency standards performance, which included two Efratom Atomic Rubidium Oscillators, and a Frequency Electronics quartz oscillator. Following this effort, a change was made in the NTS tracking network to check the spacecraft clock performance, orbital accuracy employing only time difference measurements and prepare for the forthcoming NTS-2 launch. Previous NTS-1 satellite clock comparison between USNO and RGO have been reported (4) employing doppler observations to determine the NTS-1 satellite ephemeris.

Through the cooperation of the Royal Creenwich Observatory (RGO) and the Division of National Mapping (DNM) in Australia, NTS permanent ground stations have been located at the respective countries. Inputs to the NTS time difference receivers (5) are obtained from clocks that are part of cesium clock ensembles. These clock ensembles are periodically compared with the USNO UTC time scale via portable clocks and other means. Hence these stations can be used to assess the station synchronization accuracy.

Other operational ground stations are located at the NRL annex (Chesapeake Bay Division) and in the Panama Canal Zone. The NTS control center is located at NRL.

For a one month system closure test an NTS time difference receiver was located at the U. S. Naval Observatory. The receiver was driven with clock inputs from the USNO Master Clock #1. The NTS-1 measurements are collected using a Datapoint 2200 minicomputer; these measurements are subsequently entered into the General Electric International

time sharing system. Time comparisons may be routinely calculated through the use of a software program named "International Time Transfer and Station Synchronization" (ITTAS), developed at the Naval Research Laboratory.

Station Synchronization Equations

EQ(1) (USNO-REMOTE) =
$$(T-0)_{REMOTE}$$
 - $[(T-0)_{CENTRAL}$ + $\frac{d}{dt}(T-0)\Delta t]$ + $(USNO-CENTRAL)$ + CAL

Equation (1) gives the start minus stop value, denoted by (USNO-REMOTE), obtained by combining the information from (A) the ground link from the central station clock to the USNO master clock, (B) the satellite link from the central NTS station to the NTS satellite, (C) the satellite clock and orbital trajectory update of the NTS satellite to the remote station and (D) the satellite link to the remote station at the time of measurement. It should be noted that the algebraic sign convention for (USNO-REMOTE) conforms with the recommended Naval Observatory procedure (6). In Eq(1) the (T-0) remote value (3) is obtained by combining the theoretical time difference "T" computed from a measurement model (Fig. 3), which accounts for all known factors except the clock offset, with an observed value "0" (Fig. 4) obtained from the remote time difference receiver, which measures the time difference with respect to the NTS-1 spacecraft. A similar procedure is followed whenever NTS-1 is over the central site to obtain (T-0) Central. The term $\frac{d}{dt}$ (T-0) denotes the frequency of the NTS satellite with respect to the central station clock. At is the difference between the time of observation for the NTS-1 satellite as observed from each station. This procedure is illustrated in Fig. 5. The quantity (USNO-CENTRAL) is the measured (or interpolated) value of the central station clock offset with respect to the USNO master clock. The "CAL" value is obtained by measuring the delay through the antenna and receiver systems. Eq (1) may be evaluated at any time that an observation is available, however the time of closest approach (TCA) of the satellite is the preferred time of observation (Fig. 6) for reasons that will be discussed in the sequel. The (USNO-REMOTE) value obtained by the preceeding technique can then be used to set a remote clock, calculate an updated value of the remote clock frequency or incorporate with other time difference measurements to obtain a navigation solution (7).

The (USNO-REMOTE) value may then be combined to produce a

value of (USNO-ENSEMBLE), if the offset of the remote clock is known with respect to the ensemble, using Eq (2).

Eq (2) (USNO-ENSEMBLE) = (USNO-REMOTE) + (REMOTE-ENSEMBLE)

Through the use of Eq (2) for a collection of measurements, the variance of (USNO-ENSEMBLE) may be calculated. Hence a sigma value can be obtained to estimate the weight to be assigned the NTS-1 station synchronization values when incorporating remote clock ensembles in a master clock ensemble or in a time scale.

Time Transfer Geometry at TCA

A typical pass (Fig. 4) of NTS-1 yields time difference measurements with respect to the NTS-1 satellite clock for a 2.5 hour span. Hence these measurements can be combined with the satellite clock information, satellite ephemeris and central station measurements to yield the offset (USNO-REMOTE) values for a 2.5 hour data span.

Assuming the satellite link and central link information is available, Eq (1) may be evaluated for any of these measurements to produce a value of (USNO-REMOTE). For PTTI applications involving long term comparisons of time scales it is computationally efficient to produce a single value of (USNO-REMOTE), with an associated variance, that is subsequently processed in a time scale algorithm. Previous experience has indicated that the evaluation of a single number for clock offset at the time of closest approach (TCA) to the remote station is a good choice. The reasons for choosing TCA are as follows: (1) uncertainties in the ionospheric and tropospheric delays are minimum because the satellite is at a maximum elevation angle with respect to the station, (2) the data is symmetric about TCA, and (3) the contribution of the satellite position error along the satellite velocity vector is minimized because, at TCA, the range rate is zero (Fig. 6).

USNO System Closure Results

A three week system closure test was conducted at the U.S. Naval Observatory (USNO) commencing on day 89, 1976. This test is a special case of the usual procedure depicted by Fig. 7. The normal use of NTS-1 entails use of the satellite clock to transmit a time signal to a remote location, thereby requiring a satellite clock and ephemeris update to the time of the remote observation. For the USNO test, a time difference receiver was physically located at

USNO, using a 5 MHz signal and a lPPS derived from the USNO master clock #1. Because of the proximity of USNO to NRL and the NRL central station located at the NRL annex (CBD), simultaneous observations were possible from three stations. The use of simultaneous observations of the NTS-1 signal allowed time to be transferred with a zero satellite clock update time.

The station synchronization results of the three week USNO test are presented in Fig. 8, using the complete link, with a value of zero for the satellite clock update time. The results show a systematic error and noise level of much less than 1 microsecond, hence an expanded plot of the same results is presented in Fig. 9. A small systematic bias of 9 nanoseconds (ns) with a one sigma noise level of 43 ns was measured. In the plots of Figs. 8 and 9, each point represents the value obtained from one complete 2.5 hr NTS-1 satellite pass as observed from USNO and the central NRL CBD site.

These resultant values are used in Eq (1) where remote = USNO (NTS) to designate the remote receiver located at USNO. This procedure thus allowed a measurement of the NTS-1 systematic error. Analysis of Fig. 9 shows a systematic signal is present in the residuals hence analysis was continued to estimate the random component due to the measurement error. Fig. 10 presents measurements taken with receivers at USNO and CBD for a single 2.5 hr pass. The difference calculations did not include an estimate of the central station offset with respect to USNO, which was about 6.7 $\mu \rm sec$ (Fig. 10) at the time of the pass.

The very small systematic effect (note: l ft \cong l ns) displayed in Fig. 10 is thought to be due to a slight difference in antenna coordinates for each receiver, which would give a different effect depending upon pass geometry. A cubic polynomial was fitted to the data to remove the systematic error and Fig. 1l presents the random time difference measurement error due to both receivers. A one sigma value of 5 ns was measured, which results in 3 ns random error for each receiver.

Royal Greenwich Observatory (RGO) Results

Fig. 12 presents the results from RGO obtained using the NTS-1 satellite and the RGO station clock designated RGO (JP). The data span is the same used for the USNO experiment. The measurements in Fig. 12 exhibit an RMS

NATIONAL AERONAUTICS AND SPACE ADMINISTRATION GREENB--ETC F/6 14/2 PROCEEDINGS OF THE ANNUAL PRECISE TIME AND TIME INTERVAL (PTTI)--ETC(U) AD-A043 856 1977 UNCLASSIFIED NASA-6SFC-X-814-77-149 2018 AD 4043856 C man 1 110 20

value of 211 ns. A longer time span (40 days) employing satellite passes is presented in Fig. 13 to obtain better statistical significance on the measurement. The longer time span exhibits a systematic effect that will be discussed later. Fig. 14 depicts the cesium clock ensemble used to obtain UTC (RGO). Outputs from RGO (JP) are used to drive the NTS-1 time difference receiver. Hence the USNO ensemble can be compared to the RGO ensemble via the NTS-1 satellite using the values of (RGO(JP)-UTC(RGO)) as given by Fig. 14. Eq (2) can be used to evaluate this comparison at any convenient epoch. This was done for day 108, 1976 at 00hr and yielded a value given by Eq (3).

Eq (3) UTC(USNO MC#1)-UTC(RGO)=-3.578 μ SEC(-0.0509 μ SEC/D)* (T-108).

The accuracy of this result can be estimated by using interpolated values from portable clock closures. The first of two closures was on MJD42702.3(17 Oct 1975) with a value of $-2.2(\pm)$ lµSEC. The other closure, given in USNO series 7, #447, on MJD42965.5 (6 July 1976) has a value of $-4.4(\pm)$ lµSEC. Interpolation to day 108, 1976 yields a value of -3.726µSEC. Comparison with the NTS-1 determination gives a difference of -148 nanoseconds, with respect to NTS-1.

The (USNO-RGO(JP)) measurements exhibited a noise level of 211 ns., which is considerably larger than the value obtained with zero satellite clock update. Further analysis of the data indicated that a small equipment problem was present during this data span which effectively increased the measurement noise from a nominal value of 3 ns up to 10-20 ns. This increase accounts for only a small part of the 211 ns. The additional factors include the satellite clock and ephemeris update, and the use of a single frequency time difference measurements at a nominal frequency of 335 MHz. Previous analysis (3) indicates that the use of single frequency measurements, which prevent accurate measurement of ionospheric delay, is the dominating factor for the 211 ns. noise level.

The (RGO-RGO(JP)) measurements exhibited a one sigma noise level of 12 ns for the 30 day time span from day 90 to day 120, 1976. (Fig. 15) The (RGO-RGO(JP)) noise level is small as compared to the (USNO-RGO(JP)) noise level, therefore, the approximate value of the (USNO-RGO) one sigma value is 211 ns. Hence the (USNO-RGO) time comparisons are to be assigned a weight of 211 ns when incorporating the individual measurements in a time scale algorithm.

Australia Division of National Mapping (DNM) Results

Previous satellite time comparisons between USNO and DNM have been reported (8) employing the low-altitude TIMATION-II satellite. Fig. 16 presents a comparison between USNO and the DNM clock designated as AUS(205) for a time span that overlaps the three week span at USNO. Fig. 17 presents a composite plot of 60 days of (USNO-AUS(205)) measurements. Fig. 18 presents a plot of 40 days of data that used predicted ephemeris with a more recent epoch. The value of (USNO-AUS(205)) to be used for comparison with a remote linkage closure to USNO on day 114, 1976 is an extrapolated value using the (USNO-AUS(205)) measurements given in Fig. 18. The value of (AUS(205)-AUS) was supplied by the Division of National Mapping to be -77.270 µSEC for day 114, 1976. Eq (4) gives the NTS-1 determination for (USNO-UTC(AUS)) for an epoch of day 114, 1976.

EQ (4) UTC(USNO MC#1)-UTC(AUS)=-23.112 μ SEC-(0.0717 μ SEC/D) *(T-114)

The closure on day 114 gives a value of -23.23 µSEC. This closure was obtained by several links to the DNM/NTS station. Comparison of this value with the NTS-1 determination yields a difference of +118 ns, with respect to NTS-1.

A one sigma noise level of 265 ns was measured for the (USNO-AUS(205)) during the 40 day span given in Fig. 18. Significant statistics on the (AUS(205)-AUS) noise level were not available hence it is assumed that the noise level is small as compared to the (USNO-AUS(205)) sigma value. The approximate (USNO-AUS) noise level for the NTS-1 is 265 ns.

Ephemeris Prediction Results

The comparison of two remote time scales via NTS-1 permits calculation of noise levels for the time scale comparisons, such as one sigma values for (USNO-RGO) and (USNO-AUS). Analysis of the complete link from USNO to a remote site permits link errors to be estimated assuming that the time scales involved are more stable than the satellite link. The technique of calculating comparisons at TCA minimizes the satellite ephemeris contribution along the satellite velocity vector, however the measurement remains sensitive to the two remaining components of ephemeris position. Each individual residual from a collection of time comparisons yields an error along the radial vector

given in Fig. 6. Successive observations for different satellite passes occur at different elevation angles with respect to the station, hence successive observations span the plane perpendicular to the velocity vector at TCA. According to Eq (1) evaluated at the times of central and remote observation, differences in the satellite trajectory enter in to (USNO-REMOTE) values. Then using Eq (2) the measurements may be referenced to the difference in the stable time scales.

The satellite ephemeris used to calculate the (USNO-AUS(205)) values given in Fig. 16 was 60 days from epoch (9). The (USNO-AUS(205)) values given by Fig. 18 have a more recent epoch, hence the decrease in one sigma noise level from 689 ns (Fig. 16) to 265 ns (Fig. 18) can be attributed to improved satellite ephemeris. Reference to Fig. 17 shows that combining measurements from the two ephemerides results in a small change in (USNO-AUS(205)). This small difference is further illustrated by comparing the values of (USNO-AUS(205)) calculated from the measurements given by Fig. 18 and Fig. 16 for an epoch of day 129, 1976. A small difference of 440 ns is attributed to the 60 day satellite ephemeris update. This result verifies that long term orbital predictions with small error are possible as indicated by previous NRL analysis (10).

Conclusions

- 1. The NTS-1 Worldwide station synchronization accuracy, using predicted satellite ephemeris calculated using only 335 MHz time difference observations, is 10 ns for stations near the central station and increases to about 100 ns for stations half-way around the earth.
- 2. The one sigma synchronization noise level depends on satellite clock update time. A one sigma value of 43 ns was measured with zero satellite clock update; the largest value measured was 265 ns (Fig. 19).
- Time difference measurements exhibit a one sigma value of 3 ns.
- 4. Long term (60 day) satellite ephemeris predictions have been verified for two components of satellite position.
- 5. Work is continuing on this project and further improved accuracy and precision is expected to be obtained with the launch of the NTS-2 spacecraft (Fig. 20) in 1977.

Acknowledgements

The authors acknowledge the technical support of Mr. D. W Lynch, NRL, Mr. Dick Anderle, NSWC and the guidance of Mr. R. L. Easton, NRL NAVSTAR GPS Program Manager.

Further acknowledgement is given to the personnel from NRL, USNO, RGO and DNM who assisted with their efforts in data collection and processing. Special recognition is given to Mr. Hugh Warren and his colleagues from the Bendix field engineering.

References

- 1. Smith, D. and Criss, W., "GPS NAVSTAR Global Positioning System", Astronautics and Aeronautics, April 1976.
- 2. Buisson, J. and McCaskill, T., "Timation Navigation Satellite System Constellation Study", NRL Report 7389, June 27, 1972.
- 3. McCaskill, T. and Buisson, J., "NTS-1 (TIMATION III) Quartz and Rubidium Oscillator Frequency Stability Results", NRL Report 7932, Dec. 12, 1975.
- 4. Smith, H. M., O'Hora, N. P. J., Easton, R. L., Buisson, J. A. and McCaskill, T. B., "International Time Transfer Between USNO and RGO via NTS-1 Satellite", 7th Annual PTTI, Dec. 1975.
- 5. Landis, P., Silverman, I. and Weaver, C., "A Navigation Technology Satellite Receiver", NRL Memorandum Report 3324, July 1976.
- 6. Winkler, G., "Convention for Reporting Clock Differences", Time Services Announcement, Series 14, No. 2, 30 Sept. 1968.
- 7. McCaskill, T., Buisson, J. and Buonaguro, A., "A Sequential Range Navigation Algorithm for a Medium Altitude Navigation Satellite", Navigation, Vol. 23, #2, Summer 1976.
- 8. Easton, R. L., Smith, H. M., and Morgan, P., "Submicrosecond Time Transfer Between the United States, United Kingdom and Australia via Satellite", 5th Annual PTTI, Dec., 1973.
- 9. O'Toole, J. W., "Celest Computer Program for Computing Satellite Orbits", NSWC/DL TR-3565 Oct, 1976.
- 10. Easton, R. L., "Optimum Altitudes for Passive Ranging Satellite Navigation Systems", Naval Research Reviews, Aug., 1970.

Figures

- Figure 1 Four GPS Satellites
- Figure 2 Navigation Technology Satellite #1 (NTS-1)
- Figure 3 Time Difference Measurements
- Figure 4 Typical NTS-1 Satellite Pass
- Figure 5 Station Synchronization by NTS
- Figure 6 Time Transfer Geometry at TCA
- Figure 7 Station Synchronization with Zero Clock Update
- Figure 8 USNO-USNO(NTS)
- Figure 9 USNO-USNO(NTS)
- Figure 10 USNO-NRL
- Figure 11 (USNO-NRL) Residuals
- Figure 12 USNO-RGO(JP) Day 90-112, 1976
- Figure 13 USNO-RGO(JP) Day 90-130, 1976
- Figure 14 RGO-NTS Time Link
- Figure 15 RGO Clock Ensemble
- Figure 16 USNO-AUS (205) Day 98-129, 1976
- Figure 17 USNO-AUS (205) Day 90-150, 1976
- Figure 18 USNO-AUS (205) Day 130-170, 1976
- Figure 19 NTS-1 Synchronization Noise Level versus Satellite Clock Update Time
- Figure 20 NTS-2

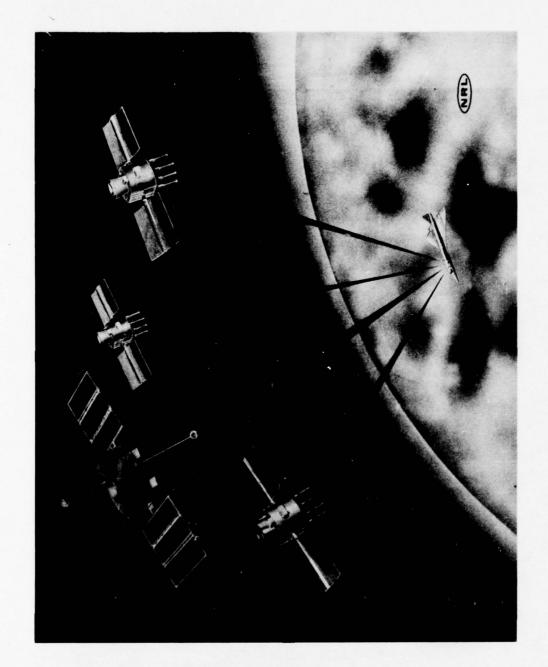


Figure 1. Four GPS Satellites



Figure 2. Navigation Technology Satellite 1 (NTS-1)

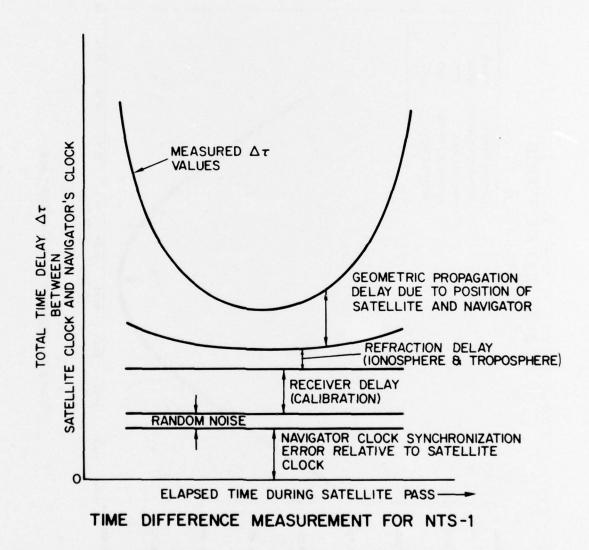


Figure 3. Time Difference Measurements

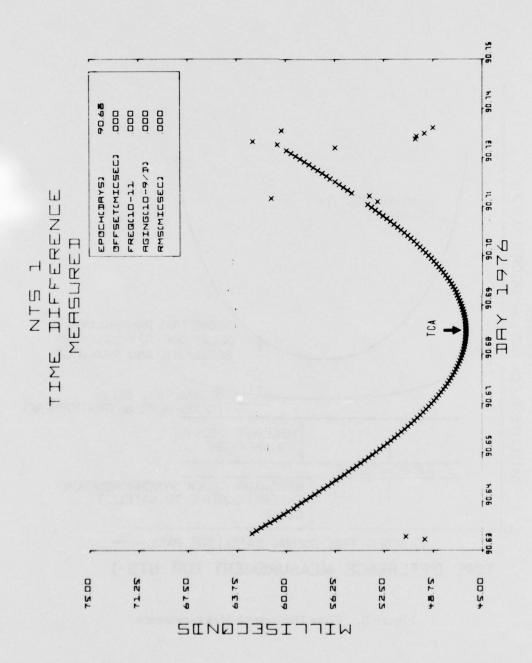


Figure 4. Typical NTS-1 Satellite Pass

NAVSTAR GPS NAVIGATION TECHNOLOGY SEGMENT STATION SYNCHRONIZATION BY TIME TRANSFER

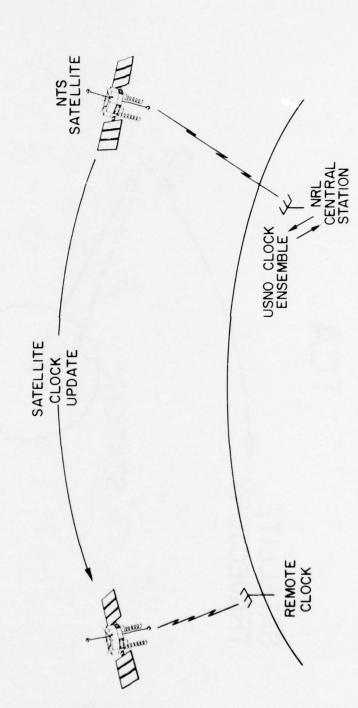


Figure 5. Station Synchronization by NTS

TIME TRANSFER GEOMETRY AT TCA

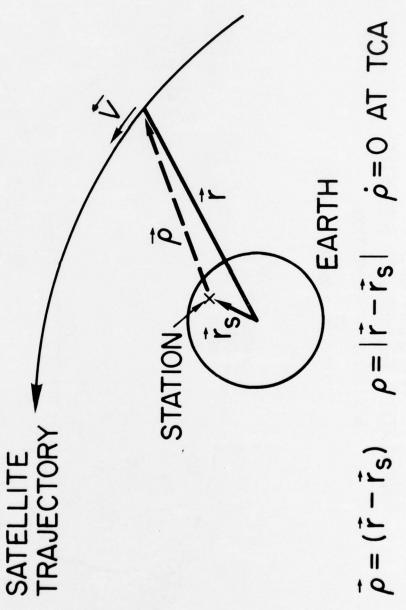


Figure 6. Time Transfer Geometry at TCA

NAVSTAR GPS NAVIGATION TECHNOLOGY SEGMENT PRECISE STATION SYNCHRONIZATION (ZERO SATELLITE CLOCK UPDATE)

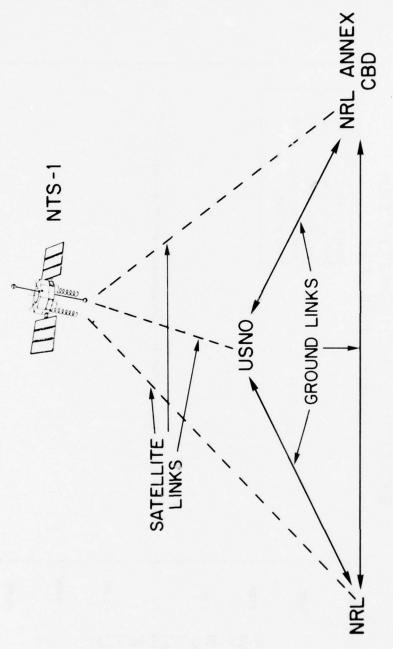


Figure 7. Station Synchronization with Zero Clock Update

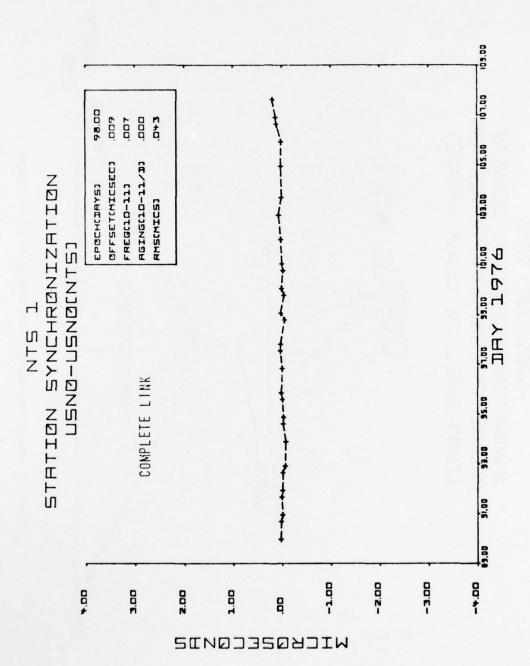


Figure 8. USNO-USNO (NTS)

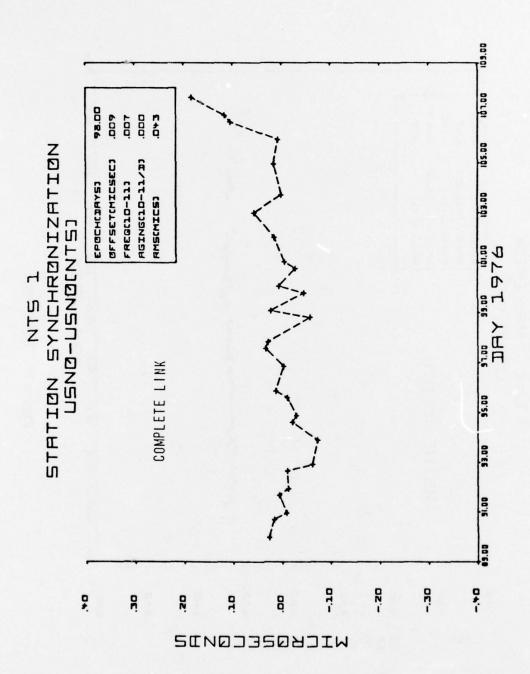


Figure 9. USNO-USNO (NTS)

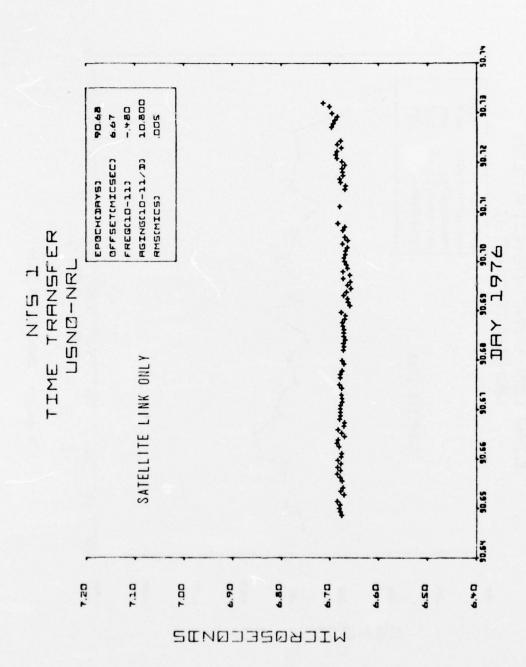


Figure 10. USNO-NRL

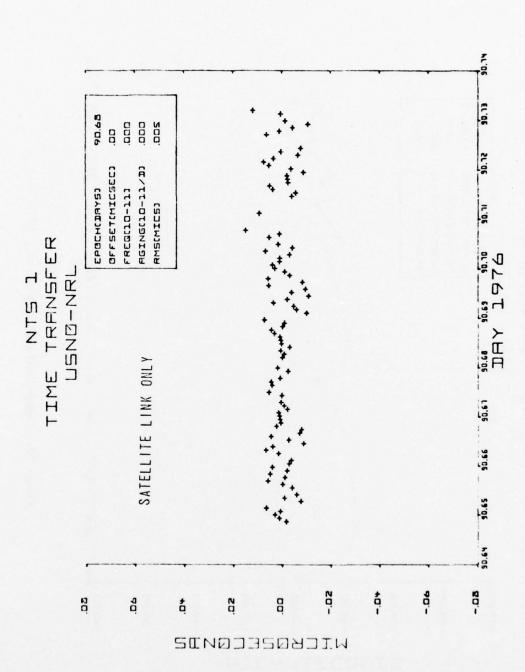


Figure 11. (USNO-NRL) Residuals

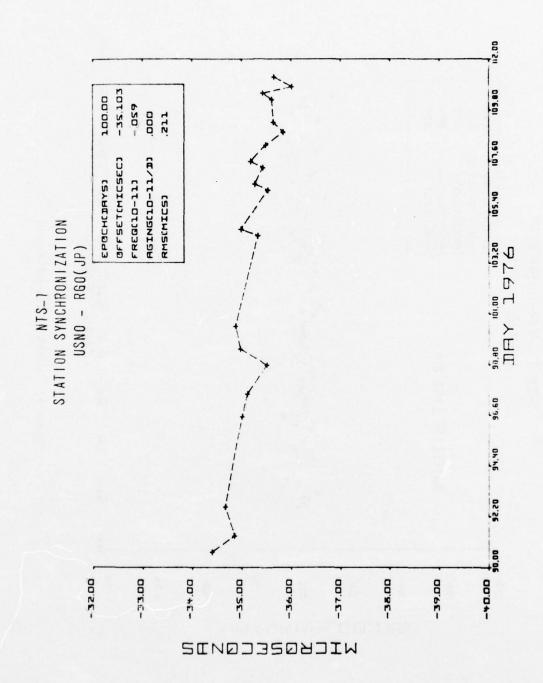


Figure 12. USNO-RGO (JP) Day 90-112, 1976

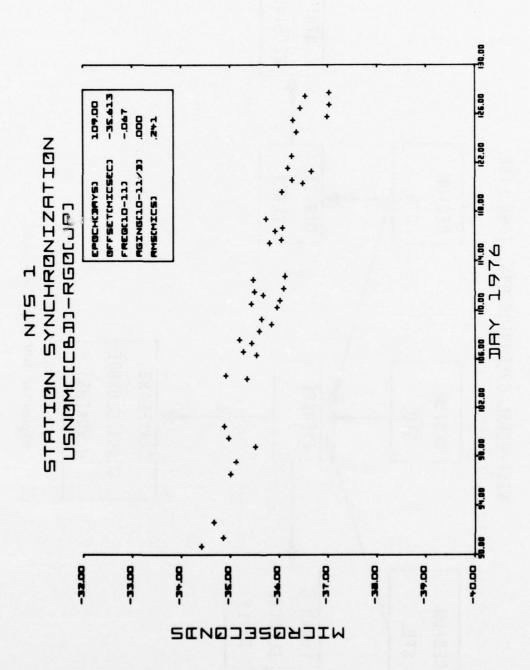


Figure 13. USNO-RGO (JP) Day 90-130, 1976

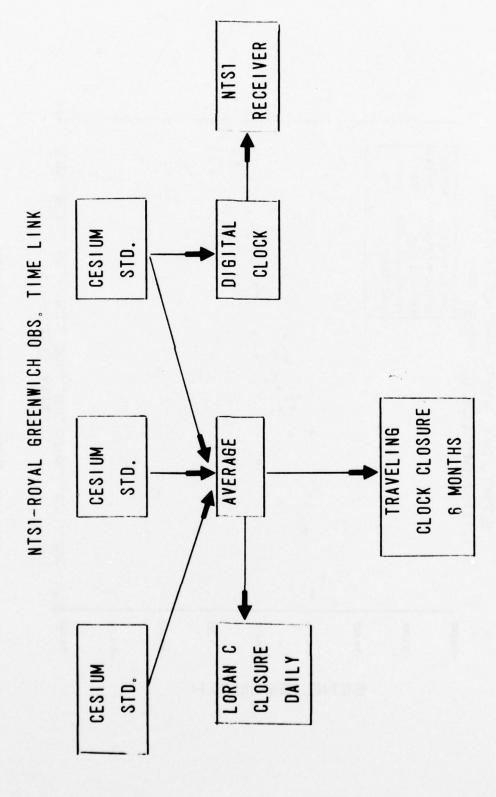


Figure 14. GRO-NTS Time Link

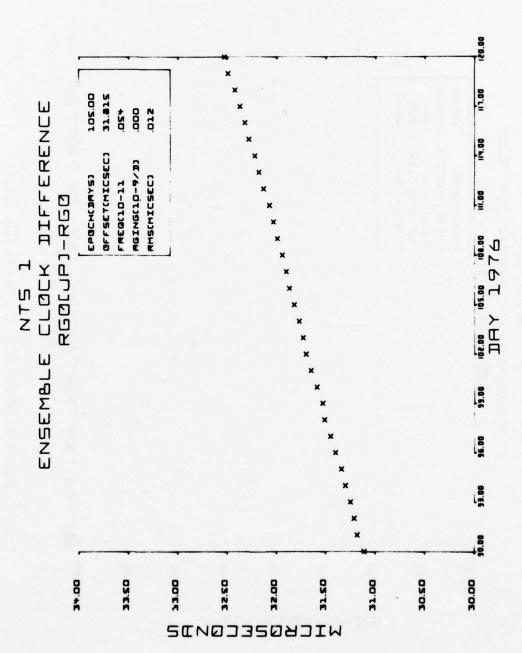


Figure 15. RGO Clock Ensemble

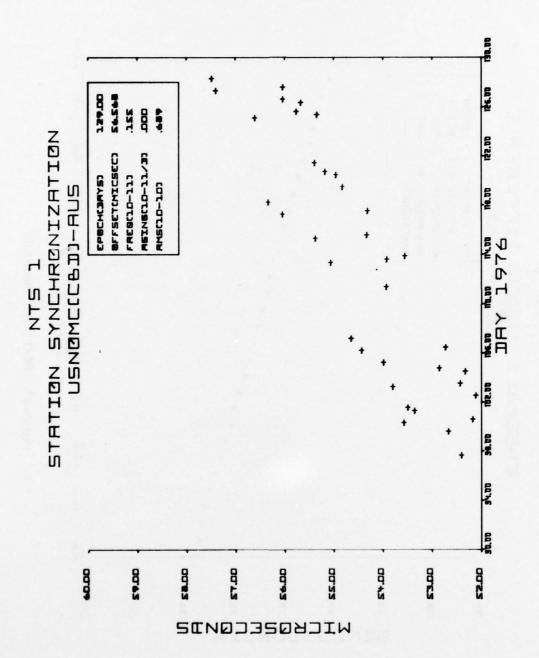


Figure 16. USNO-AUS (205) Day 98-129, 1976

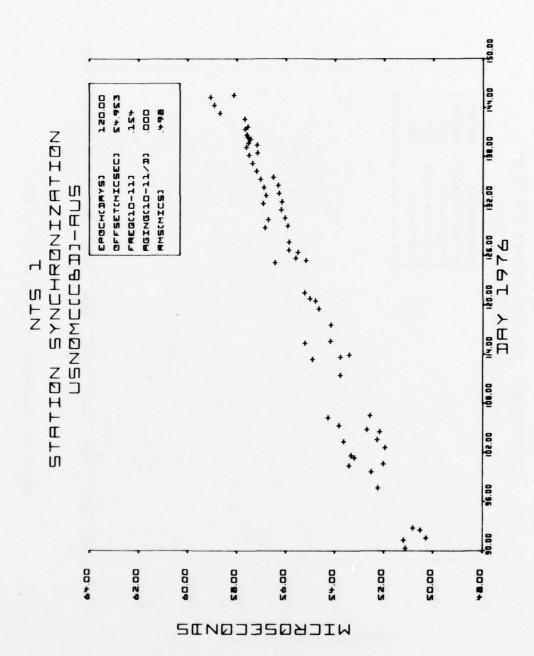


Figure 17. USNO-AUS (205) Day 90-150, 1976

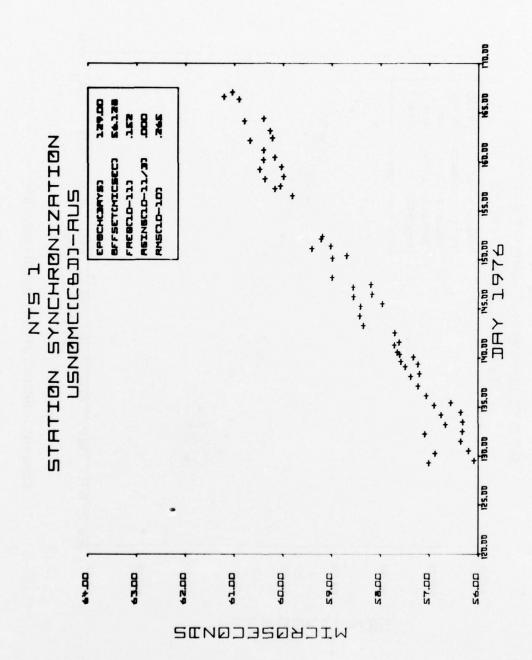


Figure 18. USNO-AUS (205) Day 130-170, 1976

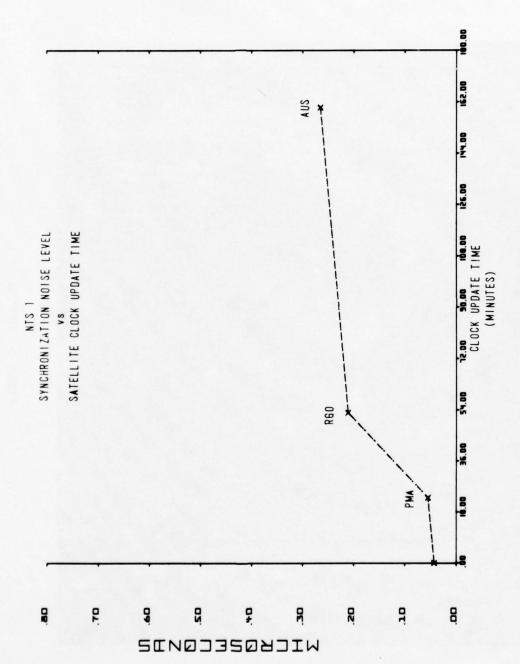


Figure 19. NTS-1 Synchronization Noise Level versus Satellite Clock Update Time

Figure 20. NTS-2

NAVIGATION TECHNOLOGY SATELLITE (NTS) LOW COST TIMING RECEIVER DEVELOPMENT*

L. Raymond, J. Oaks, and J. Osborne Naval Surface Weapons Center

G. Whitworth Applied Physics Laboratory, JHU

J. Buisson and P. Landis Naval Research Laboratory

C. Wardrip and J. Perry Goddard Space Flight Center

ABSTRACT

A compact timing receiver which receives and processes NTS ranging sidetones has been developed. In its prime operating mode, the receiver outputs a spacecraft-receiver range measurement in time units once each minute. The format of the output is compatible with the NTS data processing system, which determines the time difference between the user's clock and a reference clock at the Naval Observatory.

The receiver, which operates at P-band (335 MHz), is designed to use a minimum of RF and analog circuitry. The received ranging signals are quickly converted to low frequency, digital signals for processing under the control of an INTEL-8080 microprocessor. Receiver operation is primarily automatic, requiring only initial operator setup via front panel controls.

This paper describes the receiver and its operation, points out its advantages to a user requiring precise time at remote sites at an economical price, and describes a typical application.

^{*}The receivers were jointly developed with NASA funding by the Applied Physics Laboratory, JHU and the Naval Surface Weapons Center.

INTRODUCTION

The NASA Goddard Laser Ranging Network, which is presently being implemented, has a world wide clock synchronization requirement of \pm one microsecond to support various projects. At the present, the Network consists of one stationary Laser system located at Goddard and three Mobile systems. In addition, five more Mobile systems are being built. These eight Mobile systems will be deployed, at various times, at the locations indicated on the map. (Fig. 1) The Laser systems will have an overall ranging accuracy or capability of several centimeters.

In order to make use of the highly accurate ranging data, it is necessary to time tag the data very accurately. In applications where the data from two or more stations will be merged to determine baselines, polar motion, crustal motion, etc., it is necessary that the Laser clocks at the several stations be synchronized to within + one microsecond.

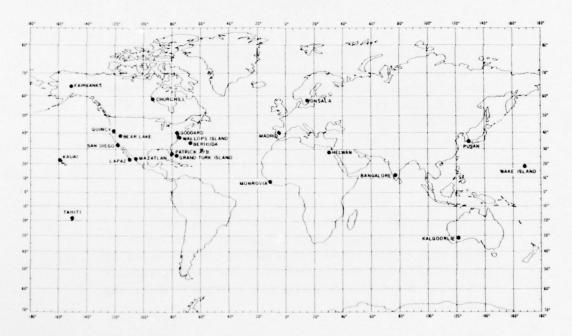


Figure 1. Tentative Laser Network

This requirement arises from the fact that a satellite moving in a typical low orbit travels about 0.7 cm per microsecond. Thus, if time is known to within one microsecond the peak error in spacecraft position due to time will be 0.7 cm.

Goddard personnel have over the years evaluated and used many techniques of time transfer including HF, VLF, dual VLF, radio navigation systems, the use of satellites such as GEOS, ATS and more recently the Navigational Technology Satellite to mention a few.

Recognizing, on a global basis, that microsecond clock synchronization is not practically achieveable by conventional means such as Loran-C or extended portable clock trips, Goddard concluded that between now and the early 1980's that the use of the NTS satellites would best provide the global coverage needed and the degree of clock synchronization required. Beyond the early 1980's NASA hopes to use either its own Tracking Data Relay Satellites (TDRSS) or the Global Positioning System to meet submicrosecond needs.

In 1975 NASA initiated the development of a signal frequency receiver for use with the NTS satellites for time transfer to within a microsecond. These receivers will be used in the Laser Ranging Timing Systems. A Laser Ranging Timing System is shown in Figure 2 and consists of a Cesium Beam Frequency Standard (004 Option), WWV and LORAN-C receivers and the NTS time transfer receiver plus signal distribution, etc.

This paper describes the NTS satellite time transfer receiver and the technique by which a user determines his time with respect to a master clock such as the U.S. Naval Observatory.

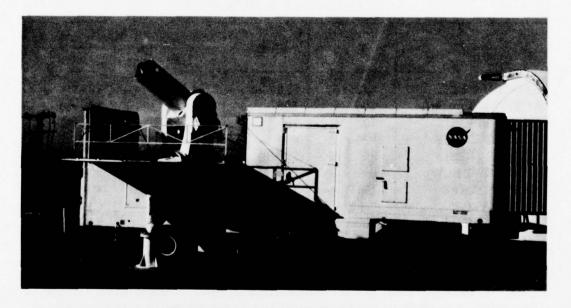


Figure 2. Laser Van

NTS Satellites

The NTS-1 spacecraft is the third satellite in a series of advanced research and technology satellites built and operated by the Naval Research Lab. Table 1 presents pertinent information of each spacecraft. The primary objectives of the missions are advanced clock development, satellite navigation and orbit determination; but a natural by-product of such work is the precise transfer of time using remote receiver sites.

For a precise time transfer to obtain maximum accuracy the following parameters are required to have minimum uncertainity:

- 1. Radial Location of Satellite
- 2. Satellite Clock
- 3. Ground Station Clock
- 4. Ground Station Antenna Position
- 5. Transmission Path

Any or all of the above five parameters could be solved for, but should be readily available in time transfer experiments.

TABLE 1
TECHNOLOGY SATELLITES

	Т-І	T-II	T-III	
			NTS-1	NTS-2
LAUNCH DATE	5/31/67	9/30/69	7/14/74	1977
ALTITUDE (N. MI.)	500	500	7400	10,900
INCLINATION	70°	70°	125°	63°
ECCENTRICITY	0008	002	007	0
WEIGHT (LBS)	85	125	650	950
D.C. POWER (W)	6	18	100	300
FREQUENCIES	UHF	VHF/UHF	UHF/L BAND	UHF/L1L2
OSCILLATOR	QTZ	QTZ	QTZ/RB	Cs
$\Delta F/F(DAY)$ PP10 ¹³	300	100	5-10	2-5

Figure 3 depicts a typical ground station time transfer configuration. Range observations are made at two or more sites by processing signals transmitted from the spacecraft. When the observations are combined and the satellite

NAVISTAR GPS NAVIGATION TECHNOLOGY SEGMENT

STATION SYNCHRONIZATION BY TIME TRANSFER

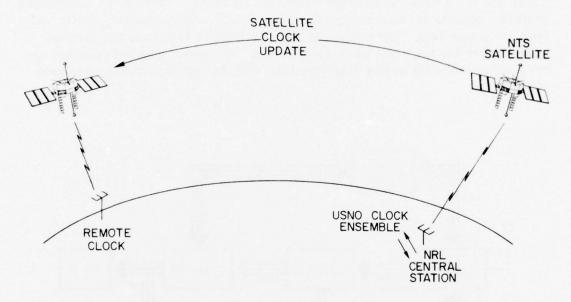


Figure 3. Time Transfer Configuration

oscillator drift is updated to allow for the time difference of the observations, the difference between the two ground clocks is obtained.

Data presented in this paper was obtained using the NTS-1 spacecraft. The receiver described will also operate with the NTS-2 satellite which is to be launched in early 1977. A more detailed explanation of the time transfer technique can be obtained in ref (1).

Time Transfer Receiver, Functional Description

The purpose of this receiver is to determine the range to a satellite in terms of the time required for its transmitted signal to reach the receiver. This is accomplished by the technique of sidetone ranging. In sidetone ranging phase comparisons are made between satellite transmitted tones and receiver generated tones of the same frequency. Both sets of tones are derived from very

stable frequency sources so that the phase differences represent mostly propagation delay with some error due to small frequency drifts in the sources, ionospheric diffraction, and propagation of the signal through receiver components. Propagation delay in the receiver is significantly constant for each tone and is calibrated out. The other errors are dealt with in the data processing performed external to the receiver.

There are three basic subsystems within the receiver. These three subsystems perform separate but interrelated functions which, acting together, derive the ultimate output data. The functional diagram (Figure 4) depicts the receiver broken down into the three basic subsystems. The major data path through the receiver is indicated in this diagram along with the output parameters of each subsystem.

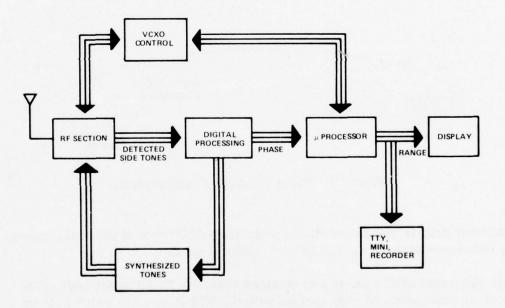


Figure 4. Rx Functional Diagram

The radio frequency (RF) subsystems's major function is to acquire and lock onto the signal transmitted by the satellite and to extract a stable intermediate frequency (IF) for subsequent mixing to the final output signal.

The digital subsystem performs two major functions. One is to synthesize the various sidetones at the proper time and in the same sequence as the satellite's transmitter. In order to do this, the digital subsystem must maintain precise

time correlation with the ground station clock. The synthesized sidetones are used by the RF subsystem to extract an output signal containing phase information. The second major function of the digital subsystem is to measure the phase of this signal and send the data to the microprocessor.

The microprocessor subsystem performs a large number of functional tasks. Its major task is to accept, analyze, and store data. Recall that the receiver's ultimate output is the range of the satellite expressed in terms of time. The microprocessor derives this range by solving a rather complex equation involving phase data.

The microprocessor performs another major task which is to control the various modes of operation of the receiver. In this task the microprocessor acts as a man-machine interface allowing the operator to select and control several functions and options including tests and calibration.

This receiver is compatible with the NTS family of satellites. These satellites transmit tones once a minute on both UHF and L bands. The UHF signals are the ones accepted by this receiver. The time of transmission by the satellite can be controlled from the ground, that is to say that the tone burst may be selected to be transmitted at any time during the minute. This means that the receiver must be initially synchronized to the time of transmission of the satellite, hence the connection to the station or master clock.

The NTS satellite's signal format is depicted in Figure 5. The receiver synthesized tones are compared to those of the satellite to get phase information.

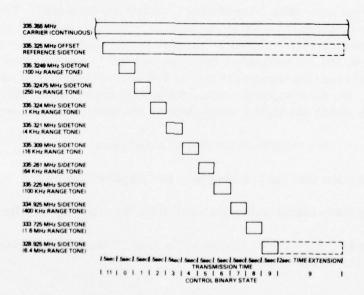


Figure 5. NTS Signal Patterns

That data is used to derive the range, which is then displayed. Phase data may also be displayed at the option of the operator.

The receiver includes several features. Meters are included to display received signal level and receiver tracking error. An alphanumeric display presents data and indicates the operational mode, data entry, clock synchronization and other functions. There is also a keyboard and a set of function switches provided for operator interaction with and control of the receiver. The keyboard and display are functionally related in that the display provides a means of monitoring pushbutton entries prior to that entry's insertion into the microprocessor memory.

This brief functional description should provide some preparation for the detailed explanations which follow. Insofar as it is possible each functional section of the receiver will be treated separately for clearer appreciation of the detail.

RF Subsystem

The RF subsystem was designed to accept the UHF transmitted from the space-craft and convert the ranging sidetones to a form suitable for processing in the digital subsystem. The subsystem uses a frequency tracking phase locked loop to generate the necessary internal signals to remove carrier doppler from the received ranging sidetones. Signals generated by the digital subsystem are then used to convert the received sidetones to a common 30 kHz frequency, containing individual sidetone doppler and in TTL waveform for processing by the digital subsystem.

The RF subsystem is capable of operating in either of two modes: The normal "carrier" mode in which the continuous carrier is tracked and used as the doppler reference; or in a "reference" mode. In this mode, whether the carrier is present or not, the RF subsystem acquires and tracks the received reference tone which is present only during the 5.5 or 7.5 second tone burst. In either of these modes, the tracking loop voltage controlled crystal oscillator (VCXO) may be tuned by either the digital subsystem or manually for quick acquisition.

The RF subsystem also outputs to the digital subsystem:

- (1) an indication that the tracking loop has acquired the signal
- (2) a short pulse signal indicating each time the tracking loop loses lock;
- (3) the tracking loop VCXO frequency for use by the VCXO tuning function within the digital subsystem.

For purposes of verifying proper functioning of the digital subsystem, the RF section has capability for inserting calibration sidetones into the sidetone channel. These are generated from signals derived from the digital subsystem.

A simplified block diagram of the RF subsystem is shown in Figure 6. The signals appearing at the antenna terminals consist of the carrier at 335.355 MHz, a reference tone at 335.325 MHz and ten sequentially occurring tones from 335.324900 MHz through 328.925000 MHz. These signals may contain doppler proportional to frequency.

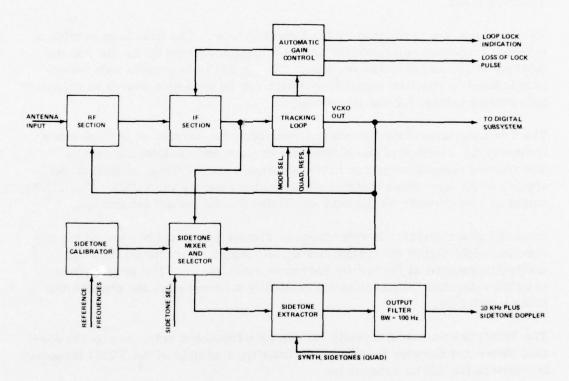


Figure 6. RF Subsystem

RF Section:

In the RF section, this band of frequencies is amplified, passed through an image and interference reject filter, and converted to an IF in which

the tracked component frequency and its doppler are reduced by about 9/10. This reduction in doppler comes about because the local oscillator for the first conversion mixer is obtained by frequency multiplying the tracking loop voltage controlled crystal oscillator (VCXO) by 9.

IF Section:

In the IF section, a 9MHz bandpass filter establishes the IF bandwidth, and AGC is applied to the composite signals. The IF outputs the full band of frequencies to both the tracking loop and the sidetone mixer.

Tracking Loop:

Two functions are performed by the Tracking Loop. The first is to provide a coherent frequency reference for use as a local oscillator by the RF and the Sidetone Mixer and Selector sections. The second is to provide a dc voltage proportional to received signal level which can be used as a source of automatic gain control voltage for the IF section.

The Tracking Loop is configured to track either the carrier or the reference frequency by selection of one of two narrow passband predetection filters. The tracked component is then downconverted a second time, amplified and applied to the loop phase detector whose output controls the VCXO. The VCXO output is used directly as the local oscillator for the second conversion.

Since the phase detector is referenced by signals generated by, and which are coherent with, digital subsystem timing, all doppler is removed from the tracked component at the second downconversion mixer. The proper phase detector reference frequency is automatically selected when the predetection filter is selected.

The VCXO is then output directly for use as a frequency reference by the Sidetone Mixer and Selector Section. Additionally, a sample of the VCXO frequency is output to the digital subsystem.

The Tracking Loop circuitry also contains a coherent amplitude detector which generates a low level unfiltered dc voltage proportional to the amplitude of the tracked signal. This voltage is output to the Coherent AGC Section.

Automatic Gain Control:

The output of a coherent amplitude detector in the tracking loop is routed to the Coherent AGC section where it is filtered and amplified. When the loop is tracking (or "locked"), the AGC circuit establishes a control voltage proportional to received power of the tracked frequency. This voltage is used to control the gain of the IF AGC amplifier. When the loop is not locked, the gain of the IF amplifier is limited to that corresponding to the weakest expected received signal level.

The AGC section also generates a loop lock signal which is sent to the digital subsystem and a front panel light which is lit continuously when the loop is tracking. This section also generates a short TTL pulse when the loop loses lock. This pulse is also output to the digital subsystem.

Sidetone Mixer and Selector:

The IF output is routed to the Sidetone Mixer which uses the tracking loop VCXO frequency as its reference. The output of the Sidetone Mixer consists of components corresponding to and bearing the doppler and phase information contained in the received reference and ranging sidetones. It should be noted that the doppler remaining on the sequentially received sidetones is proportional to the difference between the transmitted sidetone frequency and the transmitted frequency of the component tracked by the loop. This is because the RF portion of the doppler (or "carrier doppler") has been removed in the coherent down-conversion processes. A switch selects either the sidetones from the receiver or calibration sidetones derived from the digital subsystem. The selected sidetones are distributed to the sidetone extractor and filter section.

Sidetone Extractor:

The sidetones output sequentially by the Sidetone Mixer and Switch are routed to the Sidetone Extractor and Filter where they are converted to a common 30 kHz frequency. This is accomplished by a combination of double sideband and single sideband mixing processes using synthesized sidetones from the digital subsystem. The synthesized sidetones, which are coherent with digital subsystem timing and therefore contain no doppler, are switched sequentially with the received sidetones. Thus the output frequency is offset from the nominal 30 kHz by the doppler associated with the received sidetones. The phase of the output is directly related to the phase of the received sidetone. The 30 kHz sinusoidal signal is converted to TTL and output to the ditital subsystem as the primary output of the RF subsystem.

Sidetone Calibrator:

The Sidetone Calibrator provides a means of supplying calibration tones to the digital subsystem. This section generates a burst of tones similar to the received burst but which are controlled in phase since they are derived from the digital subsystem.

Detailed Processor Description

The following description will refer to the processor functional block diagram in Figure 7. In the diagram the microcomputer is shown as one block and is connected by inputs and outputs to various digital subsections. The microcomputer controls these subsections which interface the processor to the RF subsystem, station clock, and operator.

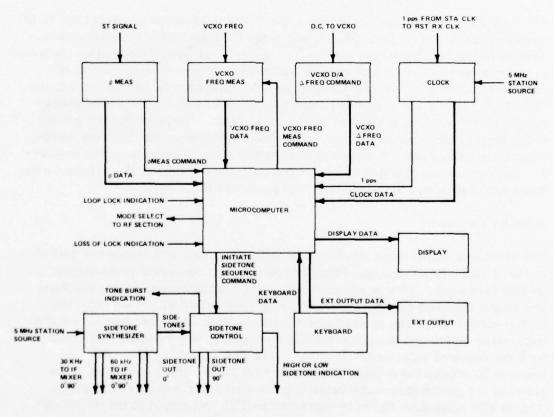


Figure 7. Processor

Phase Measurement

The signal input to the processor from the RF subsystem is at 30 KHz and contains the doppler of the sidetones. The phase of this signal is measured by a time-interval counter at the command of the microcomputer. The data upon conclusion of the measurement is available at a microcomputer input.

VCXO Control

The microcomputer has the capability of controlling the VCXO frequency through the use of a VCXO frequency measurement counter and a digital to analog converter. Upon command of the microcomputer, the VCXO frequency measurement counter counts the number of VCXO cycles which occur in one second. This VCXO frequency data is made available to the microcomputer at an input after the one second measurement. The analog output of the D/A converter is continually summed with the VCXO control voltage. The digital input to the D/A is controlled by an output which remains constant until changed by the microcomputer.

Sidetone Synthesizer and Sidetone Control

The sidetone synthesizer derives from the station 5 MHz source all the necessary mixing signals required by the RF subsystem to mix out the desired signal. The 30 KHz and 60 KHz signals are available to the RF subsystem continually for IF mixing. The synthesized sidetones are continuously fed into a sidetone control circuit which selects and sequences the tones at the command of the microcomputer. The sequence first provides a d.c. level for a half second then ten tones ranging from 100 Hz to 6.4 MHz for a half second each. The selected tone is provided to the RF subsystem in quadrature for the lower four tones and in duplicate for the upper six tones. When the sequence is complete, a d.c. level is maintained at the sidetone output to the RF subsystem. The tone burst indication output lights a front panel LED during the sidetone sequence. The high or low sidetone output is provided to indicate to the RF subsystem when the low four sidetones are sequenced.

Clock

The clock derives seconds and milliseconds data from the station 5 MHz source. An external reset provides the capability of synchronizing the receiver 1 pps to the station source 1 pulse per second (1 pps) to within an accuracy of 200 nanoseconds. The milliseconds data is fed into an input and the 1 pps into an interrupt of the microcomputer.

Mode Select, Loop Lock, and Loss of Lock

The mode select output is an indication to the RF subsystem and front panel LED as to whether the carrier or reference only mode of the receiver has been selected. The loop lock indication is an input from the RF subsystem and is active whenever the receiver is locked on a signal. The loss of lock is another input from the RF subsystem that provides a pulse whenever the receiver loses lock.

Keyboard/Display, and External Output

A sixteen button hexidecimal keyboard is provided for inputting data to the microcomputer. A four button keyboard provides the additional input functions "interrupt", "clear", "enter", and "continue". A thirty-two character alphanumeric gas discharge display is provided to output data and messages to the operator from the microcomputer. The external output duplicates all data and messages that appear on the display and is intended to be used in interfacing the receiver with an external device.

Phase Determination

The receiver's primary mode of operation for processing data is in the reference mode using automatic acquisition. This is the mode in which the data processing will be described. First the microcomputer waits until the time at which the tones are transmitted. While waiting it holds the VCXO at the desired initial acquisition frequency previously entered. When the tone transmission occurs, the VCXO D/A output is left at its last value and the synthesized tone burst sequence is initiated in the receiver. The microprocessor begins to sample the phase of the first tone through the phase measurement circuit. For each tone 81 samples of phase are taken at a 200 Hz rate, and a linear least squares fit is made to these points. In this fit the following equation is realized.

$$\phi_{\mathbf{i}} = \mathbf{M}_{\mathbf{i}} \mathbf{t}_{\mathbf{i}} + \mathbf{B}_{\mathbf{i}} \tag{1}$$

where ϕ_i is the phase of the ith sidetone, M_i is the phase rate of the ith sidetone, B_i is the phase of the ith sidetone at the time its sampling was begun, and t_i is the time of the phase relative to when the sampling was begun. Time is normalized to one unit equals 5 msec for simplicity. In equation (1) the values of M_i and B_i are calculated from the least squares approximation as follows:

$$\mathbf{M} = \frac{\mathbf{S_0S_4 - S_1S_3}}{\mathbf{S_0S_2 - S_1^2}} \quad \mathbf{B} = \frac{\mathbf{S_2S_3 - S_1S_4}}{\mathbf{S_0S_2 - S_1^2}}$$

where,

 $S_0 = number of samples = 81$

 $S_1 = sum of the times for each sample = 0 + 1 + 2 + 3 + . . . + 80 = 3240$

 $S_2 = \text{sum of the times squared for each sample}$ = $0^2 + 1^2 + 2^2 + 3^2 + \dots + 80^2$ = 173,880

S₃ = sum of the phases including integer wavelengths as measured from the time of the first sample

 S_4 = sum of the phases multiplied by the sample times

Substituting for the constants that result from fixing the number of samples gives,

$$M = .00002258 S_4 - .0009033 S_3$$
 (2)

$$B = .0484 S_3 - .0009033 S_4$$
 (3)

The values of S_3 and S_4 are accumulated during the sampling of each tone, and B_i is calculated and saved for each tone. Since M_i is the phase rate of each tone due to doppler, if the doppler is assumed to be constant throughout the tone burst sequence, then all of the tone phase rates are equal to the phase rate of the highest tone multiplied by a constant as follows,

$$\mathbf{M_i} = \mathbf{K_i} \,\mathbf{M}_{10} \tag{4}$$

where K_i is a constant unique for each tone, and M_{10} is the phase rate of the 6.4 MHz tone. M_{10} is calculated and saved for the 6.4 MHz tone.

In determining range the phase of each sidetone is projected to the point in time that the range is desired. Equations (1) and (4) may be combined to give,

$$\phi_{\mathbf{i}} = K_{\mathbf{i}} M_{10} t_{\mathbf{i}} + B_{\mathbf{i}}$$
 (5)

The ϕ_i in equation (5) must be corrected for propagation delay through the receiver so an error term is added giving,

$$\phi_{\mathbf{i}} = K_{\mathbf{i}} M_{10} t_{\mathbf{i}} + \phi_{\mathbf{E}\mathbf{i}} + B_{\mathbf{i}}$$
 (6)

where ϕ_{Ei} is the calibration error. Equation (6) is used to determine the phase of each sidetone at the end of the tone burst, and these in turn are used to determine a range.

Range Determination

The phase differences determined represent propagation delay and clock error between the satellite clock and the receiver clock. These phases are interpreted in terms of observed range to the satellite in milliseconds. The phases of the lower tones are used to get a rough range and those of the higher tones are used to resolve range to nanosecond accuracy. In resolving range equation (7) is used:

$$R_{i} = \frac{\phi_{i} + INTEGER \left[R_{i-1} f_{i} + \frac{1}{2} - \phi_{i}\right]}{f_{i}}$$
(7)

where,

 ϕ_i is the phase of the ith tone f_i is the frequency of the ith tone R_i is the range in seconds whose accuracy is based on the phase of the ith tone.

The phases of each tone are determined to an accuracy of 1%, and the accuracy of a range based on the phase of a tone is 1% of the tone's period. The accuracy of the final range is 1% of the 6.4 MHz tone period or 1.56 nsec. After the range is calculated, the phase of each tone may be displayed as well as range if the operator desires. Upon conclusion of display of the phases, real time and the last range are continually displayed until the next sequence of data is processed.

Operation

The receiver is shown in Figure 8. Inputs required are 1 pps and 5 MHz from the station clock. The receiver's final output is observed range to the satellite in milliseconds. This data is displayed on the front panel and also appears at an external output which may be interfaced with a teletype, minicomputer, or data recording device.

When the receiver is initialized, the operator first synchronizes the receiver clock with the station clock, enters a predicted satellite frequency which is

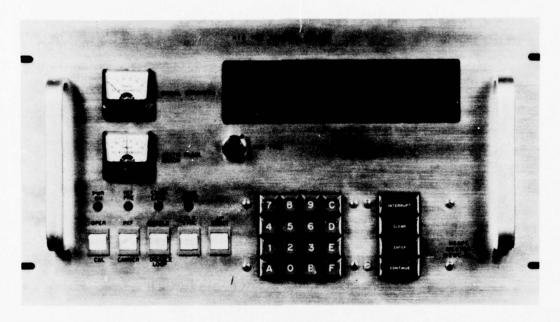


Figure 8. Rx

maintained by the microcomputer, and then waits for aquisition of the satellite. During the tone burst if there is an affirmative lock indication, the VCXO frequency is measured and replaces the initial frequency input by the operator. The VCXO is held to this frequency by microcomputer control until time for the next burst of data. Again upon lock of the signal a new frequency is measured, and the sequence continues enabling the receiver to track the satellite throughout its doppler range. The microcomputer continues the sequence of taking data until interrupted by the operator.

Field Test

The receiver shown in Figure (8) was taken to a NASA tracking station at Rosman, N.C. A time transfer was performed as shown in Figure 9. Time at Rosman was compared to that at an NRL tracking station at Chesapeake Beach, Md. Time at the NRL site was known relative to USNO time by portable clock measurements. In performing a time transfer, a range observation is made at Rosman and at Chesapeake Beach. The observation at Rosman is corrected for oscillator drift in the satellite clock during the time between the two measurements. The observation at Cheaseapeake Beach is corrected to USNO time and the difference is taken between the two stations.

NTS REMOTE CLOCK SYNCHRONIZATION

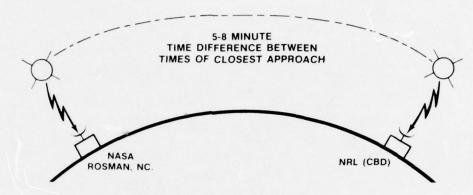


Figure 9. Time Transfer with Rosman

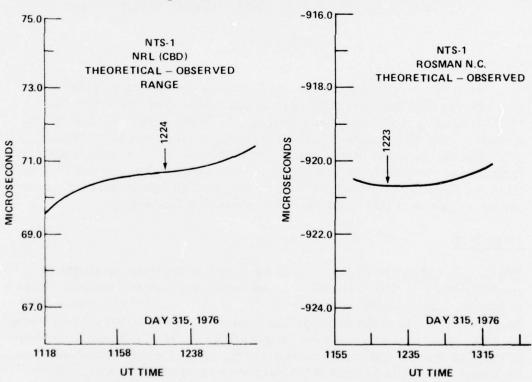


Figure 10. CBD Pass

Figure 11. Rosman Pass

Figure 10 and Figure 11 show one particular satellite pass with observations made at Rosman and Chesapeake Beach during the test. The data used in the time transfer are taken at the time of closest approach and are pointed out with arrows. Twelve such passes were taken and each time transfer is plotted in Figure 12. The noise in the data has a RMS of 86 nsec. A portable clock measurement was made before and after the field test. These points are plotted and a line drawn between the two falls very close to the time transfer data. The conclusion of the test was a time transfer accuracy better than 100 nsec.

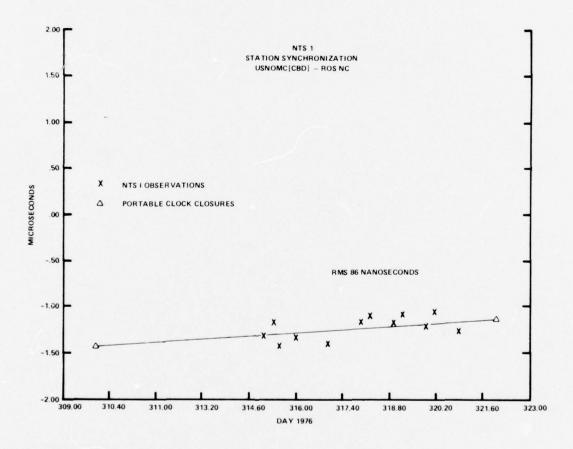


Figure 12. Time Transfer Plot

Reference:

 NRL Report 7703, April 18, 1974 "International Time Transfer Between USNO and RGO via TIMATION 2 Satellite"; R. Easton, D. Lynch, J. Buisson and T. McCaskill.

A TIME CODE FROM NOAA'S GEOSTATIONARY OPERATIONAL ENVIRONMENTAL SATELLITES

D. W. Hanson, J. V. Cateora, and D. D. Davis National Bureau of Standards, Boulder, Colorado

ABSTRACT

In support of the environmental data collection by the National Oceanic and Atmospheric Administration's (NOAA's) Geostationary Operational Environmental satellites (GOES), a time code has been incorporated by the National Bureau of Standards (NBS) into an interrogation message from these satellites. This message is directed to data-collection platforms engaged in seismic, Tsunami, hydromet and other related monitoring activities. The NBS has developed this time-code system to serve environmental data users who require only a few tenths of a second accuracy as well as those who need a more accurate time reference.

The time code is available continuously from two geostationary satellites and provides a coverage of the Atlantic and Pacific Ocean Basins as well as the North and South American Continents. The time code includes the necessary information to compensate for free-space propagation delays between the master clock located at Wallops Island, Virginia, and the user. Preliminary results indicate a timing resolution of $10~\mu s$. The accuracy is very much dependent upon the quality of orbital information supplied to NBS by NOAA. This is presently being evaluated.

The time-code system is supported by atomic clocks maintained at Wallops Island, Virginia, the point of origin for all signals to be sent through the satellites. A data-logging system monitors three television networks and Loran-C to provide a comparison link between the Wallops Island clocks and reference standards at the NBS.

A microprocessor "smart" clock has been developed for the user that automatically corrects for path and equipment delays and places its recovered time in synchronism with Coordinated Universal Time (UTC) generated by NBS. This clock and associated recovery equipment will also be discussed in the presentation.

INTRODUCTION

A time code has been added by the National Bureau of Standards (NBS) into a communications channel between the National Oceanic and Atmospheric Administration's (NOAA's Geostationary Operational Environmental Satellites (GOES) and remote environmental data-gathering platforms. The time code is continuously available throughout the entire Western Hemisphere offering easy accessibility and moderately high accuracy at low cost. The time code contains Coordinated Universal Time (UTC) information and Universal Time (UTI) corrections. In addition to the time code, the satellite's position is included for free-space propagation time corrections. These position data are presently in the form of the satellite's longitude, latitude, and range from the earth's center. The UTC and UTI information is a permanent feature of those satellites and will remain fixed in format. The satellite position information may undergo changes in form in an attempt to improve its performance.

GOES SYSTEM DESCRIPTION

There are three GOES satellites in orbit, two in operational status and the third serving as an in-orbit spare. The two operational satellites are located at 135° and 75° W with the spare at 105° W longitude. The earth coverages are shown in figure 1.

The mission for the GOES satellites includes (1) continuous photography of the earth's surface, (2) collection of data on the space environmental Sun/Earth interaction, and (3) collection of remote-sensor data including flood, rain, snow, Tsunami, earthquake, and air/water pollution monitoring. It is in this third function that a need for a time code was realized since in many cases the data would be of greater value if it were labeled with the date as it is collected.

Some of these remote sensors are equipped with both a receiver and transmitter. Upon command from the satellite, these sensors, called data collection platforms (DCP's), are activated to transmit stored data to the satellite. The satellite relays these data to the NOAA Command and Data Acquisition (CDA) station at Wallops Island, VA, for processing and dissemination to users. The communications channel used to activate this response is called the interrogation channel. This channel is continuously relaying interrogation messages through the satellites. Its format is shown in figure 2.

The interrogation message is exactly one-half second in length or 50 bits, the data rate being 100b/s. The interrogation message is binary and phase modulates a carrier ± 60 degrees after being Manchester-encoded; i.e., data and data clock are modulo 2 added before modulating the carrier. An interrogation message consists of the first four bits representing a BCD word of the time code beginning on the one-half second

followed by a maximum length sequence (MLS) 15 bits in length for message synchronization and ending with 31 bits as an address for a particular DCP. When a DCP receives and recognizes its unique address it transmits its data to the satellite. Sixty interrogation messages are required to send the 60 BCD time-code words constituting a time-code frame. The time-code frame begins on the one-half minute and requires 30 seconds to complete.

TIME CODE SYSTEM

The time code is generated and integrated into the interrogation message at the CDA for transmission to the GOES satellites. The time-code generation system, shown in figure 3, is completely redundant and fully supported by an uninterruptable power supply. There is a communication interface between the equipment and NBS/Boulder using a telephone line. Over the telephone line, satellite position information is sent to the CDA and stored in memory for eventual incorporation with the time code and interrogation message. Data are also retrieved from the CDA via the telephone line to Boulder. These data include the frequency of the atomic oscillators and the time of the clocks relative to UTC as compared to TV transmissions from Norfolk, VA, and to the Loran-C transmissions from Cape Fear, North Carolina. These data are stored for retrieval in a Data Logger similar to that described in reference [1]. The Data Logger also measures and stores the time of arrival of the signals from both the Western and Eastern GOES satellites as received at the CDA. Besides the time and frequency monitoring functions, the Data Logger provides the information necessary for NBS staff at Boulder to remotely determine if and where malfunctions exist and how to correct for them by switching in redundant system components.

The interrogation message rate, 100b/s, is generated by the atomic oscillators in the time-code system. The interrogation message is one-half second in length or 50 bits. The time-code frame repeats every 30 seconds and begins on the one-half minute as shown in figure 4. The time-code frame contains a synchronization word, a time-of-year word (UTC), the UTl correction, and the satellite's position in terms of its longitude, latitude, and radius. The position information is presently updated only on the half hour.

The satellite position information is generated at Boulder using a CDC 6600 computer and orbital elements furnished by NOAA's National Environmental Satellite Service (NESS). NESS generates these orbital elements weekly from data obtained from their trilateration range and range rate (R&RR) tracking network. That network is illustrated in figure 5. The tracking data are obtained by measuring the R&RR to the Western satellite from the CDA, and sites in the states of Washington and Hawaii. The Eastern satellite is observed from the CDA, Santiago, Chile, and Ascension Island in the South Atlantic. The sites used in the R&RR network other than the CDA are known as turn-around ranging stations (TARS).

RECEPTION

The interrogation channel signals are briefly characterized in figure 6. Typical antennas include simple low gain helixes or yagis. A receiver is shown in figure 7 as three modules; an RF/IF module, an L.O. injection module and a demodulator module. A block diagram of this receiver is shown in figure 8. This receiver is a coherent, synchronous digital receiver utilizing a phase-lock loop for demodulation and L.O. generation and a bit synchronizer for detection purposes.

The outputs of the receiver, data and data clock, are the inputs to a decoder clock (see reference 2 for a complete description of this clock). The decoder clock shown in figure 9 uses a four-bit microprocessor to demultiplex the data, extract the proper four bits of the time code every one-half second, and reconstruct the time-code frame. Once decoded, this time is loaded into Random Access Memory (RAM) and updated by incrementing the RAM clock in 10 ms steps by counting the data clock, a 100 Hz squarewave.

A prototype of a "smart" clock is shown in figure 10. This is essentially an addition of a second microprocessor to the decoder clock for the calculation of the free-space propagation delay from the CDA to the clock via the satellite. This delay value is then used with a delay generator to compensate for the free-space path delay.

PERFORMANCE

The equation relating the time recovered from the satellite to the master clock at Wallops Island is given in figure 11. Term 1 is known to better than 1 µs using the Data Logger at the CDA which compares the CDA clocks to Loran-C and TV-line 10. Using the measurement setups of figure 12, the smart-clock output on the chart recorder would draw a straight line if the orbit predictions are accurate and all equipment delays are constants; i.e., terms 2, 4, 5, and 6. Figure 13 shows raw data for 28 days. Each data point represents an average of measurements taken in one day at one-half-hour increments totaling 48 measurements per day. Figure 14 shows the same data with the CDA clock drift removed and the two jumps in delay which have been attributed to equipment changes at the CDA. The orbit predictions used to generate these data were derived from three sets of orbital elements extrapolating as much as 22 days beyond their date.

The results indicate a consistency in orbit determination and in the stability of equipment delays of about 10 μs for the period under study. A claim for accuracy cannot be made, however, until the equipment delays at the CDA and in the receiving equipment have been evaluated and more measurements of this type are taken at points separated by large geographical distances.

Portions of the actual charts producing the data just discussed are shown in figure 15. The output, uncorrected for the free-space delay shows a 24-hour diurnal due to the satellite's orbit inclination and eccentricity. The corrected output, one point every half hour, lies in a straight line at least to a few microseconds on the average. Because the satellite position data are updated only every half hour, the corrected output deviates from a straight line between the half-hour updates at the same rate shown for the uncorrected output.

CONCLUSIONS

The time code has been broadcast from the two GOES satellites for more than one year. It has proven itself to be a reliable, low cost, and extremely simple system for moderately high accuracy time. The time code is now considered a permanent feature of the GOES satellites and should see an expanding list of users for many purposes within the Western Hemisphere.

The results presented in this paper indicate a potential accuracy of 10 to 20 microseconds. These figures need to be verified, however, by additional observations at points widely separated geographically. Equipment delays need further study. The clock drift and the effect of equipment changes at the CDA need to be offset or eliminated to make the time-code system a true one-way time transfer technique.

REFERENCES

- D. Davis, "A Microprocessor Data Logging System for Utilizing TV as a Time/Frequency Transfer Standard," Precise Time and Time Interval (PTTI) Applications and Planning Meeting, November 30 -December 2, 1976.
- J. V. Cateora, D. D. Davis, and D. W. Hanson, "A Satellite-Controlled Digital Clock," NBS Technical Note 681, June 1976.

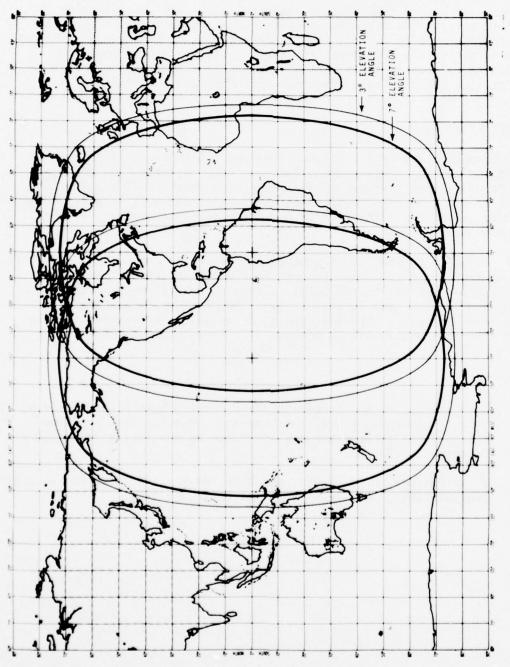


Fig. 1-GOES coverage

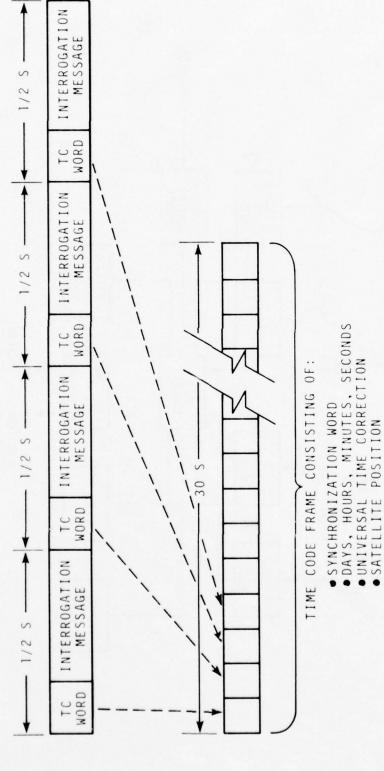


Fig. 2-Interrogation message format

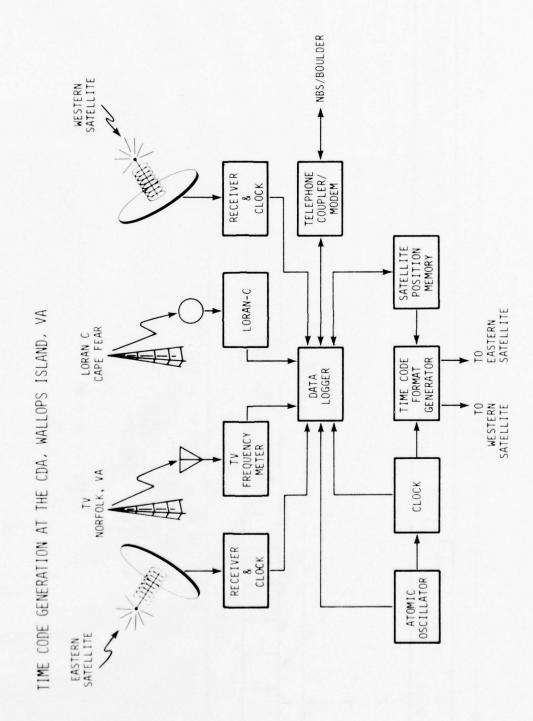


Fig. 3-Time code generation equipment at the CDA Wallops Island, VA

TIME CODE FORMAT

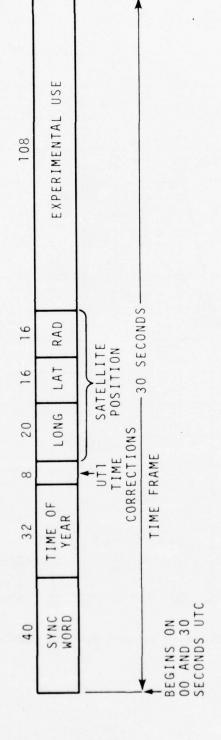


Fig. 4-Time code format

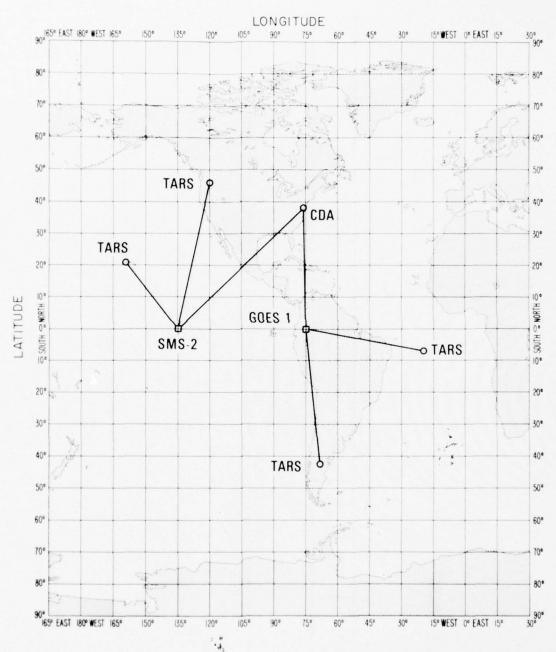


Fig. 5-Tracking network for the GOES satellites

INTERROGATION CHANNEL SIGNAL CHARACTERISTICS

			Ι	I	Γ	1		
EASTERN SATELLITE	468.8375 MHz	RHCP	CPSK (± 60°)	100 BPS	75° W	-139 dBm	MANCHESTER	400 Hz
WESTERN SATELLITE	468.8250 MHz	RHCP	CPSK (± 60°)	100 BPS	135° W	-139 dBm	MANCHESTER	400 Hz
	FREQUENCY	POLARIZATION	MODULATION	DATA RATE	SATELLITE LOCATION	SIGNAL STRENGTH (OUTPUT FROM ISOTROPIC ANTENNA)	CODING	BANDWIDTH

Fig. 6-Interrogation channel signal characteristics

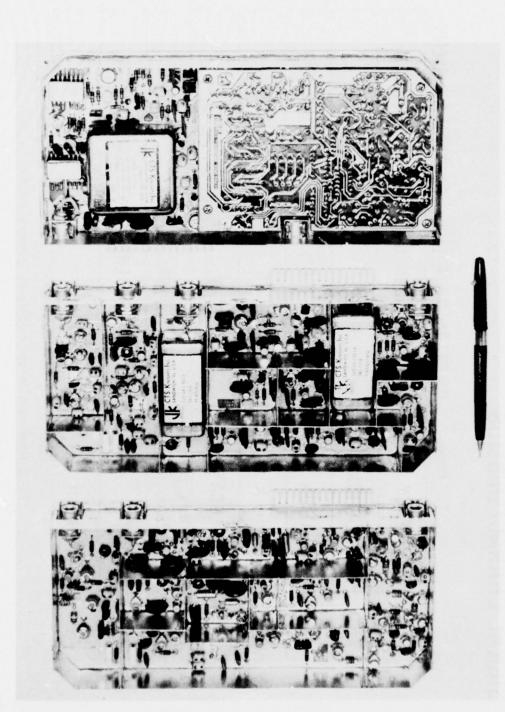


Fig. 7-Interrogation channel receiver

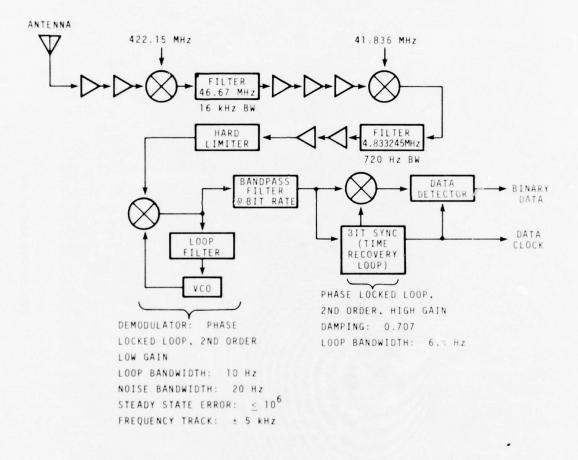


Fig. 8-Interrogation channel receiver block diagram



Fig. 9-Decoder clock

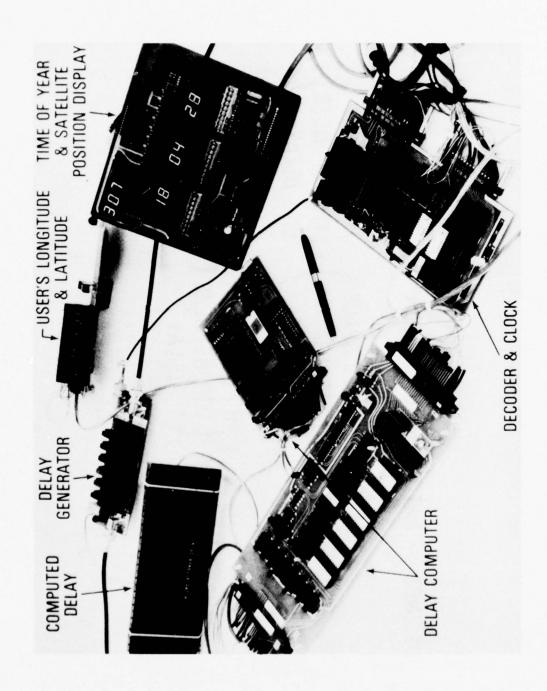


Fig. 10-Smart clock

Fig. 11-UTC(NBS)-SAT/NBS

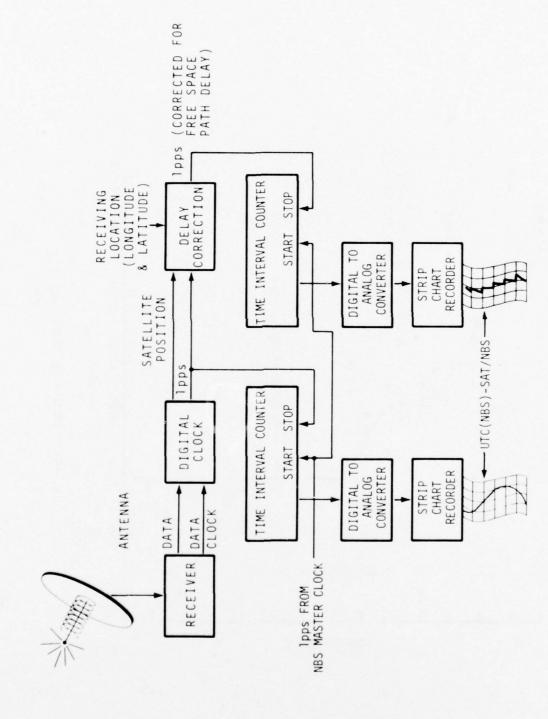


Fig. 12-Measurement of UTC(NBS)-SAT/NBS

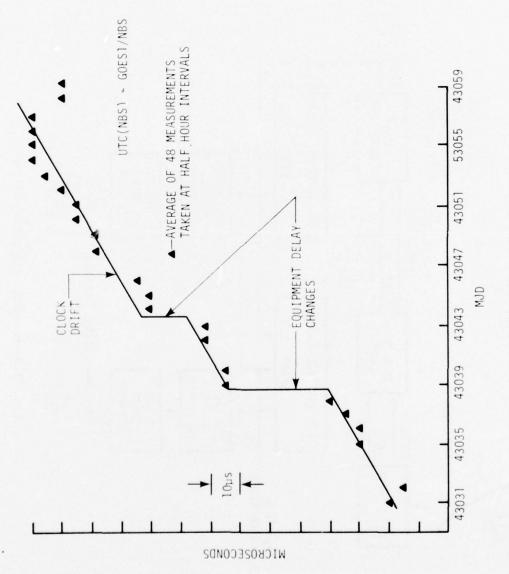


Fig. 13-UTC(NBS)-GOES 1/NBS; raw data

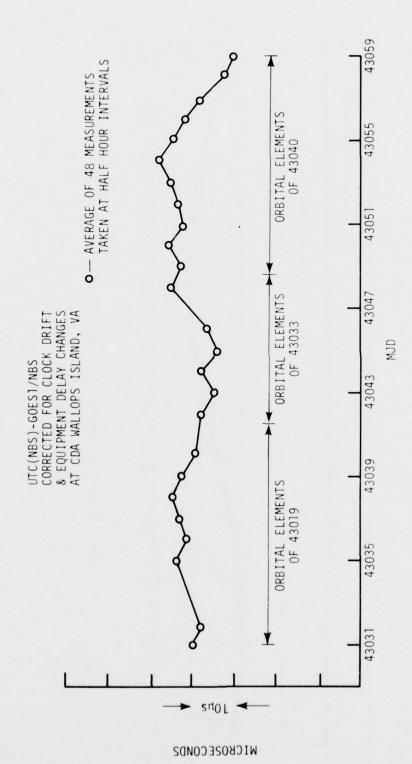


Fig. 14-UTC(NBS)-GOES 1/NBS; clock drift and equipment delay changes removed

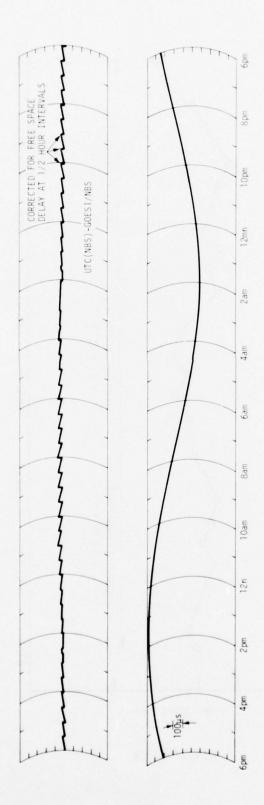


Fig. 15-Satellite output: corrected and uncorrected

LOW NOISE MULTI CHANNEL SPACE COMMUNICATION OSCILLATORS

M. Bloch, M. Meirs, and M. Rosenfeld Frequency Electronics Inc.

(Paper not Received)

A SYSTEM FOR NEAR REAL-TIME CRUSTAL DEFORMATION MONITORING

Peter F. MacDoran
Radio Interferometry Technology Applications Group
Jet Propulsion Laboratory
Pasadena, California 91103

ABSTRACT

It is proposed to demonstrate a near real-time monitoring system for study of vertical crustal deformation such as the Palmdale Bulge. This monitoring will be achieved by independent station radio interferometry techniques with a pair of small antennas (2.5m), illuminated by ALSEP S-band signals from the moon or other artificial radio signal sources. Although the ALSEP will allow only fringe frequency observations and measurement of equatorial baseline components, 82% of vertical deformation can be sensed. This system will occupy sites previously measured in three dimensions by ARIES (Astronomical Radio Interferometric Earth Surveying) and monitored thereafter by this small antenna system. By comparing the ARIES equatorial baseline components, derived from quasar positions, with those determined by ALSEP signals it will also be possible to relate lunar motions relative to the quasar reference frame with approximately 0.1 arc sec.

INTRODUCTION

The ARIES (Astronomical Radio Interferometric Earth Surveying) technique, as presently constituted, is sophisticated and cumbersome to operate because of the quasar sources are weak signals when received at the earth. However, the quasars compose a virtually time-invariant frame of reference because of their great distances and thus are free of orbit computational challenges.

The ALSEP (Apollo Lunar Surface Experiments Package) units placed on the moon by Apollo Flights 12, 14, 15, 16 and 17 represent a valuable resource of radio illumination for earth-based interferometers. Such interferometry has been accomplished by several investigators (ref. 1, 2, and 3) although, no use has been made of the ALSEP signals for terrestrial geodesy.

Unlike the quasars which emit very wideband radio spectral noise, the ALSEP is spectrally narrow being composed of telemetry signals from lunar-based scientific instruments. The ALSEP's are not radio transponders of the type used aboard interplanetary spacecraft. The ALSEP does accept uplink commands from earth to control certain functions, however, no coherent response occurs from the device.

Although the ALSEP spectrum is narrow, about 6 KHz at 3 db, the radio flux arriving at the earth is equivalent to 50,000 Jansky ($10^{-26}~\text{w/m}^2/\text{Hz}$). By comparison, in ARIES experiments a strong quasar is considered to be a source of 5 or more Jy. This factor of 10^4 difference in flux is then available to be traded-off to achieve a simpler radio interferometry system but at the expense of having introduced radio source dynamics into the problem. Fortunately, LURE (Lunar Ranging Experiment) ref. 4 and the ALSEP/Quasar $\Delta VLBI$ experiments, ref. 5, have been successfully dealing with such problems and now represent a valuable resource for achieving the desired radio interferometric geodesy simplifications.

FRINGE FREQUENCY OBSERVABLES AND VERTICAL COMPONENT SENSITIVITY

The RF spectral narrowness of the ALSEP's does represent a limitation relative to the extremely wide RF continuum emissions of quasars. A broad RF emission spectrum allows the interferometer to precisely measure the delay function by signal cross-correlation within 0.1 nanosecond, but a narrow spectrum allows only the time rate of delay change to be precisely measured (ref. 6). Three dimensional geodesy requires interferometry delay measurements from at least two quasars at substantially different declinations. In actual practice, ARIES experiments use ten to twenty quasars observed over periods of 8 to 26 hours because of a need for an alternate solution strategy caused by frequency system instabilities.

Having access to only delay rate data, also called fringe frequency, results in the interferometer being sensitive to only the two equatorial components (X and Y) of the baseline vector. The Z component insensitivity results in a loss of 18% of the information and some uniqueness of interpretation. More specifically, consider the effect of applying the rotation matrix (valid for latitude 35°) to transform a unit local vertical displacement into geocentric baseline components:

$$\begin{pmatrix} -.26 & .88 & -.39 \\ -.49 & -.47 & -.73 \\ -.83 & 0 & .56 \end{pmatrix} \begin{pmatrix} 0 \\ 0 \\ 1 \end{pmatrix} = \begin{pmatrix} -.39 \\ -.73 \\ .56 \end{pmatrix}$$

Thus, a one meter increment in the local vertical appears as a 39 cm decrease in the gocentric X component (direction toward Greenwich) and a 73 cm decrease in the Y component (90° E of Greenwich). The spin axis component, which will not be sensed by this system, experiences a 56 cm increase.

REAL-TIME DATA TRANSFER

The narrow RF spectrum of ALSEP does offer an important advantage of being easily recorded or transferred via telephone. A 3 KHz information bandwidth is suitable from signal to noise ratio considerations and quite reasonable for telephone circuit transmission for real-time cross correlation signal detection processing.

The phone lines have instabilities that need frequent calibration. This can be accomplished by time-formatting the data in the usual Very Long Baseline Interferometry (VLBI) manner at each station. Each of the 2.5m antenna stations will have a cesium clock which can be synchronized to the other clock within one microsecond or better and thus the phone line delay can be determined well within the 3 KHz bandwidth restrictions of the line. Figure 1, illustrates the conceptual elements for monitoring stations 100 km apart at Pearblossom and Palos Verdes, California. The Pearblossom site is in the maximum zone of the uplift associated with the San Andreas Fault in Southern California and known as the Palmdale Bulge (ref. 7). There is reason to believe that these uplifts can occur relatively rapidly (i.e. few months) and therefore the interest in near real-time automated monitoring.

TELECOMMUNICATIONS ASPECTS

Consider two or more 2.5 meter (\sim 8 ft.) diameter dish antennas with efficiencies of 50%, 200 Kelvin S-band receiver operating temperatures, 3 KHz bandwidth, 10 second coherent integration time and receiving ALSEP signals equivalent to 5 x 10^4 Jy. The signal to noise ratio (SNR) of the cross correlation output is then 27, (ref. 8).

By deriving the interferometer phase every 10 seconds over an 800 second interval it will be possible to extract the fringe frequency with a precision of 50 to 100 $\mu\rm Hz$ of S-band. Several 800 s. samples of the fringe frequency over a wide range of sky visibility for the ALSEP's will allow the amplitude and phase of the diurnal signature to be determined along with the frequency system offset. Thus, equatorial baseline components can be measured (ref. 6 and 8). Having 50 $\mu\rm Hz$ data quality every 800 sec. implies 10 cm baseline precision.

FREQUENCY SYSTEM REQUIREMENTS

The independently operated atomic frequency systems at each station introduce another error source. Ideally, a frequency system such as a

hydrogen maser could be used with virtually no contribution to the error budget. However, cost aspects make it important to consider other frequency sources for this study where unattended remote station operations are highly desireable. At 800 sec. the HP 5061, option 4.5 cesium frequency system has a stability of about $^{\Delta f}/f=1.6 \times 10^{-13}$ which at S-band causes a 350 $\mu\rm Hz$ noise level. Incoherently combining these 350 $\mu\rm Hz$ observations over a 10 hour observation period allows improvement to an effective 50 $\mu\rm Hz$ observation which is equivalent to about a 10 cm baseline precision.

CALIBRATIONS

A. Phase Stability

Because the equatorial baseline information is inherently diurnal in nature, special care must be taken to either stabilize the receiving system or to explicitly measure possible thermal phase variations over the tracking pass. Such phase calibration can be performed and transmitted along with the time-formatted video data (ref. 9).

B. Lunar Orbit

Based upon LURE data (ref.10) the lunar ephermerides are believed to be internally consistent to within approximately 0.01 arc sec. Considering the two small antenna stations to be deployed 100 Km apart at established ARIES sites, for example, one on the Palmdale Bulge maximum (Pearblossom) and the other near Tidal Bench Mark 8 (Palos Verdes). A 0.01 arc sec lunar position internal error causes a 0.5 cm baseline error. Possible angular rotations between the lunar frame and the quasar frame might be present and could be sensed at about the 0.1 arc sec level by this 100 Km baseline.

C. Tiansmission Media

- Ionosphere a 100 Km baseline is short enough that diurnal variation are self-cancelling in the differential measurement that is intrinsic to interferometry. Residual effects due to ionospheric clouds of scale <100 Km are estimated to be 10 cm per pass and random on a pass to pass basis.
- 2. Troposphere twice daily radiosonde weather balloon flights are available to calibrate both of the proposed sites. Edwards Air Force Base can be used to calibrate the Pearblossom site 35 Km away with both in the Mojave desert environment. Los Angeles Inter-

national Airport is 15 Km away from Palos Verdes site and both are coastal locations. It is also possible to transmit surface meteorology through the phone line. The radiosonde calibrations will be accurate to 3 cm at zenith and considering that tracking data will be taken to only 20° elevation angles, the baseline will be affected at about the 10 cm level on a single pass basis. Water vapor radiometers could calibrate the wet tropospheric delay effects within 2 cm to 10° elevation angles, however, such instruments are relatively expensive and may be non-optimal for continuous monitoring on a time scale of months to years.

Figure 2, summarizes the random and systematic errors that allow about a 21 cm performance from a single 10 hour pass and about a 7 cm accuracy given the statistical combination of nine passes of ALSEP/interferometer data.

SUMMARY

A radio interferometry scheme has been proposed which uses the relatively strong S-band radio signals coming from the ALSEP stations on the moon. These strong signals have allowed several simpifications to independent station radio interferometry such as small 2.5 m antenna sizes and real-time cross correlation. The frequency system requirements of $\Delta f/f=2 \times 10^{-13}, \tau=800$ sec, remain fairly sophisicated but obtainable commercially. Stations of the type discussed could be implemented and operated at comparatively low cost and could make important geophysical contributions to the determination of crustal deformations.

ACKNOWLEDGEMENTS

The author gratefully acknowledges useful discussions with JPL colleagues: K. M. Ong, R. A. Preston, G. M. Resch, M. A. Slade III, D. J. Spitzmesser, J. B. Thomas, and J. G. Williams.

This paper presents the results of one phase of research carried out at the Jet Propulsion Laboratory, California Institute of Technology, under Contract No. NAS 7-100, sponsored by the National Aeronautics and Space Administration, Office of Applications, Earth and Ocean Dynamics Applications Program.

REFERENCES

- 1. Counselman, C. C., III, Hinteregger, H. F., and Shapiro, I. I., "Astronomical Applications of Differential Interferometry," Science, Vol. 178, pp. 607-608, 1972.
- Counselman, C. C., III, et al., "Lunar Baselines and Libration from Differential VLBI Observations of ALSEPS," The Moon, Vol. 8, pp. 484-489, 1973.
- 3. Slade, M. A., MacDoran, P. F., and Thomas, J. B., "Very Long Baseline Interferometry (VLBI) Possibilities for Lunar Study," in The Deep Space Network, Technical Report 32-1526, Vol. XII, pp. 35-39, Jet Propulsion Laboratory, Pasadena, Calif., 1972.
- 4. Bender, P. L., et al., "The Lunar Laser Ranging Experiment," Science, Vol. 182, pp. 229-238, 1973.
- 5. Slade, M. A., Preston, R. A., Harris, A. W., Skjerve, L. J., and Spitzmesser, D. J., "ALSEP Quasar Differential VLBI," in the Deep Space Network Progress Report, 42-33, Vol., pp. 37-47, Jet Propulsion Laboratory, Pasadena, Calif., 1976.
- 6. Williams, J. G., Very long baseline interferometry and its sensitivity to geophysical and astronomical effects, The Deep Space Network, Space Programs Summary, Tech. Rep. 37-62, Vol. 2,p. 49, Jet Propulsion Laboratory, Pasadena, Calif., 1970.
- 7. Castle, R. O., Church, J. P., and Elliott, M. R., Aseismic uplift in southern California: Science, Vol. 192, pp. 251-253, 1976.
- 8. MacDoran, P. F., "Radio interferometry for international study of the earthquake mechanism," Acta Astronautica, 1, pp. 1427-1444, 1974.
- 9. Personal communications, A.E.E. Rogers, Haystack Radio Observatory.
- 10. Williams, J. G., "Lunar Laser Ranging: Present Results and Future Plans," EOS, Trans., Am. Geophys. Union, Vol. 56, 970, 1975.

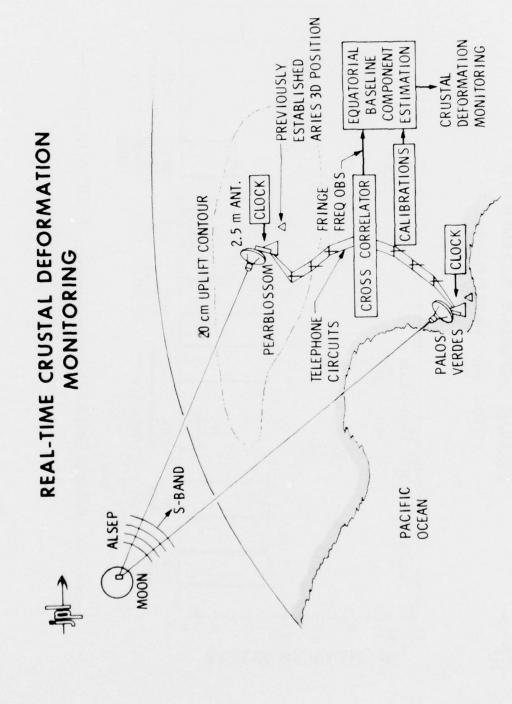
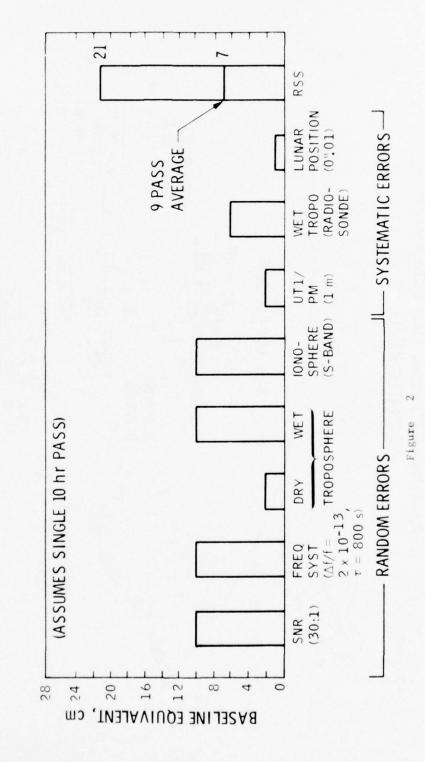


Figure 1

REAL-TIME CRUSTAL DEFORMATION MONITORING ERROR SOURCE ESTIMATES

(100 km BASELINES)



Quartz Clocks Synchronized by LF Time Signals

J. Bonanomi and P. Schumacher, Observatoire Cantonal, Neuchâtel, Switzerland

Abstract

The general availability of LF time signals, the compactness and simplicity of the receivers, and C-Mos integrated circuits make it possible to design reliable, inexpensive and unattended synchronized clocks. Battery-operated models have an autonomy of 3 years and an accuracy of 10 msec. Models with temperature-controlled crystal oscillators have an accuracy of 100 µsec.

Introduction

There are 5 LF-stations, 4 of which are in Europe [1], transmitting time signals and precision carriers continuously (fig. 1); several more stations transmit time signals regularly but not continuously (Japan, USSR). All these transmitters can be used to synchronize clocks in a straightforward way. It is the purpose of this paper to show that such clocks can be made very reliable and at low cost.

The clocks to be described here are quartz clocks, which are synchronized by the time signals and run with the rate of their quartz in the absence of a useful signal.

Frequency	Call sign	Country		nat o minu					
40 kHz	JG2AS	Japan	_						
50 kHz	OMA	Czech.							
60 kHz	MSF	England							
60 kHz	WWVB	USA				1	1		
$66^2/3$ kHz	RBU	USSR		1	1		4	1	1
75 kHz	HBG	Switz.							
77,5 kHz	DCF	Germany			1				
100 kHz	LOR.C		57	58	59	0	1	2	3

Fig. 1: Time Signal Transmitters in the LF-Band.

Properties of LF-time signals

The accuracy of LF-time signals is in the 100 µsec range; this modest accuracy is sufficient for a great number of public and industrial applications.

 $\underline{\text{Range}}$. With antenna powers around 10 kW, the useful range of the transmitters is 3000 km. Thus transmitter WWVB covers the contiguous United States adequately, whereas

the 4 European transmitters are in effect largely redundant.

Receivers. LF-waves can be received inside most buildings and penetrate many meters underground. The antenna can therefore be mounted on the same printed circuit board as the receiver (fig. 4), and only in rare cases is it necessary to separate antenna and receiver by a cable.

Noise and interference. A distinct advantage of the LF-band compared to short waves is the nearly total absence of mutual interference, because of the small number of transmitters. Fading is also either nonexistent or so slow as to be harmless. Noise, on the contrary, is abundant in the LF-band, and it is both man-made and natural (from thunderstorms). Fortunately strong and steady noise sources are rare; the typical steady background noise is equivalent, in a 10 Hz bandwidth, to a field strength of 100 μ V/m in a noisy building, 30 μ V/m in a city street, and 1 μ V/m in rural areas.

Reception of the time signals is not continuous but intermittent, even in the vicinity of the transmitter. There are several reasons for this: 1) Scheduled shutdowns of the transmitters are necessary for maintenance, and accidental failures do occur. 2) Noise, man-made or natural, may temporarily obliterate the signal. 3) Beyond 3000 km a useful signal is available only at night. 4) Fading may occasionally cancel the signal at distances as short as 500 km, especially at sunrise and sunset.

The intermittent character of the received time signals was taken into account in the specifications of our ${\rm clocks}^{[2]}$: a useful signal must be present only about 10 % of the time and interruptions as long as a few days may occur.

The local time base of a synchronized clock must therefore be able to bridge an interruption of the signal during a few days and restore correct synchronization when reception of the signal is resumed.

A quartz clock without temperature control will drift by several parts in 10^5 in the worst case. This means a drift of several seconds, but <u>less</u> than 30 seconds even

during an interruption lasting several days. Thus the clock will be correctly updated if it locks itself to the nearest minute. However, it would clearly fall out of step if it were simply locked to the nearest second pulse. Its "normal" accuracy, during continuous reception, will of course be much better, say + 10 msec.

For applications where a millisecond accuracy must be preserved also during interruptions of the time signals, we must impose rather severe specifications on the local time base. Since less than one millisecond in several days means a frequency accuracy of the order of one part in 109, the local oscillator will have to be a very good quartz, with digitally memorized frequency control.

We will discuss below in more detail these two cases.

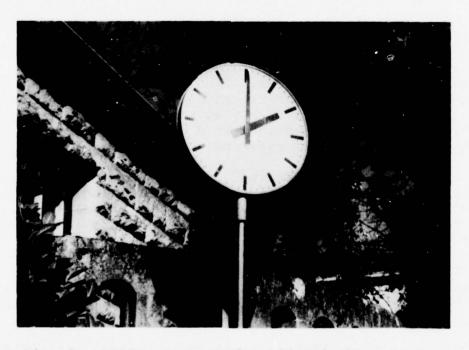


Fig. 2 : Battery operated public clock.

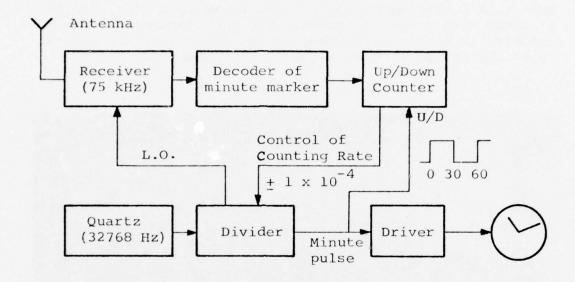


Fig. 3: Schematic diagram of public clock.

Street Clock

The first clock is for general time display to the public (figs. 2, 3). The clock has two dials with a diameter of 90 cm; its advantage is that it is completely autonomous and does not need any connecting wires from outside. It is powered by 3 type D dry cells and has an autonomy of about 3 years. The electronic part consists of one printed circuit board (fig. 4), including receiver, antenna, internal clock, and an output stage to drive the hands. The internal time base is an uncompensated quartz at the watch frequency of 32768 Hz. The receiver is designed to be as simple and compact as possible: The antenna, a ferrite rod, is followed by a preamplifier stage at 75 kHz and two IF-stages at 1272 Hz. The local oscillator frequency is derived from the time base oscillator, the tuned circuits are ferrite pot cores, the overall bandwidth is 12 Hz. The minimum field strength for correct operation is 50 µV/m, a sensitivity sufficient for HBG throughout

Europe. A better sensitivity, down to about 2 μ V/m, can be achieved with a better antenna, but the increase in cost and size is hardly warranted, as the lower limit is generally set by external noise rather than by receiver noise.

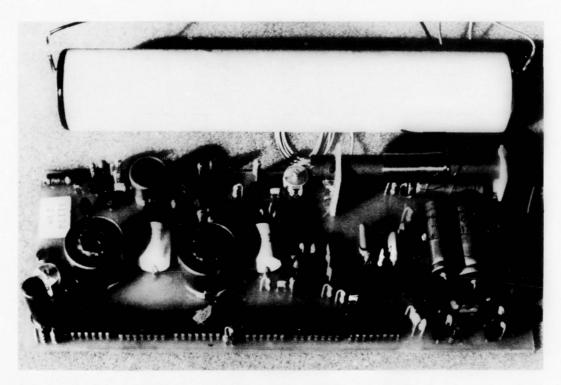


Fig. 4: Electronic module of a synchronized clock.

The envelope of the carrier is detected and the minutemarker is identified among the second pulses. The format of the minute markers is different for each transmitter.

The quartz frequency is divided down to the minute; the divider has two counting rates, one faster and one slower than the nominal by 1 part in 10⁴. If the minute pulses from the transmitter precede the minute pulse of the local time base, the divider is maintained in the fast sta-

te, and vice versa. Synchronization is thus approached at the rate of 0.36 second per hour. In the presence of noise or in the absence of the signal, spurious minute markers will be detected. To discriminate against these, the incoming minute pulses are counted in an up/down counter, up during the first half of the hour and down during the second half; at the end of the hour the sign of the resulting count is transferred to control the rate (fast or slow) of the time base divider. Since the spurious minute signals are random in time, their effect will cancel.

The power consumption of the electronic part, excluding the output stages, is 50 μA at 4 Volts. The output stages which drive the hands consume about four times more. The stepping motors which drive the minute hands or, in another model, the second hands, are conventional secondary clock movements.

The number of components has been kept as low as possible, to improve reliability and also to minimize costs. There are about 100 components, including 15 transistors and 6 C-Mos integrated circuits. The failure rate, as estimated from a sample of 300 clocks, operated during three years in different climates and environments, is 2 % per year and per clock.

The printed circuit board requires about half an hour to assemble. The low cost of this clock is apparent from the fact that the cost of the electronic module (typically \$100) is only a small part of the total hardware, i.e. casing, dials and hands.

In what respect could this public clock be improved?

First, the autonomy of 3 years can be prolonged. It is now limited by the power needed to drive the hands and by the shelf life of alcaline dry cells. The longer shelf life of lithium batteries would be an advantage, but these are not yet available at reasonable cost. The efficiency of the electromechanical motors could also be improved. Liquid crystal displays are a more remote possibility.

Second, all integrated circuits could be replaced by one single custom made chip. But, even if it becomes economical, this solution is warranted only if receiver and

antenna can also be substantially miniaturized. This is a distinct possibility which could lead to the design of small table clocks[3].

The radiated power of the LF-transmitters is now about 10 kW. One might think that increasing this power would be helpful to the users. The experience we have accumulated over several years with more than 500 clocks in several countries indicates that there was no instance where power was the limiting factor. The few cases, where signal was insufficient because of shielding by the building, were solved by placing the antenna in the vicinity of a window, but they could not have been solved by a tenfold increase in power. Increasing the power thus appears as a useless waste of energy.

Summer Time

An important option which is available with the type of clock discussed above is the automatic setting of daylight saving time. With a coded message from the HBG transmitter the clocks are advanced or retarded by exactly one hour. As the dates of the time change are not the same in different countries in Europe, each country is addressed by a different code. The code consists of 8 bits produced by lengthening to 0.2 sec the second pulses number 3 to 10 of each minute. It is repeated each minute during the night of the time change.

The decoder in the clock is made in such a way as to receive the correct message with a fair probability also in the presence of noise, but so as to make it nearly impossible for strong noise to simulate a spurious order for a time change. This system has been tested and installed successfully in several European countries.

Time Codes

Several LF-transmitters, including WWVB, transmit a time code in addition to the time signals. These time codes convey once every minute the complete information about time, date and year in a BCD format, by prolonging the

second pulses by varying amounts. These time codes are intended for the timing of events without the need for a complete clock. We contend that these time codes bring more drawbacks than advantages:

- Although a clock which is set by a time code does not need an initial setting as is required by a clock that is locked on the nearest minute marker, the former clock is much more complex and therefore less reliable than the latter. Experience shows that if the latter is set correctly when switched on, it will never fail unless a component fails, and in this case updating by a time code would not be a remedy either.
- In some cases the time code impairs the quality of the minute markers. Indeed, the format of the minute markers should have the two properties, of being easily recoverable in the presence of noise but not easily simulated by noise. The minute markers of WWVB are particularly unfavorable in this respect, due to the presence of the time code.
- A time code fills up the information channel available to the LF-transmitter. This information capacity could be used more efficiently to broadcast less redundant messages of general public interest, e.g. automatic forewarnings of storms and other emergencies for many different regions which can be addressed individually or collectively.

Clock with 100 microsecond accuracy

An accuracy of 100 µsec in a noisy environment can be obtained with an automatic receiver clock, at the cost of an approximately tenfold increase in complexity and price. Fig. 5 is a schematic diagram of one of our designs; we will not discuss it in detail but only outline its main features:

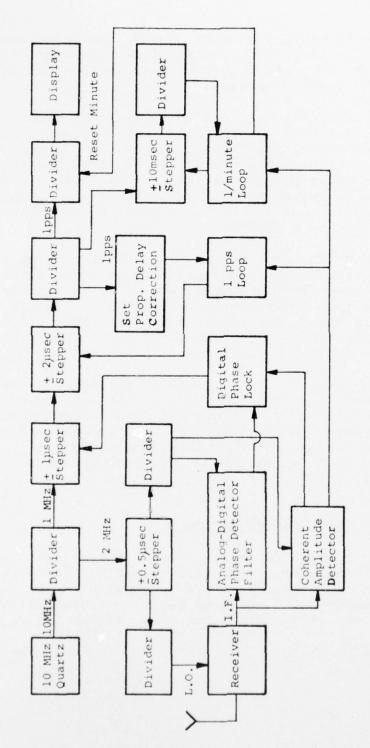


Fig. 5 : Schematic Diagram of 100 µsec Receiver Clock.

- Temperature controlled 10 MHz oscillator with aging rate less than 1 part 10^9 per day.
- Digital frequency control of the local time base, to hold the frequency during interruptions of the signal.
- Wide band receiver.
- Coherent detection of the carrier envelope.
- Separate handling of the second markers and minute markers.
- Slow correction rate of 1 part in 10^6 (1 µsec per second).

This clock has been implemented with about 60 C-Mos integrated circuits. Work is in progress to achieve the same goal by means of a microprocessor, but there are no results to report yet; the difficulty is due to the fact that C-Mos microprocessors, necessary here because of their low power drain, are not yet sufficiently sophisticated to allow a significant simplification of the clock.

Loran-C Clocks

We have also designed quartz clocks tied to the Loran-C signals (fig. 6). Since even the very best crystal oscillators will not hold the correct cycle of 100 kHz during an interruption of the transmitter, our clocks contain two quartz oscillators, each locked to a different Loran-C station. If one station goes off, the corresponding oscillator locks to the other oscillator. Since simultaneous failures of two Loran-C stations are extremely unlikely, the resulting clock is very reliable. Its low power consumption (0.5W), low cost and submicrosecond accuracy cannot be matched by any commercial atomic clock.

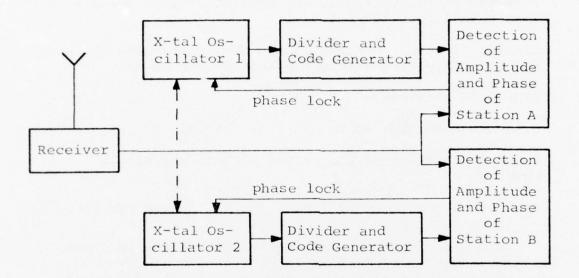


Fig. 6: Schematic Diagram of Loran-C clock tied to two different Loran-C stations.

References

- 1) Bureau International de l'Heure, Observatoire de Paris.
- 2) J. Bonanomí et P. Schumacher, La Suisse Horlogère No. 11, March 1976.
- 3) J. Fellrath, Suisse Horlogère et Revue Internationale de l'Horlogerie, No. 1, March 1969.

IMPROVED TIME REFERENCE DISTRIBUTION FOR A SYNCHRONOUS DIGITAL COMMUNICATIONS NETWORK

Harris A. Stover Defense Communications Engineering Center

ABSTRACT

A Time Reference Distribution Technique for synchronizing a digital communications network has been previously described. In that technique, time reference information from the highest ranking node in the network was supplied to all other major nodes over the best available path to each one, and provision was made for reorganizing the network to accommodate failures. By referencing the highest ranking node to a time standard such as UTC, that standard of time is made available at all major nodes with an accuracy dependent on the time transfer capabilities of the transmission paths. However, that technique fails to apply much of the information that could be used to provide a more accurate and stable (low phase fluctuation) system.

The improved Time Reference Distribution Technique described here also selects the highest ranking clock as master. In it, the natural hierarchy determined by the network connectivity is employed; instead of only supplying timing information over the best path to each node, the nodes determine the error in their local clocks either by using information from all neighboring (directly connected) nodes higher in the hierarchy than the local node or by using information from all neighboring nodes not lower in the hierarchy. To do this, information is exchanged between neighboring nodes and there are a set of procedures or rules for applying this information. These are presented and discussed.

Introduction

Digital communications have been growing at a very rapid rate and are being more widely applied. Switched digital communications networks in which the signals remain in digital form throughout the network are being developed. The problem of synchronizing such a network is much more complex than the synchronization of individual point-topoint digital communications systems. In digital point-to-point communications, it is only necessary that the receiver be correctly synchronized to the received bit stream and there is no need to synchronize the transmitters. In a network employing time division multiplexers and/or time division switches, each bit must be available at the multiplexer at the correct time to fill its assigned time slot in the interleaved bit stream. Since the bits to be interleaved at a time division multiplexer or switch originate at many locations throughout the network, it is important that their sources be adequately synchronized. Variable storage buffers can be placed in all received bit streams to act as reservoirs in which the bits are temporarily stored until they are needed. These buffers can accommodate variations in the transit time of the signal from one node to another and also small errors in the nodal clocks. However, it is preferable to use only a small portion of the available buffer capacity in normal operations and reserve most of its capacity for contingency situations. One suggested method of providing the desired transmitter synchronization is to distribute an accurate time reference through the network to all of its nodes [1, 2, 3, 4].

A switched digital communications network is normally made up of duplex (transmission in both directions simultaneously) digital transmission links which interconnect the nodes of the network. These duplex transmission links employ synchronization codes to allow the receivers to be easily synchronized to the received signals. The codes are chosen so as to be unlikely to occur as a part of the data sequence. This can be accomplished either by selection of unique patterns or by transmitting the synchronization code with a greater regularity than it would randomly occur. Since synchronization of the receiver for each individual transmission link to its received signal is required, such a network has a natural basis for the distribution of a time reference. Each node can use its local clock to control the time of transmission of the synchronization code from the local node. It can use the same local clock to measure the time of reception of the synchronization code from the other end of the transmission link. If the nodes at the two ends of the link exchange these measurements, they both can determine the difference between the two clocks with the effects of the signal transit time removed (except for usually small asymmetry in the two directions of transmission and instrumentation errors) [1, 2, 3, 4]. This is accomplished by simply subtracting one measurement from the other and dividing by two. This time comparison of clocks at neighboring nodes can be used to pass a time reference from the master to other nodes of the network.

A number of advantages for using an accurate time reference for synchronizing a digital communications network are given in references [1, 4].

Desirable Characteristics for a Digital Communications Timing Subsystem

Quite a large number of desirable characteristics can be listed for the timing subsystem of a large digital communications network [4]. Although it cannot be proved that these characteristics are necessary, many of them are widely accepted as desirable. These include: (1) Any node should be able to obtain all required timing information from its neighbors (directly connected nodes) without need to communicate with more distant nodes; (2) The timing subsystem should accommodate failures or destruction of major parts of the network and still remain operational; (3) Timing perturbations at a node should not propagate to other parts of the network (i.e., when one node makes a correction or other change in its clock, it is not desirable for this to propagate through the network like falling dominoes); (4) There should be no closed timing loop that could potentially contribute to system instability; (5) The timing subsystem should permit systematic selfmonitoring to provide early detection of malfunctions so that they can be corrected before they interrupt communications traffic; (6) The communications timing subsystem should be compatible with other timing subsystems such as those employed for navigation; and (7) The timing subsystem should be self-organizing, initially and following failures.

A time reference distribution technique for a digital communications network as described earlier [1] provided these desirable characteristics, but did not consider one other important characteristic. An error in a clock at any level of the timing hierarchy should not affect the measurement of the clock error at any node lower in the hierarchy. Further, the selection of the paths for distribution of the time reference and the measurement of the error in the local clock should be independent of the correction of the errors in any of the other nodal clocks. This permits error correction in any clock to be made with minimum perturbations of the network while still not interfering with the accurate measurement of the error in any other clock. This can be accomplished very simply by having each node in the network inform its neighbors of the measured but uncorrected error in its own clock [2].

Distribution of the Time Reference Through the Network

Figure 1 will be used as an example digital communications network for the discussion of time reference distribution through the network.

The internodal connections of this example network, as shown by the straight lines, represent one third of the total possible internodal connections for a 12 node network. If any single node of such a network is selected as the master for the entire network, for timing purposes, the internodal links of the network cause the nodes of the network to fall into a natural hierarchy with the selected master at the highest level of the hierarchy. The second level of the hierarchy comprises all nodes connected to the master; the third level consists of all nodes connected to the second level but not to a level higher than second; etc. Figure 2 shows this hierarchy for the network of Figure 1 when node A is selected as the master, while Figure 3 shows the hierarchy when node E is chosen as the master.

In the time reference distribution technique described in earlier papers [1, 2, 3, 4], a simple set of rules was employed at each node. Some of these rules were used to determine the relative error in the clocks at neighboring nodes. Other rules were employed to establish the best paths to the master from each node. The rules used to establish the best paths were essentially the rules described by Darwin and Prim [5] for self-organizing master-slave timing systems. In order to apply these rules, each node is assigned a unique rank to be used in determining the order of succession to master and to help resolve ambiguities that could occur. Each transmission link is assigned a demerit value and each node chooses to receive its time reference through the particular neighbor that will provide the lowest demerit path between the local node and the master. When the numbers next to the individual links of Figures 2 and 3 are used to represent the demerit values for the individual transmission links, the best (lowest demerit) path from each node to the master is shown by the dashed lines in these figures.

It is obvious that for many nodes there are a large number of possible paths between that particular node and the master. In Figure 2, paths from the master to node I for which there is no backtracking through levels of the hierarchy include: ACI, ADI, AFI, AECI, AFCI, ABDI, ACFI, AEJI, AFJI, ACEJI, ACFJI, ABGJI, AFCEJI, AECFJI, and ADBGJI. By combining timing information passed over these various paths, it is possible to provide greater timing accuracy. Also, the network does not have to be reorganized following some types of failure that would require reorganization if only the best path to each node were used for the time reference distribution. However, for effective use of this information from many different paths a set of rules or procedures is needed.

Each transmission link used for a time reference transfer within the network will introduce some error in the comparison of clocks at the two ends of the link. For a large number of links of a given type, these errors in the comparison of the clocks can be assumed to be

random with a mean value of zero. Therefore, the inaccuracy of a link can be characterized by the standard deviation (or variance) of the expected error. (Inaccuracy as used here refers to the inaccuracy, or error, of a clock error measurement.) Figure 4 illustrates a tandem connection of five links. Since the error (in the measured difference between two clocks) associated with each of these links (in other parts of the text these errors are referred to as inaccuracies of clock error measurements) is assumed to come from a random distribution with zero mean, the errors (inaccuracies) statistically add as the square root of the sum of the squares. Therefore the error for the tandem connection can be characterized as equation (1), where the E's represent the standard deviations and ${\sf E}^2$ is a variance.

$$E_{AF} = E_{AB}^{2} + E_{BC}^{2} + E_{CD}^{2} + E_{EF}^{2}$$
 (1)

Figure 5 illustrates two nodes connected by two paths in parallel. In this case, we would expect a combined accuracy that would be statistically better (based on more samples) than that of either path by itself. Let the measurement made over the first of the two paths be $M_1 = V + E_1$, where V is the true value and E_1 is the error introduced by the first path. Similarly, let the measurement over the second path be $M_2 = V + E_2$. It is desirable to weight and combine these two measurements in such a way as to obtain the statistically most accurate measurement. See equation (2).

$$M_{AB} = W_1 M_1 + W_2 M_2 = W_1 (V+E_1) + W_2 (V+E_2)$$
 (2)

The weighting factors W_1 and W_2 apply to both the true values and the errors. Although the weighted true values add linearly, the weighted error values (being random) add as the square root of the sum of the squares, so that:

$$M_{AB} = (W_1 + W_2) V + \sqrt{W_1^2 E_1^2 + W_2^2 E_2^2}$$
 (3)

Since it is desired that the combined result M_{AB} be the true value with a statistically minimum error, W_1 plus W_2 must be equal to 1, and the expression under the radical sign must be made minimum by the selection of W_1 and W_2 . Substituting (1- W_1) for W_2 in (3) and finding the value of W_1 that minimizes the statistical error gives (4), and subtracting this value of W_1 from 1 gives W_2 as shown in (5).

$$W_1 = \frac{E_2^2}{E_1^2 + E_2^2} \tag{4}$$

$$W_2 = \frac{E_1^2}{E_1^2 + E_2^2} \tag{5}$$

Putting these weighting factors in (2) gives (6):

$$M_{AB} = \frac{\frac{M_1}{E_1^2} + \frac{M_2}{E_2^2}}{\frac{1}{E_1^2} + \frac{1}{E_2^2}}$$
(6)

By using this combined value as given by (6) as one member of a new parallel pair, computing a new combined value, and repeating this procedure until the total number of parallel paths are included, the desired weighting factor for the measurement from the path p of n parallel paths can be written as (7).

$$W_{p} = \frac{\frac{1}{E_{p}^{2}}}{\frac{1}{E_{i}^{2}}}$$

$$(7)$$

The resulting statistical error for the combined measurement based on n parallel paths as found by substituting the weighting factors of (7) into (3) is given by (8).

$$E_{c} = \frac{1}{\sum_{i=1}^{n} \frac{1}{E_{i}^{2}}}$$

$$(8)$$

The information of equations (1) through (8) can be applied in combining timing information passed over several different paths. This will improve the timing accuracy at some nodes of the network, but the application of the information should follow a suitable set of rules.

Rules for Time Reference Distribution Via Multiple Paths

Some basic considerations that influence the choice of timing information to be transferred within the network and the selection of a particular set of rules for using this information will be discussed prior to the presentation of a suitable set of rules.

Rather than transferring all timing information to a single location where a common processor can be used for all timing information from all nodes, it is much simpler and more reliable if each node of the network can receive all required timing information from its neighbors (directly connected nodes) and use this information in a rather simple local processor (microprocessor). In a network employing a centralized processor, the common processor becomes a point of high vulnerability that reduces network reliability and survivability; and the efficiency of utilization of transmission facilities is reduced because of the large amount of information that must be transferred to and from the central processor in order to serve nodes throughout the network. Therefore, it is desirable that all timing information required by any node either be stored at that node or be supplied by its neighbors without any need for any node to communicate with nodes more distant than its own neighbors.

Consider combining timing information at node B of Figure 6 that comes over the paths AB and ACB. If this combined measurement at node B is then used to determine a combined timing measurement at node C, this new node C measurement could then be used to determine a new combined measurement at node B which could be used to determine a new one at C, etc. The resulting iterative process would change the timing at nodes B and C over a large number of iterations without introducing any new measurements from node A. The passing of information back and forth between nodes B and C cannot improve its accuracy, but could possibly introduce additional error due to the link BC each time the link is traversed. It is desirable to provide rules that will make effective use of combined timing information from multiple paths while preventing such iterations. These iterations can be avoided if each node is prevented from using timing information that has been previously influenced by that same node. To accomplish this and still make effective use of timing information over many multiple paths, two classes of timing information can be maintained at each node. Class 1 timing information (clock error measurements and inaccuracy

values for those measurements) is based only on information received from nodes higher in the hierarchy than the local node, while Class 2 timing information is based on information received from all nodes not lower in the hierarchy (those at the same level in addition to those higher). If only Class 1 information is used, there will be no closed feedback paths, but useful information from other nodes at the same level in the hierarchy will not be used in determining the clock errors. If, when deriving Class 2 timing information a node uses Class 2 information from other nodes higher in the hierarchy but is restricted to only Class 1 information from nodes at the same level in the hierarchy, the closed paths will still be avoided and the undesirable iterations will be avoided. Some of the other considerations in selecting the particular system were listed in a previous section.

In order to provide an effective self-organizing method of accurately distributing a time reference through a digital communications network, information is exchanged between neighboring nodes. This information is applied in compliance with a set of rules. These rules are discussed in the text after the following list of information which is transmitted by each node to its neighbors:

- INFO 1. Rank of the clock used as the master time reference for the local clock. (This information is used to assure that the highest ranking clock in the network is used as master and to establish the order of precedence to master when a master fails.)
- INFO 2. Number of links between the local node and its master time reference. (This information is used to establish the desired hierarchy.) ("Local node" is used in this discussion as a particular node under discussion which transmits information to its neighbors and receives information from them.)
- INFO 3. Time of the clock at the remote end of the link (including the effect of the time required for the signal to transit from the remote node to the local node) as measured by the clock at the local node. (This information is used to determine the difference between the clocks at the two ends of the link with the signal transit time removed from the comparison.)
- INFO 4A. Measured but uncorrected error in the local clock based on information from those neighbors higher in the timing hierarchy than the local node. (The term measured error as used here includes errors obtained by mathematically

combining other measurements and the error in this measured error will be called its inaccuracy.) (The resulting Class 1 error information is passed to all neighbors not lower in the timing hierarchy than the local node and can be used by neighbors at the same level to determine their Class 2 errors, or by nodes at higher levels to aid in system monitoring.)

- INFO 4B. Same as 4A, except based on information from those neighbors not lower in the hierarchy than the local node (Class 1 information from the same level and Class 2 from higher levels). (The resulting Class 2 error information is passed to all neighbors lower in the hierarchy than the local node for use in determining their Class 1 errors.)
- INFO 5A. Estimated inaccuracy, stated as a variance (or standard deviation), of the local clock based on information from all neighboring nodes higher in the hierarchy than the local node. (The resulting Class l information is passed to all neighbors not lower in the timing hierarchy than the local node, and it can be used by neighbors at the same level to determine weighting factors (see discussion of equation 7) for combining INFO 4B information from their neighbors into a Class 2 measured error.)
- INFO 5B. Same as 5A except based on information from all neighbors not lower in the timing hierarchy than the local node. (This resulting Class 2 information is passed to all neighbors lower in the timing hierarchy than the local node for use in determining weighting factors (see discussion of equation 7) for combining INFO 4A information into a Class 1 measured error.)

Notice that the two classes of information under item 4 and the two classes of information under item 5 are distinguished by the sources of information used to obtain them and also by the nodes that make use of them. When the rules for their use are also considered, it will be observed that they prevent the formation of the closed feedback paths.

Each node applies the following set of rules for the use of the information received from its neighbors.

Rule 1 A node initially entering the network will use its own clock as its time reference until a better reference can be deter-

mined. Its own clock provides a basic time reference to which the node always returns when it has no better reference available. Under these conditions, the local node supplies the rank of its own clock to its neighbors as INFO 1.

RULE 2 The first type of information received from neighboring nodes, INFO 1, provides the local node with the rank of the clock used as the master time reference by each of its neighbors. If one or more neighbors' reference clocks outrank the local clock, the node will select those neighbors (or the single neighbor) referencing the highest ranking master and use them (or it) in determining its own time reference, i.e., measuring the error in its own clock. The rank of the master time reference used by the selected neighbors will be supplied to all neighbors as INFO 1, i.e., the rank of the clock used as master for the local node. Continued application of this rule by all nodes will result in all nodes referencing the same highest ranking master clock.

RULE 3 If the local node is referencing its own clock there are no links between the local node and its master reference and this information is supplied to its neighbors as INFO 2. The second type of information, INFO 2, as received from its neighbors provides the local node with information about the number of links between each neighboring node and that neighbor's master time reference. Unless the clock at the local node outranks the master reference of all of its neighbors, the number of links between the local node and the master is greater by one than that of the neighbors (or neighbor) selected by rule 2 which have the least number of links between themselves and their master. This information is supplied to the neighboring nodes as INFO 2. Continued application of this rule will result in establishing the desired natural hierarchy such as shown in Figures 2 and 3. INFO 2 information as transmitted to neighboring nodes and as received from them indicates the position in the hierarchy of the local node relative to each of its neighbors.

RULE 4 The third type of information, INFO 3, as received from neighboring nodes provides the local node with the time difference between the local clock and the clock at each neighboring node (including the signal transit time from the local node to the neighboring node.) INFO 3 as transmitted to the corresponding neighboring node is subtracted from this information, and the difference is divided by 2. This provides a measurement of the actual time difference (no transit time included) between the local clock and the clock at each neighboring node [1, 2, 3, 4].

RULE 5 Each neighboring node <u>not</u> higher in the hierarchy than the <u>local</u> node transmits to the <u>local</u> node, as INFO 4A, the Class I measured but uncorrected error of its own clock, i.e., the error

determined using information from that neighbor's neighbors that are higher in the hierarchy than the neighbor. Similarly, each neighbor higher in the hierarchy than the local node transmits to the local node, as INFO 4B, the Class 2 measured but uncorrected error in its own clock, i.e., the error determined using information from that neighbor's neighbors that are not lower in the hierarchy than the neighbor. As received, this information gives a measured but uncorrected error for each neighboring node. To this is added the difference between the local clock and each neighboring clock as determined by rule 4. The result is a set of error measurements for the local clock based on information from each of its neighbors. (The reason for using Class 1 information from some neighbors and Class 2 information from others is to avoid closed feedback paths while still making very effective use of the available information.)

Rule 6 Each neighboring node not higher in the hierarchy than the local node transmits to the local node, as INFO 5A, the estimated inaccuracy, stated as a variance (or standard deviation), of its Class I measured error. Similarly, each neighboring node higher in the hierarchy than the local node transmits to the local node, as INFO 5B, the estimated inaccuracy, stated as a variance (or standard deviation), of its Class 2 measured error. This information, as received, is the estimated inaccuracy of the measured but uncorrected error associated with each neighboring node. Add to each member of this set of information (directly if stated as variances or as the square root of the sum of the squares if stated as standard deviations) the estimated inaccuracy of the link between each neighbor and the local node as determined during engineering design. The result is a set of inaccuracies for the set of measured errors in the local clock based on information from each neighbor.

The estimated inaccuracy attributed to the link between the local node and a neighbor as established during engineering design includes several parameters. It includes an effect due to the differences in signal transit time in the two directions of the duplex link which includes delay differences in the transmitters and receivers at the two ends of the link. It also includes inaccuracies in the equipment used to measure timing differences between the received signal and the local clock.

Rule 7 From the set of error measurements for the local clock as determined by rule 5, and the associated inaccuracies determined by rule 6, only those for neighbors higher in the timing hierarchy than the local node are selected. These error measurements are combined according to equation (6) to determine a Class of the error in the local clock, i.e., one based on neighbor in the hierarchy than the local node. This is supplied

NATIONAL AERONAUTICS AND SPACE ADMINISTRATION GREENB--ETC F/G 14/2 PROCEEDINGS OF THE ANNUAL PRECISE TIME AND TIME INTERVAL (PTT1)--ETC(U) AD-A043 856 1977 UNCLASSIFIED NASA-6SFC-X-814-77-149 NL 3 0 8 AD A043856 8 -磁 the measured error in the local clock, to all neighbors \underline{not} lower in the timing hierarchy than the local clock.

Rule 8 From the set of inaccuracies determined by rule 6 only those for neighboring nodes higher in the hierarchy than the local node are selected. These are combined according to equation (7) to determine the inaccuracy for the measured error in the local clock based on information from neighbors higher in the hierarchy than the local node. This information is supplied as INFO 5A to all neighbors not lower in the timing hierarchy than the local node.

Rule 9 From the set of error measurements for the local clock as determined by rule 5 and the associated inaccuracies determined from rule 6, all those for neighbors not lower in the hierarchy than the local node are selected. These error measurements are combined according to equation (6) to determine a Class 2 measurement of the error in the local clock, i.e., one based on all those neighbors not lower in the timing hierarchy than the local node. This is supplied as INFO 4B, the measured error in the local clock, to all neighbors lower in the timing hierarchy than the local clock.

Rule 10 From the set of inaccuracies determined by rule 6 all those for neighbors not lower in the timing hierarchy than the local node are selected. These inaccuracies are combined according to equation (7) to determine the inaccuracy for the measured error in the local clock based on information from all those neighbors not lower in the timing hierarchy than the local node. This inaccuracy information is provided as INFO 5B to all neighbors lower in the timing hierarchy than the local node.

The combining of information over several different paths, in addition to providing more accurate time measurements at many nodes remote from the master, reducing the need for massive reorganization of the network following some failures as required when using only the best path, also provides the possibility for quantitative evaluation of the fitness of the timing subsystem. Since each time error measurement (the term measurement as used here includes the mathematical combination of measurement information from different sources) has a corresponding estimated inaccuracy, these time error measurements and their corresponding inaccuracy estimates can be used to provide a quantitative alarm system. This leads to rule 11.

Rule 11 Rule 5 provides a set of error measurements for the local clock based on information from each neighboring node. Rule 6 provides a corresponding set of inaccuracies for these error measurements. Rule 9 provides a combined measurement for the error in the local clock. Rule 10 provides a corresponding inaccuracy for the

combined measurement. The combined measurement as determined by rule 9 is subtracted from each member of the set of error measurements determined by rule 5. The resulting set gives the difference between each individual measurement and the combined measurement. The inaccuracy (stated as a variance) determined by rule 10 is added to each member of the set of inaccuracies obtained by rule 6 (also stated as a variance) and the square root of each member of this set is taken to obtain a set of estimates of the standard deviations of the clock error measurements based on information from each neighbor relative to the combined clock error measurement. Each member of the set of differences between individual measurements and the combined measurement is divided by the estimate of the corresponding standard deviation to obtain a normalized set of ratios. The lowest level alarm could be activated when the ratio reaches 2. This would not be very significant because this ratio would have approximately a 5% probability of occurrence in a normally operating system. A second level alarm when the ratio reaches 3 should be quite significant since its probability of occurrence in a normally operating system should be only about 0.3%. A third level alarm when the ratio reaches 4 should initiate some form of a problem investigation since its probability in a normally operating system should be less than 0.01%. A fourth level alarm when the ratio reaches 5 should initiate definite corrective action since its probability in a normally operating system might be expected to be less than one in a million.

There are also other capabilities for checking for an erroneous information exchange. For example, the node serving as master should reference its own clock and inform its neighbors that there are zero nodes between itself and its master. Every node connected directly to the master should inform its neighbors that it has one link between itself and its master. If any neighboring node tells the master that there is other than one link between itself and the master, the master can interpret this as detection of a problem. For every node in a stabilized operating system, either each neighboring node should be reporting the same number of links between itself and the master as the local node, or it should be reporting one more or one less than the local node. Any node receiving a report from one of its neighbors that the neighbor's distance from the master differs by more than one from the local node's distance from the master has detected a problem that should either cause reorganization of the network or other corrective action.

The procedure presented here for providing a very good time reference distribution through a digital communications network is based on an assumption that the different paths passing the time reference between two nodes are independent, i.e., do not share any of the same transmission links. Although this independence does not always exist, the degradation due to the dependencies that do exist should generally be

acceptable. It is this assumption of independence that makes it possible to provide an accurate time reference distribution through the network by the application of simple procedures and calculations at each node using only simple information from neighboring nodes. In order to allow fully for dependent paths through the network, it would be necessary to keep a record of all dependent paths and make the necessary information available at every location where a calculation involving a particular dependent path is made. This would impose a very great increase in both communications and computation support to the timing subsystem. Because of the extensive increase in computation and communications required to permit full consideration of dependent paths, it is recommended that the independence assumption be made and that the simple procedures described above be applied to obtain improvements over time reference distribution via only the best path. The assumption of independent paths will indicate an apparent accuracy which is somewhat greater than the actual accuracy. The actual accuracy will usually lie somewhere between the accuracy obtained using only the best path and the accuracy indicated by using the above rules. One method of partially compensating for the effect of dependent paths might be to select a typical network arrangement using typical link inaccuracies, calculate the inaccuracy at each node by the above rules and also calculate it taking dependent paths into consideration. The average difference between the two methods could be determined for each level in the hierarchy and stored at every node. Then this average value for the local node's level in the hierarchy could be added to the value obtained using the set of rules above. The result might be expected to be statistically more accurate than just accepting the value using the assumption of path independence with no attempt to compensate.

Table I shows the inaccuracies, expressed as variances, for the measurement of the local clock errors for each node of Figure 1 when node A is the master as shown in Figure 2. Table II shows the inaccuracies when node E is the master as shown in Figure 3. These evaluations were obtained using the link inaccuracies (expressed as variances) shown in Figures 2 and 3 by applying the rules given above. The application of the rules requires that the Class 1 inaccuracy at a node is obtained from the Class 2 inaccuracies of nodes higher in the hierarchy than the local node while the Class 2 inaccuracy at a node is obtained by combining the Class 2 inaccuracies of neighboring nodes higher in the hierarchy than the local node with the Class 1 inaccuracies of neighbors at the same level in the hierarchy as the local node. In each case the local clock error measurement with Class 2 inaccuracy is available for use at the local node. As observed from the tables, the local clock error measurement with Class 2 inaccuracy is nearly always more accurate than that obtained using the best path. Because dependent paths were not taken into consideration the actual inaccuracy is probably between these two.

TABLE I. ERROR ESTIMATES FOR NETWORK OF FIGURE 2

<u>No de</u>	Error Estimate for Time Reference Via Best Path	Class 1 Error Estimate	Class 2 Error <u>Estimate</u>
Α	0	0.000	0.000
В	2	2.000	1.333
С	1	1.000	0.652
D	2	2.000	1.333
Ε	1	1.000	0.833
F	1	1.000	0.750
G	3	1.645	1.243
Н	2	1.833	1.833
I	3	0.931	0.647
J	2	1.082	0.618
K	3	1.699	1.123
L	4	3.243	1.473

TABLE II. ERROR ESTIMATES FOR NETWORK OF FIGURE 3

Node	Error Estimate for Time Reference Via Best Path	Class 1 Error Estimate	Class 2 Error Estimate
Α	1	1.000	0.833
В	3	2.833	1.326
С	2	4.000	1.333
D	3	2.833	1.086
E	0	0.000	0.000
F	2	0.848	0.693
G	4	2.143	1.193
Н	1	1.000	1.000
I	3	1.773	0.850
J	2	2.000	2.000
K	2	2.000	1.440
L	3	1.383	1.383

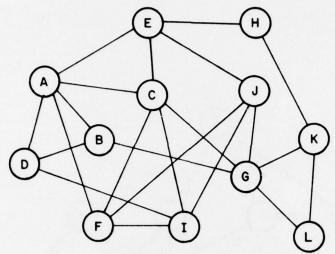
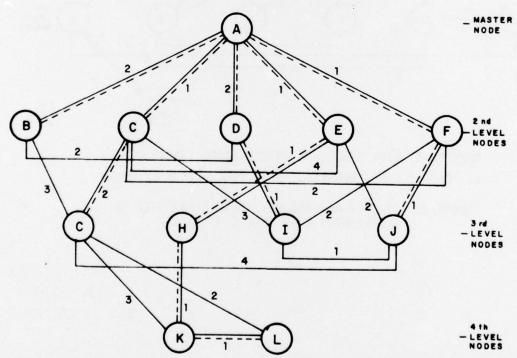
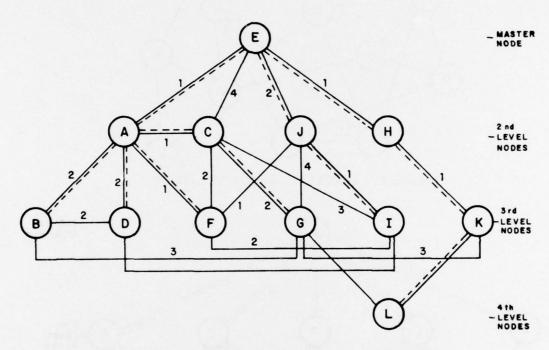


FIGURE 1. EXAMPLE OF A 12 NODE NETWORK



NUMBERS BY LINK LINES ARE INACCURACIES (VARIANCES)
---- DASHED LINES REPRESENT BEST TIME REFERENCE PATHS
FIGURE 2. EXAMPLE NETWORK OF FIGURE 1 ARRANGED IN
A HIERARCHY WITH NODE A AS MASTER



NUMBERS BY LINK LINES ARE INACCURACIES (VARIANCES)
---- DASHED LINES REPRESENT BEST TIME REFERENCE PATHS

FIGURE 3. EXAMPLE NETWORK OF FIGURE 1 ARRANGED IN A HIERARCHY WITH NODE E AS MASTER

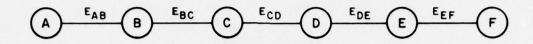


FIGURE 4. TANDEM LINK EXAMPLE

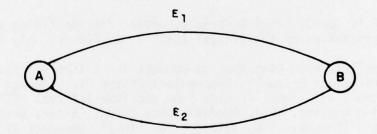


FIGURE 5. PARALLEL LINK EXAMPLE

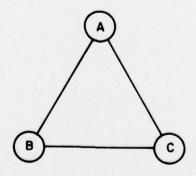


FIGURE 6. EXAMPLE THREE NODE NETWORK

ACKNOWLE DGEMENT

The author wants to thank Dr. Eugene P. Kaiser, Mr. Allen C. Trainer, and Mr. Franklin R. Wiesman for their editorial suggestions, and Mrs. Anita J. Hughes for preparing the manuscript.

REFERENCES

- DCASEF TC 39-73, "Time Reference Concept for the Timing and Synchronization of the Digital DCS", H. A. Stover, July 1973.
- "A Time Reference Distribution Concept for a Time Division Communications Network", Proceedings of the Fifth Annual NASA Department of Defense Precise Time and Time Interval (PTTI) Planning Meeting, NASA, Goddard Space Flight Center, Greenbelt, Maryland (December 4-6, 1973), H. A. Stover, December 1973.
- "Coordinated Universal Time (UTC) As A Timing Basis for A Digital Communications Network", H. A. Stover, EASCON 1974 Record.
- 4. DCEC TR 43-75, AD-A021934, "Communications Network Timing", H. A. Stover.
- 5. "Synchronization in a System of Interconnected Units," Darwin and Prim, U.S. Patent No. 2,986,723, May 30, 1961.

A MICROPROCESSOR DATA LOGGING SYSTEM FOR UTILIZING TV AS A TIME-FREQUENCY TRANSFER STANDARD

D. D. Davis
National Bureau of Standards
Boulder, Colorado

ABSTRACT

The TV network color subcarriers have been used for several years as frequency transfer standards. Additionally, a time transfer method using TV line-10 is presently used for maintaining clock synchronization at the microsecond level. This paper describes an NBS-developed microprocessor data logging system that automates both functions in a relatively inexpensive package.

Three of these systems are in routine use to collect the color subcarrier and line-10 data published in the NBS Time and Frequency Services Builetin. Two additional systems are used to monitor the station clocks of WWV/WWVB and the GOES satellite clock at Wallops Island, Virginia.

BACKGROUND

NBS has developed several techniques that allow time and frequency users to calibrate an oscillator using the TV network color subcarriers as transfer standards [1,2]. These techniques take advantage of the fact that the TV networks use 5 MHz rubidium or cesium standards and synthesize the color subcarrier by using the ratio:

$$3.57954545...MHz = \frac{63}{88} \times 5 MHz$$

User equipment starts with 10, 5, 2.5, or 1 MHz and synthesizes 3.579545...MHz by using the 63/88 ratio. The locally generated 3.58 MHz may then be phase compared with the color subcarrier from a TV receiver using one of several techniques. The least expensive technique uses a colored vertical bar on the TV screen as a phase indicator. Since the TV networks' rubidium standards are offset by approximately -3 x 10^{-8} (30ns/sec), the user must adjust his oscillator until the indicated phase changes 360° in about 9.3 seconds. A calibration accuracy of 1 x 10^{-9} can usually be achieved in a few minutes, limited primarily by the user's ability to accurately time the phase changes.

More expensive digital calibrators measure this "9-second" beat note period and compute and display this offset on the TV screen. The standard deviation of 15-minute averages is typically less than 2×10^{-11} .

In order to provide user traceability to NBS, we measure the frequency offsets of the six primary network standards (three in New York and three in Los Angeles). The microprocessor data logging systems were developed to provide the capability of continuous averaging of the color subcarrier offsets on up to four channels. A "line-10" time transfer capability was originally included to allow calibration of the reference used with the processor on Lookout Mountain (overlooking Denver). Later, we switched all published line-10 measurements to Lookout (where continuous network microwave feeds are available) because one of the local network stations went to all tape delay.

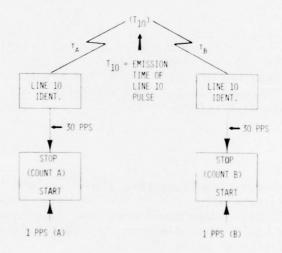


Fig. 1-The TV line-10 time transfer technique

The "line-10" time transfer technique is illustrated in figure 1. Two cooperating locations are in common view of a TV station or network. Both locations start their time interval counters at an agreed-upon second, and the counters are stopped by the common TV signal, within 1/30 second. The difference of the counter readings defines the relationship between the 1 pps signals.

COUNT A = 1 PPS(A) -
$$(t_a + T_{10})$$

COUNT B = 1 PPS(B) - $(t_b + T_{10})$

COUNT A - COUNT B = 1 PPS(A) - 1 PPS(B) - $t_a + t_b$

CLOCK DIFFERENCE PROPAGATION PATH DIFFERENCES

The counter difference includes the propagation path difference between the locations and the T_{10} source; so for absolute measurements, the path must be calibrated-most practically with a portable clock. If the line-10 technique is to be used only to measure rate differences of (A) and (B), absolute measurements are not required. All that is necessary is to determine the counter differences on successive days or weeks to determine the relative rates of the two clocks.

LOGGING SYSTEM FUNCTIONS

The logging system performs two basic functions: It averages 3.58 MHz fractional frequency offset data and it measures line-10 time difference readings. These functions are illustrated in figure 2 and described below.

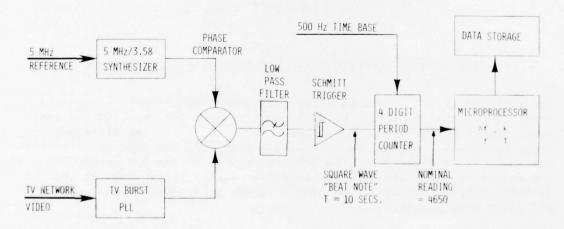


Fig. 2-Block diagram, 3,58 MHz fractional frequency measurements

3.58 FRACTIONAL FREQUENCY OFFSET MEASUREMENTS

The fractional frequency offsets of the network color subcarriers are measured using the "beat note" method. Network video is applied to a

phase-locked loop to regenerate the 3.58 MHz from burst. The regenerated network 3.58 MHz and a locally synthesized 3.58 MHz are applied to a balanced mixer phase comparator. The resultant beat note is processed through a low-pass filter and Schmitt trigger to recover a square wave of the beat note. The beat note period (nominal 10 seconds) is measured by a 4-digit counter. Each time a 10-second measurement cycle is completed, the processor converts the time measurement "T" into an offset value by dividing "T" into a constant. For the 500-Hz time base used, the constant required is 1396825. The resultant frequency offset (6 digits) is checked for validity. The microprocessor checks the validity as follows:

Each network has a "screen word" stored in memory. When the processor services a channel, it fetches the screen word for testing the validity of the measured offset. The format of the screen word, stored in random access memory, is:

101 x 10 12 DIFFERENCE IS LESS THAN "IP" - ACCEPT DATA

For each "10-second" measured offset, the measured value is subtracted from the expected offset. The difference between the measured and expected value is then compared to the "1 P" window. If the difference is less than the 1 P window (in this case 2 x 10^{-10}), the data is accepted-otherwise it is discarded. The primary purpose of the 1 P screening process is to eliminate outliers caused by sudden phase jumps of the 3.58-MHz network signals. The window is set to accept at least 98% of all valid data points.

Two additional screening processes for "10 P" and half-hour averaged data are used to eliminate any data that may originate from other than the network primary rubidium standard. The final half-hour screening operation only accepts data that is within \pm 1.9 x 10-11 of the expected value. The entire screen word may be changed by keyboard entry to accommodate different expected offsets and frequency stabilities.

The processor accumulates one-half hour averages throughout a full 24 hours. At midnight, the processor computes the daily offset average for each network and stores this average, along with the count of one-half hour samples used to arrive at the daily average. The expected offsets in the screen words are also compared with the actual daily averages and the screens are either incremented or decremented by 1×10^{-12} -unless less than 10 half-hour samples were accumulated for the day, in which case the screens are not changed.

Up to 32 days of daily averages for four channels are stored in a "wrap-around" memory for recall by keyboard command. A printout of the Lookout Mountain data for eight days is shown.

		rHA	LF HOUR
	YEAR	DAY	MINUTE
CLOCK - TIME OF PRINTOUT:	1976000	1-0 0 3 1 3 3 1	2 7
	ABCE	CBSE	NBCE
TODAY'S VALUES:	29-2999.70	26-2998.55	28-3022.54
YESTERDAY:	47-2999.82	34-2998.60	46-3022.77
	45-2999.79	47-2998.70	46-3022.53
	45-2999.71	42-2998.86	43-3022.68
	45-2999.97	42-2998.90	43-3922.66
	44-3000.27*	45-2998.69	40-3022.79
	37-3000.30	40-2998.50	38-3022.39
	48-3000.10	47-2998.73	43-3022.56
OLDEST DATA:	45-2999.97	32-2998.94	35-3022.54
		OFFSET	x 10 ⁻¹¹
		NUMBER OF HAL	F-HOUR SAMPLES

*ABCE CESIUM STANDARD WAS ADJUSTED.

Fig. 3-Eight-day printout of data from Lookout Mountain

The printout of daily averages provides the basic data needed for determining the frequency offsets of the network subcarriers. Also, the number of half-hour samples indicates how much network programming was available on a given day. However, users without a similar system are not likely to bother to accumulate 15 to 20 hours of data averages per

day. Provision was therefore made for readout of the half-hour averages in the form of differences from the expected value. A typical printout is shown below.

CLOCK: 1976000002803201

SCREEN WORD: ABCE 2999802000600198

HALF~HOUR +02+04+04+**+**+**+08+**+**-00-00+09+04+08-01

DIFFERENCES: -01+04+01-01-00-05-04+08-02+05+03-01+10+01+07+05

× 10⁻¹² +01+02+09+**+12-00-02+01+08+07+**+09+01+02+03+**

The clock indicates the time of printout; that is,

Each two-digit number indicates the amount by which the actual half-hour average differed from the expected value in the screen word (29998 x 10^{-12}) in parts in 10^{12} . The sign preceding indicates whether the actual value was higher (+) or lower (-) than the expected value. All numbers are rounded off to the nearest part in 10^{12} . That is, if the difference is - 00.4×10^{-12} , it is rounded to - 00, + 00.5×10^{-12} is rounded off to + 01. A double asterisk, +**, indicates either less than 900 seconds of valid data or the difference is greater than the 10 P window of $\frac{1}{2} \times 10^{-12}$.

The half-hour difference storage is "wrap around" so the data are always current for the preceeding 48 half hours. By reference to the clock printout, we know the processor is working in half-hour 32 and has already updated half-hour 31. The half hours are counted 0 through 15 on the first line, 16 through 31 on the second line, and 32 through 47 on the third line, with "0" indicating midnight to 12:30 a.m.

The availability of the half-hour difference data allows us to tell when the network was on the primary rubidium and whether other standards that are within \pm 60 x 10^{-12} were used for program origination. In the past year, only NBC East Coast has used a second rubidium that was identifiable. This occurred during the evening hours (8:00 - 10:00 EST) and the unit differed by about 40×10^{-12} from the primary rubidium.

Fractional frequency offset stability for the measured data show consistent results for the six network paths. Typical results computed using the pair variance are tabulated below.

	MEASURE	D AT DENVER, COL	ORADO	MEASURED AT ABC HOLLYWOOD		
	ABCE	CBSE	NBCE	ABCW	CBSW	NBCW
$\sigma_{y} (2,\tau)$ $\tau = 1 \text{ DAY}$	1.2 × 10 ⁻¹²	1.3 × 10 ⁻¹²	1.4 × 10 ⁻¹²	0.4 × 10 ⁻¹²	1.1 × 10 ⁻¹²	0.7 × 10 ⁻¹²
σ _y (2,τ) τ = 30 MINS	5 × 10 ⁻¹²	4 × 10 ⁻¹²	4 × 10 ⁻¹²	2.5 × 10 ⁻¹²	2.2 × 10 ⁻¹²	3 × 10 ⁻¹²

Fig. 4-Typical measurement results

All measurements include the stability of the frequency standards at each end of the measurement path except for the ABCW data, where a common reference is used within the plant. The value for $\sigma_{\gamma}(2,\tau)\,(\tau=1\text{ day})$ for ABCW is therefore representative of the best stability to be expected for one-day averages. Although we do not infer the measured daily stabilities are due to any one cause, the frequency standards used in these measurements are not in a well-controlled environment. The cesium reference on Lookout Mountain (Denver) is located in a completely enclosed, unheated equipment room, with temperature excursions of at least 20°C. The ABC cesium standards are in air conditioned equipment rooms, and as far as we know, so are the CBS and NBC rubidium standards.

Fractional frequency offsets for the network color subcarriers are published as weekly averages in the monthly NBS Time and Frequency Services Bulletin. Uncertainty for the published weekly averages is indicated as $\pm 2 \times 10^{-12}$ for ABCE and ABCW and $\pm 4 \times 10^{-12}$ for the other networks. These uncertainty estimates allow some margin for frequency drift of the network rubidiums.

The feasibility of the 3.58 MHz portion of the microprocessor data logging system has been proven in almost one year of on-line operation for the Denver and Los Angeles units. We had two failures of 741 operational amplifiers in the Los Angeles unit (out of four 741's in the unit). The problem was diagnosed over the telephone and with the able assistance of the ABC technical staff, the unit was repaired without a "service call" from Boulder to Los Angeles.

LINE-10 MEASUREMENTS

Daily line-10 readings for the three commercial networks are published by NBS and USNO [4]. The line-10 method has demonstrated a time transfer capability at the microsecond level on continental paths [5] and easily provides \pm 0.1 μs when both users are within view of a common TV transmitter. The primary disadvantage of the line-10 method is the necessity of making measurements at a prescribed second on each network, each day.

The microprocessor data logging system on Lookout Mountain automates the line-10 measurements and stores up to eight days of line-10 data in the following format (only two days of data are shown):

			TIME OF MEAS	UREMENT, UTC			
20:25:00	20:31:00	20:26:00	20:32:00	20:27:00	20:33:00	20:28:00	20:34:00
AB	CE	СВ	SE	NB	CE	КМ	GH
02845534	02143283	03057606	02355350	00006951	02641371	03015894	02310001
01216367	00514109	01428530	00726275	01712462	01010204	02271490	01565647

The three sets of network measurements are made directly off the three network microwave feeds. The KMGH-TV measurement is made off the air and is used to calibrate the Lookout Mountain 1 pps.

KMGH	KMGH	KMGH	KMGH
00358430 02989205	01032188 00326298	01705946 01000057	03021337 02315446
02950669 02244827	00287755 02918578	00961506 00255662	02276918 01571076

Simultaneously, a microprocessor system at the Boulder Laboratories makes measurements using the UTC(NBS) 1 pps as reference.

	AB	CE	СВ	SE	NB	CE	KM	IGH
11/09	28516.40	21493.91	30637.12	23614.58	00130.57	26474.79	00054.43	00054.45
11/08	12224.58	05202.01	14346.21	07323.67	17185.53	10162.96	00054.28	00054.29

The Boulder processor accepts the data from Lookout over a dial-up data link, uses the 20:28 and 20:34 KMGH measurements to compute the Lookout clock correction, adds a fixed 6.63 μs correction, and prints out the final published line-10 values. A microprocessor system identical to the Boulder unit is used at Ft. Collins to reference the WWV station clock back to UTC (NBS).

The Boulder and Ft. Collins processors measure and store eight line-10 readings each day. The Ft. Collins unit reduces this data to eight clock difference readings per day for eight days.

Both the Lookout-Boulder and Boulder-Ft. Collins processor pairs may be used in an "immediate" line-10 mode to determine clock difference readings. A printout of two sets of "immediate" difference readings between Lookout and Boulder is shown below.

IMMEDIATE LINE-10 DIFFERENCE READINGS - MICROSECONDS DIFFERENCE

-00054.44 -00054.45 -00054.45 -00054.45 -00054.45 -00054.45 -00054.45 -00054.45

To obtain these readings at Boulder, the user dials up the data line to Lookout, places a switch on the front panel of the Boulder unit in "line-10 multiprocessor" mode, and types in a 4-character command. The command goes from the keyboard to Lookout and is "echoed" back to the Boulder processor. The Lookout processor responds to the command by sending six sets of line-10 readings on six successive seconds to the Boulder processor. The Boulder processor makes simultaneous line-10 readings, computes, and prints out the differences as shown.

Single reading resolution of the automated line-10 system is limited to ± 10 ns by the 100 MHz time base in the associated time interval counters. Long term stability is limited by variations in envelope delay of the TV tuners. Periodic comparison of the automated line-10 system with a manual back-up system indicates a peak-to-peak delay variation between the units of 40 ns. Since the long term delay variations of the implemented line-10 systems are at least as large as the single reading resolution, no attempt has been made to improve the resolution of published line-10 data by averaging multiple readings.

HARDWARE

The data logging system was designed around the 4-bit INTEL 4040 micro-processor. Although not as fast as later-generation 8-bit machines, it was available, relatively inexpensive, and already in wide use. Figure 5 is a block diagram of the major elements in the Lookout Mountain processor. All blocks inside the dotted lines are on the CPU card.

Three types of memory are used: 2048 bytes of read only memory for the program, 1024 bytes of read/write (ram) for data storage, and sixteen 16-digit ram registers for arithmetic scratchpad operations.

The CPU uses a hardware 1 pps \longrightarrow 1 ppm clock (\div 60) with minutes, hours, days, and months counted by software. Use of the 1 ppm hardware clock allows the processor to perform relatively long Input/Output (I/O) operations without missing a software clock update.

A "beat note" phase compare, 4 digit time interval counter is provided for each of the three networks. Each of the three channels uses five integrated circuits. 5 MHz from a cesium standard, synthesized to 3.58 MHz, is used as a reference for the three phase compare channels.

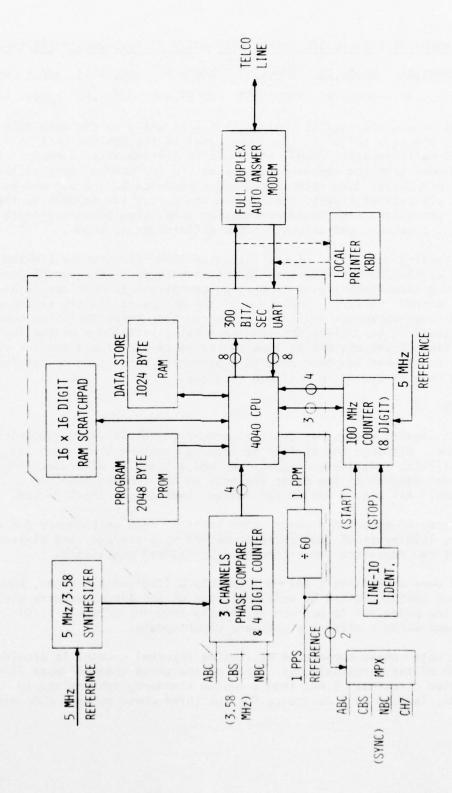


Fig. 5-Block diagram of Lookout Mountain microprocessor data logging system

I/O operations are performed at 300 bits/second (30 characters/second), full duplex through a standard RS-232 interface. A local printer/key-board may be plugged into this interface; however, for our remote installations, an auto answer modem is used with a telephone company data access arrangement (Model CBS DAA).

Line-10 measurements utilize the circuits and inputs shown at the bottom of figure 5. Stripped sync at TTL level is multiplexed under processor control to a line-10 indentification circuit. The line-10 ident provides a 30 pps output, coincident with the trailing edge of the tenth line horizontal sync pulse of field one (odd field). A 100-MHz 8-digit time interval counter makes the line-10 difference measurements under CPU control. A battery back-up supply (not shown) provides up to two hours of operation for the CPU and memory in case of power failure.

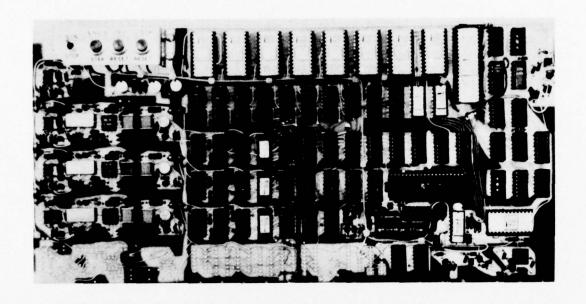
A photograph of the CPU card, with the major elements identified, is shown in figure ϵ .

Figure 7. is a photograph of the 100-MHz counter used in the system. Interface of the counter to the CPU requires four data and three control lines. The control lines are "counter reset", "multiplex clock" (CPU COUNTER), and "count available" (CPU COUNTER).

Each of the five data logging systems now in use has a slightly different configuration for both hardware and software. The previously described configuration is used at Lookout Mountain. The system at ABC Los Angeles has no line-10 capability but has four channels for 3.58-MHz subcarrier measurement (ABCW, CBSW, NBCW, ABCE). The system at Wallops Island, Virginia, has three channels of 3.58 MHz, three channels for line-10, and five channels for measuring the time difference between the master 1 pps and other 1 pps system inputs. The systems at Boulder and Ft. Collins (WWV) measure line-10 only, with no 3.58-MHz capability.

LOOKOUT MTN.	ABC, L.A.	WALLOPS ISLAND	BOULDER - FT. COLLI N S
3 - 3.58 MHz 4 - LINE 10	4 - 3.58 MHz 0 - LINE 10	3 - 3.58 MHz 3 - LINE 10 5 - 1 PPS	0 - 3.58 MHz 1 - LINE 10

CONFIGURATION OF 5 SYSTEMS



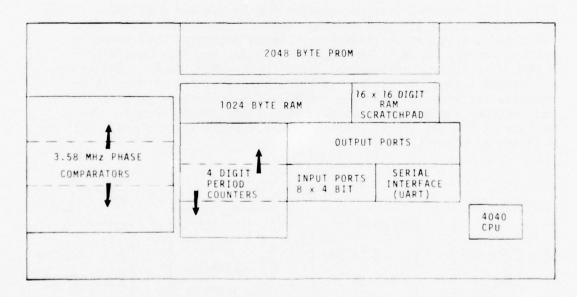
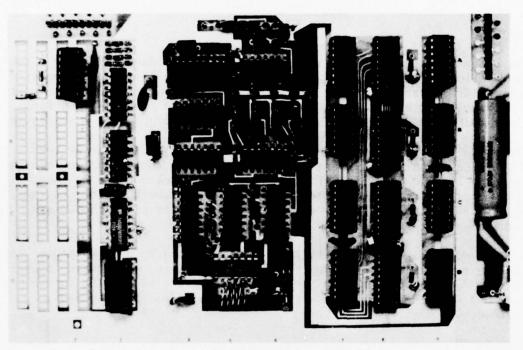


Fig. 6-Photograph of microprocessor card with functional elements identified



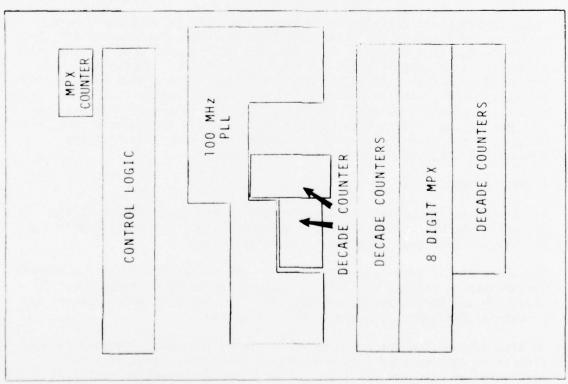


Fig. 7-Photograph of 100-MHz counter with functional elements identified

SOFTWARE

The programs used in the data logging systems were developed over a two-year period. The first program was about 1500 bytes long and processed only color subcarrier data. About two man-months were required to write and assemble it by hand. The program is stored in eight 1702A EPROMS. Since each 1702A stores 256 bytes, a total of 2048 bytes were available.

The prototype system was operated for approximately one year at the Boulder Laboratories. Program modifications were then added to incorporate the line-10 function. This increased the program size to about 1900 bytes and required another man-month for assembly of the program. Minor modifications of this "master" program tailor it to the unique requirements at each location.

Since a complete annotated listing of the software is over 60 pages long, it is not included in this paper. Anyone interested may obtain comprehensive documentation of the hardware and software by writing to the Time and Frequency Services Section, National Bureau of Standards, Boulder, CO 80302.

CONCLUSION

The microprocessor data logging systems described in this paper have proven to be reliable and relatively trouble free. Measurement stability of $\sigma_{Y}(2,\tau)\,(\tau$ = 1 day) of less than 2 x 10 $^{-12}$ worst case for the color subcarrier data is sufficient for most applications. Operational use between Boulder-Ft. Collins and Boulder-Wallops Island have demonstrated the system works well in "real world" on-line applications. If interest warrants, NBS would consider making the on-line (dial-up) link available for general use. Users with similar systems could then obtain immediate subcarrier and line-10 data without manual data reduction from the monthly NBS Time and Frequency Services Bulletin.

ACKNOWLEDGMENTS

Our thanks to the Hewlett-Packard Company (Santa Clara Division) for providing the West Coast line-10 measurements that are published in the monthly NBS Time and Frequency Services Bulletin.

Placement of the data logging systems at ABC Hollywood and at the KMGH-TV transmitter on Lookout Mountain is crucial to our TV measurements. Our thanks to the participating organizations who provided space, power, and occasional emergency maintenance help at no cost.

We also acknowledge the cooperation of the TV broadcast industry in our efforts to develop useful time-frequency techniques using TV. In particular we cite the excellent cooperation of the ABC-TV technical

operations staff over the past six years. Many individual TV broadcast stations have also been generous with their assistance.

REFERENCES

- [1] Davis, D. D., Calibrating Crystal Oscillators With TV Color-Reference Signals, Electronics, March 20, 1975.
- [2] A New Frequency Calibration Service of the National Bureau of Standards, Time and Frequency Services Section Brochures, 1975.
- [3] NBS Time and Frequency Services Bulletin, published monthly.

 Available upon request from Time and Frequency Services Section,
 National Bureau of Standards, Boulder, CO 80302.
- [4] USNO Time Services Bulletin, Series 4, published weekly. Available upon request from Time Services Division, USNO, Washington, DC 20390.
- [5] Allan, D. W., Blair, B. E., Davis, D. D., and Machlan, H. E., Merrologia, Vol. 8, No. 2, Apr. 1972, pp. 64-72.
- [6] Davis, D. D., Blair, B. E, and Barnaba, J. F., Long-Term Continental U. S. Timing System Via Television Networks, IEEE Spectrum, Vol. 8, No. 8, Aug. 1971, pp. 41-52.
- [7] Davis, D. D., Frequency Standard Hides in Every Color TV Set, Electronics, May 10, 1971, pp. 96-98.

THE ATOMIC HYDROGEN MASER*

Norman F. Ramsey Harvard University, Cambridge, Massachusetts

ABSTRACT

The basic principles of the atomic hydrogen maser will be described. Since a hydrogen maser emits a highly stable radio frequency signal, it can be used not only for accurate atomic measurements but also in other fields, such as navigation and radio astronomy where a highly stable clock is required. Results of hydrogen maser measurements are given.

INTRODUCTION

The atomic hydrogen maser depends on hyperfine transitions of atomic hydrogen in its electronic ground state.

The energy levels of atomic hydrogen in its electronic ground state are shown in Fig. 1. In weak magnetic fields the higher energy F=1 states correspond to the electron and proton spins being parallel while the spins are antiparallel in the F=0 state. With the hydrogen maser the transitions between the various hyperfine energy levels of Fig. 1 have been studied under various conditions.

The Hydrogen Maser

The atomic hydrogen maser was first developed at Harvard University by Kleppner, Goldenberg, and Ramsey [1-4]. A schematic diagram of the hydrogen maser is shown in Fig. 2. Since ordinary hydrogen that comes in a storage tank is molecular hydrogen (H₂) rather than atomic hydrogen (H), it is first necessary to convert the molecular hydrogen to the atomic form. This is done by admitting the molecular hydrogen into a small quartz or Pyrex bulb which forms the atomic hydrogen source. This bulb is surrounded by a coil of wire which is excited with a standard radio-frequency oscillator such as is used in a small radio broadcasing station. The oscillating field from this coil establishes a gas discharge in the bulb similar to the familiar gas discharge in a neon advertising sign. In this gas discharge the molecules of hydrogen are broken up into atoms, and most of what emerges from a small hole in the source bulb is atomic hydrogen.

The atoms of hydrogen emerge into a vacuum region which is exhausted to a low pressure (less than 10^{-6} Torr). In such a low-pressure region

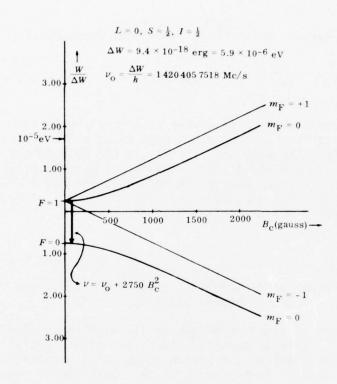


Fig. 1. Atomic hydrogen hyperfine structure showing the dependence of the energy levels on the strength of an external magnetic field. The heavy arrow indicates the transition ordinarily used in stable atomic hydrogen oscillators.

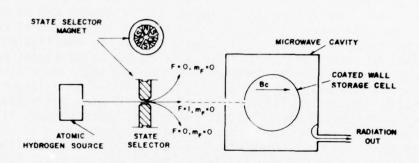


Fig. 2. Schematic drawing of atomic hydrogen maser

the atoms will travel in straight lines unless acted upon by a force. In particular, some of the atoms will go straight through the state selector magnet, as shown in Fig. 2. The state selector magnet has six poles, half on which are north poles and half south poles, arranged as shown schematically in the cross section in the upper portion of Fig. 2. By symmetry, the magnetic field must be zero on the exact central axis of the magnet. On the other hand, if the atom goes slightly off the central axis, the magnetic field will rapidly increase. Consequently, then energy of the atom will change when it is off axis. If the atom is in the F = 0 state, its magnetic energy will decrease as the atom gets farther off the axis as can be seen from Fig. 1. Since atoms prefer to go in the direction where the energy is lower, an atom of hydrogen in the F = 0 state which is off the central axis will be subject to a force pulling it still farther off the central axis. Therefore, such atoms will be defocused by the state selector magnet. On the other hand, the energies of the $M_F = + 1$ and 0 states for atoms with F = 1 increase as the atom gets farther off the axis. Consequently, the force on it pushes it back toward the axis; i.e., it is focused. The dimensions of the magnet are selected in such a fashion that the F = 1 atoms are focused on a small hole in a 6-in.-diam Teflon-coated quartz storage bulb.

As a result of the above focusing action on the F = 1 state and the defocusing action on the F = O state, the quartz bulb is dominantly filled with atoms in the higher-energy $F \approx 1$ state. The bulb is also surrounded by a microwave cavity tuned to the 1420-MHz frequency, characteristic of atomic hydrogen. Since the atoms in the bulb are dominantly in the higher-energy state, this arrangement satisfies all the requirements for maser amplifications. Indeed, such a device can be used as an amplifier. Moreover, if the amplification is sufficient it can also be a self-running oscillator. It is easy to see how oscillation can be established in such a device. If there is a weak noise signal present at the appropriate 1420-MHz frequency, stimulated emission will exceed absorption and the original signal will be amplified to a larger one which will be further amplified. The signal will thus get bigger and bigger up to the point where most of the energy being brought into the bulb by the atoms in the higher-energy state is absorbed. At this condition an equilibrium steady-state oscillation will be established. Although the power in the oscillation is quite weak -- about 10^{-12} W -the oscillation is highly stable and is concentrated in an unprecedently narrow frequency band. Consequently the signal can easily be seen despite its low total power. Ordinarily the atoms are stored in the bulb for about one-third of a second, during which time each atom makes over 10,000 collisions with the wall of the containing vessel.

An electrical coupling loop is inserted into the cavity so that some of the microwaves' oscillatory power can be coupled out for observation. The signal that emerges from such a maser proves to be unprecedentedly stable. This highly stable signal provides the basis for the experiments which will be described in the latter portion of the present report.

A photograph of a hydrogen maser is shown in Fig. 3. The entire device is about 4 ft. tall. The vertical cylinders are vacuum pumps, and the large cylinder with a horizontal axis is the tuned microwave cavity. Inside that cylinder is the Teflon-coated quartz bulb containing atomic hydrogen dominantly in the high-energy F = 1 hyperfine state. In normal use the microwave cavity is further surrounded by three successive concentric layers of molypermalloy, which shields the apparatus from the magnetic disturbances in the room.

A photograph of the six-pole focusing magnet used in the hydrogen maser is shown in Fig. 4. The six Alnico magnets are shown in the photograph. The poles of the magnets alternate successively north and south. The atomic beam goes along the axis of the cylinder.

The unprecedentedly high stability of the maser microwave oscillation arises from a combination of four desirable features, all of which contribute to increased stability. These factors include:

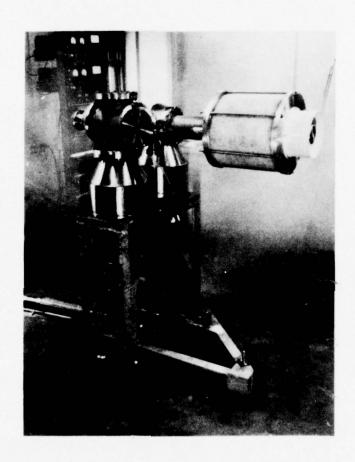


Fig. 3. Photograph of hydrogen maser

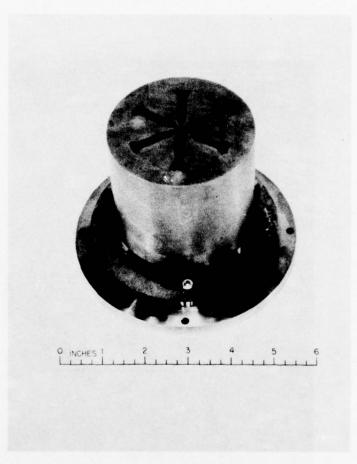


Fig. 4. Photograph of six pole focusing magnet

(a) The atoms reside in the storage bottle for a much longer period of time than the atoms remain in a normal molecular beam apparatus. Consequently the characteristic resonance line is much narrower and the output signal is more stable, since the peak of a narrow line can be much more accurately located than the peak of a broad line. The narrowing of the line is just that to be expected from the Heisenberg Uncertainty Principle. According to this principle, a longer observation time makes possible a narrower resonance and consequently a more stable frequency. The narrowness of the resonance also diminishes the pulling of the maser frequency by any mistuning of the microwave cavity; in addition the cavity can be accurately tuned by adjusting its tuning to be such that the output frequency is independent of the intensity of the beam of hydrogen atoms [3,5]. It has been shown by Crampton [5] that this method of cavity tuning eliminates the effect of a spin exchange frequency shift except for a small measurable shift of a few

parts in 10^{13} due to the change in hyperfine frequency during the time of the collision [5].

- (b) The atom is relatively free and unperturbed while radiating, unlike an atom in a resonance experiment using liquids, solids, or gases at relatively high pressure. Consequently, all atoms will have the same characteristic frequency, and the resultant resonance will not be broadened as it would be if it consisted of a superposition of a number of resonance at slightly different frequencies. Unfortunately the atoms of hydrogen are not totally free, since they must collide at intervals with the Teflon-coated wall of the storage bulb. This produces a shift in the maser frequency of about 2 parts in 10^{11} . This correction, however, can be experimentally determined by observing the frequency of the output with bulbs of two different sizes and then by extrapolating to a bulb of infinite diameter as discussed later in greater detail.
- (c) A further advantage of the hydrogen maser is that the first-order Doppler shift is greatly reduced. With the very-narrow-line characteristic of the atomic hydrogen maser, the relevant quantity for the Doppler shift is the ratio of the <u>average</u> velocity of the hydrogen atom to the velocity of light. Since the hydrogen atoms enter the storage bulb through a small hole, and then stay in the storage bulb for about 1 sec. before finally emerging from the same hole, the average velocity is zero, or close to zero. Consequently the first-order Doppler shift is completely negligible. There is a small second order Doppler shift due to the relativistic slowing down of any moving clock or oscillator. Since the second-order Doppler shift depends upon the velocity squared, it is not averaged to zero while the atom is in the bulb. On the other hand, the second-order Doppler shift is a correction that can be exactly calculated if the temperature and hence the mean square velocity of the atom is accurately known.
- (d) A final advantage that contributes to the high precision of the atomic hydrogen maser is the low-noise characteristic of maser amplification. Since the amplifying element is an isolated simple atom, there is little opportunity for any extra noise to develop beyond the theoretical minimum noise. As a result, the maser is a very-low-noise amplifier, and the oscillation will be much more stable since the frequency is less likely to drift to a nearby noise peak.

For the above four reasons the hydrogen maser frequency should be very stable. This prediction has been confirmed experimentally and the stability, as measured by the Allan variance, is about 2×10^{-15} . For many experiments stability is all that is required for the desired measurements. On the other hand, often the observer wishes to know the absolute rate of the oscillation in terms of those of a totally free hydrogen atom. In such cases the correction for the wall shift must be known. This correction can be determined by making measurements with storage bulbs of two different sizes, the necessity for making the

correction usually degrades the accuracy and a further degradation of the accuracy of absolute measurements come from the necessity of measuring the cesium hyperfine structure as the standard of time. The wall shift correction can, however, be made more reliably if a single storage bulb is used whose shape can be deformed to change the ratio of the surface area to the volume, as discussed further in section.

Large Storage Box Hydrogen Maser

In the previous discussion it has been mentioned that the principal source of uncertainty in the hydrogen maser measurements arises from the necessity of making a wall shift correction for the effect of the wall upon the hydrogen atom when the atom is in the vicinity of the wall. Although this correction can be made by extrapolating results on masers with a different sized storage bulbs, the uncertainty in the determination of the wall correction remains the principal source of uncertainty in many of the maser measurements. Zitzewitz [11,12] and Vessot [13] are undertaking experiments to reduce this uncertainty by finding a wall-coating material that is superior to Teflon. So far, however, Teflon remains the best wall-coating substance.

An alternative means of reducing the effect of the wall shift has been accomplished by Uzgiris [10] in our laboratory. He has constructed a maser with a storage box that is ten times larger in diameter than the normal 6-in.-diam. storage bulb. Since the atom will strike the wall only one-tenth as frequently in such a storage box, the wall shift will be ten times less. In addition, a longer total storage time can be arranged, which makes the resonances even sharper.

A schematic diagram of the large storage box hydrogen maser is shown in Fig. 5. The arrangement of this maser is necessarily different from that of previous hydrogen masers and a number of new principles involved. In particular the cavity can no longer surround the entire storage box, since the wavelength of the radiation is small compared to the diameter of the storage box. However, an equally narrow resonance is obtained if the cavity in which the maser oscillation occurs surrounds only a portion of the storage box, provided the atoms make a number of transits between the small storage box and the large box before finally exiting through the entrance cavity of the large box. Since the atoms are in the region of the cavity only for a very short period of time, it is necessary to have a higher level of excitation than would occur from simple spontaneous maser oscillation. As a result two cavities are used, each surrounding a small portion of the storage box and about 80 dB of amplifier gain is provided between the two cavities. In this manner the atoms are placed in a superradiant state by the intense oscillations in the high-level driving cavity and are thereby able to produce spontaneous maser oscillation in the low-level cavity, which in turn is amplified to the high-level driving cavity.

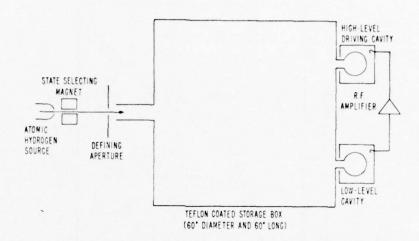


Fig. 5. Schematic diagram of large box hydrogen maser

Wall and Gas Collisions

Zitzewitz and Ramsey [11,12] have studied the Teflon wall shifts at different temperatures with the results shown in Fig. 6. One interesting result was the observation that at about 80°C the wall shift passes from positive to negative values and consequently vanishes at the crossing temperature. This feature is of value in maser experiments that are limited by the wall shift. Zitzewitz [11,12] also found that the abrupt changes with temperature in the slope of the wall shift curve in Fig. 6 are correlated to known phase changes in Teflon.

Until recently all frequency shifts due to wall collisions were measured by extrapolation with the use of Teflon-caoted storage bulbs of different diameters. However, Zitzewitz, Uzgiris, and Ramsey [11] showed that the accuracy of this extrapolation was reduced by the differences in the wall coatings on the different bulbs. Brenner [14] pointed out that this difficulty could be overcome by the use of a single flexible storage bulb whose volume could be altered while keeping the same surface. This technique was further developed by Debely [15] who used a storage cylinder, one of whose ends was a thin conical sheet of Teflon which could be in either of the two positions shown in Fig. 7. With

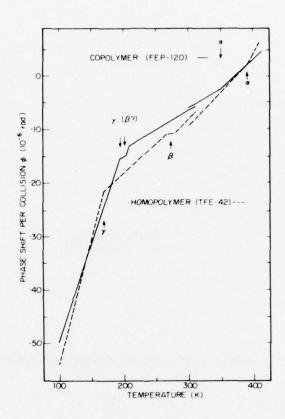


Fig. 6. Experimental phase shift per collision versus temperature

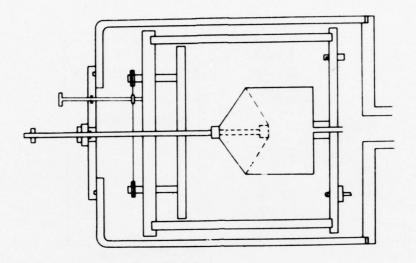


Fig. 7. Deformable bulb H maser [15]. The conical surface can be in the positions indicated by the full or dashed lines.

this deformable bulb technique the wall-shift measurements are all made on the same surface.

Reinhardt [16] has adapted this deformable bulb technique to the large box hydrogen maser by using the configuration shown in Fig. 8. An alternative to the use of the deformable bulb technique has been suggested by Vessot [13] who has proposed operating a hydrogen maser at the temperature where the wall shift vanishes [12] and using the deformable bulb to locate that temperature experimentally, i.e., to operate at the temperature for which the output frequencies are the same in the two different deformable bulb configurations. Peters has used a variable volume maser in the form of a bellows.

Bender [18] first pointed out that spin exchange collisions of hydrogen atoms might produce a significant frequency shift in the hydrogen maser, but Crampton [19] noted that the normal tuning technique would cancel out such an effect. Later Crampton pointed out the existence of a smaller additional spin exchange effect that would not be cancelled by the normal tuning method. This effect was omitted in earlier

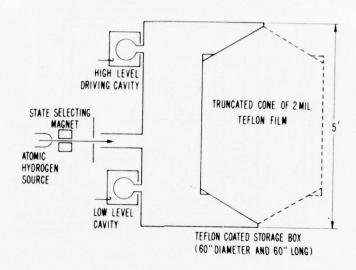


Fig. 8. Large storage box H maser with deformable bulb for measurement of wall shift [16].

theories due to their neglect of the contribution of the hyperfine interaction during the time of the short duration of the collision. Crampton developed a technique for measuring the spin exchange effect. Crampton also pointed out the existence of a small frequency shift due to magnetic field inhomogeneities; this small shift is often called the Crampton effect. Both of these effects are so small they did not effect past measurements and they can be further reduced by suitable apparatus design.

Applications

The hydrogen maser has been used both for precision measurements of the properties of the hydrogen atom and its isotopes and as a highly stable clock when other quantities are measured.

Some of the principal results of measurements of the properties of the hydrogen atom are given in Fig. 9.

ATOMIC ¹H, ²D, and ³T

 $\Delta \nu_{\rm H}$ = 1,420,405,751.7680 ± 0.0015 Hz

 $\Delta \nu_D = 327,384,352.5222 \pm 0.0017$ Hz

 $\Delta \nu_{T} = 1,516,701,470.7919 \pm 0.0071$ Hz

 $\mu_p = 0.00152103221$ (2) Bohr magnetons

 $\mu_{\rm J}$ (H) $/\mu_{\rm J}$ (D) = 1.0000000722 (10)

 $\mu_{\rm J}$ (H) $/\mu_{\rm J}$ (T) = 1.0000000107 (20)

Fig. 9. Some results of maser measurements of atomic hydrogen (H), deuterium (D) and tritium (T). $\Delta \nu$ is the hyperfine separation of the atom, μ_D is the magnetic moment of the proton and μ_J is the magnetic moment of the indicated atom.

The hydrogen maser has been used extensively as a high stability clock in long base line interferometry in radio-astronomy. It has also been used in various radio-astronomy tests of the theory of relativity. Vessot [21] has recently used a hydrogen maser in a high altitude rocket to test the equivalence principle in the theory of relativity.

References

- 1. H. M. Goldenberg, D. Kleppner, and N. F. Ramsey, Phys. Rev. Letters 5, 361 (1960).
- 2. D. Kleppner, H. M. Goldenberg, and N. F. Ramsey, Phys. Rev. 126, 603 (1962).
- 3. N. F. Ramsey, Prog. Radio Sci., 7, 111 (1965).
- 4. D. Kleppner, H. C. Berg, S. B. Crampton, N. F. Ramsey, R. F. C. Vessot, H. E. Peters, and J. Vanier, Phys. Rev. <u>138</u>, A972 (1965).
- S. B. Crampton, Phys. Rev. <u>158</u>, 57 (1967); (private communication, 1971).

- 6. S. B. Crampton, D. Kleppner, and N. F. Ramsey, Phys. Rev. Letters 11, 338 (1963).
- 7. R. Beehler, D. Halfoud, R. Harrach, D. Allan, D. Glaze, C. Snider, J. Barnes, R. Vessot, H. Peters, J. Vanier, L. Cutler, and M. Bodily, Proc. IEEE (correspondence) 54, 301 (1966); H. E. Peters, J. Holloway, A. S. Bagley, and L. S. Cutler, Appl. Phys. Letters 6, 34 (1965); R. Vessot, H. Peters, J. Vanier, R. Beehler, D. Halfoud, R. Harrach, D. Allan, D. Glaze, C. Snider, J. Barnes, L. Cutler, and M. Bodily, IEEE Trans. Instrum. Meas. IM-5, 165 (1966); H. Hellwig, R. F. C. Vessot, M. Levine, P. W. Zitzewitz, H. E. Peters, D. W. Allan, and D. J. Glaze, IEEE Trans. Instrum. Meas. IM-19, 200 (1970).
- 8. B. S. Mathur, S. B. Crampton, D. Kleppner, and N. F. Ramsey, Phys. Rev. 158, 14 (1967).
- S. B. Crampton, H. G. Robinson, D. Kleppner, and N. F. Ramsey, Phys. Rev. 141, 141 (1966).
- 10. E. Uzgiris and N. F. Ramsey, IEEE Journal of Quantum Electronics, 2E-4, 563 (1968).
- 11. P. W. Zitzewitz, E. Uzgiris, and N. F. Ramsey, Rev. Sci, Instrum. 41, 81 (1970).
- 12. P. W. Zitzewitz and N. F. Ramsey, Phys. Rev. A 3, 51 (1971).
- 13. R. F. C. Vessot (private communication, 1971).
- 14. D. Brenner, Bull. Am. Phys. Soc. <u>14</u>, 443 (1969), J. Appl. Phys. <u>41</u>, 2942 (1970).
- 15. P. Debely, Rev. Sci. Instrum 41, 1290 (1970).
- 16. V. Reinhardt, Ph.D. Thesis, Harvard University, (1974).
- 17. D. Wineland and N. F. Ramsey, Phys. Rev. A 5, 821 (1972).
- 18. P. L. Bender, Phys. Rev. <u>132</u>, 2154 (1963).
- 19. S. B. Crampton, Phys. Rev. 158, 57 (1967).
- 20. S. B. Crampton, J. A. Duvivier, G. S. Read, E. R. Williams and H. T. M. Wong, Phys. Rev. A 12, 1305 (1975); Bull. Am. Phys. Soc. 18, 709 (1973) and 19, 83 (1974).
- 21. R. F. C. Vessot, private communication.

FIELD OPERABLE HYDROGEN MASER DESIGN

Victor S. Reinhardt, Harry E. Peters, Lawrence A. Birnbaum NASA/Goddard Space Flight Center, Greenbelt, Maryland 20771

INTRODUCTION

The principal elements of a NASA field operable hydrogen maser are shown in Figure 1. This paper will not dwell on the details of NASA hydrogen masers, this has been discussed elsewhere. ^{1,2,3,4} Instead, this paper will discuss the design principles involved in two important aspects of NASA hydrogen masers: the elongated microwave cavity and storage bulb and the use of automatic flux tuning.

ELONGATED DESIGN

The elongated design has many advantages. Cavity and bulb elongation tends to reduce magnetic inhomogeneity effects, improves operating parameters, and increase the microwave cavity's mechanical stability. The reduction of inhomogeneity effects is caused by the stretching out along the longitudinal direction of both the cavity field lines and the storage bulb. The principal advantages of the elongated design for improved operating parameters comes from the increased bulb volume and the increased filling factor, η' .

An elongated storage bulb has a larger volume than a spherical storage bulb with the same wall collision rate. This increases the efficiency with which hydrogen atoms are focussed into the storage bulb because the larger bulb volume allows the use of a bulb collimator with a larger entrance aperture to achieve the same bulb escape time.

The filling factor, η' , is an important parameter in determining maser performance. ⁵ Figure 2 shows the optimum η' as a function of cavity elongation for various storage bulb shapes. The storage bulb shapes are shown in Figure 3. For a rounded cylindrical bulb in a two to one cavity, optimum η' is 0.511. This represents a 32% improvement over a spherical bulb in a one to one cavity which has an optimum η' of 0.387. Notice also that even for a one to one cavity, the rounded cylindrical bulb yields an optimum η' of 0.461 which is 19% better than that of a spherical bulb.

To aid others in making their own η' calculations, the authors have collected some of the equations and results of their η' calculations in the Appendix to this paper.

The elongated cavity offers another advantage besides improved η' : reduced sensitivity to end plate motion. Figure 4 shows the sensitivity of the frequency of a TE_{011} cavity at 1.42 GHz to changes in cavity length. The length sensitivity of a two to one cavity is about 3 MHz/inch, a factor of ten smaller than the 30 MHz/inch sensitivity of a one to one cavity. Reduced end plate sensitivity is important because mechanical instability problems such as creep at joints, differential expansion effects, and ambient pressure sensitivity effect the cavity frequency through end plate motion.

AUTOMATIC FLUX TUNING

Automatic Flux Tuning or autotuning is used to keep the microwave cavity in a hydrogen maser tuned while the maser is operating. When the flux of atoms in a hydrogen maser is changed, the maser's output frequency will change in proportion to the mistuning of the microwave cavity. ⁵ An autotuner utilizes this change as an error signal in a servo loop to keep the cavity tuned. There are two types of autotuner, a proportional type which utilizes the magnitude of the frequency change, and a sign averager type which only utilizes the sign of the frequency change. The sign averager type is used in the NP masers and has been discussed in a previous paper. ⁴ Present NASA masers use the proportional type. The present discussion will be limited to this type.

The block diagram of a proportional autotuner is shown in Figure 5. The control register continuously steps the hydrogen maser between high and low flux and measures the change in maser frequency against a reference oscillator. The control register output in a proportional autotuner is:

$$\Delta N = \frac{2(R-1)}{r(R+1)} y + \frac{n_3}{r}$$

where R is the tuning factor, 5 y is the average maser fractional frequency offset, r is the resolution of the register, and \mathbf{n}_3 is the measurement noise. The control register outputs $\Delta \mathbf{N}$ every τ_0 seconds. In a well designed system, most of τ_0 is spent measuring the difference in frequency, typically 80% of τ_0 , with the rest of the time used to allow the maser to stabilize after the change in flux. This is important because amplitude to phase conversion in the maser receiver can lead to apparent frequency shifts while the maser amplitude is still settling. In a practical system, it is useful to limit the size of $\Delta \mathbf{N}$ to keep large noise transients from detuning the maser. The measurement noise, \mathbf{n}_3 , comes from the reference oscillator and the maser itself. Since only differences in frequency are measured, only changes over the time τ_0 will affect \mathbf{n}_3 .

The output of the control register is summed in a digital integrator, which for times long compared with τ_0 , produces an output given by:

$$N = \frac{1}{\tau_0} \int \Delta N \, dt$$

This output controls a tuning register which controls the cavity frequency. The tuning register output changes the average maser frequency by:

$$y_c = -SN$$

Since the maser frequency changes with time, a noise term, \boldsymbol{n}_1 , is added to \boldsymbol{y}_c to give the maser output:

$$y = y_c + n_1$$

Putting these equations together, we obtain a loop equation which in differential form is:

$$\frac{d}{dt}y = \frac{d}{dt}n_1 - Gy + \frac{S}{r\tau_0}n_3$$
 (1)

where G, the loop gain is:

$$G = \frac{2S(R-1)}{r\tau_0(R+1)}$$
 (2)

The reciprocal of the loop gain for this first order loop is the loop time constant:

$$T = G^{-1} \tag{3}$$

One can solve these equations for the different noise processes associated with n_1 and n_3 to obtain the rms fractional frequency fluctuations of the maser output $(y^2)^{1/2}$. No matter what noise processes effect the maser and the reference oscillator, n_3 is effectively a white noise process because of the way the control register operates. Also, if data from both high to low and low to high flux is used, reference drift will not enter into n_3 . In analyzing n_1 processes, one need only consider long term processes since the loop time constant is usually such that only long term noise processes are affected by the servo loop. The servo loop turns long term non-stationary noise processes into stationary processes, so $(y^2)^{1/2}$ exists for these processes. Table 1 lists $(y^2)^{1/2}$ for n_3 noise, n_1 drift, n_1 random walk of frequency noise, and n_1 flicker of frequency noise.

Noise processes are not fully described by $\langle y^2 \rangle^{1/2}$; from the equation of motion, one must obtain the autocorrelation function or the spectral density from which the Allan variance can be derived. Table 1 also lists the Allan Variance, $\sigma_y(\tau)$, for each process. Notice that the autotuner converts both n_3 noise and n_1 frequency random walk noise into random telegraph noise whose Allan Variance is:

$$\sigma_{\rm v}^2(\tau) = \langle {\rm y}^2 \rangle \, {\rm h} \, ({\rm G} \tau)$$

where

$$h(\tau) = \frac{2\tau + 4e^{-\tau} - e^{-2\tau} - 3}{\tau^2}$$

Figure 6 shows a plot of $h(\tau)^{\frac{1}{2}}$. Notice that for $\tau \gg 1$:

$$h(\tau) \simeq \frac{2}{3} \tau - \frac{1}{2} \tau^2$$

which looks like random walk of frequency noise, and for $\tau \gg 1$:

$$h(\tau) \simeq \frac{2}{\tau} - \frac{3}{\tau^2}$$

which looks like random walk of phase noise. Also notice that $h(\tau)$ is quite flat over several orders of magnitude in the intermediate range of τ . This may explain flicker like behavior of some frequency standards due to slow random telegraph modulation of the frequency. Finally, notice that the autotuner converts flicker of frequency noise into flicker of phase noise when $\tau \gg G$.

Table 1 Autotuner Noise Properties

1. n₃ noise:

$$\langle y^2 \rangle^{1/2} = \frac{\sigma_r(R+1)}{2(R-1)} \sqrt{\frac{\tau_0}{2T}}$$

$$\sigma_r^2 = 2(\sigma_{maser}^2 + \sigma_{ref}^2)$$

Table 1 (Continued)

where $\sigma_{\rm maser}^2$ and $\sigma_{\rm ref}^2$ are the appropriate two sample Allan Variance for total sample time $2\tau_0$.

$$\sigma_y^2(\tau) = \langle y^2 \rangle h(G\tau)$$
$$h(\tau) = \frac{2\tau + 4e^{-\tau} - e^{-2\tau} - 3}{\tau^2}$$

2. n₁ drift:

$$Y = DT$$

D = free drift rate

3. n₁ frequency random walk:

$$\langle y^2 \rangle^{1/2} = \sigma_w \left(\frac{3T}{2} \right)$$

$$\sigma_{\rm W}(\tau) = {\rm free} \, \sigma_{\rm V}(\tau)$$

$$\sigma_y^2(\tau) = \langle y^2 \rangle - h(G\tau)$$

$$h(\tau) = \frac{2\tau + 4e^{-\tau} - e^{-2\tau} - 3}{\tau^2}$$

4. n₁ frequency flicker:

$$\langle y^2 \rangle^{1/2} = \frac{\sigma_f}{2} \left[\frac{\ln(1 + \omega_c^2)}{\ln 2} \right]^{1/2}$$

$$\sigma_{\rm f} = {\rm free} \, \sigma_{\rm y}(\tau)$$

 $\omega_{\rm c}$ = angular cut off frequency of autotuner mixer

for $\tau \ll T$:

$$\sigma_y^2(\tau) = \sigma_f(\tau)$$

for $\tau \gg T$:

$$\sigma_{y}^{2}(\tau) = \frac{\sigma_{f}^{2} T^{2}}{4\pi(\ln 2) \tau^{2}} \left[\frac{9}{2} - \ln 2 + 3 \ln \left(\frac{\pi \tau}{2T} \right) \right]$$

Let us define optimum performance for any n₁ process as minimizing:

$$\langle y^2 \rangle_{n_1} + \langle y^2 \rangle_{n_3}$$

For each n_1 process, these $\langle y^2 \rangle_{\rm opt}^{1/2}$ are listed in Table 2. Using these values, Figure 7 shows the stability of NASA hydrogen masers calculated for various reference oscillators.

Table 2 Optimum Performance

1. n₁ drift:

$$\langle y^2 \rangle_{\text{opt}}^{1/2} = \sqrt{\frac{3}{2}} \left(\frac{\sigma_r^2 D \tau_0 (R+1)^2}{16(R-1)^2} \right)^{1/3}$$

$$T_{\text{opt}} = \left(\frac{\sigma_r^2 \tau_0 (R+1)^2}{16(R-1)^2 D^2} \right)^{1/3}$$

2. n₁ frequency random walk:

$$\langle y^2 \rangle_{\text{opt}}^{1/2} = \left(\frac{\sigma_r \, \sigma_w(3\tau_0) \, (R+1)}{2(R-1)} \right)^{1/2}$$

$$T_{\text{opt}} = \frac{\sigma_r \, \tau_0}{\sigma_w(3\tau_0)}$$

3. n₁ frequency flicker:

$$\langle y^2 \rangle_{\text{opt}}^{1/2} \simeq \frac{\sigma_f}{2} \left[\frac{\ln(1 + \omega_c^2)}{\ln 2} \right]^{1/2}$$

$$T_{\text{opt}} \ge \frac{3\sigma_r^2 (R + 1)^2 \tau_0 \ln 2}{4(R - 1)^2 \sigma_f^2 \ln(1 + \omega_c^2)}$$

APPENDIX

FILLING FACTOR FACTS

The filling factor η' is given by:⁵

$$\eta' = \frac{V_b}{V_c} \frac{\langle H_z \rangle_{bulb}^2}{\langle H_r^2 + H_z^2 \rangle_{cavity}}$$

For a ${\rm TE}_{011}$ cavity of length d and radius a:

$$H_{z} = J_{0} \left(S_{01} \frac{r}{a} \right) \sin \left(\frac{\pi z}{d} \right)$$

$$H_{r} = -\left(\frac{\pi a}{S_{01} d} \right) J_{1} \left(S_{01} \frac{r}{a} \right) \cos \left(\frac{\pi z}{d} \right)$$

$$S_{01} = 3.8317$$

$$J_{1} (S_{01}) = 0$$

$$\omega = c \left[\left(\frac{S_{01}}{a} \right)^{2} + \left(\frac{\pi}{d} \right)^{2} \right]^{1/2}$$

$$d = \frac{pc}{\omega}$$

$$a = \frac{pc}{g\omega}$$

$$g = \frac{d}{a}$$

$$p = \sqrt{S_{01}^{2} g^{2} + \pi^{2}}$$

At the hyperfine frequency:

$$\frac{c}{\omega} = 3.359142360 \text{ cm}$$

For centered cylindrical bulbs of radius ρ and length ℓ :

$$\eta' = \left(\frac{16}{S_{01}^2 \pi}\right) \frac{J_1^2 \left(S_{01} \frac{\rho}{a}\right) \left(\frac{d}{\ell}\right) \sin^2 \left(\frac{\pi \ell}{2d}\right)}{\gamma + \delta/g^2}$$

$$\gamma = 0.25481$$

$$\delta = 0.17129$$

At optimum η' for cylindrical bulbs:

$$\frac{\rho}{a} = 0.450$$

$$\frac{\ell}{d} = 0.7423$$

$$J_1^2 \left(S_{01} \frac{\rho}{a} \right) = 0.33856$$

$$\eta'_{opt} = \frac{0.133675}{\gamma + \delta/g^2}$$

$$\eta'_{opt}(g = \infty) = 0.5246$$

For any shape bulb, if one makes the scale change on both the bulb and the cavity (see Figure 8):

$$z = Gz'$$

 η' will scale as:

$$\eta'(g) = \left(\frac{\gamma + \delta/4}{\gamma + \delta/g^2}\right) \eta'(g = 2)$$

For elliptical bulbs, this is extremely useful since the scale change takes elliptical bulbs into elliptical bulbs. Figure 9 is a contour chart of η' for ellipsoidal bulbs in a g=2 cavity. The second digit of η' is printed on the chart. The first digit can be inferred from the zeros on the graph which are filled in to emphasize

the changes in the first digit. For example, the optimum ellipsoid bulb in this chart has $\eta'=0.46$. The horizontal scale is the semi minor axis of the ellipsoid divided by a from 0 on the left to 1 on the right. The vertical scale is the major axis of the ellipse divided by d from 0 on the top to 1 on the bottom. Using the scaling law and this chart, η' can be determined to two digits for any ellipsoidal bulb for any g.

For rounded cylindrical bulbs, optimum η' occurs as follows:

g	η'	ℓ/d	ρ/a
2	0.461	0.85	0.50
3	0.498	0.80	0.50
4	0.511	0.78	0.50

For a g = 2 cavity, Baker 6 has numerically determined the shape of the bulb which optimizes η '. For this bulb, $~\eta$ '= 0.462.

REFERENCES

- 1. V. Reinhardt, D. Kaufmann, W. Adams, J. De Luca, and J. Soucy, "NASA Atomic Standards Program An Update," Proceedings of the 30th Frequency Control Symposium, USAEC (Atlantic City, 1976).
- 2. Harry E. Peters, "Characteristics of Advanced Hydrogen Maser Frequency Standards," Proceedings of the Fifth NASA/DOD Precise Time and Time Interval Planning Meeting, NASA Doc. X-814-74-225, pg. 283 (Greenbelt, 1973).
- 3. Harry E. Peters, "Topics in Atomic Hydrogen Standard Research and Applications," Proceedings of the Frequency Standards and Metrology Seminar (Quebec, 1971).
- 4. H. E. Peters, T. E. McGunigal, and E. H. Johnson, "Hydrogen Standards Work at Goddard Space Flight Center," Proceedings of the 22nd Frequency Control Symposium, USAEC (Atlantic City, 1968).
- 5. D. Kleppner, H. C. Berg, S. B. Crampton, N. F. Ramsey, R. F. C. Vessot, H. E. Peters, and J. Vanier, "Hydrogen Maser Principles and Techniques," Phys. Rev. 138, No. 4A, A972 (17 May 1965).
- 6. W. Davenport and W. Root, "Random Signals and Noise," McGraw-Hill (New York, 1958).
- 7. D. Gray, ed., AIP Handbook, McGraw-Hill (New York, 1972).
- 8. R. Vessot, M. Levine, L. Mueller, and M. Baker, "Design of an Atomic Hydrogen Maser System for Satellite Experiments", Proceedings of the 21st Frequency Control Symposium, USAEC (Atlantic City, 1967).

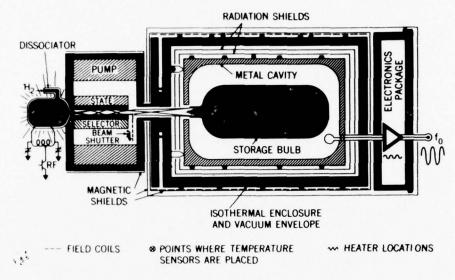


Figure 1. Principal Elements of a NASA Hydrogen Maser

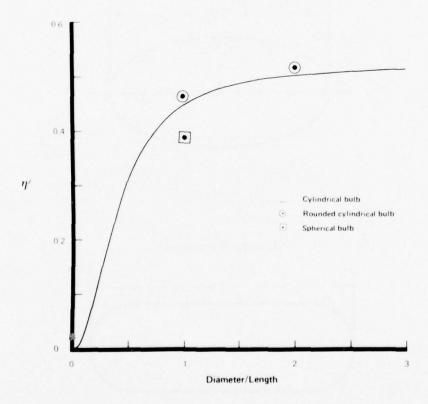
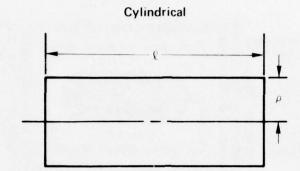
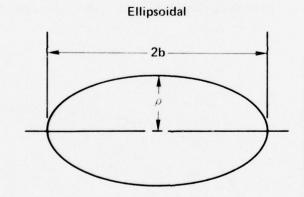


Figure 2. Optimum η' for Various Bulb Types as a Function of Cavity Elongation





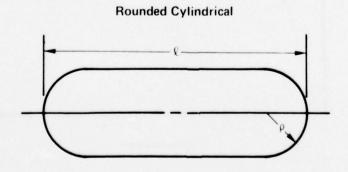


Figure 3. Types of Storage Bulbs

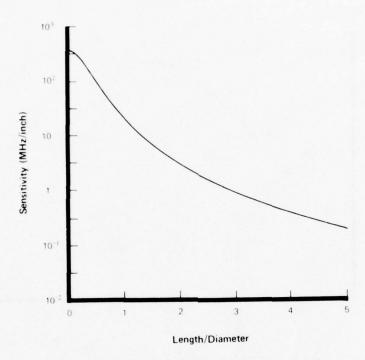


Figure 4. Length Sensitivity Versus Cavity Elongation for a ${\rm TE}_{0\,1\,1}$ Cavity at 1.42 GHz

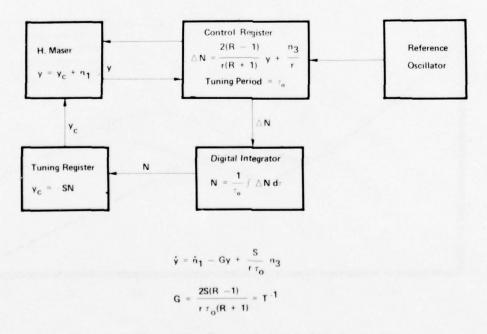


Figure 5. Proportional Autotuner

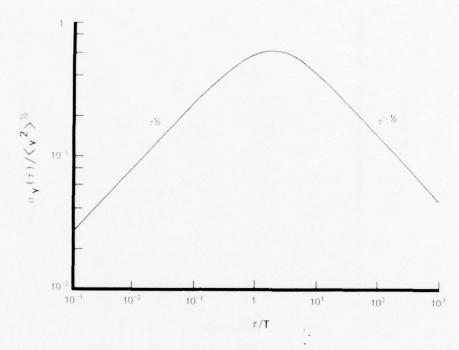


Figure 6. Random Telegraph Allan Variance

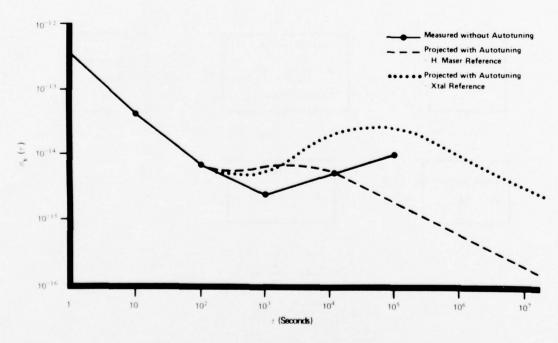


Figure 7. NASA Hydrogen Maser Stability

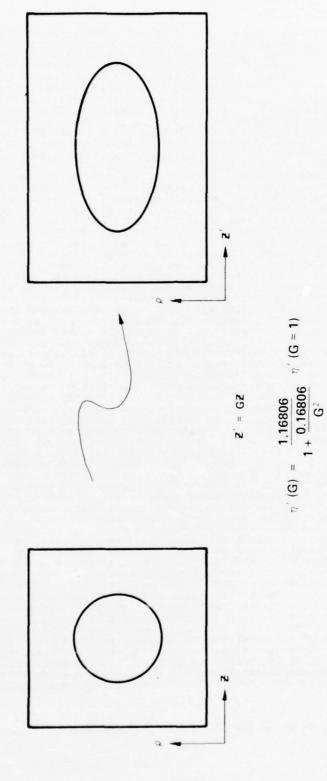


Figure 8. Effect of Scale Change on η'

```
♦♦♦♦♦♦11111112222333344444555566666666777777777777666666665555554444433332
••••••111112223334445556667777888889999999999999999999999938888777666655554443333222211
♦♦♦♦♦1111122233344455666778889999₹♦♦♦♦11111111110♦♦♦♦999988777666555544433322221
◆◆◆◆◆111122233344555667788999◆◆◆11112222222222221111◆◆◆99988777665554443332222
◆◆◆◆◆1111222334455666778899◆◆11122233333333333333222111◆◆◆99887776655444333222
♦♦♦♦11122233445566778899♦♦11222333444455555555444433322211♦♦♦998077665544433322
●●●●11112223344556778899●112233444555566666666665555444332211●●99897766554433322

●●●●111122334455667889●●112334455566677777777777766655544332211●9989776655443332

●●●1112233445667889●●12234455667788888897998888877766554433211●988776655444332
♦♦♦♦1112233445567789♦♦12234456677888999♦♦♦♦♦9999888776655433211♦♥9887665544332
●●●1112233445667899●1223455678899●●111111111111●●●29887655433211●998776554433

●●●111223345567889●1223455678899●●11122222222111●●29887665443211●297776554433

●●111223344566789●●12345567889●●11223333333333322211●●288766543321●98876654433

●●111223344567889●12345567899●112233444445544444332211●278766543321●27876655443
♦♦♦11122334556789●1223456789♦♦122344455566666555554433221●♦9876654321!●9877655443
♦♦♦11122334566789♦123456789♦♦1233455566677777766655443321●♦9876544321●9987665443
●●▶1112234456789●●134567899●1234456677778888887776655543321●99876543211●987765543
●●1112234456789●123456789●123455677888899999990887765544321●9876554321●98765544

●●1112334556789●12356789●123455678999●●●●●●●●99988776544321●987654321●98765544

●●111233456789●12345678●123455678899●●11111111●●●99877654321●987654321●98765544

●●112233456789●12346789●1234567899●●112222222111●9987654321●987654321●98765544
●●112233456789●1245678●123456789●●112223333332211●●9887654321●97654321●98776544
•••112234456789•2345689•13456789••122333444443332211•987654321•98765421•99876554
♦♦♦11223455678♦1234678912345789♦♦12334444555544433211♦987654321987654321♦9876554
♦♦♦11223456789♦1235679♦13456789♦12334455556555554433211♦98765321♦98654321♦9876554
●●11223456789●1345689●2346789●12334556666666665544321●98765432●98764321●9876554
♦♦♦11223456789♦234578♦1245679♦12334556677777773655543321♦9876432198765321♦9876654
♦♦♦112234567891234679♦1345789♦12345567788888887776654321♦98765421♦9765431♦9876654
●●112334567891235689●235678●123456678899999888776554321●9865431●9865432●9876554

●●112334567891235689●235678●13455678899999999988776554321●9876432●987543219877654

●●1123345679●124578●134578●12345678899●●●●●999877654321●876532198754321●877654
●●11123345689●134679●234679●1345678899��●111●●●9987665421●9865421●8764321●987654
◆◆11123445789◆234679◆2356891234567899◆◆1111111◆◆998765432◆9875421◆8764321◆987654
◆11123456789◆235689124578◆124567899◆1112222111◆9876543219875431◆9765321◆987654

◆11123456789◆235689124679◆13456789◆11222222211◆998765421◆876431◆9765321◆987654

◆11123456789123568◆134679◆2346789◆◆1222333322211◆98765431◆976432◆9765321◆987654
••11123456789124578•13568912356789•11223333333221•99865432•976532•9765321•987654
◆●11223456789124578●23568●1245689◆●122333444333211◆9876432●986532●9765321●987654
♦♦1122345678♦|24579♦24578♦1346789♦|223344444433221♦98765321986532♦9865321♦976654
••1122345678•134679•24579•2346789•1233444444443321•98765421986532•9865321•976554
   1122345678€134679124679€235679€112344455544433211€9765421986532€9865321€876554
●●1122345678●1346791246791245689●123344555555443221●9865421●87532●9765321●876544
●1122345679●1346891346891245789●12334555555443321●9865421●87532●97653219876544
●1122345679●1346891346891345789●12344555555543321●9875421●87532●97653219876544
●●1122345679●13568●13568●13467891223445556555544321●9875421●86532●976432●9876543
●1122345679●23568●13568●134678●1233455566655544321●9875421986532●976432●9876543
◆◆1122345679◆23568◆13578◆134679◆1234455566665544321◆9875421986532◆976432◆9876543
••1122345679•23568•13578•235679•1234455666665544321•9865421986532•876431•9876543
••1122345679•23568•23578•235679•1234455666665544321•9865421986531•875431•9876543
●1122345679●23568●23578●235679●1234455666665544321●9865421986431●875421●9765543
●1122345689●23568●23578●235689●1234455666655543321●976532●9764319865421●8765443
◆●1122345689●23568●23578●235689●1234455666655543321●976532●976421986532198765443
●●1122345689●23578●23578●235679●123445556655554432219876432●875421986532198765433
●●1122345689●23568●23578●235679●123345555555544321●9876431●87542●976432●98765433
●●1122345689●23568●23578●235679●123344555555544321●9875421●86532●976431●98765432
```

Figure 9. η' for Ellipsoidal Bulbs With g = 2

HYDROGEN MASER FREQUENCY STANDARDS FOR THE DEEP SPACE NETWORK

Peter R. Dachel, Roger F. Meyer, Samuel M. Petty, Richard L. Sydnor Jet Propulsion Laboratory California Institute of Technology

ABSTRACT

JPL has been operating two experimental hydrogen maser frequency standards at the Deep Space Network (DSN) stations at Goldstone, California since 1970. Based on operating experience gained with these units and with a test bed maser system at JPL, a field operable production maser has been developed for use in the DSN. The first maser of this new design was installed at the DSN 64meter station near Canberra, Australia in December 1975. Second and third units are presently under construction for the remaining DSN 64-meter stations at Madrid, Spain and Goldstone, California. While these DSN masers remain similar in basic configuration to the earlier experimental units, many design changes have been incorporated in both physics and electronics systems to effect improvements in the following areas: 1) short and long term frequency stability, 2) RF isolation of maser output lines, 3) lifetime of active physics components, 4) automatic fault detection and location, and 5) performance and reliability of the receiver/synthesizer system. Frequency stability measurements of the DSS 43 maser, using an updated experimental maser as a reference, resulted in a fractional frequency stability of 3.8×10^{-15} long term (T = 90 seconds) and 1.1×10^{-13} short term ($\tau = 1 \text{ second}$).

INTRODUCTION

In 1965, the Jet Propulsion Laboratory (JPL) initiated a development program for a field operable hydrogen maser to meet the future requirements of the Deep Space Network (DSN). Two experimental hydrogen masers (Ref. 1) were subsequently built and installed at the DSN stations at Goldstone, California during 1970. Based on operating experience gained with these units and with a test bed maser system at JPL, a prototype hydrogen maser was recently developed for use in the DSN. This paper describes some of the unique features of this maser, and presents life expectancy, frequency stability, and other

performance data obtained to date.

The DSN hydrogen maser (Fig. 1) consists of two assemblies; a physics unit and an electronics rack. The physics unit is mounted on a shockabsorbing base and consists of the maser vacuum system, microwave front end, and four electronics modules that are associated with the hydrogen glow discharge. All other electronics, including the operating controls for the physics unit, are contained in the electronics rack.

PHYSICS UNIT

A simplified cross-sectional diagram of the physics unit is shown in Figure 2, and characteristics are listed in Table I.

High Output Power

Maser frequency stability in the time interval $0.1 - \tau - 10$ seconds is primarily determined by maser signal/noise ratio, and therefore maser output power. The DSN requirement is such that an output power level of at least -90 dBm is needed (see Figure 5) This is achieved by increased hydrogen flow rate at the expense of ion pump element lifetime and hydrogen spectral line broadening. The DSN maser has a nominal power output of -88 dBm at an operating hydrogen pressure of 10^{-6} Torr. Ion pump lifetime is calculated to be 3 years at this pressure.

Long Term Stability Without Cavity Tuning

For maximum reliability, it was decided that the long term frequency stability specification (time interval $\tau \ge 30$ seconds) should be met without the aid of the automatic cavity tuner. This constraint, and the large hydrogen linewidth caused by high flux operation, placed stringent requirements on 1) the frequency stability of the RF cavity, and 2) the stability of the hydrogen flow rate.

These requirements were satisfied in the DSN maser (see Figure 2) by 1) surrounding the RF cavity with a temperature regulated oven placed inside the vacuum, 2) providing low thermal conduction standoffs between RF cavity, inner oven, vacuum housing, ion pump, and support frame interfaces, 3) use of low temperature coefficient Cer-Vit¹ in the RF cavity assembly, 4) surrounding vacuum housing, microwave front end, and ion pump with thermal insulation, and 5) maintaining a stable hydrogen flux level by closed loop control of the palladium valve with an oven-stabilized Pirani pressure gauge.

¹Trademark of Owens-Illinois Corp.

Maintenance

The separation of physics and electronics functions permits maximum access to the physics unit for maintenance, troubleshooting, etc. Components have been grouped into replaceable modules or assemblies wherever possible. Viton O-ring seals are used throughout and have proved satisfactory.

The time required for two field technicians to replace any physics unit component (excepting the ion pump body), and then again achieve vacuum, is one day or less. Perhaps the most complex and time consuming maintenance task would be replacement of an RF cavity component. This job requires one full day for disassembly and reassembly, and does not require hoists or other mechanical aids.

The repair of the physics unit requires specialized knowledge and skills which are not available in the DSN repair facility as yet, so development personnel normally will travel to the field station to make repairs of items inside the vacuum housing. All other repairs and maintenance will be handled in the normal manner.

The most lengthy portion of a maintenance task is the time necessary for the maser to reach thermal equilibrium after reassembly is completed and vacuum pumping is resumed. If the inner oven can remain on during maintenance (as in replacement of ion pump elements, hydrogen source assembly, palladium valve, Pirani gauge, or any electronics assemblies), long term stability is obtained a few days after initial vacuum pumpdown. If, on the other hand, the vacuum housing must be opened, then the inner oven must be baked out at elevated temperature during pumpdown, and 4 to 5 weeks are required to obtain normal long term stability (use of autotuner can possibly reduce this time).

Life Expectancy

A number of physics components have displayed limited life expectancy in the past, and efforts to increase these figures have been a continuing goal. One purpose of the two experimental masers operating at Goldstone has been to evaluate the operating life of various components which are destined for use in the DSN maser. The results of these tests are described below:

At JPL, quartz storage bulbs are prepared by applying a single coat of FEP/TFE teflon mixture. After coating, they have not shown degradation as a function of time or number of exposures to air. The bulbs in the two experimental masers have each accumulated five years of operating time (and numerous exposures to air) with no noticeable

degradation and no recoating necessary.

The hydrogen glow discharge bulbs in the two experimental masers have been operating $4\ 1/2$ years and $1\ 1/2$ years respectively since last cleaning. These bulbs have been exposed to air during many periods of maser modification and maintenance.

The palladium valves and copper plated RF cavities in the experimental masers have not shown degradation in 5 years of operation.

Ion pump lifetime is calculated to be 3 years for the present output level of $-88~\mathrm{dBm}$. The experimental masers have logged 2 $1/4~\mathrm{and}$ 1 $3/4~\mathrm{years}$ respectively.

Reliability

The single DSN maser now in the field has experienced two failures. Immediately after installation, electrical vacuum feedthru seals, which rely on epoxy for the seal bonds, developed vacuum leaks. Temperature cycling of other units proved these seals to be unreliable. New non-magnetic seals of tungsten-glass and alumina are now being evaluated to solve this problem. Also, a matching capacitor in the glow discharge RF circuitry failed. This is the first failure to occur in more than 13 years of accumulated hours among 5 units. This failure is not believed to be design-related.

ELECTRONICS RACK

The power, control, receiving, synthesis, status, and alarm functions are provided by the electronics rack (Fig. 3) which contains 32 precalibrated plug-in assemblies that can be easily serviced by field technicians.

Physics Unit Control and Monitoring

The upper half of the electronics rack (Fig. 4) contains ten plug-in control modules and the ion pump power supply. These units provide all monitoring and control functions for the physics unit. (Two other modules in this group, "Status Indicator" and "Autotuner," will be discussed separately.) Table II lists the various functions of these modules.

Status and Alarm System

Many control modules generate alarm signals if operating parameters exceed pre-set limits. The Status Indicator module displays these alarms in three forms: 1) a dynamic indication which is on only when the alarm condition exists, 2) a "latched" indication which remains

on until a field technician notes the problem and resets, and 3) an audible alarm which is derived from the "latched" indication. The particular subsystem which is, or was, in an alarm condition is identified on the front panel.

Automatic Cavity Tuner System

The automatic cavity tuner ("Auto-tuner") uses an available station rubidium, cesium, or second hydrogen maser standard as a reference, and has a resolution of 0.004 seconds per 100 second period $(\Delta f/f=4\times 10^{-15}~\rm for~100~\rm MHz~inputs)$. It produces a varactor correction voltage proportional to the observed tuning error (integrated). The desired system loop gain is switch-selected and the linear drift component of either the maser or reference standard does not affect the output. The auto-tuner has the ability to ignore unusually large or "noisy" counts, and can provide an alarm of this occurrence.

It was decided that neither the maser frequency, nor the reference frequency (usually a station rubidium or cesium standard multiplied to 100 MHz) should be offset by the required 0.01 Hz necessary for auto-tuner operation. Therefore, an offset frequency generator is being developed at JPL which synthesizes, for auto-tuner use, a signal precisely 0.01 Hz offset from the standard maser 100 MHz output. It is expected that this will be accomplished without significant degradation of the original frequency stability.

Additionally, the auto-tuner provides a valuable troubleshooting and monitoring capability to the station since it can be used off line to measure frequency stability (at τ = 100 seconds) between any two 5 MHz or 100 MHz inputs.

Phase-Lock Receiver

The triple-conversion phase-lock receiver consists of 18 standard DSN modules in the lower half of the electronics rack and the modified Dana synthesizer at the top of the rack. The synthesis section provides 24 standard outputs ranging from 0.1 MHz to 1400 MHz at 13 dBm and 70 to 100 dB isolation. The output frequencies are adjustable over a range of $\pm 2 \times 10^{-7}$ with a resolution of 7 x $\pm 10^{-18}$. Other specifications are listed in Table II.

Reliability

Major electronics failures during DSN maser production have occurred in three commercial components: the high resolution synthesizer, the 1400 MHz multiplier, and the ultra-stable low voltage power supplies. These problem areas have been dealt with by 1) JPL redesign and

testing assistance to the manufacturer, 2) JPL quality assurance and source inspection, and 3) a 2000 hour burn-in to aid in establishing a high confidence level.

PERFORMANCE

Frequency stability measurements for the early experimental hydrogen masers, and for the first DSN maser (using an updated experimental maser as a reference), are shown in Fig. 5. Only two measurements have been obtained thus far for the DSN maser: 1.1 x 10^{-13} for τ = 1 second, and 3.8 x 10^{-15} for τ = 90 seconds. Detailed characteristics for the physics and electronics units are shown in Tables I and II.

FIELD OPERATION

The physics unit is prepared for shipment by attaching a cover to the shock-absorbing mounting base. A battery pack inside the cover supplies power to the ion pump to maintain vacuum during shipment. Since the ovens are off during shipment, normal long term stability is not achieved until four weeks after turn-on. Upon installation at the station, power is obtained from a station-wide 120 VAC uninterruptable power supply system. The electronics rack is placed with other station electronic equipments where it is monitored by field technicians on a weekly basis. The physics unit is placed some distance away in an isolated area where vibration and magnetic interference are under control.

PLANS, PRESENT AND FUTURE

At the present time, the two experimental hydrogen masers continue to operate at Goldstone, California. The prototype DSN maser has been operating at the DSS 43 64-meter station near Canberra, Australia since December 1975. A second DSN maser was just completed and is undergoing testing at JPL. In 1977, it will replace the experimental maser located at the DSS 14 64-meter station at Goldstone. A third maser will be built and shipped to the remaining 64-meter station near Madrid, Spain (DSS 63) in late 1977. The second experimental maser (updated), which is mounted in a trailer, will continue to be used as a portable maser system available to all Goldstone stations.

Presently the DSN has committed hydrogen masers for use in the Jupiter/Saturn outer planet missions, Very Long Baseline Interferometry (VLBI) experiments, portions of the current Viking mission, and station time-sync calibrations. Each hydrogen maser installation will have an auxiliary back-up standard consisting of a modified, high performance Hewlett-Packard 5061A Cesium Standard. Each DSN hydrogen maser/cesium pair will interface with a microprocessor-based monitor and control

system. This system will monitor many operating parameters of both standards, periodically measure stability between the two standards, and make an automatic phase-coherent switchover (with time loss ≤ 10 nanoseconds) to the back-up standard in the event the on-line standard degrades beyond pre-programmed limits.

ACKNOWLEDGEMENT

The authors wish to make a special acknowledgement to Hubert Erpenbach, recently retired. Mr. Erpenbach was responsible for the successful solution of many physics problems, including the quartz bulb coating technique, RF cavity plating technique, and the long life hydrogen source asembly.

REFERENCE

1. C. Finnie, R. Sydnor, and A. Sward, "Hydrogen Maser Frequency Standard," in Proc. 25th Annual Symposium on Frequency Control, pp 348-351, April 1971.

TABLE I. PHYSICS UNIT CHARACTERISTICS (nominal unless otherwise stated)

UNLOADED CAVITY Q 55,000 min.

LOADED CAVITY Q 35,000

CAVITY Copper plated Cer-vit cylinder with aluminum

end plates and 250 gram quartz storage bulb

DISSOCIATOR POWER 125 MHz, 4 watts ave., 18 watts max.

COLLIMATOR 400 hole, 50 micron diameter per hole

BEAM SHUTTER 1 mA taut-band meter movement

STATE SELECTOR Hexapole permanent magnet, Alnico 8

ATOMIC LINE WIDTH 2 Hz

CAVITY POWER OUTPUT -89 dBm min.

SIGNAL TO NOISE RATIO 84 dB/Hz

ION PUMP CAPACITY 200 liters/second

ION PUMP POWER INPUT 4200 volts @ 2.4 mA

HYDROGEN PRESSURE 1×10^{-6} Torr VACUUM BACKGROUND 1×10^{-7} Torr

HYDROGEN SUPPLY 2.25 liters @ 1250 psig initial pressure

DC MAGNETIC FIELD 500 microgauss

MAGNETIC SHIELDS Quantity 4
Shielding Factor (dc) 1000

FIELD WINDINGS One main, two trim, 0 to + 10 mA

CAVITY TUNING Type

Coarse Mechanical 2.4×10^{-10} /turn 20 turns Medium Mechanical 1.5×10^{-11} /turn 20 turns

Fine Varactor $2.0 \times 10^{-12}/\text{volt}$ 10 volts max

TABLE II. ELECTRONICS UNIT CHARACTERISTICS

1.420405751 GHz Three-Conversion Phase-Lock Receiver

BANDWIDTH Preselector 30 MHz 20, 4 MHz I.F. 4 KHz Loop (2nd order) 100 Hz

INPUT SIGNAL LEVEL maximum -71 dBm FROM PHYSICS UNIT nominal -90 dBm minimum -110 dBm

GAIN CONTROL manual 39 dB automatic 20 dB

VCO FREQUENCY 100 MHz

NOISE FIGURE 4.0 dB

STABILITY $(\pm 5^{\circ}\text{C AMBIENT})$ 6 x 10⁻¹⁶

1.42 GHz PHASE NOISE 5 x 10⁻⁶ radians RMS/Hz (10 Hz off-

AGC AM to PM CONVERSION 0.16°/dB

PHYSICS UNIT MONITOR AND CONTROL

FRONT PANEL CONTROLS

Palladium valve temperature
Hydrogen discharge RF power level
Beam shutter attenuation
Magnetic field coil currents

Magnetic field coil currents Varactor voltage (manual mode)

QUANTITIES CONTINUOUSLY DISPLAYED

Ion pump current, voltage
Hydrogen discharge forward and
reflected power
Varactor voltage (dial calib.)
Magnetic field coil currents
(dial calibration)

(dial calibration) Maser output power

QUANTITIES AVAILABLE FOR DISPLAY ON MULTI-FUNCTION DIGITAL METER

Pirani gauge output level Oven currents Palladium valve heater current Beam shutter current Field currents

TABLE II (Continued)

QUANTITIES AVAILABLE TO REMOTE MONITOR AND CONTROL SYSTEM VIA REAR PANEL CONNECTOR All above plus: Oven monitor thermistor outputs Power supply voltages Etc.

OTHER FUNCTIONS

Palladium valve "open loop" (manual control) or "closed loop" (controlled by Pirani gauge)

Varactor diode "manual" (front panel digital control) or "automatic" (controlled by Auto-tuner)

Automatic turn-off of ion pump and/or palladium valve if certain potentially damaging failure modes occur

STATUS INDICATOR AND ALARM

Status and alarm system powered by self contained uninterruptible power supply (UPS) system.

UPS DURATION

12 hours

TRANSIENT SUPPRESSION DELAY

4 msec, up to 10 sec for some parameters

ALARM OUTPUTS

Audio, visual, and remote

MAIN ALARM OUTPUT

Green - operational Yellow - operational but degraded

Red - non-operational

SUBSYSTEMS AND FUNCTIONS MONITORED

Receiver lock Synthesizer lock I.F. level

Hydrogen glow discharge VSWR and temperature Hydrogen source pressure

Oven temperatures Ion pump power Auto-tuner

LIST OF FIGURES

- 1. DSN Hydrogen Maser.
- 2. Simplified Cut-away View, Physics Unit.
- 3. Electronics Rack.
- 4. Physics Unit Control Panel, Electronics Rack.
- 5. JPL Hydrogen Maser Frequency Stability.

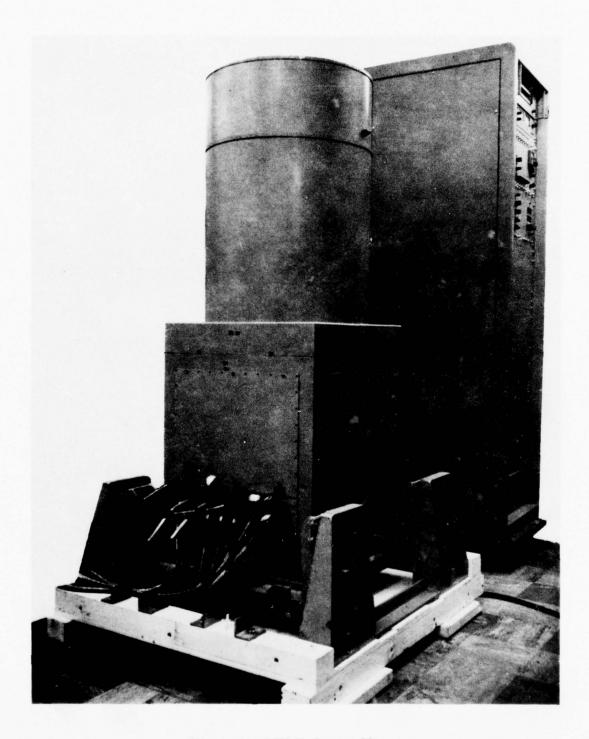


Figure 1. DSN Hydrogen Maser

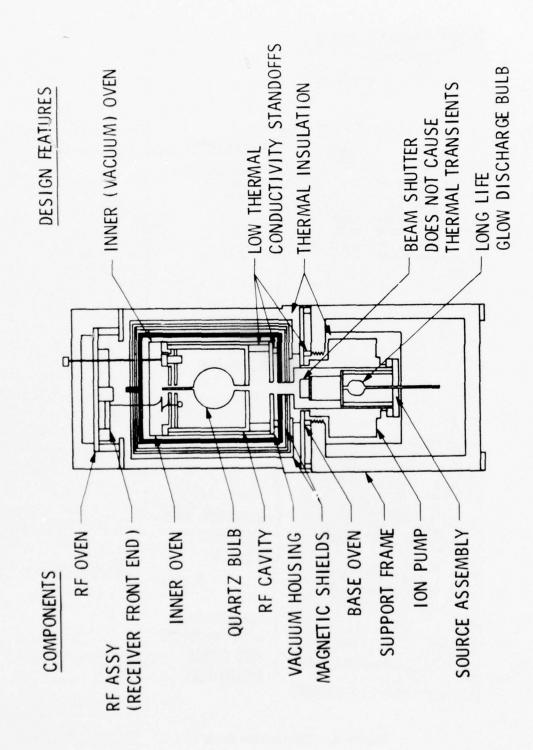


Figure 2. Simplified Cut-away View, Physics Unit

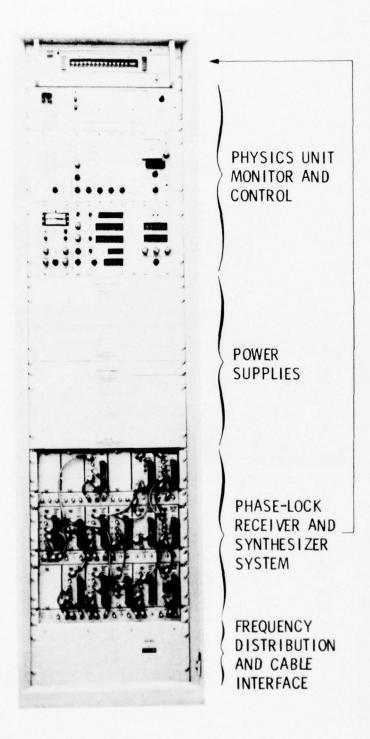


Figure 3. Electronics Rack

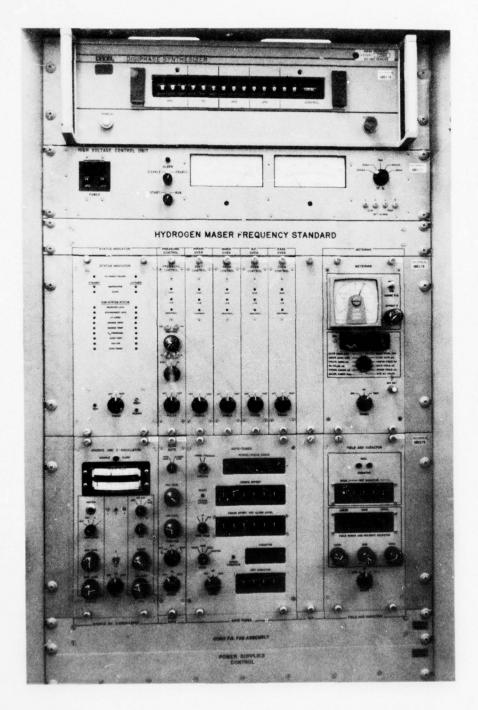
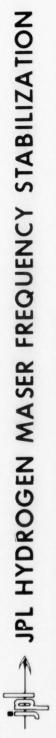


Figure 4. Physics Unit Control Panel, Electronics Rack



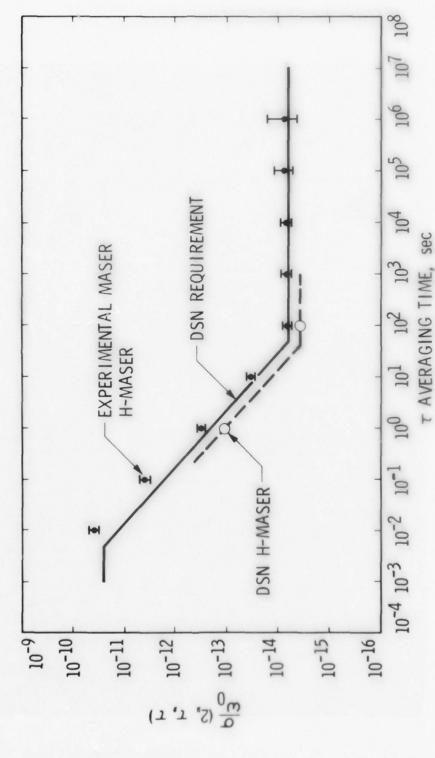


Figure 5. JPL Hydrogen Maser Frequency Stability

HYDROGEN MASER DESIGN AT THE LABORATOIRE DE L'HORLOGE ATOMIQUE

Pierre Petit, Jacques Viennet, Roland Barillet, Michel Desaintfuscien et Claude Audoin, Laboratoire de l'Horloge Atomique, Equipe de Recherche du C.N.R.S., Université Paris-Sud, 91405 Orsay France

ABSTRACT

A description is given of some specific features of the Laboratoire de l'Horloge Atomique masers, together with a discussion of the reasons of their choice. The performances achieved are given, with and without action of a classical autotuning system. Some possible improvements are also described.

INTRODUCTION

Besides two experimental hydrogen masers, two reference hydrogen masers are in operation at the Laboratoire de l'Horloge Atomique since 1972. Fig. 1 shows a schematic drawing of these masers, designed for operation in laboratory conditions. We describe their specific features and the performances obtained. The technical choices are discussed, as well as possible improvements.

SPECIFIC FEATURES OF THE REFERENCE MASER

Three major points will be considered: the production of the beam of atomic hydrogen, with a difference of population between the levels involved in the maser transition, the storage of the atoms in the microwave cavity, and the maser signal processing.

PALLADIUM PURIFIER

It is designed to give a fast response time to the hydrogen flow regulator, so that the dead time while the cavity is tuned by varying the beam intensity is very small.

a. Low thermal inertia palladium purifier The palladium-silver alloy, shaped as a glove finger, is heated directly (Fig. 2) $^{(1)}$. The hydrogen gas under high pressure (3 x 10 5 Pa (3 bars)) is located inside the palladium tube, so that the heat transfer to the surrounding is minimized. The working pressure of 7 Pa (5 x 10 $^{-2}$ torr) is obtained with a current of 2.5 A in the glove finger. The corresponding heating power is 0.4 W only; the measured thermal inertia of the palladium leak equals 4 s.

b. Source pressure regulator

A pressure gauge is made with a thermistor, with a small thermal inertia. A simple electronic system maintains constant the value of its electrical resistance, and therefore the value of its temperature for all the useful values of the hydrogen pressure. This electronic system provides to the thermistor the electric power which compensates its thermal losses. The heating current is alternating, with a frequency of 15 kHz, in order to avoid the drifts associated with the operation of a DC current pressure gauge. The emf of the source providing the power to the thermistor, which is a function of the hydrogen pressure, is detected at a high signal level and compared to an adjustable reference voltage in order to serve the heating current of the palladium leak and to maintain the source pressure at the desired level.

The time constants in the servo loop are the time constant of the palladium (4 s), the time constant of the pressure gauge (10^{-2} s) , the pumping time of the gas in the source (1.5 s) and the transit time of the gas between the palladium and the gauge (0.5 s).

c. Performances

Fig. 3 shows the response of this pressure regulator to steps of the reference voltage. The pressure, measured by the gauge, is established

within 20 s. This time could be reduced by a factor of 2 by decreasing the transit time of the hydrogen gas between the palladium leak and the discharge tube ⁽¹⁾.

The stability of the pressure source is quite good: the drift is smaller than 1 % per day for a working pressure of 13 Pa (0.1 torr).

HYDROGEN DISSOCIATOR

Molecular hydrogen is dissociated in a cylindrical discharge tube, 2 cm in diameter and 20 cm long. The mean time spent by a molecule in the discharge is long, so that its dissociation probability is very high.

The atomic beam is issued from a single cylindrical tube, coaxial with the discharge tube. This design is easy to implement, and does not significantly affect the directivity of the beam and the efficiency of the dissociation: the measured atomic concentration in the beam is of the order of 0.6 for a working pressure of 13 Pa (0.1 torr) (2).

STATE SELECTOR

The pole tips of the hexapole are shaped in order to fit the theoretical equipotential curves (3). The measured field repartition in the magnet is very close to the theoretical field repartition, as shown in fig. 4. Consequently, the effective diameter of the magnetic lens is very close to the physical diameter of the magnet, allowing an efficient use of the atomic flux issued from the source, and the optical properties of the magnetic lens can be calculated for a given velocity distribution in the beam (4).

CAVITY PULLING

In order to lower the cavity pulling effects, it is necessary, for a given atomic line width, to reduce the thermal coefficient of the cavity, to control its temperature, and to tune it properly.

a. Thermal compensation of the cavity

The cavity is made of quartz, with metallic compensation rods. The compensation is adjusted in order to be effective for the cavity loaded by the storage bulb. The cavity is enclosed in a thermal shield situated inside the vacuum tank. In a recent realization, the measured thermal coefficient is of the order of 0.1 kHz ${\rm K}^{-1}$.

b. Thermal control of the cavity

The temperature of the cavity is regulated within 10^{-3} K for 20 days and 10^{-2} K for four years.

The thermal control is provided by three concentric ovens; each of them being divided into three independently regulated parts:

- the magnetic shield n° 2 (the two end caps and the lateral wall). Its temperature is maintained at about 28° C.
- the magnetic shield n° 5 (the two end caps and the lateral wall). Its temperature is maintained at about 43° C.
- the copper tank enclosing the cavity. The lateral part of the tank and the upper part of the pumping tube are maintained at 48° C. The lower part of the pumping tube, made of stainless steel, is maintained at 35° C at the level of shield n° 2.

The separation between each magnetic shield is filled with a thermal insulator.

The microwave cavity itself and the storage bulb are thermally insulated from their enclosure, being supported by quartz posts. A cupper cup is set at the top of the pumping tube, in good thermal contact with the copper vacuum tank. It prevents, as much as possible, thermal radiation exchanges with lower parts of the maser. The time constant of the temperature variations of the cavity is 15 hours about.

The temperature sensors are thermistors, which are maintained in two opposite arms of a Wheatstone bridge.

The voltage produced by temperature fluctuations is amplified by a low drift operational amplifier and determines the duty cycle of a multivibrator. The period of the pulses is about 1 ms. Their width determine the heating power.

The output transistor of the circuit is used as a switch, and the power efficiency is very good.

The heating current feeds a resistive coaxial cable. The inner conductor is a thin copper wire. The outer conductor, also made of copper, is externally insulated with teflon. The cable is glued to the wall which is to be controlled. The thermistors are in good thermal contact with the wall, and as close as possible to the heating cable, in order to reduce the delay due to the heat propagation time.

We never observed any trouble in the maser operation due to the use of pulsed heating current when every conductor inside the magnetic shields is coaxial.

The performances obtained have been measured by the cavity pulling, using a cavity with a large thermal coefficient (1.5 kHz $\rm K^{-1}$), for the 1 mK stability over 20 days, and by a direct measurement of the cavity temperature, via a platinum resistance temperature transducer for the 10 mK stability over 4 years.

MAGNETIC FIELD

The atoms are shielded from spurious magnetic field variations by six magnetic shields, all made of mumetal, with a thickness of 2 mm. The fluctuations of the magnetic field which is applied to the hydrogen atoms, due to magnetic noise in the laboratory has been measured on an experimental maser equipped with similar shields. The measurement of the frequency stability of the field dependent $\Delta F = 1$, $\Delta m = 1$ transition (5) showed that the fluctuations are of the order of 10^{-11} T (0.1 microgauss) only.

COLLISIONS WITH RESIDUAL GASES AND WITH THE WALL OF THE STORAGE BULB

Collisions with paramagnetic gases may have important effects on the atomic frequency and relaxation times (6).

The best way to get rid of these spurious effects is to maintain as good as possible a vacuum. This is the reason why we use two vacuum pumps and two separate vacuum chambers, made of stainless steel or

copper (inside the magnetic shields). Only metallic gaskets are used.

MICROWAVE SIGNAL PROCESSING : ELECTRONIC CIRCUITS WITH NO SPURIOUS PHASE SHIFT ASSOCIATED WITH VARIATIONS OF THE SIGNAL LEVEL

When a hydrogen maser is used as a frequency or time standard, its cavity is tuned by the classical "frequency method" tuning. In this method, the atomic linewidth is modulated and the cavity is tuned in order to cancel any frequency modulation associated with the linewidth modulation. The level of the oscillation varies with the atomic linewidth. If the receiver introduces phase shifts related to the level of the signal, these phase shifts affect the short term frequency stability of the frequency standard.

Furthermore, the application of an alternative method for the cavity tuning critically depends on the use of electronic circuits showing, as far as possible, a level independent phase shift. In this application, the level correlated spurious phase shift must be smaller than a few 10^{-3} degree for amplitude variation of 3 dB.

These phase shifts are due to non linearities in bipolar transistors parameters and to thermal effects.

It has been shown ⁽⁷⁾ that the non linearities of the transistor parameters are proportional to the square of the voltage amplitude and to the phase lag in the considered circuit.

In low frequencies amplifiers, the thermal effects result of the variation of the electrical parameters of the transistors which are induced by the variations of the power dissipated in the transistors. This variation has a component in quadrature with the collector current, owing to the thermal inertia of the device. An amplitude dependent phase shift may result.

This effect can be avoided if the transistor is polarized for an mum (maximum) power dissipation: the fundamental of the parameters variations then disappears.

We have built 5.75 kHz amplifiers (Fig. 5) according to the following design rules:

- transistors with a large transition frequency are used
- the collector to base voltages are high enough to reduce the voltage dependence of the collector to base capacitor
- the high frequency cut-off is as large as possible, and the low frequency cut-off as small as possible
- the collector is polarized for the maximum value of the dissipated power
- feedback in the emitter circuit reduces the distorsion rate and linearizes the input impedance
- the output voltage must not be too large : the maximum amplitude is 1 V at 5 kHz and 0.1 V at 500 kHz.

On the other hand, it is known that phase comparators are not ideal devices and that a modulation of the amplitude of the signal induces a modulation in the D.C. output, even when the signal and the reference are very close to the quadrature condition. Consequently, the use in the phase-lock loop of an amplitude limiter showing a level independent phase shift is of prime importance when the maser oscillation level is modulated.

Such amplitude limiters, at a working frequency of 5.75 kHz, have been built (Fig. 6), according to the Franck's (8) analysis of the wave form dependent phase shift.

Various tests on amplifiers and amplitude limiters give confidence that the achieved amplitude correlated phase shift is much smaller than 10^{-2} degree for amplitude variations of 3 dB.

PERFORMANCES OF THE TWO REFERENCE MASERS

We have not yet performed a direct precise measurement of the wall shift in our reference masers. Such a measurement will be possible in a near future, using the double bulb device described later.

FREQUENCY STABILITY WITHOUT AUTOTUNING SYSTEM

The signals delivered at the output of the 1420 MHz low noise amplifier of the two reference masers are mixed and applied to the input stage of an electronic heterodyne receiver. After detection, the beat note is filtered in a low pass filter, with a bandwidth of 6 Hz. The difference in frequency between the two masers is set between 0.1 and 1 Hz by adjusting the magnetic field.

Fig. 7 shows a plot of the root mean square of the Allan variance of each maser, the statistical properties of which being assumed to be identical.

For each value of the averaging time τ , ($\tau < 10^4$ s) each experimental point is determined from a series of more than 100 samples. The uncertainty in the estimation of the Allan variance is then less than 10 % (9).

The fractional frequency stability is $4 \times 10^{-13}/\tau$ for 1 s < τ < 40 s and 3 x 10^{-15} for τ = 1000 s (for that last figure, 600 non selected data points of a continuous run have been used to compute the Allan variance). The daily frequency fluctuations equal a few parts in 10^{14} .

FREQUENCY STABILITY WITH AN AUTOTUNING SYSTEM

A classical autotuning system has been built and tested. The frequency of the 5 MHz quartz crystal, phase locked to the maser under tuning, is measured for high flux and low flux.

The difference between the two results is used to tune the cavity. In this device, the frequency is not measured while the flux changes (the dead time equals 30 s, which is longer than the time needed for the pressure change in the source).

Fig. 7 shows the frequency stability of the phase locked 5 MHz quartz crystal oscillators multiplied up to 400 MHz. The frequency stability measurement data are taken continuously, even when the flux is varying, and without correlation with the atomic flux modulation. The short term frequency stability could be improved by using better frequency multi-

pliers in the phase lock loop.

POSSIBLE IMPROVEMENTS

ADIABATIC RAPID PASSAGE

This device, which reduces the spin exchange relaxation rate without affecting the density of useful atoms in the bulb has been successfully tested in the past in an experimental maser (10)

PHASE METHOD FOR THE TUNING OF THE CAVITY

It has been shown ⁽⁵⁾ that if the level of the maser oscillation is varied, without affecting the atomic linewidth (for instance, by varying the beam composition without affecting the total beam flux), the phase of the maser oscillation varies, unless the cavity is tuned to a particular value.

$$\Delta\omega_{(\Delta\phi=0)} = 2 \epsilon_{\rm H} \gamma_{\rm 2e} \tag{1}$$

where $\epsilon_{\rm H}$ = (4.04 ± 0.35) 10⁻⁴ at room temperature ⁽⁶⁾. $\epsilon_{\rm H}$ is the parameter describing the effect of the duration of hydrogen-hydrogen spin exchange collisions ⁽⁶⁾, and $\gamma_{\rm 2e}$ is the transverse relaxation rate associated with spin exchange.

On the other hand, the classical linewidth method tuning leads to an oscillation angular frequency $\omega_{(\Delta F=0)}$ which differs from the atomic angular frequency by the quantity :

$$\Delta\omega_{(\Delta F=0)} = -2 \epsilon_{H} \gamma_{20}$$
 (2)

where $\gamma_{20}^{}$ is the transverse relaxation rate not depending on the atomic density in the storage bulb.

The values $\Delta \omega_{(\Delta F=0)}$ and $\Delta \omega_{(\Delta \varphi=0)}$ can be measured within 10 % since $\epsilon_{\rm H}$ is known within this error (6) and γ_{20} and γ_{2e} can be measured with

an uncertainty of a few percents $^{(11)}$. This uncertainty on the value of $\Delta\omega_{(\Delta F=0)}$ and $\Delta\omega_{(\Delta \varphi=0)}$ leads to a relative uncertainty of a few parts in 10^{14} on the maser frequency.

Consequently, the phase method can be used as well as the classical method. One must keep in mind that the oscillation frequency of the maser tuned by the phase method slightly depends on the density in the bulb: a γ_{2e} fluctuation of 0.1 s⁻¹ leads to a fractional frequency fluctuation smaller than 1 part in 10¹⁴ at room temperature.

The difference between the two frequencies $\omega_{(\Delta \varphi=0)}$ and $\omega_{(\Delta F=0)}$ is :

$$\omega_{(\Delta \Phi = 0)} - \omega_{(\Delta F = 0)} = 2 \varepsilon_{H} \gamma_{2}$$
 (3)

(it is worth noticing that this formula could be used for a measurement of the $\epsilon_{_{\rm H}}$ parameter).

The phase method has been successfully tested: the modulation of the level of oscillation was obtained by modulating the beam composition. This was accomplished by switching on and off a DC current in a coil, coaxial to the beam, and located between the state selector and the storage bulb entrance. The period of the modulation was 4 s.

The experiment was made possible by the use of the electronic circuits described in the previous section.

The experimental results are shown in Fig. 8 where the phase variation $\Delta \phi$ is referred to the maser oscillation frequency of 1.42 GHz.

The origin of the horizontal axis is set at the frequency $\omega_{(\Delta\!F=0)}$ delivered by the maser tuned according to the classical method. The errors bars are determined from the level of residual noise affecting the measured voltage.

The line crosses the horizontal axis for $\Delta f/f_0 = (0.25 \pm 0.8) \times 10^{-13}$ whereas the fractional frequency shift should be 2.8 x 10^{-13} as given by equation (3). This apparent small discrepancy is likely connected to the joint effect of inhomogeneities in the static magnetic field and the microwave field (6) as already observed for the classical method of tuning of the cavity (12).

The fundamental advantage of the phase method should be a large reduction of the period of modulation (i.e. 4 s instead of 300 s when the beam intensity is modulated). Consequently, the flicker noise of frequency of a crystal frequency source, if used as a frequency reference in the autotuning system, would contribute to a smaller extent to the noise in the error signal which is used to tune the cavity.

DOUBLE STORAGE BULB DESIGN

The standard method for measuring the frequency shift due to the atomic collisions on the wall of the storage bulb consists in measuring the maser oscillation frequency as a function of the collision frequency by using bulbs of various diameters. It is also possible to vary the collision frequency by using a single bulb with a variable shape (13). These last devices imply the use of a flexible teflon sheet which is submitted to different stresses for the different configurations. We are studying a double configuration bulb without any flexible sheet and which allows a large variation of the collision frequency. Fig. 9 shows the principle of this bulb. The two collision frequencies are obtained, for a given temperature, for the two positions of the valve. They differ by a factor of 1.85.

The oscillation is maintained for the two positions of the plate, and for bulb and cavity temperature between 293 and 393 K with a good frequency stability.

This work has been sponsored by C.N.R.S. and B.N.M.

REFERENCES

- (1) J. Viennet, P. Petit and C. Audoin, Journal of Physics E : Scientific Instruments <u>6</u> 257 (1973)
- (2) M. Desaintfuscien, Revue de Physique Appliquée 2 235 (1967)
- (3) C. Audoin, Le Journal de Physique appliquée 26 71A (1965)
- (4) C. Audoin, M. Desaintfuscien and J.P. Schermann, Nuclear Instruments and Methods 69 1 (1969)
- (5) C. Audoin, J.P. Schermann, P. Grivet, Advances in Atomic and Molecular Physics 7 1 (1971)
- (6) S.B. Crampton and H.T.M. Wang, Physical Review A 12 1305 (1975)
- (7) R. Barillet and C. Audoin, C.P.E.M. Boulder 1976. To be published
- (8) R.L. Franck, Proc. of the IEEE 58 257 (1970)
- (9) P. Lesage and C. Audoin, IEEE Transactions on Instrumentation and Measurement IM-22 157 (1973); IM-24 86 (1975); IM-25 270 (1976)
- (10) C. Audoin, M. Desaintfuscien, P. Petit, J.P. Schermann, Electronics Letters 5 292 (1969)
- (11) M. Desaintfuscien, C. Audoin, Le Journal de Physique 35 829 (1974)
- (12) P. Petit, J. Viennet, R. Barillet, M. Desaintfuscien and C. Audoin, Metrologia 10 61 (1974)
- (13) D. Brenner, Journal of Applied Physics 41 2942 (1970)
 P.E. Debely, The Review of Scientific Instruments 41 1290 (1970)
 H.E. Peters, Proc. of the 29th Annual Symposium on Frequency Control 362 (1975) Fort Monmouth, N.J.

FIGURE CAPTIONS

- Fig. 1 Simplified representation of the structure of the masers
- Fig. 2 Mechanical assembly of the palladium-silver leak
- Fig. 3 Response of the pressure regulator to steps of the reference voltage
- Fig. 4 Measured magnetic field variations as a function of the distance to the axis of the hexapole magnet
- Fig. 5 Amplifier at 5.75 kHz with a gain of 40 dB
- Fig. 6 Basic circuit for amplitude limiter
- Fig. 7 Plot of the root mean square of the Allan variance
 - 1) for the reference masers without autotuning
 - 2) for the reference masers with an autotuning system
- Fig. 8 Experimental results for the test of the phase method for the cavity tuning
- Fig. 9 Double storage bulb set-up

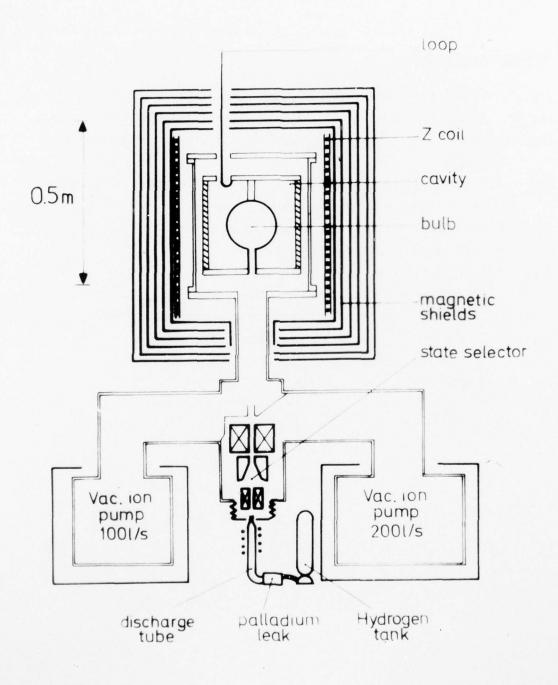


Fig.1_Simplified representation of the structure of the masers

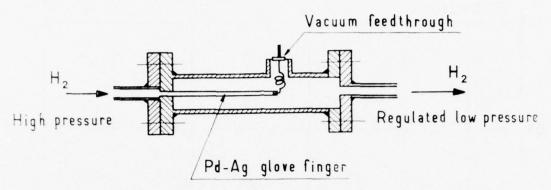


Fig 2 _ Mechanical assembly of the palladium-silver leak

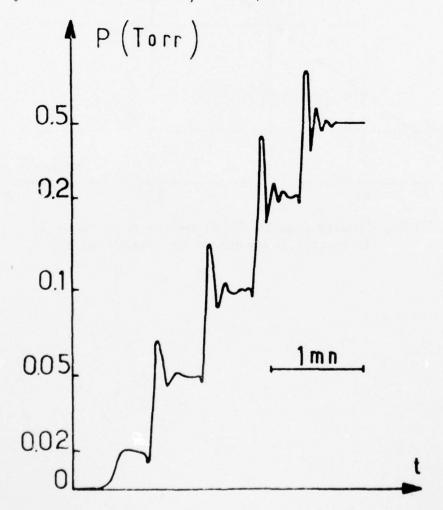
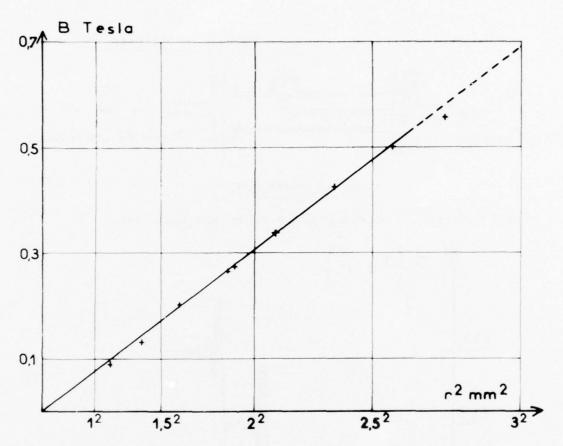


Fig. 3-Response of the pressure regulator to steps of the reference voltage



 $\label{eq:Fig.4} Fig. 4 \ \underline{\quad \text{Measured magnetic field variations as a fonction of the distance to the axis of the hexapole magnet}$

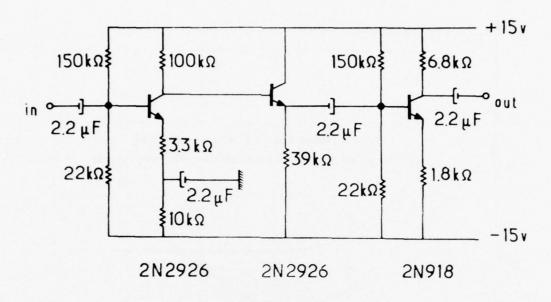


Fig.5 _ Amplifier at 5.75kHz with a gain of 40dB

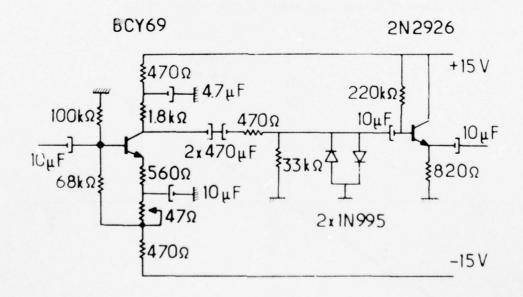
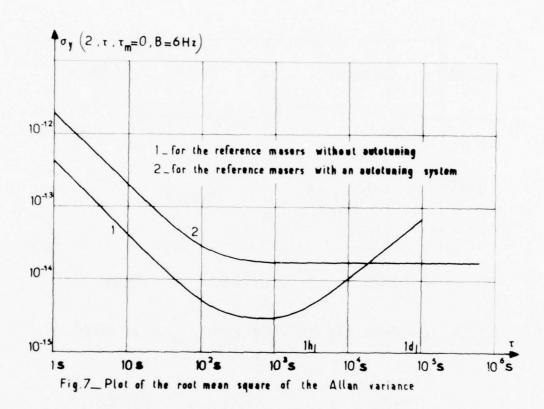


Fig. 6 - Basic circuit for amplitude limiter



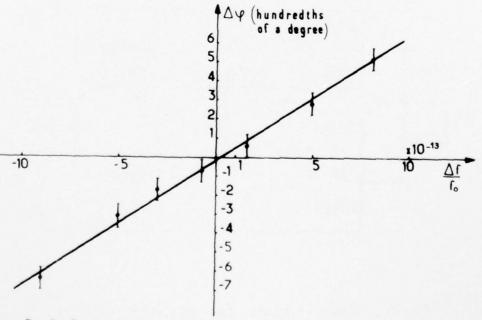


Fig. 8 _ Experimental results for the test of the phase method for the cavity tuning

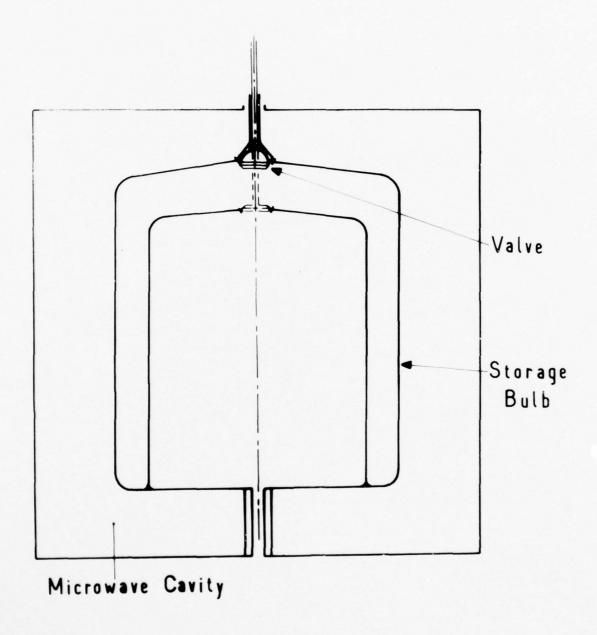


Fig.9 _ Double storage bulb set-up

A HYDROGEN MASER DESIGN FOR GROUND APPLICATIONS

M. W. Levine, R. F. C. Vessot, E. M. Mattison, E. Blomberg, T. E. Hoffman, G. Nystrom, D. F. Graveline, R. L. Nicoll, C. Dovidio, and W. Brymer, Smithsonian Astrophysical Observatory

ABSTRACT

A new hydrogen maser for ground-based applications has been designed at the Smithsonian Astrophysical Observatory. The mechanical, thermal, and electronics design philosophy of the VLG-II series is described, and comparisons with previous SAO masers are detailed. The VLG-II masers incorporate many of the lessons learned during the redshift rocket-flight program, in which a rugged, reliable, lightweight hydrogen maser was successfully operated after being boosted to an altitude of 10000 km by a Scout rocket. Preliminary test data and projections of stability performance are included, as well as photographs of the maser system during the construction phase.

THE EVOLUTION OF THE NEW VLG-11 MASERS

The design of the Smithsonian Astrophysical Observatory (SAO) ground masers and the SAO gravitational redshift space maser is the result of an unbroken evolution of ideas that began in 1960 shortly after the invention of the maser by Kleppner, Goldenberg, and Ramsey. In 1962, the National Aeronautics and Space Administration/Marshall Space Flight Center (NASA/MSFC) sponsored the development of hydrogen masers with the goal of producing a transportable self-contained device to serve as a frequency standard for ground-based operation. 2,3 This development continued and a spacecraft design was begun, the new goal being to measure the gravitational redshift by using a 24-hour ellip-

tically orbiting payload ⁴ launched by a Titan 3C system. The design later evolved into the VLG-10 and 10A masers after this initial entry into the field of relativistic measurements was temporarily abandoned owing to the high cost of the program.

In 1969, the development efforts, begun at Varian Associates and continued under Hewlett-Packard at Beverly, Massachusetts, were successfully transplanted to SAO in Cambridge, where the first of a series of VLG-10 masers was built for the U. S. Naval Research Laboratory and the radio-astronomy community for use in very long-baseline interferometry. In 1970, the redshift program was revived, and the former space-borne design was now embodied in nine VLG-10 and 10A masers, three of which were to be used as ground masers for the SAO/NASA redshift experiment. 5

The new redshift program has been enormously more demanding, in that the probe maser's weight had to be considerably less than 100 lb, in contrast with the 400-lb design for the previous program. The fourstage solid-fuel Scout rocket system, when separated from the fourth stage, has the ability to loft a 200-lb payload to 10000 km. This would provide a total time aloft of 2 to 3 hours and would attain a predicted redshift of some 4 parts in 10^{10} , 60% of the redshift available from the earth's gravity.

The flight maser was required to survive the trauma of a rocket launch and to operate within specifications immediately following burnout. The qualification model was therefore subjected to an intensive series of shock, acoustic, vibration, spin, and magnetic-field tests. During 9 months of testing, the probe maser was operated practically without interruption in preparation for its successful 2-hour mission in space, which took place June 18, 1976. Obviously, a complete rethinking of the space-maser design was necessitated, particularly because of the low weight and the very stringent mechanical constraints imposed by the Scout rocket system.

Again, as had previously occurred, many aspects of the design of the space maser found their way into the new design for the ground maser, now designated as the VLG-11. In particular, the vexing problem of RF dissociator failure that plagued the VLG-10 design in its early days has been rectified by using the probe-maser dissociator design. This design has been retrofitted to eight out of the nine VLG-10s now in use. The remaining one, having been in continuous operation since 1973, will be refitted in July 1977 as part of its modification to the VLG-10A configuration.

Another mysterious and equally vexing design problem with the VLG-10 has been the effect of barometrically induced stress on the cavity resonator through the motion of the bell-jar base. In 1974, the problem was rectified and by July 1977, all but two of the nine VLG-10 masers now in use will include the appropriate modifications. The VLG-11 series incorporates the mechanically rugged cavity designed for the flight maser, as well as the barometric-isolation system used in the VLG-10A masers.

DESIGN PHILOSOPHY OF THE VLG-11

The VLG-11 is housed in the same 22" x 30" x 52" cabinet used for the VLG-10 masers. The device is intended to be a stand-alone system, requiring 24 to 30 volts DC to operate and providing output frequencies at 60, 5, and 1 MHz. This package weighs 650 lb, is mounted on casters, and requires no special handling nor transportation facilities. Normally the package can be shipped cold if the time between available power is less than about 3 days. For longer times of transit or storage, a stand-by power supply for the ion pump is recommended.

The design emphasizes extreme ruggedness and mechanical stability, especially for the very critical cavity-bulb assembly, in order for the

maser to withstand high levels of shock and vibration during shipment without requiring cavity tuning. In addition to rugged construction, the cavity is made of CER-VIT, a material of unbeatable dimensional stability and long-term resistance to dimensional creep. A low thermal coefficient of the cavity resonator frequency is achieved by using CER-VIT-101, with a thermal coefficient of 2 to 5 x $10^{-7}/^{\circ}$ C. The major remaining contribution to thermal mistuning of the cavity has been found to be the temperature coefficient of the dielectric constant of the quartz storage bulb within the resonator. A typical value for the resonator-bulb combination for the VLG-10 series is

$$\frac{1}{f} \frac{\Delta f}{\Delta T} = -1000 \text{ Hz/°C}$$

By reducing the thickness of the bulb (but maintaining the stiffness-to-weight ratio), we have

$$\frac{1}{f} \frac{\Delta f}{\Delta T} = -300 \text{ Hz/}^{\circ}\text{C}$$

for the VLG-11 series masers without having to use any differential compensating mechanism that might be vulnerable to temperature gradients. By having intrinsically passive thermal stability in the most sensitive components, we believe we can then use thermal-control techniques effectively and thereby provide exceptional thermal stability for long periods of time. Figure 1 shows the cavity-bulb assembly for the VLG-11 maser.

Provisions are made for using an autotuner, which is highly recommended if tuning is to be done in the field by personnel who are inexperienced with hydrogen masers or if mechanical and thermal environmental circumstances are severe enough to require relatively frequent retuning.

^{*} Powens-Illinois.

PHYSICS PACKAGE DESIGN

In order to describe the design evolution from the VLG-10 and 10A masers to the VLG-11 maser, we present a series of sketches, starting with the inner cavity-bulb assembly. It will be seen that the differences are chiefly in the direction of more rugged structural and more careful thermal design and better magnetic shielding. The two major departures of the VLG-11 from either the VLG-10 or the space-probe maser are the lightweight bulb and the torrispherical magnetic shields.

Figure 2 describes the cavity-bulb assembly, including the output coaxial line and the isolator; the latter is properly part of the cavity resonator. Figure 3 shows the cavity structure and outlines the major load paths. Possible cavity-stress changes owing to the expansion coefficient of the external cylinder holding the cavity together are taken up by the Bellville washer. Similar thermally induced radial stress in the base is relieved by the rollers. Strains on the bell jar owing to barometric-pressure change are isolated from the cavity by the double-base structure.

The magnetic-shield oven assembly surrounding the ball jar is seen in Figure 4. Here the VLG-11 differs greatly from the VLG-10 and 10A, in that torrispherical shields have foam-glass insulation at their ends for support. These shields are under far less local stress than are the flat-ended outer shields and have much improved lapped joints at the lower cover (the upper cover is not removable). Figure 5 shows the magnetic shields. The VLG-11 solenoid follows the design used in the probe even though it is considerably larger in size. The multilayer printed-circuit design allows very complete cancellation of spurious magnetic fields and provides a rugged, close-fitting, and simple coil system located immediately inside the innermost magnetic shield. Figure 6 shows the VLG-11 solenoid.

Figure 7 illustrates the thermal-control system. Design experience with the space maser has shown us that temperature gradients are a problem that can be solved by including separate zones of thermal control for the bell jar and the oven. In addition, the pump-dissociator assembly is also controlled so as to stabilize the RF lines, the dissociator, and the isolator; this last item is located within the pump shields along with the temperature-sensitive electronics systems. The pump-dissociator assembly is temperature controlled by means of recirculated temperature-controlled air from a heat-added system and a heat exchanger, at the rear of the cabinet, that dumps unwanted heat to the ambient environment. Maximum added power of 14 watts is required to operate this system over an ambient-temperature range of 20° to 30°C.

The ion-pump manifold and the dissociator/state selector for the VLG-10, 10A, and 11 masers are shown in Figure 8. The source glassware for both items follows the space-maser design. The chief differences between this design and the initial VLG-10 design include the size of the dissociator glassware and the layout of the RF coil. Ever since these modifications were made, we have had no recurrence of dissociator failure. We believe that the improvement is the result of the change in dissociator size, from 1" diameter \times 1.4" long to 1.4" diameter \times 2" long, which increases the volume by a factor of 3. These dimensions coincide almost exactly with those used with excellent success by the Jet Propulsion Laboratory maser group. The ion-pump manifold and neck assembly is shown in Figure 9.

The VLG-11 RF oscillator includes a voltage regulator and an RF-level monitor. The condition of the discharge color's brightness, determined by studying the relative strengths of the atomic hydrogen Balmer- α (6562 Å) red line and an adjacent molecular-band spectrum, provides a measure of the dissociator efficiency.

DESIGN OF THE VLG-11 ELECTRONICS

All the electronics systems for the VLG-11 masers are of new design in both their circuitry and their packaging. Design aspects of particular significance are discussed in the following sections.

Phaselock Receiver

An RF preamplifier, immediately following the isolator, has been incorporated into the VLG-Il receiver. The noise figure of the amplifier is less than 5.0 db, which compares very favorably with the 10.0-db noise figure at the balanced-mixer input of the earlier VLG-IO receivers. The preamplifier is temperature controlled within the isolator enclosure to help stabilize the input impedance so as to present a more constant impedance at the isolator output.

A first IF frequency of 340 MHz has been selected to permit the use of a low-Q image-rejection filter at the input to the first mixer. This filter removes the noise contribution at the image frequency and further improves the effective noise figure of the receiver.

The output frequency of the master crystal oscillator at the receiver is 60.0 MHz, which is multiplied to 1080 and 360 MHz for the first and second local-oscillator frequencies, respectively, and divided to 20, 5, and 1.0 MHz for the third local-oscillator frequency and for utility outputs. Buffered isolated outputs are provided at 360, 60, 5.0 (two independent outputs), and 1.0 MHz.

The upper unit in Figure 10 is the receiver package, shown mounted into the maser frame. The large square box in the right center of the receiver is the oven-controlled multiplier-divider assembly. The IF amplifier, buffer amplifiers, and phaselock circuits are located in the shielded plug-in modules to the left of the oven.

NATIONAL AERONAUTICS AND SPACE ADMINISTRATION GREENB--ETC F/6 14/2 AD-A043 856 PROCEEDINGS OF THE ANNUAL PRECISE TIME AND TIME INTERVAL (PTTI) -- ETC(U) 1977 UNCLASSIFIED NASA-6SFC-X-814-77-149 NL 4 of 8 AD 43856 1000 100 00 4

Digital Synthesizer

The digital synthesizer for the VLG-11 maser has been specifically designed for maser applications. It is tunable from 405750.000 to 405753.999 Hz in discrete steps of 0.001 Hz. The synthesizer concept combines both direct and indirect synthesis techniques. The four tunable digits are generated by divide-by-N phaselock loops, which are carefully designed to minimize spurious outputs. All reference carrier frequencies are 5 kHz or greater to simplify the problem of suppressing reference-frequency modulation of the loop's voltage-controlled oscillator.

All the digital logic within the synthesizer is CMOS, offering the twin advantages of very low power consumption and freedom from switching transients. The highest internal frequency within the synthesizer is 5.0 MHz, the clock signal. The absence of high-frequency signals simplifies circuit-board and backplane wiring and permits the use of card extenders for servicing.

The digital synthesizer requires approximately 6 watts at +28 volts for operation and can be operated directly from an emergency battery system. The short-term stability of the synthesizer has been measured at 4 \times 10 $^{-13}$ for a 100-sec Allan variance, which corresponds to an overall maser-system contribution of approximately 1.2 \times 10 $^{-16}$ at 100 sec. It should be noted that these stability measurements indicate only an upper bound — instrumental limitations establish a noise floor at about 1 \times 10 $^{-13}$ for our measurements at 405 kHz.

Figure 10 shows the mechanical packaging of the synthesizer, directly below the receiver unit. Five of the seven individually shielded printed-circuit boards are shown installed. Each shielded module can be operated on a board extender to facilitate troubleshooting and servicing.

Maser Control Systems

Exhaustive thermal testing of the probe maser clearly demonstrated that thermal gradients along the vacuum tank are the primary contributor to the ambient-temperature sensitivity of the maser cavity. Increased thermal gain or improved preamplifier stability alone is ineffectual in attacking this problem; however, division of the tank (and oven) surface into independently sensed and controlled zones has shown itself to be a powerful technique for minimizing gradient problems. Accordingly, the vacuum tank is divided into three zones - dome, cylinder, and base each of which has its own sensing thermistor, amplifiers, and heater windings. Each zone can respond independently to external thermal loads without materially affecting the temperature of other zones. To minimize the thermal stress on the vacuum-tank controllers, the oven is divided into a dome-cylinder zone and a base zone; each of these is independently controlled. The isolator-preamplifier box is a separate thermal zone. making a total of six distinct thermal-control zones. The circulating air, which controls the temperature of the pump, the dissociator, and the upper maser electronics, is an entirely independent system with selfcontained sensors and electronics.

Hydrogen for operation of the dissociator is furnished from a two-liter gas bottle pressurized to approximately 100 psi. The relatively low pressure permits the use of a small, thermally agile palladium valve. Hydrogen pressure within the dissociator is sensed by a thermistor Pirani gauge, which is incorporated into a resistance bridge along with an identical thermistor that senses the high-vacuum side of the pumping system. The bridge output, which is independent of ambient temperature variations to first order, drives a servo system that controls the dissociator pressure by varying the temperature of the palladium valve.

The pressure and thermal-control electronics are housed in a controller assembly mounted on the maser cabinet frame. The controller

assembly can be seen at the top of Figure 11, with one of the individually shielded printed-circuit boards plugged into the back plane. The critical preamplifiers for the three zones of the vacuum-tank heater are located within the maser physics package in the thermally controlled upper maser electronics assembly. Figure 12 shows the controller assembly swung out on its hinges. The hinge arrangement permits convenient access to the rear of the assembly for maintenance and service without interruption of power or signal.

A rear view of the maser (Figure 13), taken early in the fabrication phase, shows the power-amplifier assembly, which mounts the power transistors for the thermal and pressure controls.

Monitoring System

The VLG-11 provides front-panel analog metering for 32 functions. All metering, including eight receiver/synthesizer functions, is centralized on the monitor panel, which is visible at the top of the rack in Figure 11. LED lamps provide a quick-look indication of the status of the subsystems, while a small LED numerical readout continuously displays the four least-significant digits of the synthesizer output frequency.

In addition to the conventional panel meter with selector-switch monitoring, the VLG-11 provides an internal telemetry system. Thirty-one channels of voltage or current data are normalized to a standard 0- to +5.0-volt range, buffered, and brought out to a 61-pin cylindrical connector on the front panel. In addition, five monitoring thermistors are accessible through this connector to permit convenient measurements of vacuum tank and oven temperatures.

PERFORMANCE AND STABILITY DATA OF THE VLG-10A AND EXPECTED DATA FROM THE VLG-11 MASER

VLG-10A Data

The most critical environmental tests on VLG-10A masers published so far have been made under the direction of Dr. A. Rogers of Haystack Observatory using two VLG-10As and a Goddard NP series maser. 7 The following parameters, taken from that publication, are for the SAO VLG-10A maser serial number P-4:

Temperature:

Comments

$$\frac{1}{f} \frac{\partial f}{\partial T} \sim -5 \times 10^{-14} / ^{\circ}C$$
 ~ 1 -day time constant

Pressure:

$$\frac{1}{f} \frac{\partial f}{\partial P} < 1.7 \times 10^{-14} / \text{"} \text{ Hg}$$

 $\frac{1}{f} \frac{\partial f}{\partial P} < 1.7 \times 10^{-14} / \text{" Hg}$ beyond limit of sensitivity for 0.15" Hg pressure modulation

Magnetic field:

$$\frac{1}{f} \frac{\partial f}{\partial B} \sim 1 \times 10^{-12}/\text{gauss}$$

Stability data are shown in Figure 14.

VLG-11 Data

From data obtained from tests on the VLG-11 maser during assembly, we can make the following projections about systematic effects:

A. Thermal insensitivity will be improved by a factor of at least 3, since the intrinsic thermal sensitivity of the cavity-bulb assembly has been found to be about 3 times lower, and we can also expect a considerable improvement from the thermal redesign.

- B. The axial shielding factor will see an improvement by a factor of about 1.6. Our tests on torrispherical shields indicate a 40% improvement in the ratio of axial to transverse shielding for a single shield. From operating tests of the physics package of the VLG-11 maser, we observe that we can operate the maser at a field of 0.350 mgauss (500-Hz Zeeman frequency). This allows a direct two-fold improvement in magnetic sensitivity, which, combined with the improved shielding factor, should yield a net improvement by a factor of 3.
- C. The modified VLG-10A cavity design exhibits a barometric-pressure sensitivity that is lower than can be measured adequately within the ambient-pressure range available at the Haystack Observatory. The VLG-11 cavity structure is more rugged and better isolated than the VLG-10A, as the strain relief of the attached coaxial cables has been improved, so we expect better performance from the new design. To verify the improvement in barometric sensitivity, a special chamber is under construction at SAO to permit testing over an ambient-pressure range of ± 0.0 to ± 2.0 " Hg (approximately 1 psig).
- D. Improvement of the noise figure of the maser receiver/synthesizer by a factor of about 5 will result from using a preamplifier with a 5-db noise figure instead of the 13-db effective noise figure of the diode mixer in the VLG-10A system. The short-term stability in the T^{-1} portion of the Allan variance, which is associated with additive white phase noise, will be reduced by $\sqrt{5}$, or about 2.

Figure 14 shows the anticipated performance of the VLG-11 with all the above factors taken into account.

ACKNOWLEDGMENT

This work was supported in part by Contract NAS8-27969 from the National Aeronautics and Space Administration.

REFERENCES

- D. Kleppner, H. Goldenberg, and N. Ramsey, Theory of the hydrogen maser. Phys. Rev., vol. 26, pp. 603-615, 1962.
- R. Vessot, Frequency stability measurements between several atomic hydrogen masers. In <u>Quantum Electronics III</u>, ed. by P. Grivet and N. Bloembergen, Columbia Univ. Press, New York, pp. 409-417, 1964.
- 3. R. F. C. Vessot, H. E. Peters, and J. Vanier, Recent developments in hydrogen masers. In <u>Proceedings of the 18th Annual Symposium on Frequency Control</u>, U.S. Army Electronics Command, Ft. Monmouth, N.J., pp. 299-307, 1964.
- 4. R. F. C. Vessot, M. W. Levine, L. Mueller, and M. Baker, Design of an atomic hydrogen maser system for satellite experiments. In <u>Proceedings of the 21st Annual Symposium on Frequency Control</u>, U.S. Army Electronics Command, Ft. Monmouth, N.J., pp. 512-542, 1967.
- 5. R. F. C. Vessot and M. W. Levine, Performance data of space and ground hydrogen masers and ionospheric studies for high accuracy frequency comparison between space and ground clocks. In Proceedings of the 28th Annual Symposium on Frequency Control, U.S. Army Electronics Command, Ft. Monmouth, N.J., pp. 408-414, 1974.
- 6. R. F. C. Vessot and M. W. Levine, A preliminary report on the gravitational redshift rocket-probe experiment. In <u>Proceedings of the Symposium on Experimental Gravitation</u>, Pavia, Italy, in press.
- 7. A. E. E. Rogers and A. R. Whitney, A comparison of various hydrogenmaser frequency standards. In <u>Proceedings of the Eighth Annual</u> <u>Precise Time and Time Interval Applications and Planning Meeting</u>, U. S. Naval Research Laboratory (this volume).

FIGURE CAPTIONS

- Fig. 1 VLG-11 cavity-bulb assembly.
- Fig. 2 VLG-10A and VLG-11 cavity-bulb assembly.
- Fig. 3 VLG-10A and VLG-11 cavity structure and stress load paths.
- Fig. 4 VLG-10A and VLG-11 magnetic shields and oven assembly.
- Fig. 5 VLG-11 magnetic shields.
- Fig. 6 Two-sided printed-circuit solenoid for VLG-11 maser.
- Fig. 7 VLG-10 and VLG-11 thermal-control system.
- Fig. 8-VLG-10 and VLG-11 ion-pump vacuum manifold and dissociator state selector.
- Fig. 9 VLG-11 ion-pump and neck assembly.
- Fig. 10 VLG-11 receiver and synthesizer.
- Fig. 11 VLG-11 maser front view.
- Fig. 12 VLG-11 maser front view showing electronics assemblies opened for inspection.
- Fig. 13 Rear view of VLG-11 maser showing power-amplifier assembly and heat sink.
- Fig. 14 VLG-10 maser stability data and projected VLG-11 performance. Error bars show the spread between a number of individual data sets. Crosses are for a single data set.

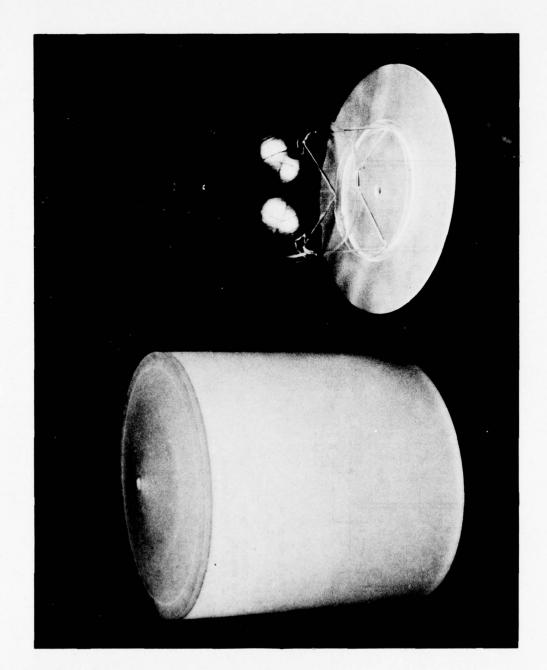
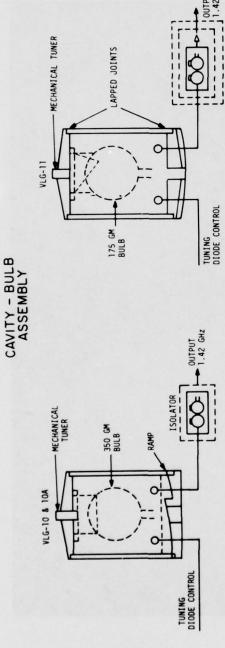


Fig. 1 VLG-11 cavity-bulb assembly.



CERVIT-101
LENGTH CUT TO ACCOMODATE BULB
CERVIT-107
LENGTH CUT TO ACCOMODATE BULB
ELOST COMPANIES TO TO TO ACCOMODATE BULB
ENDS LEPPED OVER TOTAL CIRCUMFERENCE
7" SPHERE — TEFRAHEDRAL STRUTS TO
CYLINDRICAL SKIRT
COATING 0.22" x 1.5" INTEGRAL COLLIMATOR
FEP TEFLON
BULB WEIGHT 175 GRAMS
MECHANICAL TUNER 200 KHZ
ELECTRONIC 7 KHZ DIODE INLOOP

QL ~ 42,000
QL ~ 42,000
QL NK 20,030
QL ~ 60,030
COOTO COAMIAL LINE
60 db 0.5 db LOSS
THERMALLY CONTROLLED — 2 LEVELS
MAGNETICALLY SHIELDED
20 db AMPLIFIER N.F. 4.5 db

 $_{8}^{01}$ $_{\sim}^{\sim}$ 35,000 LINE Q $_{\sim}$ 1.3 $_{\times}$ 10⁹ $_{8}^{0}$ $_{\sim}^{\circ}$ 0.3

CAVITY

TUNING COARSE ~ 10 MHz FINE (MECHANICAL) 100 KHz ELECTRONIC 15 KHz-0.5-10V DIODE IN LOOP FERRITE ISOLATOR 60 db 0.5 db LOSS THERMALLY CONTROLLED -1 LEVEL EXTERNAL MAGNETIC SHIELD

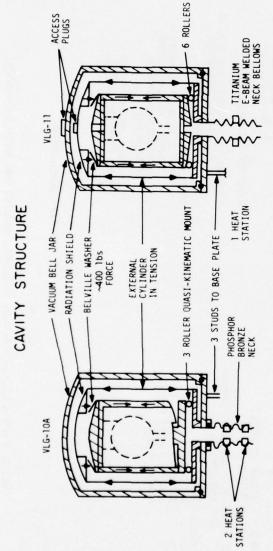
CONNECTION TO DIODE AND RF COUPLING 0.085" 0.0. COAXIAL

Fig. 2 VLG-10A and VLG-11 cavity-bulb assembly.

BULB 7" SPHERE-CYLINDRICAL SKIRT MOUNTING 0.22" x 1.5" INTEGRAL COLLIMATOR

COATING FEP TEFLON BULB WEIGHT 350 GRAMS

CAVITY MATERIAL CER-VIT 101
TUNABLE ON INTERRUPTED
THREAD



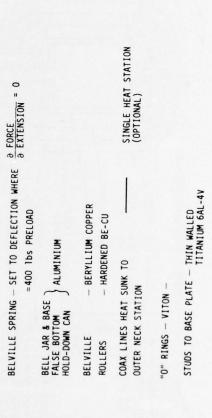
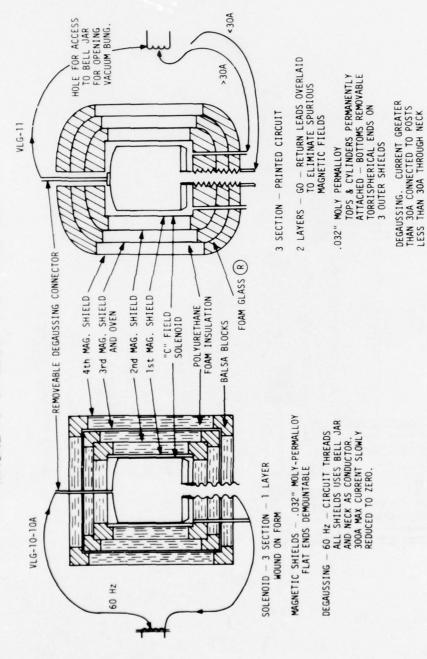


Fig. 3 VLG-10A and VLG-11 cavity structure and stress load paths.

MAGNETIC SHIELDS - OVEN ASSEMBLY



(R) PITTSBURGH-CORNING

Fig. 4 VLG-10A and VLG-11 magnetic shields and oven assembly.

Fig. 5 VLG-11 magnetic shields.

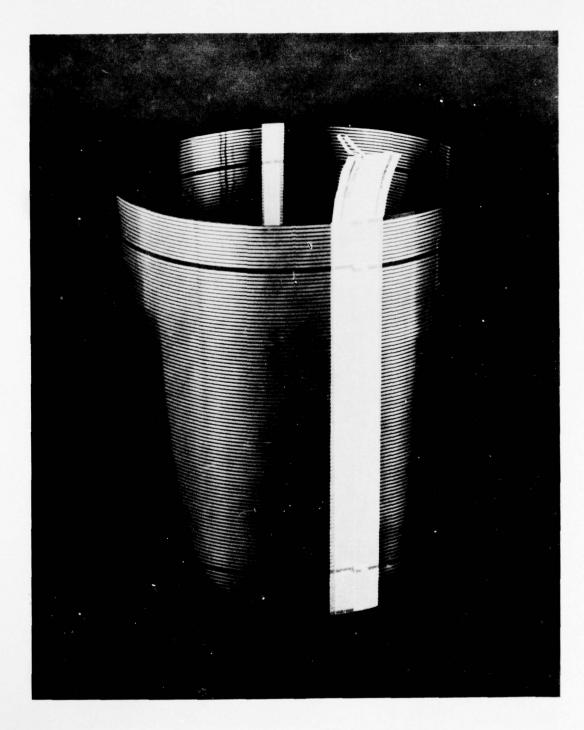
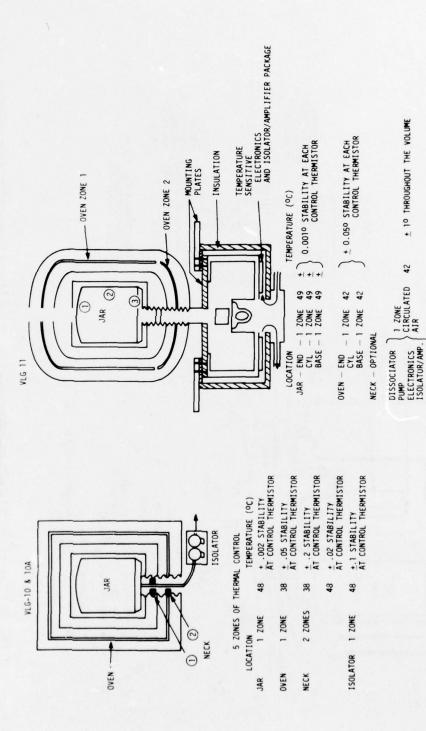


Fig. 6 Two-sided printed-circuit solenoid for VLG-11 maser.

THERMAL CONTROL



+ 0.01 STABILITY AT THE CONTROL THERMISTOR 49

ISOLATOR/AMP. 1 ZONE (WITHIN ABOVE ZONE)

Fig. 7 VLG-10 and VLG-11 thermal-control system.

+ 10 THROUGHOUT THE VOLUME

42

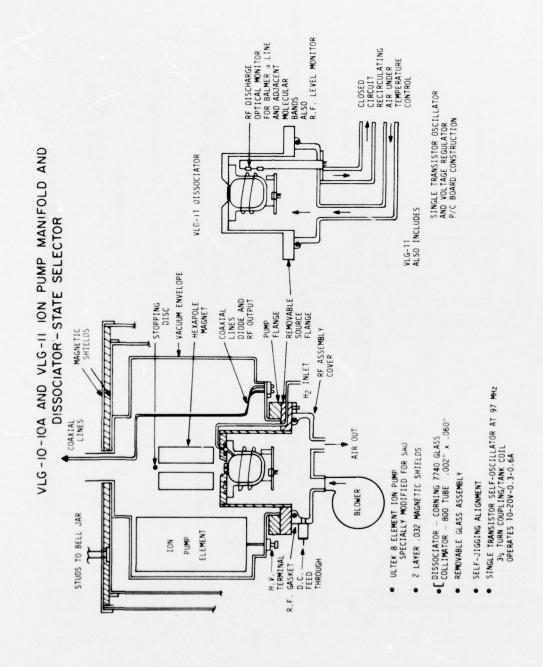


Fig. 8 VLG-10 and VLG-11 ion-pump vacuum manifold and dissociator state selector.

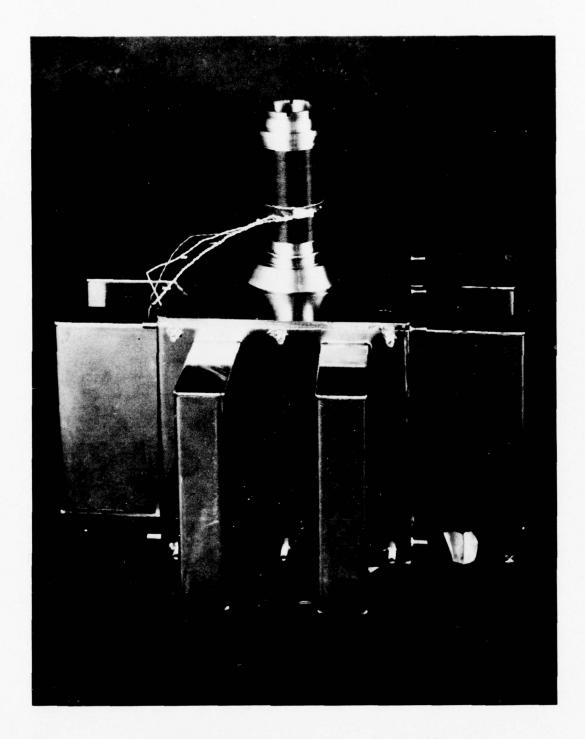


Fig. 9 VLG-11 ion-pump and neck assembly.

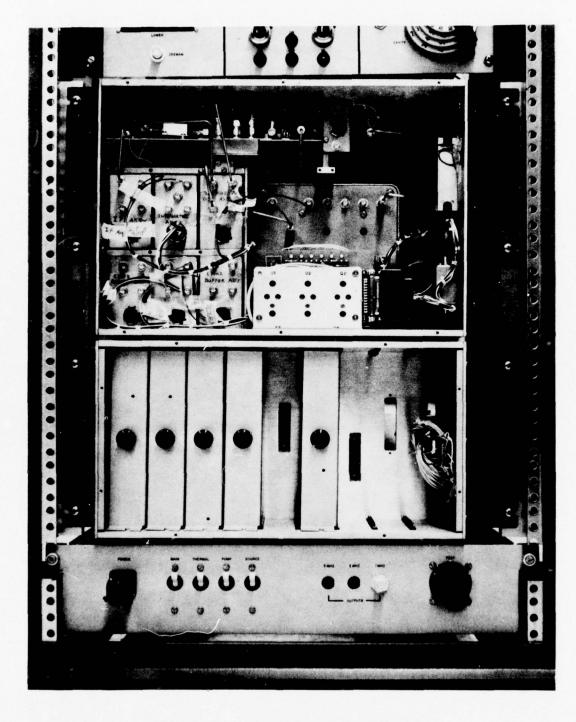


Fig. 10 VLG-11 receiver and synthesizer.

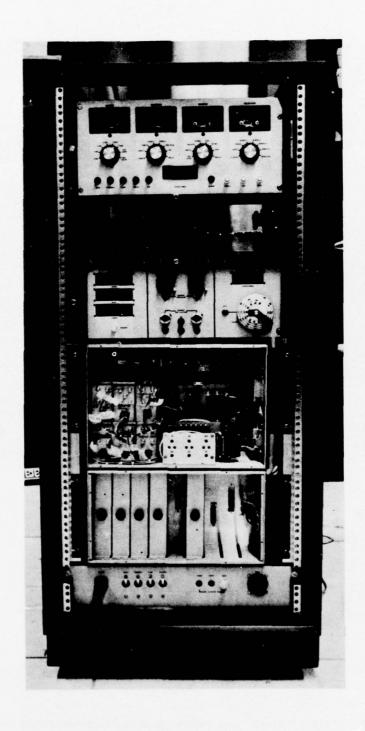


Fig. 11 VLG-11 maser front view.

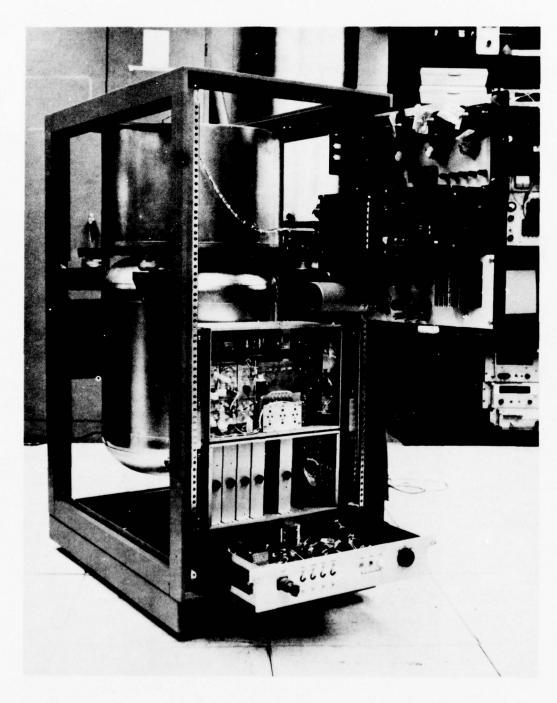


Fig. 12 VLG-11 maser front view showing electronics assemblies opened for inspection.

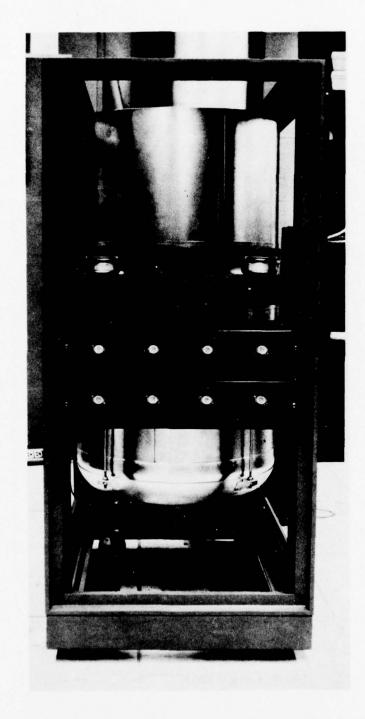
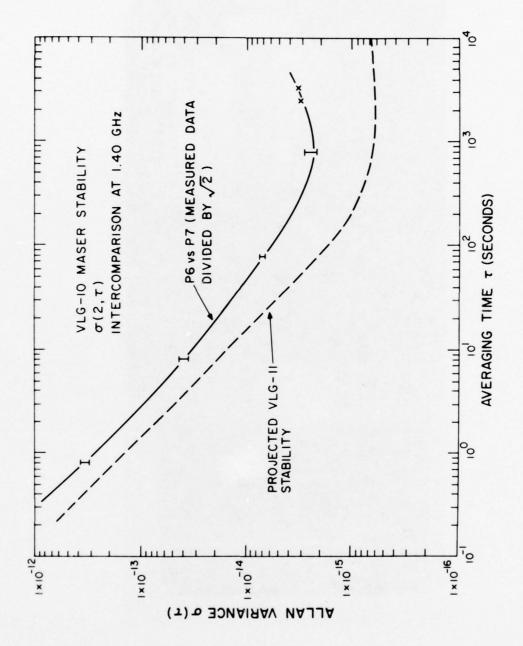


Fig. 13 Rear view of VLG-11 maser showing power-amplifier assembly and heat sink.



show the spread between a number of individual data sets. Crosses are for a single data set. Fig. 14 VLG-10 maser stability data and projected VLG-11 performance. Error bars

SPACE-BORNE HYDROGEN MASER DESIGN

R. F. C. Vessot, M. W. Levine, E. M. Mattison, T. E. Hoffman, E. A. Imbier, M. Tetu,* and G. Nystrom (Smithsonian Astrophysical Observatory),
J. J. Kelt, Jr., H. F. Trucks, and J. L. Vaniman (Marshall Space Flight Center)

ABSTRACT

The gravitational redshift rocket probe experiment, with a specially developed space-qualified hydrogen maser as the principal component of the payload, was successfully flown July 18, 1976. The experiment strategy and the requirements for the maser are reviewed, and the design features developed to meet the requirements are described. Stability data of the space maser taken during the flight with a three-link doppler canceling system are discussed.

INTRODUCTION

The objective of the gravitational-redshift experiment is to compare the rate of a space-borne clock (representing the "proper" clock of idealized relativity "gedanken" experiments) moving over a wide range of gravitational potential against a set of clocks in a constant gravitational potential. This experiment was realized June 18, 1976, by using a clock launched into space in a nearly vertical trajectory whose apogee altitude was about 10000 km. This paper will concentrate on the design aspect of the space maser used in that experiment.

The gravitational-redshift rocket-probe experiment was performed jointly by the Smithsonian Astrophysical Observatory (SAO) and the

^{*}Currently at Laval University, Quebec City, Canada.

George C. Marshall Space Flight Center of the National Aeronautics Space Administration (NASA/MSFC). At the present time, although the final data have yet to be generated, the experiment has successfully met its objectives. The following is an account of some aspects of the design of the maser for space and the rationale behind some technical decisions made to meet a very stringent set of environmental and weight restrictions. In addition, this paper serves to update an early description of the maser published in 1974 ; in the hardware description of that report, the fourth-stage rocket motor was still to remain attached to the spin-stabilized payload.

The gravitational-redshift rocket-probe experiment evolved from the originally proposed 24-hour eccentric-orbit experiment powered by a Titan 3C system²⁻⁴ in order to make use of the far more modest Scout D propulsion system. The experiment became a one-shot up-down comparison of a probe oscillator with a ground oscillator, and the strategy for the experiment became considerably more demanding than originally planned for the orbital mission.

From the dynamics of a body falling nearly vertically in the gravity field of the earth and from the known behavior of atomic hydrogen masers, we can establish a very rough optimum situation, based on the following considerations:

- A. Allow enough time aloft to stabilize whatever launch-induced perturbations may occur and minimize the effect of such thermal and mechanical perturbations so that the maximum possible stable operating time is available.
- B. Keep the payload in communication with the ground station throughout the mission, concentrating on obtaining data from apogee down to altitudes as low as possible at the end of the mission.

Owing to the 1/R gravity potential acting on a freely falling body, the time available for measurements near impact is a relatively insensitive function of the time aloft, and the strategy therefore is to obtain a minimum period of about 2 hours, attaining apogee redshift values greater than 4 parts in 10^{10} . The upward branch of the trajectory would also contain some data; however, because of the propulsion phase and payload stabilizing time, these data will be of less value than the data from the later, downward branch.

Obviously, no time would be available for the more conventional spacecraft outgassing and thermal stabilizing. Furthermore, since it would be a one-shot mission, both the space and the ground equipment would have to operate without interruption and with the required stability throughout the mission. The experiment had to start from a very stable operating condition before launch and maintain thermal and mechanical stability throughout. This plus the weight limitations resulting from the vehicle constraints placed rather stringent design requirements on the experiment.

The hypothesis being tested is that the rate of the proper clock will vary according to the expression

$$\frac{\Delta f}{f} = \alpha \frac{\Delta \phi}{c^2} ,$$

where $\Delta f/f$ is the fractional shift observed in the proper clock, $\Delta \phi$ is the variation in the gravitational potential of the clock, and c is the velocity of light. The parameter α is taken as unity according to the principle of equivalence, and departures from unity in this test will be given by ϵ , where α = 1 \pm ϵ . The best previous test, made over a 75-ft vertical distance by using the Fe₅₇ Mossbauer effect, was done in the early 1960s by R. V. Pound, G. A. Rebka, and J. L. Snider, who placed a 1% limit on ϵ .

Our goal is to test the above expression for $\Delta\phi/c^2$ to as high a precision as possible. Ignoring all other perturbations in the system, the maximum objective is limited by the relative stability of the maser clocks, which, for 100-sec averaging intervals and beyond, is assumed to be 1 part in 10^{14} . Therefore, for $\Delta\phi/c^2 \sim 4 \times 10^{-10}$, the precision of the test is constrained to a 25-ppm upper limit. The system for removing the first-order and ionospheric doppler effects is shown in Figure 1.

The design strategy for the experiment is to make all other contributions of system instability well below 1 part in 10^{14} for time intervals from 100 sec to the end of the flight.

MASER DESIGN REQUIREMENTS

The first requirement is that of survival through the vibration, shock, acoustical pressures, and decompression of launch by the four-stage, solid-fueled Scout system into a zero g and spinning condition while in space. Of the total payload equipment, the hydrogen maser and the newly designed ammonia cooling system for the transponder are the only types of items that had not previously been flown in space.

At the outset, we allowed about 90 lb for the maser and adhered as closely as possible to this limit. The requirements for its survival and operation in space were as follows:

- A. The maser-frequency fixed-frequency offset resulting from the trauma of launch should be small, less than 5 parts in 10^{12} , stabilizing within about 10 min to an overall stability of 1 part in 10^{14} for the remainder of the mission.
- B. Thermal, zero g, spin, and pressure effects from the transition into space causing possible longer term instability must be less than 1×10^{-14} either by calibrating for various environmental factors during

preflight simulation tests or by engineering the maser to cope with its immediate environment at this level of stability.

C. The maser should be built so as to operate continuously for about 9 months to allow time for its qualification testing and calibration and to permit it to operate, without alteration, as a piece of flight hardware; this includes several weeks of preflight stabilization.

MASER FREQUENCY PERTURBATIONS

The principal systematic frequency variation of hydrogen masers is described by the following expression:

$$\frac{\Delta f}{f} = \frac{1}{f} \left[\frac{Q_c}{Q_{\ell}} (f_c - f_0) + 2750 B^2 \right] . \tag{1}$$

The first term is the cavity-resonance mistuning, or "pulling," effect, and the second is the second-order magnetic-field dependence of the atomic hydrogen hyperfine transition F = 1, $M_F = 0 \rightarrow F = 0$, $M_F = 0$. Q_C is the cavity resonator Q_C , and Q_R is the Q_C of the atomic transition, which depends on the geometry of the hydrogen-maser storage bulb, the quality of the wall coating, and the collision rate of the atoms among themselves (spin-exchange processes). This last process is a function of beam input flux, which, in turn, can be represented in terms of the maser output power level.

Two aspects of the cavity-resonance shift especially concern us: 1) the variation in Δf_{C} during the mission, and 2) the average magnitude of Δf_{C} as a result of the combination of shake, shock, and zero gravity that occurs from earth-bound conditions through to the free-fall condition after powered flight ceases. The effect of cavity-resonance variations is obvious in equation (1). However, if there is also a large fixed offset $(f_{C}-f_{0})$, we are further subject to output frequency

variations due to variations in \mathbf{Q}_{ℓ} resulting from changes in atomic hydrogen flux during the mission. These changes in flux result in changes in power level W, and the measured power level was used as a measure of the beam flux for calibration.

In the probe maser, the cavity-resonance frequency is subject to many changes — in the gas pressure P of the enclosure surrounding the cavity vacuum system, in temperature T, in rotation rate Ω (centrifugal stretching), and in the magnetic field B of the microwave ferrite isolator in the output radio-frequency line from the maser cavity. This last effect, found during magnetic calibration of the probe maser, was traced to the isolator ferrite's magnetic resonance; it turns out that this resonance is affected by external fields despite what had previously seemed to be adequate levels of magnetic shielding about the isolator.

The expression describing all the known perturbations to the output frequency of the maser is

$$\frac{df}{f} = \frac{1}{f} \left[\frac{Q_c}{Q_{\ell}} \left(\frac{\partial f_c}{\partial P} dP + \frac{\partial f_c}{\partial T} dT + \frac{\partial f_c}{\partial \Omega} d\Omega + \frac{\partial f_c}{\partial B} dB \right) \right] + Q_c \Delta f_c \frac{\partial (1/Q)}{\partial W} dW + \frac{\partial f}{\partial B_0} dB_0$$

In the magnetic calibration of the maser, we found that the cavity effect dominated, and the calibration correction includes both effects simultaneously.

The magnetic-field behavior was measured by simulating the magnetic history of the payload before launch, during launch, and throughout the flight. A standard initial-condition state magnetization of the magnetic shields was ensured by a pregaussing operation performed before the vehicle-erection phase of both the actual flight and the magnetic simulation of the flight. We had previously obtained the magnetic

conditions from a survey of the launch area and from measurements at the position of the maser in the launcher while the launcher was being erected. The fields during liftoff and into the trajectory were obtained from earth field models, and the effect of the spinup of the probe at the appropriate earth field is incorporated in the simulation. The simulation of the rapid ascent into the vacuum of space was also included at the appropriate time in the sequence.

The magnetic field encountered during the flight has been determined from standard earth models. At present, only the axial component appears to be important. The algorithm developed for the magnetic influence on the probe output frequency has two branches, owing to hysteresis effects in the magnetic shields. The following algorithm was developed in the magnetic calibrations:

$$\frac{\Delta f}{f} = -5.899 \times 10^{-13} B_{\text{axial}} \text{ ascending} ,$$

$$\frac{\Delta f}{f} = -12.721 \times 10^{-13} B_{\text{axial}} \text{ descending} .$$

The sign convention is that the plus direction of field enters the earth at its north magnetic pole.

The effect of temperature variations was measured via telemetry in terms of the aft-oven heater voltage. The frequency variation due to this effect was determined during tests, with the following algorithm for frequency versus aft-oven voltage:

$$\frac{\Delta f}{f} = -3.6 \times 10^{-14} \Delta V \qquad .$$

The effect of pressure variations measured in the dome enclosing the forward assembly of the maser was determined by calibration to be as follows:

$$\frac{\Delta f}{f} = -2.9 \times 10^{-12} \Delta P$$

where ΔP is in psi. The pressure was measured by telemetry.

The effect of spin-rate variations on the output frequency of the maser was measured during tests, from which we developed the following algorithm:

$$\frac{\Delta f}{f} = -4.547 \times 10^{-17} \, \Omega^{2.05}$$

where Ω is in rpm. The spin sensor provided rotation-rate data through the telemetry system.

The effect of the power-level variation is

$$\frac{\Delta f}{f}\Big|_{V,\Omega,P}$$
 = 1.22 × 10⁻⁷ $\Delta f_c \Delta W$,

where ΔW is in ergs/sec and f is in Hz. In these calculations, values of Q = 3.4 \times 10⁴ and Q = 1.11 \times 10⁹ were determined for the probe for conditions of flight operation.

During prelaunch testing at MSFC, we established the offset frequency between the probe maser and the ground masers under the conditions at which the probe would be operated. This fixed offset was chiefly due to wall-shift variations in the bulb coatings and to the differences in bulb temperatures, which caused differences in second-order doppler shifts from the stored hydrogen atoms. The importance of this calibration lies in our being able to measure the cavity shift $\Delta f_{\rm C}$ when the probe was at apogee, where the time variation of the output beat frequency from the doppler canceling system was least. This estimate of $\Delta f_{\rm C}$ enabled us to set the value for the frequency shift due to flux

changes as observed from power changes given by $\frac{\Delta f}{f}\Big|_{V,\Omega,P}$ above. The frequency offset at apogee due to relativity must be assumed to be as predicted by the equivalence principle at slightly better than the 1% level for this determination. Our first cut at determining the cavity offset revealed that the cavity was mistuned in frequency by about -36 Hz, which makes

$$\frac{\Delta f}{f}\Big|_{V,\Omega,P} = -4.4 \times 10^{-6} \Delta W$$

MECHANICAL DESIGN

The Cavity-Bulb Structure

The mechanical and thermal requirements of the cavity itself were met by making it of CER-VIT. * Details of the design will follow in later sections; for the present, we must recognize that the overall thermal coefficient of the resonance frequency of the cavity-bulb assembly is about -800 Hz/°C.

At the outset, we realized that the thermal design of the maser would impose a special set of problems, and we established very demanding requirements for temperature excursions at the critical areas near the cavity assembly. Estimates of the temperature variation on the mounting points and the conditions of radiative coupling into space provided the boundary conditions for computer solution at MSFC to help provide design information to SAO for thermal control of the maser.

The maser bulb is a 7"-diameter quartz sphere attached to a cylindrical mounting skirt, also of quartz, by four 1" welds. The

^{*} Bowens-Illinois.

skirt, in turn, is fastened to the CER-VIT end plate by means of torr-seal epoxy. The bulb collimator is integral to the bulb structure.

The bulb is coated with FEP-120 Teflon. The cavity cylinder, made of CER-VIT 101, is ll" in diameter and 9 1/2" long and has an 0.2" wall. The cavity end plates are press moulded of CER-VIT and have reinforcing ribs on the outer surfaces for lightness and stiffness. All interior conducting surfaces of the cavity are coated with evaporated copper about 0.0003" thick. This thin coating is ductile and prevents the cavity from being distorted by thermal expansion of the copper.

The cavity is cut to the appropriate length and the joints lapped for mechanical stability. Before the bulb end plate was released for final assembly, it was shock and vibration tested under vacuum to verify the integrity of all joints — particularly those between the quartz cylinder and the sphere. The cavity is assembled within the vacuum enclosure, as shown in Figure 2, by using a special press that forces the upper end of the vacuum tank to close against the Bellville spring. The previously calibrated behavior of force vs. deflection in the spring was verified during assembly by observing the cavity resonance as the spring was compressed. The CER-VIT cavity in this case acted as a load cell to monitor the applied force. When appropriate load and deflection were achieved, the vacuum tank was welded shut and the tank was removed from the press.

The lower part of the cavity is supported by 12 beryllium copper (BeCu) tangentially oriented rollers seated on a hardened BeCu ring to allow for differential thermal expansion of the aluminum tank cover and the CER-VIT. In the upper assembly, this function is done by the Bell-ville spring. The vacuum tank has an access port for cavity fine tuning by means of a mechanical adjustment. Electronic fine tuning is done via a loop and varactor diode located in the lower cavity end plate. Dia-

^{*} BouPont.

metrically opposite this is the output coupling loop. The cavity components are shown in Figure 3.

The thermal-control system for the probe maser is shown in Figure 4 and discussed in detail in a later section.

Magnetic shielding for the probe maser is interleaved between and supported by layers of machined polyurethane foam insulation, as shown in Figure 5. There are four layers of 0.014" molypermalloy magnetic shields, which, strangely enough, offer better shielding than we can get from 0.032" molypermalloy. The 0.014" thickness is very difficult to handle, very unstable, and easily dented and deformed, all of which can severely deteriorate the shielding factor. The effect of stress is illustrated in Figure 6, which describes the change in shielding factor resulting from stress in the exterior shield.

Figure 7 shows the preamplifiers and voltage-reference electronic boards mounted on the aft-oven cover.

Finally, to complete the description of the cavity-bulb assembly, Figure 8 shows the lightweight C-field solenoid, located inside and close to the innermost magnetic shield. It is wound in three sections; each section is in two layers wound with the same pitch and having the plus and minus leads carefully superimposed to minimize stray magnetic fields from nonsolenoidal current distributions.

The Midplane-Plate Assembly

The main structural member of the experiment — and the structural interface with the spacecraft — is the aluminum midplane plate, shown in Figure 9. The midplane-plate assembly, 18" in diameter and 1.91" deep, weighs 3.1 lb. The electronics are located in 12 triangular bays, 11 of which house the major portion of the electronics; each bay contains two

printed-circuit cards. The temperature-sensitive electronics are placed on the oven cover just forward of the midplane plate, within the temperature-controlled zones previously described. The remaining bay, which has a test connector at its outermost radius, serves to pass interconnections between the forward and the aft assemblies. The bays are then covered with an 0.062"-thick aluminum plate on which the ancillary equipment aft of the midplane plate is mounted. The aluminum plate provides a precision outside diameter to engage a bore in the spacecraft's mounting plate so that, when the two plates are mated, radial definition is established in two planes. The midplane plate also has 12 mounting holes for securing the experiment in the thrust axis. Figure 9 shows the plate with its wire harness.

The Vacuum Manifold

The aft vacuum assembly (see Figure 10) is a two-pump system: an SAES Getters (Italy) Sorbac cartridge shown in Figure 11 and a Varian 0.2-liter ion pump. The former pump, which works by chemically entrapping hydrogen atoms to form hydrides of zirconium, is the prime hydrogen pump. If the cartridge should become saturated, i.e., unable to pump hydrogen, it can be regenerated by high-temperature bakeout by applying an external voltage to its internal resistance heater and by connecting the maser to a laboratory pumping system to remove the released hydrogen.

The 0.2-liter ion pump is used for noble-gas pumping. Its capacity is sufficient to maintain a system pressure of less than 1 x 10^{-6} torr for the 9 months before launch. The ion pump also serves as a pressure gauge for the evacuated envelope since the ion current can be correlated with gas pressure.

The aft vacuum assembly also contains a hexapole magnet, mounting ports for the Pirani gauges, and ionization glassware and hydrogen-introduction apparatus.

The hexapole magnet, which was developed by Frequency and Time Systems, Inc., Danvers, Massachusetts, weighs about 2 lb and has a bore of 0.125", a length of 3", and a pole-tip field strength of about 8 kgauss. An 0.050"-diameter glass stopping disk mounted on a tungsten wire at the exit plane of the magnet serves to remove unwanted particles from the beam entering the bulb, such as 1) atoms in the lower magnetic hyperfine levels that are not sufficiently deflected, 2) hydrogen molecules, 3) gases other than hydrogen, and 4) ultraviolet light from the dissociator, which has a strong 1216 Å component that shines directly along the beam through the pores of the collimator and strikes the Teflon coating at the apex of the bulb. Such relatively high-energy ultraviolet light has a very destructive effect on Teflon and in time can break down the long-chain carbon fluorine copolymer.

The dissociation of molecular hydrogen to atomic hydrogen is done in a Pyrex* 7740 glass bulb, 3.5 cm in diameter and 4.5 cm long. Excitation is by a three-turn coil, which is the tank coil for a single-transistor self-oscillator operating at 97 MHz with about 5-watt DC power input. Since we had been having a number of problems with earlier dissociator designs of smaller dimensions, we followed the dimensions successfully used by the maser group at the Jet Propulsion Laboratory. This design has proved to be completely successful and was subsequently used to retrofit all the VLG-10 and 10A ground masers.

To maintain the atomic hydrogen flux level within close limits, we took precautions to keep the temperature very constant by using a forced-air convection circuit. Optical monitoring of the intensity of the dissociator plasma discharge was done with a photodiode and interference-filter combination to measure the strength of the Balmer- α (6562 Å) red line and the light from a spectrally adjacent molecular-hydrogen-band structure. The efficiency of dissociation and the inten-

^{*} Ocorning.

sity of the RF were monitored in this manner. The brightness of the two spectral components, the voltage and current in the dissociator oscillator, the hydrogen pressure, and the maser-signal output were all part of the telemetry information returned to earth during the mission for comparison with data taken during 9 months of continuous and varied tests that were part of the qualification testing program.

Figure 12 describes the assembly of the dissociator, the hydrogen supply, and the pressure control. One of the problems of confining a quantity of hydrogen is the weight of the usual gas bottles. We found that we could use about I mol of lithium aluminum hydride (LiAlH,) to supply up to 2 mol $\,$ of $\,$ H $_{2}$ with a net weight of 38 g. Since thermal dissociation of molecular hydrogen from $LiAlH_{\Delta}$ is very easily done, we were able to get about 1 mol of H_2 at about 80 psi from approximately 29 g of $LiAlH_4$, controlling the hydrogen flow (and also filtering out impurities and LiAlH $_{\Delta}$ dust) with a palladium silver diaphragm. Figure 12 shows the pressure-control system used in the probe with the combined thermistor Pirani gauge and vacuum reference gauge, the locations of which can be seen in Figure 10 under the two parallel tubes pointing upward from the aft vacuum bulkhead. Figure 10 also shows the LiAlH $_{\Delta}$ container in the right-hand foreground. The canister with large holes in it in the left foreground of the photograph is the supporting structure that surrounds and secures the LiAlH $_{\Delta}$ container.

The assembled payload with its shroud removed is shown in Figure 13. All the components are mounted on a honeycomb plate. The inverted U-shaped structure in the foreground is the radiator that controls the dissociator forced-air temperature-stabilizing system.

PAYLOAD-MASER ELECTRONICS SYSTEMS

The payload electronics systems can be divided, for convenience of description, into seven functional groupings, as follows:

- A. Active thermal control and measurement.
- B. Atomic hydrogen source control and measurement.
- C. Cavity tuning and magnetic-field control.
- D. Ion-pump power supply and measurement.
- E. Telemetry signal conditioning.
- F. Telemetry PCM processor.
- G. Auxiliary measurement functions (pressure, spin).

Each of these groupings varies in complexity, in subfunctions required, and in the extent to which support is provided for on-board systems other than the maser itself. Command capability for operating the maser is done by an umbilical cable up to the moment of launch. No in-flight command capability is provided.

Thermal Control

The thermal-control requirements for the maser resonator are extremely stringent. After thermal stabilization on the launch pad, the vacuum-tank temperature at each of three points on the surface of the tank cannot vary by more than 0.01°C throughout the flight. Figure 14 shows a block diagram of the payload-maser electronics assembly.

The thermal-control system serves an additional function: to help maintain the pressure within the outer pressure enclosure constant to within ±0.01 psi. The pressure of the fixed volume of air within the pressure enclosure responds predictably to the temperature of the surface. Therefore, the surface temperature must be closely controlled to minimize pressure changes on the vacuum tank from the trapped air.

A multizone, multilevel, thermal-control system is employed to satisfy the temperature-variation and gradient requirements of the maser. The innermost level of control is the vacuum tank, which immediately

surrounds the maser cavity. The vacuum tank, in turn, is divided into three zones: the forward dome, the tank cylinder, and the aft dome. Each zone is independently controlled with separate thermistor sensors, heater windings, bridge preamplifiers, and power amplifiers. Sensor location, bridge set points, and thermal gains are adjusted to minimize both thermal gradients and changes in thermal gradients with variations in ambient conditions.

The vacuum tank is thermally guarded by the next level of control, the oven. The oven is divided into two zones, the aft-oven cover and the oven forward dome/oven cylinder. Again, each of the zones is independently controlled with sensors located so as to reduce the effects of the ambient temperature on the gradients across the oven. Thermal gains and insulation values are selected so that the oven absorbs the bulk of the ambient-temperature fluctuations, providing a relatively stable environment for the more critical vacuum-tank controllers.

Surrounding the oven is the pressure-can heater. Although this level of control provides some additional thermal isolation for the vacuum tank, its primary function is to maintain the enclosed air in the pressure can at a constant temperature, and therefore at a constant pressure. The pressure can is a single zone, with the sensor location selected to minimize gradients along the can.

All six thermal controllers are virtually identical in electrical design, except for variations in bridge set points and amplifier gains to accommodate different requirements. Figure 15 is a block-diagram representation of a typical controller.

Temperature is sensed by a selected "oceanographic" thermistor, which forms one leg of a bridge; the other three legs are very low-temperature coefficient ($\pm 5~\rm ppm/^{\circ}C$) wire-wound resistors. Unbalance of the bridge is detected and amplified by a type 725A integrated-circuit amplifier — an exceptionally stable and low-noise device — and the

output of the 725A is fed back to the bridge. The feedback is positive when the bridge is far off balance, producing an "infinite-gain" or self-oscillating controller. Close to balance, the preamplifier is a true proportional controller with anticipatory feedback.

All the preamplifiers, with the exception of the pressure-can unit, are mounted on the aft-oven cover shown in Figure 7. This volume is controlled to within $\pm 1\,^{\circ}\text{C}$, contributing further to the overall stability of the controllers and minimizing spurious thermoelectric and 'thermocouple voltage variations on the thermistor leads.

Each of the preamplifiers feeds a pulse-width-modulated power amplifier with a maximum power capability of 11 watts at minimum battery voltage. The pulse-width-modulated amplifiers operate at a constant pulse rate of approximately 40 kHz; the width of the pulses is proportional to the amplifier input voltage. Thus, the average output voltage is directly proportional to the input voltage, although the power transistors are always operating in a pulse mode, fully on or off. The output of the amplifier is carefully filtered at the output of the final power stage so that only the DC component appears across the output terminals.

The switching amplifier is quite compact and efficient. Overall efficiency is greater than 80% at full load, independent of voltage over the allowable variation in battery voltage. The high efficiency eliminates the requirement for a massive heat sink for the power transistor and permits it to be mounted directly to the amplifier's printed-circuit board. This arrangement simplifies the interconnection wiring and permits the construction of a simple, readily shielded amplifier assembly.

The six thermal-control power amplifiers are mounted on pie-shaped boards, which plug into compartments in the electronics ring as shown in

Figure 16. A simple U-shaped bracket secures the amplifier board and provides a thermal conduction path to the frame of the payload.

The pressure-can preamplifier, which has a much lower stability requirement than the oven or vacuum-tank controllers, is mounted on the aft vacuum assembly.

Thermal Controller Performance

The temperature sensitivity of the thermal-control preamplifiers has been bench tested over a 0° to 60° C range. The maximum allowable variation in bridge-balance temperature is 0.001° C per degree of ambient-temperature change. Typical values are in the order of 0.0001° C/°C, ensuring that the temperature sensitivity of the preamplifiers in the $\pm 1^{\circ}$ C aft-oven-cover area does not contribute significantly to the overall temperature sensitivity of the payload maser.

Under more realistic conditions in the thermal-vacuum tests, the thermal-control system maintains the vacuum tank within $\pm 0.01^{\circ}\text{C}$ under all test conditions.

RF Oscillator Control

The variable-voltage supply for the oscillator collector is furnished by a pulse-width-modulated power amplifier functionally and physically identical to those used in the thermal-control system. The control voltage for the power amplifier is generated by the coarse-control circuitry, also located on a printed-circuit board in the electronics ring. The source control is essentially a 4-bit digital-to-analog converter in which the four digital switches are magnetically latched relays. The relays are set and reset only from the external ground-station equipment. Subsequent payload power interruptions or transients cannot affect the state of the relays.

Hydrogen Pressure Servo

The pressure of the molecular hydrogen gas is in the range of about 1 to 2 millitorr and regulated by a closed-loop servo system. The pressure of the gas is sensed by a Pirani gauge at a point just before the gas line enters the dissociator bulb. The Pirani gauge is a small thermistor bead suspended in the gas volume on two very slender, 0.001", wires. The thermistor forms one leg of a self-balancing bridge. The bridge circuitry causes sufficient current to flow through the bead to make the bead temperature rise to approximately 200°C; at this temperature, the resistance of the bead is such that the bridge is balanced. At very low pressure, little current is required to balance the bridge; at higher pressures, the thermal conductivity of the gas is increased and higher current is required to balance the bridge. Thus, the current required to balance the thermistor bridge is, for a given species of gas, a direct measure of the gas pressure. In order to minimize the effects of ambient-temperature variations of the gas-pressure measurement, a second self-balancing reference bridge is provided. This reference Pirani gauge, which is specially matched to the measurement Pirani, is installed in the high-vacuum side of the vacuum system and exposed to the same ambient temperature as the measurement Pirani. Fluctuations in bridge current are electronically subtracted from the measurement bridge current to provide a temperature-compensated pressuremeasurement output.

The pressure-measurement output serves two functions; first, the output level is conditioned and used for telemetry monitoring of hydrogen pressure, and second, it forms one input to the pressure comparator. The other input to the pressure comparator is the pressure-set-point voltage, which is controlled from the GSEE. The pressure comparator provides a voltage output proportional to the difference between the measured pressure and the pressure set point. This voltage output, in turn, serves as the input to the pressure power amplifier.

The power amplifier, identical to the thermal-control power amplifiers, regulates the power input to the LiAlH₄ heater and thus completes the feedback loop. The voltage across the canister heater is monitored through the telemetry-signal conditioning system and provides a continuous telemetry record of canister heater power.

The pressure-set-point voltage is generated by a 5-bit digital-to-analog converter. The digital switches are magnetically latched relays that can be operated only from the GSEE system. The two self-balancing bridges, the pressure comparator, and the 5-bit digital-to-analog converter are mounted on the pressure-control assembly, which, in turn, plugs into the electronics ring.

Optical Monitor

The hydrogen-gas discharge in the dissociator bulb must be monitored to obtain information as to the state of dissociation in progress. Two photodetectors are a substitute for direct observation and provide a quantitative, objective measurement of the quality and brightness of the discharge. Each photodetector is an integrated photodiode-amplifier device.

Both the "atomic" and the "molecular" outputs of the optical monitor are signal conditioned and processed for telemetry transmission.

Cavity Tuning and Magnetic-Field Control

The maser cavity is tuned by varying the reverse voltage on a varactor diode mounted within the cavity. The uniform magnetic field imposed on the cavity and storage-bulb area is adjusted by varying the current through a main field winding and two trim windings on the printed-circuit solenoid. These four controllers, one tuning and three magnetic field, are all physically identical and all are installed in the electronics ring.

The cavity-tuning subsystem is shown in block-diagram form in Figure 17. One side of the tuning diode must be frame grounded for RF shielding; therefore, the controller and its associated power supplies must be isolated from frame ground and all other power-supply returns in order to avoid ground loop problems.

The cavity-tuner power supply consists of a DC-to-DC converter that generates +15 and -15 volts, both isolated from ground, from the main battery supply at 24 ± 3 volts. The tuner power supply is mounted on the aft vacuum assembly and is carefully filtered at both the input and the output to avoid injecting noise into the critical cavity-tuning circuitry. This power supply furnishes the operating voltages for the cavity-tuner voltage reference. The reference is essentially an extremely stable voltage regulator generating +10 volts, isolated from ground. The tuner voltage-reference board is located in the temperature-controlled aft-oven-cover area. The +10-volt output of the reference is the input to the cavity-tuner controller, which is a binary 10-bit digital-to-analog converter whose ladder network is a precision thin-film device with a resistance-temperature-tracking coefficient of less than 5 ppm/°C. The digital switches are magnetically latching relays controlled from the payload GSEE. No in-flight command capability is provided.

The 10-bit controller provides an output of 0 to 10 volts to the cavity-tuning varactor with a resolution of approximately 10.0 mvolts per bit. Absolute accuracy is not important, but excellent temperature stability of the varactor voltage is a strong requirement. The temperature coefficient of the voltage reference is 10 ppm/°C; the sensitivity to power-supply variations is essentially zero. The temperature coefficient of the voltage-division ratio of the tuner controller is less than 5 ppm/°C over the temperature range 0° to 70°C.

The current through each of the three windings on the printedcircuit solenoid is adjusted by means of three separate 10-bit binary digital-to-analog converters, each physically identical to the cavity-tuning controller described above.

Since each winding has a very low resistance, less than 10 ohms, the 0- to 10-volt range of the voltage divider is converted to 0- to 1-mA current by the addition of a 10-kilohm thin-film resistor. An additional relay, not used for the cavity-tuning function, reverses the direction of current flow through the solenoid winding. All 11 magnetically latching relays are controlled directly from the payload GSEE. As before, no switching capability is available after the umbilical cable is removed from the spacecraft.

The 10-bit controller provides an output of 0 to 1 mA through the winding with a resolution of approximately 10 μ A per bit. Stability of the current is determined principally by the temperature coefficient of resistance of the series resistor, approximately 50 ppm/°C, over the range 0° to 60°C.

Ion-Pump Power Supply and Measurements

The appendage ion pump requires a power source furnishing approximately 2500 volts at 50 μ A maximum. A small DC-to-DC converter, manufactured by MIL Electronics, Lowell, Massachusetts, is mounted directly to the pump bracket. The power-supply high-voltage terminal is adjacent to the pump feedthrough, and the entire high-voltage cavity is potted with a silicone rubber compound after wiring.

The power supply is regulated at 2500 volts $\pm 1\%$ over an input voltage range of 24 \pm 3 volts. Current is electronically limited to 50 μ amp by internal protective circuitry.

The ion-pump current, which is also a means for measuring the condition of the vacuum, is monitored by measuring the voltage across a

resistor in series with the ground return of the power supply. This voltage is filtered to eliminate converter switching noise and signal conditioned for telemetry transmission. No provision is made to monitor the ion-pump supply-voltage output.

Telemetry Measurements and Signal Conditioning

Signal conditioning to a standard 0- to 5.0-volt range for all channels is provided by the maser's signal-conditioning subsystem for all payload, spacecraft, and vehicle fourth-stage functions. Telemetry for the fourth-stage accelerometers and pressure gauge is routed through the payload-maser telemetry processor to save the weight and power ordinarily allocated to a dedicated vehicle processor and transmitter.

Signal conditioning for the tank-temperature-monitor thermistor is integral to the thermal-control system, as described earlier. Eight additional temperature-measurement bridges are provided within the signal-conditioning subsystem of the payload maser, seven of which are designed for thermistor sensors at various parts of the payload. The eighth, the antenna-temperature monitor, utilizes a platinum resistance thermistor (RTD). All eight temperature-measurement circuits are physically identical except for the choice of bridge resistances. In each, the thermistor or RTD forms one leg of a resistance bridge. The unbalance voltage, which is a function of the temperature of the sensor, is amplified so that the full temperature range appears as a voltage varying from 0 to +5.0 volts.

The translator/transponder's monitor-channel buffers amplify the static phase error, the automatic gain control (AGC), and the status signals from both the translator and the transponder. These are routine measurements except for the translator AGC, which must be monitored with very high resolution to detect small changes in maser power output. The

translator AGC signal conditioner contains provisions for selecting a small segment of the translator AGC output and expanding this portion to the full 0- to 5.0-volt range. The final adjustment of the translator AGC signal-conditioning circuitry provides a full-scale range from -116 to -110 dbm, established during calibration of the probe maser.

Eight channels of voltage measurements are provided for battery voltage, battery current, and six payload-maser heater voltages.

Three channels for in-flight calibration checks of the telemetry system are included: full scale, +4.980 volts; midscale, +1.00 volts; and ground.

Six measurement channels to monitor maser performance are also incorporated. Two of these monitor the voltage and current of the source RF oscillator. The remaining four — hydrogen pressure, ion-pump current, "atom" level, and "molecule" level — were discussed in previous sections.

The payload-maser signal-conditioning subsystem provides reference voltages and buffer amplifiers for the Scout fourth-stage head pressure gauge. The three Scout fourth-stage accelerometers are internally conditioned; their outputs are routed through the signal conditioner to the telemetry processor.

Telemetry PCM Processor

The telemetry processor is an 8-bit, 37-channel pulse-code-modulated (PCM) system operating at 1000 bps. Each main frame has eight subframes 128 bits in length: 21 providing subframe sync, 3 giving subframe identification (ID), and 104 making up 13 8-bit data words. In turn, four data words are multiplexed, yielding 32 channels per main frame. The remaining five data words are used for high-repetition-rate data as

follows: the translator AGC voltage is sampled once each subframe (eight times each main frame), and the four Scout channels are sampled twice each subframe (16 times for each main frame).

The major components of the telemetry processor consist of an analog-to-digital converter, a main-frame multiplexer, four subframe multiplexers, and a timing and sync generator.

All telemetry-processor circuitry is mounted on eight pie-shaped boards that plug into the electronics ring. The processor's timing circuitry generates the following clock signals for the telemetry system: the bit-rate clock (1000 bps), the coordinate clock (125 bps), and the subframe clock (7.8125 bps). All clocks are derived from, and harmonically related to, the subcarrier oscillator frequency of the transponder's telemetry modulator.

The subcarrier crystal oscillator in the transponder generates a 2.048-MHz signal, which, divided by 2 within the transponder, generates the 1.024-MHz telemetry subcarrier. The 2.048-MHz signal is also routed through the maser/spacecraft interface to the pulse-shaper board, which amplifies the signal and regenerates standard +10-volt COS/MOS logic levels. The 2.048-MHz signal is then digitally divided to 1000 Hz by COS/MOS integrated circuits on the pulse-shaper board. The 1000-Hz clock is routed to the telemetry timing board in the electronics ring.

The pulse shaper contains an auxiliary oscillator operating at approximately 1980 Hz. A clock detector on the pulse shaper detects the absence of an incoming pulse stream from the transponder and automatically switches the auxiliary oscillator on line. The auxiliary oscillator frequency is divided by 2, to 990 Hz, to replace the divided subcarrier oscillator signal for testing or in the event of subcarrier-oscillator failure.

The telemetry timing board, in the electronics ring, consists of several COS/MOS divider chains, delay circuits, and buffer amplifiers, which generate all clock frequencies required for telemetry-system operation. In addition to the major clock signals, the timing board generates a number of auxiliary clocks that are either delayed in time with respect to the main clock or have suppressed pulses for internal system timing applications.

The sync board generates the subframe sync and subframe ID words under control of the timing subsystem. The subframe sync word is a standard Goddard Space Flight Center 21-bit code; the subframe ID is a 3-bit octal word. The subframe sync word is stored in a 21-bit parallel-in, serial-out shift register. The bit pattern is hard-wired into the parallel-input parts. The sync board also accepts data input from the analog-to-digital converter board, assembling the sync word, subframe ID, and data words into a single bit stream at a uniform 1000-bps rate.

The analog-to-digital converter digitizes 0- to +5-volt data into 8-bit data words that are stored in serial-output shift registers. The converter is a completely integrated, 256-level, successive-approximation circuit, requiring 13 digitizing clock cycles for a single digitizing operation. To permit the converter to complete a full cycle of operation in less than eight main-clock cycles, the digitizing clock runs at 32 kbps, derived from the timing-board divider chains. The +4.980-volt reference for the analog-to-digital converter is generated on the source-control/telemetry reference board. The stable +10.0 volts required for operation of this board, in turn, is generated by a separate reference supply, which is installed on the temperature-controlled aft-oven cover.

The main-frame multiplexer accepts 13 analog (0 to +5.0 volts) inputs — four from the subframe multiplexers, one from the translator AGC signal conditioner, and two from each of four Scout measurements — and switches its output to each input in succession. The switching

devices are COS/MOS transmission gates, which are under the control of an on-board counter, and a four- to 16-line converter, which, in turn, is controlled by the timing board.

The subframe multiplexers are mounted on the same circuit boards as the signal-conditioning circuitry. Each subframe multiplexer board contains an eight-channel COS/MOS transmission-gate analog switch and the signal-conditioning circuitry associated with those eight telemetry channels. The transmission gates are controlled by a three- to eight-line digital demultiplexer, which is controlled by the subframe ID-word generator on the sync board.

Pressure and Vehicle Spin-Rate Measurements

Two specialized in-flight measurements are provided for correction of the maser cavity's frequency. The resonant frequency of the maser cavity is a function of the gas pressure within the pressure can, the vehicle spin rate, and the cavity temperature. The last of these is monitored through telemetry by observing the aft-oven-cover heater voltage, but the first two require specific instrumentation provisions.

The sensitivity of maser frequency to pressure within the pressure can is approximately $3.9 \times 10^{-12}/\mathrm{psi}$. Therefore, a very precise, very high-resolution pressure measurement is required to correct the maser frequency to within $\pm 1 \times 10^{-14}$. This requirement is met by the use of a very stable diaphragm-type pressure transducer and highly stabilized bridge-sensor electronics. The transducer and the electronics package are mounted within the temperature-controlled pressure can at the forward end. Figure 18 is a block diagram of the pressure-measurement assembly.

The pressure transducer, a Bell and Howell type CEC1000, uses thinfilm strain gauges and bridge resistors to minimize the differential temperature coefficients of the bridge elements. The bridge excitation voltage is controlled to within ± 10 mvolts to minimize self-heating errors in the bridge balance point. The bridge amplifier, an Analog Devices type AD521S instrumentation amplifier, has a very low-voltage offset coefficient and a high common-mode-rejection ratio. The entire assembly is temperature controlled to better than $\pm 1^{\circ}\text{C}$ owing to its location within the pressure-can heater system.

The required resolution is obtained by limiting the dynamic range of the measurement to 1.0 psi so as to operate from 17 to 18 psia. In order to obtain 0-volt output from the pressure monitor at 17 psia, it is necessary to offset the bridge amplifier electronically. The effect of changes in the offset voltage on the overall stability of the pressure measurement is minimized by using the bridge excitation voltage as the source of the offset voltage. To first order, changes in the excitation voltage cancel completely at 17 psia and produce only a very small residual error at 18 psia. The resolution of the system, as observed through the 8-bit telemetry system, is approximately 0.004 psi per step of the least-significant digit.

The sensitivity of maser frequency is approximately 1×10^{-14} /rpm at 115 rpm. A very high-resolution spin-rate monitor is therefore required; unfortunately, however, the actual in-flight spin rate cannot be accurately predicted.

The problem of combining high resolution with a wide dynamic range is solved by a sun-sensing dual-resolution monitor that automatically switches from high resolution to a wide-range low-resolution mode for every tenth measurement. A block diagram of this monitor is given in Figure 19. The sun sensor shown in the figure is mounted on the space-craft honeycomb plate, where it views the sun and the outside world through a small hole in the side of the thermal shield. Each time the vehicle rotation brings the sun into the field of view of the sensor, a pulse is generated, amplified, and used to energize a Schmitt trigger

circuit. A digital division by 2 then generates a gate, the duration of which is equal to the period of the rotation rate; the gate pulse is further divided by 10 to generate a multiple-period gate pulse, which is the average of 10 rotation periods. The multiple-period gate serves two functions: the positive-going edge triggers the sequence control counter, while the pulse opens the main gate, allowing 1000-bps clock pulses to flow to the main counter.

The binary number stored in the 8-bit main counter is a measure of the duration of 20 periods of the vehicle's rotation rate. At the end of each multiple-period gate, a transfer pulse is generated that jamtransfers the contents of the main counter into the storage register and resets the counter to zero. The output of the storage register is the input to an 8-bit digital-to-analog converter, identical to the one used in the telemetry processor's analog-to-digital converter. The analog output of this converter is amplified and routed to the appropriate telemetry subcarrier multiplexer for processing.

The main counter's most-significant digit frequently overflows during a high-resolution measurement cycle, resulting in an ambiguity regarding the absolute value of the measured spin rate; the full-scale range of the sensor is approximately 6 rpm within the range centered near 114 rpm, i.e., 111.61 to 117.19 rpm. To resolve this ambiguity, the sequence switches the clock pulses through a divide-by-10 for one measurement cycle after every 10 high-resolution measurement cycles. The unambiguous range of the sensor is much larger at the lower clock rate than at the higher rate, thus making it possible, by using both sets of data, to determine the rotation rate of the vehicle.

Since the payload's telemetry processor has no provision for direct entry of digital data, it is necessary to convert the digital rotation-period data to analog form and redigitize them in the telemetry processor. The error buildup that might be inherent in such a process is

minimized by using a small full-scale range, a precise reference derived from the telemetry reference board for the digital-to-analog-converter reference voltage, and the crystal-controlled subcarrier oscillator as the source of the 1000-Hz main counter clock.

As noted earlier, the spin sensor is mounted on the spacecraft's main honeycomb plate and is thus the only component of the maser electronics system that is not physically installed on the maser itself. The resolution of the spin sensor, in its design range, is approximately ± 0.02 rpm; the estimated overall accuracy is approximately 0.05 rpm, including the quantizing error.

Payload Ground Support Electronics Equipment

Two major items of equipment are required for direct support of the payload maser during qualification tests and on the pad before launch; these are the payload control rack and the SAO frequency standard, both of which are installed in the support trailer used for normal operations. The payload control rack houses facilities for operating the relays in the payload for field, source, and cavity during control, for decoding spacecraft telemetry, and for displaying quick-look digital and analog data of selected telemetry channels. The frequency standard provides facilities for measuring the frequency stability of the payload maser at the output frequency of the translator, 2203.078 MHz.

Figure 20 is a photograph of the payload control rack. The three functional groups within the rack are the Zeeman-frequency audio oscillator, the controller group, and the quick-look telemetry group. The magnetic field within the maser cavity can be measured by applying an audio-frequency field across the cavity structure and observing the frequency at which the maser output level dips (nominally between 500 and 1000 Hz) owing to Zeeman transitions induced between the $M_{\rm F}=\pm 1$ and

O sublevels of the upper energy state of the hydrogen atom. The audio-frequency source in the payload control rack is a Hewlett-Packard Model 651B audio oscillator. A printed-circuit loop on the vacuum tank is wired to the oscillator output through the umbilical cable.

Payload Controls

The magnetic-latching relays in the payload are controlled by pushbutton switches on the payload control rack, each switch controlling one relay in a binary sequence. The six sets of push-button controls comprise three for the magnetic fields, one for cavity tuning, one for hydrogen pressure, and one for source oscillator voltage.

The extremely simple relay-control circuitry is designed to avoid spurious relay operation caused by power failure or electronic malfunction and to provide nonvolatile memory between times when the payload is energized. The operator presets the desired binary number into push buttons for a particular function. A green indicator lamp in the bottom half of each preset button indicates which switches have been depressed; no power can be applied to the relays at this point. After the preset number has been verified, the operator momentarily depresses the set switch to apply power to the relay coils. A red indicator lamp in the top half of each preset switch signals when the set control is operating properly.

The relays can be energized from the power supply on the payload control rack only if the set switch is depressed; otherwise, the relay coils are completely disconnected from the GSEE. Each relay coil line is brought out individually, through the umbilical cable, to the control rack without involving the spacecraft electronics in any way; thus, no malfunction aboard the spacecraft can alter the state of the relays once they are set from the GSEE payload control rack.

Quick-Look Telemetry

The control rack houses a Coded Communications Corp. Model ECO-1 PCM decoder, a digital-display unit, and an analog-display unit.

The decoder accepts the payload's PCM bit stream and a 1000-bps clock. Both signals are provided by special balanced line drivers on the maser payload and are routed through the umbilical cable to balanced line receivers in the payload control rack and then to the input of the PCM decoder. The balanced signal lines enhance the common-mode noise rejection of the quick-look telemetry system and also preserve the ground isolation of the payload electronics. The output of the PCM decoder is a parallel 8-bit natural binary data word, a 6-bit parallel word ID, and a 3-bit subframe ID. The decoder output cycles through all 218 8-bit main-frame words in 1.024 sec; each word is identified by the appropriate word and subframe IDs.

The data bus, the word ID bus, and the subframe ID bus are routed to the digital-display unit. The system also provides for selective digital-to-analog conversion on four channels for real-time monitoring on strip-chart recorders.

CONCLUSIONS

At the time of writing this paper, the data-reduction phase of the experiment is in full swing. The reduction process consists of comparing the frequency of the relativity signal obtained from the system shown in Figure 1 with predictions of what this signal frequency should be from currently accepted relativity theory. The input data for the predictions depend on tracking the position and velocity of the probe to very high accuracy and deriving from these data the relativistic frequency predictions, including redshift, second-order doppler, and earth-motion effects. From the data processing, still in progress, we

can recover the Allan variance of the output data taken at maximum range, shown in Figure 21. These data include the effects of more than 30000 km of propagation and three passes through the earth's atmosphere and ionosphere. These data are quite similar to maser-comparison data taken in the laboratory over a few meters of cable!

For the longer term data taken during the mission, Figure 22 shows the residual frequency between observation and predictions based on a preliminary trajectory determination. The discrepancies near the ends are still not understood in detail; however, in the present analysis of the tracking data used in determining the trajectory, there appears to be an incorrect representation of the payload's dynamics during the flight, and a more complete computation is required to obtain the probe's trajectory. We look forward to presenting a total picture of the outcome of this experiment in the near future.

ACKNOWLEDGMENT

This work was supported in part by Contract NAS8-27969 from the National Aeronautics and Space Administration.

REFERENCES

- R. F. C. Vessot and M. W. Levine, Performance data of space and ground hydrogen masers and ionospheric studies for high accuracy comparisons between space and ground clocks. In <u>Proceedings of the</u> <u>28th Annual Frequency Control Symposium</u>, U.S. Army Electronics Command, Ft. Monmouth, N.J., pp. 408-414, 1974.
- 2. D. Kleppner, R. F. C. Vessot, and N. Ramsey, The orbiting clock experiment to determine the gravitational redshift. Astrophys. Space Sci., vol. 6, pp. 13-32, 1970.

- 3. R. F. C. Vessot and M. W. Levine, Measurement of the gravitational redshift using a clock in an orbiting satellite. In <u>Proceedings of the Conference on Experimental Tests of Gravitation Theories</u>, ed. by R. W. Davies, Jet Propulsion Lab. Rep. 33-499, pp. 54-64, 1971.
- 4. R. F. C. Vessot, Lectures on frequency stability and clocks and on the gravitational redshift experiment. In Experimental Gravitation, ed. by B. Bertotti, Academic Press, New York, pp. 111-162, 1974.
- 5. S. Petty, R. Sydnor, and P. Dachel, Hydrogen maser frequency standards for the deep space network. In <u>Proceedings of the Eighth Annual Precise Time and Time Interval Applications and Planning Meeting</u>, U.S. Naval Research Laboratory (this volume).
- 6. M. W. Levine, R. F. C. Vessot, E. M. Mattison, E. Blomberg, T. E. Hoffman, G. Nystrom, D. F. Graveline, R. L. Nicoll, C. Dovidio, and W. Brymer, A hydrogen maser design for ground applications. In Proceedings of the Eighth Annual Precise Time and Time Interval Applications and Planning Meeting, U.S. Naval Research Laboratory (this volume).

FIGURE CAPTIONS

- Fig. 1 Doppler canceling system.
- Fig. 2 Schematic of the cavity support system.
- Fig. 3 Cavity components.
- Fig. 4 Probe-maser thermal-control system.
- Fig. 5 Magnetic shields and insulation.
- Fig. 6 Redesign of external magnetic shield showing the effect of stress.
- Fig. 7 Control electronics located on the aft-oven cover.
- Fig. 8 Two-sided printed-circuit C-field solenoid.
- Fig. 9 Main mounting frame with electronics bays.
- Fig. 10 Aft vacuum manifold assembly.
- Fig. 11 SAES Sorbac cartridge used for hydrogen scavenging.
- Fig. 12 RF dissociator and hydrogen system.
- Fig. 13 Payload assembly.
- Fig. 14 Block diagram of the probe-maser electronics assembly.
- Fig. 15 Block diagram of a typical controller.
- Fig. 16 Typical electronics board.
- Fig. 17 Cavity electronics tuning system.
- Fig. 18 Block diagram of the pressure transducer assembly.
- Fig. 19 Block diagram of the dual-resolution payload spin sensor.
- Fig. 20 Payload-maser ground support control rack.
- Fig. 21 Allan variance of the redshift beat frequency near apogee, taken from the system shown in Fig. 1.
- Fig. 22 Data from the preliminary payload trajectory.

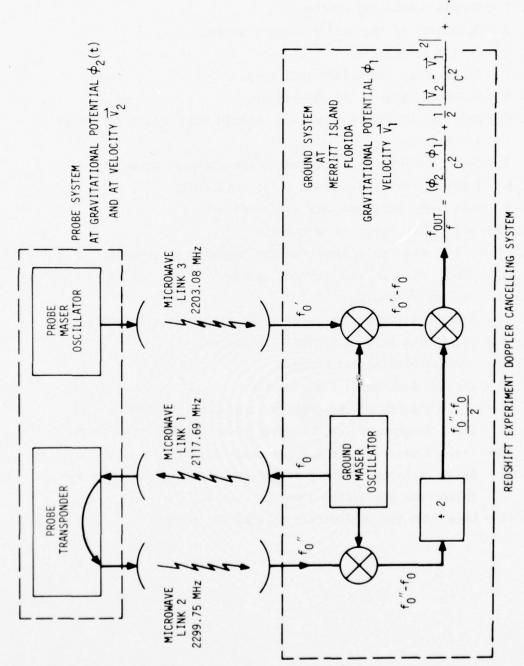


Fig. 1 Doppler cancelling system.

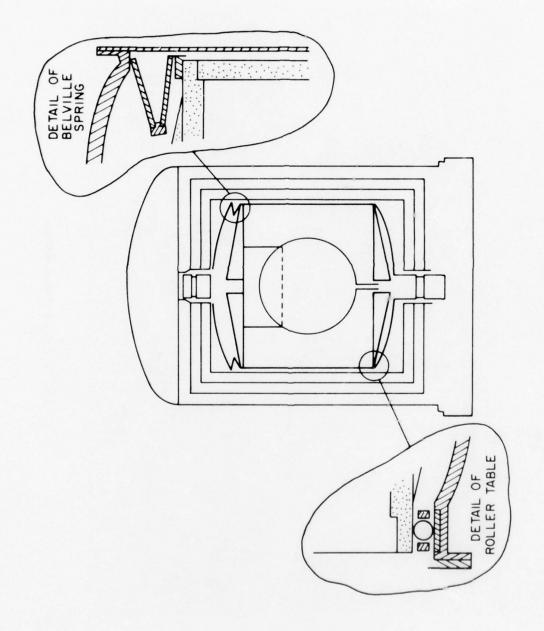


Fig. 2 Schematic of the cavity support system.

Fig. 3 Cavity components.

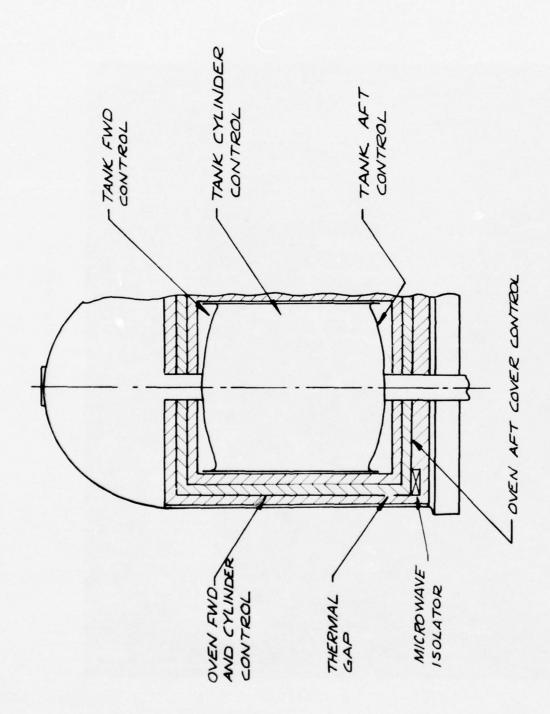


Fig. 4 Probe-maser thermal-control system.

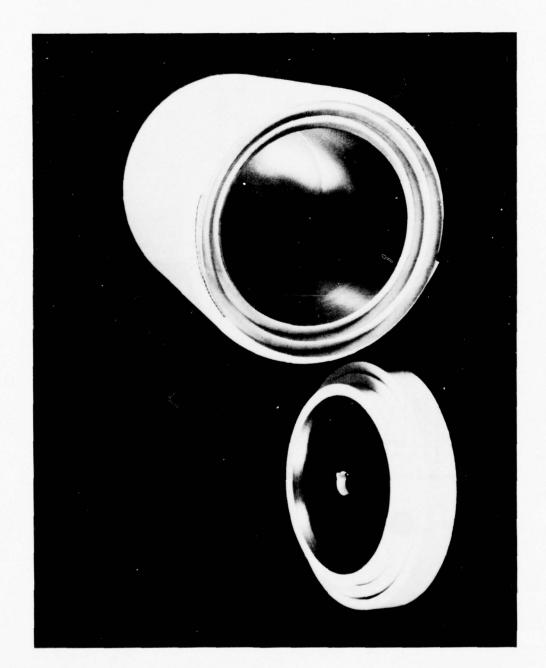


Fig. 5 Magnetic shields and insulation.

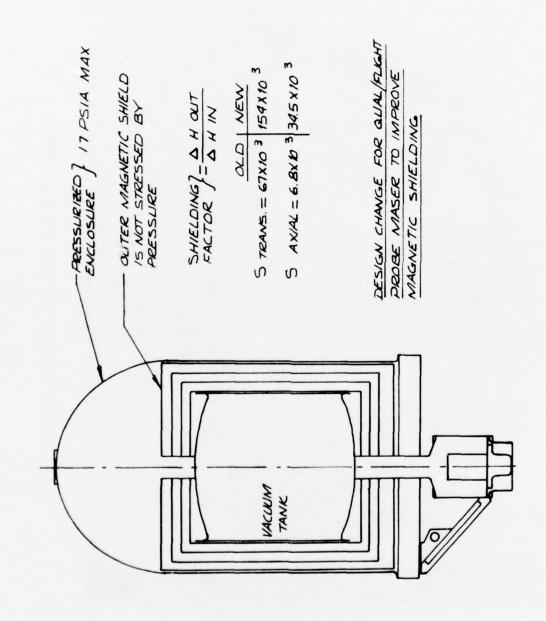


Fig. 6 Redesign of external magnetic shield showing the effect of stress.

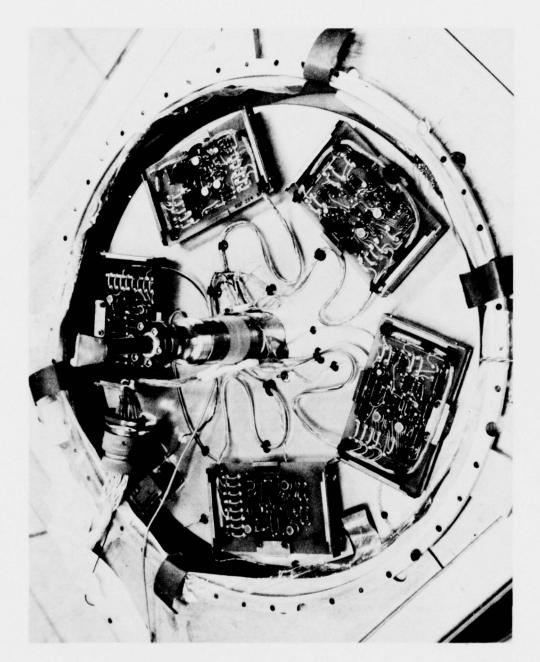


Fig. 7 Control electronics located on the aft-oven cover.

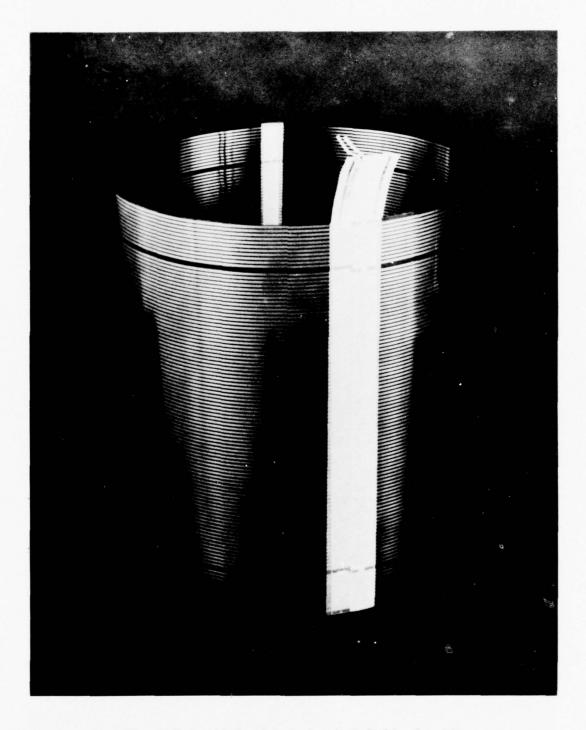


Fig. 8 Two-sided printed-circuit C-field solenoid.

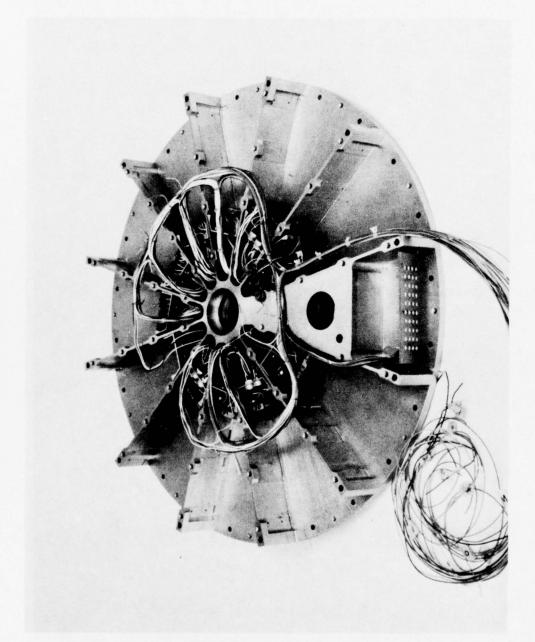


Fig. 9 Main mounting frame with electronics bays.

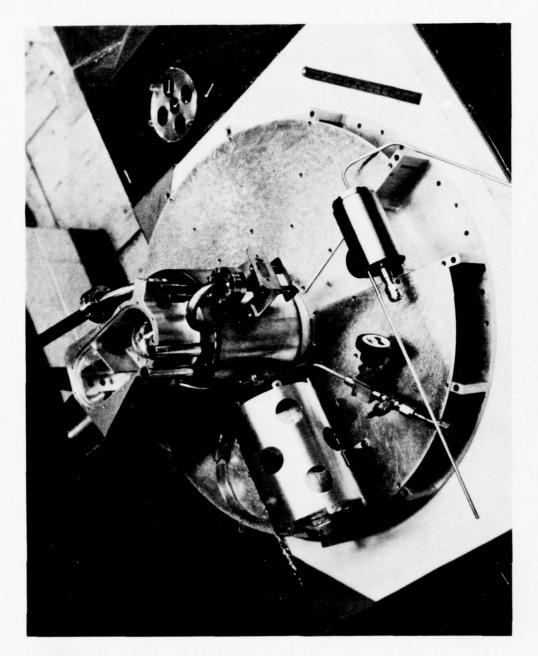


Fig. 10 Aft vacuum manifold assembly.

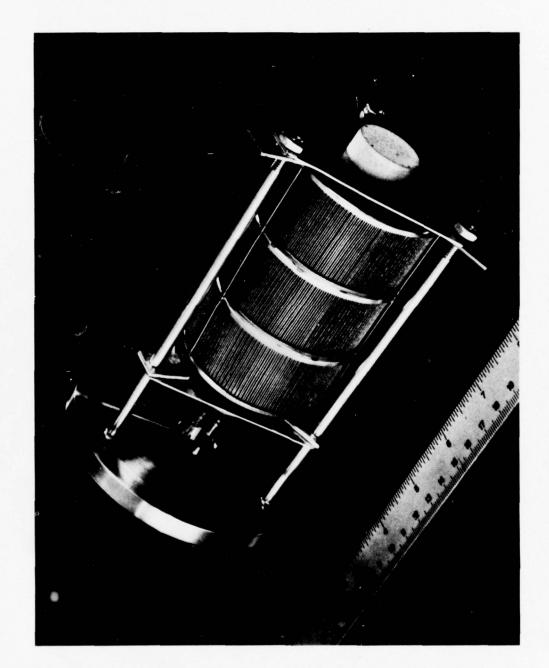


Fig. 11 SAES Sorbac cartridge used for hydrogen scavenging.

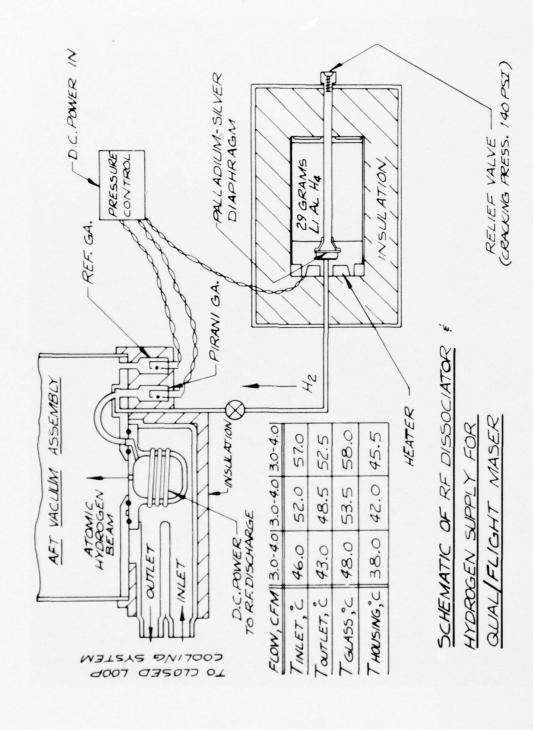


Fig. 12 RF dissociator and hydrogen system.

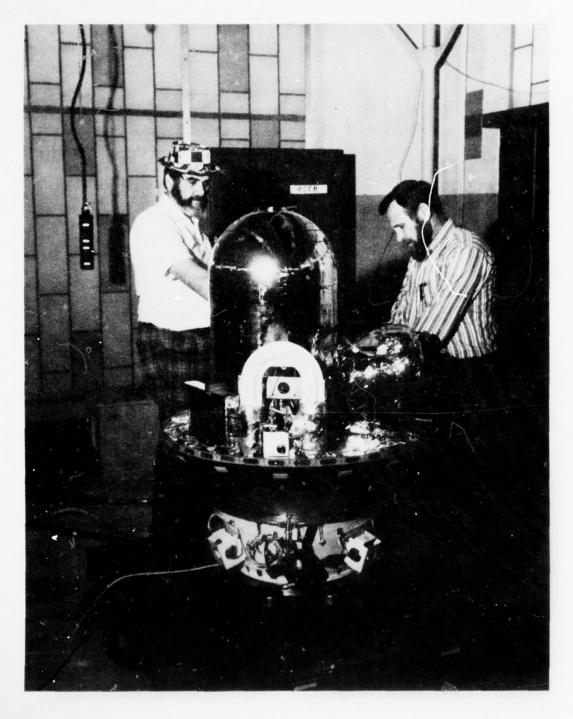
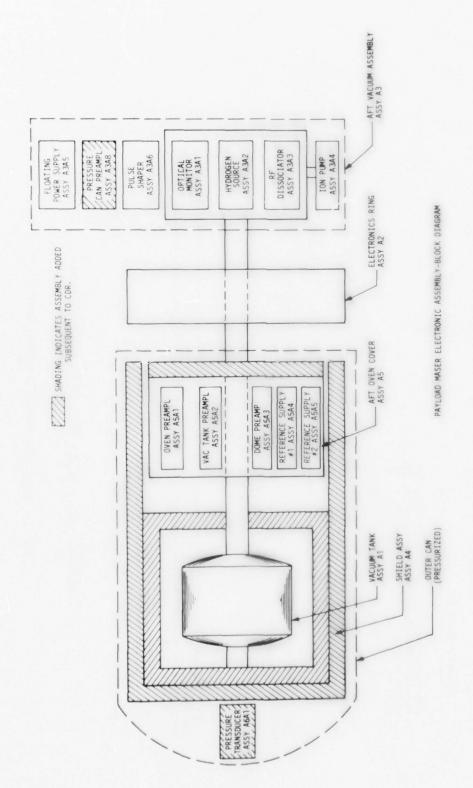
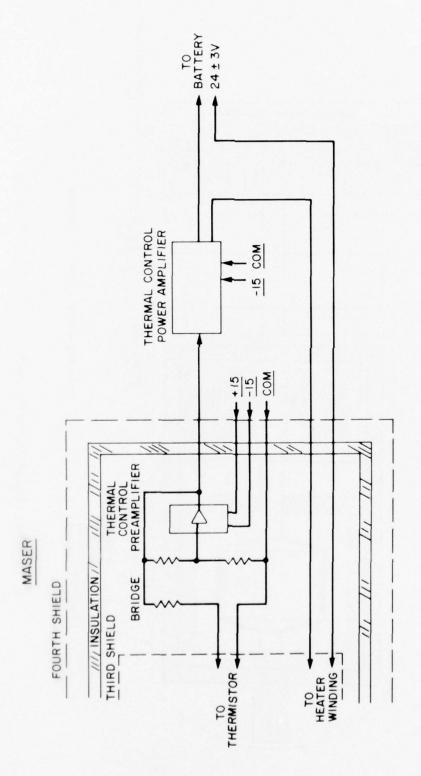


Fig. 13 Payload assembly.



i i

Fig. 14 Block diagram of the probe-maser electronics assembly.



THERMAL CONTROLLERS BLOCK DIAGRAM

Fig. 15 Block diagram of a typical controller.

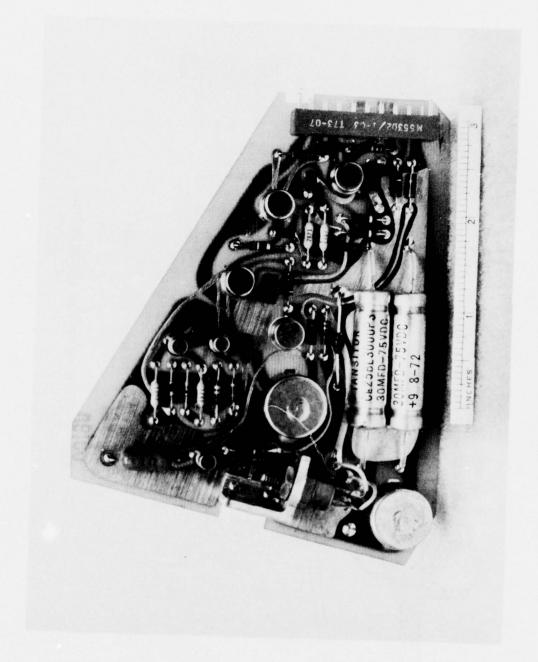


Fig. 16 Typical electronics board.

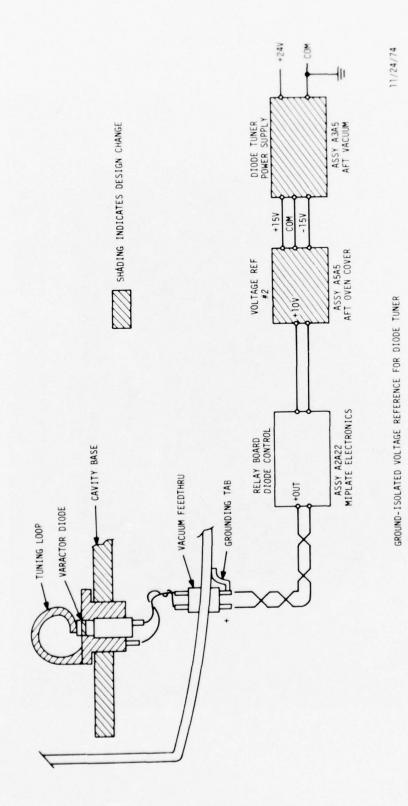
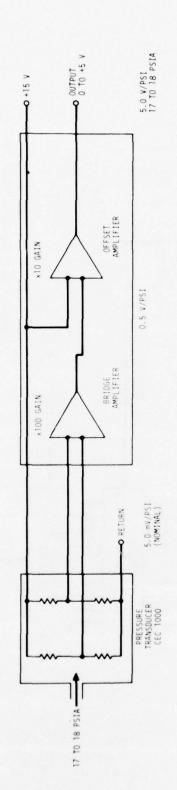


Fig. 17 Cavity electronics tuning system.



PRESSURE TRANSDUCER ASSEMBLY

Fig. 18 Block diagram of the pressure transducer assembly.

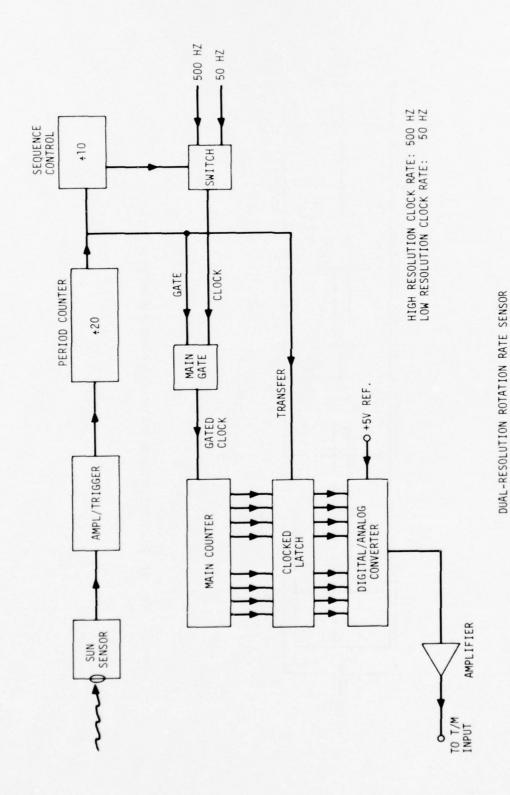


Fig. 19 Block diagram of the dual-resolution payload spin sensor.

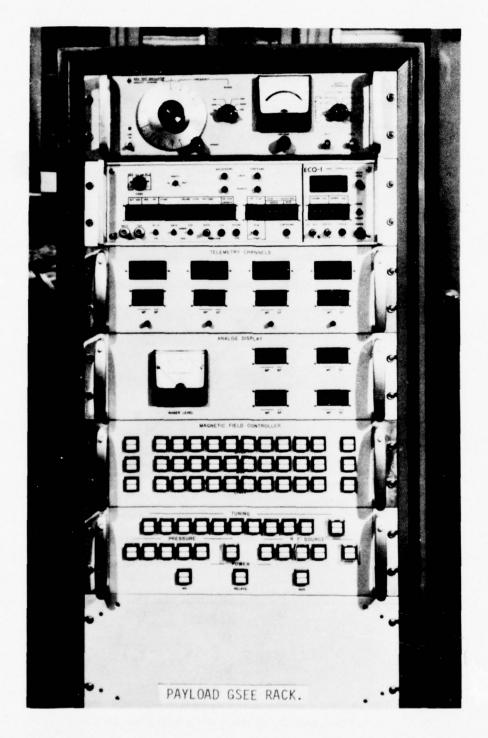


Fig. 20 Payload-maser ground support control rack.

ALLAN VARIANCE OF PROBE AND GROUND MASER COMPARISON USING 300 SECONDS OF DATA NEAR APOGEE

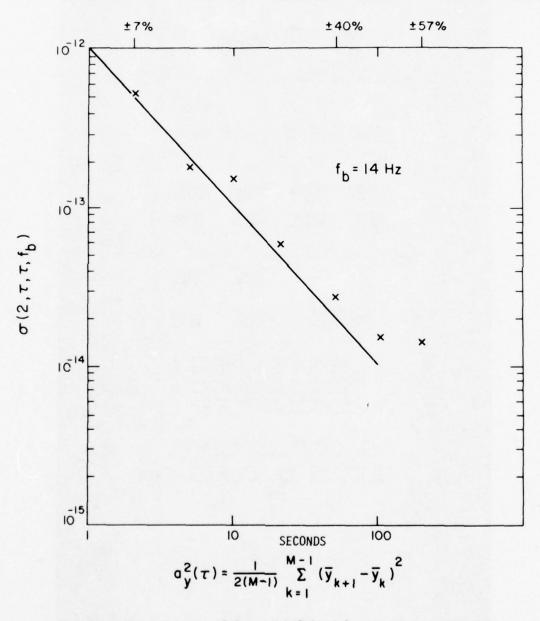


Fig. 21 Allan variance of the redshift beat frequency near apogee, taken from the system shown in Fig. 1.

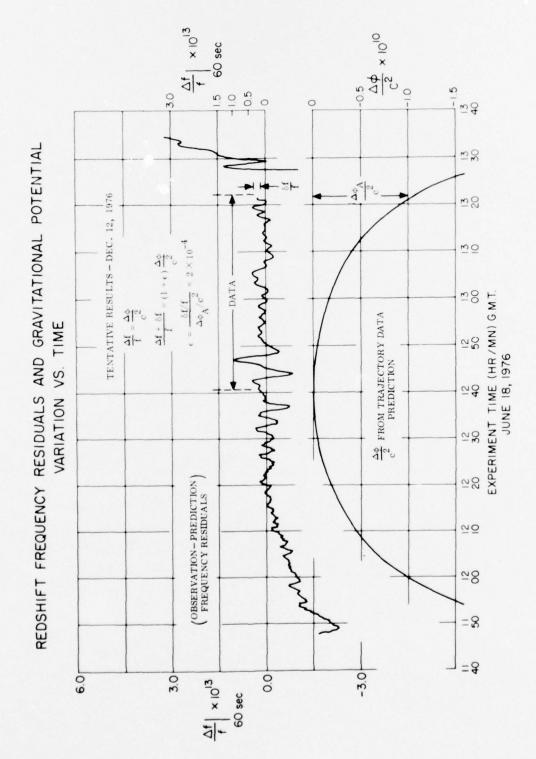


Fig. 22 Data from the preliminary payload trajectory.

VARIABLE VOLUME MASER TECHNIQUES

Victor S. Reinhardt NASA/Goddard Space Flight Center Greenbelt, Maryland 20771

INTRODUCTION

The hydrogen maser achieves its extremely good frequency stability principally by confining the masing atoms for long periods in a teflon coated storage bulb. Because of this confinement, the frequency of the hydrogen maser is shifted due to collisions of the atoms with the walls of the storage bulb. This is shown in Figure 1. The wall shift is given by:

$$f = \frac{\phi V}{2\pi} \cdot \frac{A}{4V}$$

where ϕ is the average phase shift per collision, v is the average atomic speed, and (4V/A) is the mean free path between wall collisions, λ .

In order to use the hydrogen maser as a primary frequency standard, one must correct for the wall shift. The obvious method to do this is to vary λ by operating hydrogen masers with different size storage bulbs, and to make frequency comparisons between the masers. This has been done many times², but has not produced good results because ϕ has not reproduced well from bulb to bulb.

In 1969, Douglas Brenner proposed another approach.³ If one were to make a maser with a flexible storage bulb, one could vary λ but keep ϕ constant. This would allow for the correction of the wall shift without the uncertainties associated with changing bulbs. The technique is outlined in Figure 2. This method has been a fruitful one, leading to several devices and increasing degrees of success. This paper will discuss this variable volume technique and the strengths and weaknesses of the devices which have been based on this technique.

THE VARIABLE VOLUME TECHNIQUE

The first variable volume maser was built by Douglas Brenner.⁴ He used several types of flexible bulbs with a variety of wall coatings. One of his teflon bulbs is shown in Figure 3. As shown in Figures 1 and 2, Brenner's technique relies on one's knowledge of B, the ratio of the bulb volumes, and the fact that both the value of ϕ and the value of f_0 , the corrected frequency, remain constant

during the change of volume. With careful measurement, B can be determined to the 0.1% level. 4.5 How this effects the error, however, is strongly dependent on the size of B. As B approaches unity the uncertainty in determining f_0 goes to infinity for given errors in measuring B, f_1 , and f_2 . The size of B in Brenner's device is limited severely by the fact that the filling factor 1 is degraded in the compressed volume. Brenner achieved values of 1.18 to 1.37 for B.

The value of ϕ is effected by both changes in the atomic density in the bulb and changes in the surface properties of the bulb. If the relative rate at which atoms strike the bulb surface change when one changes the volume, ϕ may change. In a bulb with good communication between sections, this effect can be made negligeably small.4,5,6 Changes in the surface properties of the teflon during the measurement process can be induced by the changes in stress that occur when the bulb volume is changed. Brenner discussed this problem and estimated that the stress effect would change ϕ by 0.25%. The major weakness of his device, however, is in the uncertainty caused by lack of knowledge of the effects of stress on his storage bulbs.

Changes in f_0 during the measurement process come from shifts in the maser frequency other than the wall shift: the doppler shift, magnetic shifts and spin exchange shifts. It has been determined that to one part in 10^{14} of the hyperfine frequency the atomic velocities are thermalized to the bulb temperature. One therefore can correct for the doppler shift by measuring the bulb temperature.

The principal magnetic shift can be corrected for by measuring the zeeman frequency. Magnetic inhomogeneity shifts can cause errors as large as parts in 10^{12} . These shifts are a function of the average inhomogeneity over the storage bulb and so change when the storage bulb volume is changed. Inhomogeneity shifts can be corrected for, but unfortunately Brenner was unaware of these shifts when he performed his measurements, so he did not correct for them.

Spin exchange shifts come from collisions of the radiating hydrogen atoms with other hydrogen atoms and with other paramagnetic gases. 1,8,10,11 The principal part of the hydrogen spin exchange shift is corrected out with flux tuning. An anomalous part is not. This shift is 4×10^{-4} of the non-hydrogen spin exchange part of the atomic linewidth. In a variable volume maser, except for contributions from magnetic inhomogeneities and from background gases, the non-spin exchange linewidth is proportional to the inverse bulb volume just as the wall shift is, 12 so most of the anomalous spin exchange shift is corrected for by the same process which measures the wall shift. The background

contribution to the linewidth can be kept small by keeping the partial pressure of paramagnetic gases small,⁸ and the magnetic linewidth can be kept small by reducing the size of magnetic inhomogeneities. One should therefore be able to keep uncertainties due to the anomalous spin exchange shift below the 10⁻¹⁴ level.

VARIABLE VOLUME DEVICES

To overcome the stress problems associated with the Brenner flexible bulb, Norman Ramsey proposed using a thin flexible teflon cone attached to a rigid cylinder as the variable volume storage bulb. This idea was implemented by Pierre Debely 13 and is shown in Figure 4. The great advantage of this configuration is that a thin cone can be inverted in such a way that only the edges of the cone are stressed. This reduces the region of possible stress effects to a negligibly small area, eliminating the uncertainty due to surface stressing. The volume ratio achieved by Debely was limited to 1.3 because of difficulties in obtaining maser oscillation with the cone inverted. The accuracy of the Debely device was limited to 2.4 x 10^{-12} because of the small value of B, drifts in the reference maser, and areas in the cone which became exposed when the cone was inverted. The asymmetrical bulb also made Debely's device especially susceptable to magnetic inhomogeneity shifts which he did not consider.

To overcome the problems associated with the Debely device, Norman Ramsey proposed combining the flexible cone with the large storage box hydrogen maser. This was implemented by the author 12,14 and is shown in Figure 5. In this device, the flexible cone is outside the microwave cavity, so the size of B is not limited by oscillation requirements. Magnetic inhomogeneity problems are also reduced. Because the device has a linewidth a factor of ten narrower than a conventional hydrogen maser, anomalous spin exchange effects are correspondingly reduced. The present configuration of the device achieved an accuracy limit of 2.4 parts in 10^{13} , but this was due to a large measurement uncertainty for B and a long term stability floor of a part in 10^{13} caused by the necessity of using an amplifier in the maser feedback loop. With passive maser techniques, 16 an accuracy of a part in 10^{14} should be achievable.

Another device which shows much promise is the concertina hydrogen maser developed by Harry Peters.⁶ The device is shown in Figure 6. In this device, the variable volume storage bulb is a flexible bellows of teflon film. There are stress effects, but to first order they cancell due to the bellows configuration. This device also has the great advantage of allowing measurement over a continous range of calibrated volumes. Stress effects will be determined by curve fitting the frequency shift data and by using bellows of differing thickness. The assymetrical arrangement of the storage bulb in the microwave cavity makes

this device very susceptable to magnetic inhomogeneity problems, but these can be measured and calibrated out for each volume setting. Preliminary measurements with the concertina maser have been consistent with hydrogen hyperfine measurements using the flexible bulb-large storage box maser, 17 and with a recent compliation of wall shift measurements. A very interesting side result of this measurement is that at $40\,^{\circ}\text{C}$, ϕ for type L FEP film 19 is a factor of four smaller than ϕ for FEP teflon sintered on a quartz storage bulb.

FURTHER DEVELOPMENTS

In 1970, Paul Zitzewitz and Norman Ramsey^{20,22} discovered that the wall shift goes through zero at approximately 100°C. This was later verified by Robert Vessot and Martín Levine.^{21,22} Based on this, a device using a variable volume storage bulb as a null detector for the zero wall shift point was proposed by Vessot and Levine.^{21,22} The great advantage of this device is that one need not know B accurately to calibrate out the wall shift, and because one actually operates with a zero wall shift, the device can be operated in an automated fashion.²²

One can generalize this idea to take advantage of dropping the necessity of measuring B without having to go to the zero wall shift temperature. This generalization is demonstrated in Figure 7. Since the value of ϕ changes with temperature, one need only change the temperature of a variable volume device while making measurements at the same two volumes. By extrapolating to the point where the curves for each temperature intersect, one can determine the zero wall shift point without actually reaching it. As discussed previously in the context of determining stress effects, 6 if one makes measurements at at least three temperatures, by the scatter of the intersection points, one can estimate the errors due to assumptions of constant ϕ or due to changes in f_0 .

One need not even have a linear measure of the inverse volume or λ^{-1} for the method to work. Since the wall shift is homogeneous in ϕ , for any monotonic function $X(\lambda^{-1})$, the intersection point of a family of curves in ϕ can only occur at zero wall shift. Also because the wall shift is homogeneous in ϕ , one can make a single point transformation λ^{-1} (X) where X is the measurement parameter such that the frequency change linear in λ^{-1} . One can therefore arbitrily mark two points, X_1 and X_2 , on the ordinate axis of a graph and linearly extrapolate to $\lambda^{-1}=0$ which is experimentally determined by the intersection of the straight lines.

Based on this method and the knowledge gained from previous devices, a new variable volume device is being developed at NASA's Goddard Space Flight Center. It is shown in Figure 8. The device will have a flexible cone variable

volume element outside the cavity to avoid the problems associated with a variable storage bulb inside the microwave cavity. It will also not have any electronic feedback to avoid the instabilities associated with amplifiers in the feedback loop. Figure 9 demonstrates that a reasonable external volume can be achieved without electronic feedback. The extra filling factor obtained with the elongated cavity design used in NASA masers has proved instrumental in achieving this. The plans are to operate this device either as a zero wall shift maser or in the generalized mode just described. Recent experiments have shown that FEP teflon film, after a bake out at 120°C, has a low enough vapor pressure at 100°C to allow a zero wall shift maser to function. With this device and future developments with some of the others outlined here, the promise of 10^{-14} accuracy should become a reality in the near future.

ACKNOWLEDGEMENTS

The author would like to acknowledge Dr. Peter Cervenka of Phoenix Corporation for providing Figure 9 and for his theoretical work demonstrating the feasibility of the external bulb variable volume maser.

REFERENCES

- 1. D. Kleppner, H. Goldenberg, and N. Ramsey [1962], Theory of the hydrogen maser, Phys. Rev., Vol. 26, 603
- 2. VANIER, J., LAROUCHE, R., and AUDOIN, C. [May 1975] The hydrogen maser wall shift problem. Proc. 29th Annual Symposium on Frequency Control (U.S. Army Electronic Command, Ft. Monmouth, N. J. 07703, May 28-30, 1975), in press (Electronic Industries Association, Washington, D. C. 20006).
- 3. BRENNER, D. [1969] Bull Am Phys. Soc., Vol. 14, 943.
- 4. BRENNER, D. [1970] Absolute frequency of the hydrogen maser using a flexible storage bulb. J. Appl Phys., Vol. 41, 2942.
- 5. REINHARDT, V. [1973] Flexible bulb-large storage box hydrogen maser. Proc. 5th Annual Precise Time and Time Interval Planning Meeting (NASA, Goddard Space Flight Center, Greenbelt, MD).
- 6. PETERS, H.E. [May 1975] The concertina hydrogen maser. Proc. 29th Annual Symposium on Frequency Control (U.S. Army Electronic Command, Ft. Monmouth, N. J. 07703, May 28-30, 1975), in press (Electronic Industries Association, Washington, D.C. 20006).
- 7. PETERS, H. E. [1971], Topics in Atomic Hydrogen Standard Research and Applications, Proceedings of the frequency standards and metrology seminar (Quebec).
- 8. CRAMPTON, S. B. and WANG, H. T. M. [May 1974] Density-dependent shifts of hydrogen maser standards. Proc. 28th Annual Symposium on Frequency Control (U.S. Army Electronics Command, Ft. Monmouth, N. J. 07703, May 29-31, 1974), pp. 355-361 (Electronic Industries Association, Washington, D. C. 20006).
- 9. REINHARDT, V. and PETERS, H. [May 1975] An improved method for measuring the magnetic inhomogeneity shift in hydrogen masers. Proc. 29th Annual Symposium on Frequency Control (U. S. Army Electronics Command, Ft. Monmouth, N. J. 07703, May 28-30, 1975), in press (Electronic Industries Association, Washington, D. C. 20006).
- 10. BERG, H. [March 1965], Spin exchange and surface relaxation in the atomic hydrogen maser. Phys. Rev. A., Vol. 137, A1621.

- 11. CRAMPTON, S. B. and WANG, T. M. [October 1975], Duration of hydrogen-atom spin-exchange collisions. Phys. Rev. A, Vol. 12, A1305.
- 12. REINHARDT [March 1974], The flexible bulb-large storage box hydrogen maser. Thesis (unpublished), Harvard University.
- 13. DEBELY, P. E. [1970] Hydrogen maser with deformable bulb. Rev. Sci. Inst., Vol. 41, 1290.
- 14. REINHARDT, V. [1973] Flexible bulb-large storage box hydrogen maser. Proc. 5th Annual Precise Time and Time Interval Planning Meeting (NASA, Goddard Space Flight Center, Greenbelt, MD).
- 15. UZGIRIS, E. E. and RAMSEY, N. F. [1970] Multiple region hydrogen maser with reduced wall shift. Physical Review A, Vol. 1, page 429.
- 16. WALLS, F. L. and HELWIG, H. [1976] A new kind of passively operating hydrogen standard, 30th Symposium on Frequency Control (USAEC, Ft. Monmouth, N. J.).
- 17. REINHARDT, V. S. and LAVANCEAU [1974] A comparison of the cesium and hydrogen hyperfine frequencies by means of portable clocks and Loran C, 28th Symposium on Frequency Control (USAEC, Ft. Monmouth, N. J.).
- 18. HELWIG, H. et. al. [1970] Measurement of the unperturbed hydrogen hyperfine transition frequency, IEEE Trans., Vol. IM-19, 200.
- 19. Dupont Trademark.
- 20. ZITZEWITZ, P. W. and RAMSEY, N. F. [1971] Studies of the wall shift in the hydrogen maser. Physical Review A. Vol. 111, page 51.
- 21. VESSOT, R. and LEVINE, M. [October 1970] A method for eliminating the wall shift in the hydrogen maser. Metrologia, Vol. 6, No. IV, pp 116-117.
- 22. VESSOT, R., et. al. [1971] Recent developments affecting the hydrogen maser as frequency standard. NBS Special Publication 343, Precision measurements and fundamental constants, August 1971. pp 22-37. (See also U. S. Patent No. 370-2972, Atomic hydrogen maser with bulb temperature control to remove wall shift).

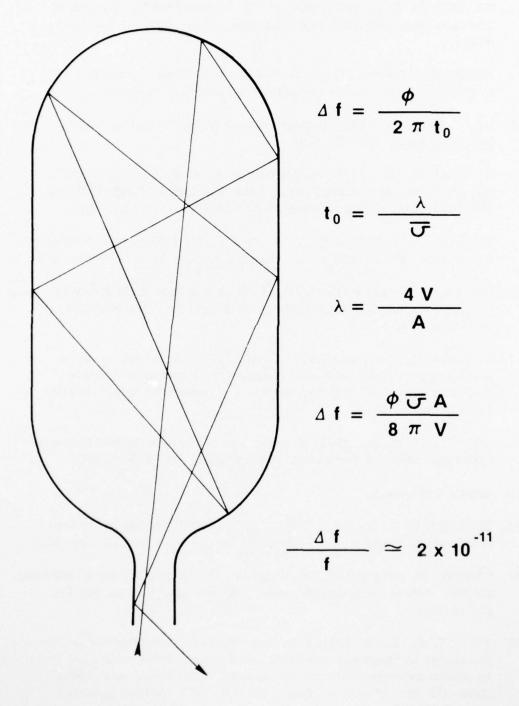


Figure 1. The Wall Shift

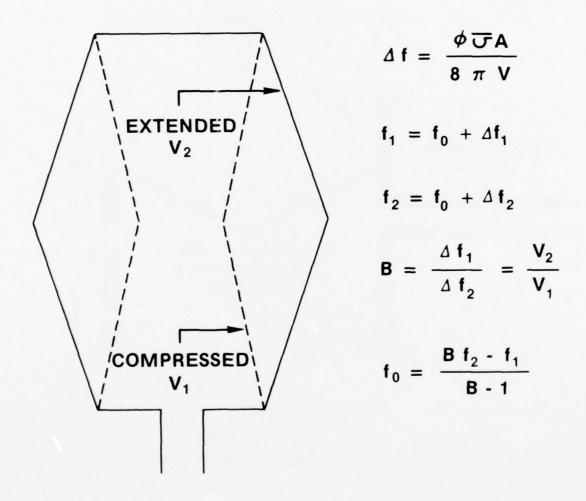


Figure 2. The Variable Volume Technique

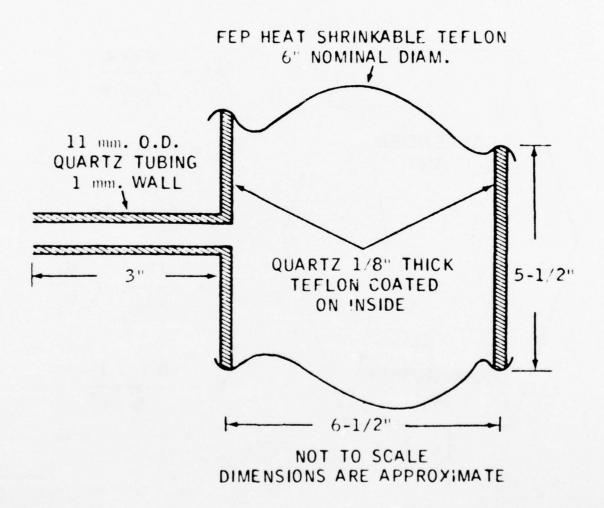


Figure 3. Brenner Variable Volume Storage Bulb (Reprinted From: D. Brenner [1970], J. Appl Phys., Vol. 41, 2942).

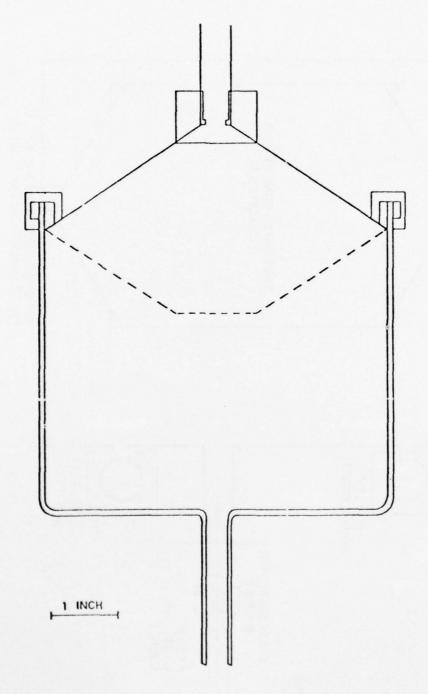


Figure 4. Debely Variable Volume Storage Bulb (Reprinted From: P. E. Debely [1970], Rev. Sci. Inst., Vol. 41, 1290)

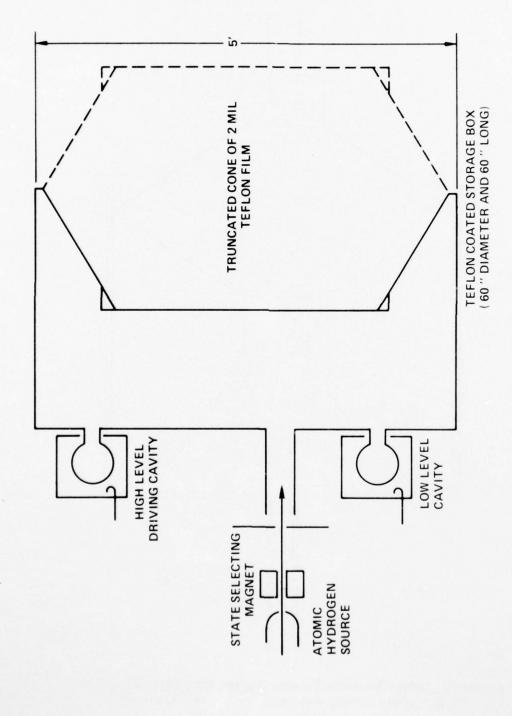


Figure 5. The Flexible Bulb-Large Storage Box Hydrogen Maser

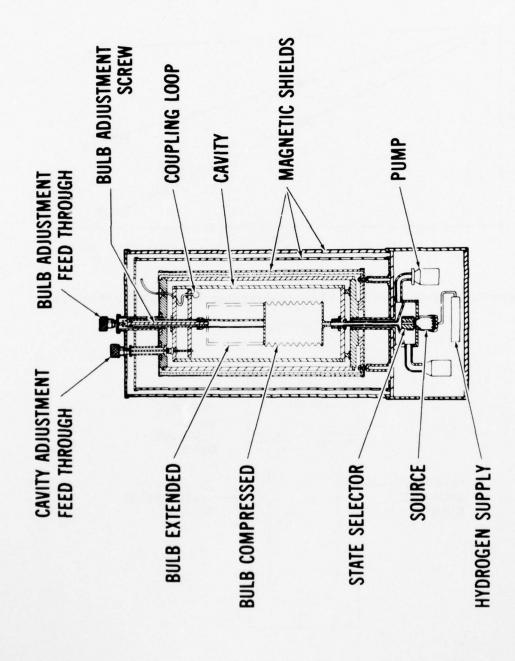


Figure 6. The Concertina Hydrogen Maser

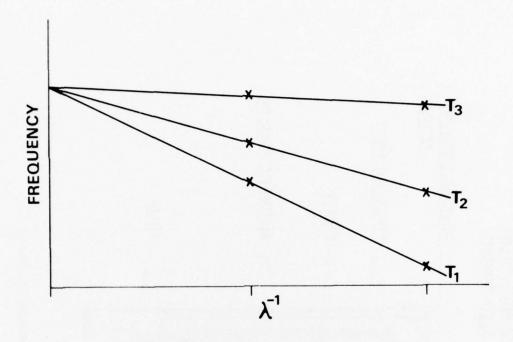


Figure 7. Extrapolation Method for Determining the Zero Wall Shift Point

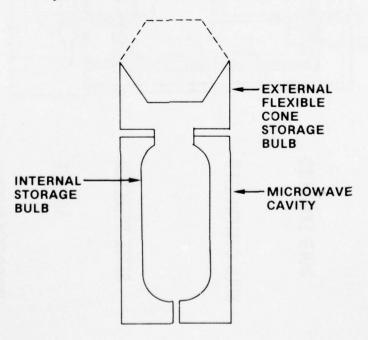


Figure 8. The External Bulb Variable Volume Maser

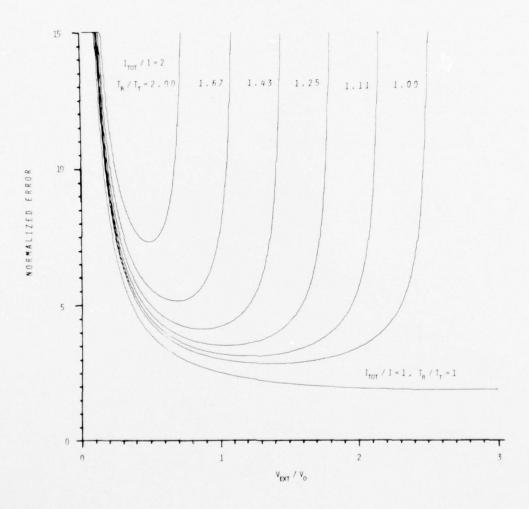


Figure 9. External Bulb Variable Volume Maser Error

PROBLEMS IN HYDROGEN MASER DESIGN AND SUGGESTED IMPROVEMENTS

Stuart B. Crampton
Harry T. M. Wang
John L. Barrett
Williams College
Williamstown, Massachusetts

ABSTRACT

Frequency shifts due to changing magnetic field inhomogeneities can limit the stability of atomic hydrogen maser standards. They can be minimized by careful design of the magnetic shields, by centering the storage bottle in the microwave cavity, and by operating at relatively high ambient magnetic fields, so as to make these frequency shifts less than one part in 10-13 and the instabilities due to changes of field much smaller than 10^{-13} . The inhomogeneity shift is also reduced by increasing the atom storage time, as are both the instabilities due to changes of cavity tuning and the amount of hydrogen atom flux required for self-sustained oscillation. Strategies for improved atom storage times include new surface materials and improved collimation techniques.

INTRODUCTION

Atomic hydrogen maser frequency standards are normally operated at very low average magnetic fields, in order to take advantage of the quadratic dependence of frequency on magnetic field so as to minimize errors due to changes of the average magnetic field. Unfortunately, in low average magnetic fields the hydrogen maser oscillation frequency is subject to appreciable errors due to changes of gradients in the magnetic field. Motion through static and microwave magnetic field gradients by the radiating atoms induces hyperfine transitions which pull the oscillation frequency by amounts which can vary as the static magnetic field gradients change over time. And the static magnetic field gradients change over time. This report provides rough estimates of frequency shifts to be expected because of this mechanism and suggests strategies for minimizing the effects on long term frequency stability.

MOTIONAL FREQUENCY SHIFTS

Changes $\delta v_{\rm osc}$ of the spin exchange tuned hydrogen maser oscillation frequency due to changes of static magnetic field gradient are of the order of 3

$$\delta v_{\rm osc} \simeq \pm (3 \text{ to } 6) \times 10^{-3} (\pi T_{\rm B})^{-1} (\rho_{11} - \rho_{33})_{\rm 0} \left[1 + (1.5 \times 10^{-5} \omega_{\rm g})^{4}\right]^{-\frac{1}{2}} \delta (\pi T_{\rm M})^{-\frac{1}{2}} . \tag{1}$$

 $(\pi T_{\rm R})^{-1}$ is the contribution to the atomic resonance linewidth from the rate at which atoms escape from the storage bottle. It can be reduced by using a small effective exit area, but it cannot be reduced much below the contribution $(\pi T_W)^{-1}$ to resonance linewidth from wall collision relaxation plus the contribution $(\pi T_M)^{-1}$ from motion through static magnetic field gradients, without limiting the oscillation power level and spin exchange timing range. $(\rho_{11} - \rho_{33})$ is the net average electron polarization of the hydrogen atom beam as it enters the storage bottle. It can be reduced with some loss of oscillation power and tuning range by driving Zeeman transitions in the atomic beam before it enters the storage bottle, or it can be reduced without loss of power or tuning range using the double focusing technique to eliminate atoms in the uppermost hyperfine state from the atomic beam. 4 , 5 ω_z is the angular frequency of the ΔF=0 Zeeman transitions and is directly proportional to the static magnetic field averaged over the storage bottle. The contribution $(\pi T_M)^{-1}$ of magnetic field gradient relaxation to the atomic resonance linewidth is proportional to the mean square deviation of the static magnetic field from its average, so that $\delta(\pi T_M)^{-\frac{1}{2}}$ is proportional to the change of amplitude of the static magnetic field gradient. $(\pi T_M)^{-1}$ depends on ω_z roughly as $[1+(1.5\times10^{-5}\omega_z)^4]^{-1/2}$, so that $\delta v_{\rm OSC}$ falls off with increasing static magnetic field roughly as ω^{-4} and can be made arbitrarily small by operating the hydrogen maser at relatively high magnetic fields such that ω_2 is large compared to the rate at which atoms bounce back and forth across the storage bottle. In that case care must be taken to precisely measure and make relatively large corrections for the magnetic field dependence of the oscillation frequency in such high magnetic fields. The factor $\pm (3 \text{ to } 6) \times 10^{-3}$ in eq.(1) depends in sign and magnitude on the correlation between static magnetic field inhomogeneities and the configuration of the microwave magnetic field in the hydrogen maser cavity. Carefully centering the storage bottle in the cavity eliminates oscillation frequency pulling from first and all odd order static magnetic field gradients.

Eq.(1) predicts frequency shifts which are small enough to be hard to detect yet large enough to contribute to long term frequency instability. For example, for $(\pi T_M)^{-1}{}^{\simeq}0.1$ Hz. a change of static magnetic field gradient of 10% may give a shift of order $5{\times}10^{-1}{}^4{\rm of}$ the oscillation frequency. The shift may be larger or smaller depending on the configuration of static magnetic field gradient,

but model calculations based on plausible field configurations suggest this order of magnitude at very low average magnetic field and $(\rho_{11} - \rho_{33})_{\mathbb{Q}} \cong 1/2$. Of course, this source of oscillation frequency instability can be reduced by reducing changes of static magnetic field gradient by careful magnetic shield design, or by reducing any of the other factors in eq.(1).

INCREASED HYDROGEN ATOM STORAGE TIME

We have been doing experiments to maximize hydrogen atom storage time using multitube collimators to confine the atoms in the storage bottles longer, thereby reducing both the factor $(\pi T_B)^{-1}$ in eq.(1) and the overall linewidths at which the hydrogen maser is tuned and operated. Lower overall linewidth means less oscillation frequency instability due to drifts of the microwave cavity tuning. The beam intensity required for oscillation is also less, so that requirements of pumping speed and pump element life are eased. The only disadvantage is that the oscillation power level is reduced, so that longer averaging times are required.

Table one shows a comparison between relaxation rates and relative beam intensities measured for two 5" diameter spheres coated with FEP Teflon, one of which had a conventional stem to limit egress by the atoms and the other a multitube collimator in place of the stem.

TABLE ONE

	With	Stem	With Collimator
$(\pi T_B)^{-1}$ $(\pi T_O)^{-1}$.67	Hz	.27 Hz
$(\pi T_O)^{-1}$.87	Hz	.49 Hz
I	1		.27
V _C	5.16	cm ³	.1 cm ³

The stem was 7.54 mm I.D. by 115.6 mm long and was coated with FEP Teflon. The collimator was a bundle of tubes having .05 mm pore diameters by 1 mm long and said by the manufacturer to have 50% transparency before being coated with fluorinated drifilm. The $(\pi T_B)^{-1}$ contribution to the resonance linewidth due to atom escape from the storage bottle was substantially reduced for the bottle with the collimator. The overall density-independent linewidth $(\pi T_O)^{-1}$, including $(\pi T_B)^{-1}$, $(\pi T_M)^{-1}$ and wall collision relaxation was also substantially reduced but by a smaller ratio because similar .2 Hz contribution by wall collision relaxation cases. Comparing the measured $(\pi T_B)^{-1}$ for the bottle collimator to what would be predicted by geometry. The relative input beam intensity I for

NATIONAL AERONAUTICS AND SPACE ADMINISTRATION GREENB--ETC F/6 14/2 PROCEEDINGS OF THE ANNUAL PRECISE TIME AND TIME INTERVAL (PTTI)--ETC(U) 1977 AD-A043 856 UNCLASSIFIED NASA-6SFC-X-814-77-149 NL 5 OF 8 AD AO43856

was even less than .38, probably due to alignment problems. Despite the alignment loss, the ratio of maximum available resonance linewidth to $(^{\Pi}T_{O})^{-1}$, which determines the spin exchange tuning range, was 1.2 times greater for the bottle with the collimator because of the much longer storage time. The volume V_{C} of the collimator, which is an important factor in the motional averaging frequency shifts discussed by Brenner, was only .02 as large as the volume of the stem.

These results are promising, and we plan to try some collimators having larger pore diameters for easier alignment and better transparency after coating but with some increase of volume. We also plan to try some new coating materials, in order to reduce the contribution to $(\pi T_{\rm O})^{-1}$ from wall collision relaxation, but we have not yet found anything better than FEP Teflon.

REFERENCES

- * Research supported by National Science Foundation Grant PHY74-12226 AO1, NASA Contract 23520, and The Research Corporation.
- D.Kleppner, H.C.Berg, S.B.Crampton, N.F.Ramsey, R.F.C.Vessot, H.E.Peters and J.Vanier, Phys. Rev. 138, A972 (1965).
- 2. S.B.Crampton and H.T.M.Wang, in <u>Proceedings of the 28th Annual Frequency Control Symposium</u> (Electronics Industries Association, 2001 Eye St. N.W., Washington, D.C., 20006, 1974), p 355.
- S.B.Crampton, E.C.Fleri and H.T.M.Wang, to be published in Metrologia.
- C.Audoin, M.Desaintfuscien, P.Piejus and J.P.Schermann, <u>Proceedings of the 23rd Annual Frequency Control Symposium</u>, p. 288 (1969).
- 5. R.F.Lacey and R.F.C.Vossot, op. cit., p.279.
- Galileo Electro-Optics Corp. Galileo Park, Sturbridge, Mass. 01518.
- 7. D. Brenner, Phys. Rev. 185, 26 (1969).

NEW TE111-MODE HYDROGEN MASER

Edward M. Mattison, Martin W. Levine, and Robert F. C. Vessot, Smithsonian Astrophysical Observatory

ABSTRACT

We describe the construction and discuss the properties of a TE_{111} -mode hydrogen maser resonant cavity that has achieved maser oscillation. The TE_{111} -mode cavity is about half the size of traditional maser cavities and combines the electromagnetic resonator and the hydrogen storage region in a single structure. The measured line Q of the operational cavity is $Q_{\chi} = 8.5 \times 10^8$, and the probability for hydrogen-atom relaxation on the Teflon-coated walls is approximately $5 \times 10^{-5}/\text{impact}$. We also discuss a possible modification to the cavity that would increase the magnetic filling factor.

INTRODUCTION

The minimum size of a hydrogen maser is determined by the size of its electromagnetic resonant cavity, which must have a resonance frequency of 1420 MHz. Typical ${\rm TE}_{011}$ -mode resonators traditionally used in masers are approximately 28 cm long and 28 cm in diameter. The cavity, in turn, is surrounded by a vacuum envelope, temperature-controlling ovens, thermal insulation, and several layers of magnetic shields. A lower size limit for ${\rm TE}_{011}$ -mode hydrogen masers appears to be represented by the maser that flew in the probe rocket of the recent gravitational redshift experiment 1 ; this maser was 0.6 cm long and 0.5 m in diameter and weighed 40 kg.

We have investigated the possibility of using different types of cavities to reduce the size of hydrogen masers. 2 In particular, we have shown that a new type of cavity, the cylindrical ${\rm TE}_{111}$ -mode resonator, is capable of sustaining maser oscillation, and we have constructed and successfully operated such a cavity in a maser.

The ${\rm TE}_{111}$ -mode cavity, which is compared with the ${\rm TE}_{011}$ -mode cavity in Figure 1, is roughly half the length and diameter of the ${\rm TE}_{011}$ resonator. It is divided into two equal storage volumes by a Teflon-coated septum, with half the hydrogen beam entering each volume. A separate storage bulb is not used; rather, the inside walls of the resonator are coated with Teflon and, together with the Teflon septum, constitute the hydrogen-confining surface. Thus, the resonator and "bulb" are a single structure.

OSCILLATION CRITERION

In a hydrogen maser, hydrogen atoms are confined to a region of constant-phase RF magnetic field within an electromagnetic resonant cavity. To produce self-oscillation, the field amplitude must be great enough to stimulate emission from the atoms at a rate that overcomes the electrical losses in the cavity. The necessary condition for oscillation thus involves both the resonator Q and the geometrical distribution of RF fields within the hydrogen storage volume. The oscillation criterion is given by 2

$$S \equiv Q_1 n' \ge 5.9 \times 10^3$$
 (1)

where the parameter S is the product of Q_L , the loaded cavity Q_n and η' , the storage-bulb filling factor. The filling factor is defined by

$$n' = \frac{V_b}{V_c} \frac{\langle H_z \rangle_b^2}{\langle H^2 \rangle_c} \qquad \text{for the TE}_{011}\text{-mode cavity}$$
 (2a)

$$\eta' = \frac{2V_b}{V_c} \frac{\langle H_z \rangle_b^2}{\langle H^2 \rangle_c} \qquad \text{for the TE}_{111}\text{-mode cavity}$$
 (2b)

where V_b = volume of a single storage region,

V_c = total cavity volume,

 $\langle \rangle_{b}$ = average over storage region,

 $\langle \rangle_{c}$ = average over cavity, and

H and H_z = RF magnetic field.

The value of Q_L depends on the materials and construction of the cavity, as well as on its size, shape, and electromagnetic mode; η' , on the other hand, is a function only of the storage-bulb and cavity geometries.

Figure 2 shows S_0 , the value of S for an uncoupled resonator, as a function of shape for a silver-coated TE_{111} -mode maser cavity. Such a cavity with a length-to-diameter ratio L/D=1.25 has a calculated filling factor of $\eta'=0.42$. With a loaded Q of 24000, attainable in practice, this gives S=10000, almost twice the threshold value, indicating that the cavity should support oscillation.

PROPERTIES OF THE TE_{111} -MODE MASER

A prototype TE_{111} -mode cavity, 18 cm long and 16 cm in diameter, is shown in Figure 3. For convenience of construction it was made of OFHC copper, rather than of low-expansion ceramic, and is divided into

four sections. The division parallel to the longitudinal cylinder axis allows the left and right halves to clamp a thin Teflon sheet that separates the two atom-confining regions, while the division perpendicular to the axis permits the cavity's resonance frequency to be set by machining the cavity to the proper length. These dividing planes were chosen to coincide with zero-current lines of the TE_{111} mode so that good electrical contact between the sections is not a critical requirement.

The cavity was mounted on a modified maser that contains a hydrogen source, magnetic shields and solenoids, and thermal controls. The resonance frequency was adjusted during operation by varying the cavity's temperature and by moving a copper rod within a small Teflon-coated glass dome that extends into the cavity. A similar dome houses the RF pickup loop.

The characteristics of the TE_{111} resonator are given in Table 1, The unloaded cavity Q is quite close to its theoretically calculated value, the high value probably being due to the use of a solid copper cavity with 1 cm walls and proper dividing planes, which combine to prevent RF leakage. The measured Q_L , together with the calculated η' , gives a value for the oscillation parameter S that is 1.9 times its threshold value, as predicted. The oscillating TE_{111} -mode maser has an RF power output of

$$P_{out} \simeq -102 \text{ dBm} = 6.3 \times 10^{-11} \text{ mw}$$

and a measured line Q of

$$Q_{\varrho} = 8.5 \times 10^{8}$$

Table 1. TE₁₁₁ cavity parameters.

Measured

Loaded Q: $Q_L = 27 \times 10^3$ Coupling parameter: $\beta = 0.12$

 $Q_0 = 30 \times 10^3$ Unloaded Q:

Calculated

 $Q_0 = 33 \times 10^3$, $\frac{Q_0(\text{meas})}{Q_0(\text{theo})} = 0.9$ Unloaded Q:

Filling factor: $\eta' = 0.419$

Oscillation Criterion

 $S = Q_L(meas) \times n'(calc) = 11.3 \times 10^3$

 $\frac{S}{S_{\text{thresh}}} = 1.9$

The hydrogen-atom relaxation time was measured to be 0.34 sec, while the calculated geometrical lifetime is 1 sec, giving a wallcollision relaxation rate of 2 sec⁻¹. This corresponds to a relaxation probability of approximately 5×10^{-5} /impact, which agrees with other relaxation measurements on FEP Teflon.³

MODIFIED CAVITY DESIGN

In the TE_{111} resonator discussed above, the hydrogen atoms sample the RF magnetic field throughout the cavity, including near the ends, where the field is transverse rather than longitudinal. If the atoms were restricted to the center region of the cavity, the filling factor of the resonator could be increased and frequency instabilities caused by changes in the transverse RF and DC magnetic-field gradients could be reduced.

One method of confining the hydrogen atoms to the center is to fill the ends of the cavity with a solid dielectric material such as quartz. A second method is to form the ends of the hydrogen storage volume with transverse septa of thin, Teflon-coated quartz, as shown schematically in Figure 4. Shortening the storage region by the latter technique increases the filling factor by approximately 15% for a storage region that is three-fourths the length of the cavity (Figure 5). Both methods of shortening the storage region have the disadvantage that the dielectric would decrease the cavity's Q and increase its sensitivity to temperature change (although the use of very thin quartz septa could minimize these effects), and thus neither method is likely to be practical if employed solely to increase the filling factor. However, the second method may be useful for investigating, and possibly reducing, the inhomogeneity frequency shifts.

ACKNOWLEDGMENT

This work was supported in part by Contract N00014-71-A-0110-0003 from the Department of the Navy, Office of Naval Research, administered by the U.S. Naval Research Laboratory.

REFERENCES

- R. F. C. Vessot, M. W. Levine, F. M. Mattison, T. E. Hoffman, E. A. Imbier, M. Tetu, G. Nystrom, J. J. Kelt, Jr., H. F. Trucks, and J. L. Vaniman, Space-borne hydrogen maser design. In <u>Proceedings of the Eighth Annual Precise Time and Time Interval Applications and Planning Meeting</u>, U.S. Naval Research Laboratory (this volume).
- E. M. Mattison, R. F. C. Vessot, and M. W. Levine, A study of hydrogen maser resonators and storage bulbs for use in ground and satellite masers. In <u>Proceedings of the Seventh Annual Precise Time and Time Interval Applications and Planning Meeting</u>, Goddard Space Flight Center, Greenbelt, Maryland, pp. 243-263, 1976.

- 3. M. Desaintfuscien. Ph.D. Thesis, University of Paris, Orsay, 1975.
- 4. S. B. Crampton, Effects of atomic resonance broadening mechanisms on atomic hydrogen maser long term stability. In <u>Proceedings of the 2nd Frequency Standards and Metrology Symposium</u>, National Bureau of Standards, Boulder, Colorado, pp. 589-613, 1976.
- 5. V. J. Folen. Naval Research Laboratory Report, to be published.

FIGURE CAPTIONS

- Fig. 1 TE_{011} and TE_{111} maser cavities. Section views are drawn to the same scale; the actual inside dimensions of typical cavities are TE_{011} , 25-cm length x 29-cm diameter; TE_{111} , 19-cm length x 15-cm diameter.
- Fig. 2 Oscillation parameter ${\rm S}_0$ for uncoupled ${\rm TE}_{111}$ -mode maser cavity as a function of cavity shape.
 - 3 Photograph of experimental TE $_{111}$ -mode cavity on test-bed maser.
 - 4- Section view of TE $_{111}-$ mode maser cavity with shortened hydrogen storage volume.
- Fig. 5 Filling factor of TE_{111} -mode cavity with shortened storage volume.

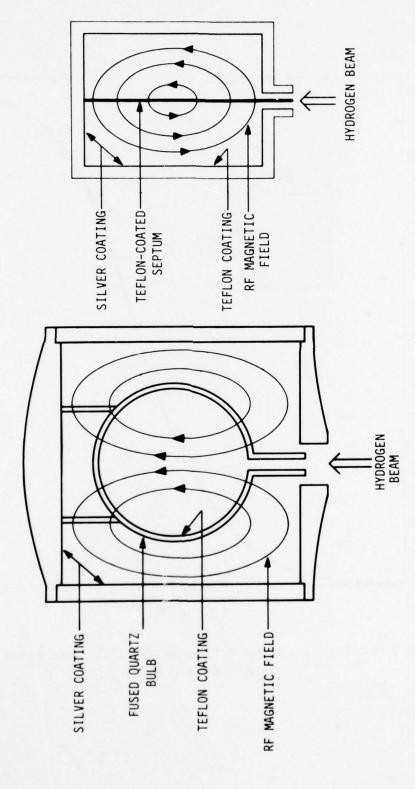


Fig. 1-TE $_{011}$ and TE $_{111}$ maser cavities. Section views are drawn to the same scale; the actual inside dimensions of typical cavities are TE $_{011}$, 25-cm length x 29-cm diameter; TE $_{111}$, 19-cm length x 15-cm diameter.

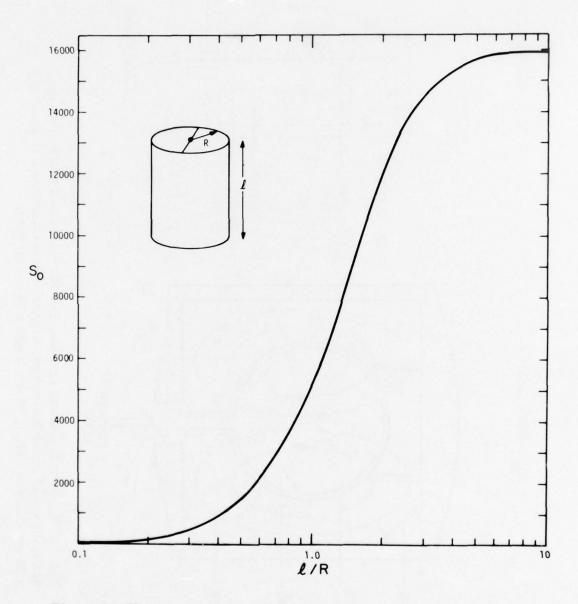


Fig. 2-Oscillation parameter ${\bf S_0}$ for uncoupled ${\bf TE_{111}}{\text{-}}{\bf mode}$ maser cavity as a function of cavity shape.

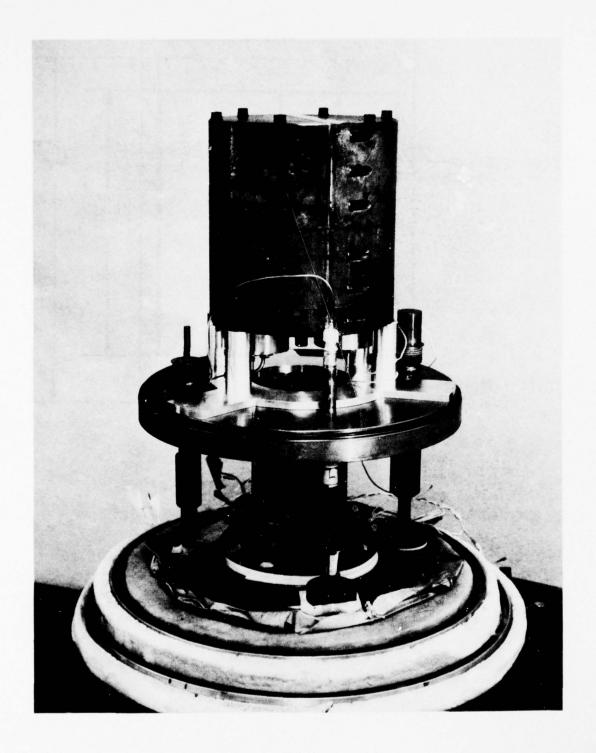


Fig. 3-Photograph of experimental $\mathrm{TE}_{111}\text{-}\mathrm{mode}$ cavity on test-bed maser.

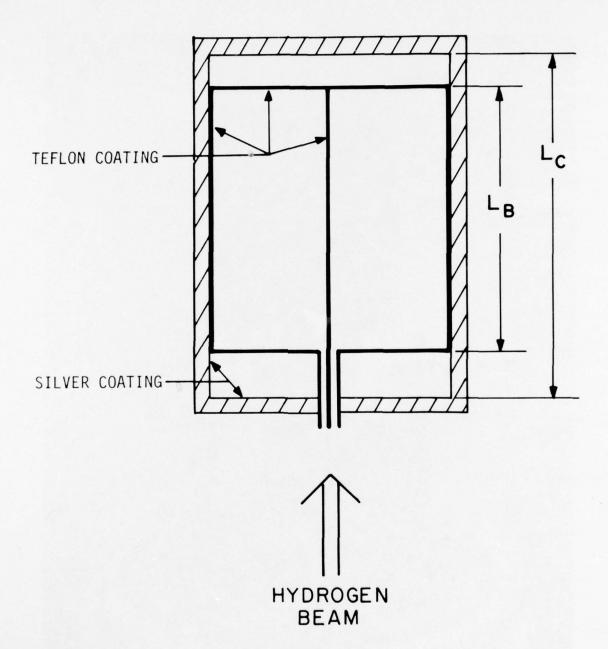


Fig. 4-Section view of ${\rm TE}_{\rm 111}{\rm -mode}$ maser cavity with shortened hydrogen storage volume.

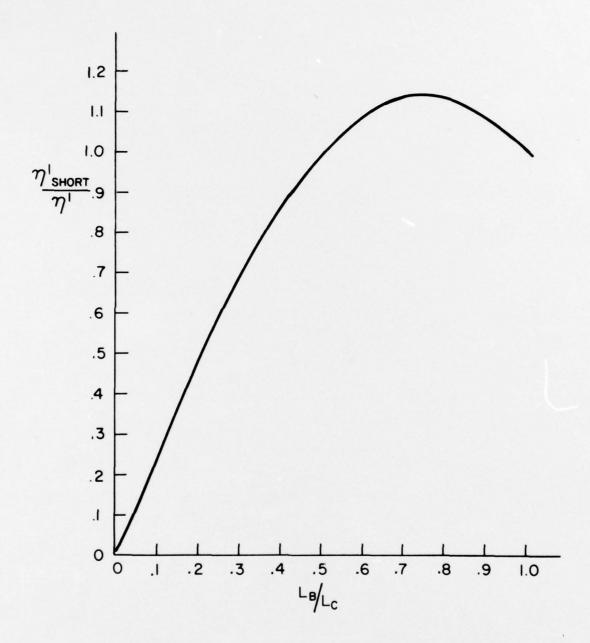


Fig. 5-Filling factor of $\mathrm{TE}_{111}\text{-mode}$ cavity with shortened storage volume.

DESIGN AND RESULTS FROM A PROTOTYPE PASSIVE HYDROGEN MASER FREQUENCY STANDARD

F. L. Walls

Frequency & Time Standards Section National Bureau of Standards Boulder, Colorado 80302

ABSTRACT

The basic design of a prototype passive hydrogen maser frequency standard is very briefly described and its unique features outlined. The latest results on its long-term stability and environmental sensitivity will be given. The present results indicate that $\sigma_{\mathbf{y}}(\tau) \leq 2 \times 10^{-7} \text{ for averaging times between 40 s and } 15000 \text{ s}, \sigma_{\mathbf{y}}(15000) \sim 1.4 \times 10^{-7} \text{ . Over a fourteen-day period the rms daily time fluctuations was 2 ns while the least squares fit to a linear frequency drift over the fourteen days was 6 x 10 /day, which is within the measurement noise. These results are particularly noteworthy for those interested in clocks for timekeeping applications as they were obtained without temperature control of any of the electronics and only a single oven on the cavity. Further improvements in the electronics including temperature stabilization of critical control circuits should reduce the daily variations by a factor of five to ten and also improve the already excellent long-term stability.$

The design principles illustrated by this prototype can also be used to realize a miniature passive hydrogen maser frequency standard with little compromise in long-term stability [1].

Fig. 1 shows the block diagram of the present prototype passive hydrogen maser frequency standard. This present configuration is intended to show feasibility of achieving GPS specifications for time keeping stability of 10 ns over a 10 day prediction period, and to allow monitoring of various parameters which might affect its performance. The microwave cavity, atomic hydrogen source, and magnetic field configuration are similar to designs used in active masers. The 5 MHz crystal controlled oscillator is distributed through five -120 dB isolation amplifiers. Three outputs are for measurement purposes and two drive internal electronics. The 5 MHz signal is phase modulated at 12.2 kHz and $^{\circ}$.4 Hz, multiplied to 1440 MHz and then mixed with a synthesizer signal to produce the hydrogen resonance frequency. The .4 Hz phase modulation probes the hydrogen resonance which produces amplitude modulation at .4 Hz, the size of which is proportional to the frequency offset between

the probe signal and the hydrogen resonance. This signal is detected as .4 Hz amplitude modulation of the 20 MHz signal. After amplification and filtering, this signal is demodulated to produce an error signal which is used to correct the frequency of the 5 MHz oscillator. The attack time of this frequency lock loop is typically a few seconds.

In a very similar way the cavity detuning from the probe frequency is sensed by detecting the 12 kHz amplitude modulation on the 20 MHz signal. This 12 kHz signal is amplified, filtered, and demodulated to produce an error signal which is used to correct the cavity frequency. Since the probe signal is automatically steered to the center of the hydrogen resonance frequency via the .4 Hz servo, this produces a clean way of tuning the cavity frequency to the hydrogen resonance frequency. The 12 kHz sidebands due to the phase modulation are -10 dB relative to the carrier and equal in amplitude to several parts per million. The signal-to-noise in the cavity servo loop is such that the cavity frequency can be detected with a resolution of 5 Hz in only a few seconds. The present servo attack time is 10 s which allows rapid correction of cavity offset due to any environmental perturbation be it changes in pressure, aging of the cavity coating, deformation of the cavity due to strain or sudden shock, or even changes is cavity pulling due to changes of the coupling to the amplifiers. This cavity servo scheme should have virtually no effect on the hydrogen resonance line due to the small size of the 12 kHz sidebands and their high symmetry about the hydrogen resonance.

The ability of the cavity servo to correct for cavity changes is very clearly illustrated by Figure 2. The lower portion shows the cavity correction vs time after a 1°C change in cavity temperature. The sensitivity is about 1 volt per 1 kHz change in uncorrected cavity frequency. The upper portion of Figure 2 shows the frequency of the fully locked up passive hydrogen frequency standard over the same period of time. The frequency changed fractionally by about 7×10^{-14} due to a .7°C change in cavity temperature over the period in which the data was taken. This corresponds to an open loop change of about 700 Hz in cavity frequency. This fractional change of 7×10^{-14} is probably due to a combination of a change in the wall shift and the second order Doppler shift, rather than an error in the cavity servo. Without the cavity servo the frequency would have changed fractionally by ∿ 10⁻¹ results mean that the cavity servo can correct for cavity changes of order 100 Hz or larger and still hold the perturbation to the output frequency below 1×10^{-14} . This relaxes the requirement of temperature . This relaxes the requirement of temperature stability of the cavity approximately a factor of 100 compared to any present stand alone active cavity maser design. The required cavity temperature stability for the passive maser is determined by the second order Doppler shift of $1.3 \times 10^{-13}/^{\circ}\text{C}$ and the temperature dependence of the wall shift. This limit is about ± .070°C for a fractional change of ± 1 × 10-14

Other parameters which might affect the frequency of such a passive hydrogen maser are variations in hydrogen beam density and variations in microwave power. Fig. 3 shows the data taken to measure the spin-exchange shift. A 33% increase in beam intensity produced a change of $^{\simeq}$ 6 $^{\pm}$ 4 x 10 $^{-14}$. Similarly it was found that a change in microwave power of -2 dB caused a shift of about 8 $^{\pm}$ 4 x 10 $^{-14}$. Both these effects are small enough that they should not affect the stability on the 10 $^{-14}$ level in the final design. The time domain stability of the passive hydrogen maser for 2000 s < $_{\rm T}$ < 2.9d was measured against two high-performance cesium tubes in a three-corner hat arrangement, i.e., three pairs of beat frequency data were used to assign a stability to each clock. See Fig. 4.

Figure 4 shows primarily that the frequency stability of the passive hydrogen maser is substantially better than that of Cs 324 and Cs 323, over the region from 2000 s to 64000 s. For example, the data at 2000 s and 4000 s, which have the best confidence, indicate that the short-term stability of the passive hydrogen is \sim 6 \pm 27 x 10 $^{-1/2}$. Unfortunately, there just was not enough time to take more data in order to reduce the uncertainty in the measurement.

The data of passive hydrogen versus NBS-6, one of our primary cesium standards is shown in Fig. 5. This data shows that the stability of the pair is $^{\circ}$ 2.2 x 10⁻¹² $_{\tau}$ 7⁻¹/₂ (38 s < $_{\tau}$ < 15000 s) and hence provides an upper limit on the stability of the passive hydrogen and NBS-6. The long-term frequency stability of the passive hydrogen maser was assessed by comparison against the UTC (NBS) time scale comprised of nine cesium standards including our primary cesium standards NBS-4 and NBS-6. The 5 MHz output from the passive maser was divided down to 1 pulse per second and compared to a similar 1 pulse per second tick originating from member clocks of the time scale. Daily time differences were recorded with an accuracy of = 1.5 ns. In this way the frequency of the passive maser at one-day and longer averaging times could be measured. Frequency stability plots of this data are shown in Figs. 5 and 6. The fractional frequency stability data is shown at the bottom of Fig. 6 along with variou. notes of prevailing experimental conditions. As noted this data was taken over several days following ~ 1°C change in cavity temperature. The data over the days 8-9 and 9-10 were anomalously low and an examination of the various monitors indicated that the crystal oscillator servo loop was exceeding its dynamic range part of the time. The crystal oscillator was then re-set within its normal range. The frequency then returned to its nominal average of the first eight days. The morning of day 14, the laboratory suffered a short power outage which caused some troubles in the electronics and the analysis was terminated.

The square root of the Allan Variance derived from the data of Fig.6 is shown in Fig. 5 [2]. It is quite apparent that there is a more or less daily variation in the frequency due to some environmental influence, which is above the level of white frequency fluctuations expected on the basis of the data from 38 s to 15000 s.

In spite of this, the stability at 3 days is $8.4\pm5 \times 10^{-15}$ and at 4 days it is $2.2\pm1.8 \times 10^{-15}$. It is expected that the noise level near 1 day, which acts like some sort of phase modulation can be reduced by temperature control of the critical servo control electronics and some of the filters. At the present time none of the electronics is temperature controlled. A least squares fit to the data of Fig. 6 yields a linear drift of 6×10^{-16} /day which is within the measurement noise of the two end points. From the frequency stability data of Fig. 6 it can be shown that the expected time keeping accuracy over a 10-day prediction period has a 10 uncertainty of less than 10 ns. In fact over the 8-day period where continuous data exists, the maximum time excursion was 4 ns using an after the fact average frequency, which of course can't be done for true time prediction.

The <u>long-term</u> frequency stability data presented in Figs. 4 to 6, and especially the low drift are to my knowledge, the best that have ever been documented for a single stand alone hydrogen frequency standard, and it is as good as that observed with multiple hydrogen masers which are autotuned against one another or against a separate hydrogen maser [3-7].

This excellent long-term stability has been accomplished with a relatively standard physics package - only the electronics design is new and it isn't even temperature stabilized yet. Therefore, stabilities of this level or better could be achieved with many existing active masers by converting the electronics to the passive approach outlined in Fig. 1. The main requirement is that the cavity have 2 coupling ports.

The passive electronics will also be used with a small dielectric cavity measuring ~ 6 " diameter and 6" long. It is expected that 10-day stabilities exceeding 1 x 10^{-14} can also be achieved with the small cavity. This coupled with the other advantages of the passive approach, e.g., low hydrogen beam requirements, should make possible a hydrogen maser of exceptional stability measuring less than 15" dia and 36" long.

Moreover it should be reiterated that the sensitivity of the passive hydrogen maser to environmental purturbations is greatly reduced over that of the present stand alone active masers because of its rapid active cavity control, the lack of threshold conditions on beam flux, and its ability via equalization of the populations of the three upper spin states, to greatly reduce the magnetic field inhomogeneity shift (Crampton effect) without reducing the safety margin above a threshold condition [1].

ACKNOWLEDGMENTS

It is a pleasure to acknowledge the assistance of H. Hellwig, D.W. Allan, H.E. Machlan, S.R. Stein, D.J. Wineland, D.A. Howe, H.E. Bell, and J. Valega.

I am also grateful to Drs. P. Franken and J. Small for making the facilities of the Optical Science Center of the University of Arizona available and to E. Strittmatter and R. Sumner of the Optical Science Center for machining and delivery of the ULE cavity used in this work.

REFERENCES

- [1] F. L. Walls and H. Hellwig, Proc. 30th Annual Frequency Control Symp., Ft. Monmouth, NJ (1976).
- [2] J. A. Barnes et al., IEEE Trans. on Instr. and Meas. IM-20, No. 2, p. 105 May 1971.
- [3] D. Morris and K. Nakagiri, Metrologia 12, 1, (1976).
- [4] Octav Gheorghiu, Jacques Viennet, Pierre Petit et Claude Audoin, C.R. Acad. Sc. Paris t. 278, 1059, June 1974.
- [5] C. Finnie, R. Sydnor and A. Sward, Proc. 25th Annual Freq. Control Symp., Ft. Monmouth, NJ, 348 (1971).
- [6] M. W. Levine, R.F.C. Vessot, E.M. Mattison, D.F. Graveline, T.E. Hoffman and R.L. Nicoll, Proc. 8th Annual Precise Time and Time Interval Applications and Planning Meeting, Washington, DC (1976).
- [7] S. Petty, R. Sydnor and P. Dachel, Proc. 8th Annual Precise Time and Time Interval Application and Planning Meeting, Washington, DC (1976).

FIGURE CAPTIONS

- Fig. 1 Block diagram of passive hydrogen maser frequency standard.
- Fig. 2 Top: Beat period between NBS-6 and passive hydrogen maser during temperature transient of 0.7°C.

 Bottom: Cavity correction during a 0.7°C temperature transient.
- Fig. 3 Beat period between passive hydrogen maser and NBS-6 at 5 MHz for hydrogen pressure of 4.11 Pascals (0.309 Torr) and 5.47 Pascals (0.411 Torr).
- Fig. 4 Stability plot for three concurrent beat frequencies between Cs 323, Cs 324, and passive hydrogen. This data was then used to estimate an independent stability for the passive hydrogen maser prototype. The dotted lines are only shown to provide a reference. The data spanned 6 days.
- Fig. 5 Summary of time domain stability for the present passive hydrogen maser. The data vs. NBS-6 (38 s \leq τ \leq 150 00 s) provides an upper limit for the stability of the passive hydrogen maser. The passive H estimate is from Fig. 4, while the stability of the passive H maser vs. UTC(NBS) was calculated from the data shown in Fig. 6. See text.
- Fig. 6 Top: Time error of passive hydrogen maser vs. UTC(NBS) assuming an average frequency difference of 8900 ns/day (rms time error 1.8 ns).
 - Bottom: Rate of passive hydrogen vs. UTC(NBS). Note the indication of various experimental conditions during the 14 days.

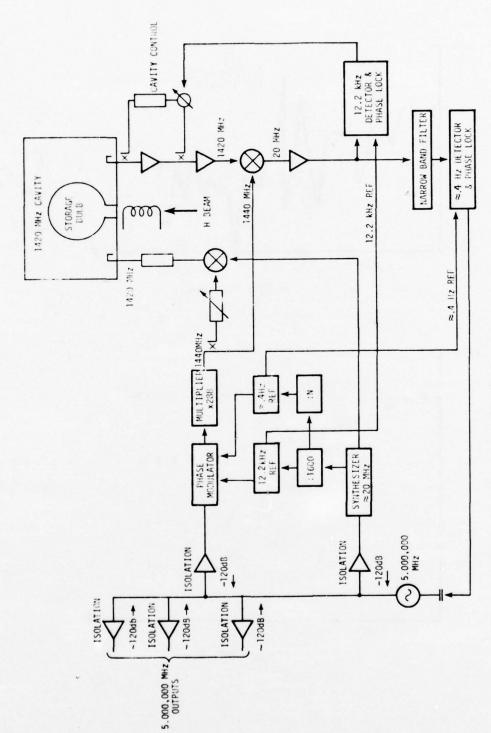
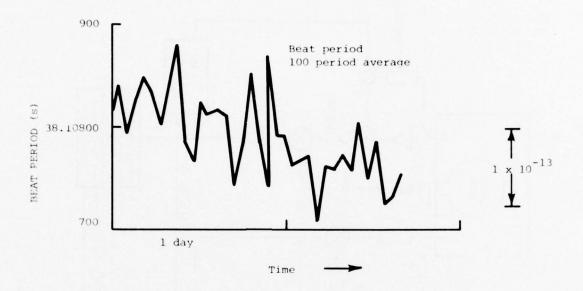


FIGURE 1



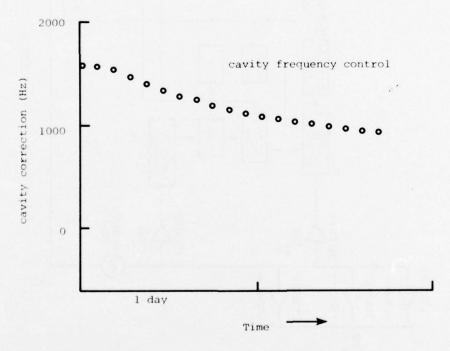
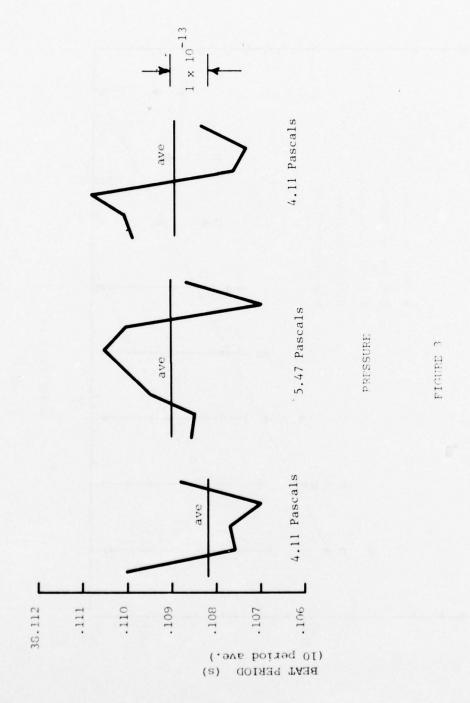
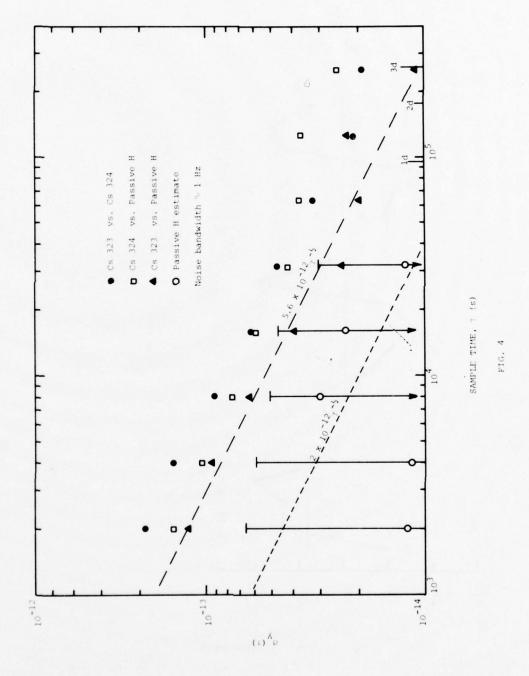


Fig. 2





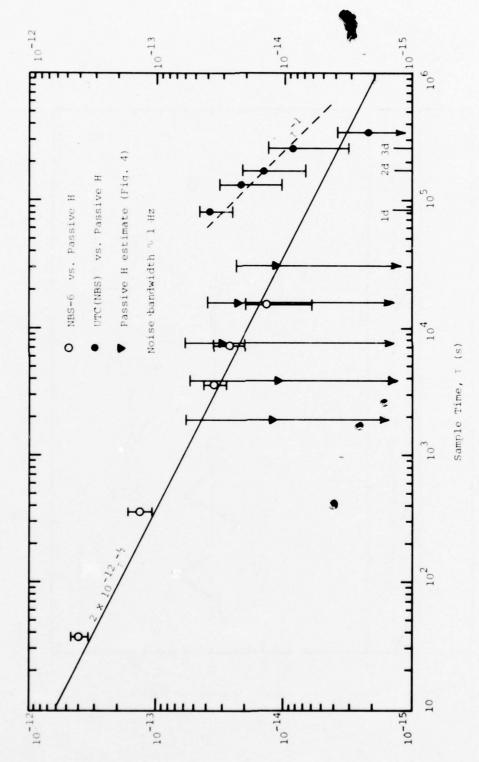
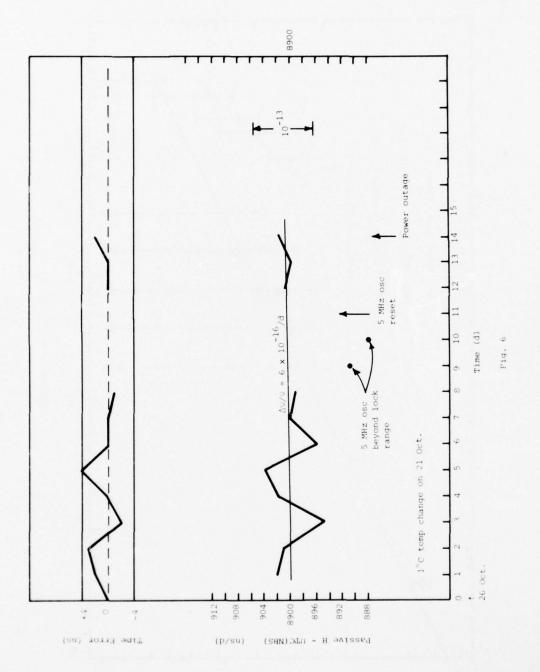


Fig. 5



PANEL A

Relative Merits of Different Hydrogen Maser Designs and Their Evaluation

Panel Members

Norman F. Ramsey Stuart Crampton Harry Peters Victor Reinhardt Richard Sydnor Robert Vessot

Michel Desaintfuscien

Fred Walls

Harvard University Williams College

Consultant

Goddard Space Flight Center Jet Propulsion Laboratory

Smithsonian Astrophysical Observatory

Universite of Paris

National Bureau of Standards

PANEL A DISCUSSION

DR. RAMSEY: That brings us to the end of this portion of the Session. The next, I believe, is to be sort of a panel, or long table discussion. I think the tables are being set up now. I might make a couple of comments while we are getting this set up. In fact, while we are setting up why don't we start since we are running a little behind time. I would suggest for the first perhaps 10 or 15 minutes that the various panel members ask questions amongst themselves, then we will throw it open to the floor for questions.

Will the speakers then please come forward.

To start this, since I think the first initial discussion will be amongst the panel members I think I will take advantage of my position as chairman to ask two questions. Since I probably will be busy, I'll think of other things as we go along.

The first is perhaps more of a comment and even a suggestion to Bob Vessot in his somewhat rounded shields which he pointed out he had to make the inner shield cylindrical and use some of the advantage of this for the purpose of being sure he gets a uniform magnetic field.

In fact, you can still do it with a spherically shaped shell provided you put windings on the upper portion of the spherical shape and with a constant pitch. So, if there is any great advantage it seems you could benefit from that.

DR. **VESSOT**: We have a torusspherical end so that might complicate the winding a little further and are uncertain whether the net permeability of the shield is uniform.

DR. RAMSEY: Independent of what the shape of the end or cavity may be, provided the pitch is uniform as you go up you get a uniform magnetic field.

The second question or comment, Dr. Desaintfuscien, on the, your version of how you measure the wall shift, namely, being able to put a plug in with a different one as opposed to the distorted shape.

Seems to me there you lost one of the big advantages of the distorted shape in that when you put the plug in, you have different portions of the wall exposed and consequently, you are not as free of the properties of the wall, one of the attributes of the others is that it is independent of the same wall coating.

DR. RAMSEY: Yes

DR. DESAINTFUSCIEN: But we can verify that the wall has the same properties by measuring the ratio of the wall — the two configurations and verify the ratio is the same as the one from the geometric — from geometrics.

DR. RAMSEY: But I think at least what we have found in some of the earlier ones that let us be interested in the variable shape has been the fact that, well, if you do it, yours is an intermediate kind of wall. We have done it with separately coated bottles, when you do that one time and another we find there is a variation from one time to another.

I think it is a suspicion, not a confirmation, that you get some degree of variation even within different portions of a single wall, so it is clearly better in that regard than totally separate decoding processes.

DR. VESSOT: Perhaps the first thing might be to say, why the torusspherical shield in the first place. We found, it was an accident, most good things are. We had to make a torusspherical pressure vessel which in our search for light weight we elected to combine with the magnetic fields.

All I can say about that idea is, don't do it.

But we had torusspherical magnetic fields and wanted to find out what they did. What we simply did was measure against equivalent sized flattened shield and found we had about 40 percent less inhomogeneity in the longitudinal shielding factor combined with the transverse shielding factor.

Transversely where you are looking at the field lines going sideways through a cylinder you have very good, closed and continuous path the lap joints don't bother and one has, I think, intrinsically a better shield.

The sharp corners on the covers and reluctance of the gaps of the joints themselves is the main problem. Generally you have almost 20 to 1 less shielding factor in the axial direction than in the transverse direction.

The other improvement, I feel, is that the flat plane of an oilcan-like end is subject to much strain and this degrades the shield very much.

So, by eliminating the sharp corners and keeping a radius of curvature, you have a far more structurally acceptable configuration. Just handling these things, it is obvious that the thing is really quite strong. So that was why we tried it.

Of course, the next game is how do you make the field uniform inside, and this is the real question.

DR. RAMSEY: In fact, one of the things I found very pleasing and impressive were the actual large number of new improvements that have come within, or even new ideas for improvements that have been coming in the whole field within roughly the last couple of years.

You might think it would be by now saturated. I think it is apparent from the discussion there are really quite a number of these.

My own belief is that this gives a lot of mutual stimulation to each other. In many cases I think they can be adopted.

For example, in the case of the passive hydrogen maser which, I think, is a very valuable development to have, I think many of the advantages you get from that can indeed be taken over in the other and likewise in the vice versa direction.

There are, however, still some very real differences, I think time will tell which is the best. But I think whichever proves to be best in the long run, I think that the development of each will be extremely valuable because of the particular features pushed one system versus another and then recognizing the value of that. Frequently you can do the equivalent thing, a good example being, I think, the much greater planning of use of various automatic tuning techniques.

You get some advantages doing it with this, if you do it - you can get many of these advantages back in the passive, in the active maser.

DR. WALLS: Well, in the passive maser it is clear it will not be a good device from, say, ten to a thousand seconds because it comes down as square root of Tau because it is incoherent.

So, I don't think it will be useful in the short term as phase comparisons, for example, as the active masers have done exceptionally well. But in the long term for a stand-alone system where you are not able to do auto tuning against another hydrogen maser, and

with the present limitations we have on quartz crystals, I think that the passive system will do much better because of the active control, and you can make the storage time very, very long because you don't have to oscillate.

So, you can run down the storage times, you get so little power out it doesn't oscillate so you have a narrow line, cavity pulling goes down.

- **DR. CRAMPTON:** Just a minor point, as a diagnostic tool since you can make measurements now with very much greater atom confinement, then you have a chance to look at surface properties, relaxation on the surfaces.
- **DR. REINHARDT:** One comment I would like to make is that I think the real power, the passive technique, is that it frees you from geometry limitations. I think where it will really pay off is in terms of variable volume masers and experimental devices which, since you have the stability, you have demonstrated, you can build it any size or shape you want and not worry about oscillation.

You don't need two cavities, you don't need the amplifier in between. For any of these masers, for example the Concertina maser, the external bulb maser, where I showed we were pushing the limit of filling factor we can use the same technique here.

I think it should always be kept in mind it is sort of an ace-in-the-hole that you have, if our external bulb maser doesn't oscillate, we can always use it as a passive maser.

DR. VESSOT: We shouldn't be too mesmerized by the concept of a single standalone maser. I think anyone who relies on one clock is on terribly dangerous ground. In fact, even the British Navy in its early days would never sail without three chronometers on board if they were serious about getting there, and they were.

But to acquire more than one maser, I realize, may be a terrible economic problem.

- DR. RAMSEY: How many masers did you have in your shot that went up in the air that you used for testing relativity?

 (Laughter.)
- **DR. VESSOT**: That was a budget constraint. We had more than one on the ground, however. That was a constraint we were not in favor of, but nonetheless had to live with.
- DR. RAMSEY: I think, though, there are many instances when you will, in fact, have that constraint for one reason or another, so I think there are real advantages to having them both do well alone and do well the other way.
- **DR. REINHARDT**: One comment, there has been some comments about the reliability of masers but the masers proved more reliable than the tracking stations in this case.
- DR. VESSOT: I am glad you said that because you guys at GSFC ran the tracking stations. I would like to investigate the past history of some equipment including the individual characteristics of a certain circuit breaker. But I must say the people who ran the station were able to find that circuit breaker in one minute, eight seconds from the time it tripped, which I think is a track record considering the number of circuit breakers involved in the very complicated station.
 - MR. PETERS: I wanted to comment first on the magnetic shielding.

One of the things everyone has observed in early hydrogen masers, those with very large holes in the shields, is that they have very large inhomogeneity and require trim coils and so forth.

As we have experimented with masers, smaller and smaller holes in them, it appears most of the inhomogeneity is due to the large holes in the shields.

In the later masers which we have we do not even need trim coils. They have no effect upon the ability to go to low fields, and, of course, this also implies a terrific improvement in the inhomogeneity when you have small holes in your magnetic shields.

It goes as a very strong power as the distance from the bulb to the shields and I think this is probably, in the practical world, assuming you have enough shields outside, inhomogeneity is more important than any fact of life, in magnetic shielding.

I did have one other comment, but it is not directly related to magnetic shielding. Several people have mentioned film used in hydrogen maser, Teflon film, it's been used in the big box maser, it's used in several conceptions of the TE11 mode maser and used in the variable volume maser.

I think one of the most exciting things and it hasn't been really documented or published, but it's becoming so well known, I would like to mention at this time, and because it is being used in a hydrogen maser design which hasn't been published I would like to mention it because what is so exciting in conjunction with the measurements on wall shift which Victor Reinhardt has made is that the film material can be made into a bulb, a cylindrical bulb. This has been actually measured at Goddard Space Flight Center originally right after the variable volume, Concertina maser was first designed, what has been measured is that the pulling, due to a one-mil Teflon cylindrical bulb is about 300 kilocycles.

This is a factor of 200 less than the pulling due to a quartz bulb. If one designs a maser where the thin bulb is at the peak of the Bessel function for the electromagnetic field in the cavity, you can reduce further any geometrical variations due to a film by at least a factor of a hundred if you calculate the slopes.

So one can get on the order of ten to the fourth less pulling and less perturbation due to a film bulb in a maser than you can with a quartz bulb.

Of course, this is a very good solution to dialetric pulling, and thermal effects and things like that. There was one other point in conjunction with a factor of four or less wall shift as measured by Victor recently and this is quite exciting as it bears upon one aspect of wall shifts which has seemed possible to me. There is a good chance that much of the wall shift is not due to the Teflon molecule chain or due to interactions itself as such, but due to impurities in the material or exposure of the wall through the Teflon film.

This tends to support this conjecture, also lends credence to the possibility of achieving much longer storage times with a film bulb. Hopefully a homogeneous bulb might have much more uniform properties, certainly — than a sintered on material.

So, I think this is an exciting development and can possibly contribute to a good factor of improvement in hydrogen masers whether they be passive, TE111 or TE011 and I am still somewhat in favor of a TE011 maser at the moment but that may change.

DR. REINHARDT: I would like to make one comment on the film bulb. What is also very exciting about this is that because the pulling is so much smaller you eliminate one of the big production problems with hydrogen masers, that is, you can't get the quartz bulbs reproduced well enough so you have to do some last minute trimming on the cavities. From Harry's calculations it looks like if you could hold the tolerances on machining for these cavities, there is no reason why you couldn't spit these cavities out one after another and just put the bulbs in and not worry about trimming them up after the fact.

MR. PETERS: It is also very light, whereas quartz weighs 800 grams, this weighs less than a gram; it is very applicable to lightweight hydrogen masers.

DR. RAMSEY: Other comments or questions from one panel member to another? Including to himself.

DR. DESAINTFUSCIEN: I would like to make a comment about, "The warped shape is not due to Teflon." I'm not sure you are right. I found that Teflon on wall shift — closed area at peak temperature range. Perhaps it is due to impurity, but it is a property of the Teflon.

DR. WALLS: I think that is fairly clear from measurements that have been made that show that phase transitions in the Teflon are related to changes in slope, in relaxation, in other things. So I think that is fairly clear, that Teflon has to play a role with — perhaps a major portion of it, but not all of it.

DR. VESSOT: I would like to strengthen Dr. Desaintfuscien's argument, by saying that every measurement we have made of wall relaxation seems to come out to be about 6 x 10 to the minus 5 probability of loss per collision at the temperature we operate, which is dangerously close to the data you get. It's quite independent taken on many separate instances.

So, I believe the properties of Teflon intrinsically are what are governing. This doesn't say the end groups of Teflon cannot be considered a property of the Teflon, but if you consider that to be impurity, I think you have to define pretty well what the Teflon really is in the first place. I wouldn't be surprised if the end group did contribute, and the thought now is to polymerize the material in place.

There is even the remote possibility — and this is really very remote — that the Teflon could be made without end groups, by simply joining the things into hoops so they would be like Spaghetti-O's and lie on the surface in some random manner like a pile of rubber inner tubes all over the place on a garage floor.

DR. REINHARDT: One comment I would like to add to that is that in the type L film we use to make these measurements — the principal difference between it and FEP film is the higher molecular weight, so there are fewer end groups. The correlation with the change of state, if it is due in fact to the end, or impurities, could correlate with dimensional changes in the latter that occur.

You could expose more or less of the chains or spread the ends out as you change the density of the Teflon, rather than a direct effect of the Teflon itself.

DR. CRAMPTON: Looking ahead a little bit to things that don't work yet but might work in the future in that line, it seems to me possible, with variable temperature of hydrogen masers like the one developed at Orsay, to look at quite different kinds of wall coating materials. After all, the length of the Teflon chain doesn't do you any good except to help the thing lie down on the wall.

There are some advantages to going to other kinds of materials which you can't form into walls unless you go to lower temperatures. We are working on this ourselves, and I'm sure there may be some work like that at Orsay where they have already a low-temperature hydrogen maser.

DR. RAMSEY: Are there any other questions that members of the panel want to address to each other?

MR. PETERS: It might be worth mentioning, since all the masers which have been described, I think, today, and mostly in the past, have used hexapolar state selectors, which are ideal when you have maximum efficiency of the state selector is far from the bulb, that the latest designs at Goddard have used quadrupole state selector.

Under certain circumstances these have a very great advantage. For example, when you have small holes in your magnetic shields, and you can put the state selector within two or three inches of the bulb itself — (it's five inches in some of the NASA masers that have already been built) without any disturbance you can measure. The atoms captured an a quadripole state selector nearly all enter the bulb due to the geometry.

So you don't need to worry about exact focusing, as happens in a hexapolar state selector.

A quadripolar state selector as designed, has much greater pumping speed sideways from the pole tips because of their design, but most important there is at least a 20-percent improvement in the peak magnetic field.

But more significant than that, particularly for small size hydrogen masers, is not the focusing properties but the defocusing properties. In a hexapolar state selector, the magnetic field and gradient goes to zero as you go to the center of the focusing magnet. In a quadripole it is a constant from the center out.

Therefore, you have an exit angle, you are defocusing the wrong state atoms, very strongly, whereas if you put the source and state selector close to the bulb with a hexapolar system you can get a significant proportion of other state atoms into the bulb with that particular geometry.

So, for small hydrogen masers we do have extremely high efficiency in utilization of the hydrogen due to going close to the bulb, but a quadripole state selector is very desirable under those conditions.

DR. RAMSEY: Well, I think it's becoming apparent that the members of the panel can keep going until 12:30 just questioning and making comments amongst each other. I think maybe I would like to summarize my own personal view in reaction to the meeting this morning and, in fact, in contrast to some meetings that have occurred in the past.

I am just terribly impressed by the sort of amount of fertile developments that are going on in the field from all sides; also, particularly impressed by the extent to which most of these can be taken from one to another. I mean, each of the kinds of masers, or passive and active, each have certain features, each I think can benefit from some of the improvements that have occurred in the other.

I think there is great optimism of considerably and very marked improvement in the period to come and also shows the benefit of the fair number of people working on it. I think most members of the panel probably agree on this, so we can end on a statement with which we can all agree, and I think at this stage we should throw the discussion open.

Actually, one question was submitted in advance. Dr. Reder would like to ask a question, so to make sure he has not forgotten, I would like to call on him as the first question.

"Considering expected 'mean time before failure' cost, status of cesium techniques, environmental effects and requirements, what is the justification for large H maser effort?"

DR. REINHARDT: I will stick my neck out a little on this one. As Dr. Reder knows, we did present some data on mean time between failure with the NASA NP masers which looked quite favorable and compared quite favorably with the cesium standards.

I think the justification for expenditure is really that H masers, in certain ranges of time intervals, can outperform cesium masers in terms of stability. Obviously, cesium standards are smaller. Right now they are cheaper. You can buy them off the shelf as production items; hydrogen masers you still can't. Price might get lower if produced on a production level.

But in terms of short-term stability, I think the VLBI people show that they just can't do with anything but H masers. I think for long-term stability, too, because of the smaller line width, that they will outperform cesium.

I have heard a lot of comments about hydrogen masers with poor long-term stability,

but JPL has demonstrated 1 x 10⁻¹⁴ stability, out to 10⁶ seconds.

I have not seen commercial cesium standard which will do this. That competes favorably with the best laboratory cesiums at NBS or the other national labs, and on full ensembles where the cost is quite comparable. So I think in terms of a cost-to-performance ratio, that justifies the expenditure.

Does that somewhat answer your question?

DR. REDER: Well, I wonder, is there anyone here from the cesium manufacturers who would like to say something?

DR. RAMSEY: There is a question there.

DR. C. COSTAIN: This is not exactly in the line of Dr. Reder's comments, and I also would like to question the fact that cesium standards are always smaller.

But one of the things that worried me in the presentations, with rare exceptions was, it seemed to me, a complete lack of indexing in the measurements. In fact, a stability measurement of parts in 10 to the 15, I question what is it against. We have measured a pair of hydrogen masers independent with autotuner will keep time to a nanosecond a week, but we know in comparison with our primary standards that they were both drifting several nanoseconds a day.

We have measured it, it doesn't say it happens in all H masers, but we have on one of ours very carefully indexed data over 18 months giving six parts in 10 to the 13, decrease in frequency per year, about two parts in 10 to the 15 per day, monatomic drop. We don't

really know why.

Over five years it has been three parts in 10 to the 12.

DR. VESSOT: I understand, Cecil, what you are saying. We agree the hydrogen maser in fact has some intrinsic long-term effect with the bulb. You have seen it, I think, very vividly, and I think the causes that give yours the magnitude you have are probably well understood by you.

I think it's a question of how they are built and how they are outgassed to avoid contaminations that lead to whatever is going on in the bulb. This long-term effect, I believe,

is real and I understand that Dr. Winkler has also observed it.

So, as far as long-term stability, I, too, question the accuracy over a period of time in the order of years. I believe we will have a systematic change. No amount of autotuning or massaging is going to change that. That is a property of the interaction of the bulb and hydrogen atom.

As far as the other question of having the masers in different environments, I believe there have been enough experiments between masers to say that the systematics between one environment and another, I believe, have been removed.

I don't want to steal Alan Rogers' thunder, but there are enough tests, I think, that say it's unlikely that in the 10³ to the 10⁴ second domain we are dealing with correlated phenomena. In the very long term, yes, I think definitely that the wall coating is going to have some effect, and we'd better learn to either cope with it, eliminate it, or live with it.

DR. REINHARDT: I would just like to comment on the last statement before we move on to a question.

I think the wall shift drift or change is a limitation, but I think that is where the importance of the variable volume maser comes in. All the other parameters are evaluatable in the hydrogen maser as in primary cesium. The wall shift was the last one.

In fact, at NASA we are planning to do three- or four-year experiments where we will continuously evaluate our field masers with the Concertina maser on the part in 10 to the 14 level.

But one other thing I would like to comment about this wall shift drifting with time is that Harry Peters did do a three-year experiment in which he did measure several masers against each other and TAI and found they reproduced over three years to within two parts in 10 to the 13. The resolution there is limited by what happened to TAI in two years. I think that is probably a question that has to be answered.

It's the same problem you get when you evaluate a primary standard. At a certain point, you have to use theory to make evaluations. You cannot just build two identical standards and put them at separate parts of the world. You should, as a check, but you must rely on theory at a certain level.

The problem that you always encounter when you build the most stable standard: What are you going to measure it against?

- MR. PETERS: It seems to me that the wall shift drift with time is a problem of atomic contamination, which is not necessarily inherent. It's a function of the design.
- DR. RAMSEY: May I make one comment, too? I think some of these new proposed designs, for example, being able to use less beam intensity can affect this problem, which has been a relatively new one.
- DR. WALLS: I think that is very clear. We, in the past, have not had a chance to measure hydrogen masers against the uniform time scale that was sufficiently smooth that we could evaluate these things down to a part in 10^{14} . As we get better time scales, and have more experience, and look at aging (perhaps of the wall shift if it is real as a function of temperature) as a function of cleanliness and other things, we will have a chance to evaluate it.

In order to do so, it's imperative that we have a smooth time scale that we all agree on that we can make measurements against.

So, I would like to encourage everyone here and in the audience that hydrogen masers that are run for a long time be reported and referenced against TAI so we can try and start to make a time scale which is quite smooth.

The other comment is that the measurements in long-term have been made with the active masers, and Victor Reinhardt, I think showed rather nicely that even with autotuning there is an offset which is proportional to the drift of the maser over the attack time of the autotuning loop, whereas with the passive maser we can, in principal, make the attack time not 1000 seconds, as it often is in the active masers, but a millisecond.

Currently, we are running at 10 seconds. And across 8 days or 14 days one has only a limited amount of data and one shouldn't stick his neck out. But I think we can still say the drift is exceptionally small in our present prototype, and I think we will find it even smaller.

DR. RAMSEY: I think Dr. Winkler has been trying to get the floor back there.

DR. WINKLER: I would like to continue the discussion with Mr. Reinhardt. You gave as justification for the massive effort and support for H maser work that it outperforms cesium standards in a large range of talents, and I think that is a very valid argument, and I completely accept it.

But how about the superconducting cavity masers which outperform the H masers in the same region? Are we giving commensurate support to that effort?

DR. REINHARDT: One statement I want to make: I agree with you, and I think superconducting cavities should be supported.

First of all, I would like to say I don't think their is massive support for hydrogen masers. If you look at the support for cesium over the years, it would be comparable. How much is the support in rubidium in dollars all commercial labs produce? There are still only a few labs in the country doing work on hydrogen. You have got them all here.

Another comment on the superconducting cavities: Yes, I think a lot of support should go into that, but the superconducting cavity has a basic limitation, that it's no good as a primary standard. It's still just basically like a crystal. It relies on dimensional stability and you cannot use it as a primary standard.

I think with the variable volume techniques you have the possibility of getting a primary standard with part in 10 to the 14 level accuracy.

DR. VESSOT: The point about aging in the case of walls is that it is quite likely they will age of themselves in that if we put a material down that is basically amorphous, I see no reason why, in time, it couldn't crystalize.

The question is what happens to the wallshift during this process. I don't think we know. We do know, however, that there is a difference between amorphous and crystalized teflon and that it is substantial.

So maybe the thing we ought to do to get out the aging is to have the Teflon in the least energy condition which is to have it in crystalized form.

The other thing I believe is quite important is that ultraviolet light, however it gets into the bulb, can be quite dangerous to the teflon; and we all know that the molecular binding energy is well below 1216 angstrom the principal U.V. component from the hydrogen dissociator.

So I suggest maybe we should use the stopping disc as an ultraviolet dodger.

MR. PETERS: If I may just say one sentence, it is not as interesting as relativity which I am also interested in; but I think there is a misconception when you speak of ultraviolet

light interacting with the bulb from the source, because the area which it hits is less than a part in 10 to the 4th.

If you change the entire wall shift by that fraction, the total effect could be no more than a part in 10 to the 15 so I don't believe it is really a serious consideration whatsoever.

DR. VESSOT: It can be reflected, however, and the deterioration occurs at the place where the atoms first bounce.

MR. RUEGER: Rueger from Johns Hopkins.

I would like to pose a question to the general panel of how we can make intercomparative measurements of the various designs so we will know where we stand with who is doing the best job in the various environmental effects and in the overall performance.

I wanted to pose the question to the panel of how we might intercompare these various standards insofar as their sensitivities to environmental effects and other parameters that might let us understand better how each is working and where it is working best.

DR. RAMSEY: I will make an initial comment on that one which is I think indeed these kinds of comparisons are coming forward and should be coming forward fairly soon. I think one of the reflections of the fairly small amount of support that has been available up until the recent period of time is that here haven't been many masers for which there could be these intercomparisons.

It is only in the last period of time they were there.

We at Harvard have indeed had some, but also had to do everything with graduate students who were also looking at thesis and certainly weren't primarily directing themselves towards intercomparisons of this nature.

I think now with the various organizations that are developing, I think there will be many such standards on a high quality and you can really find out what this is.

I guess the answer is they should be indeed intercomparing and getting together with the intercomparison people.

DR. REINHARDT: At NASA we are going to be getting a frequency standard and test facility so we can make this kind of long-term test comparison.

I think one of the problems in the past is that since BIH needs long-term data without interruption and we are limited in the number of masers, we just can't leave them alone for two or three years; we haven't been able to do this.

But at NASA we hope we are going to have a three-year or more experiment on longterm stability in conjunction with the Concertina masers and hope to contact you sometime in the future about reporting our data to the TAI.

- **DR. VESSOT**: That is a role for the Bureau of Standards and these people ought to be the arbitrators of whatever happens. They have done so in the past, and should continue.
- **DR. WALLS:** We hope to get two of the passive design hydrogen masers on our time scale within the next year or a little more. And so we fully intend to do that. But it has been really a limit in terms of funds.

We haven't had funds in the past to make hydrogen masers, but developmental work had to be done on some new concepts.

We would like very much to have masers from other laboratories come to our place and sit in a quiet corner and let us make measurements, but they haven't been offered because they weren't available. And we haven't had the money to purchase them.

Perhaps that is something that ought to be taken care of.

DR. CLARK: A comment to Gernot's question earlier and in part extend that to another question that may impact a little on our thinking of the user's standpoint this afternoon.

Much of the dollars that have gone into H maser work is because various users have required H masers now in order to be able to do their program. Tracking networks, the astronomics community, they need these things now. It is not we need the boxes five or ten years from now after additional research goes on and another technique to find out which one of those two ends up being the best.

Much of the driving force, because of that other funding, has been to get some of these masers out to certain of the critical stations to do these various semioperational or R&D programs that are being done at those stations. Because that is the place where most of these masers are in fact now located, and techniques like very long baseline interferometry, offer good intercomparison techniques for comparing frequency standards which may be located around the world, there exists the possibility of using the VLBI technique as part of the intercomparison which should be then fed into the BIH.

So this is a place where I think this morning's discussion and this afternoon's discussion really overlap. As one of the users, to be armed for this afternoon, I would like to ask one question, though.

We find even hydrogen masers aren't good enough for many of the things we are doing. What are the ultimate limitations on frequency standards? Even using combination techniques of masers and the cryogenic cavities or some of the additional development work that is going on in the laboratory now, what stability levels from the one second out to hundred thousand second levels can we expect of frequency standard performance in the next five years?

DR. RAMSEY: I can make some comments on it. Others might want to make some also.

First place, I think as far as the stability, certainly one limit you eventually run into in most devices is second order broadening from the second order Doppler shift.

This sort of comes in at regions of parts in 10 to the 15 or so depending on how accurately you make that determination. There are a couple of bright ideas that may, in principle overcome this by trapping techniques with ions, and so-called resonant cooling.

Maybe Dave would want to speak to that a bit or someone else here. I think these devices are down to that limit now. I think there are, actually, with the kinds of things that are currently going on including the passive maser, I could conceive it getting down there.

I think for the shorter periods of time, it is quite clear that it is hard to beat power for getting stability. The ideal device for that is the superconducting cavity. I think this is an absolutely superb technique for the short period of time.

At one time I had thought about ways of making the H maser also function down there by having beams coming in from all sides, huge quantities of hydrogen since it is a matter of power. It is clear that is not the best way and I think I would agree with the comment that you want to be a little specialized with what you want to need.

On the other hand, for longer periods of time it is my impression, and it is reenforced by the discussions and papers presented today, that there are quite a large number of opportunities for major improvements in the basic active and passive hydrogen maser techniques over the next year or two up to where you start to get really into serious problems with this rather fundamental limitation that affects all things, lasers and everything else, of the second order Doppler shift.

DR. WALLS: Let me amplify the comments of Professor Ramsey slightly.

In short term it really is a matter of power. If we compare the H maser with, say, a line width of one hertz and a power of maybe a 100 minus 85 dbm or so, 10 to the minus 11 watts, with a superconducting cavity which at X band has also a line width of about 1 hertz, but its power is a milliwatt or can be as large as a milliwatt.

So you can beat KT a whole lot easier and one might expect stabilities in the 10 to the minus 16 level to be routine from perhaps a few seconds out to, I don't know, a thousand seconds or more.

MR. D. WINELAND: A couple questions, on hydrogen.

One was on surface. As I recall, Professor Ramsey 10 years ago talked about using different surfaces, for instance, lithium fluoride. Maybe some comments on different surfaces besides Teflon can be made.

The other question was to solicit some opinions on absolute accuracy of hydrogen masers. I presume the limitation is the wall shift. And, whatever it is, maybe some comments on what future accuracies of hydrogen masers could be.

DR. VESSOT: Dave, I think the limitation is less likely to be the wall shift than it is to be the knowledge of the absolute temperature of the atoms, and the determination of the second order Doppler shift.

I think the wall shift problem can be beat into the ground by many, many techniques, some of which we have seen.

With relation to the question of ultimate stability, I think it is entirely a question of signal to noise. I just made myself a note, you could couple up Niagara Falls to a monstrous magnetron and you would get superb stability, very short term to be sure.

These are questions I don't think have an answer and should only be responded to in the context of the use to which the device is being put. In my opinion, right now VLBI, as Professor Clark mentioned, has a clear and pressing need, and I don't think we could have done a redshift experiment over two hours without having a device that would develop stability at a time substantially shorter than two hours.

I really think if you should look at the application and then decide what kind of an animal you are going to need in order to cope with the problem.

DR. ROGERS: I am Allen Rogers from Haystack Observatory.

I would like to ask the panel a question about having a high flux mode in the masers which would not necessarily be used a high fraction of the time. For many, many applications you only need very good short-term stability for a very short period, like maybe a few hours experiment, even, which might be carried out, say, once every two months, or maybe a couple of days, say, every two months. Maybe we could afford to have a high flux mode that we could use for special experiments without impacting the lifetime of the maser.

Could you comment on how much flux would be needed to make the maser as good as the superconducting cavity oscillator at a thousand seconds? And is that technically feasible?

DR. VESSOT: I can't answer the second question but I believe it would be difficult to get at 1-10 seconds.

In most of the equipment that is in the field, certainly in the case of the ones we have produced, there is in fact a switch with two settings for the hydrogen flux level. If you need the stability you turn up the wick, and, get more power out.

I don't know how much more power you would need in a maser in order to compete with a cavity. If one increases power output, one automatically diminishes line width so you're really trading off short term stability against the long term stability.

It is really a question of how long do you want to integrate the correlations that you're seeking, and what level of stability do you expect. And it is clearly going to be some kind of optimum solution for each kind of oscillator.

DR. RAMSEY: Also, I think it is an excellent suggestion, and typical of the fact that the sort of what masers that have been handed out have usually been incidental to some other purpose.

I think you certainly could do even more explicitly than was done, maybe by accident in some of your masers, by making an adaptation by deliberate design. That you could, indeed, adapt them to have a mode which could be pushed to the most favorable in that direction.

My impression is that with that, and for periods of the orders of thousands of seconds, this could be reasonably comparable to the best obtainable with the others. If you want it on the other hand for periods of a tenth of a second, it's got to be a pretty formidable switch.

I think there, there is no question that for periods of time on the order of tenths of second or even a second, this high stability ought to be achievable from the superconducting cavity or in certain cases even from a copper cavity, that has a lot of power too and for a short enough period of time, can be a very good one.

But I think your point is excellent, I think people who are particularly planning things, especially for some of the uses such as Haystack where I understand full well the desirability sometimes for quite long-term stability, and sometimes for sort of medium term stability. I think you could do a great deal by making the design bear that in mind, and I think it could be a more multipurpose device without sacrifice.

DR. REINHARDT: I would just like to add my comments to this.

You mention the 100 to 1000 seconds as short term. But I don't think any of the masers are limited by that kind of short-term noise that could be decreased by increasing the power at 100 to 1000 seconds.

The JPL maser which runs at tremendous power compared to ours you can say has comparable results.

I think you're limited by your multipliers chains, and other things in that range. You wouldn't get any advantage except, as Professor Ramsey pointed out, for about a tenth to one second.

DR. RAMSEY: In passing, I think there could indeed be a bit of extra work on the electronics.

In many cases the electronics has had to be rigged up with certain limitations, costs and otherwise, in mind.

DR. CRAMPTON: I would like to comment on these questions of development on the one hand and ultimate obtainable accuracy on the other. And whether it will be possible to get these devices together to see who is doing how well.

It seems to me that the development effort has been, at some places that have been playing with them for the physics, namely Harvard, Williams, and a few other places.

Beyond that, development has been done primarily by clock people. It seems to me that where the development is needed is in between there where people are willing to go back and work more with the basic physics of how you make a better standard. I think the best job of that has been done at Orsay. But I think the effort is needed to go back, and Teflon is terrible stuff. I think more work needs to be done on a basic level. Frankly, my personal view is that that kind of development work and cross-comparison of how well you are doing ought to be done at the Bureau of Standards.

DR. RAMSEY: Again, I would like very much to emphasize this.

I am really a very great believer and have been for a long time, that Teflon isn't neces-

sarily the best substance, particularly the kind of Teflon we normally put on.

On the other hand, for a long period of time there was simply no one to work on it and it's not easy to persuade a graduate student even such as Stuart Crampton to delay his Ph.D. experiment a couple of years while he investigates various forms of Teflon and other materials. I think now there are places such as Orsay and now I think the Bureau of Standards and other places working on it where I think this kind of development — I think it has a great future.

It's to be remembered, that Teflon was essentially the first thing ever tried. So there is no reason to believe that we are all that clever just because frying pans are made that way.

DR. REINHARDT: I think something we can all agree on is that no matter what field we are in, whether hydrogen maser or cesium or crystals, we all need more money.

MR. ENGLISH: Tom English, from EFRATOM, California.

One of the obvious requirements for military applications of frequency-type standards is nuclear radiation hardening.

I would like to ask the panel perhaps to comment on what they think might happen for example to the wall shift if you had nuclear radiations present.

I don't know if anything has been done on this or not, but it's certainly a problem all standards have to look at least in some point of the development.

DR. WALLS: I won't comment on the Teflon itself because I don't know that much about it.

But nuclear radiation clearly is going to cause major structural changes, perhaps. So active cavity control I think would be essential. If it still worked, then you could worry about what happened to the Teflon on the wall.

MR. PETERS: I don't have the data, but I think there have been some discussions on the effect of nuclear radiation on the wall material. I am thinking primarily of the wall shift.

But I believe the flux rates you anticipate, we don't think it's a large effect, but it certainly needs to be measured.

DR. VESSOT: Well, there was a quantitative estimate made, I think, some time ago. I think Dr. Winkler was responsible for its inception, to determine levels of nuclear radiation from the normal environment would be expected inside the maser. I believe the Naval Research Labs were involved in this, too.

They came to a conclusion that the radiation over five years, using what they saw as shielding materials, namely the molypermalloy shields and quartz or whatever the bulbs are made of and the cavities, that they felt confident that this would not cause significant drift at the five year level.

DR. ALLEN: Dave Allen, National Bureau of Standards.

Good accuracy ultimately translates to good long-term stability, looking futuristically at hydrogen, if in fact Bob Vessot is right and you can beat the wall shift down into the dirt, would it then be good to beat the second order Doppler down by looking at the low temperature cavity type materials?

DR. RAMSEY: My first comment on that is yes, by all means.

In fact, there are several advantages you could have with low temperatures.

You just have to be sure that you aren't getting the atoms sticking to the walls too much.

But I think there is a great deal of research to be done in that.

One graduate student of mine, Bob — Paul Zitzewitz, that Paul Zitzewitz, did some studies of temperature effect on wall effects.

Actually, one of the things we wanted to do was go to really low temperatures, but there simply wasn't the funds for the work.

DR. CRAMPTON: There has been some work done at lower temperatures at Orsay and it shows that as you go down some to liquid nitrogen temperature, for example, there are some real advantages, things work okay.

If you try to go very below that you get into trouble. But liquid nitrogen is a very attractive temperature, it's very good to stay at. I think more work needs to be done on that.

- **DR. DESAINTFUSCIEN:** Teflon becomes a real solid at temperature below 200 K. Perhaps it is possible to create another kind of Teflon whose properties would be different.
- **DR. RAMSEY**: In this connection, as soon as you can afford to do anything in the way of going to very low temperatures you open up many possibilities of totally different surfaces.

In fact, practically from the beginning even almost before we tried Teflon, my definition of the ideal surface for many purposes was a solid helium surface at appropriately low temperature because this is something in which there would be very little sticking characteristics, and you would get it in a very pure form. I think the solid helium might be a little hard to achieve. I would be very optimistic about things like argon as a possible surface material. Are there any other questions from the floor?

- MR. CHI: I wonder before you close the panel discussion, could you leave a clear and optimistic prediction of the performance of hydrogen maser, assuming all the problems which have been identified, that have been highlighted, what would be the performance and who are the people who might be interested in doing those kinds of activities?
- **DR. RAMSEY**: In the first place, I think you should give realistic estimates and optimistic estimates.
- **DR. VESSOT:** We are going out to a big limb, but we are betting we will see data consistently below 1 part in 10 to the 15 for average in times beyond 10³ seconds. We have been tantalized with data that has been at the 1 in 10 to the 15 levels occasionally.

DR. WALLS: How long?

- **DR. VESSOT:** That challenging voice was Walls saying for how long and the answer is I don't know how long but I suspect you would have to go to about 2000 to 4000 seconds to get it. It will probably go roaring up right afterwards, too.
- MR. PETERS: I would like to make another independent estimate of this lower limit. I really feel that parts in 10 to the 16 which may be another way of saying better than a part in 10 to the 15, but I think we will be closer to part in 10 to the 16, possibly better than that. I don't see why. But it's the long-term systematic phenomena we're being limited by, of course, this is all a function of what averaging time we are talking about. And this is right where the limit is set now. But a continued study of these I feel should get us lower than Bob feels he will get.
- DR. WALLS: We are counting on the Bureau of Standards doing for ten days and beyond in the very low parts in 10 to the 15. I expect to do a part in 10 to the 14 per year. We may not quite make it or we may be better. I think a lot of it's going to depend on what is really going on with the wall shift. I am not quite so worried about the second order Doppler effect, but I am worried about the long-term stability of the wall shift. If we have troubles, it's just more research. You use a different coating, use a different temperature, whatever. I don't see it's fundamental, but it takes time and money and people.

DR. RAMSEY: Does anyone else want to make a comment?

DR. REINHARDT: I think one question that has sort of been missed a little, one part of it that has been missed a little in talking about the Doppler shift, we have ignored some of the magnetic shifts and other problems we face. The real way to get better stability is narrower lines.

I think until you get some narrower lines that you might have some problem with parts in 10 to the 16.

It's the same problem with cesium and with all the standards. When you start to split these lines by 100,000 or so, you run into all kinds of systematic problems. If we can get a factor of 10 or more improvement in lines, then I think we can get parts in 10 to the 16.

MR. PETERS: I think part of my optimism arises because I think we may get storage times which are much longer, possibly with new materials or different size bulbs and we possibly can improve the line Q significantly.

DR. RAMSEY: Is that an answer to your question? You sort of have to average over these numbers, but certainly part in 10 to the 15 and maybe beyond that point.

Is there any other very important question?

More important than lunch?

I guess lunch wins in which case I would like to thank the panel members and the audience both.

(Whereupon, at 12:38 p.m., the meeting was recessed.)

A COMPARISON OF VARIOUS HYDROGEN-MASER FREQUENCY STANDARDS

A.E.E. Rogers and A.R. Whitney, (NEROC, Haystack Observatory),
L.B. Hanson, (Lincoln Laboratory, Millstone Hill Field Station),
Wesford, Massachusetts
01886

ABSTRACT

Comparisons have been made between several hydrogen-maser frequency standards of different design to test their sensitivities to changes in environmental factors. These comparisons are carried out with one maser placed in the standards' room of the Haystack Observatory and the other in a special room at the Westford antenna, about 1.2 km distant. A phase stable link connects the two facilities. The room at Westford allows the pressure, temperature, and magnetic field to be changed and controlled within certain limits. The room at Haystack is controlled in temperature, but is unshielded from variations in magnetic field and atmospheric pressure. Results will be presented from pairwise comparisons between four hydrogen masers, one each of the NP2 and NX2 design, built at Goddard Space Flight Center, and one each of the VLG10-P2 and VLG10-P8 design, built at the Smithsonian Astrophysical Observatory.

INTRODUCTION

Earlier tests¹ of hydrogen maser frequency standards at the Haystack Observatory had shown maser standards to be quite sensitive to temperature, pressure and magnetic field. Over the past few years several improvements have been made in hydrogen maser standards. SAO has eliminated the pressure sensitivity evident in the original VLG masers and NASA has decreased the temperature and magnetic field sensitivity evident in the NP masers with a new generation of masers to be based on the NX-2 design.

Recently three hydrogen masers have been operated simultaneously at the Haystack Observatory. Long term stability still appears limited by environmental sensitivity of the masers but drifts of less than a part in $10^{1\,3}$ have been observed for periods extending over several days.

ENVIRONMENTAL SENSITIVITY MEASUREMENTS

The sensitivity of various frequency standards to temperature, pressure and magnetic field have been measured by placing the standard in an enclosure at the Westford facility 1.2 km away from the reference standard at Haystack Observatory. The pressure within the enclosure at Westford can be changed by $\sim\!0.15"$ Hg by changing the Westford antenna "balloon" radome pressure from low to high limits. Figure 1 illustrates the small but noticeable effect of cycling the pressure (with a 3-hr period) at Westford upon the frequency of the SAO built VLG-10-P2 maser using the NASA NP-2 as reference. A pressure sensitivity coefficient can be determined by synchronously averaging many pressure cycles.

Table 1 summarizes the enviornmental sensitivities measured from early 1975 to the present; the data was obtained by cycling one environmental parameter at a time.

¹A.R. Whitney, et al., "Applications of very-long-baseline interferometry and geodesy: Effects on accuracy of frequency-standards instability", Proc. of 6th Annual DOD/NASA PTT1 Planning Meeting, Wash., D.C., 1974.

The SAO VLG masers were originally quite sensitive to barometric pressure. Modifications* have been made to the base plate of the vacuum chamber which have reduced the pressure sensitivity to the point where it is now not possible to see correlation between frequency and barometric pressure variations.

Figure 2 shows the long term frequency variations between NP-2 and NX-2. For these measurements NP-2 was located at Haystack and NX-2 at Westford. Frequency comparisions were made using a 5 MHz phase comparator and electronically compensated cables. Each point is the average frequency for a time interval of 900 seconds. The variations present are highly correlated with temperature variations in the room in which NP-2 was operating, although the correlation is somewhat complicated by the action of the NP-2 maser autotuner which attempts to correct the cavity tuning with a time constant of several days. A temperature coefficient of -3 x 10⁻¹⁴ (°C) -1 was measured using a 3 hour temperature cycle period. However the temperature coefficient derived from the data in Figure 2 is almost -1 x 10⁻¹³ (°C)⁻¹ because the maser's thermal time constant is sufficient to smooth out the variations in a 3 hour cycle, but not over the much longer time span presented in Figure 2. NX-2 appears to have a thermal time constant as long as 3 days and the coefficient given in Table 1 was derived using a 24 hour temperature cycle. The temperature coefficient of NX-2 derived from observing the effect of a temperature step after 2 days is approximately $5 \times 10^{-14} (^{\circ}\text{C})^{-1}$. Note that there is no correlation with the large barometric pressure changes associated with hurricane "Belle" as neither maser is measurably sensitive to barometric pressure.

CONCLUSIONS

While many improvements have been made in the latest generation of hydrogen masers, their long term stability may still be limited by variations in the environment in which the maser is operated. Currently it is possible to maintain long term drift within 1×10^{-13} provided room temperature is held within 1°C . Continued intercomparison of masers in separate environments may be useful in further evaulation of environmental effects and long term aging which have so far been undetected. Improved hydrogen maser performance is

^{*}R.C. Vessot - Private Communication

⁺For all the measurements reported the NP masers were autotuned against an HP105 crystal oscillator.

important in the development of increasingly accurate geodesy and astronomy using very-long-baseline interferometry (VLBI).

AKNOWLEDGEMENT

We thank Drs. T.A. Clark, V. Reinhardt, D. Kaufmann, C. Wardrip and R. Coates of Goddard Space Flight Center for making the NP-2 and NX-2 hydrogen maser standards available for use at Haystack Observatory. In addition we thank Dr. Irwin Shapiro of the Earch and Planetary Science Department of the Massachusetts Institute of Technology for suggesting this evaluation of hydrogen maser frequency standards. The most recent test VLG-10-P4 given in Table 1 was conducted with assistance of Dr. E. Mattison of SAO and Dr. J. Ellder of Onsala Space Observatory, Sweden.

FIGURE CAPTIONS

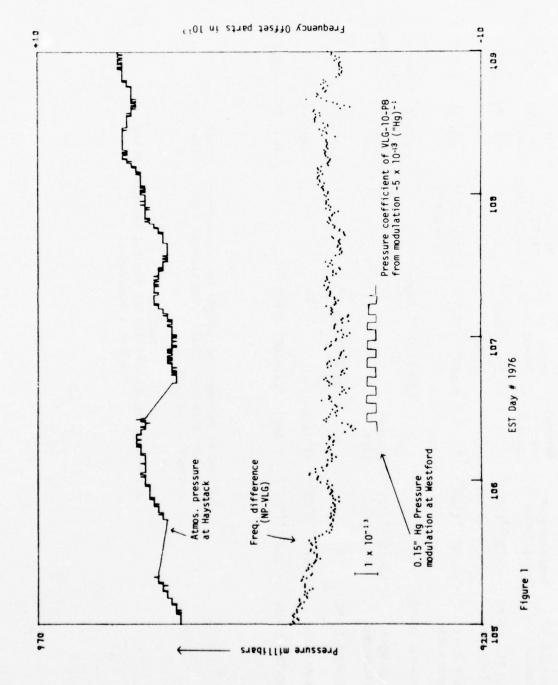
Figure 1. The effect of barometric pressure changes on the frequency of the SAO VLG-10-P2 maser before modification. (After modification the effect of 0.15" Hg pressure modulation on maser frequency were not detectable - see Table 1.)

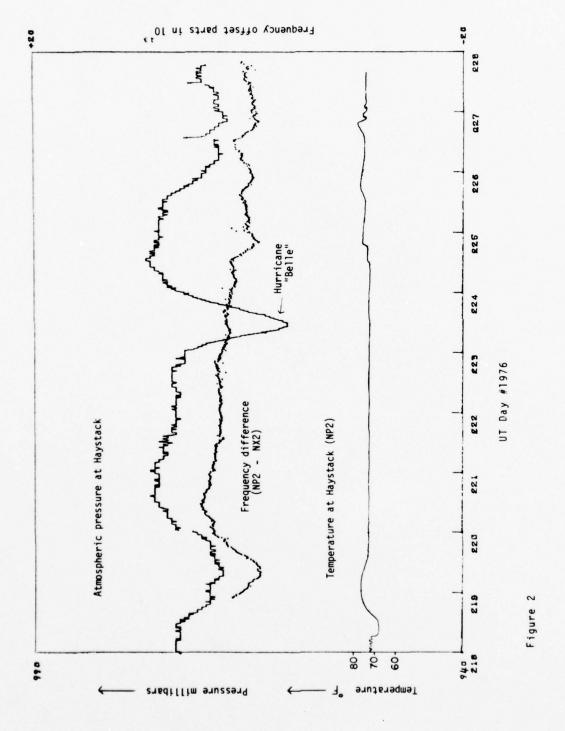
Figure 2. The effect of temperature variations on the frequency of the NASA NP-2 maser.

Ref. Standard	NP-3	Jan. 75 VLG-10-P2	NP-2	Apr. 76 VLG-10-P8	NP-2	NP-2	Nov. 76 VLG-10-P2
Date of Measure- ment	Jan. 75	Jan. 75	Apr. 76 NP-2	Apr. 76	Jul. 76 NP-2	Sept 76 NP-2	Nov. 76
Magnetic Field Sensitivity	1×10^{-12} (Gauss)-1	5×10^{-12} (Gauss) ⁻¹					
Pressure Sensitivity	$-3.5 + -6.0 \times 10^{-13}$ ("Hg) ⁻¹	<4x10 ⁻¹⁴ ("Hg) ⁻¹	$-5 \pm 1 \text{x} 10^{-13} ("Hg)^{-1}$		<4×10 ⁻¹⁴ ("Hg) ⁻¹		$-5x10^{-14} (^{\circ}C)^{-1}$ 1 day <1.7x10 ⁻¹⁴ ("Hg) ⁻¹
Thermal time constant				Several days		≈3 days	1 day
Temperature* Sensitivity	-1x10 ⁻¹³ (°C) ⁻¹	-2x10 ^{-1 \(\(^{\circ}\)C)^{-1}}		-3x10 ⁻¹⁴ (°C) ⁻¹ Several days		2x10 ⁻¹⁴ (°C) ⁻¹ ≈3 days	-5x10 ⁻¹⁴ (°C) ⁻¹
Frequency Standard	SAO-VLG-10-P2 before mod.	NASA NP-3 before mod.	SAO-VLG-1@-P8	NASA NP-2 before mod.	SAO-VLG-10-P2	NASA-NX-2	SAO-VLG-10-P4

*NP and NX masers have larger temperature sensitivity when the effect of their long thermal time constant is removed - see text

TABLE 1 Environmental Sensitivity of Several Hydrogen Maser Frequency Standards





PANEL B

User Experience and Requirements of Hydrogen Masers

Panel Members

Hugh Fosque
Roger Easton
Peter MacDoran
Thomas Clark
Alan E. Rogers
Rudolph Decker

NASA Headquarters
Naval Research Laboratory
Jet Propulsion Laboratory
Goddard Space Flight Center
Massachusetts Institute of Technology
Rurshall Space Flight Center

PANEL B DISCUSSION

MR. FOSQUE: Would the panel members come forward, please.

Gentlemen, I would like to open this panel discussion by asking certain individual members if they will perhaps relate the user experience that they have had in a general way, that is to provide a background for the discussions, then we will move into some more specific questions.

I think I will just start over on my right with Mr. Rogers, and then proceed across the table. If you would be so kind, perhaps you could speak to us in a general way about your experience with the hydrogen masers and the uses that you put them to.

DR. ROGERS: Our main use is for very long baseline interferometry, and for geodesy and astronomy work it is extremely important to have frequency standard stability that is very good in sort of the medium term, that is, between say 10 and 10,000 seconds.

The reason why it is important in that time scale is that we make observations of a number of radio objects during a course of a typical observing session, and some of these objects act as calibrators. So really, what is important is that the frequency standard acts as a flywheel to carry us between the time that we observe one particular source, through, say, a number of other sources and back again, say, to the same source. One could, of course, carry this to an extreme and have a system with multiple antennas where one set of antennas are always looking at a particular radio source, in which case that would sort of become the Clarke star.

However, that is extremely costly in order to do that because in order to see the radio sources you need very large antennas. Our experience with hydrogen masers has been quite good. Our early experiences were not that good. We have used H-10 masers which have quite good stability at a hundred seconds. But seem to degrade very rapidly beyond that, mainly because of their extreme sensitivity to environmental factors, we think. At that time we were not really seriously measuring the sensitivity of the maser to various different environmental factors. Also, we had some difficulties with masers failing.

Early design masers had problems with the disociator and the lifetime of the disociator, and they used to develop the disease known as the whites. However, I am pleased to say that in more recent design masers, I don't think we have ever seen a case of the whites. We would, I think, like to see somewhat better, or less sensitivity to environment than we have now, although we are of course working to improve the rooms in which we operate these standards. But even so, it is very difficult to hold the temperature of a room much better than two-tenths of a degree C, and even that perhaps is optimistic, if you are going to have people going in and out to check this.

So certainly we would like to see improvements in this area. Dr. Clark indicated that we really could benefit by even better performance. I think better stabilities, in the range 10 to 10,000 seconds; and I think that is true.

We might want to set a goal of maybe a part in 10 to the 15. Our experiments become limited by the atmosphere probably at this level, although we are working on systems for calibrating the atmosphere that may mean even better frequency standard stability than a part in 10 to the 15 could in fact benefit us in the future.

MR. FOSQUE: I would like to ask Dr. Clark if he would comment on his experience.

DR. CLARK: Well, I should preface this by saying that Alan Rogers and I are really from the same group, although our affiliations are different. There has been a group of astronomers and radioscientists on the East Coast of the United States that have merged together to do a number of types of VLBI programs a long time ago, and we still continue to be working together. So, to some extent Al and I speak together; so we are getting twice as much time as any of the other people.

I thought it might be a little bit useful to trace in slightly more detail the history that we have had with hydrogen masers, just so you can see that our experience is fairly widely based. And I will take off some of the different kinds of units that we have used along the way.

The first masers which were used as Alan said were H-10s. The Haystack has its own H-10. We managed to pick out of the box with Harry Peters' help an H-10 that went to Green Bank, West Virginia.

The earliest use of two hydrogen masers at VLBI was on that particular baseline. Subsequent to that time we have had additional experience with the masers that Dick Sydnor has built and used them at the Goldstone tracking station in California. We have used the NP design masers of Harry Peters in a number of facilities, in California, Sweden, Alaska, in Massachusetts; and have gained quite a bit of experience and confidence in those units. And the Smithsonian masers were of the current generation masers, have been the only ones that have been "commercially" available. Commercially is said in quotes here because I don't think Bob Vessot would like to think of himself as a factory, but he did make at least a limited number of masers for sale to the astronomy community for VLBI purposes.

Currently such are in use at Green Bank, West Virginia; Maryland Point; Haystack; and one at the Onsala Observatory in Sweden and at Ft. Davis, Texas.

So based on that kind of set of experience, I think you can see that we have seen masers all around the world. The Goddard masers have also been used on VLBI in Australia and are currently also in use — Pete MacDoran just walked in and I am sure he will make comment on the use of it within another VLBI program in NASA.

One of the environmental effects which Alan showed on his slide which was not expanded upon, perhaps as much as it should have been, which I think is a particular type of environment effect that we are very concerned about, long baseline interferometry work, is magnetic field effects.

The reason that this is of concern to us is that we typically use these masers at facilities that have large dish antennas which amount to large amounts of steel overhead which move to point at various directions in the sky, altering the earth's magnetic field in the environs of the masers.

Since the signatures we are trying to observe from the radio sources are in fact diurnal sinusoids, which the motion of the antennas with a diurnal period to track the radio sources could very easily mask themselves into erroneous geophysical and astronomical results.

So magnetic field effects have been of particular concern to us. In fact, based on Alan's testing at the Haystack observatory and reexamination of the shielding properties of the NP masers, Goddard Space Flight Center has recently embarked on a program to add additional magnetic shielding to the NP maser series. Two of those have now been upgraded, and additional ones are going through the mill having additional shields added.

We have seen such interesting effects as waste baskets and chairs alongside of hydrogen masers do in fact change tuning and hence the baseline results. That is certainly the kind of thing you do not want to see affecting high accuracy geophysical results.

So I think in terms of the reliability and requirements for masers, Alan indicated that levels of the order of parts in 10 to the 15 of a thousand seconds are certainly very desirable numbers for us. We do like to have longer term stability too, up to the one day level. Past one day it is relatively unimportant for most of the VLBI applications because our very long term time base is in fact TAI derived from LORAN-C.

However, since we are observing phenomena due to the rotation of the earth, we do like to be able to come back and observe that phenomena today and tomorrow, hopefully without any untoward behavior of the clock. Hence, time scales up to about 10 to the

5th seconds are of some importance to us.

Very short-term time scales are required, fairly good stability, though not past the level of the crystal oscillators included inside the H masers because we use them for local oscillators also.

So our most critical type regime is in the 100 to 10,000 second range with somewhat

less criticality with one times 10 to the 5th range.

That is the reason for Alan's comment. In terms of the way the masers have operated, I think we have found at least two brands of masers currently available have shown very high degrees of reliability and movability. Not portability because then you think of a suitcase and these certainly aren't suitcases.

But the masers from Goddard and Smithsonian astrophysical observatory have both been moved around to a large number of places in the world and usually you can plug them in and they work when you get there at about the same level of transportability and

reliability as cesium standards.

We have grown to trust them very much and have had very few failures. I think the question was asked this morning on mean time to failures. I think our experience has been very good. The worst failures we usually see are light bulbs burning out.

MR. FOSQUE: I would like to pause a moment before we go on and make sure that we ask Major Kittler of SAMSO to come forward if he is in the audience.

I guess he didn't come in late. Well, then, I would like to pass the microphone on to Mr. Easton and see if he will give us some flavor for his experiences with hydrogen masers and their uses.

MR. EASTON: We have had two different requirements for hydrogen masers.

Originally we started wanting one to compare rubidium and cesium standards to. For this purpose we got the first VLG10 ever built. And as Dr. Rogers has said, these had some problems with the disociator. But after the disociator was changed, it gave no further problems. We had another problem with the isolation amplifier, and when that was fixed, the thing has run now for a year with no problems. So we are quite pleased with the present VLG10, and our next use for hydrogen masers though is quite different.

We were now worried about flying them, so we are critically interested in small size,

weight, power, but still have long life.

So I have been very encouraged today to hear that some of these standards have run for five years. That is about the order of life we would like to see. So I think, all in all, we are encouraged and think we can build good and long-life masers for space applications.

MR. DECKER: I am from Marshall Space Flight Center, and we have recently used four masers built by SAO in a redshift experiment.

These were three ground masers and one probe maser. These masers have undergone quite some severe tests especially the probe maser of course. Further there has been travel

between SAO Wallops Island and the station at Cape Canaveral and have to work quite often in rather difficult environments. We have not experienced any reliability problem, any difficulties and these masers showed excellent short-term stability.

Our main concern for this experiment was stability over a period of about three hours because this was the main operational time required during the experiment. Our requirement was less than 1 part in 10^{14} drift.

You heard this morning from Mr. Bob Vessot about the design of those masers. The flight maser was tested in a vacuum chamber and its design was rather similar to the ground masers.

It was tested, for vibration, shock, ambient pressure changes between vacuum and atmospheric pressure; environments as you experience it in space, centrifugal force since we had a spinning payload and some variation of magnetic field, as well as combination of these various factors. In addition we did not only test but calibrated the maser for changes in these parameters during flight; we simulated the flight environment in the chamber and calibrated its various effects.

Through all these activities we never experienced any problem with a maser, and as you heard this morning, experiments worked very well and all the masers performed perfectly. I guess maybe we will come back later to talk about future requirements.

MR. FOSQUE: Maybe we could get Mr. MacDoran to give us some of his experiences, and I know he has had experience both in the areas of VLBI and spacecraft tracking. I will ask him if he would please make a few comments in both areas.

MR. MACDORAN: Thank you, Hugh. Well experience at JPL started out in the spacecraft navigation area, and the — some of the particular system elements that I was involved in was the effect of the time and frequency system upon the accuracy of the estimation of the Doppler signal and its decomposition to deduce the right ascension and declination of the spacecraft.

One of the elements that comes in that is generally foreign to the experience of most of the individuals involved in PTTI is the notion of long, round trip light time. People involved with, say, satellite timing, or something like that, are kind of used to the notion of, about a quarter second of round trip light time, out to geostationary orbit when you are talking about spacecraft tracking. In particular, my experience came with Mariner 6 and 7; where we were setting out ranging signals and waiting at that time for 45 minutes for them to get back from the spacecraft transponder.

And, as more ambitious missions are coming up, we have Mariner-Jupiter-Saturn that is getting ready to launch next year, and there some of those light times are going to be measured in hours.

The reference that you use for demodulating telemetry when you receive the return signal or the range code or the Doppler, you are obviously looking at a replica of what frequency system was doing three hours ago. And that is a very strange kind of environment in which to live.

So, you end up looking at a different kind of perspective of the way this error source gets into the data. For example, if this turned around very fast, you can tolerate a pretty poor kind of stability, you know, because it is going to be just differenced out in the next instant.

But, when you are looking at hours of round trip light time, obviously, the requirements are changed quite a lot. Not only is the Doppler the prime data type in the Mariner-Jupiter-Saturn mission, but some new things have come up. One is that the declination of

the planets, the outer planets at least like Jupiter and Saturn, are what they are. You might feel that you wish that it wasn't so close to zero declination, if you go through and write out the equations of Doppler, you will see that at zero declination, you don't have any sensitivity in a Doppler data system. So if you are talking about a flyby to a planet, and the planet is near zero declination, you have a very bad time estimating just where it is in that direction, relative to the equatorial plane of the earth.

There is now a move to try and determine angles by differential range. Now that differential range starts to put on another series of requirements, because if you are talking about range, good to a meter, there you are having to face now something like three nanoseconds of synchronization between two stations that are probably at intercontinental

separations.

And my colleague, Brooks Thomas, was going to address that, but the press of work back at the laboratory prevented him from being here. But, there are lots of ways that this is being looked at. There are some schemes that are called near simultaneous ranging where you can sort of trade the fact that you can interpolate the orbit just a little bit and pretend as if it were simultaneous and, therefore, you don't have to have the synchronization on the ground.

But there is a lot of thought being given to synchronization at the subnanosecond level to do the navigation. The rippling effect this has on the design of a mission is really amazing. Ultimately, it goes right back down to what it is that you are going to fly. For example, if you have an ambitious kind of scientific package, you want to fly, but it is kind of too heavy, then it comes onto the trade-off with the propulsion people, just how much weight are you going to get; how much propellant are you going to off-load to put on this instrument. That goes back to the navigation and says, "Well, how well are you going to put me by the planet so I can decide what kind of motor burn I am going to have to do when," and it's a tremendous rippling effect and you see it coming down to: "Well, how well is the PTTI going to be done?"

The requirement's coming up for the Mariner Jupiter Saturn sync@onization of something like 10 to 13 and it looks like VLBI is going to play a prime role both in the synchronization of the oscillators, as well as the epoch of the clocks, in the time interval of the

Mariner-Jupiter-Saturn mission.

With regard to ARIES and the transportable VLBI work, the experience we have had now is with quite a few major systems, started out in 1971 doing experiments using two of the developmental JPL masers, and the very valuable experience, and we began to get a better handle on just what it was that we had to have.

From that experience and the experience of using rubidium, we managed to develop observing strategies that would allow us to live with some of the peculiarities of the rubidium system relative to a hydrogen maser. We then had an experiment in which we had an SAO maser in Madrid, which Bob Vessot very kindly took the maser to Madrid for us. And — he just smiles over there. And we got some very interesting data there. We were getting synchronizations of the oscillator rates that were equivalent to a part in 10 to 13. And the two components of the equatorial baseline between Goldstone and Madrid were precision of about one meter and agreement at about the two meter level with Doppler determination sustention positions. Then, about a year ago, we started doing experiments using a rubidium and ARIES station and modified H-10 masers at Owens Valley and almost 12 months ago, we started using a Goddard hydrogen maser in the ARIES transportable then.

The experience with the Goddard maser has been very gratifying. Our data reduction goes ever so much more smoothly that we don't have to figure out exactly what rubidium

was doing in order to kind of back our way through the analysis. It is a very well behaved system. I think it is even NP-1 that we have in the station, so it, by no means, is the latest of the Goddard technology.

We have made all the moves successfully, and there have been a total of six moves that we have made during the last 12 months. And the Goddard maser has worked well. Once I have to admit the van got overly hot, and I guess we lost phase lock in one of the loops or something but we got the air conditioning back on and things settled down and it came right back up. But that is certainly not a problem with the maser; we had a truck break down and it was summertime and the thing got very hot and so on. But the maser has done very well.

And as we look forward to other systems, I guess we would like to see a maser that would settle down in just a period of a couple hours or something after a move and I don't know what the implications are for a system design for that kind of a wish. Synchronization needs for us are something like about 10 microseconds to get this started in the cross process, so we don't have to search too large a space and frequency synchronization, about one part in 10 to the 11 and then stability, once wherever the maser is going to be running or wherever the frequency device is of about one part in 10 to the 14 will sort of do everything we need to do, even up to X-band on regional baselines up to, say, 1000 kilometers. Or probably even more than that.

Even intercontinental baselines part in 10 to 14 will do it but let me not mislead you with a statement like that. When we are talking about transportable geodesy, what we are after are three baseline components, three dimensional relationship between the two stations and in instrumental terms. For that I will just mean something that looks like a clock synchronization and something that looks like a synchronization of the rates. So we are solving for just five parameters. In some of the work that Tom and Roger are concerned with, they have a more ambitious kind of solution problem. Not only do they have to do the five I just described, but they are talking about picking up you the one, polar motion, radio source positions and so on.

MR. FOSQUE: I wonder if at this time, there are some questions that the various panel members wish to bring up among themselves. If not, I think we can probably stimulate some discussion by opening the panel to questions from the floor.

I see Dr. Winkler with his hand up there. Perhaps we could let him have the first question.

DR. WINKLER: Can I ask the last speaker, MacDoran, would you repeat your statement about the planets being on declination zero? I am old enough to have seen most of the planets, declinations as high as 23-1/2 degrees up and down. I think there must be something wrong.

MR. MACDORAN: Okay, the problem is that outer planets will do those kind of things. You just have to wait around long enough. For the inner planets, sure, you don't have to wait too long to watch Venus kind of go through its whole range of declinations, but if you want to wait around to watch Pluto go through its whole range of declinations, it might chew up a lot of time.

If you have got a mission and you have got the funding and have everything put together, you are going to launch. And the planet you are going to go to, you are going to fly by the declination that it happens to reside in. If it turns out it is a declination of five or six degrees, rather than 20, that makes quite a lot of difference in the sensitivity

of the Doppler tracking and its ability to estimate the declination of the spacecraft as it approaches the planet. Have I answered the question?

MR. FOSQUE: Other questions from the floor? I see Victor Reinhardt.

DR. REINHARDT: Victor Reinhardt, Goddard Space Flight Center. I was just wondering if you could sort of sum up your needs for the future in terms of frequency stability, environmental sensitivity, longer term stability, just to get some sort of consensus or, and also synchronization. I heard three nanoseconds here which raised my eyebrows a little bit considering past statements.

I am just wondering if any of you would just make some projections for the future about your needs and would likes.

DR. ROGERS: I will try and get my set of numbers. A crucial time scale, as we have already mentioned is 10 to 10,000 seconds. I think one needs to have a better than part in 10 to the 14. Perhaps, as good as a part in 10 to the 15, if we make the improvements in atmospheric calibration that we may be able to make. So somewhere between a part in 10 to the 15 and part in 10 to the 14 for that time scale.

I think we would like to have that same stability extending out to a day. As far as the environmental sensitivity, I think you can really just take that number and as I say, I think we can hold the room temperature to, well, two-tenths of a degree, which means that the kind of temperature coefficients we have now have a few parts in 10 to the 14 are just good enough. But one could, again, go for some improvement. As far as synchronization is concerned, I think I am not sure you quite understood what Peter MacDoran said on that,

The initial requirement for synchronization, I don't think, is anything like nano-seconds. I think it is the order of microseconds, and it is merely a matter of convenience. In fact, we have done some experiments where we did not know the initial clock synchronization to better than a millisecond, and one can search for the clock synchronization, but it does take processing time. I think that we can, through the very long baseline interferometry technique, provide very good synchronization at, I think, the nanosecond level, once we calibrate our antenna systems correctly.

We have now subnanosecond synchronization, but only relative from one experiment to another. We have unknown constants in the synchronization that we have yet to calibrate out at the nanosecond level.

DR. CLARK: I might expand on this just slightly. The tracking stations and radio astronomy facilities that are involved in doing long baseline interferometry work using hydrogen masers probably constitute the biggest challenge for frequency standards for very high technology frequency standards anywhere in the world. And the fact that these can be synchronized by the interferometric techniques, that can essentially become a very high accuracy network of time available to the users.

One point when we get around to the questions going in the other direction that I would like to make is the idea of in some way having the astronomical facilities doing long baseline interferometry serving as a worldwide grid of time. So, I am posing that a little bit early but it goes along with what Alan just said here.

MR. FOSQUE: I guess we have a question here, I think we will take the question, and then come back to the panel views on requirements again.

QUESTION: Samuel Ward, Jet Propulsion Lab.

Would MacDoran or the panel like to discuss the problem of establishing calibration and nanosecond level and maintaining sync for long periods, like five to eight years?

Most of the users at the panel are only doing this for a period of a few hours.

MR. **FOSQUE**: Who wishes to speak to that? Pete MacDoran?

MR. MACDORAN: Well, the synchronization on the scale of years comes down to, what level of synchronization you need. I am going over in my mind what the interplanetary flight would really need, say, nanosecond over that kind of time frame and I can't see any driving requirement at the nanosecond level for years. You know for time spans continuously for a scale of years.

I could see it certainly during the differential ranging to get around the zero declination degeneracy and parameter estimation but that extends over a tracking path; that is in the scale of hours.

Now, you have a problem of clocks going down, you have to restart, you have a synchronization problem there; but I see that problem being solved by the VLBI technique itself, where for initial conditions you have sychronization of oscillator rates at about the part in 10 to the 11, which you can do by VLF techniques or whatever; and you have for convenience, initial clock synchronization at the few microsecond level.

Once you have those as initial conditions, you start then with the VLBI; and probably, as the JPL deep space network is now considering, they are going to bring that back either on a so-called high speed data line at rates of about 50 kilobits per second, or maybe through a satellite communications circuit, and do synchronizations at the nanosecond level of clock epoch. And from changes of epoch to deduce rate.

So, I see what you mean on scale of years, but I don't see that translating into nanoseconds. I see it much more at parts in 10 to the 13th, as I mentioned before, for the Doppler tracking with long-return-trip light-times. That is where I see the driving requirements coming from.

MR. FOSQUE: I would like to go back now again to the question of future requirements and ask our other panel members who are not involved in the VLBI, if they would address what they see in terms of future requirements.

I will start with Mr. Easton.

MR. EASTON: Our requirement, as Fred Walls made quite clear this morning, is not frequency stability requirement; it is a time requirement. We would like to keep a maser in space having unknown errors no greater than about 10 nanoseconds, when compared to Dr. Winkler's 32 hydrogen masers, which, I am sure, he will have in the near future.

MR. DECKER: If we talk about maser application in space, of course, size, weight and space requirements are very critical. Particularly, long operation lifetime without maintenance or with automatic control from the ground.

If we consider future relativity experiments to measure some higher order effects — we would like to see a frequency stability of 10 minus 16 or better over at least a period of several hours; as good as you can get.

MR. FOSQUE: There is a gentleman with a question. Would you identify the panel member that you are addressing the question to?

QUESTION: I am still very unsatisfied with the answers in terms of requirements and need. I am not that familiar with the VLBI, but can you give some concrete examples of what difference it would make to you, and what specific missions, whether you can order 10 to the minus 14 or 10 to the minus 15. It is very nice to have 10 to the minus 15 or 10 to the minus 16, but is there really a need and does it make a difference?

You would like to have 10 nanoseconds but in terms of applications, in terms of real need, now, what difference, what system would it make any specific difference whether

you have 10 nanoseconds or 20.

There may be a substantial expenditure to achieve such a result. It is all very nice to have it, you know, but it still costs money to get it. Is it worth it, I mean to go from 10 minus 14 or 10 minus 15?

MR. EASTON: The reason why we want and need 10 nanoseconds is that at that level, the error budget due to the clock becomes large, compared to the other errors in the system. And very soon the system starts going to pot. This is the GPS system. So, that is why 10 nanoseconds is important.

MR. DECKER: In terms of time synchronization or time, the requirement is not very critical for the relativity experiment.

MR. FOSQUE: I think he's asking you about the level of stability that is required.

MR. DECKER: This depends on the type of measurements you want to make. If we go, for example, to the sun, we can with the present maser design do some very good measurements on relativity experiments. That depends how close you can come to the sun, how much change in the gravitational potential you can experience with a maser.

But there are some other experiments where you would like to get up to about 10

minus 16, if you can.

Does this answer the question?

DR. VESSOT: I can answer that question.

Prof. Kenneth Nordtvedt has just calculated what would happen if you did a solar grazer, not a solar plunger. That is a device that goes in a parabolic trajectory within four solar radii of the center of the sun and is measured at an angle of 45 degrees to its trajectory in the plane of the ecliptic, so you are not looking out of the plane appreciably.

He comes out with the following results. If you had a clock at one part ten to the 14th, you would get that value of the redshift would be on the order of 10 to the second-8, and the value of beta the second-order redshift would come out at about 10 to the minus 5 from the trajectory determination. You would measure beta from the second order redshift directly at about 10 to the minus 1. You would measure gamma, I think, at about 10 to the minus 6 level; that is the parameter that has to do with the way the spatial part of relativity is altered by the presence of the solar mass.

The oblateness of the sun could be measured at about 10 to the minus 10 level, that

is the fact that the sun is flattened owing to its rotation.

There is also an experimental test of the frame dragging, which is the property space has when it is near moving matter, in this case the rotating matter of the sun where the actual coordinate frame is dragged by the rotating object, and that Lense-Thirring Effect. This effect would be measured at about .6 to .2 level — enough to see its existence.

Your question can be answered by saying all of these can be improved by a factor of 10 if you got to 10 to the 15th, instead of part 10 to the 14th, where, I think, we are now at. These are all measurements which, I think, are very, very important to people in astronomy, relativity and astrophysics in general.

MR. FOSQUE: I think we will take the gentleman real seriously and ask all our panel members if they can sharpen up their requirements and identify how they come about. So, let's go now to our VLBI contingent.

MR. MACDORAN: After having heard the implications of the general relativity aspects, I would like to acquaint you with a much more prosaic problem: one of solid waste management. You think I am putting you on, but I am not.

There is a mission that is about to fly called SEASAT. SEASAT is going to carry a radio altimeter and it is going to measure the ocean's surface from orbit. One of the driving requirements of SEASAT is to find the open ocean circulation. That happens because there is something called geostrophic flow because when the water sort of turns a corner, it stacks up.

The assumption is that by flying over you will be able to see the stacking up of the water and identify the center of the thing called the amphidrome. That is the oceanographic aspect.

The geodetic aspect is that there is a systematic problem with the apparent sloping of mean sea level.

Something is inconsistent. It doesn't seem to be on the level.

MR. MACDORAN: Unless you can figure out what is happening there, you will get confused between what is systematic slope and what is the open ocean circulation.

Now, ARIES Project with the transportable VLBI is involved now with the National Geodetic Survey in developing a relationship between differential leveling and geometric geodesy.

Now, we come back to the positions requirement. How good do you have to do this thing? And the answer is about 10 centimeters. What is 10 centimeters, what does that actually translate into when you look at even a simple solving for five parameters? And you keep going through this, and what you end up with is about a part in 10 to the 14th stability.

So, now we have traced it back to a frequency stability requirement and that have to do with open ocean circulation and dumping of solid waste from the coastal states and how long it takes before it washes up on your beaches.

It wasn't a put-on.

DR. ROGERS: Are you people looking for an actual number?

VLBI is basically differential ranging, and we are hoping to be able to measure strains on the crust of the earth of the order down to the centimeter level across the continent and we hope perhaps down to the millimeter level for around a hundred kilometers, and we have already done the millimeter level on distances of about one kilometer. If you just take one millimeter and you say, you want to get down to one millimeter, and let's say, your antenna takes a thousand seconds to move from one object to another, you want the frequency standard to drift an equivalent to one millimeter, which is the

order of one picosecond in a thousand seconds. That is a part in 10 to the 15th right there. That is the kind of calculation that is a very crude calculation, but that's the kind of numbers you come up with.

DR. CLARK: I was going to amplify a little on Alan's analogy. There are a number of the geometric turns. He was talking about the one where you make a differential measurement between two different radio sources to determine differential arrival time from the two sources at the two stations so that is, in a sense, a double difference measurement he was describing there, which required that kind of level of stability.

But if the kind of numbers we are trying to get down here are down in these centi-

meter and subcentimeter category then it's another story.

Let's talk about the one-day level of stability briefly. If we are talking of about a part in 10 to the 14th over 10 to the 5th seconds, that is a nanosecond per day. We all know a nanosecond is a foot. So, if we have instabilities at the part in 10 to the 14th level at the one-day level, that means that there is 30 centimeter type noise that is masked in all of the rest of the stuff we are really trying to observe.

Some of that noise, if it averages out, really doesn't hurt us very much. But the thing that we are trying to observe with the very long baseline interferometry techniques, we use the quasars up in the sky as inertial reference frame. They are very fixed; we haven't much worry about their stability. We are trying to measure the geometry of the earth

underneath those quasars.

We see that geometry change once per day as the earth rotates underneath the quasars and the apparent geometry of the baseline, as seen from the quasar then rotates once a day. Therefore, what we get as an output signature for the observable from one source is a sinusoid that varies over a period of time of one day.

But we can't observe it over a full day because the earth isn't transparent, unless we find some very specialized sources that are up all of the time and all of the antennas that

are involved, which doesn't happen.

So, what we are trying to observe is over a significant fraction of a day, and hopefully come back the following day and make sure the measurement lies on top of that first measurement, be able to stack all of these things together, coming out with that numbers that are accurate at the centimeterish level, we don't want to have, then, frequency standard effects that have diurnal signatures masked into the data.

For instance, if the frequency standards have temperature sensitivity, the temperature sensitivity in the room is going to have a diurnal signature to it typically. So that is a kind of effect that can be very bad. Similarly magnetic field effects could be diurnal because we have this big moving mass of telescope overhead, which is pointing at the different stars

and taking out the earth's rotation.

These are some of the reasons why we require all of this freedom from environmental parameters at the same kind of level Alan showed for the double difference measurements. So, it does convert to a requirement also for precision out at the nearly one-day level or one-day level.

Now, obviously, we could then do what Pete did, and say what is the implications of

measuring these distances to that level.

Well, that obviously has implications in earthquake prediction areas and things like that.

I don't think we want to go into the economic benefits. Pete already did in his dumping of waste matter analogy.

MR. FOSQUE: Any questions?

DR. REINHARDT: I would just like to make a comment in line with what the BIH people said about wanting hydrogen masers. And our problem at the laboratory has been holding on to them long enough.

Since the VLBI are using the masers and use them for long periods and have the network, the ideal place for reporting to TAI is the masers at the VLBI stations rather than at the laboratories that are doing the research on the masers themselves.

MR. FOSQUE: Other questions?

DR. KNOWLES: Steve Knowles, NRL.

The questions about the supercooled oscillators I have heard about. What is the current state of the art on those; who makes them; and is there a possibility of a prototype being available for use at a VLBI telescope? I would certainly like to see that. We all have good facilities for testing oscillators.

MR. FOSQUE: Who wants to tackle that problem?

DR. **CLARK**: We have some of the NBS people here in the audience.

MR. FOSQUE: It has been suggested we have people very knowledgeable in the audience. Perhaps Mr. Allen might, if you give him a microphone, maybe he could comment on that.

DR. **ALLEN**: The best results to my knowledge that have been obtained at Stanford by Dr. Stein, and Dr. Turneaure. Those results have been published.

We have not yet - had systems operating to the point where we can compete with those. Those results are, one-second stabilities.

DR. WALLS: Now seconds -

DR. ALLEN: Yes, 4 and 10 to the 16, 1000 seconds. One-second stability, as I recall, is about 10 to the minus 14, going down, one over Tau. That is what has been documented. As far as their availability, we are not interested in a production unit. The thing that needs to be done is for someone to pick that up and try to capitalize on what research has been done. We have high hopes for the superconductor cavity.

I think one thing has to be kept in mind, and that is that if I understand the need in VLBI, it is the total accumulated phase over whatever integration period is of interest, whether it is 1000 seconds or whatever.

And if you talk about that, then you talk about the stability at that sample time. If it is at 1000 seconds, then, due to the environment sensitivity of superconducting cavity you nominally have comparable stability between hydrogen and superconducting cavity.

So that is an important point I think that needs to be brought out.

MR. MACDORAN: I guess going back about a year and a half ago I had a meeting with Turneaure when we thought we were in better financial shape than we are.

We talked about the possibility of putting together a transportable device which he thought he could do. My recollection, it was something like, at that time at least, around the 50 K category for a demonstration field unit. And there were some really fascinating possibilities with it.

The fact that you have to go down to below the usual for Kelvin liquid helium temperature, you have to pump it down I guess 1.6 or something. It is cold, cold outside. But not much. Being from Southern California, it is a real shock to me. But one of the other things you could get, a kind of synergy going is with the cryogenic traveling wave maser.

In the masers now used in the deep space network, there is a bath that runs about 4 Kelvin, and — or maybe a little cooler. So there is this traveling wave maser structure so what you begin to envision is the structure and this Gunn diode running in this resonant cavity and it is all one integrated unit.

When you take the maser from 4 degree Kelvin, the maser gain is something like 45 dB, but when you pull the maser down to about 1.6 Kelvin, the gain goes to about 90 dB and it is just fantastic, so you get visions of this tremendous receiver one could have operating, you know, probably at around 10 Kelvin for the operating temperature of the receiver with an integrated local oscillator. The Gunn diode wants to run at X-band anyway so you don't have to do any multiplication.

Frankly, I think one can see stabilities that we haven't even thought about how we were going to exploit them if they were available because our thinking has been restricted right now to what we can get or by whatever means we obtain, to use what is physically available. But that is going to be changing, I think, in the next few years.

DR. ROGERS: I would like to just comment on Pete's statement and, those kind of stabilities.

I think we know we are limited by atmospheric stability a long time before the part in 10 to the 16 level.

DR. FOSQUE: Are there other questions?

DR. WARD: I would just like to add something to Pete's statement. He forgot that that maser also has a superconducting magnet.

MR. MACDORAN: That's right.

MR. FOSQUE: Any more questions?

Well, I have a piece of paper here which somebody gave us a written question. I think I would like to turn that over to the panel now.

The question is: what are hydrogen maser user experiences in comparison with cesium and rubidium standards? And have these different devices really been compared on an equal basis, or under equal conditions?

I will start over here on my left and see what comment the gentlemen would like to make on that.

MR. DECKER: I don't have any experience. We have no comparison.

MR. EASTON: Well, we have had experience with all of them but I don't know how to say equal bases, since they all use different types of atoms.

There is no doubt that the hydrogen maser is the most stable. The cesium is right now the most accurate. Rubidium has very good short-term stability and not so good long-term stability.

We are in hydrogen masers because we were told to look into them. And, strangely enough, it now appears to be a very good decision. But it wasn't one we had to make.

MR. FOSQUE: Would you gentlemen care to comment?

MR. MACDORAN: Well, a year ago PTTI, the paper I had in there, discussed specifically how we had used an HP50-65 to get baseline solutions at S-band, where the requirements are less severe than going to X.

We evolved observing strategies so that the frequency system would not do us in. But that doesn't mean those strategies were not compromised to what it is we ultimately want to do. You know, it was good to begin to demonstrate a feasibility, to develop software and the whole systems analysis.

Now that we have had experience with the hydrogen maser in the transportable station, we are looking at covariance limits right now, sort of the best we could do theoretically from the data quality being generated, and those covariance limits are in the range of three to five centimeters. We have some other systematic things going on that are kind of limiting us at 10 or 12 centimeters right now, but we think we will get those cleared up within the next few months. So I think we will start moving down where we can get out the three to five centimeters and that will be in the time scale of the next year.

The hydrogen maser plays a prime role in that. It is kind of interesting. If you don't have a really clean data system, or a clean frequency and time reference, then the entire system, and ARIES is a very multidisciplinary kind of thing, and if you are getting confused right at the time and frequency level you have trouble distinguishing what your dependences are on the radio source positions or the ability to do the transmission media calibration, both the charged particle effects and the neutral atmosphere, or the ability to do the modeling. Enumerable numbers of things.

So it sure is a real blessing to us with the hydrogen maser that now we can get in there and say we just don't have the problem from the time and frequency system and now these other errors are so much more clearly standing out and amenable to a systematic solution.

DR. ROGERS: We have had a little experience with rubidiums. The HP50-65A at Haystack Observatory is in fact used as the primary source of five megahertz.

In fact, we lock the rubidium to the maser.

That, we may change. That was somewhat historic because we wanted to keep that five megahertz on line at all times.

We have had rubidiums going in and out of our standards room as we switch from one rubidium to another. We have seen very good stability with that particular HP standard. It approaches a part in 10 to the 13. I think at about 1000 seconds.

I have a sigma tau plot. I have it in my briefcase if anybody would like to see it afterwards.

We did have a cesium supertube that Dr. Klepczynski brought to Haystack Observatory, but unfortunately we were only to look at it for a matter of about an hour.

It came as part of a clock synchronization service, normally we would just look at the second tickout to synchronize our clocks, but we tied it into a frequency comparison system. It looked like it was not too good at all at 100 seconds. Worse than the rubidium.

It was about a part in 10 to the 12 at 100 seconds. I am not quite sure why that was so. Maybe he would like to comment on that. But that is the only test I know of a supertube cesium.

The older cesiums we know are totally inadequate for any kind of VLBI application. Stability at 100 seconds is totally inadequate. We can't even get coherence at X-band.

DR. CLARK: There was one supertube cesium experience we had on the air that I think Allen may have forgotten about. It was at a time when we were running VLBI between Haystack and the Goldstone Tracking Station and the normal site maser was not available at that time.

So we did take one of the very early supertubes that Goddard had bought to the Goldstone Tracking Station to use as a local oscillator. Our on-the-air experience with that, very early one, was that it gave stabilities at the critical time scales for VLBI roughly comparable with what we would have gotten with the rubidium.

In terms of answering this question, in terms of a geodesy application, Pete gave part of the answer. There are some errors which are instrumental errors which are independent of baseline length. There are others, VLBIers, which are proportional to baseline length.

The fact we don't know before the fact the geometry of earth, which way is the pole pointing and how fast is the earth rotating, that introduces errors to us.

On very long baselines, the way in which the frequency standard maps into our ability to measure these terms, it will introduce a few centimeters of uncertainty if the frequency standards depart in the 10 to the 14 level.

That uncertainty goes essentially — that is for the critical numbers around 1000 seconds.

Therefore, if we are talking about a part in 10 to the 13, that is introducing 30-centimeters errors and it gets very difficult to do 5-centimeter geodesy if you have 30-centimeter clock-error noises masking themselves into the data.

So I think the VLBI applications for high accuracy astronomy and geophysics, to produce numbers at the output at the subdecimeter level clearly require hydrogen masers or comparable performance from some other technique, whatever that Brand X technique might end up being, and I don't see any way around that.

MR. EASTON: Perhaps there is one thing that has not been brought out.

The reason the hydrogen maser is so good compared to cesium and rubidium is that the bandwidth of the line is so narrow. It is about one hertz in the ordinary hydrogen maser — and in the passive maser, Fred, what is it, a quarter?

DR. WALLS: It could be.

MR. EASTON: Something like a quarter of a hertz. With the very long tube cesium, 30 hertz?

VOICE: 25.

MR. EASTON: With the ordinary run of the mine, 500 hertz.

Perhaps this gets to the point of this question. If we are comparing a hydrogen maser to an equivalent cesium standard, it is perhaps 300 meters long, and even the H10s weren't that big.

DR. KLEPCZYNSKI: Bill Klepczynski, National Observatory.

Tomorrow we will be reporting on a paper which is co-authored by the people from NRL, Ken Johnston being one of them.

We did do some experiments with radio astronomy where we have results where we were comparing rubidium on a maser and cesium on a VLBI experiment.

As expected, you find the maser is the superior performer.

However, according to specs as you see them, the short period term, rubidium outperforms cesium, about 1000 seconds. In this instance the cesium did pretty well.

You will see some of those results tomorrow concerning the one problem. We had the cesium up at Haystack a while back; I don't really know how to answer that because I think Dr. Costain is going to make a comment.

DR. COSTAIN: We had the same thing at NRC before we came to Haystack.

We were doing a phase comparison there against their cesium 5. We found very good agreement with it.

I was surprised at the performance we were getting at Haystack with this particular cesium.

It is within the spec, though, of what HP prints.

I was expecting, and when we got back the closure indicated the cesium itself had performed a lot better than it did, the time of the performance of the phase track we were doing.

So I am not completely sure about what happened there.

MR. FOSQUE: I believe we have a question over on my left, Dr. Costain.

DR. COSTAIN: There still is a question in our mind as to the place of cesium. Certainly we use the hydrogen maser still to, in our evaluation of our primary cesium standards. But we are beginning to wonder that if we can — we think we can or have achieved a part in 10 to the 14 stability in about three hours which is just going outside the requirement of many of these; but we think that is maintained for a year.

I think there is probably, certainly in the time-keeping business, it's going to be wide open, long-beam cesium standard type.

It's in my mind still a question in operational conditions — of whether the absolute long-term stability is not going to be an important factor.

Or the question is, is it going to be an important factor with sort of timekeeping of a microsecond per year?

I would just give a brief comparison. We have, against some high performance at Hewlett-Packard for selected intervals. This is not in performance seen between our primary standard and the high performance figures down into the several parts in 10 to the 15.

MR. FOSQUE: I believe there is a question down here on my right. Mr. Peters.

MR. PETERS: I think it's pretty important or I wouldn't bring up perhaps what might be a touchy subject.

But as the question of accuracy relating to the type of standard has been brought up, when we are talking about accuracy with cesium superior to that of hydrogen masers, we are always referring to the National Standards Laboratory cesiums.

The available cesiums which are used as standards in the field, the commercial cesiums, I'm sure everyone will confirm this, are not specified in accuracy to near the accuracy capability documented for the usual hydrogen maser. Typically, five parts in 10 to the 12.

We are talking about fundamental accuracy now, and in the sense that they can be evaluated. I would like to question the statement that cesiums are more accurate than hydrogen in the sense that they are referred to the National Standards Laboratories and are even in their specifications. So for hydrogen in that sense, its capability at present is more accurate by a factor of 2 to 5 at least, I believe; as everyone is well aware, or should be.

MR. FOSQUE: I will take a question from Dr. Winkler first, then come back to Dr. Costain.

DR. WINKLER: I have no question. I have to make a comment.

I think I begin to see the point of Dr. Decker, that accuracy is becoming a much abused and misunderstood word.

I have to say I honestly begin to see the reason why it would be better to refer, to split the meaning which is inherent in that word, split away the part which he considers as uncertainty of a standard. Whatever that may be, Peters is of course correct. If you talk about uncertainty of a standard, you mix together several unknown systematic effects. If you talk about the other benefits which were inherent in your discussion here of long-term stability, you talk about your control over systematic effects which may come in over long periods of time. These are really two different things, I think, which one has to consider, and I believe maybe we shouldn't talk so much about accuracy and consider more the systematic effects.

There is something which Harry has said two days ago or three days ago at NCIR meeting which may be useful to mention here. That is the ability to model these long-term systematic effects; it may be here that there is an advantage in the hydrogen maser. Maybe Peters would like to make a comment on that.

This, of course, is ridiculous and a complete misunderstanding of the meaning of band width, and long-term performance.

The reason why the hydrogen maser is a — standard at least in a region of sigma tau plot, certainly between ten seconds, and somewhere, tens of thousands of seconds, I would certainly agree with that, there is no question about it, is that there is — it is inherently phased stable — coherent phase output avoids the random accumulation of steps or what we call the random walk-in phase which is inherent in the performance of a cesium standard; which is why frequency noise dominated, as opposed to the hydrogen maser, which is why phase noise dominated until it reached the frequency — so I think it is completely wrong to make that comparison.

I wish that you, Roger, would recant immediately, and -

I think it would be very interesting if you would comment on the ability, your expectation of modeling the systematic effects in the hydrogen masers.

I think this is a thing which is definitely pertinent here.

Of course, as Dr. Winkler has brought out, there is a problem in comparing hydrogen masers to cesium standards.

One is an oscillator and one is not.

Or one can be an oscillator and hydrogen maser can either be an oscillator or a filter like cesium.

But if you were referring to equal band widths, and as I recall the question there was some equality, equal conditions, you would certainly have to have a very long cesium standard to have the same line width as you have with a hydrogen maser.

That was my only point.

DR. WINKLER: The question refers to equivalent or equal environmental conditions, please?

MR. FOSOUE: Do you want to make a comment?

DR. CLARK: I was going to add another Winkler-type comment, that perhaps instead of one meter tube, we are talking about 10 to the 4th 100-meter tubes.

MR. FOSQUE: I guess I still have the question Dr. Costain wanted to bring up, but so we won't lose the thought Dr. Winkler made I would like Harry Peters to comment on that first.

MR. PETERS: Well, I think it's clear from the performance of hydrogen masers and — and many other standards, that the statistical properties at one second, ten seconds, a thousand seconds typically, at least for H masers, particularly in this range, are important. However, in the long term at about 1000 seconds and beyond, we are subject mostly to the environmental problems, the sensitivities of the device to the environment, magnetic field, and various and sundry things. And that was one of the main efforts of the NASA research at Goddard, was to identify these and as well as to try to illustrate operation of ground-based hydrogen masers. I do feel that by testing and quantifying the systematic sensitivities that we should be able to identify those things which are causing us to, say, flicker out, is the usual word; but I really don't believe in that idea of flickering out because typically I think of this as saddle point, and that is where the systematic things begin to take over and typically — so we always see a low point in the curve.

But by changing the temperature or magnetic field of the maser, it's being done much better now than we really did or should have done when we made our hydrogen maser. This type of thing can give coefficients and quantify the systematic sensitivities and perhaps show us how we can get down into the 10 to the minus 16. I don't know if I answered that exactly in the right way, but I think this is a very important area of research.

It's important also for cesium or any other standard I think that we can likely identify the systematic effects, and that such things as just a random measure of frequency instability without identifying what its physical cause is may at least occur at a lower level than it does at present.

MR. FOSQUE: Thank you, Harry.

I would like to take Dr. Costain's question, and then perhaps any comments generated from Harry's.

DR. COSTAIN: I think it's probably, better that I comment on what Harry Peters says, in reference to the National Standards Laboratories on primary cesiums.

We are beginning to think perhaps it's time to take the primary cesiums into the field or at least get online with communications and navigations systems from the Standard Laboratories.

MR. FOSQUE: I want to take Mr. Allen's comment or question first, then go to Dr. Winkler.

DR. ALLEN: The point that Harry Peters makes I think is an extremely valuable one. The long-term flicker floor as it's sometimes called I think really is almost always environmentally induced. If you can characterize this, it's an extremely important thing.

Along those lines the comment I really wanted to make is that if all of these very nice hydrogen masers that have long life, that exist at these various observatories, could be tied into the international time scale, this would be very valuable in understanding their long-term performance, what kind of environmental sensitivities and drifts they have.

I think this would do two things. One, it would help us to understand their long-term performance. It would also help them when they go to decorrelate the data because they are synchronized and they know where they are in time; it takes less computer time to search to know where they are because all of the clocks in the system, as it were, are synchronized to the same scale.

I think there are those two advantages.

One further point that I would like to make is that I think there is a little bit of comparison of apples and oranges, when we talk about the same basis that Dr. Reder is, I think, referring to.

We must keep in mind that most of the cesiums out are commercial cesiums. It's really not quite fair to compare a production model with these hydrogen devices which are put together by experts. The people who are not production line operators.

MR. FOSQUE: Dr. Winkler; Professor Ramsey, Dr. Winkler defers to you.

DR. RAMSEY: This was a minor comment on Allen's comment. It's quite true, this is a very major difference in comparisons; but the argument goes both ways. I think in many respects the commercial ones, those in commercial development, have many advantages. One of the things hydrogen masers have suffered most from has been that their has not been until quite recently any major effort. They have been essentially hand-produced ones.

In our lab at least experts do rather less well than the routine people. Since this is Naval Research Laboratory, this was certainly true when I was involved in radar work at MIT. Navy sailors could do a lot better with production radars than we could ever do in the lab when we were developing them.

MR. FOSQUE: I think Dr. Winkler wishes to speak.

DR. WINKLER: I completely agree with Professor Ramsey about that. It is a two-way affair and there are advantages and disadvantages. But one — going back to Dr. Klepczynski's remarks, if you take a high performance cesium clock to the lab and immediately start making performance checks, you will be immediately disappointed. In the first couple hours there is a temperature shock usually involved and you have shifts in the various circuits imposed upon whatever performance disturbances you may have. So I would discount that completely.

But, Dr. Costain, how much would be a five meter long cesium if we would ask you to produce one, how much would it be?

DR. COSTAIN: We are going the other way, essentially two meter overall.

DR. WINKLER: Maybe you do get into the cesium business and you become a competitive producer. Honestly, do you have any estimate for the amount of money which was necessary to put together a large standard?

DR. COSTAIN: I think a long beam primary standard could be produced at the scale of a dozen or so for \$120,000, \$130,000.

MR. FOSQUE: Well, this has been very interesting and certainly enlightening to me and I hope to many of you in the audience.

I see that we have already overrun our time by a few minutes, and as much as we might wish to continue for a few more questions, I believe unless there is, as Professor Ramsey said, a really important question out there in the audience, perhaps we better fold up this panel.

I thank you, gentlemen, for participating in the panel discussion.

We will, I think we have a coffee break now; then we will resume in session 5. (Recess.)

SPECIAL PURPOSE ATOMIC (MOLECULAR) STANDARD*

David J. Wineland, David A. Howe, and Helmut Hellwig

Frequency & Time Standards Section National Bureau of Standards Boulder, Colorado 80302

ABSTRACT

A special purpose frequency standard and clock is being developed featuring a novel combination of stability and accuracy performance, shock and temperature insensitivity, instant turn on characteristics and featuring low weight, power consumption, and potentially low fabrication costs.

This new device is based on the well-known 3-3 transition in ammonia (~ 23 GHz) which provides the frequency reference for a ~ 0.5 GHz oscillator. The oscillator signal is multiplied in one step to K-band and injected into a waveguide cell containing ammonia. The absorption feature is used to frequency lock the 0.5 GHz oscillator to line center. A fixed output frequency between 5 and 10 MHz is provided by direct division from 0.5 GHz. The 0.5 GHz oscillator is a novel strip-line transistor oscillator of high spectral purity. It may not only be important for our standard but also for other atomic standards where acceleration and irradiation problems are encountered. The absorption device may well be able to fill a metrology need not satisfied by presently available atomic and quartz crystal standards.

Design goals of the present project are 10^{-10} stability from ~ 10 sec. to 10^4 sec, and 10^{-9} absolute accuracy. The rather broad linewidth of ammonia (~ 100 kHz) reduces overall resolution but allows a short (< 1 ms) servo attack time thus reducing the acceleration sensitivity of the primary 0.5 GHz oscillator. Working at low pressure (< 10^{-4} Torr $\simeq 1.33 \times 10^{-2}$ Newton/m²) reduces temperature sensitivity to an acceptable level. Power consumption should be < 3 W and expected size of a working device ~ 10^{-3} cm³.

^{*} This research was supported by the Advanced Research Projects Agency of the Department of Defense and was monitored by ARPA under Contract #3140.

INTRODUCTION

The Special Purpose Atomic Standard Project has developed from a need for a frequency standard satisfying specific requirements not found in other precision oscillators. Briefly, currently available precision oscillators can be divided into two classes: the quartz crystal oscillators and atomic "clock" oscillators. The quartz crystal oscillators, while having good short-term stability and low cost (\$0.5K to \$2000 for high-quality units) suffer three major drawbacks: (1) The frequency is not fundamental and is related only to the macroscopic dimensions of the quartz crystal. Therefore, calibration is required initially and subsequent recalibration is required due to "aging" of the crystal. Aging rates of 1 part in 10^8 (fractional frequency change) per year are considered good. (2) The crystal oscillator is sensitive to vibration and shock. These environmental factors affect the macroscopic dimensions of the crystal and therefore can cause step shifts in frequency. (3) The quartz crystal oscillator is temperature sensitive and requires significant warm-up time to achieve a stable output frequency.

Atomic oscillators provide stabilities from one part in 10^{10} to one part in 10^{13} per year. Their cost ranges from \$3,000 to above \$20,000 depending upon performance. Their high frequency stability and accuracy make recalibration unnecessary for most applications. However, the use of presently available atomic oscillators in place of crystal oscillators for the purpose of avoiding recalibration routines or reducing environmental sensitivity is technical "overkill," since the excellent performance of today's atomic oscillators (obtained at high cost) is not required for many applications. In addition, their warm-up time is slow; and their performance under severe environmental conditions (acceleration, vibration, temperature, barometric pressure and magnetic fields) is inadequate for some applications.

Therefore, a special purpose oscillator or clock with frequency accuracy in the 10^{-9} range and frequency stability in the 10^{-10} to 10^{-11} range would satisfy the needs of many technical applications if low cost and insensitivity to environment could be obtained. Fig. 1 (solid line) shows the frequency stability desired in the present work.

In order to meet the above requirements we might hope to look for a system which incorporates the desirable features of both the atomic oscillators (high accuracy, stability) and crystal oscillators (low cost) and includes features of environmental insensitivity and possible fast warm-up. Since we do not require ultimate accuracy and stability, we might make sacrifices in this regard. We have chosen as the frequency reference the (3-3) transition in ammonia $\rm N^{15}H_3$ gas (\sim 23 GHz) which is contained in a simple closed cell. Historically, this same scheme was used in the first "atomic" clock in 1948 [2]. Research on this basic device was pursued until about 1955 but was discontinued

then because new methods, although more complicated, promised better accuracies and stabilities than a gas cell absorption device. In 1955, the accuracy of an ammonia device was about 5 parts in 10^8 with approximately 1 part in 10^8 stability, and the apparatus was quite complicated and expensive, suitable only as a laboratory instrument [3]. However, since that time, vast improvements have been made in RF and microwave electronics; these coupled with new insights into the electronic and physical problems encountered suggest that the ammonia absorption cell idea could be used to provide the "special purpose" oscillator described above.

The basic scheme used for the standard is shown in Fig. 2. For simplicity and economy, the primary oscillator in the system is at \sim .5 GHz. With this, one can multiply in one step to \sim 23 GHz with ample output power to detect the ammonia transition. In addition, one can directly divide the .5 GHz signal to produce a fixed output frequency between 5 and 10 MHz, which is harmonically related to the ammonia transition frequency.

APPROACH

It might be possible to use an existing atomic oscillator (rubidium, hydrogen, cesium) to accomplish the goals of the special purpose frequency standard. However, the increased complexity and sophistication of these devices which results in their superior performance are just the factors which increase their cost and decrease their reliability in an adverse environment. This sophistication is introduced primarily to make the reference transition free from first-order Doppler broadening. This results in increased line-Q and therefore increased accuracy and stability. In the approach chosen here we contain the reference "atom," the ammonia molecule, in a closed waveguide cell. The linewidth is limited by Doppler broadening to give a fundamental upper limit on line Q $_{\rm w}$ 3 x 10 $^{\rm 5}$. This can be compared to the line Q's of the high performance atomic oscillators [4]:

Q(Rb)
$$\sim 3 \times 10^7$$
 Q(H) $\sim 10^9$ Q(Cs) $\sim 3 \times 10^7$.

Therefore, sacrificing resolution, we obtained a much simpler system resulting in a significantly reduced cost and increased reliability. Also, the lower line Q allows fast servo loops within the standard, thus reducing acceleration sensitivity.

(a) Microwave Source

In specifying a possible fundamental oscillator for the standard, one has reasons for not using a microwave oscillator. They are: (1) Fundamental oscillators at K-band draw too much power, are too expensive, and are not stable enough (by a factor of at least 10) in short term to be useful as a primary oscillator. (2) In order to compare an output frequency of between 5 and 10 MHz to the ammonia transition

frequency we require a multiplier chain. (Note that few dividers exceed 1 GHz input frequency; therefore, we could not divide directly from $\sim\!23$ GHz.) The development of a special $\sim\!.5$ GHz oscillator is more practical as shown in the diagrams of Figs. 2 and 3.

(b) Gas Cell

The advantages of using the ammonia gas cell as a reference

- are:
 (1) The microwave transition of interest provides an absorption signal which is orders of magnitude stronger than those of other interesting molecules or atoms [5]. This is a significant advantage because it means that the desired signal-to-noise is obtained without resorting to impractically large microwave cell sizes as would be necessary for amost any other gas.
- (2) Since ammonia remains in the gas phase for the temperature range of interest $(-40^{\circ}\ \text{to}\ +60^{\circ}\ \text{C})$ the device has instant turn-on capability. One must, however, note the existence of a pressure (therefore temperature) dependent frequency shift; this is discussed more fully below.
- (3) The frequency of the ammonia transition is fundamental in nature and therefore essentially eliminates the need for calibration of the device.
- (4) The ammonia transition linewidth is fairly broad ($\sim 100~\text{kHz}$). This is a disadvantage in terms of the ultimate accuracy obtainable, but it allows the primary oscillator to be locked to the ammonia reference in very short times (< 1~ms). The advantage is that the vibration sensitivity of the primary $\sim .5~\text{GHz}$ oscillator is reduced by as much as the open loop gain of the servo system at the vibration frequency of interest. Such a technique is not feasible with other currently available high precision oscillators because of the inherent narrow linewidths.

RESULTS

(a) Introduction

For ease of discussion and clarity, it is convenient to divide the system into four components:

- (1) ~.5 GHz primary oscillator and divider.
- (2) ~.5 GHz to 23 GHz multiplier,
- (3) ammonia gas cell.
- (4) servo electronics and integrated system.

(b) .5 GHz primary oscillator and divider

In reviewing the possible oscillator designs, it appeared that an oscillator using a simple LC resonator should be investigated. Advantages to this design include:

- (1) wide tunability,
- (2) continuous operation under very adverse conditions (shock, vibration),
- (3) good short-term stability,
- (4) low cost.

An oscillator was developed operating at about 0.5 GHz and having a free-running stability as shown in Fig. 1. The curves include a divider chain (\pm 100) after the .5 GHz oscillator. These data were computed using the two-sample variance for different averaging times [1]. The bandwidth of the measurement system affects the variance in the case of white and flicker of phase type noise; therefore, two curves are plotted around the averaging times of interest (\sim 10 ms). The oscillator features a P.C. board etched strip as a transmission line resonator (stripline resonator). In the design of a high-performance stripline oscillator, we must address three principal problems [6]:

- (1) minimization of resonator losses,
- (2) minimization of additive transistor noise, and
- (3) shock and vibration isolation of the resonator.

There are other problems which must be looked at, but these three represent the major contributors to degradation in stability.

Radiative loss is minimized by adopting a three-layer sandwich etch technique. In this design, two ground planes are used on the top and bottom surfaces of the P.C. board with the stripline centered in the dielectric. Fig. 4 shows a cross-section of the line. Fiberglass-teflon is used for the dielectric which has a small loss tangent of about 10^{-3} , thus keeping loss at a minimum. The stripline itself is a 7 cm length of copper which is 1 cm wide and 2 mm thick. Contact resistance is minimized by using silver-solder on all connections. The unloaded Q of the line resonator at .5 GHz is about 400. Loaded Q of the resonator is maximized by the use of a field-effect transistor as the active element [7]. It is chosen to have a high forward transconductance and a high cut-off frequency.

Additive transistor noise is due primarily to low frequency (near carrier) flicker noise behavior and high frequency (far from carrier)

white phase noise. Flicker behavior is difficult to characterize in many instances. Helpful in the reduction of flicker noise is a transistor which is manufactured with care and in a clean environment, since flicker noise may relate to sporadic conductance through the device due to impurities. White phase noise is usually associated with thermal noise due to operation of the device at room temperatures. One can then resort to devices capable of higher current densities in order to increase signal-to-noise. A tradeoff exists between white phase and flicker noise, however, since higher device currents usually aggravate the flicker noise problem. "sually, we arrive at a compromise solution which depends directly on the application of the oscillator. The curves shown in Fig. 1 represent a much higher device drive level than is common in, say, quartz crystal oscillators.

At frequencies around .5 GHz, transistor package parameters (inductance and capacitance) and stray parasitic elements such as connecting lead inductance and stray capacitance all contribute to the fundamental resonance. If one is to achieve a relative frequency stability approaching 1×10^{-9} , then it is imperative to maintain resonator inductance and capicatance values stable to this level. The greatest deterrent to maintaining high inductive and capacitive stability is vibration sensitivity of the oscillator. This problem of microphonics has been reduced by using the three-layer P.C board and rigidly mounting all components and leads with a low-loss doping compound. The oscillator is in turn rigidly fixed to an aluminum block which acts as the shield for the components. The test block weighs about 3 kg. Depending on the application, one can rigidly mount or soft mount the oscillator into a system. If rigidly mounted, structure-born vibration is directly applied to the oscillator. A soft mount designed to isolate the oscillator from vibration can reduce the transmitted vibration at higher frequencies at the cost of increasing the vibration sensitivity at a lower frequency. Damping material can also be used to alter the vibration response.

In the ammonia standard, the problem of vibration sensitivity of the fundamental oscillator is only significant in extreme cases of shock and vibration where the dynamic range of the servo system is exceeded or the period of the vibration is shorter than the servo attack time. The servo attack time can be smaller than .1 ms, since the NH3 resonance is wider than 10 kHz. Thus, the design of the oscillator mount should yield a vibration response in which frequencies of 10 kHz and above are suitably attenuated.

(c) Step recovery diode multiplier

It is desirable to make a multiplier module with fairly low output Q (Q $_{\rm Z}$ 10) and output power $_{\sim}$ 100 $\mu W. We have used state-of-the-art step-recovery diodes in a waveguide multiplier module. In simplest terms, the problem is one of impedance matching for both the input and output frequencies. For example, for the input circuit (<math display="inline">_{\sim}$.5 GHz) the

dynamic diode impedance is Z $_{\rm 2}$ l Ω . Therefore, two π section transformers were cascaded to match to the 50Ω output impedance of the .5 GHz amplifier. Approximately 0.5 to 0.75 W input power is needed to "snap" the diode properly. To accomplish this, a microstrip hybrid class "C" amplifier was used. The amplifier, microstrip matching circuit and multiplier module were integrated into one package in order to avoid instabilities due to connections. The output circuit is composed of a shorting stub and iris coupling to form a cavity Q $_{\rm 2}$ 10 with the diode matched to the characteristic impedance of the narrow height waveguide. In the interest of rigidity and simplicity, shims were used rather than movable plungers. With $_{\rm 0.6}$ W input power to the diode, output power as shown in Fig. 5 was obtained. This power is more than 5 times what is needed in the system.

(d) Ammonia gas cell

The ammonia gas cell is straightforward in principle but must be refined to compensate for those effects which influence frequency stability and accuracy. For initial experiments, relatively short cells (50 cm - 100 cm long) were constructed of K or X band waveguide. In order to study pressure related effects (i.e., broadening and shifts), a flow system was constructed as shown in Fig. 6. The waveguide cells are sealed using mica windows and indium seals.

(e) Pressure problems

It should be noted that standard X or K band cells with copper surfaces are not suitable for anal permanently sealed cells. This is because ammonia sticks to most surfaces (including copper). This accentuates the pressure shift because the gas density also increases with temperature. If there were no pressure shift, we would like to operate at a pressure as high as possible but not have the line be broadened by pressure. This occurs for p $_{-}$.4 N/m² (1 Torr $_{-}$ 133 N/m²). We have measured the shift, and it has been previously reported [9] that the fractional frequency shift due to pressure is:

$$\frac{v - v_0}{v_0} \approx 1.5 \times 10^{-7} \text{p}$$

where p is in N/m^2 . Therefore, if we operated at a pressure of .7 N/m^2 we incur an absolute frequency shift of 10^{-7} . In order to obtain 10^{-9} accuracy, we would need to know the pressure to 1 percent. For the long-term stability goal of 10^{-10} , we would have to hold the temperature of the gas to 0.3° C (assuming no sticking of ammonia to the walls).

Three approaches exist to overcome these basic pressure effects:

- (1) We must first ensure that sticking on the walls is kept to a minimum. To minimize this effect, a suitable "non-sticky" surface will be sought; for example, tests have begun using teflon- and paraffin-coated cell walls.
- (2) The temperature effect can also be reduced by operating at a lower pressure. This degrades signal-to-noise but can be compensated by increasing cell size. If we operate at a pressure of 1.3 x 10^{-2} Newton/m² (~ 10^{-4} Torr) and if ammonia "sticking" can be kept to a minimum, we would expect a basic temperature sensitivity of 6 x $10^{-11}/^{0}$ C. This is to be compared to the basic (uncompensated) temperature sensitivity of the rubidium atomic clock, which is about 1 x $10^{-10}/^{0}$ C.
- (3) Compensation schemes can be used whereby the pressure is sensed and compensation is made in the output frequency.

Since the projected cell size may be as large as 1000 cm³, we must employ schemes to make it convenient in a compact package. A straightforward way to make the cell larger is to make it longer. We can then form it into a spiral. Our preliminary experiments use glass tubes which are metal plated on the outside (forming circular cross-section waveguide) and are formed into spirals (~25 cm diameter) and mated to standard waveguide flanges.

Servo electronics and integrated system

Although the performance of the device is not high when compared to a state-of-the-art atomic clock, the demands on the servo system in the final system are rather high. This is because we are trying to resolve the rather broad resonance feature (i.e., "split the line") to about 10⁻⁵ or 0.001 percent. This is within an order of magnitude of the servo requirements on a laboratory cesium standard. This means we must be particularly careful about harmonic distortion in the FM modulation used and about D.C. offsets in the feedback integrators. The most important problems which we face are: (a) frequency pulling due to frequency dependence in the source output power and detected power (source-detector profile), (b) frequency pulling due to the resonant cavity seen by the ammonia (cavity pulling). (c) frequency pulling due to ammonia line distortion, and (d) frequency pulling due to offset voltages and distortions in the servo electronics (servo offsets). In Fig. 2, the basic scheme is illustrated. FM modulation (1-10 kHz) is used on the .5 GHz oscillator; the servo demodulates the detected microwave signal and forces the multiplied oscillator to line center.

(a) Source-detector-profile

The source power output and detector efficiency are, in general, frequency dependent; thus the observed transition rides on top

of a broad profile. Because this background may have a slope and curvature at the transition frequency, it may distort the line slightly and cause a frequency shift. Since this background profile may change in time (due, for example, to temperature change), it affects both long-term stability and accuracy. To solve this problem, we borrow a technique used in stabilized laser work [10]. We can demodulate the third harmonic of the FM rather than the fundamental. By doing this we can null the third derivative of the slope to a high degree rather than first. This is useful because it lowers the profile pulling by approximately the square of the ratio of the background curvature to the curvature of the resonance line. The effects of such a 3rd harmonic lock are shown in Fig. 1, where a definite improvement in stability is observed (until other effects dominate).

(b) Cavity pulling

This is a familiar problem in all atomic clocks to varying degrees and has been documented elsewhere [11]. Very simply, the ammonia and microwave cavity form a system of coupled oscillators. Therefore, varying the frequency of one (say the cavity) changes the observed frequency of the other (ammonia transition). We have

$$\vee$$
 (observed) - $\vee_0 = K \frac{Q_c}{Q_R} (\vee_C - \vee_0)$

where v_0 = unperturbed ammonia frequency,

 $Q_c = microwave cavity Q,$

 Q_{ℓ} = ammonia transition Q.

 v_c = cavity frequency, and

K = a parameter near 1 which depends on the FM harmonic observed and on the FM amplitude.

Ideally, the pulling effect could be eliminated by using a cell consisting of a piece of waveguide terminated by its characteristic impedance at all frequencies. However, the difficulty in designing such apparatus due to various parasitic effects present under practical conditions precludes the use of such a cell. The importance of this effect can be illustrated by example: if $Q_{\rm C} \simeq 50$, $Q_{\rm k} \simeq 2 \times 10^5$ we would have to tune the cavity to .02 percent of its linewidth to achieve 10^{-9} accuracy; temperature sensitivity would be $\sim 10^{-8}/^{\circ}{\rm C}$ for a copper cavity. Both of these problems are circumvented by servoing the center of the cavity to line center. This can be accomplished, knowing that K in the above expression is different, if we lock to the 3rd harmonic rather than the 5th harmonic (extension of the 3rd harmonic technique).

Therefore, as shown in Fig. 3, we use the 3rd harmonic to lock the oscillator to the apparent line center, then use the 5th harmonic to lock the cavity to the oscillator. This ensures that $(v_{\rm C} - v_{\rm O}) = 0$ in the above expression and therefore eliminates cavity pulling.

(c) Fundamental line distortion

The $\rm N^{14}H_3$ (3-3) transition is slightly asymmetric due to quadrupole hyperfine structure in the molecule [5]. Therefore, the apparent center frequency of the line depends on FM amplitude and microwave power; stability is correspondingly affected as these parameters change. We therefore use the (3-3) transition in $\rm N^{15}H_3$, which is free of these fundamental distortions and for which a well-defined center frequency exists. (Initial tests have also used the $\rm N^{14}H_3$ isotope.)

(d) Servo offsets

At the present time, 2nd harmonic FM distortion, voltage offsets and voltage offset drifts in the servo system along with the pressure shift problem seem to limit long-term stability. For example, an offset voltage can exist on the input of the first integrator in the third harmonic loop (see Fig. 3). With the system locked, a residual 3rd harmonic signal must be present to provide a D.C. level out of the mixer to compensate this offset. To reduce these offset problems, digital demodulators are being investigated.

ENVIRONMENTAL FACTORS

Sensitivity to environmental factors is most easily determined experimentally, and this will be straightforward once some of the obvious problems limiting long-term stability are solved. Nevertheless, theoretical estimates can be made of magnetic field and electric field sensitivity, and other remarks are appropriate for vibration and temperature sensitivity.

Magnetic fields

First-order Zeeman effects cause a splitting of the line on the order of 10 MHz per Tesla. This splitting is symmetric and therefore causes only (usually negligible) broadening except that some asymmetry may be present due to slight differences of the Zeeman effect (uncoupling of the spins) in the two inversion levels. This asymmetry may be of the order of 1 Hz at 10^{-4} Tesla. Measurements need to be made to quantitatively assess this effect. The worst anticipated outcome is the need for one simple magnetic shield for some applications in very high fields. The second-order Zeeman effect is, of course, exceedingly small: the relative shift is about 2 x 10^{-7} H² (H in Tesla) and thus is negligible).

Electric fields

Electric fields are only of importance in the construction details of the gas cell where thermo-electric and contact potential problems may be present. A worst estimate can be based on the most sensitive hyperfine component of the (3-3) line; for this we have a relative shift of about 10^{-9} E² (E in V/cm). Since electric fields surely can be limited to less than 0.1 V/cm, we do not anticipate any problems.

Temperature sensitivity

This has already been discussed above. For best performance it may be necessary to provide some minimal temperature compensation (i.e., a frequency compensation based on the temperature). At least a factor of ten improvement could be expected here; this would then reduce the overall temperature sensitivity by a factor of ten.

Vibration sensitivity

It is difficult to predict a priori what the limits to vibration sensitivity will be, since in many cases they vary with mechanical construction imperfections which are most easily eliminated directly. However, some general comments could be made in this regard. To a high degree the ammonia cell and servo electronics should be vibration insensitive. We can expect then that the vibration sensitivity of the 500 MHz primary oscillator should be reduced by the open loop gain of the feedback servo. Therefore, if the attack time of the servo is τ = 0.1 ms, then the vibration sensitivity of the locked oscillator at say 100 Hz should be reduced by a factor of approximately 10^4 over the free-running oscillator.

OVERALL PHYSICAL PARAMETERS

Power requirements

The basic electric components of the present standard configuration are shown in Fig. 2. At the present time, power requirements for specific portions are:

(1)	.5 GHz oscillator, .5 GHz amplifier with multiplier	5.5 W
(2)	divider chain (÷ 100)	1.0 W

(3) detector amplifier and servo $\frac{1.0 \text{ W}}{7.5 \text{ W}}$

The .5 GHz power amplifier is the major drain on the power supply. The multiplier step-recovery diode needs about 1 W input, and the efficiency of our present amplifier is about 20 percent. In an actual system we could expect total power requirements to be approximately half of their present value, or ~ 3 W.

Size requirements

The lower limit on size will primarily be limited by the size of the ammonia cell. It is expected that the cell should occupy no more than 1 liter volume; hence, the overall package may be from 1-2 liters in volume.

Weight requirement

With proper choice of materials the expected final package weight should be less than 3 Kg. For operation in extreme magnetic fields, shielding may have to be included; this will increase weight by approximately 1/2 Kg.

ACKNOWLEDGMENTS

The authors are indebted to Michael B. Mohler for development of the step recovery multiplier and other electronics and to Howard E. Bell for construction of the vacuum and cell components.

REFERENCES

- [1] For characterization of frequency stability see, for example: ALLAN, D. W., "Statistics of Atomic Frequency Standards," PROC. IEEE, <u>54</u>, February 1966, pp. 221-230.
- [2] LYONS, H., Annals New York Acad. Sci., <u>55</u>, 831 (1952).
- [3] SHIMODA, K., "Atomic Clocks and Frequency Standard on Ammonia Line I" and "III," J. Phys. Soc. Japan $\underline{9}$, June 1954, pp. 375-386 and pp. 567-575.
- [4] HELLWIG, H., "A Review of Precision Oscillators, "National Bureau of Standards Technical Note 662, February 1975.
- [5] TOWNES, C. H., SCHAWLOW, A. L., Microwave Spectroscopy, McGraw-Hill Book Co., New York, 1955.
- [6] HODOWANEC, G., "Microwave Transistor Oscillators, "RCA Application Note AN 6291.
- [7] OXNER, E., "High-Performance FETs in Low Noise Oscillators," Siliconix Incorporated, December 1973.
- [8] See, for example: "Ku-band Step Recovery Multipliers," Hewlett- ackard Application Note 928. Also: "Harmonic Generation Using Step Recovery Diodes and SRD Modules," Hewlett-Packard Applications Note 928, 620 Page Mill Road, Palo Alto, CA.
- [9] SHIMODA, K., "Ammonia Masers," IRE Trans. Instr. and Meas., IM-11. December 1962, pp. 195-200.
- [10] WALLARD, A. D., J. Phys. E., 5, 927 (1972).
- [11] See, for example: VIENNET, J., AUDOIN, C., and DESAINTFUSCIEN, M., "Discussion of Cavity Pulling in Passive Frequency Standards," Proc. 25th Annual Symposium on Frequency Control, U. S. Army Electronics Command, Ft. Monmouth, NJ, April 1971, pp. 337-342.

LIST OF FIGURES

- 1. Frequency stability plots showing the two sample variance (σ_y) for different averaging times (τ). B.W. \equiv measurement system bandwidth.
- 2. Simplified block diagram of system. Frequency lock servo is used employing 1-10 kHz FM on $\sim\!.5$ GHz oscillator.
- 3. Detailed block diagram of system. Multiplier tuned for $\rm N^{14}\ H_3$ isotope.
- 4. Cross-section of stripline resonator.
- 5. Plot of multiplier output power.
- 6. Vacuum pumping station.

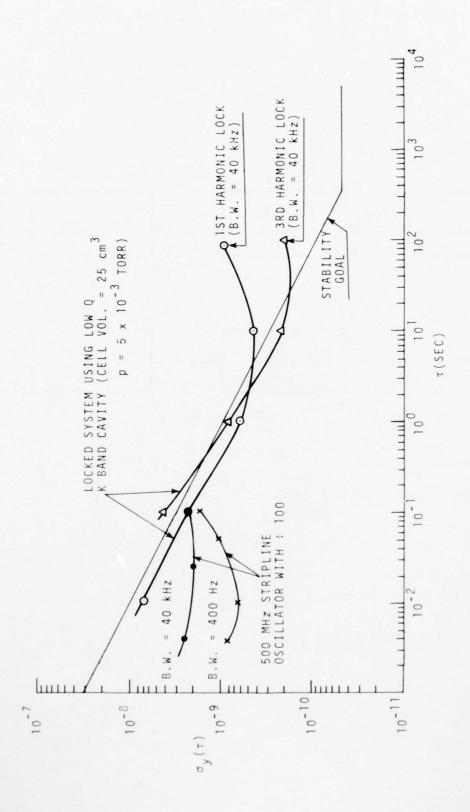


Fig. 1

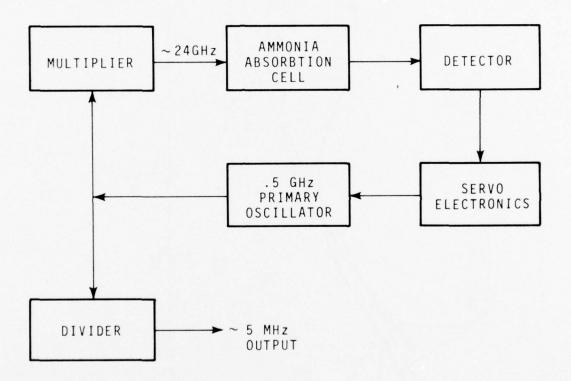


Fig. 2

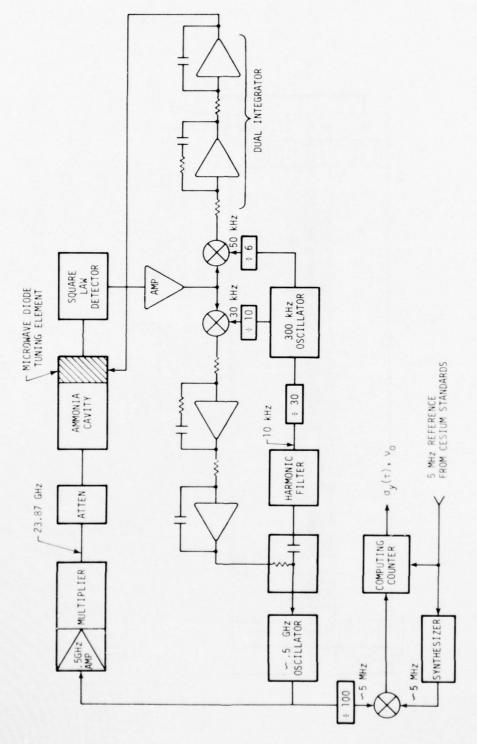
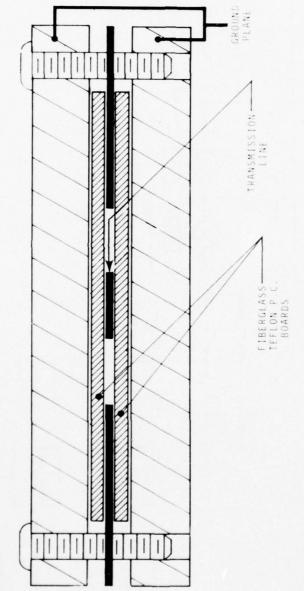
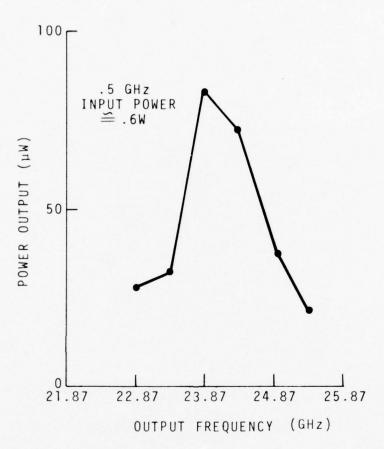


Fig. 3





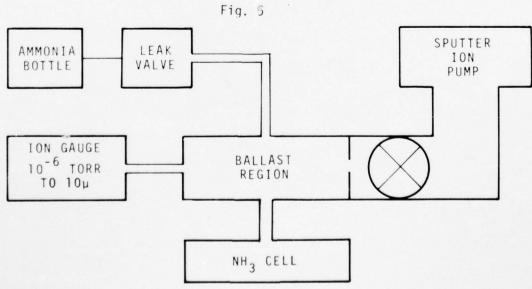


Fig. 6

CALCULATION OF OMEGA PROPAGATION GROUP DELAY AND APPLICATION TO LOCAL TIME STANDARD MONITORING

R. Grover Brown, R. L. Van Allen, USAF, and Kim Strohbehn
Electrical Engineering Department
and
Engineering Research Institute
Iowa State University
Ames, Iowa 50011

ABSTRACT

The OMEGA navigation system now has seven transmitting sites strategically located throughout the world. All transmissions are derived from cesium-beam standards, and each station transmits time-multiplexed coherent bursts at 10.2, 11 1/3, and 13.6 kHz. Thus, an observer at some distant location has an opportunity to track the phase of three coherent precision transmissions rather than just a single frequency as is usually the case (e.g., WWVB, Ft. Collins). It is shown that by using the phase information received on all three frequencies, the observer can compute a synthetic group delay referred to any arbitrary frequency in the 10-14 kHz range. By coincidence, it works out that the group velocity (and thus group delay) at 12.5 kHz is about the same for nominal day and nighttime conditions. Thus, the group delay at this frequency has a natural insensitivity to diurnal variations. This invariance to diurnal shifts is demonstrated with actual OMEGA data.

In a monitoring application, it is suggested that there might be an advantage in compensating for propagation lag with group delay rather than the usual predicted phase delay. Most of the low-frequency diurnal error is eliminated in the synthetically-formed group delay, leaving only relatively high-frequency components to be filtered in the residual error. This, of course, simplifies the filtering problem. It is shown that complementary filter theory can be applied to advantage in this application.

INTRODUCTION

The OMEGA navigation system now has seven transmitting sites strategically located throughout the world. When the eighth station (Australia) commences operation, the system will be fully operational with world-wide coverage [1]. In addition to its primary purpose as a

navigation system, it also provides the world with a common precision time/frequency reference system. All transmissions are derived from cesium-beam standards, and each station transmits time-multiplexed coherent bursts at 10.2, 11-1/3, and 13.6 kHz. This makes OMEGA unique as a time reference system, because the observer at a remote location has an opportunity to track three coherent transmissions within a narrow frequency range, rather than the usual single frequency (e.g., WWVB, Ft. Collins). The availability of phase information on multiple frequences enables the observer to compensate for propagation variations on-line, if he so chooses. For example, the well-known diurnal shift is due to a change in the effective height of the ionosphere from day to night. The same mechanism that causes the velocity of propagation to change also causes different phase shifts at different frequencies. So, one can reverse the reasoning and infer something about the change of velocity of propagation from the measured phase shifts on two or more frequencies.

A number of on-line OMEGA compensation schemes have been proposed, but it is not clear as yet which is to be preferred [2]. On-line compensation (in contrast to prediction) is especially attractive in the navigation application because it has the potential of mitigating unusual situations, such as sudden ionospheric disturbances (SID), as well as the usual diurnal shift. It is suggested here that some of these compensation ideas might be applied to advantage in the precise time/frequency application.

Before proceeding, a simple example should help put the precise timing problem in perspective. Obviously, the observer at a remote location would like to have the equivalent of an expensive cesium-beam standard in the form of a simple radio receiver. Unfortunately, though, the propagation delay is somewhat "rubbery" and relatively large errors can occur over short time periods. To illustrate this, consider tracking a 10 kHz single-frequency source. For long paths, a total phase shift from day to night of one full cycle would not be unusual; and, if this took place over a span of two hours, the apparent frequency error during this period would be about one part in 10^8 -- a totally monsterous error when dealing with precision systems. Obviously, if one leaves the diurnal shift uncorrected, very long averaging times are needed for precise work. The culprit, of course, is the "rubberiness" of the propagation medium. Would it not be nice to be able to "stiffen" the medium someway? The remainder of this paper will be directed toward online (in contrast to predictive) methods of accomplishing this.

VLF Wave Propagation

Wave propagation in the VLF range is usually explained in terms of waveguide theory, with the earth's surface and the ionosphere forming the waveguide boundaries. For simple waveguide modes, the phase and group velocities vary with frequency as shown in Fig. 1 [3]. In the

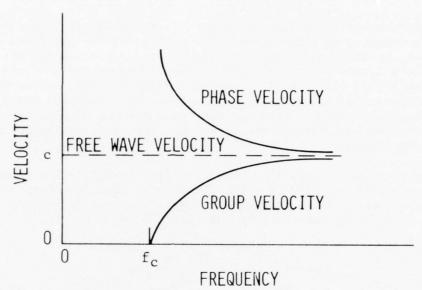


Fig. 1. Phase and group velocities for parallel-plane waveguide.

NIGHT

DAY

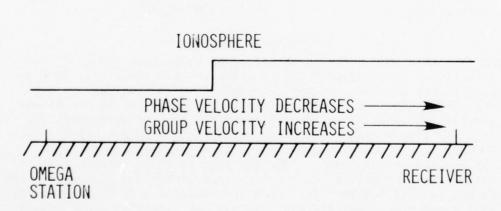


Fig. 2. Flat earth model.

OMEGA case, the waveguide height dimension is considerably greater than the wavelength, so the lowest order mode is considerably above the cutoff frequency, $f_{\rm C}$. Thus, the phase velocity is only slightly greater, and the group velocity slightly less, than the free wave velocity. The change in ionospheric height that occur from day to night (typically, from 70 to 90 km) do, however, cause a shift in cutoff frequency that results in changes in the phase and group velocities of the order of a few tenths of a percent. The sketch of Fig. 2 shows a simplified "flatearth" model illustrating the transition from day to night. It should

be apparent that if the phase and group velocities change by equal amounts in opposite directions, then the average of the group and phase delays would be invariant from day to night. Compensation for the transit time from transmitter to receiver with a blend of phase of group delays should then eliminate the diurnal variation. This method of on-line compensation was first suggested by J. A. Pierce [4] and is now known as composite OMEGA. Without going into all the details here, two phase measurements on nearby frequencies are needed to accomplish the desired compensation.

A number of variations on Pierce's original compensation scheme have been proposed recently [5,6,9]. These have been necessary because the original idea of an equal blend of phase and group delays did not take into account the curvature of the earth as shown in Fig. 3. It can

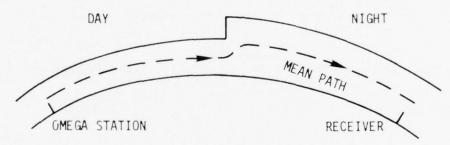


Fig. 3. Curved earth model.

be seen that even though the phase and group velocities change in opposite directions, the average delay is still not invariant because the mean path length increases as the ionospheric height increases. This suggests giving group delay more weight than phase delay in the blending, and this is borne out by recent investigations by Mactaggart [6]. Carrying this line of reasoning a bit further, there might exist a condition where the increase in path length in going from day to night would be exactly proportional to the increase in group velocity. This is confirmed by theoretical curves of group velocity vs. frequency given by both Hampton [7] and Watt [8] which are reproduced in Figs. 4 and 5. Note that these plots indicate that the day and nighttime group velocities should be the same for a frequency somewhere in the 12.5 to 13.0 kHz range. This crossover phenomenon is unique with group velocity (in contrast to phase velocity) and only occurs at one frequency. Quite by coincidence, this crossover frequency occurs within the spectral range of the OMEGA system. This has obvious implications in terms of eliminating the diurnal shift. In principle, all one need do is observe the envelope of a modulated wave at say 12.5 kHz and its transit delay should be relatively invariant from day to night. This is easier said than done, though.

There is very little direct experimental evidence supporting the theoretical curves shown in Figs. 4 and 5. No doubt this is due to the difficulty in making precise envelope time-of-arrival measurements in

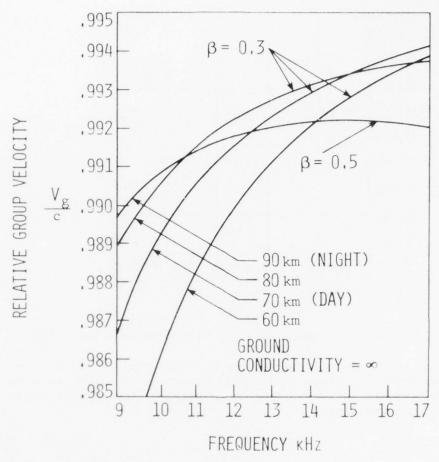


Fig. 4. Variation of group velocity with frequency (Hampton [7]).

the VLF range. However, by making simultaneous phase measurements on three or more coherent transmissions on nearby frequencies, one can infer indirectly the group delay referred to any desired frequency. The procedure for doing this will now be illustrated for the three-frequency case. The extension to more than three frequencies is obvious.

Computation of Group Delay from Phase Delays

As a matter of review, the phase velocity of a traveling wave is the speed at which the fine structure (individual cycles) appears to move. It is given by the equation

$$v_p = \frac{\omega}{\beta}$$
 (1)

NATIONAL AERONAUTICS AND SPACE ADMINISTRATION GREENB--ETC F/G 14/2 PROCEEDINGS OF THE ANNUAL PRECISE TIME AND TIME INTERVAL (PTTI)--ETC(U) AD-A043 856 1977 UNCLASSIFIED NASA-6SFC-X-814-77-149 NL 6 OF 8 AD43856

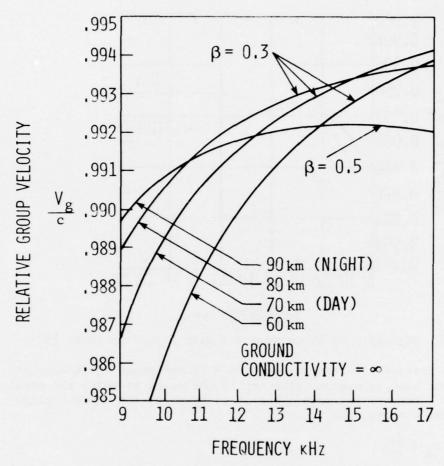


Fig. 4. Variation of group velocity with frequency (Hampton [7]).

the VLF range. However, by making simultaneous phase measurements on three or more coherent transmissions on nearby frequencies, one can infer indirectly the group delay referred to any desired frequency. The procedure for doing this will now be illustrated for the three-frequency case. The extension to more than three frequencies is obvious.

Computation of Group Delay from Phase Delays

As a matter of review, the phase velocity of a traveling wave is the speed at which the fine structure (individual cycles) appears to move. It is given by the equation

$$v_{p} = \frac{\omega}{\beta} \tag{1}$$

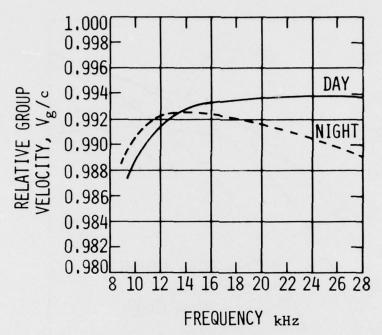


Fig. 5. Variation of group velocity with frequency (Watt [8]).

where ω is frequency in radians/sec and β is the phase shift constant. On the other hand, the group velocity is the speed at which the envelope (modulation) appears to travel, and it is given by the inverse slope of the β versus ω curve, i.e.,

$$v_{g} = \frac{d\omega}{d\beta} \tag{2}$$

Now assume we have three phase delay measurements, T_1 , T_2 , T_3 , corresponding to the three OMEGA frequencies, ω_1 , ω_2 , ω_3 . Each of these time delays represents a ratio of total phase shift to frequency, i.e.,

$$T_1 = \frac{\phi_1}{\omega_1} = \frac{\beta_1^d}{\omega_1} = \frac{d}{\omega_1/\beta_1} = \frac{d}{v_{p_1}}$$
 (3)

$$T_2 = \frac{\phi_2}{\omega_2} = \text{etc.} \tag{4}$$

$$T_3 = \frac{\phi_3}{\omega_3} = \text{etc.} \tag{5}$$

where d is the distance from transmitter to receiver. It is tacitly assumed from here on that lane ambiguities (whole number of wavelengths)

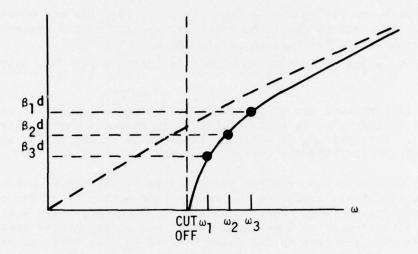


Fig. 6. Phase shift versus frequency.

for all three frequencies have been resolved. In effect, the three phase measurements give us three points on the βd vs. ω curve as shown in Fig. 6. Now assume that βd can be approximated as a quadratic function of ω over a reasonable range of ω ; i.e., let

$$\beta d = C_2 \omega^2 + C_1 \omega + C_0 \tag{6}$$

Next, we will choose the coefficients C_0 , C_1 and C_2 such that βd goes through the measured ϕ_1 , ϕ_2 , ϕ_3 points as shown in Fig. 6. Thus, the coefficients are determined by

$$c_0 + c_1 \omega_1 + c_2 \omega_1^2 = \phi_1 \tag{7}$$

$$c_0 + c_1 \omega_2 + c_2 \omega_2^2 = \phi_2 \tag{8}$$

$$c_0 + c_1 \omega_3 + c_2 \omega_3^2 = \phi_3 \tag{9}$$

Omitting the algebra, it is obvious that Eqs. (7), (8), and (9) can be solved explicitly for C_0 , C_1 , and C_2 in terms of the measurements ϕ_1 , ϕ_2 , and ϕ_3 .

Returning now to Eq. (6), the group delay can be found as

$$T_{g} = \frac{d}{v_{g}} = \frac{d}{\left(\frac{d\omega}{d\beta}\right)} = \frac{d(\beta d)}{d\omega} = 2C_{2}\omega + C_{1}.$$
 (10)

If the solutions for C_1 and C_2 from Eqs. (7), (8), (9) are substituted into Eq. (10), and if the frequencies ω_1 , ω_2 , and ω_3 are assumed to be in the exact ratio 9:10:12, the following equation results

$$T_g = \left(60 \frac{\omega}{\omega_2} - 66\right) T_1 + \left(-100 \frac{\omega}{\omega_2} + 105\right) T_2 + \left(40 \frac{\omega}{\omega_2} - 38\right) T_3$$
 (11)

Equation (11) enables one to compute a group time delay, referred to any arbitrary frequency ω , in terms of the three measured phase delays, T_1 , T_2 and T_3 . Note that T_g in a <u>linear</u> function of T_1 , T_2 and T_3 and that the sum of the coefficients (weight factors) is unity.

Also note that the measured phase delays T_1 , T_2 and T_3 are simply the measured phases, including the appropriate multiples of 2π , divided by the frequencies (i.e., Eqs. 3, 4, and 5). However, phase must be measured with respect to some local reference, so an unknown constant will appear in each term on the right side of Eq. 11. The sum of the coefficients is unity, so this same additive constant will appear with T_g . This additive term will be assumed to be constant for the moment, but, in any event, it certainly is not dependent on the propagation medium.

Returning now to Eq. (11), it is of special interest to look at variations in the coefficients of T1, T2, and T3 with frequency. These three coefficients will be designated as K_1 , K_2 , and K_3 (i.e., T_g = $K_1T_1 + K_2T_2 + K_3T_3$), and they are plotted in Fig. 7. Note that in the 12.0 - 12.5 kHz range none of the coefficients exceeds 6. Purely random errors in the phase delay measurements do, of course, get "amplified" by the coefficients, so large values are undesirable. How undesirable, though, is a matter of degree, but certainly factors of 4 or 5 are not unreasonable. Pursuing this further, if one assumes the three measurement errors associated with T1, T2, and T3 to be independent and each having unity variance, the resultant rms error in T_g would be as shown in Fig. 8. It should be apparent that the best choice of reference frequency involves a compromise between the induced measurement noise error shown in Fig. 8 and the diurnal-shift error. This will not be pursued further from a theoretical viewpoint. Instead, we will proceed directly to some experimental results that demonstrate these concepts.

Experimental Examples

A formula for computing a synthetic group delay at any desired frequency in the OMEGA range was derived in the previous section. This, along with experimental phase measurement data on 10.2, 11-1/3, and 13.6 kHz, should provide a means of verifying the theoretical curves of Hampton [7] and Watt [8], reproduced in Figs. 4 and 5. These curves were worked out for a single mode with idealized boundary conditions, so we should not expect exact correspondence. Qualitatively, though, we would expect to find the group delay to be greater during the day than at

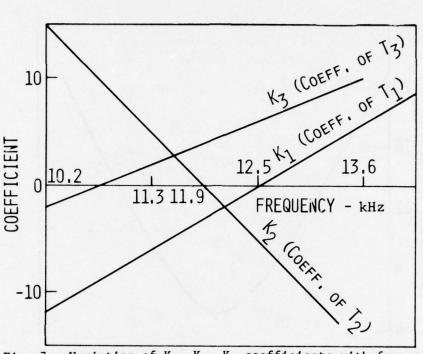


Fig. 7. Variation of K₁, K₂, K₃ coefficients with frequency.

$$(T_g = K_1 T_1 + K_2 T_2 = K_3 T_3).$$

night for frequencies less than the crossover, and then the day and night delays should approach each other as the frequency is increased to the crossover frequency around $12.5\ kHz$.

A limited amount of experimental data was obtained from the U. S. Coast Guard OMEGA Navigation System Operations Detail (ONSOD), which gathers phase measurement data from various monitoring sites located around the world. Phase difference measurements were in the form of strip-chart recordings and covered the time period from March 10 through March 31, 1975. Two transmission paths, Trinidad to North Dakota and North Dakota to Hawaii were selected as examples for presentation he e. In both cases, the monitoring sites were close to the local transmitters, so the recorded phases can be considered as "one-way" phase measurements. Phase data at all three OMEGA frequencies were read from the charts at a rate of one sample per hour, and then these data were used to compute group time delays at various reference frequencies in accordance with Eq. 11.

Results for the Trinidad to North Dakota path (B-D) are shown in Fig. 9. Twenty-two days of data are shown superimposed in each of the four parts of the figure. In order to establish a perspective, the uncompensated phase delay at 10.2 kHz is shown in the upper-left corner.

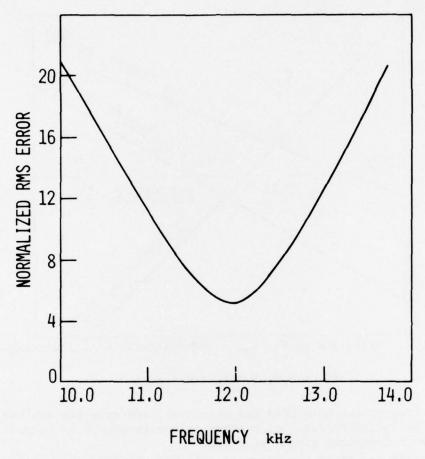


Fig. 8. Normalized RMS error due to measurement noise.

As expected, the diurnal shift is quite large, roughly about 75 microseconds or about 3/4 cycle at 10.2 kHz. The other three parts of Fig. 9 show the group delays computed at 11.5, 12.0 and 12.5 kHz. Note that the average day and night delays do tend to equalize as the reference frequency is increased to 12.5 kHz. The random fluctuations also increase dramatically as the reference frequency is increased, especially at night. It is tempting to explain this as being due to phase measurement errors being amplified by the K_1 , K_2 , and K_3 coefficients, which do increase somewhat in going from 12.0 to 12.5 kHz. However, the daytime portion of the curves does not show a similar increase in randomness with an increase in reference frequency. Thus, a more reasonable explanation would seem to be the basic instability at night due to modal interference.

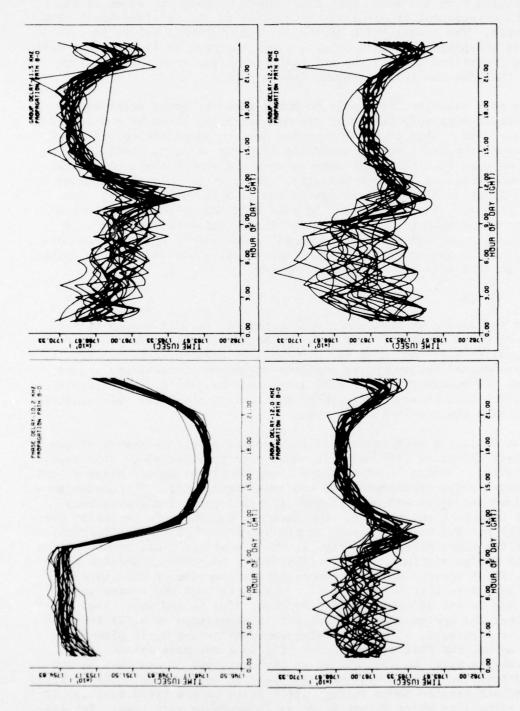


Fig. 9. Phase and group delays for Trinidad-North Dakota path for 10-31 March 1975.

Results from the North Dakota-Hawaii (D-C) path are shown in Fig. 10. The arrangement of the plots is similar to the Trinidad-North Dakota example. The equalization of the day and nighttime delays is not quite as conspicuous in this case, because the path is largely east-west and the transition between day and night is spread over a longer time period than for the Trinidad-North Dakota path.

In both examples, it should be noted that the group delay variations are considerably less than diurnal variation shown by the raw 10.2 kHz phase data. This is to be expected because Hampton's curves (Fig. 4) indicate the day-to-night variation in group velocity should only be about one part in a thousand, whereas we would expect about three times this much variation in phase velocity. Thus, group delay has a natural insensitivity to diurnal variation in the 11.5 to 13 kHz range. For timing purposes, it is important to note that the large 24-hour component error has been virtually eliminated at a reference frequency of 12.5 kHz, leaving only relatively rapidly fluctuating noise. Presumably, this should be easier to filter than the relatively low-frequency 24-hour error, so this will now be pursued further.

Filter Example

In the timing problem under consideration, we will assume that we have a received CW signal from a remote source (OMEGA) and a corresponding signal from a local source. Both will be assumed to be referred to the same nominal frequency via whatever frequency synthesizers and/or dividers are necessary. The local source may be just a simple crystal oscillator, but, in any event, there must exist some local reference to compare with the received OMEGA signal.

The filtering problem here falls into the general category of complementary filtering [10], so a few words are in order about this type of filtering. Figure 11 shows three forms of filtering operating on two independent noisy measurements of the same signal s(t). The contaminating noises are $n_1(t)$ and $n_2(t)$. Note that all three implementations lead to identical end results. The designer's problem is to choose the best Y(s) for the noises present in his particular physical situation. Each of the block diagrams in Fig. 11 lends a slightly different insight into the design problem. The straightforward two-channel version shown in Fig. 11(a) clearly shows the complementary feature of this type of filtering. Note that the signal s(t) passes through the system undistorted and is not affected by the choice of Y(s) in any way. Fig. 11(b) shows that the design problem reduces to a separation of n1(t) from n2(t). For example, if n1 is low-frequency noise and n2 is high-frequency noise, the obvious choice for Y(s) is a low-pass filter. This will preserve $n_1(t)$ to some degree of accuracy, and it can then be subtracted from the first measurement to yield an improved estimate of s(t). The feedback version shown in Fig. 11(c) is to be preferred over (a) or (b) in situations where either n_1 or n_2 is unstable with time. The lin-

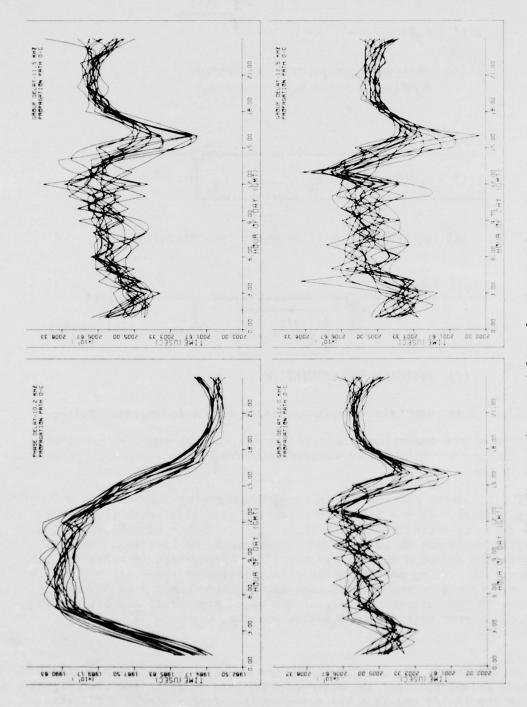


Fig. 10. Phase and group delays for North Dakota-Hawaii path for 10-31 March 1975.

$$s(t) + n_1(t) \longrightarrow 1 - Y(S) + \hat{s}(t)$$

$$s(t) + n_2(t) \longrightarrow Y(S)$$

(A) COMPLEMENTARY FILTER. IN COMPLEX DOMAIN: $\hat{S} = S + N_1(1 - Y) + N_2Y$

$$\frac{s(t) + n_1(t)}{s(t) + n_2(t) + n_1 - n_2} \xrightarrow{\hat{s}(t)} \hat{s}(t)$$

(B) DIFFERENCING - FEEDFORWARD IMPLEMENTATION.

(C) FEEDBACK IMPLEMENTATION.

Fig. 11. Three equivalent implementations of a complementary filter.

ear range of the operations indicated in (a) and (b) might be exceeded in this case, but this can be avoided with the feedback implementation shown in (c).

The linearity restriction just mentioned really only applies in analog systems. If the filter is operating on digital data (i.e., numbers) there is virtually no such restriction. Either continuous analog or digital data may be encountered in the timing application. Obviously, with the aid of a digital processor and appropriate interfacing, all sorts of interesting possibilities exist, including computation of group delay referenced to any desired frequency in accordance with Eq. 11. However, in the interest of keeping the discussion brief and simple, we shall be content with a simple analog example.

To illustrate the benefit of the group-delay approach (in contrast to phase delay) consider the observed OMEGA signal to be the beat signal between the 11-1/3 and 13.6 kHz transmissions from a single OMEGA sta-

tion. We will assume that the electronic circuitry is such that it produces an analog CW signal at the difference frequency of 2-4/15 kHz. This can also be thought of as the envelope of a single modulated wave whose carrier is midway between 11-1/3 and 13.6 kHz, or 12.46---kHz. The envelope travels at group velocity, so the phase of the envelope is delayed by the group delay, in this case referenced to about 12.46 kHz. Note, by coincidence, this is very near the day-night crossover. Thus, the phase-delay characteristics of the beat signal between 11-1/3 and

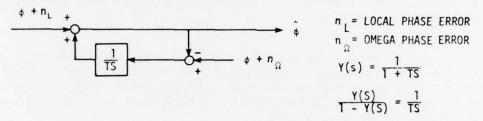


Fig. 12. First-order filter example.

13.6 kHz should be close to those shown in Figs. 9 and 10 for the 12.5 kHz reference frequency. That is, the major part of the diurnal variation should be eliminated, leaving only the more rapidly varying phase error. The beat signal at 2-4/15 kHz can now be compared directly with the phase of the local source suitably divided down to the same frequency. Thus, in this example, there is no need to "compute" a synthetic group delay, because a sinusoidal wave with essentially no diurnal shift can be obtained directly in analog form.

The filter block diagram for this example is shown in the "feedback" configuration in Fig. 12. In this case we might expect the residual propagation error associated with the OMEGA source to be relatively high frequency noise. On the other hand, one would expect unstable, low-frequency drift error in the local reference. The spectral characteristics of these two error sources are quite different, so we can expect the complementary filter to do a respectable job of separating the two. A low-pass filter is the obvious choice for Y(s). For purposes of illustration let Y(s) be of the form

$$Y(s) = \frac{1}{1 + TS}$$

where T is the time constant of the filter. This is the simplest possible low-pass filter. Some commercial systems are capable of operating with a time constant of about one day, so we will choose this as the time constant T in this example. We shall then compare the complementary filter outputs with raw 10.2 kHz OMEGA as the reference on one hand, and with the 2-4/15 kHz beat signal as the OMEGA reference on the other. Five days of actual B-D OMEGA data for 3-7 March 1975 with a

sampling rate of one sample per 10 minutes was used as the remote reference in the simulation. The local reference for this example was assumed to be a relatively high quality source with a drift rate of 1 part in 10^{10} .

The results for the 5-day simulation are shown in Fig. 13. The first two or three days may be ignored as the transient period, but note as the system approaches steady-state, the simulation with the beat signal as reference has considerably smaller fluctuations than the raw 10.2 kHz phase-reference system.

There was no attempt to optimize the filter in this example. Rather, the filter form and time constant were chosen to conform with current state-of-the-art phase-tracking time/frequency systems. Application of optimal filtering techniques should provide even further reduction of the residual error.

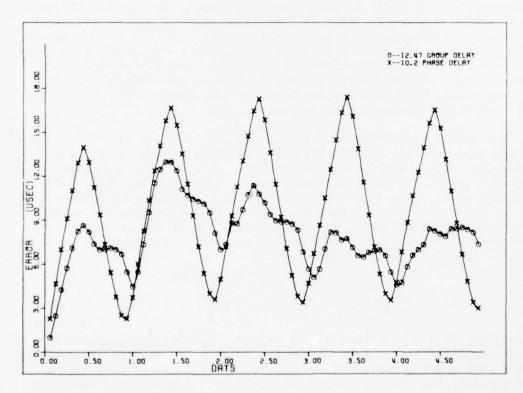


Fig. 13. Comparison of errors for phase- and group-reference systems.

Summary

It has been demonstrated that group delay in the 12.0 to 12.5 kHz range exhibits much less diurnal variation than the corresponding phase delay. Thus, if the local reference is coupled to the remote reference via group delay rather than phase delay, then the local filtering problem is less severe. Also, the resulting filtering problem was shown to fit within the framework of complementary filter theory. Once this is recognized, a considerable body of both optimization theory and experience can be brought to bear on the problem. Thus, the OMEGA system with its three coherent transmissions shows considerable promise as the long-term reference in a precise time/frequency system.

Acknowledgements

The authors are particularly indebted to the U. S. Coast Guard OMEGA Navigation System Operations Detail (ONSOD) for furnishing the strip chart data used in this analysis. We also acknowledge the Iowa State University Engineering Research Institute for financial support of the project.

Reference

- 1. J. E. Bortz, R. R. Gupta, D. C. Scull, and P. B. Morris, "Omega Signal Coverage Prediction," J. of the Inst. of Navigation, Vol. 23, No. 1, Spring 1976, pp. 1-9.
- 2. A. N. Beavers, Jr., D. E. Gentry, and J. F. Kasper, Jr., "Evaluation of Real-Time Algorithms for OMEGA Propagation Prediction," J. of the Inst. of Navigation, Vol. 22, No. 3, Fall 1975, pp. 252-258.
- 3. R. G. Brown, R. A. Sharpe, W. L. Hughes, and R. E. Post, <u>Lines</u>, Waves, and Antennas, 2nd Ed., Ronald Press, 1973.
- 4. J. A. Pierce, "The Use of Composite Signals at Very Low Radio Frequencies," Harvard University Technical Report 552, February 1968.
- W. Papousek and F. H. Reder, "A Modified Composite Wave Technique for OMEGA," J. of the Inst. of Navigation, Vol. 20, No. 2, pp. 171-177.
- 6. D. Mactaggart, "An Empirical Computed Evaluation of Composite OMEGA," Proc. of the Second OMEGA Symposium (Sponsored by the Inst. of Navigation), November 1974, pp. 131-138.
- D. E. Hampton, "Group Velocity Variations of V.L.F. Signals," Royal Aircraft Establishment Report No. 65282, December 1965.

- 8. A. D. Watt, VLF Radio Engineering, Pergamon Press, 1967, p. 383.
- R. G. Brown and K. L. Van Allen, "Three Frequency Difference OMEGA," Proc. of the National Aerospace Symposium (Sponsored by the Inst. of Navigation), April 1976, pp. 117-124.
- 10. R. G. Brown and J. W. Nilsson, <u>Introduction to Linear Systems Analysis</u>, John Wiley and Sons, N. Y., 1962, Chapter 15.

OMEGA SYNCHRONIZATION: CURRENT OPERATIONS AND FUTURE PLANS

Howard J. Santamore U.S. Coast Guard, Washington, D.C.

Roger N. Schane, Stephen F. Donnelly, The Analytic Sciences Corporation, Reading, Massachusetts

ABSTRACT

Modern estimation techniques are applied to the problem of synchronizing OMEGA VLF signal transmissions from geographically-remote transmitter stations. Each OMEGA transmitter is controlled by its own bank of four cesium beam atomic frequency standards. A synchronization computer program SYNC2* combines models of cesium clock error dynamics with OMEGA phase timing measurements to estimate and control inter-transmitter synchronization offsets (both phase and phase rate) to an accuracy on the order of 1 µsec rms.

Auxiliary algorithms perform OMEGA phase measurement preprocessing, including: compensation for propagation anomalies, reciprocal path phase differencing, automatic outlier rejection, dynamic measurement-quality weighting, and time-correlation modeling. Alternative timing measurements (including: satellite/TV, Loran-C, and portable clock) are utilized, as available, to synchronize the entire transmitter system to Coordinated Universal Time (UTC) as maintained by the United States Naval Observatory (USNO).

Future plans for OMEGA synchronization include: increased use of non-VLF propagation models, and active participation by the Japanese Maritime Safety Agency (JMSA) in Program SYNC2 operation.

^{*}This program was developed at The Analytic Sciences Corporation (TASC) for the U.S. Coast Guard OMEGA Navigation System Operations Detail (ONSOD) under Contract No. DOT-CG-23735-A.

INTRODUCTION

OMEGA is a long-range, all-weather, radio navigation system consisting of eight transmitter stations, strategically located around the world. Each transmitter generates continuous-wave, phase-locked, very-low-frequency (VLF) signals between 10.2 and 13.6 kHz. OMEGA provides a unique combination of worldwide navigation capability and bounded position errors, typically on the order of 1 to 2 nm rms.

VLF signals propagate in a natural waveguide between the earth's surface and the ionosphere, and maintain a nearly linear relationship between signal phase and distance from each transmitter. Phase difference measurements from pairs of transmitters define earth-referenced hyperbolic lines-of-position (LOPs) which are used for position determination. Certain geophysical factors (e.g., variations in solar illumination, geomagnetic field, and ground conductivity) tend to distort this linear phase/distance relationship and, thus, limit position accuracy. Models have been developed [1] to partially compensate for VLF phase propagation variations, and tables of Predicted Propagation Corrections (PPCs) have been computed [2] and published [3].

Use of phase differences for OMEGA navigation requires precise phase synchronization of signals from all OMEGA transmitters. (A six microsecond synchronization offset between two transmitters can result in a 1 nm position error.) phase of each OMEGA transmitter is controlled by its own online cesium clock (and several backup clocks). A cesium clock determines precise time intervals by counting oscillation periods of a cesium-beam atomic frequency standard. For two clocks to be perfectly synchronized, their frequency standards must match perfectly in both phase and frequency. In general, there are small uncontrollable differences (on the order of 0.03 to 0.3 µsec/day) in the cesium frequencies of different online clocks. These relative frequency offsets result in inter-transmitter phase (or timing) offsets that can increase with time, if uncorrected.

To prevent uncontrolled time offset growth in the OMEGA system, internal synchronization is accomplished by periodically adjusting the epoch (i.e., time or phase) of each OMEGA transmitter to the average epoch of all transmitters (Mean OMEGA System Time). External synchronization, which is not necessary for navigation, but is for time dissemination, is established by maintaining Mean OMEGA System Time at a known constant offset from UTC as maintained by the U.S. Naval Observatory (USNO).

Transmitter phase (epoch) adjustments are computed weekly by processing both internal and external timing measurements. Internal measurements indicate the relative timing offsets between pairs of OMEGA transmitters. External measurements indicate the time offsets between individual transmitters and UTC(USNO), and are currently available from four independent sources: VLF phase monitored at USNO, satellite/TV, Loran-C, and portable clock. Non-VLF measurements provide significantly increased accuracy over conventional VLF techniques, but are not currently available on a regular basis for all OMEGA transmitters.

This paper describes an integrated dynamic synchronization process currently implemented as Computer Program SYNC2. The program employs a linear data-mixing filter that appropriately combines mathematical models of cesium clock error dynamics with VLF and non-VLF timing measurements to estimate and control transmitter radiated phase and phase-rate The data-mixing filter has the inherent capability offsets. of optimizing OMEGA synchronization by making the best possible use of all available information including quantitative statistical descriptions of: cesium clock frequency uncertainties, timing measurement uncertainties, and measurement error time correlations. The discussion includes: cesium clock error modeling, measurement preprocessing, data-mixing filter formulation, synchronization adjustments, program input and output, and future plans for OMEGA synchronization.

Program SYNC2 is currently run each week by the U.S. Coast Guard OMEGA Navigation System Operations Detail, and is used to control OMEGA system synchronization to an accuracy on the order of 1 μsec rms. A block diagram of the overall synchronization process is shown in Fig. 1.

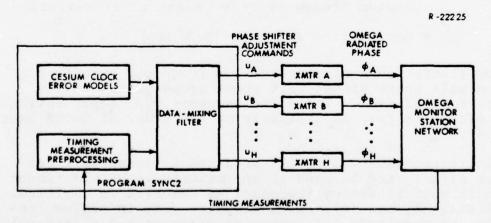


Fig. 1 - Integrated Synchronization Process

CESIUM CLOCK ERROR DYNAMICS

Program SYNC2 employs cesium clock error models to extrapolate transmitter synchronization offsets (both phase and phase rate) between times when synchronization measurements are available. Ignoring, for a moment, any phase shifter adjustments, the phase or time offset in μsec of transmitter I (I = A, B, ..., H) relative to Mean OMEGA System Time can be represented by a standard cesium clock error model [4] at time t_{n+1} , i.e.,

$$\left[\delta\phi_{I\Omega}\right]_{n+1} = \left[\delta\phi_{I\Omega}\right]_{n} + \Delta T \left[\delta f_{I\Omega}\right]_{n} + \left[\mathbf{w}_{I\Omega}^{\phi}\right]_{n}$$
 (1)

and the phase rate (cesium frequency) offset in $\mu sec/day$ relative to Mean OMEGA System Time is given by

$$\left[\delta f_{I\Omega}\right]_{n+1} = \left[\delta f_{I\Omega}\right]_{n} + \left[w_{I\Omega}^{f}\right]_{n}$$
 (2)

where

 $\mathbf{w}_{\mathbf{I}\Omega}^{\Phi}$ = zero-mean, white gaussian sequence corrupting the phase offset $\delta\Phi$ caused by uncorrelated fluctuations in clock cesium frequency (phase rate)

 $\mathbf{w}_{\mathbf{I}\Omega}^{\mathbf{f}}$ = zero-mean, white gaussian sequence corrupting the phase rate $\delta \mathbf{f}$ caused by uncorrelated fluctuations in clock cesium frequency rate (phase acceleration)

 $\Delta T = computation interval (0.5 day)$

Random fluctuations in clock cesium frequency result in a random walk phase offset that grows proportional to the square root of time. The white sequence $\mathbf{w}_{1\Omega}^{\Phi}$, representing this effect in (1), is typically on the order of 0.019 µsec rms [4].

The white sequence $w_{I\Omega}^f$ in (2) produces a random walk frequency offset, and is used to approximate long-term random jumps in nominal cesium frequency as observed in empirical clock data [5] and [6]. Each discrete jump in cesium frequency, of magnitude $\Delta\delta f$ occurring after an N-day interval,

is approximated by a series of small jumps of magnitude $\Delta\delta f/2N$ occurring twice each day. The rms value of w^f_{Ω} appropriate for this approximation, is given by

$$\sigma_{\text{wf}} = \Delta \delta f(2N)^{-\frac{1}{2}} \tag{3}$$

For a typical frequency jump magnitude of 0.03 µsec/day and a typical interval between jumps of 15 days, (3) yields a σ_{wf} of 0.0055 µsec/day. Since there is a lower bound on the uncertainty in an estimate of a random walk process [7], employing the white sequence w_{1}^{f} in the clock model effectively prevents the data-mixing filter from becoming overly-confident in the accuracy of its cesium frequency estimate. Consequently, the filter is more responsive to any sudden change in the synchronization measurement trend brought about by a cesium frequency jump.

MEASUREMENT PREPROCESSING

The basic <u>internal</u> synchronization measurement involves a pair* of transmitters each with an associated monitor station. The associated monitor pair measures the VLF phase delay in each direction along the "reciprocal propagation path" between the transmitters as illustrated in Fig. 2. The monitors are close to, but not collocated with, their respective transmitters. Signals received at each monitor from the two transmitters are used to generate phase difference measurements. At monitor j, which receives signals from transmitters I and J, the <u>phase difference measurement</u> (I-J) is given by

$$\Delta \phi_{\text{IJ}}^{j} = \phi_{\text{Ij}} - \phi_{\text{Jj}} + \varepsilon_{\text{j}} \tag{4}$$

where

 $\phi_{I,j}$ = phase of transmitter I received at monitor j

 ϕ_{Ji} = phase of transmitter J received at monitor j

 ε_{i} = instrumentation error at monitor j

^{*}There are 28 possible transmitter pairs in an eighttransmitter system.

Fig. 2 - Typical Reciprocal Propagation Path

Compensation for Propagation Anomalies - The $\Delta \phi_{IJ}^J$ in (4) are corrected for propagation variations using a PPC value, and compared to a nominal phase difference (proportional to geodesic path length to the transmitters) to obtain an observed synchronization offset between transmitters I and J:

$$OBS_{IJ}^{j} = \Delta \phi_{IJ}^{j} + PPC_{IJ}^{j} - NOM_{IJ}^{j}$$
 (5)

R-11144

The quantity OBS_{IJ}^{j} in (5) is called an "observed" offset because it includes not only the actual synchronization offset between I and J, but also instrumentation errors and residual propagation errors (i.e., errors due to unpredicted propagation variations). PPC errors are typically the dominant error source with magnitudes on the order of 3 to 12 µsec.

Reciprocal Path Phase Differencing - A significant portion of the PPC error in (5) is independent of direction along the path (i.e., the PPC error for propagation from transmitter I to monitor j is approximately equal to the PPC error for propagation from transmitter J to monitor i). This fact can be used to advantage by differencing the two observed synchronization offsets measured in each direction to yield

$$z_{IJ} = \frac{1}{2} \left(OBS_{IJ}^{j} - OBS_{JI}^{i} \right) \tag{6}$$

Direction-independent PPC errors (e.g., solar illumination and ground conductivity) tend to cancel out in $(6)^*$. The

^{*}This technique was originally developed in [8].

quantity z_{IJ} is a relative synchronization offset measurement for transmitters I and J. It is shown in [9] that z_{IJ} is of the form

$$z_{IJ} = \delta \phi_{IJ} + v_{IJ} \tag{7}$$

where $\delta\phi_{IJ}$ is the actual phase (or time) offset between transmitters I and J, and v_{IJ} is a measurement error, typically on the order of 1.0 - 2.5 μsec rms, which includes only direction-dependent PPC errors and uncorrelated instrumentation errors.

Outlier Rejection - Program SYNC2 includes a comprehensive algorithm designed to detect and reject VLF measurement outliers as described in Appendix A.

Measurement-Quality Weighting - SYNC2 includes a special routine to estimate VLF measurement errors for use in specifying measurement quality in the data-mixing filter. Each VLF measurement error is approximated by the rms "fit error" between actual synchronization measurements and those predicted by SYNC2 models over each previous three-week period. Specifically, the measurement fit error at time t_n is defined as*

$$\left[\delta z_{IJ}\right]_{n} = \left[z_{IJ}\right]_{n} - \left[\hat{z}_{IJ}\right]_{n} \tag{8}$$

where the predicted measurement is

$$\left[\hat{\mathbf{z}}_{\mathbf{I}\mathbf{J}} \right]_{\mathbf{n}} = \left[\delta \hat{\boldsymbol{\phi}}_{\mathbf{I}\Omega} \right]_{\mathbf{n}} - \left[\delta \hat{\boldsymbol{\phi}}_{\mathbf{J}\Omega} \right]_{\mathbf{n}}$$
 (9)

and $\delta\hat{\phi}_{\text{IQ}}$ is the filter estimate of the internal phase (or time) offset of transmitter I relative to Mean OMEGA'System Time. SYNC2 computes the rms fit error over the three-week period prior to each daily measurement, and repeatedly updates this statistic after each daily measurement is processed. The mean square fit error is used to define a measurement noise covariance matrix R_n which accounts for measurement quality in the data-mixing filter.

^{*}The overhat (^) denotes an estimated parameter.

Time-Correlation Modeling - VLF measurement errors are generally correlated in time due to residual diurnal (daily) and seasonal propagation variations not removed by published PPCs. Analysis of empirical data [10] indicates that the normalized autocorrelation function of the daily measurement errors v_{IJ} in (7) can be approximated by an exponential function of the form*

$$R_{v}(\tau) = E\left\{v(t) \ v(t+\tau)\right\} / E\left\{v^{2}(t)\right\} \approx \exp(-|\tau|/\tau_{o})$$
 (10)

where τ is time shift in days, and τ_O is determined from empirical data. (A "best fit" is obtained for $\tau_O \approx 2.5$ days.) From (10), the daily measurement error is modeled as a first-order markov process:

where ΔT = 0.5 day is the computation interval, and η_{IJ} is a zero-mean, white, gaussian sequence representing the uncorrelated components of v_{IJ} . The variance of v_{IJ} is denoted by σ_{IJ}^2 , and is approximated by the mean square value of the measurement fit error over each previous three-week period. The corresponding variance of η_{IJ} is computed as [7].

$$\left[\sigma_{IJ}^{\eta}\right]_{n}^{2} = \left[\sigma_{IJ}\right]_{n}^{2} \left\{1 - \exp\left(-4\Delta T/\tau_{0}\right)\right\}$$
 (12)

EXTERNAL TIMING MEASUREMENTS

External timing measurements for synchronization to UTC(USNO) are currently available for four of eight OMEGA transmitters. OMSTAS Liberia, Trinidad and North Dakota are linked to UTC by one-way VLF phase measurements; OMSTA Hawaii has been linked via satellite/TV, Loran-C, and several portable clock visits each year [11]. A Loran-C timing link between OMSTA North Dakota and UTC is planned for the near future.

^{*}The symbol E(·) denotes expected (or ensemble average) value.

An external synchronization measurement of UTC relative to transmitter I (I = A, B, ..., H) is expressed in the form

$$z_{RI} = \delta \phi_{RI} + v_{RI}$$
 (13)

where $\delta \varphi_{RI}$ is the actual external phase (or time) offset of transmitter I, and v_{RI} is the measurement error. For filter mechanization, (13) is expressed in an equivalent form in terms of the internal phase offset $\delta \varphi_{I\Omega}$ of transmitter I (relative to Mean OMEGA System Time) and the external offset $\delta \varphi_{RO}$ of UTC relative to Mean OMEGA System Time, i.e.,

$$z_{RI} = \delta \phi_{R\Omega} - \delta \phi_{I\Omega} + v_{RI}$$
 (14)

Internal and external measurement errors, as modeled in the data-mixing filter are summarized in Table 1. External VLF phase measurements are generally not as accurate as internal VLF measurements since the reciprocal path differencing technique in (6) cannot be employed for one-way propagation. However, external VLF bias errors are dynamically calibrated and removed by comparing them to more-accurate non-VLF measurements when available. Non-VLF measurement errors are discussed in detail in [11].

TABLE 1 SYNCHRONIZATION MEASUREMENT ERRORS

Synchronization Measurement Type	RMS Error (µsec)		
Internal VLF phase	1.0 - 2.5*		
External			
VLF phase	1.1 - 2.6*		
Loran-C	0.21 or 0.28		
Satellite/TV	0.11 or 0.21		
Portable clock	0.07 or 0.19 [†]		

^{*}Typical values dynamically computed for each daily measurement based on 3-week rms fit error as defined in (8).

[†]Accuracies reflect dynamic and static calibration, respectively, of the phase advance between each transmitter's radiated signal and its online cesium clock.

ESTIMATION ALGORITHM

System State Equation - The clock error dynamics model in $\overline{(1)}$ and $\overline{(2)}$ is expressed in a vector-matrix system state equation for all eight OMEGA transmitters (A,B,...,H) at time t_n as

^{δΦ} ΑΩ ^{δΦ} ΒΩ • • • • • • • •	0 1	0	ΔT	0	$\delta \phi_{\mathbf{A}\Omega}$ $\delta \phi_{\mathbf{B}\Omega}$	$\begin{array}{c} \mathbf{w}_{\mathbf{A}\Omega}^{\varphi} \\ \mathbf{w}_{\mathbf{B}\Omega}^{\varphi} \\ \vdots \\ \vdots \\ \mathbf{w}_{\mathbf{H}\Omega}^{\varphi} \end{array}$		
δ¢ _{RΩ} =	0	1	0	ΔΤ	$\delta \phi_{\mathbf{R}\Omega}$	$+$ $\frac{\overline{\mathbf{w}_{\mathbf{R}\Omega}^{\phi}}}{\mathbf{w}_{\mathbf{R}\Omega}}$	0	1
δf _{AΩ}			1 0		δfAΩ	wf An	0	
€1 _{BΩ}			1		δfBΩ	$w_{B\Omega}^f$		
	0	0		0			1 .	
			•			1 .	1 .	1
· 6f _{HΩ}			0 .		· δf _{HΩ}	$\frac{\mathbf{w}_{H\Omega}^{\mathbf{f}}}{\mathbf{w}_{H\Omega}}$	0	
^{6f} RΩ n+1	0	1	0	1	δf _{RΩ}	$n = \frac{\overline{\mathbf{w}_{R\Omega}^f}}{\mathbf{w}_{R\Omega}}$	0	n

(15)

or, more compactly*

$$\underline{x}_{n+1} = \Phi \underline{x}_n + \underline{w}_n + \underline{u}_n \tag{16}$$

where Φ is the state transition matrix, and the control vector \underline{u}_{n} accounts for phase shifter adjustments applied to each clock during the computation interval $\Delta T.$ The elements $\delta \varphi_{R\Omega}$ and $\delta f_{R\Omega}$ represent the external phase and frequency offsets, respectively, of UTC relative to Mean OMEGA System Time.

Measurement Equation - The internal synchronization measurements in (7), and the external measurements in (14) are combined as

^{*}A bar beneath a symbol denotes a vector.

ZAB		1 -1				δ¢ _{AΩ}	v _{AB}
ZAC		1 0 -1 0				δΦBΩ	VAC
			0	0	0		•
ZAH	=	1 0 0 -1				• +	V _{AH}
z _{BC}		0 1 -1				$\frac{\delta \phi_{\mathbf{R}\Omega}}{}$	^v BC
z _{BD}		0 1 0 -1				δf _{AΩ}	v _{BD}
			0	0	0	δf _{BΩ}	
z _{BH}		0 1 0 0 -1					v _{BH}
		•				δf _{HΩ}	-
1:			0	0	0	δf _{RΩ}] _n	
z _{GH}		0 0 1 -1	0	0	0	2 311	v _{GH}
0		1 1 1	0	0	0		0
z _{RA}		-1	1				v _{RA}
z _{RB}		-1 0	1				v _{RB}
		•		0	0		
1:		0 .	:				
z _{RH}	,	9 -1	1				v _{RH}
	n					n	
							(17)

or, more compactly as

$$\underline{z}_{n} + H_{n}\underline{x}_{n} + \underline{v}_{n} \tag{18}$$

The measurement matrix H_n has 18 columns and up to 37 rows, depending on measurement availability (typically, 16 are available). If any measurement is not available at a particular sample time, the corresponding rows are deleted from (17).

Measurement Constraint - The zero element in the measurement vector z_n in (17) represents an internal "measurement constraint" which is included for convenience to avoid a singular measurement matrix. In general, for an N-transmitter system, there are N(N-1)/2 different reciprocal paths (see Fig. 2), but only N-1 paths provide independent measurements. This can cause computational difficulty in attempting to determine eight transmitter timing offsets from only seven independent measurements. One approach to this problem is to arbitrarily define the mean internal timing offset (Mean OMEGA System Time) as zero, i.e.,

$$\phi_{\Omega} = \frac{1}{8} \sum_{\mathbf{I}=\mathbf{A}}^{\mathbf{H}} \delta \phi_{\mathbf{I}\Omega} \equiv 0$$
 (19)

Then, it is possible to define, as an internal measurement constraint, an "error-free" measurement of Mean OMEGA System Time as

$$z_{\Omega} = \frac{1}{8} \sum_{I=A}^{H} \delta \phi_{I\Omega} \equiv 0$$
 (20)

The measurement constraint in (20), used in conjunction with seven independent measurements, allows a direct computation* of eight internal timing offsets.

For the complete eight-transmitter system (with 28 possible reciprocal paths), internal synchronization offsets can theoretically be determined using relative phase measurements from any seven independent paths. In the absence of measurement and propagation prediction errors, the estimation error using any seven independent paths would be zero. However, since there are always residual measurement and modeling errors, it is desirable to use redundant data from as many paths as possible to minimize the effects of these errors on system synchronization.

<u>A Priori Information</u> - Implementation of the data-mixing filter requires a priori information on: clock cesium frequency disturbances \underline{w}_n in (16), synchronization measurement errors \underline{v}_n in (18), initial state estimate $\hat{\underline{x}}_0$, and initial state estimation error \underline{x}_0 , i.e.,

^{*}Alternative techniques involve the use of a "pseudoinverse" matrix and produce identical results.

$$\underline{\tilde{\mathbf{x}}}_{0} = \underline{\hat{\mathbf{x}}}_{0} - \underline{\mathbf{x}}_{0} \tag{21}$$

Typically, the initial state estimates for the current week are set equal to the final estimates from the previous week. (For an unsynchronized transmitter, the initial estimates are set to zero.) The remaining parameters, \underline{w}_n , \underline{v}_n and $\underline{\tilde{x}}_0$, are described statistically in terms of the diagonal covariance matrices:

$$Q = E\left\{\underline{w}_{n}\underline{w}_{n}^{T}\right\} \tag{22}$$

$$R_{n} = E\left\{\underline{v}_{n}\underline{v}_{n}^{T}\right\} \tag{23}$$

$$P_{0} = E\left\{ \frac{\tilde{\mathbf{x}}}{0} \frac{\tilde{\mathbf{x}}}{0} \right\}$$
 (24)

The elements of Q, R_n and P_0 are given in Table 2.

TABLE 2 A PRIORI STATISTICS

Covariance Matrix	Diagonal Element	Value	Units
Q	σ <mark>2</mark> w φ	3.6 × 10 ⁻⁴	usec ²
	σ ² _{wf}	0.3 × 10 ⁻⁴	(µsec/day) ²
R _n	$\left[\sigma_{\mathrm{IJ}}\right]_{\mathrm{n}}^{2}$	See Table 1	µsec ²
Po	$\left[\sigma_{1\Omega}^{\phi}\right]_{0}^{2}$	Final values from previous week*	usec ²
	$\left[\sigma_{1\Omega}^{f}\right]_{0}^{2}$		(µsec/day) ²

^{*}For an unsynchronized transmitter, typical values are 100 μsec^2 phase uncertainty and 0.75 $(\mu sec/day)^2$ frequency uncertainty.

Data-Mixing Filter - A linear dynamic estimation algorithm for computing OMEGA synchronization offsets can be formulated in terms of the basic system model defined in (16) and (18). The resulting formulation is referred to as a Kalman (data-mixing) filter [7] and is summarized in Fig. 3. The diagonal elements of the covariance matrix P_n in Fig. 3 provide an indication of the uncertainty associated with each synchronization estimate $\frac{\hat{\mathbf{x}}_n}{\hat{\mathbf{x}}_n}$. Implementation of these equations in Program SYNC2 is discussed in detail in [12].

Measurement Correlation - A necessary condition for implementation of the data-mixing filter in Fig. 3 is that the measurement errors \underline{v}_n in (18) are <u>uncorrelated</u> in time (i.e., a white sequence). However, VLF measurement errors are, in fact, time-correlated. This problem is circumvented by employing a <u>measurement-differencing</u> technique as outlined in [13]. This technique produces differenced measurement errors that are uncorrelated in time, and allows the resulting system model to be written in a form equivalent to that defined in (16) and (18).

OPTIMAL ESTIMATE				
$\hat{\underline{x}}_{n}^{-} = \Phi \hat{\underline{x}}_{n-1}^{+} + \underline{u}_{n-1}$	EXTRAPOLATION BETWEEN MEASURE- MENTS	(25)		
$\hat{\underline{x}}_{n}^{+} = \hat{\underline{x}}_{n}^{-} + K_{n} \left[\underline{z}_{n} - H_{n} \hat{\underline{x}}_{n}^{-} \right]$	MEASUREMENT UPDATE	(26)		
$K_{n} = P_{n}^{-}H_{n}^{T}\left[H_{n}P_{n}^{-}H_{n}^{T} + R_{n}\right]^{-1}$	WEIGHTING	(27)		
ESTIMATION ER	ROR COVARIANCE			
$P_n^- = \Phi P_{n-1}^+ \Phi^T + Q$	EXTRAPOLATION BETWEEN MEASURE- MENTS	(28)		
$P_n^+ = \left[I - K_n H_n \right] P_n^-$	MEASUREMENT UPDATE	(29)		

Fig. 3 - Data-Mixing Filter Formulation

SYNCHRONIZATION ADJUSTMENTS

OMEGA synchronization control is physically implemented by periodically adjusting the phase shifter of each transmitter's online cesium clock. Two types of adjustments are applied: a weekly adjustment to correct for the phase (or time) offset existing at the beginning of each week, and a four-hour adjustment (i.e., applied every four hours) to correct for expected phase drift (due to cesium frequency offset) during the week.

The synchronization control task is complicated by communications delays between the eight transmitter/monitor stations and the OMEGA Data Processing Center in Washington, D.C. Additional delays are introduced in data processing, resulting in a time lag of 40 hours between the last synchronization measurements taken each week and the application of new weekly and four-hour adjustments. This lag can be significant if the computed four-hour adjustment command for a particular cesium clock changes significantly from one week to the next. A special adjustment is made to compensate for this effect as discussed below.

The weekly adjustment for transmitter $I(I=A,B,\ldots,H)$ consists of two basic components: an estimated external phase offset (UTC-transmitter I) based on the latest available measurements, and special compensation (if necessary) for ten obsolete four-hour adjustments applied during the 40 hour lag discussed above. The four-hour adjustment for transmitter I is simply the external frequency offset estimate (UTC-transmitter I) in $\mu \sec/4$ -hr.

SAMPLE OUTPUT

A typical time history of internal synchronization measurements print-plotted by Program SYNC2 is shown in Fig. 4. Both 10.2 and 13.6 kHz reciprocal-path phase-difference measurements of transmitter pair DG (north Dakota minus Trinidad) are given for the period from 24 November 1975 to 5 January 1976. SYNC2 adjustment commands were used to control system synchronization throughout this period. The last three weeks of measurements in Fig. 4 have a standard deviation on the order of 1 μsec and mean value on the order of -1 μsec . This -1 μsec bias represents either a measurement bias error, an actual phase offset between transmitters D and G, or some combination of both. SYNC2 employs the measurement fit error computation in (8) to account for measurement bias errors (which, in this case, were -0.4 μsec).

TRANSMITTER PAIR DG 1=10.2 KHZ 3=13.6 KHZ B=ROTH PREQUENCIES

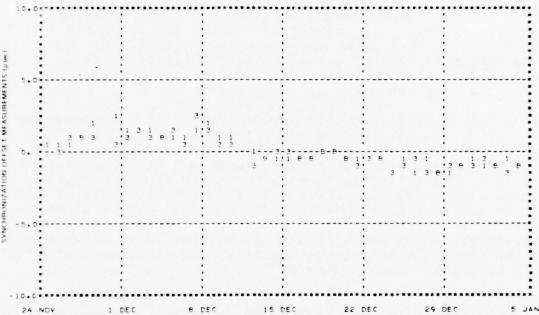


Fig. 4 — Synchronization Measurements (North Dakota Minus Trinidad)

A time history plot of synchronization offset estimates (both phase and cesium frequency) computed for \overline{OMSTA} North Dakota (transmitter D) is shown in Fig. 5. Estimates immediately after each twice-daily measurement update are shown for the same six-week period indicated in Fig. 4. The abrupt change in the phase offset estimate from (-0.5 to 0.0 $\mu sec)$ on 26 November reflects a weekly phase shifter adjustment. The abrupt change in the frequency offset estimate (from 0.08 to -0.6 $\mu sec/day)$ on 15 December reflects a replacement of the online clock for transmitter D by one of its backup clocks. (Frequency offset estimates for backup clocks are computed in a separate algorithm by least-squares fit to online clock data.)

The rms uncertainties for the estimates in Fig. 5 are derived from (28) and (29) and are plotted in Fig. 6. SYNC2 automatically increases the frequency offset uncertainty to 0.2 µsec whenever an online clock is replaced, as shown in Fig. 6. In general, as more measurements are processed, estimate uncertainties (both phase and cesium frequency)

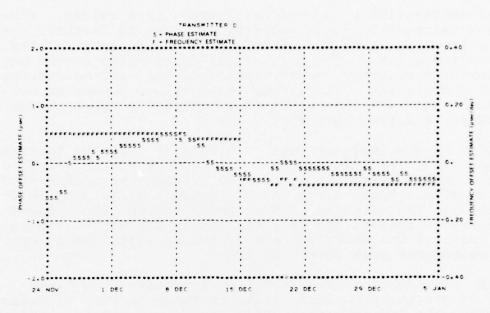


Fig. 5 — Synchronization Estimates

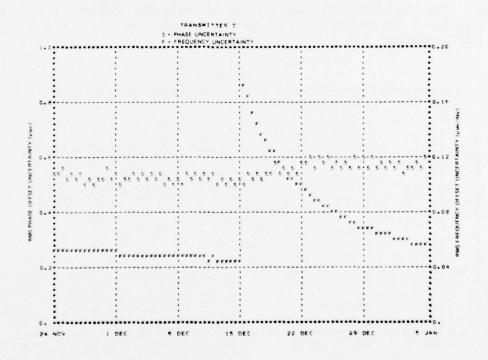


Fig. 6 - Estimate Uncertainties

decay exponentially to non-zero steady-state values. (The slight increase in phase uncertainty after 15 December, results from the large frequency offset uncertainty for the new online clock.) The exponential decay rates depend on: measurement accuracy, measurement interval, and measurement error correlation. The steady-state values depend on measurement accuracy and random fluctuations in clock cesium frequency and frequency rate.

Figures 5 and 6 indicate that on 5 January 1976 the internal phase offset for transmitter D was -0.3 ± 0.6 µsec relative to Mean OMEGA System Time, and the transmitter online clock had a natural phase drift rate (frequency offset) of -0.08 ± 0.06 µsec/day relative to Mean OMEGA System Time. Based on these estimates, the internal weekly adjustment was on the order of 0.3 µsec, and the four-hour adjustments for the subsequent week were 0.01 µsec.

A time history plot of external measurements (UTC minus Hawaii) via Loran-C timing links is shown in Fig. 7. These measurements indicate that OMSTA Hawaii was synchronized to UTC within an accuracy on the order of 1 µsec for the period 13 September to 25 October 1976. External non-VLF measurements (when available) provide an excellent means of checking (as well as maintaining) synchronization accuracy of the OMEGA system.

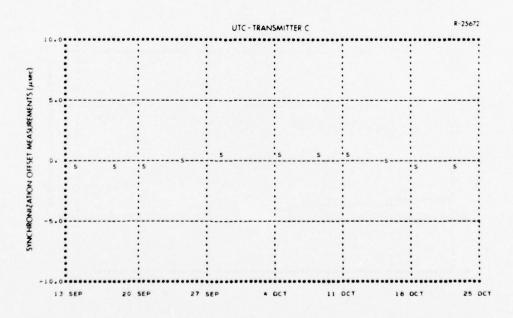


Fig. 7 - Loran-C Measurements (UTC Minus Hawaii)

FUTURE PLANS

Timing Measurements - Reciprocal VLF timing measurements in (7) are generally accurate to a few µsec when directiondependent propagation prediction errors are small. tional experience has revealed two situations where these errors are, in fact, significant: near the magnetic equator and near the geographic poles. Recent portable clock measurements [14] and [15] indicate propagation anomalies on the order of 3-9 usec in some VLF measurements for OMSTA Reunion (which is south of the magnetic equator). Polarpath synchronization measurements involving OMSTA Norway are significantly degraded in the spring and fall due to changing solar illumination conditions. In order to minimize adverse effects of the above phenomena, future efforts related to OMEGA synchronization accuracy will most likely follow two basic avenues: accuracy improvement via refinement of existing VLF propagation prediction models [2], and accuracy verification (and improvement) via increased use of non-VLF timing links such as satellite/TV, Loran-C, and portable clock measurements.

Leap Second Offset - Mean OMEGA System Time currently leads UTC(USNO) by five seconds. Although operational procedures do exist for inserting leap second timing adjustments at each OMEGA transmitter, there are currently no plans to eliminate this offset from UTC. OMEGA leap second offset information is announced in ONSOD's Weekly Status Message and on WWV.

JMSA Participation - At the September 1976 OMEGA Technical Conference in Bergen, Norway, OMEGA Member nations supported a resolution to transfer OMEGA synchronization operations from ONSOD to the Japanese Maritime Safety Agency (JMSA). JMSA has completed test runs of Program SYNC2 and is currently maintaining data files in parallel with ONSOD on a weekly basis. After official transfer of Program SYNC2 operations to JMSA, ONSOD will maintain parallel data files to ensure a smooth transition. In order to maintain system synchronization to UTC(USNO), JMSA will continue to use UNSO data as the primary source of external timing measurements.

SUMMARY

This paper describes the application of modern estimation techniques to the problem of synchronizing the OMEGA radio navigation system to an accuracy on the order of 1 µsec rms.

In order to achieve this accuracy, extensive preprocessing is performed on VLF timing measurements to reduce the effects of VLF propagation anomalies. The noisy, time-correlated VLF measurements are then processed in a Kalman data-mixing filter that appropriately combines them with cesium clock error models to estimate OMEGA transmitter timing offsets and compute timing adjustment commands. The synchronization algorithm is mechanized in Computer Program SYNC2 which was developed by The Analytic Sciences Corporation and implemented in January 1975. Program SYNC2 is run each week by the U.S. Coast Guard OMEGA Navigation System Operations Detail to control both internal and external system synchronization.

APPENDIX A VLF OUTLIER REJECTION

SYNC2 employs an automatic outlier rejection scheme to identify and remove VLF measurements that are not "statistically representative" of the total data set. It is assumed that, on the average, 95% of the measurements are statistically representative and 5% are outliers. Prior to applying an outlier rejection test, two distorting effects are removed from the measurements: the effect of weekly phase shifter adjustments, and any nonzero trend over the previous six weeks. The resulting data set is assumed to be normally (gaussian) distributed about the trend line.

For normally distributed data, 95% of the measurements lie within 1.96 standard deviations (1.96 σ) of the trend line [16]. Typically, the <u>true</u> σ of the data set can only be approximated by a <u>sample</u> standard deviation $\hat{\sigma}$, and this approximation is good only for large data samples (i.e., 30 or more measurements). Frequently, however, due to transmitter outages, monitor outages, or previously rejected data, there may be significantly less than 30 daily VLF measurements available for a particular transmitter-pair in a given six-week period.

A more appropriate rejection criterion for this situation is developed in [16] and [17] where it is shown that for n normally distributed measurements, 95% lie within $k\hat{\sigma}$ of the trend line, where

$$k = \frac{T \sqrt{n-1}}{\sqrt{n-2+T^2}} , n \ge 3$$
 (33)

and T is the value of the Student's probability distribution function for 0.05 level of significance and n-2 degrees of freedom. As the number of daily measurements increases from 3 to a maximum of 42, k increases from 1.41 to 1.95 (k = 1.96 for $n \rightarrow \infty$).

SYNC2 employs an iterative $k\hat{\sigma}$ outlier rejection scheme that: computes a six-week sample standard deviation $\hat{\sigma}$ about the measurement trend line, rejects all measurements exceeding $k\hat{\sigma}$ from the trend line, and repeats this process until no new outliers are found.

REFERENCES

- 1. Swanson, E.R., and Brown, R.P., "OMEGA Propagation Prediction Primer," Naval Electronics Laboratory Center, Technical Note TN-2101, August 1972.
- 2. United States Coast Guard OMEGA Navigation System Operations Detail, "OMEGA Propagation Prediction Model and Computer Program Documentation," April 1973.
- 3. Defense Mapping Agency Hydrographic Center (DMAHC), "OMEGA Propagation Correction Tables," H.C. Publication Series No. 224.
- 4. Autonetics Div., North American Rockwell Corp., "Analysis of Advanced Time-Frequency National Air Space System Concept, Volume II, Time and Frequency Techniques Survey," Report No. RD-69-32, August 1969.
- 5. Hafele, J.C., "Performance and Results of Portable Clocks in Aircraft," <u>Proceedings of the Third Annual PTTI Planning Meeting</u>, November 1971.
- 6. Winkler, G.M.R., et.al., "The USNO Clock Time Reference, and Performance of a Sample of Atomic Clocks," Metrologia, Vol. 6, 1970.
- 7. Gelb, A., Ed., <u>Applied Optimal Estimation</u>, M.I.T. Press, Cambridge, 1974.
- Pierce, J.A., et.al., "OMEGA: A Worldwide Navigational System, System Specification and Implementation, Second Revision," Office of Naval Research, DDC No. AD-630-900, May 1966.

- 9. Swanson, E.R., and Kugel, C.P., "VLF Timing-Conventional and Modern Techniques," Proceedings of the IEEE, Vol. 60, No. 5, May 1972.
- 10. D'Appolito, J.A., and Kasper, J.F., "Predicted Performance of an Integrated OMEGA/Inertial Navigation System," National Aerospace Electronics Conference, Dayton, Ohio, May 1971.
- 11. Lavanceau, J.D., "OMEGA Signals and Universal Time," First OMEGA Symposium, Tokyo, Japan, June 1975.
- 12. Schane, R.N., "Linear Dynamic Estimation and Control of OMEGA Radio Navigation System Synchronization,"

 Proceedings of the 1976 IEEE Conference on Decision and Control, Clearwater Beach, Florida, December 1976.
- Bryson, A.E., and Henrikson, L.J., "Estimation Using Sampled Data Containing Sequentially Correlated Noise,"

 Journal of Spacecraft and Rockets, Vol. 5, No. 6,

 June 1968.
- 14. Fisher, L.C., United States Naval Observatory, Personal Communication, 19 July 1976.
- 15. Vannicola, V., United States Coast Guard OMEGA Navigation System Operations Detail, Personal Communication, 20 July 1976.
- 16. Cramer, H., <u>Mathematical Methods of Statistics</u>, Princeton University Press, 1974.
- 17. Swaroop, R., and West, K.A., "A Simple Technique for Automatic Computer Editing of Biodata," National Aeronautics and Space Administration, Technical Note NASA-TN-D-5275, June 1969.

ACKNOWLEDGEMENTS

The authors acknowledge the encouragement provided throughout this effort by Mr. David C. Scull of ONSOD, and the helpful suggestions of Drs. John E. Bortz and Joseph F. Kasper of TASC during algorithm development.

A BRIEF REVIEW OF FREQUENCY STABILITY MEASURES

Gernot M. R. Winkler
U. S. Naval Observatory, Washington, D. C.

ABSTRACT

A standard statistical treatment of the measurements of frequencies of clocks can be done simply by computing the mean μ and variance σ^2 of these measurements. However, drifts (aging of crystal clocks) pose a problem because they cause a troublesome dependency of μ and σ^2 on N, the number of samples. While such measures in the time domain can be made more meaningful by using the mean square successive difference instead of σ^2 as a measure of clock stability, RADAR, microwave spectroscopy and other applications require measures which give sideband to carrier power ratios (frequency domain measures). The principles of such measures and their various advantages and disadvantages will be discussed.

INTRODUCTION

This paper has been prepared at the request of the program committee which wished to have the subject of frequency stability measures emphasized as one of the issues of this year's conference. It is therefore proposed to review the subject as an introduction to more specific papers and to the panel discussion which is to follow these presentations.

There is a considerable amount of written material available which can serve as introduction to our subject. One of the best introductory coverages is given in Rovera's (IEN, 1974) lecture notes. Appended is a selected list of original contributions. Two excellent and complementary reviews are the NBS Technical Notes No. 669 (D. Allan, 1975) and No. 679 (D. Howe, 1976). One cannot expect to improve upon such lucid and exemplary expositions of the subject. One can only attempt to present it in a different style, context and accent.

We can divide our subject according to various lines of which the division short-term vs. long-term stability is only a more superficial division. By measurement techniques one can distinguish measurements in the time domain from frequency domain measurements. One can characterize stability in the time domain and in the frequency domain. Here we would like to emphasize yet another dichotomy:

- A. Trends, Systematic or Deterministic Variations of Frequency, vs.
 - B. Random Variations as Part of a Random Process.

A failure to separate the systematic variations from the random part will, in most cases, affect any characterization of a clock in a very misleading way (Barnes and Allan, 1964). On the other hand, the random part of the observed frequency variations of a clock is of the same type as the observed variables which arise from many other random processes. Such data form a time series which can be investigated and characterized with the same methods as have proved useful in other sciences. We therefore do not have to re-invent the wheel but can simply apply what we can find in the literature of Time Series Analysis etc. (Box and Jenkins, 1970, Jenkins and Watts, 1968, Wiener, 1949).

CLOCK SAMPLING

Table 1 shows the general scheme which we can follow if we sample our clock error x(t) at regular intervals h. Such sampling is the basic measurement in the time domain. We use a clock output marker (which could be a pulse or a sine wave zero crossing) and a reference clock "R" which we assume to be perfect. The sampling of the clock error of the test clock "T" is done with a time interval counter at the time t.

$$START(T) - STOP(R) = x(t)$$
 (1)

The complement of x(t) is called the clock correction, C(t) = -x(t). These measurements constitute our basic time series in which we designate the number of each measurement as the index k.

Table 1

	x Time t=t _o +kh	Clock Error x(k)	First Diff. ∀x(k)	Second Diff. $\nabla^2 x(k)$	Third Diff. $\nabla^3 x(k)$
0	t _o + Oh	x(0)	-	-	•
1	t _o + 1h	x(1)	∀x(1)	-	-
2	t _o + 2h	x(2)	∀x(2)	$\nabla^2 \mathbf{x}(2)$	10 to -10 mile
3	$t_{\circ} + 3h$	x(3)	∇x(3)	$\nabla^2 x(3)$	$\nabla^3 x(3)$
4	t _o + 4h	x(4)	∀x(4)	$\nabla^2 x(4)$	$\nabla^3 x(4)$
5	t _o + 5h	x(5)	∀x(5)	∇²x(5)	$\nabla^3 x(5)$

We assume n + 1 measurements (last k = n). We use "backward" differences ∇ because that is what we can compute in real time immediately after a measurement. The symbol ∇ may also be understood as a linear operator to be applied to a table entry z_k (cf. Hamming, 1962):

$$\nabla(z_k) = z_k - z_{k-1} \tag{2}$$

$$\nabla(\nabla^{m}(z_{k})) = \nabla^{m}(z_{k}) - \nabla^{m}(z_{k-1})$$
(3)

A similar operator is the backshift operator B:

$$B(z_k) = z_{k-1} \tag{4}$$

We have obviously the following operator equation which is true for whatever argument is chosen:

$$\nabla = 1 - B \tag{5}$$

(1 is the identify operator). A formalism such as (5) will be used in the discussions of the Box-Jenkins (1970) approach to statistical modeling. Let us apply these concepts to table 1 where we interpret the m^{th} difference as a symbolic m^{th} power of \triangledown . We use the binomial theorem:

$$\nabla^{m} = (1 - B)^{m} = \sum_{r=0}^{m} (-1)^{r} {m \choose r} B^{r}$$

$$(6)$$

 B^r means that we apply B r times. As an example we can write the general expression for the 3^{rd} difference in our table 1 by multiplying equation (6) with x(k):

$$\nabla^{3}x(k) = \sum_{r=0}^{3} (-1)^{r} {3 \choose r} x(k-r)$$
$$= x(k) - 3x(k-1) + 3x(k-2) - x(k-3)$$

FREQUENCY

The average normalized (relative) frequency departure (error) during the basic interval h is

$$\overline{y}_{h}(k) = \frac{\nabla x(k)}{h} = \frac{\Delta x}{\Delta t}$$
 (7)

Its dimension is time error per unit time, i.e. it is a dimensionless (relative) quantity. It is therefore given as parts per billion etc., whereas the time error is given as time, e.g. as microseconds (µs). Frequency F, as distinguished from relative frequency error $\overline{y}(t)$, is given in cycles (of 2π radians each) per second (Hertz, Hz). The period P is the duration of one cycle: P = 1/F. Angular frequency Ω is given in radians per second (rad/s) and we have $\Omega = 2\pi F$ and

$$\overline{y} = \frac{\Delta F}{F} = \frac{1}{\Omega} \cdot \frac{\Delta \phi}{\Delta t}, \quad x = \frac{\phi}{\Omega}$$
 (8)

where ϕ is the phase error at the frequency F.

Our timing waveform is always bandlimited since it comes from mateial circuits. Our concept of average frequency may therefore be brought to the limit for a smaller and smaller sampling interval Δt and we obtain the concept of the instantaneous relative frequency departure

$$y(t) = \lim_{\Delta t \to 0} \frac{\Delta x}{\Delta t} = \frac{dx}{dt} = \frac{1}{\Omega} \frac{d\phi}{dt} = \frac{1}{\Omega} \dot{\phi}$$
 (9)

For practical reasons our basic sampling interval h must be chosen sufficiently long so that the Δx can be resolved above the noise level of measurement. Once the measurements are recorded it is of course easy to choose any multiple of h as the averaging or integration time τ . In the general case we have

$$\tau = kh \tag{10}$$

where $k \ge 1$ is a positive integer.

Now, if our clock errors would be purely deterministic and if they followed an \mathbf{m}^{th} degree polynomial

$$x(t) = a'_0 + a'_1 t + a'_2 t^2 + a'_3 t^3 + \cdots + a'_m t^m$$
 (11)

which we could consider e.g. as the beginning of a Taylor series, then, according to the fundamental theorem of the difference calculus, the $^{\rm mth}$ difference would be a constant. By applying the operator \triangledown m times one can verify that

$$\nabla^{\mathsf{m}} \mathsf{x}(\mathsf{t}) = \mathsf{a}_{\mathsf{m}}^{\mathsf{m}} \mathsf{n}^{\mathsf{m}} \mathsf{h}^{\mathsf{m}} \tag{12}$$

If we use the index k as the argument with h=1, then the polynomial is now in powers of k

$$x(k) = a_0 + a_1k + a_2k^2 + a_3k^3 + \cdots + a_mk^m$$
 (11')

with

$$\nabla^{m} x(k) = a_{m} m! \qquad (12')$$

The (m + 1)st differences are zero. Since (12) and (12') refer to the same quantity we also can see that

$$a_{m} = a_{m}^{\dagger} h^{m} \tag{13}$$

where a_m^+ has the dimension of time $^{m+1}$. But in addition to measurement noise, our clocks are always subject to random disturbances and therefore the ∇^{m+1} will not be zero but will reflect the clock erratics. These erratics will be magnified as higher differences are taken according to (6).

These properties of the higher differences offer a possibility to obtain insight into the clock's performance. We could try to form the average difference

$$\nabla^{\ell} x(k) = \frac{1}{n - \ell + 1} \qquad \sum_{k=\ell}^{n} \nabla^{\ell} x(k) \qquad (\ell \ge 1)$$
 (14)

for successive $\ell=1,2,3$ etc. until we find a $\nabla^m x(k)$ which is not only close to zero but also shows no trends if we take different samples, i.e. which is stationary. Our clock performance would then contain a systematic part in the form of a polynomial of degree m-1 and the coefficient of the highest power term would be

$$a_{m-1} = \frac{1}{(m-1)!} \cdot \nabla^{m-1} x(k)$$
 (15)

As an example consider a quartz-crystal clock which can be modeled typically with a second degree polynomial for its clock errors

$$x(k) = a_0 + a_1k + a_2k^2 + x'(k)$$
 (16)

where x'(k) are the residuals. The third differences will average (show no trend) close to zero and we find for the aging coefficient

$$a_2 = \frac{\nabla^2 x(k)}{2} \tag{17}$$

Furthermore in this case one can use as a measure for the clock erratics (the random part) the average third absolute difference as it once was actually used by H. M. Smith in the early 50's at the RGO. Such

a measure would be written in our terms

$$V = \left| \nabla^3 x(k) \right|$$

By using the root mean square we obtain a sort of higher variance (since the average is close to zero) as it has been discussed by Kramer at the PTB (1975) who called it curvature variance. Expressed as sigma (variance $^{-1/2}$) we have

$$\hat{\sigma}_{C}(h) = \sqrt{\frac{\left[\nabla^{3}x(k)\right]^{2}}{3! h^{2}}}$$
(18)

This measure is insensitive to frequency drifts and in that regard would be superior to the pair variance (two sample Allan variance). The pair sigma, which for good reasons is the most popular frequency stability measure, is in our terms

$$\hat{\sigma}_{y}(h) = \sqrt{\frac{\left[\nabla^{2}x(k)\right]^{2}}{2! h^{2}}}$$
(19)

Formulae (18) and (19) are, in fact, just special cases of the discussion given by Audoin & Lesage (1975). A sample variance σ_y^2 , finally, can simply be obtained by averaging the $\nabla x(k)$ with a naive determination of the standard deviation and squaring it. But again, this is usually a misleading procedure if we do not first take off any trends in the record (in another way of looking at the problem this amounts to forcing the averages to zero in which case, if we have a white noise process, all of the above discussed mean square measures become variances of the same magnitude).

The simplest case in principle, and a very important one for conceptual clarification, is the case of purely random $\overline{y}(k)$'s. We call that white FM. A cesium beam atomic clock would be an example (typically for $\tau > 10s$) since the servo loop error signal coming from the atomic beam tube is shot noise fundamentally due to the arrival of individual atoms at the detector. We should have no trends in this case but the random additions of noise produce a random walk in x(t) as is shown in fig. 1. This random walk (RW) has neither a stationary mean nor a stationary variance in x(t) but of course, the differences constitute a normal process by definition. This is a major reason why the $\overline{y}(t)$ play such a large role in comparison with the x(t) which are the values one measures directly. By using differences one gets rid of not only systematics but a RW as well.

An actual clock performance as shown in fig. 2 (which gives the $\overline{y}(1^d)$ of Cs 571) exhibits always some systematic disturbances in addition and the clock errors are therefore much larger. In addition to a linear trend of +1.5 x 10^{-13} p.a. which has been removed, we see that there is some obvious correlation in the frequency residuals. It is this tendency of frequency variations to persist for a while which produces a dispersion of the time error which is greater than in the case of purely random FM.

It will be clear at this point that

- (1) The measures of clock performance based on sampling (table 1) become less sensitive to long term trends as higher differences are used for the analysis.
- (2) It would be most desirable to agree on a standard way to reduce the data to a clock performance measure which is related to the application of clocks rather than to adopt procedures such as those which led to formulae (14) and (15).

The statements (1) and (2) are in mutual conflict only at first sight because in almost all cases we do not need to go to higher than second differences if we take off any long-term trends first. This allows us to satisfy the requirement (2) in the most straightforward way.

A. Elimination of Trends

There are three main classes of approximating functions which we can consider viz.

- (1) Polynomials in t (or k) of degree m,
- (2) Fourier Series,

(3) Exponential Functions, $\sum_{i}^{-a_i t} e^{-a_i t}$

All of these transform into another function of the same kind (they are class conservative) under a transformation $t\to t+k$, i.e. we can assume that there is no special origin inherent to the problem. If any singularity is present in the record then one can't use these functions, at least not for the whole range. In the case of clock records we are not so much concerned with genuine singularities. But often we see breaks in clock rate due to a specific but usually unknown disturbance. The most natural way to handle such cases is to break the record at these points and to use a particular function for the approximation of each undisturbed part. The simplest case would be the approximation of a clock with pieces of straight lines. This can usually be done with the $\overline{y}(k)$.

Only class (1) is class conservative also under the transformation $t\to kt$. This class is therefore of major importance if no natural scale is inherent in the problem. For an extensive discussion of approximation with these mathematical functions cf. Hamming (1962). For these reasons clocks have been approximated with polynomials in the overwhelming number of cases. Quadratic and cubic polynomials are usual for the $\overline{y}(k)$ and the x(k) of crystal clocks (the cubic is to account for a changing frequency drift due to aging). For the mathematics of polynomial approximation cf. Jordan (1965) if one does not have a "canned" computer or calculator program available.

It is clear that by increasing the degree of the polynomial one can reduce the variance of the residuals but there is an absolutely essential point to be kept in mind. Any attempt to absorb the random variations in a mathematical model with a complexity greater than what is necessary for the elimination of the genuine long-term trend will lead to completely illusory gains. An apparent slight decrease of the variance of the residuals will have been obtained at the price of a representation of the trends which is useless and even dangerous for any amount of extrapolation. The same danger exists if a clear break due to a real clock disturbance occurs and is not recognized as such but incorporated into a greater complexity of the clock model. Eighth and higher degree polynomials have been used for long term clock modeling instead of breaking up the record into pieces which can be fitted with a low order polynomial. This is fundamentally wrong and dangerous. Similar is the principle of parsimony (Box & Jenkins, 1970).

However, the elimination of trends is usually extremely simple. Of greatest importance is the recognition of breaks or steps in the record. In most cases we will then find a more or less linear drift of frequency which can easily be subtracted from the record. In some cases the elimination of trends is a tricky problem and it is wise to be conservative and to take off only the most obvious overall trend instead of trying to be sophisticated. In that case one is likely to end up with a mathematical model for the low Fourier frequency components of the random part of the frequency variations.

Of course, the problem, if there is any, can always be solved by going to higher differences. Such a filtering (1st order differences) is already being done automatically by using frequency instead of phase records for evaluation. This brings us one step closer to the goal of stationarity which produces stable measures. But this is of major importance mainly in clock modeling for purposes of prediction and much less so for the characterization of performance as needed for specifications, testing etc. It is a main benefit of the pair variance that it uses second differences thereby avoiding most of the problems mentioned while still giving an objective reproducible measure which is closely related to at least one important class of applications.

B. Random Process Characterization

Assume that we have freed our record from obvious trends. A natural question will be whether the residuals x'(t) will now be purely random and/or stationary. Particularly the stationarity question has plagued the discussions because of a number of frequent misunderstandings. First we must realize that no natural process can be assumed stationary in the sense that its statistical measures are independent of time. The universe does not allow any process to go on indefinitely, therefore life time limitations and aging phenomena are commonplace. Stationarity can only be a property of models as it was pointed out so emphatically by Barnes (1976) and Barnes et al (1971). The question must then be asked whether and how one can apply stationary models.

Let us consider an example: Fig. 3 gives the daily frequencies of clock 837 after removal of a linear frequency drift of -7.2×10^{-13} p.a., in a record of more than 900 days. We can see two types of non-stationarity quite clearly:

- (i) a residual long-term frequency variation of systematic character (non-stationarity of $\mu)$ and
- (ii) an increase in the frequency variations from day to day (non-stationarity in σ^2).

If we really want to characterize fully the behavior of this clock then we must display the record as it is given in fig. 3. Any other measure of frequency stability characterization can only be done by compacting data. But this is a euphemism, we actually must throw data away. I say that after drift removal the sample variance is 4.4×10^{-26} $(\sigma = 2.1 \times 10^{-13})$ then this will give only a very general idea of the overall variations and it will be too pessimistic for most purposes. The day to day variations are really much smaller. In contrast to the sample variance which is rather useless in such a case, the pair sigma (corresponding to the two sample Allan variance) is more realistically tuned to what is useful in a time keeping application. It is only $\sigma_{\nu}(1^{\rm d}) = 4.5 \times 10^{-14}$. This datum will be even more useful if we add the explanation that this is an average value, that the sigma is better for the first two years of operation and is getting worse now. Therefore we must also realize that the stability measures have a time variability. This adds a significant complication to the problem of stability measures. We interpret our samples as pieces of stationary time series models and we state the model parameters as they change with the samples which come from later dates (when the clock ages). Since the samples are necessarily limited in time, our confidence in the statistics must be limited also (cf. Lesage and Audoin, 1973). But there is no point at all in insisting on hairsplitting perfection which is of no concern in practice since we don't have perennial clocks.

THE AUTOCOVARIANCE AND THE SPECTRAL DENSITY

As we could see in the last example, the frequency residuals $\overline{y}'(t)$ can be correlated in time (fig. 3). A purely random (uncorrelated, normal) process is easy to characterize with its mean μ and the variance σ^2 . A process with correlated distribunces z(k) can be characterized by its sample mean $\hat{\mu}$ (we use the "hat" to distinguish the estimates from the ideal population parameters):

$$\hat{\mu} = \frac{1}{n} \cdot \sum_{k=1}^{n} z(k) = \overline{z}$$
 (20)

and the autocovariance (acvf) for lag u:

$$c(u) = \frac{1}{n} \cdot \sum_{j=u+1}^{n} (z_j - \overline{z}) (z_{j-u} - \overline{z}) = \hat{\gamma}(u)$$
 (21)

and we see immediately that

$$c(0) = \hat{\sigma}^2 \tag{22}$$

The acvf is the average lagged product of the deviations from the mean and can therefore be interpreted as a quantity which originates from the variance but which is "spread out" into the lag axis. For any precision in the estimates it is clear that n will need to be large and in general will be n > 50. The normalized acvf is known as the autocorrelation function (acf) $\rho(u)$:

$$\rho(u) = \frac{\gamma(u)}{\gamma(0)} = \frac{1}{\sigma^2} \gamma(u)$$
 (23)

Obviously the c(u) or the r(u) = $\hat{\rho}(u)$ cannot be estimated confidently for greater lags than a fraction of n and in practice one should stay within u < n/2. (Jenkins and Watts recommend u < $\frac{n}{10}$). Completely random uncorrelated disturbances will have an acf which drops to zero for any u ≥ 1 . In contrast we see that actual clocks show a $r_{\overline{y}}(u)$ which indicates significant correlation for lags of many days (figs. 4 and 5). Indeed the acvf of $\overline{y}(\tau)$ gives most of the significant information of interest but it does not give it in a form which is best suited for further analysis. That is available in the Fourier transform of the acvf, the (one-sided) spectral density of the \overline{y} :

$$S_{\overline{y}}(f) = 4 \int_{0}^{\infty} \gamma(u) \cos(2\pi f \cdot u) du$$
 (24)

Since the S(f) and the acvf are a Fourier transform pair we also can go backwards to the acvf once we know the S(f):

$$\gamma_{\overline{y}}(u) = \int_{0}^{\infty} S_{\overline{y}}(f) \cos(2\pi f \cdot u) df$$
 (25)

A consequence of this last formula is

$$\gamma_{\overline{y}}(0) = \sigma^2_{\overline{y}} = \int_0^\infty S_{\overline{y}}(f)df$$
 (26)

which explains S(f) as a variance density function of Fourier frequency. Its dimension is therefore variance per Hz. One must not be misled by these simple and transparent relationships. S(f) is not directly available but must be computed from a finite sample. This can be a tricky process and Jenkins and Watts (1968) or similar references must be consulted for guidance on details. Figs. 6 and 7 show examples of $\hat{S}_{\overline{y}}(f)$ computed, however, from the acf which normalizes the plots to a $\sigma^2 = 1$.

A special caveat concerns the role of τ . For each value chosen, $\gamma_{\overline{y}}(u)$ and $S_{\overline{y}}(f)$ will be different as can be seen from (26) but also because of the measurement resolution which changes with τ . The essential point is, however, that sampling the frequency for an interval τ corresponds to a convolution with a rectangular time window. This is transformed into the frequency domain as a factor

$$K = \frac{\sin^2(\pi f \tau)}{(\pi f \tau)^2} \tag{27}$$

so that the spectral density of $\overline{y}_{\tau}(K)$ is really obtained from the spectral density of y, the instantaneous relative frequency departure, by multiplication with K:

$$S_{\overline{y}}(f) = S_{y}(f) \cdot K \tag{28}$$

A second factor K' is needed if we want to compute an estimated variance for a sample of finite data length. As explained by Cutler and Searle (1966) in great detail (their paper is indispensable for an understanding of details, unfortunately it is full of annoying misprints), sampling for a total time $n \cdot h$, cf. table l, and removing the drift and average (i.e. our elimination of systematics) corresponds to a high pass filtering with two zeros and a cutoff frequency

$$f_1 = 1/nh_{\pi} \tag{29}$$

1 :

Therefore the variance in such a sample must be expected to be smaller than the true variance. The computation achieves this with the factor

$$K' = 1 - (\sin^2 f n h_{\pi}) / (f n h_{\pi})^2$$
 (30)

and we obtain

$$\sigma_{\overline{y}}^{2}(h) = \int_{0}^{\infty} S_{y}(f) \cdot K \cdot K' \cdot df$$
 (31)

The high pass filter action of K' can usually (if we have removed the systematics) be approximated by a low frequency cutoff on the integral

$$\sigma_{\overline{y}}^{2}(h) \sim \int_{1/nh\pi}^{\infty} S_{y}(f) \cdot K \cdot df$$
 (32)

A method of obtaining $\hat{\sigma}$ from the frequency domain without sampling and digital analysis is actually based on this formula (Rutman, 1974, Rutman and Sauvage 1974).

On the other hand if we consider how we actually obtain our estimate of $S_{\overline{y}}(f)$, the $\hat{S}_{\overline{y}}(f)$, then the situation is somehow the reverse of what we have just discussed. Data acquisition for a total time h·n corresponds to a convolution of the true S(f) with a filter function $Q_C(f)$ which is the Fourier transform of the time window (the Hanning or Hamming etc. which we perform on the acvf). Therefore the true S(f) differs from the estimate $\hat{S}(f)$ which we compute:

$$E[\hat{S}] = SQ_{C}(f)$$
 (Qualifies convolution) (33)

The effect of this is a blurring of the details of S(f), making it impossible to resolve details finer than $\Delta f \sim 1/nh\pi$.

Since $S_y(f)$ is of such fundamental importance for frequency stability considerations, the accepted terminology concerning types of clock erratics often refers to it. As an important example we mention white FM, completely uncorrelated frequency disturbances, which is characterized by a $S_y(f)$ = constant between the practical limits f_L and f_h given by record length and sample interval. We have

$$f_h = 1/2h \tag{34}$$

This is related to the sampling theorem which one must also keep in mind in regard to the danger of aliasing. If the sampled process contains substantial noise at or above f_h then special filtering is advisable (cf. Baugh 1971).

GENERAL COMMENTS ON THE USE OF STATIONARY MODELS:

If z(t) (which could be a model for our x, y or any of the ∇ 's) is stationary then $\Upsilon(u)$ is an even function and the probability distribution function P(z) (pdf) is time invariant.

If z(t) is "wide sense" stationary then μ is constant and $\gamma(u)$ is only a function of u .

If z(t) is stationary and ergodic then the ensemble (stochastic) average μ is equal to the time average $\overline{z(t)}$:

$$\mu = \overline{z(t)} = \lim_{T \to \infty} \frac{1}{2T} \int_{-T}^{T} z(t)dt$$
 (35)

If we have done a sufficient job with the removal or filtering of the systematics then our averages will remain stable regardless of which part of the record we select for estimating the average:

$$\hat{\mu}(N,i) = \frac{1}{N+1} \sum_{k=i}^{i+N} z(k)$$
(36)

will be nearly constant if N is sufficiently large.

A large power of S(f) at low frequencies f is typical for trends which have not been removed (cf. figs. 3 and 7). Barnes (1976) gives an excellent discussion that in such cases the experimenter cannot make believable statistical estimates. Many learned arguments about what happens at f = 0 have simply overlooked the fact that as one runs out of data, one also loses the justification for the use of statistics. This is the real meaning of the distinction of trends from the higher frequency noise which alone is the genuine raw material for statistics. But there is also this other aspect of the separation. Most applications are concerned only with clock properties for time intervals which are shorter than a certain limit of usefulness given by the nature of the problem (e.g. re-synchronization interval, or time constant in a feedback loop etc.). Therefore measures, in order to be useful, must have been freed from long term effects (Barnes & Allan, 1964).

DISTRIBUTION OF THE y(k)

It was obvious from some of the previous examples that the actual $\overline{y}(k)$ may not be Gaussian distributed. If z be again a representative random variable, p(z) the probability density function and P(z) the probability distribution function then we have, of course,

$$P(z) \approx \int_{-\infty}^{z} p(z)dz \quad \text{and} \quad \int_{-\infty}^{\infty} p(z)dz = 1$$
 (37)

One can plot the P(z) as a function of the magnitude of the deviation preferably expressed in units of σ . Figs. 8 and 9 give an estimate of P(\overline{y}_{1d}) of our two representative cesium clocks 571 and 837. One notes the non-normal nature of the erratics of 837. Such plots seem to have only very limited usefulness compared with the plot of $\overline{y}(t)$ itself.

THE PAIR VARIANCE (TWO SAMPLE ALLAN VARIANCE)

In our examples which showed actual clock behavior (Cs 571 and 837) we could see that even in the absence of long-term trends, the determiniation of the estimates of variance $(\hat{\sigma}^2)$ depends on the number of samples taken. It was therefore proposed by Barnes and Allan (1964) to use N = 2 samples for a variance determination and to average over many such groups to improve the estimate. Such grouping produces a variance which is the limiting case of a sample variance and one idea would be to simply standardize the procedure to N = 2. However, this pair variance has additional benefits. The general sample variance depends not only on the number N but also on any deadtime T between frequency measurements and Allan (1966) introduced the notation $\sigma^2(N,T,\tau)$ for this general sample variance. In our case of x(t) sampling we have, of course, no deadtime between frequency measurements because we can compute the $\overline{y}_{\tau=kh}$, cf. our equation (10), for any selected sequence of measurements. Since the pair variance is developed by Allan as the limit for N = 2 of the general sample variance, it contains a factor of 2 in the denominator which is the only difference from the mean square successive difference of \overline{y} . The mean square successive difference was used already by von Neumann and others (1941) for the characterization of processes with a drift such as it was encountered in ballistic testing.

Allan has also introduced a variance ratio $\boldsymbol{\chi}$ (we assume zero deadtime:

$$\chi(N,\tau) = \frac{\sigma^2(N,\tau)}{\sigma^2(2,\tau)} \text{ (later also denoted } B_1(N,\mu))$$
 (38)

For purely random noise χ = 1, and this allows an easy check for the noise type present in one's data. For details one should consult Allan (1966) but it must be kept in mind that the utility of χ is primarily limited in usefulness to cases where "power law" noises predominate. We can see this from the following relationships:

$$\hat{\sigma}_{\mathbf{y}}^{2}(2,\tau) = \frac{k=n}{k=2} \sum_{k=2}^{k=n} (\overline{y}_{k} - \overline{y}_{k-1})^{2}$$
(39)

which for large n becomes approximately

$$\hat{\sigma}_{\mathbf{y}}^{2}(2,\tau) = \frac{1}{n} \sum_{k=1}^{n} \overline{y}_{k}^{2} - \frac{1}{n-1} \sum_{k=2}^{n} \overline{y}_{k} \overline{y}_{k-1}$$

$$(40)$$

If $\mu(y)$ is assumed to be zero then the first term will be the estimated variance and the second the estimated acvf for a lag of 1 (which is τ , if expressed in s):

$$\sigma_{\overline{y}}^{2}(2,\tau) = \sigma^{2}[\overline{y}(\tau)] - c_{\overline{y}}(1)$$
 (41)

since $c(u) = r(u)\hat{\sigma}^2$ we obtain as a useful approximation for large samples

$$\chi(N,\tau) \sim \frac{1}{1-r_{y}(1)} \tag{42}$$

We can see that Allan's variance ratio can be related easily to the beginning of the autocorrelation function. Considering the great simplicity of the concept and the computation of $\chi(N,\tau)$, if we restrict ourselves to the case N=n and no deadtime, it is a very useful tool in the set of the various stability measures. The pair variance $\hat{\sigma}_{\overline{V}}^2(\tau)$

which is a short hand notation for $\hat{\sigma}_{\overline{y}}^2(2,\tau)$ and much more so the pair

sigma $\hat{\sigma}_y(\tau)$ have become a standard for frequency stability specifications and measurements for averaging times greater than about Is because it is the simplest quantity to measure and it is relatively insensitive to the choice of measurement circumstances. It provides an objective measure even in the presence of some systematics in the record because it uses second differences of phase as we saw in our equation (19). In practice, the incentive to go to more sophisticated aggregates of the $\nabla^m(k)$ for $m \geq 2$ has been rarely given in view of what we said before about the necessary removal of systematics.

An excellent characterization of oscillator performance can be given in the form of sigma-tau double logarithmic plots as shown for our two Cesium clocks 571 and 837 in figs. 10 and 11. In the case of Cs 837 we can see the effect of the systematic variations in an upswing of the graph for large tau's.

MEASURES IN THE FREQUENCY DOMAIN

Up to now we have used the x(t) measures as basis for our performance characterization; we operated in the time domain and did or did not transform our results also into the frequency domain to obtain $S_v(f)$. However, for about f > 1 Hz, such measures can also be obtained directly. Since we are now dealing with relatively fast phenomena, the problem of removal of the systematics can be easily circumvented by phaselocking the oscillators together. This assures that $\phi(\mathsf{t})$ and $\dot{\phi}(\mathsf{t})$ will only vary around zero. The phaselock loop (PLL) can act as a frequency or as a phasedetector. If the time constant of the PLL is τ_1 then the error signal will be proportional to the phase error $\phi(t)$ for times $\tau << \tau_1$ and proportional to $\dot{\phi}(t)$ for $\tau >> \tau_1$. We can assume that the phase detector is operated in its linear range. A narrow-band low frequency spectrum analyzer or wave analyzer is used to scan the PLL error signal for the AC power which is contained as a function of (Fourier) frequency f. We obtain directly the sideband power of the phase or frequency variations depending on the choice of the PLL time constant. Of course, the various measures are closely interrelated (cf. table 2). However, in contrast to the long-term measures where one prefers $S_{V}(f)$ for the reasons discussed, here $S_{\phi}(f)$ is more popular because most oscillators are dominated by white phase noise in a large part of the spectrum and this gives a horizontal line in S_{ϕ} . Also in the applications, phase noise is the more fundamental concept and $S_{\phi}(f)$ is more closely related to what is measurable in the laboratory. The unit of $S_\phi(f)$ is again a variance (now in radians²) per Hz. The sideband power can also be directly expressed as a ratio in terms of the (Suppressed) carrier in db.

Therefore, we see three different phase-time spectral densities in use today: $S_X(f)$ is the time error spectral density which is independent of the signal frequency F. $S_{\varphi}(f)$ is the phase error spectral density which increases with the square of F. Finally, $\mathcal{K}(f)$ is defined variously as the single sideband to carrier power ratio per Hz in the RF spectrum assuming negligible AM. The ratio is also often given in respect to total power with little practical difference for high performance oscillators. In the latter case one can speak of a normalized density measure since the integral over the total RF spectrum (which in f-measure goes from -F to $+\infty$, since f is centered on the carrier) must be one:

$$\int_{-F}^{\infty} (f)df = 1$$
 (43)

 \gtrsim (f) was used by NBS for some time but there is general agreement today that $S_{\varphi}(f)$ is more clearly defined and more directly related to what can be measured with the usual test set-up. For small phase deviations (φ << 1 rad) we may use as an excellent approximation

$$\approx (f) = \frac{1}{2} S_{\phi}(f) \tag{44}$$

A PLL phase detector output voltage V_p (we assume $\tau_L >> \frac{1}{f}$) can be converted into the phase error (assuming the signal is kept in quadrature with the reference which is assumed noise free)

$$\phi = \frac{V_p}{V/rad} \tag{45}$$

where V/rad is the phase detector sensitivity to phase errors. The variance of ϕ at the wave analyzer setting f is per Hz:

$$\hat{S}_{\phi}(f) = \left(\frac{V_{p,rms}}{V/rad}\right)^{2}/Hz$$
 (46)

If the signal frequency is measured after a frequency multiplication of m times then $S_{\phi}(f)$ will be increased by m^2 (its db measure will increase by 20 log m).

Example: Two equal quartz crystal oscillators with a 5 MHz output are being measured at 25 MHz (m = 5) and we assume a phase detector sensitivity of 2V/rad. We measure with a wave analyzer of 1 Hz bandwidth a rms voltage of 200 nV at 100 Hz. This will give for one oscillator at 5 MHz a

$$\hat{S}_{\phi}$$
 (100 Hz) = - 140 db - 14 db - 3 db (2 oscillators)
= - 157 db/Hz

For more details cf. Howe (1976) and Shoaf et al (1973). Practical questions are discussed by M. Fischer (this volume).

Note: We have used only one-sided spectral densities S (with 0 \leq f \leq ∞). Two sided spectral densities S are more popular in theoretical work (where f goes from - ∞ to + ∞). We have

$$\underline{S} = \frac{1}{2} S \quad \text{and}$$

$$\int_{-\infty}^{\infty} \underline{S}(f) df = \int_{0}^{\infty} S(f) df$$
(47)

RANDOM PROCESS MODELING AND FORECASTING

Given a white noise process a_k with zero mean and (constant) variance $\sigma_{\bf a}^2$ we can ask how a more complicated process Z_k such as observed in the $\overline{y}(k)$ of clocks can be simulated on a digital computer. Box and Jenkins (1970) discuss several classes of models:

a) The Moving Average (MA) of order q is given by

$$Z_k = a_k + o_1 a_{k-1} + o_2 a_{k-2} + \dots + o_q a_{k-q}$$
 (48)

which can be written with the aid of our operator notation

$$Z_k = \Theta(B)a_k \text{ with } \Theta(B) = 1 + \Theta_1B + \dots + \Theta_qB^q$$
 (49)

where ⊙(B) is the MA operator.

For finite q this process is always stationary.

b) The Autoregressive Process of order p (AR) is

$$Z_k = \Phi Z_{k-1} + \dots + \Phi_p Z_{k-p} + a_k$$
 (50)

which in our short hand becomes

$$(1 - \phi_1 B - \dots - \phi_p B^p) Z_k = a_k \text{ or } \phi(B) Z_k = a_k$$
 (51)

where $\varphi(B)$ is the AR operator. The magnitude and sign of the $\varphi_{\mathbf{i}}$ determines the degree of internal correlation of the process and it is seen that a large variety of processes can be obtained since e.g. for large i and large positive $\varphi_{\mathbf{i}}$ a low frequency component of S(f)

results, whereas large negative coefficients at small i must produce high frequency components.

c) A mixed model can combine the AR with a MA to represent an $\ensuremath{\mathsf{ARMA}}$ model

$$\Phi(B)Z_k = \Theta(B)a_k \tag{52}$$

With such a model almost any spectrum can be obtained.

d) This process can be further modified to include integration (which produces a random walk type behavior in the Z_k) by modeling a difference of the process. This could be written as the <u>ARIMA</u> model of order (p, d, q)

$$\Phi(B) \nabla^{d} Z_{k} = \Theta(B) a_{k}$$
 (53)

We note that we have a stochastic trend of order d if $\nabla^d Z_k$ is stationary. In the presence of such trends, differencing reduces $\sigma^i(\nabla^i Z)$ to a minimum for ∇^d then it increases again (cf our formulae 6 and 12). This leads to our discussion around equations 14 and 15.

An equivalent formulation would be to model a random variable \mathbf{w}_{k}

$$\Phi(B)w_k = \Theta(B)a_k \tag{54}$$

and then to sum the $w_k d$ times to obtain the Z_k .

Now assume that we have found a reasonably simple model which produces clock noise of the same kind (with the same measures such as the acvf, \$, etc) as observed in the clock under test. Assume that a sufficiently long series of clock data is available and has been represented by our model Z_k up to time k. We call the $\mathring{Z}_k(\aleph)$ the forecast at k for a lead of \aleph . Under the assumption that the errors in the estimated model parameters are small and that the model remains unchanged in the future, a so-called optimum forecast can be obtained (optimum on a minimum mean square error basis):

$$E \left[Z(k + \ell) - \hat{Z}_{k}(\ell) \right]^{2} = \min.$$
 (55)

However, in practice these assumptions are rarely valid. Box and Jenkins (1970) emphasize these points:

a) It is essential to separate trends before modeling.

b) When the model is not adequate, simple visual extrapolation is the best method of forecasting.

One may also note that the above approach is completely equivalent to the "filter" approach as sketched in fig. 12. The coefficients of the digital filter (as well as the operators Φ & Θ) contain the same information as the spectral density S(f). However, as Barnes (1976) emphasizes, it is easy to go from the filter and the model to S(f) and to a time domain measure such as $\sigma_y(\tau)$ but the opposite is not possible, at least in the general case.

In summary it must be stressed that any theoretical basis available must be utilized for the removal of systematics instead of building models which are solely based on purely statistical fits. This is true even if the theoretical ideas are most general which may still be sufficient, e.g., to explain the puzzling flicker noise (cf. Percival, 1976).

Models have an important place in diagnostics, simulation and systems optimization. In this regard, Box and Jenkins (1970) also discuss the estimation of a system's transfer function from an available model.

CONCLUSIONS AND RECOMMENDATIONS

In order to obtain sound measures of clock performance it is necessary to:

- a) Specify the conditions of measurement such as f_h , the systems bandwidth; n, the number of measurements; F, the frequency of the signal; T, dead time if any, in the case of frequency measurements; the experimenters trust in the results if not expressed as confidence based on n; the environmental conditions, etc.
- b) Remove any obvious systematics such as drifts and state them separately <u>before</u> the random part of the clock performance (the erratics) is analyzed. Failure to do so leads to unnecessary complications and often to erroneous results.
- c) Determine and state, if possible, the environmental sensitivity in coefficients of sensitivity to pressure, temperature, vibration, acceleration, magnetic field, etc.
- d) State the clock erratics in the same language (time or frequency domain) in which the needs can be identified. A conversion is possible but problematic, particularly from time domain to frequency domain.

For the important case of power law spectra, conversion can be accomplished by means of Table 2. State any observed time dependency of the statistics.

- 1) <u>Time Domain</u>. The two sample Allan variance $\sigma_y^2(\tau)$ (or rather the "pair" sigma $\sigma_y(\tau)$) has become a de facto standard. A double log plot of $\sigma_y(\tau)$ contains most of the information of possible interest in timekeeping. The practical range is for $\tau > 1s$.
- 2) Frequency Domain. For τ < 1s it is generally easier and more reliable to determine $S_{\varphi}(f)$ directly with a phase detector and wave analyzer. $\varkappa(f)$ which is often used, is a practically equivalent measure; it "looks better" for a given oscillator by 3 db. $S_{\varphi}(f)$ is the recommended measure.

ACKNOWLEDGEMENT

I am obliged to Mr. Dave Allan of National Bureau of Standards, Dr. Len Cutler of Hewlett Packard Company, and Dr. U. Hübner of PTB for valuable comments and suggestions.

REFERENCES

- Allan, D. W. (1966) "Statistics of Atomic Frequency Standards", Proc. IEEE, Vol. 54, pgs 221-230.
- Allan, D. W. (1974) "The Measurement of Frequency and Frequency Stability of Precision Oscillators", Proc. 6th PTTI Planning Meeting, pgs 109-142 and NBS TN 669.
- 3. Audoin, C. and Lesage, P. (1975) "Instabilité de frequence des oscillateurs", L'Onde Electrique, Vol. 55/2, pgs 82-89.
- 4. Barber, R. E. (1971) "Short-Term Frequency Stability of Precision Oscillators", BSTJ, Vol. 50/3. pgs 881-915.
- 5. Barnes, J. A., and Allan, D. W. (1964) "Effects of Long-Term Stability etc.", Proc. IEEE-NASA Symposium on Short-Term Frequency Stability.
- 6. Barnes, J. A. et al (1971) "Characterization of Frequency Stability", IEEE Trans. I&M, Vol. 20/2, pgs 105-120.
- 7. Barnes, J. A. (1976) "Models for the Interpretation of Frequency Stability Measurements", NBS TN 683.

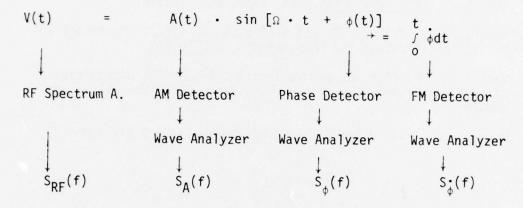
- 8. Baugh, R. A. (1971) "Frequency Modulation Analysis with the Hadamard Variance", Proc. 25th ASFC, pgs 222-225.
- 9. Box, G. E. P. and Jenkins, G. M. (1970) "Time Series Analysis, Forecasting and Control", Holden-Day, San Francisco.
- 10. CCIR Study Group VII Report 580, ITU, Geneva.
- 11. Cutler, L. S. and Searle, C. L. (1966) "Some Aspects of the Theory and Measurement etc.", Proc. IEEE, Vol. 54/2, pgs 136-154.
- 12. Fischer, M. C. (1976) "Frequency Stability Measurement Procedures", Proc. 8th PTTI Planning Meeting.
- 13. Jordan, Ch. (1965) "Calculus of Finite Differences", Chelsea, NY, (CH. VIII).
- 14. Hamming, R. W. (1962) "Numerical Methods for Scientists and Engineers", McGraw-Hill.
- 15. Howe, D. A. (1976) "Frequency Domain Stability Measurements", NBS TN 679.
- 16. Jenkins, G. M. and Watts, D. G. (1968) "Spectral Analysis and its Applications", Holden-Day, San Francisco.
- 17. Kramer, G. (1975) "Digitale Bestimmung von Schwankungsspectren", PTB Jahresbericht Teil II, p. 157.
- 18. Lesage, P. and Audoin, C. (1973) "Uncertainty Due to the Finite Number etc.", IEEE Trans. I&M, Vol. 22, pgs 157-161.
- 19. Lindsey, W. C. and Chie, C. M. (1976) "Theory of Oscillator Instability Based Upon Structure Functions", Proc. IEEE, Dec.
- 20. Loeb, H. W. (1972) "Efficient Data Transformation in Time Domain Spectrometry", IEEE Trans. I&M, Vol. 21/2, pgs 166-158.
- 21. Neumann, J. V., Kent, R. H., Bellison, H. R. and Hart, B. I. (1941)
 "The Mean Square Successive Difference", Annals of Mathematical
 Statistics, Vol. 12, pgs 153-162.
- 22. Percival, D. B. (1976) "A Heuristic Model of Atomic Clock Behavior", Proc. 30th ASFC.
- 23. Rovera, G. (1974) "Stabilità di Frequenza", Editrice Tecnico Scientifica, Pisa, Italy (Obtained from IEN, Torino).

- 24. Rutman, J. (1974) "Relations Between Spectral Purity and Frequency Stability", Proc. 28th ASFC, pgs 160-165.
- 25. Rutman, J. (1974) "Characterization of Frequency Stability", <u>IEEE</u> Trans. I&M, Vol. 23/1, pgs 40-48.
- 26. Rutman, J. and Sauvage, G. (1974) "Measurement of Frequency Stability etc.", IEEE Trans. I&M, Vol. 23/4, pgs 515-518.
- 27. Shoaf, J. H., Halford, D. and Risley, A. S. (1973) "Frequency Stability Specification and Measurement", NBS TN 632.
- 28. Vessot, R., Mueller, L. and Vanier, J. (1966) "The Specification of Oscillator Characteristics etc.", <u>Proc. IEEE</u>, Vol. 54/2, pgs 199-207.
- 29. Wiener, N. (1949) "Time Series", MIT Press (ISBN 0 262 73005 7).

APPENDIX

The Various Uses of Spectrum Analyzers

The output signal of a standard frequency generator can be written as a time varying voltage:



Notes: The center of $S_{RF}(f)$ will be at f = F. ($2\pi F = \Omega$)

The wave analyzer scans from f = 1Hz up to about 100 kHz in most practical applications.

Power Law Noise Models With Their Respective Stability Measures

Table 2

Random Walk FM -2 h ₋₂ /f ²	Flicker FM	White FM	Flicker Phase	White Phase	Noise Type
-2	느	0	_	2	δ
h_2/f ²	-1 h ₋₁ /f	h _o	h ₁ f	2 h ₂ f ²	Spectrum Sy(f) Slope Sx S
-4 -2	-3 -1	-2 0	-1 +1	0 +2	rum Slope S _x S _y
$\frac{4\pi^2}{6} \cdot h_{-2} \cdot \tau$	21n2 · h_1	h ₀ 2·τ	$[3\ln(2\pi f_{h^{\tau}}) + 1.038] \frac{n_1}{(2\pi\tau)^2}$	$\frac{3f_{h} \cdot h_{2}}{4\pi^{2} \cdot \tau^{2}}$	Time Domain $\sigma_{\mathbf{y}}^{2}(\tau)$
3/2	_	1/2		0	σ _x (τ)
3/2 1/2	0	1/2 -1/2 -1		0 -1 -2	Slope $_{\mathbf{y}}^{(\tau)} \sigma_{\mathbf{y}}^{(\tau)} $
_	0	<u>.</u>		-2	E

Notes:

- Slope refers to double logarithmic plots of S(f) or σ (τ) in which the noise types are distinguished as pieces of straight lines with the slope given.
- 2. Allan's (1965) μ corresponds with the parameter μ as it is used here. However, his α is our α - 2 because we refer to S_y instead of $S_X.$ This is the new convention.

Table 2 (Continued)

3.
$$S_{\mathbf{y}}(\mathbf{f}) = (2\pi \mathbf{f})^2 S_{\mathbf{x}}(\mathbf{f}) = \frac{1}{\Omega^2} S_{\phi}^*(\mathbf{f}) = (\frac{\mathbf{f}}{\mathbf{F}})^2 S_{\phi}(\mathbf{f})$$
4. $S_{\phi}(\mathbf{f}) = (\frac{\mathbf{F}}{\mathbf{f}})^2 S_{\mathbf{y}}(\mathbf{f}) = \frac{1}{(2\pi \mathbf{f})^2} S_{\phi}^*(\mathbf{f}) = \Omega^2 S_{\mathbf{x}}(\mathbf{f})$, See also equation (8).

Table 3

Long Term Performance of Ten Cesium Clocks at the USNO

Oscillator	Days	Linear Frequen Drift Removed (Per Year in 1	(After Drift Removed)
Cs 346/1C	1200	+ 3.5	4.0
Cs 532/1C	1200	-	2.9
Cs 549/1	1200	<u>.</u>	2.9
Cs 571/1C-2	1185	+ 1.5	0.7
Cs 591/1	1138	+ 4.1	3.1
Cs 654/1C-2	972	- 4.9	0.8
Cs 660/1C-2	952	-	6.4
Cs 783/1C-2	845	3)	14.2
Cs 834/1C-2	727	-	1.5
Cs 837/1C-2	726	- 7.2	4.4

Notes:

- 1. The data refer to the $\overline{y}(1^d)$ which are measured in reference to A.1(USNO, MEAN).
- 2. The units with a "-2" designation are high performance units (004).
- 3. The large variance of Cs 783/1C-2 is caused by a large non-linear frequency drift which was not removed.
- 4. Dashes indicate that no significant drift was found in a straight line fit.

(Data courtesy of D. Percival, USNO)

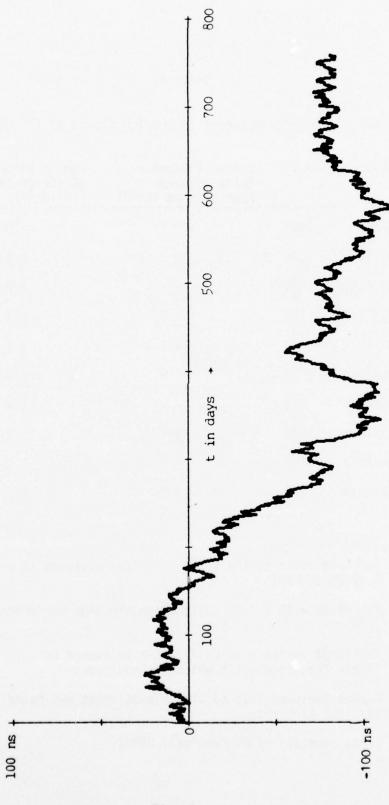
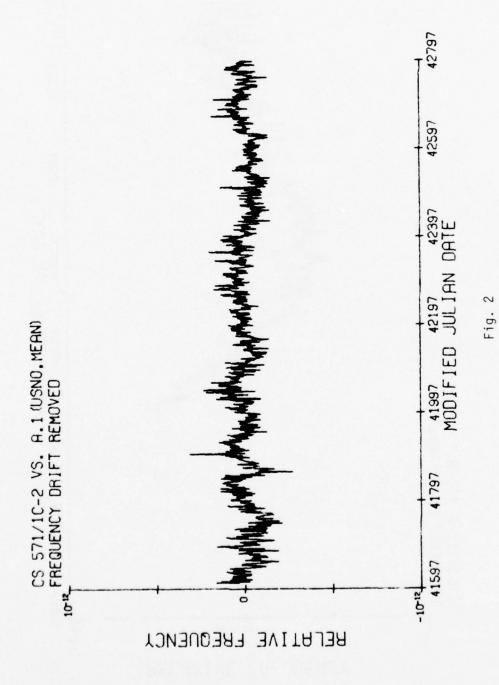


Fig. 1 516



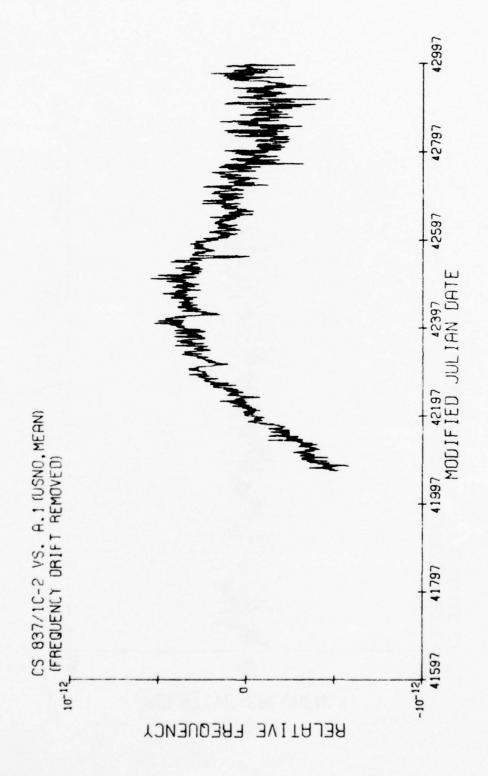


Fig. 3

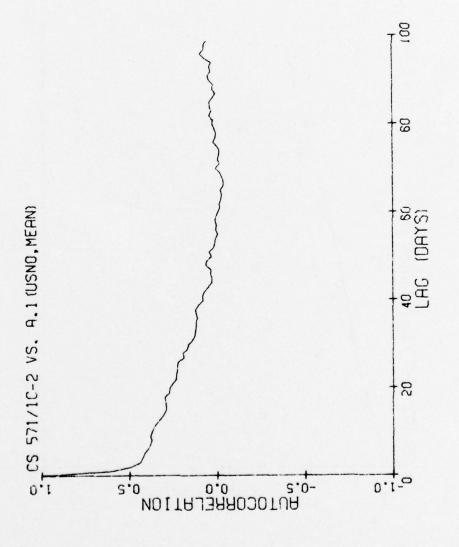
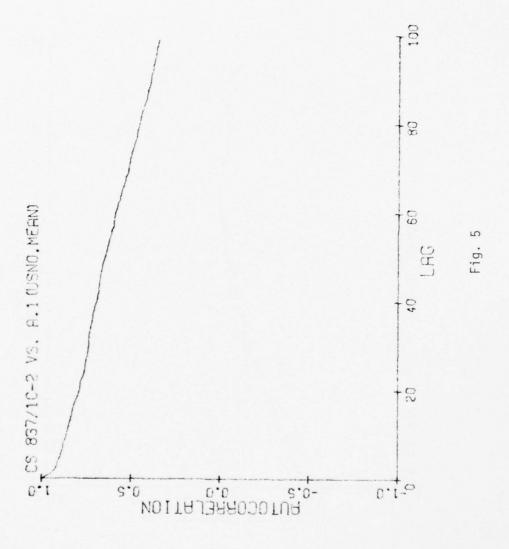


Fig. 4



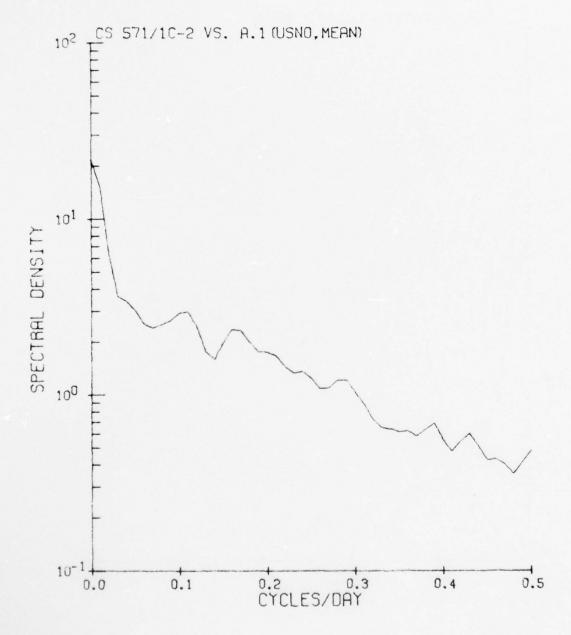


Fig. 6

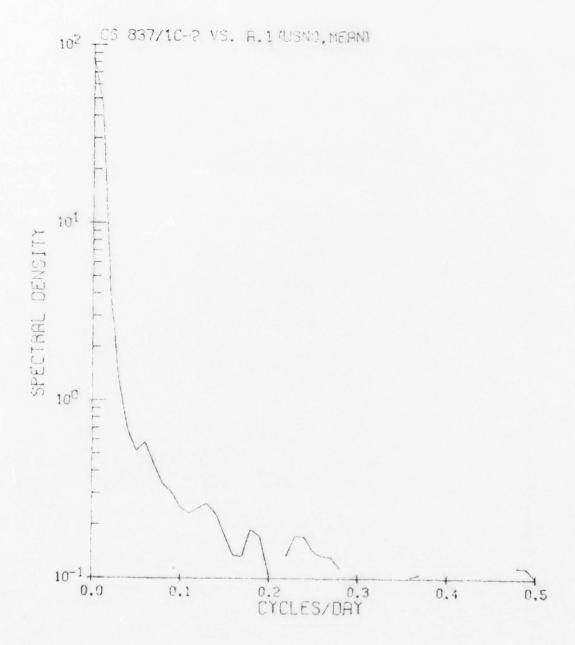
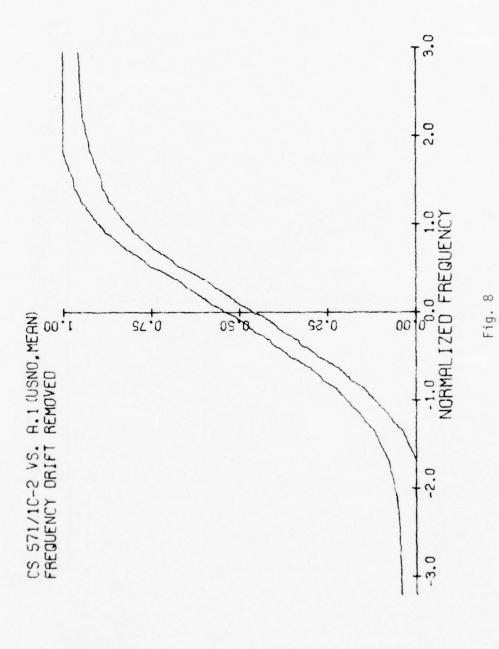
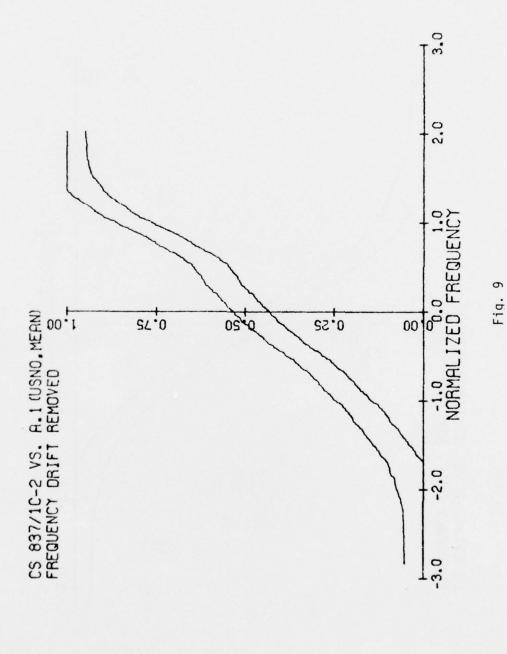
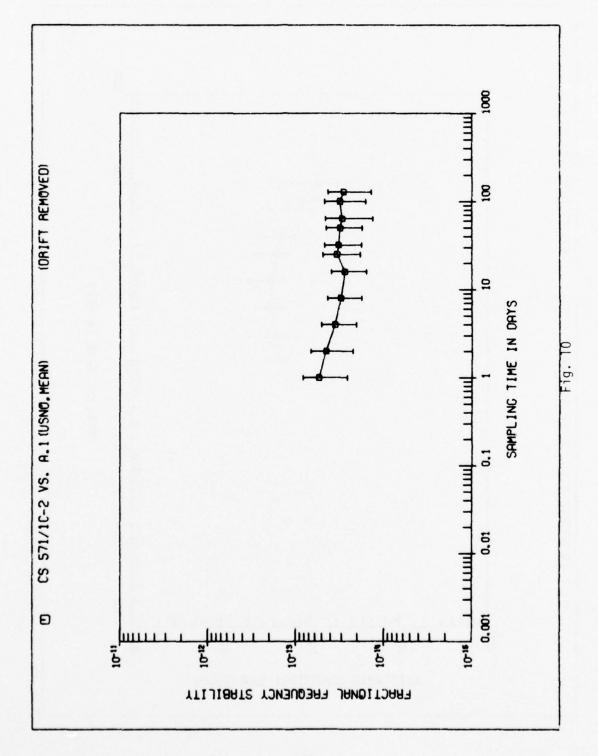
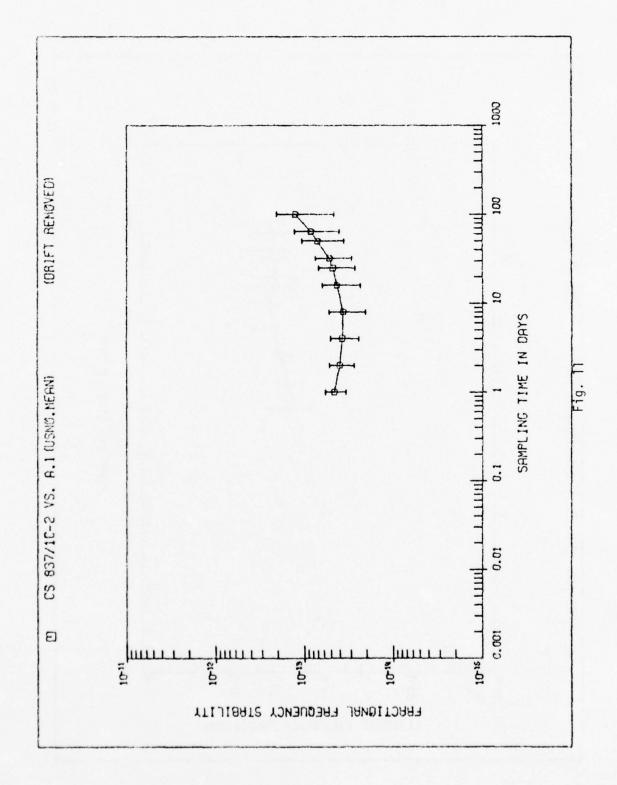


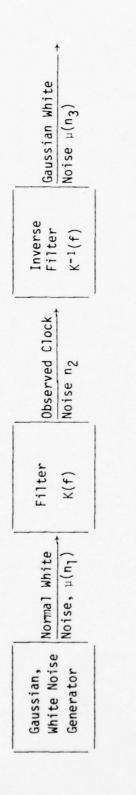
Fig. 7











DATA REDUCTION

CLOCK

Use the mean $\mu(n_3)$ as input to K(f) to obtain an optimum prediction. Use final state of ${\rm K}^{-1}$ for the initial conditions of ${\rm K}({\rm f})$ Procedure: Determine $K^{-1}(f)$ from the data ("whitening") Clock Modeling; The Filter Approach Invert K^{-1} into K(f)

FIRST RESULTS FROM A SATELLITE DATA LINK RADIO INTERFEROMETER

S. H. Knowles, W. B. Waltman E. O. Hulburt Center for Space Research Naval Research Laboratory, Washington, D. C. 20375

> N. W. Broten, D. H. Fort National Research Council Ottawa, Canada

K. I. Kellermann, B. Rayhrer National Radio Astronomy Observatory Green Bank, West Virginia

> J. L. Yen University of Toronto Toronto, Canada

> > and

G. W. Swenson University of Illinois Urbana, Illinois

Since 1967 radio astronomers have been using the Very Long Baseline Interferometer (VLBI) technique to link together radio telescopes separated by continental or intercontinental distances, forming a radio telescope with extremely high resolving power. This high resolving power has had important results in radio astronomy, and is of interest for a wide variety of possible applications including highly precise time transfer, earthquake prediction, and station location. Previous experiments have relied on recording the signals from each antenna on television-type video recorders. This technique has several disadvantages. It is limited in bandwidth and thus sensitivity, cannot produce real-time results and is inherently quite unreliable. In November 1976 our group completed the first successful demonstration of an improved method of operating a long baseline radio interferometer, using * geosynchronous satellite as the connecting data link. The experiment was carried out by an international team of Canadian and American scientists. Large radio astronomy antennas in Lake Traverse, Ontario, and Green Bank, West Virginia were connected via satellite link. The satellite used was the Communications Technology Satellite, a joint Canadian-U.S. effort. As shown

in Figure 1, signals from a cosmic radio source were received at an antenna in West Virginia, retransmitted via a wideband data link to the satellite, which sent them to a receiver at the Ontario antenna where they were correlated with the other received signal. The correlated radio source output was observed in real time on an oscilloscope. Figure 2 is a tracing of such an output for a strong radio source with one minute's integration. The width of the correlation function is about 125 nanoseconds, corresponding to the 10 MHz data bandwidth. The time difference between the two station clocks can be determined to a small fraction of this number.

Figure 3a represents the output as a function of fringe frequency when using hydrogen masers at both stations. For a brief period we replaced one frequency standard with a rubidium standard. The resulting deterioration in fringe frequency stability was easily visible (Figure 3b).

This technique, which allows real-time viewing of interferometer results, makes feasible many extensions of VLBI techniques and is of particular importance for all operational and applied uses of VLBI, including precise time transfer, earthquake prediction, and location of a moving vehicle. In all of these, the laborious and failure-prone use of magnetic tape has proved a major practical handicap. The real-time link also makes possible the simultaneous comparison and analysis of data from several stations by time or frequency multiplexing.

The real-time system also eliminates the artificial restriction placed on signal bandwidth by video tape techniques. The bandwidth of our experimental system, 10 MHz, is five times that of the currently-common "Mark II" video-tape system. Since signal-to-noise ratio for a wideband radio astronomy signal increases as the square root of the bandwidth, this results in a significant improvement. Bandwidths up to 50 MHz are possible using existing digital technology, and data bandwidths much higher yet should eventually be possible using analog correlation.

A further possibility is the development of a true phase-coherent interferometer by a two-way transmission of the local oscillator signal via the satellite, thus enabling compensation for the phase change over the satellite path. With this technique, an angular measurement precision of 10^{-4} arcseconds should be possible. This is of importance to radio astrometry and to measurements of Universal Time. We are currently developing equipment for such an experiment.

Low cost is vital to the successful use of this system by scientists. The preliminary experiment reported here was made possible by the granting of time on the CTS satellite by the Canadian Department of Communications. It is hoped that the coming Space Shuttle low-cost satellite era will permit more permanent arrangements to be made.

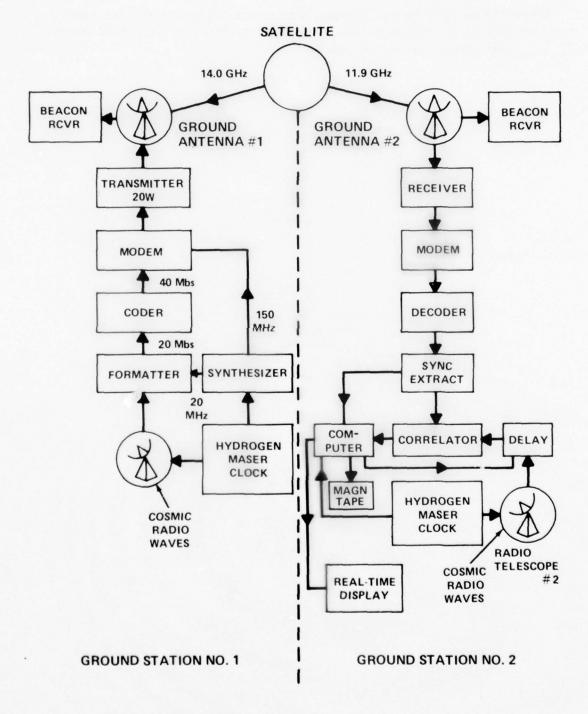


Figure 1. Satellite-Link Interferometer Block Diagram

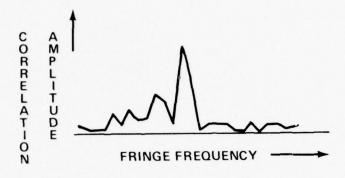


Figure 2. Correlation Amplitude vs. Delay

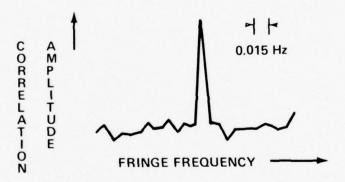


Figure 3a. Correlation Amplitude vs. Fringe Frequency --Hydrogen Masers

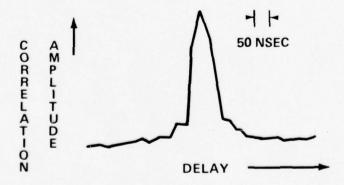


Figure 3b. Correlation Amplitude vs. Fringe Frequency --Rubidium Standard and Hydrogen Maser

INTERPRETATION AND APPLICATION OF OSCILLATOR INSTABILITY MEASURES USING STRUCTURE FUNCTIONS

W. C. Lindsey and C. M. Chie University of Southern California Department of Electrical Engineering Los Angeles, California 90007

W. E. Leavitt Naval Research Laboratory Washington, D.C. 20375

ABSTRACT

This paper is written to cast further light on issues associated with contemporary frequency and phase stability measures of an oscillator. This is accomplished by generalizing known and accepted τ -domain measures of stability through the use of Kolgomorov structure functions. Two sets of stability functions (τ -domain stability measures) are presented and it is shown how they are related to the rms fractional frequency deviation and the two-sample Allan variance. It is further shown that these τ -domain measures of oscillator instability are uniquely related to the f-domain measure $S_{\mathbf{v}}(f)$ by means of the Mellin transform.

Applications of these stability functions to specifying and predicting performance of coherent communication systems, one-way and two-way Doppler measuring, and ranging systems is used in order to emphasize the utility of the theory.

I. INTRODUCTION

A problem of current interest to statistical communication theorists, communication and radar system design engineers and other working groups, see Fig. 1,

This work was supported by LinCom Corporation under NRL Contract N000123-75-C0481. It was also supported by the Office of Naval Research under ONR No. N-00014-75-C-0519.

is that of specifying and selecting accurate and stable frequency generators for use in the implementation of radar, communication, navigation, and time service systems. Certain users of frequency generators have had to face, for the most part, the deleterious effects which oscillator instability produces upon system performance by "seat-of-the-pants" engineering. At the same time the users of frequency generators frequently ask the question: What are the stability requirements of the frequency generator(s) needed in a particular application?

In fact, it appears at present that those involved with the process of manufacturing atomic time standards, and electronic time bases have been largely concerned with the characterization of oscillator instability from the viewpoint of developing accurate and stable clocks [1], [2], [3]. This working group has measured the stability of oscillators and compared the measurements with frequency stability measures [1], [2] and suggested mathematical models [1], [2], [4] of the oscillator. On the other hand, statistical communication and radar theorists [5], [6], for the most part, have been developing mathematical models for communication, radar and tracking systems by assuming the availability of ideal (perfect sine wave) frequency generators. The net result of these disjoint ventures, see Fig. 1, is that not enough emphasis has been placed upon determining how oscillator instability degrades system performance measures or how the frequency stability measures proposed in [1], [2] can be used to assess performance. Presently, there is a real need for this in the design of current systems and planning of advanced systems.

This state of affairs, see Fig. 1, is not uncommon to find in many scientific fields where theory, manufacturing and practice are developed and used by widely dispersed workers. At the present the authors feel that there is a lack of understanding among the users pertaining to the differences between oscillator phase instability and frequency instability. There is also a lack of understanding of how to use accepted frequency instability measures. To some engineers, phase and frequency instability imply the same concept; consequently, one of the main purposes of this paper is to offer a unified mathematically characterization of phase instability (time-base jitter) and frequency instability (frequency-base jitter) of an oscillator and demonstrate the degree of sameness of the two concepts, their interconnections with frequency stability measures [1], [2], and present mathematical

formulations such that certain users can select the appropriate instability measure for their application. It is hoped that this paper will also spur and motivate a closer relationship between the working groups illustrated in Fig. 1 by providing a systematic forum for discussion.

1.1 Organization of the Paper

Structure functions* (SFs) [7] are introduced so that characterization of oscillator instability is established on a sound mathematical basis regardless of the user application. SFs provide a common mechanism by which all working groups can communicate about the instability of frequency generators. Furthermore, they represent stability functions by which system performance can be predicted or a frequency generator selected. SFs are also introduced so that users of frequency generators can see how current frequency standards enter into the performance expressions of modern communication, Doppler and range measuring systems. There are several other reasons why SFs are introduced [8], [9]. The unifying role they play with respect to frequency stability standards is summarized and their use in various applications as a means of defining system performance is given. The concepts of phase instability (time-base jitter) and frequency instability (frequency-base jitter) are introduced via phase and frequency SFs. In addition, T-domain to f-domain and f-domain to T-domain transformations are summarized in terms of Mellin transforms and SFs. Secondly, with the aid of these SFs, alternate interpretations of accepted frequency instability measures [1], [2] and their interconnections are given in hopes that the users will be able to obtain a better understanding of how "oscillator vendor data" can or cannot be used in their particular application. For the sake of brevity, emphasis on the applications have been in the communication and tracking system area.

^{*}Because of their applications, they are called stability functions in the abstract.

Next, we show the important role which the power spectral density (PSD) of the oscillator frequency process plays with respect to several user applications and emphasize (via theory) that it is the key element which is needed to access the deleterious effects which oscillator instability has on the performance of modern communications and tracking systems. In other words, we show that the PSD of the short term frequency instability is needed in order to define appropriate τ -domain system performance measures. For the engineer involved in the design of communication and tracking systems, it appears that the most important τ -domain performance measure is not always the rms fractional frequency deviation or the Allan variance but is application and performance measure (bit error probability, range or range-rate accuracy, etc.) dependent. Various system performance measures for users are presented in order to support this statement.

On the more controversial side, the authors provide discussions which lead to certain questions regarding the interpretation of the so-called rms fractional frequency deviation as a measure of frequency instability; rather the authors feel that it is a measure of phase instabil ity (time-base jitter) of an oscillator and give an interpretation to support this. On the other hand, the two-sample Allan variance has a direct interpretation in terms of frequency instability (frequency-base jitter) and, as such, provides a measure of the frequency instability of an oscillator. Use of these two measures then motivate a mathematical manipulation that shows that frequency and time are not reciprocally related for real world oscillators. User applications of the two measures are given in the system context in order to offer support for the proposed interpretation and their use [10], [11]. This is accomplished by presenting performance measures for ranging, Doppler and coherent communication systems in terms of structure functions of oscillator instability. Finally, we characterize oscillator instability in terms of SFs of the RF oscillation and show the problems which arise when one attempts to use the RF domain for direct measurement of oscillator instability.

- II. STRUCTURE FUNCTIONS (SF) IN OSCILLATOR INSTABILITY THEORY
- 2.1 SF's of the Nth Increment of the Phase and Frequency Noise Process

Let us consider the radian frequency process $\Phi(t)$ of an oscillator which we assume takes the form

$$\frac{\dot{\Phi}(t)}{\Phi(t)} = \underbrace{\frac{\omega_0}{\omega_0}}_{\text{Mean}} + \underbrace{\sum_{k=1}^{N-1} \frac{\Omega_k}{k!} t^k}_{\text{Kel}} + \underbrace{\dot{\psi}(t)}_{\text{Kel}} + \underbrace{\dot{\psi}(t)}_{\text{Cong Term}} + \underbrace{\sum_{k=1}^{N-1} \frac{\Omega_k}{k!} t^k}_{\text{Frequency}} + \underbrace{\dot{\psi}(t)}_{\text{Frequency}} + \underbrace{\dot{\psi}(t)}_{\text{Frequency}} + \underbrace{\dot{\psi}(t)}_{\text{Frequency}} + \underbrace{\dot{\psi}(t)}_{\text{Instability}} + \underbrace{\dot{\psi}(t)}_{\text{Colored}} + \underbrace{\dot{\psi}(t)}_{\text{Instability}} + \underbrace{\dot{\psi}(t)}_{\text{Colored}} + \underbrace{\dot{\psi}(t)}_{\text{Instability}} + \underbrace{\dot{\psi}(t)}_{\text{Colored}} + \underbrace{\dot{\psi}(t)}_{\text{Col$$

where $w_0 = 2\pi f_0$ is assumed to be the constant mean frequency, the Ω_k 's constitute a set of <u>random</u> k^{th} -order frequency drift rate and $\psi(t)$ is a stationary, zero mean random process used to characterize the short term oscillator instability. Integrating (2.1) from 0 to t, we have the oscillator phase noise process

$$\Phi(t) = w_0^t + \sum_{k=2}^{N} \frac{\bigcap_{k=1}^{N} t^k + \left[\psi(t) - \psi(0)\right] + \Phi(0)}{\text{Short Term}}$$
Phase Drift

(2.2)

Consider now the N increment of $\psi(t)$ defined recursively by

$$\Delta^{N_{\psi}}(t;\underline{\tau}^{N}) \stackrel{\Delta}{=} \Delta^{N-1_{\psi}}(t+\tau_{n};\underline{\tau}^{N-1}) - \Delta^{N-1_{\psi}}(t;\underline{\tau}^{N-1})$$
 (2.3)

where $\frac{\tau}{T} \stackrel{k}{\underline{\triangle}} = (\tau_1, \tau_2, \dots, \tau_k)$ is a k-dimensional vector parameter and $\underline{\triangle}\psi(t;\tau_1) \stackrel{k}{\underline{\supseteq}} \psi(t+\tau_1) - \psi(t)$, which is stationary. For the purpose of our discussion, we define the Nth SF of phase instability to be [10]

$$D_{\psi}^{(N)}(\underline{\tau}^{N}) = E\{[\Delta_{N}\psi(t;\underline{\tau}^{N})]^{2}\}$$
 (2.4)

where $E\{\cdot\}$ is the expectation operator in probability theory. When $\tau_k = \tau$, $k = 1, \ldots, N$, we shall denote $D_{\psi}^{(N)}(\underline{\tau}^N)$ by $D_{\psi}^{(N)}(\tau)$. If $S_{\psi}^{\bullet}(\omega)$ is the two-

sided PSD of the process \$\div(t)\$, then [10]

$$D_{\Phi}^{(N)}(\underline{\tau}^{N}) \approx \prod_{k=1}^{N} \tau_{k}^{2} \cdot E\{\Omega_{N-1}^{2}\} + D_{\psi}^{(N)}(\underline{\tau}^{N}) \qquad (2.5)$$

where

$$D_{\psi}^{(n)}(\underline{\tau}^n) = \frac{2^{2n}}{2\pi} \int_{-\infty}^{\infty} \prod_{k=1}^{n} \sin^2(\omega \tau_k/2) \frac{S_{\psi}(\omega)}{\omega^2} d\omega \qquad (2.6)$$

for $n \ge 1$. For M > N, (2.5) reduces to

$$D_{\Phi}^{(M)}(\underline{\tau}^{M}) = D_{\psi}^{(M)}(\underline{\tau}^{M}) \tag{2.7}$$

Analogously, the (N-1) st SF of frequency instability satisfies

$$D_{\frac{1}{4}}^{(N-1)}(\underline{\tau}) = \prod_{k=1}^{N-1} \tau_k^2 E\{\Omega_{N-1}^2\} + D_{\psi}^{(N-1)}(\underline{\tau}^{N-1})$$
 (2.8)

where

$$D_{\psi}^{(n)}(\underline{\tau}^n) = \frac{2^{2n}}{2\pi} \int_{-\infty}^{\infty} \prod_{k=1}^{n} \sin^2(\omega \tau_k/2) S_{\psi}^{\bullet}(\mathbf{w}) d\mathbf{w} \qquad (2.9)$$

for $n \ge 1$. For $M \ge N$, then

$$D_{\Phi}^{(M)}(\underline{\tau}^{M}) = D_{\Psi}^{(M)}(\underline{\tau}^{M}) \tag{2.10}$$

Equations (2.5)-(2.10) are important in several respects. First of all, if we take high enough increments, the corresponding SF is independent of the drift effect. This is evident from (2.7) and (2.10). Secondly, we note that the usual convergence problem associated with "flicker"-type PSD can be avoided in the τ -domain. For example, suppose $S_{\bullet}(w)$ behaves like $|w|^{-\nu}$ with $\nu \ge 1$ as $\omega \to 0$. For a fixed vector $\underline{\tau}^n$, the quantity $\frac{n}{k} \sin^2(\omega \tau_k/2)$ is proportional to ω^{2n} for $|\omega|$

small. So, as long as v < (2n-1) the expression for $D^{(n)}(\tau^n)$ is finite. Similarly, $D^n_{\cdot}(\tau^n)$ is finite if v < (2n+1). Hence, besides combatting the problems associated with the long term frequency drift, the SF approach is useful in treating "flicker"-type noise. An interesting example demonstrating these points is given in [9]. Thirdly, notice that all SFs are characterized in the τ -domain via the PSD $S^n_{\cdot}(\omega)$.

Equations (2.6) and (2.9) can be inverted for $S^{\bullet}_{\psi}(w)$ using Mellin transforms [10]. In particular, the PSD $S^{\bullet}_{\psi}(w)$ can be evaluated via

$$S_{\psi}^{\bullet}(\mathbf{w}) = \mathcal{M}^{-1}[\mathcal{M}_{\mathbf{f}}(\mathbf{s})]$$
 (2.11)

where the Mellin transform of the function f(+), $\mathcal{M}_{\mathbf{f}}$ is given via

$$\mathcal{M}_{f}\left(1-\sum_{k=1}^{n}s_{k}\right)=\frac{\mathcal{M}_{g}(\underline{s}^{n})}{\prod_{k=1}^{n}\mathcal{M}_{K}(s_{k})},$$
(2.12)

 m^{-1} [.] is the one-dimensional inverse Mellin transform (with inverse transform variable w), $m_{K_k}(s_k)$ is the one-dimensional Mellin transform of the functions

$$K_k(\tau_k) = \sin^2\left(\frac{\tau_k}{2}\right) \quad k = 1, ..., n$$

and $\mathcal{D}_{g}(\underline{s}^{n})$ is the n-dimensional Mellin transform of the function

$$g(\underline{\tau}^n) = \frac{\pi}{4^n} D_{\psi}^{(n)}(\underline{\tau}^n)$$
.

Alternatively,

$$S_{\psi}^{\bullet}(w) = w^{2} m^{-1} [m_{f}(s)] \qquad (2.13)$$

where now

$$g(\underline{\tau}^n) = \frac{\pi}{4^n} D_{\psi}^{(n)}(\underline{\tau}^n)$$

Unfortunately, taking the inverse Mellin transform in (2.11) and (2.13) is difficult in general and numerical techniques may be needed. For small n and $\tau_1 = \ldots = \tau_n$, a different method for inverting (2.5) and (2.8) was presented in [9]. Figure 2 summarizes τ -domain to f-domain and f-domain to τ -domain transformations which are possible by either of the two approaches.

SFs of the frequency process Φ and phase process Φ of an oscillator are fundamental to definitions or frequency standards involving oscillator instability. In the following, we give new interpretations to

the recommended definitions [1], [2] of instability in terms of the theory based upon structure functions. In particular, we discuss the conditions to be imposed on the phase or frequency process in order to attach meaning to the rms fractional frequency deviation and the two-sample and L-sample Allan variance.

2.2 RMS Fractional Frequency Deviation

For the rms fractional frequency deviation to make sense the radian frequency process $\dot{\Phi}(t)$ has to be modeled as a constant w_0 plus a stationary frequency component $\dot{\psi}(t)$ whose PSD is well behaved near w=0, i.e., $S_{\dot{\psi}}(w) \sim |\psi|^{-\nu}$, $\nu < 1$. Then,

$$D_{\psi}^{(1)}(\tau) \stackrel{\Delta}{=} E\{ \left[\psi(t+\tau) - \psi(t) \right]^{2} \} < \infty$$
 (2.14)

is the expected value of the square of the phase accumulated in τ seconds. The <u>true rms fractional frequency deviation</u> defined by Cutler-Searle can be expressed in terms of the first phase structure function as [9]*

$$\frac{\Delta f(\tau)}{f_0} = \sqrt{\frac{D_{\psi}^{(1)}(\tau)}{(\omega_0 \tau)^2}} . \qquad (2.15)$$

Furthermore, the statistical average of the measured rms fractional frequency deviation, say $\Delta \hat{f}(\tau)/f_0$, as found using frequency counted data, is easily shown to be an asymptoically unbiased estimator of $\Delta f(\tau)/f_0$. The measurement bias is expressed in terms of the first phase SF via

$$\left[\frac{\Delta f(L\tau)}{f_0}\right]^2 = \frac{D_{\psi}^{(1)}(L\tau)}{L^2(\omega_0^{\tau})^2} . \tag{2.16}$$

2.3 The Allan Variance

For the two-sample Allan variance to yield a precise meaning, the frequency process $\dot{\Phi}(t)$ must be modeled as a linear frequency drift term and if "flicker"-type noise is present $S_{\dot{\psi}}(\boldsymbol{w})$ must behave like $|\boldsymbol{w}|^{-\nu}$ for $\nu < 3$ near $\boldsymbol{w} = 0$. Then

542

^{*}In the original definitions for rms fractional frequency deviation and Allan variances [1], [2], [3], the time average, instead of the present ensemble average, was employed. However, in order to fully exploit various results on stochastic processes in the literature, the ensemble average is used in what follows. Notice that both averages are equivalent if ergodicity holds.

$$\frac{D_{\Phi}^{(2)}(\tau)}{(\omega_{0}\tau)^{2}} = E\left\{ \left[\frac{\Phi(t+2\tau)-\Phi(t+\tau)}{\omega_{0}\tau} - \frac{\Phi(t+\tau)-\Phi(t)}{\omega_{0}\tau} \right]^{2} \right\}$$
(2.17)

is the expected squared fractional deviation of the average frequency. The two-sample Allan variance $\mathrm{E}\{\sigma_A^2(2,\tau,\tau)\}$ with zero dead time between measurements can be written as [9]

$$E\{O_{A}^{2}(2,\tau,\tau)\} = \frac{D_{\Phi}^{(2)}(\tau)}{2(\psi_{D}\tau)^{2}} . \qquad (2.18)$$

Except for a factor of $\frac{1}{2}$ and the normalization constant $(w_0\tau)^2$, the two-sample Allan variance is exactly the second phase structure function. We also note for small τ that the average in (2.17) is related to the instability of the frequency process, i.e., derivative of the phase process.

If the frequency process $\Phi(t)$ does not have any drift and $S_{\bullet}(\omega)$ behaves like $|\omega|^{-\nu}$ for $\nu \le 3$, then the L-sample Allan variance [2], [3, eq. 4] is

$$E\{\sigma_{A}^{2}(L,\tau,\tau)\} = \frac{L}{L-1} \frac{1}{(\omega_{0}\tau)^{2}} \left[D_{\psi}^{(1)}(\tau) - \frac{1}{L^{2}} D_{\psi}^{(1)}(L\tau)\right] (2.19)$$

The L-sample Allan variance is not related to the two-sample Allan variance in a simple way, but rather it is an asymptotically unbiased estimator of the rms fractional frequency deviation squared provided the latter is well defined. The estimator bias is expressed in terms of the first phase SF via

$$\frac{1}{(\omega_0 \tau)^2} \left[\frac{1}{L-1} D_{\psi}^{(1)}(\tau) - \frac{1}{L(L-1)} D_{\psi}^{(1)}(L\tau) \right]. \tag{2.20}$$

2.4 Relationship Between RMS Fractional Frequency Deviation and Allan Variance

If the assumptions regarding the frequency process $\Phi(t)$ in Section 2.2 hold, then the two-sample Allan variance and the rms fractional frequency deviation form a one-to-one correspondence via

$$E\{\sigma_{\mathbf{A}}^{2}(2,\tau,\tau)\} = 2\left\{\left[\frac{\Delta f(\tau)}{\mathbf{f}_{0}}\right]^{2} - \left[\frac{\Delta f(2\tau)}{\mathbf{f}_{0}}\right]^{2}\right\}$$
 (2.21)

The equation can be inverted to yield

$$\left[\frac{\Delta f(\tau)}{f_0}\right]^2 = \frac{1}{2} E\{\sigma_A^2(2,\tau,\tau)\} + \frac{1}{2} \sum_{k=1}^{\infty} \frac{D_{\psi}^{(2)}(2^k \tau)}{2(w_0 2^k \tau)^2} . \qquad (2.22)$$

In addition, the L-sample Allan variance is related to the rms fractional frequency deviation via

$$E\{\sigma_{A}^{2}(L,\tau,\tau)\} = \frac{L}{L-1} \left(\frac{\Delta f(\tau)}{f_{0}}\right)^{2} - \frac{1}{L(L-1)} \frac{D_{\psi}^{(1)}(L\tau)}{(\omega_{0}\tau)^{2}}$$
(2.23)

Provided $D_{\psi}^{(1)}(\tau) < \infty$ for all τ , then for large L we see that the L-sample Allan variance converges to the mean squared value of the fractional frequency deviation. The authors believe that these facts have not been recognized in previous studies.

In addition, these relationships allow us to identify the bias [12, eq.15] function $\chi(L)$ as

$$\chi(\mathbf{L}) \stackrel{\Delta}{=} \frac{\mathrm{E}\left[\sigma_{\mathbf{A}}^{2}(\mathbf{L}, \tau, \tau)\right]}{\mathrm{E}\left[\sigma_{\mathbf{A}}^{2}(2, \tau, \tau)\right]} = \left(\frac{2L}{L-1}\right) \left[\frac{\mathrm{D}_{\psi}^{(1)}(\tau) - \mathrm{D}_{\psi}^{(1)}(\mathbf{L} \tau)/L^{2}}{\mathrm{D}_{\psi}^{(2)}(\tau)}\right] \tag{2.24}$$

and if $D_{\psi}^{(1)}(\tau) \ll \infty$ for all τ , then for large L,

$$\chi(L) \approx 2D_{\psi}^{(1)}(\tau)/D_{\psi}^{(2)}(\tau)$$

$$= \frac{1}{2} + \frac{1}{2} \sum_{k=1}^{\infty} 4^{-k} \frac{D_{\psi}^{(2)}(2^{k}\tau)}{D_{\psi}^{(2)}(\tau)}$$
(2.25)

III. INTERPRETATION OF OSCILLATOR INSTABILITY MEASURES

3.1 Phase (Time) and Frequency Instability

In characterizing the performance of an oscillator, it is of fundamental interest to distinguish between the notion of "instability" and 'precision" of its frequency as well as its phase. While it is relatively easy (and unambiguous) for one to agree upon a definition of the "precision" of a random quantity in terms of, perhaps, the deviation from its mean value (the relative error), there is no general agreement of what "instability" means. In what follows, we shall take "instability" to mean instability with respect to the passage of time, i.e., how a stochastic quantity behaves (in a probability sense) relative to its past τ seconds earlier. For example, an oscillator which emits a frequency that does not change with respect to time is a "stable" oscillator; the frequency it gives at any particular instant is "precise". Using these notions, we shall attempt to interpret the meanings of phase instability. Conventional measures, in particular, the rms fractional frequency deviation and Allan variance, will serve as the basis for our interpretations.

To formalize the following discussion, we shall assume the instantaneous phase and frequency of the oscillator satisfy

$$\Phi(t) = \psi_0 t + \psi(t) + \left[\Phi(0) - \psi(0)\right]$$
 (3.1)

$$\dot{\Phi}(t) = \mathbf{w}_0 + \dot{\psi}(t) \tag{3.2}$$

where $\dot{\psi}(t)$ is stationary with finite variance and $E\{\psi(t)\} = E\{\dot{\psi}(t)\} = 0$. Under these assumptions, the instability measures to be discussed are all well-defined quantities.

The instantaneous phase (time) instability of the phase noise process $\psi(t)$ is measured by the increment $\Delta\psi(t;\tau)=\psi(t+\tau)-\psi(t)$ while the rms phase instability is measured by $\sqrt{D_{+}^{(1)}(\tau)}$. Thus the rms fractional frequency deviation is related to the phase instability via (2.15). On the other hand, the instantaneous frequency instability of the frequency noise process $\psi(t)$ is measured by the increment $\Delta\psi(t;\tau)=\psi(t+\tau)-\psi(t)$ while the rms frequency instability is measured by $\sqrt{D_{+}^{(1)}(\tau)}$. The two-sample Allan variance approximates $D_{+}^{(1)}(\tau)/2\omega_{0}^{2}$ with an error

$$\frac{D_{\psi}^{\{1\}}(\tau)}{2\omega_{0}^{2}} - E\left[\sigma_{A}^{2}(2,\tau,\tau)\right] = \frac{2}{\pi\omega_{0}^{2}} \int_{0}^{\infty} \sin^{2}\frac{\omega\tau}{2} \left[1 - \sin^{2}\frac{\omega\tau}{2}\right] S_{\psi}^{*}(\omega)d\omega \ge 0$$
(3.3)

For a PSD $S_{\psi}(\omega)$ with power concentrated in the frequency region $\omega_{\tau} \ll 1$ then

$$\frac{D_{\psi}^{(1)}(\tau)}{2\omega_{0}^{2}} \simeq E\left[\sigma_{A}^{2}(2,\tau,\tau)\right] \tag{3.4}$$

Thus the two-sample Allan variance is a measure of frequency instability of the oscillator. Table I serves to summarize the results.

From (2.14), (2.15) and (3.1), it is obvious that the rms fractional frequency deviation $\Delta f(\tau)/f_0$ is an instability measure of the phase process Φ or the accuracy (relative error) of the phase increment $\Delta \Phi = \Phi_{\tau} - \Phi$. Now the frequency accuracy is related to $E\{\psi^2\}/\psi_0^2$. If (2.15) is used as a measure of frequency precision, the error introduced in interpreting (2.15) as a measure of frequency precision is

$$\frac{\mathrm{E}\{\dot{\psi}^2\}}{\overset{2}{\mathsf{w}_0^2}} - \left[\frac{\Delta f(\tau)}{f_0}\right]^2 = \frac{1}{\pi \mathsf{w}_0^2} \int_0^{\infty} \left[1 - \mathrm{sinc}^2\left(\frac{\mathsf{w}\tau}{2}\right)\right] S_{\psi}^{\bullet}(\mathsf{w}) d\mathsf{w} \ge 0 \quad (3.5)$$

where $\operatorname{sinc}(x) \stackrel{\Delta}{=} \sin x/x$. The severity of the error in this interpretation depends on the shape of $S^{\bullet}_{\psi}(w)$ weighted by the weighting function $1-\sin^2(w\tau/2)$.

3.2 Normalized Time Instability Times the Frequency Instability as a Measure of Oscillator Instability

Depending on specific applications, oscillators are used as references for making time (phase) measurements as well as in frequency measurements. Since frequency instability is fundamentally different from phase instability, it seems only fair to specify the performance of an oscillator in terms of both its frequency and phase instability in the measurement (τ) domain. For this purpose, we can define frequency instability $\delta f(\tau)$ to be the rms change in frequency over the observation time τ , through

$$\delta f(\tau) \stackrel{\triangle}{=} \frac{\sqrt{D_{\psi}^{(1)}(\tau)}}{2\pi} \cong \sqrt{2} f_0 \sqrt{E\left[\sigma_A^2(2,\tau,\tau)\right]}$$
 (3.6)

On the other hand, the time-instability $\delta T(\tau)$ can be defined as the rms change in the "time" (see (3.11)) from its mean τ , via

$$\delta T(\tau) \stackrel{\triangle}{=} \sqrt{\frac{D_{\psi}^{(1)}(\tau)}{\frac{2}{\omega_0}}} = \left(\frac{\Delta f(\tau)}{f_0}\right) \cdot \tau \tag{3.7}$$

Accepted Frequency Standard	$\Delta f(au)/f_0$
RMS Phase Instability Measure	$\sqrt{D_{\psi}^{(1)}(\tau)/(\mathbf{w}_0\tau)^2}$
Phase (Time) Instantaneous Phase Instantaneous Phase RMS Phase Accuracy Measure Instability Measure Standard	$\Delta \psi = \psi_{\tau} - \psi$
Instantaneous Phase Accuracy Measure	் - E [ம்]
Phase (Time) Process	ψ(t)

Frequency	Instantaneous Frequency Accuracy Measure	Frequency Instantaneous Frequency Instantaneous Frequency Instability Accuracy Measure Instability Measure	lency	Accepted Fre- quency Standard
• (t)			$\int_{\mathbb{Q}_{\psi}^{(1)}(\tau)/2(w_{0}\tau)^{2}} \left \operatorname{E}\left[\sigma_{A}^{2}(2,\tau,\tau)\right] \right $	$\mathbb{E}\left[\sigma_{\mathbf{A}}^{2}(2,\tau,\tau)\right]$
			$\cong \sqrt{\mathbb{E}\left[\mathbb{Q}_{\mathbf{A}}^{2}(2,\tau,\tau)\right]}$	

Dhase Incre-	Dhase Increment Dhase Increment		RMS Dhase Increment Accented Freque	Accented Freque
ment Process	Accuracy Measure	re	Instability Measure	ency Standard
Δψ (t)	[৸ব] ভ্র - ৸ব	$\Delta(\Delta \psi) = \Delta^2 \psi$	$\sqrt{b_{\psi}^{(2)}(\tau)/2(w_0\tau)^2}$	$\tilde{\mathrm{E}}[\sigma_{\mathrm{A}}^{2}(2,\tau,\tau)]$
			$=\sqrt{\mathbb{E}\big[\sigma_{\mathbf{A}}^{2}(2,\tau,\tau)\big]}$	

Interpretation of Phase and Frequency Instability and the Relationship to the RMS Fractional Frequency Deviation and Two-Sample Allan Variance. Table I.

The locus of the point $(\delta f(\tau), \delta T(\tau))$, as a function of the observation time τ , could serve as the overall stability performance guide of an oscillator and is depicted in Fig. 3.

The product: frequency instability times time instability

$$\delta f(\tau) \delta T(\tau) \stackrel{\triangle}{=} \frac{1}{f_0} \sqrt{\frac{D_{\psi}^{(1)}(\tau)}{(2\pi)^2} \cdot \frac{D_{\psi}^{(1)}(\tau)}{(2\pi)^2}}$$
(3.8)

of an oscillator serves as a parameter by which various oscillators can be compared for a given frequency of oscillation and a given observation time τ . In Fig. 3, this parameter at $\tau = \tau_1$ is equal to the area of the shaded area. For an ideal oscillator then

$$\delta f(\tau) \cdot \delta T(\tau) = 0 \tag{3.9}$$

for all τ . Thus any oscillator, which is to be used as a standard in instability measurements, should appear to the oscillator under test to satisfy (3.9) for all τ of interest. Moreover, if we use (3.4) to approximate $D_{\tau}^{(1)}(\tau)$ by the Allan variance then we can write

$$\frac{\delta f(\tau)}{f_0} \cdot \underbrace{\frac{\delta T(\tau)}{\tau}}_{\tau} \cong \sqrt{2} \sqrt{E[\sigma_A^2(2,\tau,\tau)]} \underbrace{\left(\frac{\Delta f(\tau)}{f_0}\right)}_{\text{RMS Fractional Frequency Deviation}} (3.10)$$

$$\text{The Time-Base Instability}_{\tau} = \frac{\delta T(\tau)}{\tau} \cong \sqrt{2} \sqrt{E[\sigma_A^2(2,\tau,\tau)]} \underbrace{\left(\frac{\Delta f(\tau)}{f_0}\right)}_{\tau} = \frac{\delta f(\tau)}{f_0} \times \frac{\delta f(\tau)}{f_0} = \frac{\delta$$

This equation supports our earlier claim that the Allan variance is a measure of oscillator frequency instability while the rms frequency deviation is a measure of oscillator phase (time) instability. The authors believe that the above construction has provided insight into the meaning of the Allan variance and the rms fraction frequency deviation.

To gain further insight into these performance measures, let us assume that the random process $f(\tau) \triangleq \Delta \psi(\tau)/2\pi$ and $T(\tau) \triangleq \Delta \psi(\tau)/\omega_0$ are jointly Gaussian. If the process $\psi(t)$ is stationary, it can be shown that $\Delta \psi(\tau)$ and $\Delta \psi(\tau)$ are uncorrelated. Hence $f(\tau)$ and $T(\tau)$ are uncorrelated Gaussian processes with zero mean and standard deviations $\delta f(\tau)$ and $\delta T(\tau)$. If we plot the contour of constant probability density as a function of τ as in Fig. 4, we observe the effect

of the degradation of oscillator stability as τ increases.

3.3 Is the Nominal Frequency of a Real World Oscillator Reciprocally Related to the Nominal Period?

If the oscillator phase process $\Phi(t)$ in (3.1) is used for a clock (period $T_0 \stackrel{\Delta}{=} 2\pi/w_0$), the time $T_c(t)$ registered by the clock is given by

$$T_{C}(t) = \left[\Phi(t) - \Phi(0)\right] / \omega_{0}$$
 (3.11)

During the interval $(t, t+T_0)$, the clock time accumulated is

$$\Delta T_{c}(T_{0}) = T_{0} + \frac{\Delta \psi(T_{0})}{\omega_{0}}$$
 (3.12)

The time average frequency during this time interval is

$$\overline{f}(T_0) = \frac{1}{2\pi T_0} \int_t^{t+T_0} \Phi(\xi) d\xi = f_0 + \frac{\Delta \psi(T_0)}{2\pi T_0}$$
 (3.13)

Hence the product $\Delta T_c(T_0) \times \overline{f}(T_0)$ is

$$\Delta T_{c}(T_{0}) \times \overline{f}(T_{0}) = 1 + \frac{\Delta \psi(T_{0})}{\pi} + \frac{(\Delta \psi(T_{0}))^{2}}{(2\pi)^{2}}$$
 (3.14)

which is random with mean

$$E\{\Delta T_{c}(T_{0}) \times \overline{f}(T_{0})\} = 1 + \left(\frac{\Delta f(T_{0})}{f_{0}}\right)^{2}$$

$$= 1 + D_{\psi}^{(1)}(T_{0})/(2\pi)^{2}$$
(3.15)

From (3.15), it is clear that the rms fractional frequency deviation (or first phase SF) characterizes the uncertainty in the product $\Delta T_c(T_0) \times \overline{f}(T_0)$. Since $(\Delta f(T_0)/f_0)^2$ is not zero for real world oscillators, the period and (time average) frequency are not inversely related for any physical clock. Instead the mean of the product differs from unity by the square of the rms fractional frequency deviation.

IV. EFFECTS OF OSCILLATOR INSTABILITY IN APPLICATIONS IN TERMS OF SF'S

The characterization and specification of oscillator instability must

ultimately be made in the light of its effects on the performance of systems that rely on the oscillation. The utility of SF's will now be demonstrated in terms of a number of user applications. It shall become evident that, in every application, the PSD $S_{\psi}^{\bullet}(w)$ of the stationary frequency noise is the key to predicting performance due to oscillator instability. Only a summary account is given herein; detailed analytical developments are anticipated in future articles.

4.1 Effect of Oscillator Instability on Phase-Locked Loop (PLL)
Tracking

One interesting application of SF's is found in studying the tracking behavior of a PLL. In addition to a first-order statistical characterization, i.e., the phase-error variance, the first SF of the phase error is also an important performance measure of a tracking loop. It is important in assessing the effect of oscillator instabilities on tracking performance and it is related to the average hold-in time of the PLL.

As an example, it was shown in [10] (assuming the loop bandwidth is small compared to τ , i.e., $W_{L}\tau << 1$) that the first phase-error SF of a first-order loop due to oscillator instability is given by

$$D_{\varphi}^{(1)}(\tau) = D_{\psi_{1}}^{(1)}(\tau) + D_{\psi_{2}}^{(1)}(\tau) \tag{4.1}$$

where ϕ is the loop phase error, ψ_1 represents the phase noise on the transmitted oscillation and ψ_2 represents the phase noise process produced by the frequency generation in the receiver. Notice that in this case, the phase instability measure (3.7) of the oscillators are the quantities of interest in predicting the ability of the loop to track the input process in the presence of oscillator phase noise.

4.2 Effect of Oscillator Instability on One-Way and Two-Way Doppler Measurements

In a practical Doppler measurement system, the Doppler information is usually extracted from the local phase estimate increment $\Delta \Theta(\tau)$ generated by the receiver PLL. For one-way Doppler measurements, the error contribution due to oscillator instabilities can be shown to be contained in the equation

$$D_{\Theta}^{(1)}(\tau) = \mathbb{D}_{\psi_{1}}^{(1)}(\tau) + \mathbb{D}_{\psi_{2}}^{(1)}(\tau) + D_{\psi_{3}}^{(1)}(\tau)$$

NATIONAL AERONAUTICS AND SPACE ADMINISTRATION GREENB--ETC F/6 14/2 PROCEEDINGS OF THE ANNUAL PRECISE TIME AND TIME INTERVAL (PTTI)--ETC(U) AD-A043 856 1977 UNCLASSIFIED NASA-6SFC-X-814-77-149 NL 7 OF 8 AD A043856

where Θ_e denote the error in the local phase estimate, ψ_1 represents the transmitter oscillator instabilities, ψ_2 represents the receiver VCO instability and ψ_3 represents the receiver reference instability. The quantities $\mathbb{D}_{\psi_1}^{(1)}(\tau)$ and $\mathbb{D}_{\psi_2}^{(1)}(\tau)$ denote the first SF of the loop

filtered ψ_1 and ψ_2 process which are directly related to the PSD $S_{\psi}^{\bullet}(\omega)$. Thus the key role which $S_{\psi}^{\bullet}(\omega)$ plays is again manifested.

For two-way Doppler measurements [6], the situation is more complicated. The first SF of the error in the local phase estimate due to oscillator instabilities is given by

$$D_{\Theta}^{(1)}(\tau) = D_{\psi_0}^{(1)}(\tau) + D_{\psi_1}^{(1)}(\tau) + D_{\psi_2}^{(1)}(\tau) + D_{\psi_3}^{(1)}(\tau)$$
where ψ_0 represents the transmitter oscillator instability, ψ_1 repre-

where ψ_0 represents the transmitter oscillator instability, ψ_1 represents the vehicle receiver VCO instability and ψ_2 represents the ground receiver, VCO instability, and ψ_3 represents the ground receiver reference instability [5].

In the case that: (1) the transmitter and receiver reference signals are derived from the same timing source and (2) the static phase gain and the receiver filtering—can be neglected, then the error contribution due to the reference oscillator instability $\psi_0 = \psi_3 = \psi$ alone is $D_{\psi}^{(2)}(\tau, T)$ which is explicitly (see (2.6))

$$D_{\psi}^{(2)}(\tau, T) = \frac{16}{\pi} \int_{0}^{\infty} \sin^{2}(\frac{\omega_{\tau}}{2}) \sin^{2}(\frac{\omega T}{2}) \frac{S_{\psi}^{\bullet}(\omega)}{\omega} d\omega \qquad (4.4)$$

where T is the round-trip delay time of the signal. Hence we see that the second SF of the phase noise is the important quantity to specify the performance of the reference oscillation. It can be shown that $D_{\psi}^{(2)}(\tau,T)$ is related to the two-sample Allan variance with non-zero dead time $T-\tau$ between measurements $E\{\sigma_{\Lambda}^{(2)}(2,T,\tau)\}$ via

$$E\{\sigma_{A}^{2}(2,T,\tau)\} = \frac{1}{2(\omega_{0}\tau)^{2}} D_{\psi}^{(2)}(\tau,T)$$
 (4.5)

Under the same assumptions, if the Doppler frequency shift is derived from the loop frequency estimate, the error contribution from the oscillator instability ψ is $D_{\psi}^{(1)}(\tau)$. In this case, the first SF of the frequency noise process of the reference is the instability measure of interest.

4.3 Effect of Oscillator Instability on Range Measurements

In one-way ranging, the vehicle transmits a ranging signal to the tracking station. Range from the tracking station to the vehicle can then be determined from a measurement of the local phase estimate of the receiver PLL relative to the phase of a reference. The uncertainty introduced in the range estimate due to oscillator instabilities alone is related to the variance in the phase estimate error

$$\sigma_{\varphi_{e}}^{2} = \tilde{\sigma}_{\psi_{1}}^{2} + \tilde{\sigma}_{\psi_{2}}^{2} + \sigma_{\psi_{3}}^{2} \tag{4.6}$$

where

$$\widetilde{\sigma}_{\psi_{1}}^{2} = \frac{1}{2\pi} \int_{-\infty}^{\infty} \left| 1 - H_{\varphi}(j\omega) \right|^{2} \frac{S_{\psi}^{*}(\omega)}{\omega^{2}} d\omega$$

$$\widetilde{\sigma}_{\psi_{2}}^{2} = \frac{1}{2\pi} \int_{-\infty}^{\infty} \left| 1 - H_{\varphi}(j\omega) \right|^{2} \frac{S_{\psi}^{*}(\omega)}{\omega^{2}} d\omega$$

$$\sigma_{\psi_{3}}^{2} = E\{\psi_{3}^{2}\}$$

and ψ_1 represents the transmitted reference instability, ψ_2 represents the receiver VCO instability, ψ_3 represents the receiver reference instability and $H_{\phi}(j w)$ is the receiver PLL closed-loop transfer function.

In two-way measurements, a ranging signal is transmitted to the vehicle to be tracked and is returned by it to the tracking station. Range is then determined from a measurement of the phase of the returned tone relative to a reference (possibly the same one as the original transmitted tone). The uncertainty introduced in the error in the phase estimate due to oscillator instabilities alone is related to the variance of the phase estimate error

$$\sigma_{\mathbf{e}}^{2} = \tilde{\sigma}_{\psi_{0}}^{2} + \tilde{\sigma}_{\psi_{1}}^{2} + \tilde{\sigma}_{\psi_{2}}^{2} + \sigma_{\psi_{3}}^{2}$$
 (4.7)

where the σ 's are defined by expressions similar to (4.6). Here ψ_0 represents the instability of the transmitted signal, ψ_1 represents the vehicle transponder VCO instability, ψ_2 represents the receiver VCO instability, ψ_3 represents the instability in the reference used for phase comparison.

If the effect of the PLL's are neglected and the transmitted tone and the reference tone are derived from the same oscillator, then the error contribution to the range measurement due to the oscillator phase noise ψ is related to $D_{\psi}^{(1)}(T)$ where T is the round-trip path delay. Notice that $D_{\psi}^{(1)}(T)$ is proportionate to the rms fractional frequency deviation.

If the phase error of the PLL in the tracking station is used to measure range-rate via $\Delta \phi(\tau)/\tau$ or $\dot{\phi}$, expressions similar to (4.7) and (4.8) can be obtained in terms of the appropriate quantities.

4.4 Effect of Oscillator Instability on Coherent Communication System Performance

In digital communication systems, the bit error probability [6] is an important performance measure and is related to the statistics of a random variable which depends upon [11] the phase error φ and its increment $\Delta \varphi \triangleq \Delta \varphi(T)$. Then the probability of error will depend upon the instability and the accuracy of φ . The first SF $D_{\psi}^{(1)}(T)$ given by (4.1) becomes the important parameter in determining the bit error probability. The effect of the oscillator instabilities then enters into the bit error probability evaluation through, for example, (4.1) and therefore can be used to select frequency generators for system implementation.

4.5 Application of SFs in Studying Timing Standards [9]

In timing standards, it is important to specify the instability $\psi(t)$ as well as the drift term as in (2.1). The use of SF's provides a convenient means for such measurements. The scheme is first to work with successively higher increments until the drift problem and the singularity problem associated with "flicker"-type PSD are alleviated. The "measured" SF's will then be inverted via (2.11) or (2.13) to get an estimate for S. (ω). After obtaining this estimate, one can design an optimal estimation procedure to evaluate the drift. An example of such an approach was discussed in [9].

4.6 Miscellaneous Applications of Structure Functions

All signalling schemes in telecommunication and radio engineering depend on a stable frequency reference. In a time-division multiple

access (TDMA) system, the accumulated phase noise between "marker" intervals of duration T_{τ} is an important factor in evaluating synchronization performance. The rms phase noise accumulated between marker interval is characterized by $D_{\psi}^{(2)}(\tau,T)$ which is related to the two-sample Allan variance with dead zone (see (4.5)).

In communication systems employing differential phase-shift keying (DPSK), it turns out that the second SF $D_{\psi}^{(2)}(\tau,\tau)$ of the transmitter oscillator phase noise ψ is an important parameter in specifying achievable system data rates.

Because of the path delays involved in network synchronization, the SF approach is also important in studying network synchronization and specifying the requirements on oscillator stability.

V. SF'S AND THEIR RELATIONSHIP TO THE RF OSCILLATION

Frequently the PSD of the RF oscillation is used as a means of obtaining the "PSD" of the phase noise process. Here we derive an expression for the Nth moment function of the RF oscillation and show how the SF of the phase process enters into the measurement as well as the problems associated with this approach. In order to proceed with this approach, several restrictive assumptions are required if this approach is to be tractable.

For the sake of simplicity in what follows, let us work with the complex oscillation

$$\mathbf{s}(\mathsf{t},\Phi(\mathsf{t})) = \sqrt{2P} \exp[\mathbf{j}\Phi(\mathsf{t})] \tag{5.1}$$

where P represents the mean square power of the oscillation and $\Phi(t)$ is given by (2.2). For k = 0, ..., N, let us define the random variables

$$\mathbf{z}_{k} = \begin{cases} \binom{N}{N-k} \mathbf{s} \left(t + \sum_{m=1}^{k} \tau_{m} \right) & k = 0, 2, \dots \\ \binom{N}{N-k} \mathbf{s}^{*} \left(t + \sum_{m=1}^{k} \tau_{m} \right) & k = 1, 3, \dots \end{cases}$$
 (5.2)

where ξ^* denotes the complex conjugate of ξ . Then the $(N+1)^{st}$ moment function of the random variables $\{z_0,\ldots,z_N\}$ is related to the N^{th} SF of the phase process $\Phi(t)$ via

$$E[z_{N}...z_{0}] = (\sqrt{2P})^{N+1}E\{\exp[j\Delta^{N}\Phi(t;\underline{\tau}^{N})]\}$$
 (5.3)

Notice that if the Nth increment of the phase process $\Phi(t)$ is stationary, then the quantity $E\{\exp\left[j\Delta^N\Phi(t;\underline{\tau}^N)\right]\}$ is independent of t and equal to the characteristic function of the Nth increment, say, $\Delta^N\Phi(t=0;\underline{\tau}^N)$, evaluated at unity. Furthermore, if $\Delta^N\Phi(t;\underline{\tau}^N)$ is Gaussian, then

$$E[z_{N}...z_{0}] = (\sqrt{2P})^{N+1} \exp[-D_{\overline{\Phi}}^{(N)}(\underline{\tau}^{N})/2]$$
 (5.4)

which generalizes earlier work when N > 1. As an example, if the complex oscillation satisfies

$$s(t, \Phi(t)) = \sqrt{2P} \exp\{j[\omega_0^{\dagger}t + \psi(t) - \psi(0) + \Phi(0)]\}$$
 (5.5)

then

$$E[s_{\tau}s^*] = 2P \exp[-D_{\psi}^{(1)}(\tau)/2] \exp(-j\psi_{0}\tau)$$
 (5.6)

The real part of (5.6) satisfies

$$\operatorname{Re}\left\{\mathbb{E}\left[\mathbf{s}_{\tau}\mathbf{s}^{*}\right]\right\} = 2\operatorname{P} \cos \omega_{\tau} \exp\left[-\frac{1}{2}D_{\psi}^{(1)}(\tau)\right]$$
 (5.7)

It can be shown that if $\psi(t)$ is stationary, Gaussian, then the time average correlation $\overline{E[r(t+\tau)r(t)]}$ of the process

$$r(t) \stackrel{\Delta}{=} Re\{s(t)\} = \sqrt{2P} \cos(\omega_0^t + \psi(t) - \psi(0) + \Phi(0))$$
 (5.8)

where $Re\{\xi\}$ denotes the real part of ξ , is given by [13, pp. 108-119]

$$\overline{E[\mathbf{r}_{\tau}]} \stackrel{\triangle}{=} \lim_{T \to \infty} \frac{1}{2T} \int_{-T}^{T} E[\mathbf{r}(t+\tau)\mathbf{r}(t)] dt \qquad (5.9)$$

$$= \frac{1}{2} \operatorname{Re} \{ E[\mathbf{s}_{\tau}\mathbf{s}^{*}] \}$$

$$= P \cos \omega_{0} \tau \exp[-D_{tt}^{(1)}(\tau)/2]$$

Notice that in this case, the first phase SF $D_{\psi}^{(1)}(\tau)$, which is related to phase instability, is the quantity of interest in characterizing the instability of an RF oscillation. If we now assume that $\psi(t)$ is stationary then the PSD of $\sin[\psi(t+\psi(t))]$ is given by [14]

$$S_{\mathbf{r}}(\mathbf{w}) = P[S_{\mathbf{r}_0}(\mathbf{w} - \mathbf{w}_0) + S_{\mathbf{r}_0}(\mathbf{w} + \mathbf{w}_0)]$$
 (5.10)

where

$$S_{\mathbf{r}_{0}}(\mathbf{w}) = \exp(-\sigma_{\psi}^{2}) \left[\delta(\mathbf{w}) + \frac{S_{\psi}^{\bullet}(\mathbf{w})}{2} + \frac{1}{2!} \left(\frac{S_{\psi}^{\bullet}(\mathbf{w})}{2} * \frac{S_{\psi}^{\bullet}(\mathbf{w})}{2} \right) + \frac{1}{3!} \left(\frac{S_{\psi}^{\bullet}(\mathbf{w})}{2} * \frac{S_{\psi}^{\bullet}(\mathbf{w})}{2} * \frac{S_{\psi}^{\bullet}(\mathbf{w})}{2} \right) + \dots \right]$$

$$(5.11)$$

and the symbol * denotes convolution. Obviously, the first term corresponds to unmodulated carrier and the remaining terms are due to oscillator instability. Thus, it is clear that the ''tails'' of $S_{\mathbf{r}}(\mathbf{w})$ do not correspond to $S_{\mathbf{r}}(\mathbf{w})$!

ACKNOWLEDGMENT

The authors wish to express their thanks to P. M.

Hooten, Satellite Communications Branch of the Naval Research
Laboratory, for his support, encouragement, and for participating
in various stimulating discussions throughout the course of this work.
They also wish to express their thanks to Andrew Chi of Goddard
Space Flight Center for providing us with the opportunity of presenting
this material and to Dr. Jim Mullen of the Raytheon Company for his
helpful comments and recommendations for improvements in the
presentation.

REFERENCES

- [1] "Special issue on frequency stability," Proc. IEEE, vol. 54, pp. 101-284, Feb. 1966.
- [2] J. A. Barnes et al., "Characterization of frequency stability," <u>IEEE Trans. Instrum. Meas.</u>, vol. IM-20, pp. 105-120, May 1971.
- [3] P. Kartaschoff and J. A. Barnes, "Standard time and frequency generation," Proc. IEEE, vol. 60, pp. 493-501, May 1972.
- [4] J. A. Barnes, "Models for the interpretation of frequency stability measures," NBS, Washington, D. C., Tech. Note 683, Aug. 1976.

- [5] W. C. Lindsey, <u>Synchronization Systems in Communication and Control</u>, Englewood Cliffs, N.J.: Prentice-Hall, 1972.
- [6] W. C. Lindsey and M. K. Simon, <u>Telecommunication Systems</u>
 <u>Engineering</u>, Englewood Cliffs, N.J.: Prentice-Hall, 1973.
- [7] A. N. Kolmogorov, "Dissipation of energy in locally isotropic turbulence," <u>Dokl. Nauk. SSR</u>, vol. 32, pp. 16-18, 1941. Reprinted (in English) in <u>Turbulence: Classic Papers on Statistical Theory</u>, S. K. Frielander and L. Topper, Eds., New York: Interscience, 1951, pp. 159-161.
- [8] W. C. Lindsey and C. M. Chie, "Characterization of oscillator phase noise instability," in Proc. Int. Conf. Commun., Philadelphia, Pennsylvania, June, 1976.
- [9] W. C. Lindsey and C. M. Chie, "Theory of oscillator instability based upon structure functions," <u>Proc. IEEE</u>, vol. 64, Dec. 1976.
- [10]W. C. Lindsey and C. M. Chie, "Theory of oscillator phase noise in correlative tracking systems," to be published.
- [11] W. C. Lindsey and C. M. Chie, "Performance of coherent communication system in the presence of phase noise," to be published.
- [12] J. A. Barnes, "Tables of bias functions, B₁ and B₂, for variances based on finite samples of processes with power law spectral densities," NBS, Washington, D. C., Tech. Note 375, Jan. 1969.
- [13] H. E. Rowe, Signal and Noise in Communication Systems. New Jersey: Van Nostrand, 1965.
- [14] D. Middleton, An Introduction to Statistical Communication Theory, McGraw-Hill Book Company, New York, 1960.

Figure 1. Characterization of the State-of-Affairs Among Various Working Groups and Users of Frequency Generators.

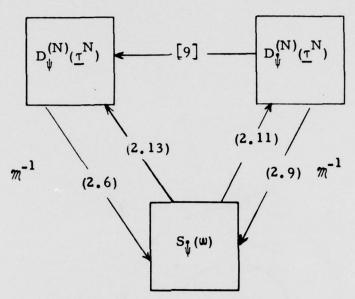


Figure 2. τ -Domain to f-Domain and f-Domain to τ -Domain Transformations.

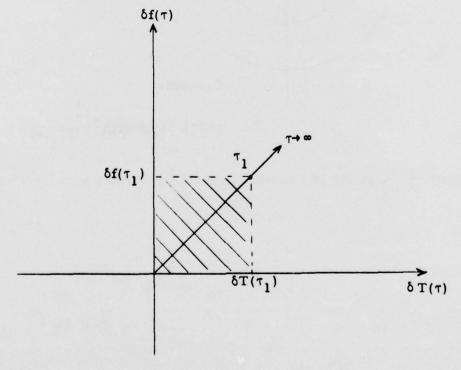


Figure 3. An Overall Frequency/Time Instability Measure.

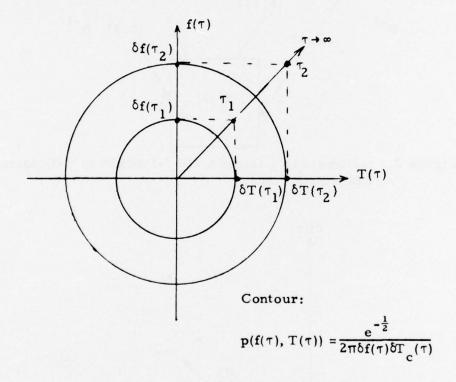


Figure 4. Contour of Constant Probability Density as a Function of τ .

IDENTIFICATION OF NOISE PROCESSES IN OSCILLATORS AND SAMPLE DATA OF FREQUENCY STABILITY OF FREQUENCY STANDARDS

Robert F. C. Vessot

Smithsonian Astrophysical Observatory Cambridge, Massachusetts

ABSTRACT

A brief and simple outline of how various noise processes affect time-domain stability and how these processes can be identified will be presented. Examples will be given of data from various crystal and atomic frequency standards.

Reference: Methods of Experimental Physics, Vol. 12, Astrophysics Part C, Radio Observations, 1976, Academic Press, New York. Chapter 5.4 "Frequency in Time Standards," by Robert F. C. Vessot.

A SIMPLE TECHNIQUE FOR HIGH RESOLUTION TIME DOMAIN PHASE NOISE MEASUREMENT

Victor S. Reinhardt and Theresa Donahoe, NASA/Goddard Space Flight Center, Greenbelt, Maryland 20771

ABSTRACT

A new time domain phase comparator is described. The device uses a novel technique to allow time domain phase measurements to be made with period and time interval counters without the use of offset reference oscillators. The device uses a single reference oscillator and allows measurements with a phase resolution greater than the noise floor of the reference. Data is presented showing a phase resolution of 0.02ps at 5 MHz with a crystal reference. The device has application in measuring the phase stability of systems where approximate phase quadrature can be maintained.

INTRODUCTION

Ideally, a frequency distribution system should not contribute any noise to the frequency being distributed. Practically, this means that the elements of a frequency distribution system should introduce negligible phase noise compared to the phase noise of the reference oscillator. To ensure this in the most precise frequency distribution systems, one must be able to measure phase noise with a resolution greater than that available from the best reference oscillators. This means that one must use a phase noise measurement technique which cancels out the phase noise of the reference oscillator.

A well known simple system which accomplishes this is shown in Figure 1. The system is based on a low noise mixer and a 90° splitter to produce a voltage proportional to the phase difference between the RF voltages at the mixer input ports. By placing one or more test devices in the R. F. signal paths, the phase stability of the test devices can be measured by analyzing the voltage out of the mixer. Because the RF source is common to both legs of the system, its phase noise does not effect the output voltage. Figure 2 shows the spectral domain phase noise resolution of such a system at 5 MHz using a Shotky diode mixer. A lock-in amplifier was used as the noise analyzer.



It is in trying to apply this simple system to time domain noise analysis that a problem occurs. The time domain measures of phase stability 1,2 , x(t) and y(t), require instantaneous measurements of the phase of a signal at periodic intervals. This is usually accomplished by superimposing the voltage carrying phase information on a low frequency beat, measuring y(t) with a period counter, and measuring x(t) with a time interval counter. Figure 3 outlines these techniques. In order to produce a beat with the simple system shown in Figure 1, two reference oscillators must be used. This, however, reintroduces the phase noise of the reference oscillators into the output. To cancel the reference oscillator contributions one must use two such systems in a dual mixer phase comparator 3 , and use a time interval counter to measure the difference in the zero crossings of the two beats.

A SIMPLE TIME DOMAIN PHASE COMPARATOR

Though the dual mixer system works quite well, it requires double the circuitry as the simple system, and requires two reference oscillators one of which must be offset in frequency. One can make high resolution time domain phase stability measurements, however, with only a single reference if one realizes that the low-frequency modulation which enables counters to be used need not come from a beat between two oscillators. As shown in Figure 4, the purpose of the beat is just to accomplish voltage to time conversion so that a period or time interval counter can measure the voltage changes which correspond to phase changes. The beat can, thus, be any stable low frequency voltage modulation which is added to the mixer output. Figure 5 shows a block diagram of such a time domain comparator based on the simple measurement system.

A convenient way to obtain a stable enough low frequency modulation is to divide down a reference oscillator output and smooth the resulting square wave with a low pass filter. Figure 6 shows the partial schematic of a time domain phase comparator using this method of obtaining the modulation. The amplifier after the mixer defines the bandwidth of the phase noise and amplifies the mixer output so the noise of the modulating voltage does not reduce the phase resolution of the comparator.

The line stretcher provides a convenient means of calibrating the system. The counter is set to time interval, and the change in time interval, $\triangle t$, is recorded as a function of the change in line stretcher length, $\triangle L$. The system calibration is then given by:

$$x = (c K)^{-1} \Delta t$$
 (Time interval)

$$y = (c \ K)^{-1} \frac{\Delta T}{T} \text{ (period)}$$

where:

$$\mathbf{x} = \frac{\Delta \phi}{2\pi \mathbf{f}}$$

$$y = \frac{\delta f}{f}$$

$$\mathbf{K} = \frac{\Delta \mathbf{t}}{\Delta \mathbf{L}}$$

and where T is the period of the modulation. Typically in the system built, at 5 MHz, (c K)⁻¹ has been about 10^{-8} so a counter resolution of 10^{-7} s will yield a phase resolution (x) of 10^{-15} s.

The simple series L and C phase shifters shown in Figure 6 were found to be quite stable. The capacitor was NPO and the inductor was ferrite core. The inductor is adjusted while monitoring the mixer output to produce phase quadrature.

RESULTS

Figures 7, 8, 9, and 10 show detailed schematics of the time domain phase comparator outlined in Figure 6. As in all ultra low noise work, care must be exercised in keeping 60 Hz interference as low as possible. In this comparitor, this was accomplished by the use of a built in voltage regulator and magnetic shielding; the whole device, the diode mixer and the inductor in the phase shifter was shielded with Co-Netic foil. The comparator is designed to use an externally supplied 10 Hz square wave for modulation. The noise bandwidth, $(4 \text{ RC})^{-1}$, is 16.7 Hz. Both the beat frequency and the noise bandwidth can be changed by changing the appropriate RC time constant. To ensure good results the comparator has its own level sensing trigger. The monitor output is a linear output which aids in adjusting the phase splitter. Both a TTL and a

pulse output are supplied for the counter. For short lines, the TTL output yielded somewhat better results. The pulse output is floating for ground loop isolation.

The device's noise resolution was measured using a Hewlett Packard 5245 counter as the 10 Hz source, an oscilloquartz B5400 5 MHz crystaloscillator as the reference, and a Hewlett-Packard 5345 counter as the time interval/period counter. Figures 11 and 12 show the results for time interval and period respectively. Figure 11 shows $\sigma_{\rm TX}$ (τ) verses averaging time, τ . $\sigma_{\rm TX}$ is defined by:

$$\sigma_{\text{TX}}^2(\tau) = \frac{1}{2} \left\langle \left[x(t + \tau) - x(t) \right]^2 \right\rangle$$

It is a measure of clock error similar to U_x (τ) used in clock modeling ⁴, but normalized to measure single point error. Figure 12 shows the two sample Allan Variance, σ_y (τ), verses averaging time. The variance is not strictly the zero dead time variance; for $\tau=0.1s$, $T=2\tau$, and for $\tau\geq 1s$, $T\simeq \tau$.

Notice the device's phase noise is approximately 0.02ps over the range measured. This compares quite favorably with the NBS dual mixer system³.

CONCLUSIONS

The simple time domain phase comparator discussed in this paper offers a means of making ultra high resolution phase stability measurements with a minimum of equipment. Though not as versatile as the dual mixer comparator, in applications where approximate phase quadrature can be maintained, the simple time domain phase comparator will yield as good or better results.

ACKNOWLEDGEMENTS

The authors would like to acknowledge David Ricci of Hewlett-Packard Corporation for the useful discussion which helped spawn the ideas for this new phase comparator. The authors would also like to acknowledge David Allan of the National Bureau of Standards for discussions on the validity of the theory of the phase comparator which encouraged us to build and test the device.

REFERENCES

- 1. J. A. Barnes, et al., "Characterization of Frequency Stability," IEEE Trans. IM-20, p. 105 (1971).
- 2. B. E. Blair, ed., Time and Frequency: Theory and Fundamentals, NBS Monograph 140, CODEN: NBSMA6, U. S. Superintendent of Documents, Catalogue #C13.44:140, Ch. 8 (1974).
- 3. D. W. Allan and H. Daams, "Picosecond Time Difference Measurement System" 29th Annual Symposium of Frequency Control (Atlantic City, 1975).
- 4. B. E. Blair, op. cit, Ch. 9.

FIGURES

- 1. A simple phase noise measurement system
- 2. Diode Mixer Phase Noise
- 3. Measuring x(t) and y(t)
- 4. Voltage to tune conversion by low frequency beat
- 5. Time Domain Measurement System
- 6. Time Domain Phase Comparator
- 7. Phase Comparator Schematic Phase Shifter Mixer
- 8. Phase Comparator Schematic Sum Circuit
- 9. Phase Comparator Schematic Trigger Circuit
- 10. Phase Comparator Schematic Voltage Regulator
- 11. 5 MHz Phase Resolution with Time Interval Counter
- 12. 5 MHz Phase Resolution with Period Counter

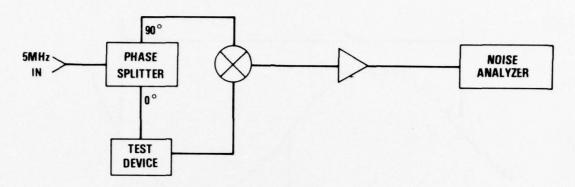


Fig. 1-A simple phase noise measurement system

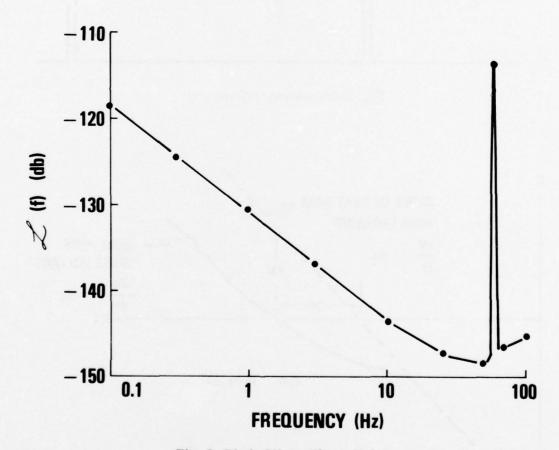


Fig. 2-Diode Mixer Phase Noise

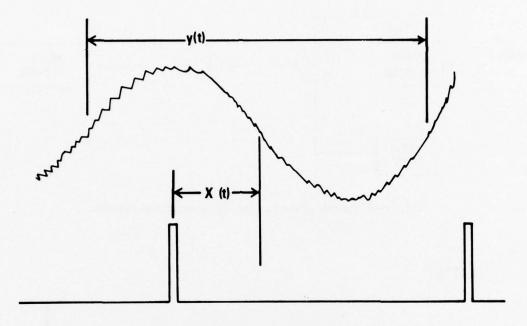


Fig. 3-Measuring x(t) and y(t)

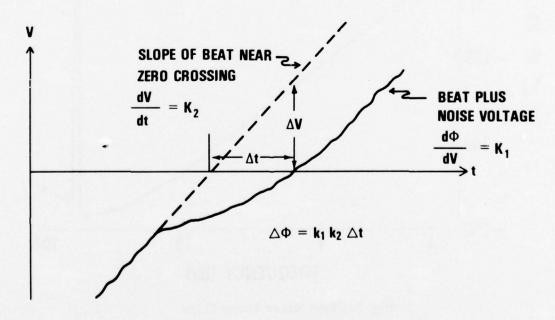


Fig. 4-Voltage to tune conversion by low frequency beat

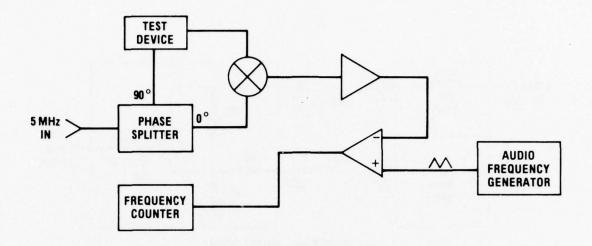


Fig. 5-Time Domain Measurement System

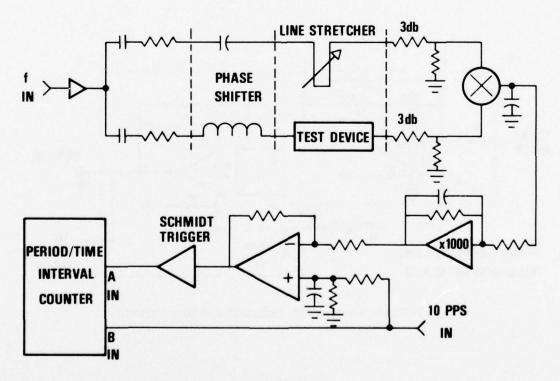


Fig. 6-Time Domain Phase Comparator

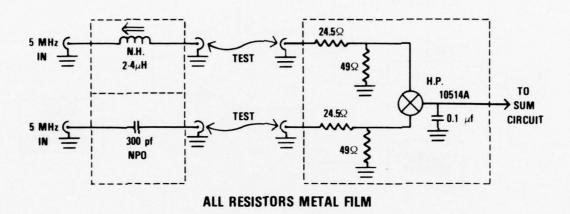


Fig. 7-Phase Comparator Schematic - Phase Shifter - Mixer

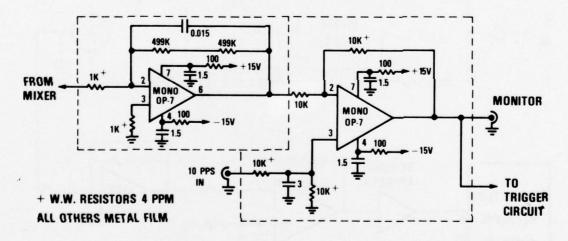


Fig. 8-Phase Comparator Schematic - Sum Circuit

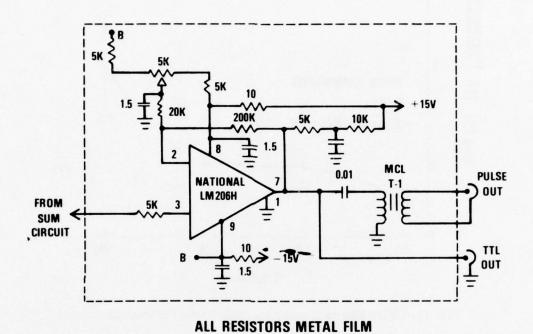


Fig. 9-Phase Comparator Schematic - Trigger Circuit

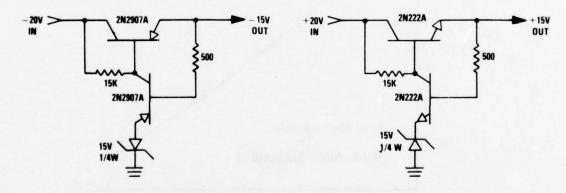


Fig. 10-Phase Comparator Schematic - Voltage Regulator

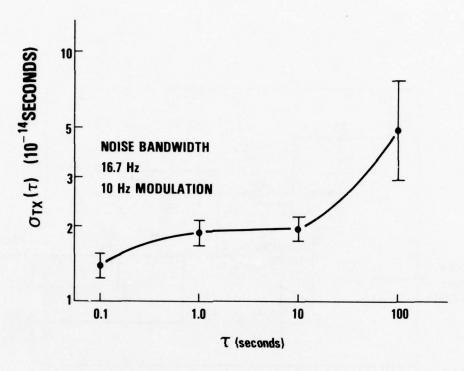


Fig. 11-5MHz Phase Resolution with Time Interval Counter

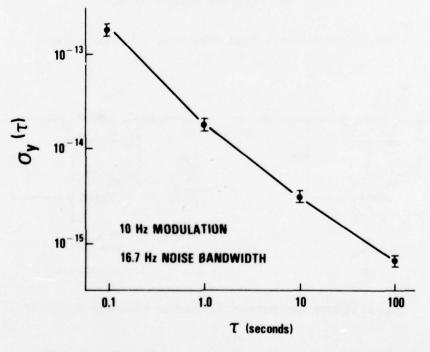


Fig. 12-5MHz Phase Resolution with Period Counter

FREQUENCY STABILITY MEASUREMENT PROCEDURES

Michael C. Fischer Hewlett-Packard Company, Santa Clara, California

ABSTRACT

This paper is intended to be a tutorial review of established techniques for workers new to this field and as a reference for those who must make these measurements infrequently. Enough background is included to remove most of the mystery, leaving rigorous mathmatical justifications to be found in the references. Special techniques for pushing measurement precision to the known limit are only mentioned briefly. It is recognized that any single application of a precision oscillator will have system requirements for which a limited range of these procedures will apply.

The measurements covered are phase modulation sidebands from 0.01 Hz to 50 kHz, and short term stability by Allan variance from 0.1 millisecond to 10^4 seconds, including the effects of non-random components such as spurs or bright lines.

Applications of a new frequency stability analyzer system are discussed in some detail also. This system is particularly suited for characterizing VHF frequencies and above.

INTRODUCTION

As an introduction to the subject of frequency stability, the first paragraphs review some basic concepts which set a context for understanding the measurement methods and results. Frequency measurements are concerned with describing changes in the phase of the output signal of an oscillator. This can be viewed as observing how uniformly in time the zero crossings occur. There are two parameters which have little to do with frequency stability as it affects a user system. These are amplitude modulation and harmonic distortion. These points will be explained next to remove them as possible confusion factors.

Amplitude Modulation

Most measurement methods and specifications ignore amplitude noise, that is unwanted amplitude modulation. This is because amplitude noise can be stripped off in an inexpensive limiter stage. Many systems use such a limiter to interface with a frequency standard input for this reason, as well as to provide gain and/or to standardize the signal level for the stages which follow. Even when not specified, AM noise sidebands in most quality sources are comparable to or better than phase noise.

Harmonic Distortions

The square wave output of a symmetrical limiter mentioned above contains large odd order harmonics which can be filtered off if the system would be perturbed by them. Where a limiter is used, odd order harmonic distortion on the output of the oscillator is of no consequence. Of more concern is even order harmonic distortion because it causes the positive half-cycles to have a different shape from the negative half cycles. This asymmetry can cause unbalanced operation in some frequency doubler circuits.

Most applications are not sensitive to moderate amounts of harmonic content. Because of this, even the highest quality sources have harmonic distortion specifications around 30 to 40 dB down. This performance is easily measured directly on a spectrum analyzer, or selective voltmeter.

To summarize: any distortion in the shape of the wave which remains unchanged from one cycle to the next, shows up as harmonic distortion. This is easily measured, and has no effect on frequency or phase stability.

FREQUENCY - PHASE, TIME

Examination of the frequency standard output waveform will now concentrate on the variations in the time of occurance of the zero crossings (1). Consider again a frequency standard signal having passed through a hard limiter. The only information remaining is the time of the zero crossings. It is here that all the stability of frequency and phase, or time, is defined. This suggests the technology of digital logic where waveshape and amplitude receive little attention, but edge timing is critical. An illustration of these points exists in the fact that Schot*ky T²L logic

circuitry can be used to process the output of a high quality source with comparable results to well designed discrete analog circuitry. Also, the action of logic circuitry meets the definition of a hard limiter.

Frequency Counters

The most familiar method of frequency measurement is the frequency counter instrument. When it is used for a standalone measurement (without use of an external reference standard) its internal time base oscillator accuracy will range from 10^{-8} for a top quality instrument on a monthly calibration schedule, to 10^{-6} for a low cost counter receiving annual checks.

In order to make frequency measurements with accuracies better than 10^{-8} , a carefully maintained house standard is usually the reference of choice in a laboratory environment. In a field or system environment, an atomic resonance stabilized oscillator can, even with significant environmental effects, still offer 10^{-11} absolute accuracy.

The resolution of the frequency counter itself represents a measurement precision limit separate from the reference source. For example a modern high performance counter may actually count a 500 MHz internal clock for a large number of periods of the input signal to be measured. Such a counter then divides the latter by the former to display a frequency result. The resolution is simply the total number of cycles of 500 MHz counted. If the operator can afford to wait 1000 seconds for a reading, then the resolution is one out of 5 x 10^{11} or 2 x 10^{-12} per increment of the least significant digit.

Frequency From Phase Rate

The difference between two frequencies can be measured by triggering an oscilloscope with one while observing the other and timing the rate of phase drift between the two with a stop watch. For instance, if during 10 seconds, four cycles pass across the center line of the graticule, then the frequencies differ by 0.4 Hz.

It is more common to time the passage of a zero-crossing of the signal as it moves across a major division of the oscilloscope screen for two reasons: First, for small

frequency errors, many minutes or even days might elapse before a complete cycle had passed. Second, frequency errors and tolerances are usually expressed in normalized or fractional notations as $\Delta f/f$. If the 0.4 Hz error above were on a 10 MHz signal, then its fractional frequency error or $\Delta f/f$ would be 4 x 10 $^{-8}$.

As an example of this method, conditions near the practical limit of its use are: a 10 nanosecond phase change during a 100 second elapsed time. This is referred to as a $\Delta t/t$ of 1 x 10^{-10} . Since a $\Delta t/t$ measured in this way equals $\Delta f/f$ directly, computation is minimal and simple. It is useful to note that this method does not involve knowledge of the carrier frequency. This can be especially convenient when the carrier frequency is a cumbersome non-integer, or for comparing errors among branches of a system where the carrier frequencies differ. A coherent synthesizer will probably be needed to serve as a trigger reference in these cases.

Phase Meter, Strip Chart Recorder

Several more orders of magnitude of resolution down to $\Delta f/f = 1 \times 10^{-14}$ can be obtained by using a phase meter with some means of recording its output. The simplest arrangement to achieve this is a vector voltmeter with its dc phase output connected to a strip chart recorder. This can resolve 0.1 nanosecond and, in less than three hours, or 10^4 seconds, the resolution becomes $\Delta t/t = 1 \times 10^{-14}$.

A time interval counter can also be used to measure phase, and can reach fractional nanosecond resolution with time interval averaging, or interpolation. Recording data from a counter can be handled with a printer, a digital to analog converter and strip chart recorder, or an interface bus to a calculator and peripherals.

A comment on the $\Delta t/t$ method is in order: The fractional frequency difference measured with this method is the average (mean) during the measurement interval t.

These techniques are recommended for the measurement of absolute frequency error, long term aging, effect of environmental changes, and house standard monitoring. Two beat frequency methods which yield extreme resolution in very short measurement times are described in HP Application

Note 52-2, page 3 (1), and, by David W. Allan, "Report on NBS Dual Mixer Time Difference System (DMTD)..." (2).

FREQUENCY STABILITY

An oscillator's inherent instabilities, other than those induced by environmental effects, can be grouped conveniently into three classes of frequency changes: monotonic, periodic, and random.

Aging

Monotonic drifts in frequency over time ranging from days upward are called frequency aging and are measured by repeated application of techniques described above for absolute frequency measurement. (3) Non-monotonic drifts also occur and can be measured by these techniques.

Periodic FM

Periodic changes in frequency amount to frequency modulation (whether or not intentional) by a sine wave and its harmonics. This is a typical problem in many applications and will be discussed along with random frequency variations and their measurements. It is worth noting at this early point that frequency modulation or phase modulation are no more than different ways of measuring the same signal. For example, should one attempt to analyze the signal coming from a black box emitting a 1.0 MHz carrier, whose frequency swings sinusoidally from 0.999 MHz to 1.001 MHz at a 1.0 kHz rate, it would be found to have FM/PM sidebands, spaced at 1.0 kHz multiples from the carrier, of amplitudes indicating a modulation index of 1.0. Correspondingly a phase meter would show that the carrier phase was swinging sinusoidally at a 1.0 kHz rate with peak excursions of 1.0 radian.

RANDOM FREQUENCY VARIATIONS, TIME DOMAIN

Possibly the most familiar measure of the randomness or scatter of any variable is the standard deviation or rms, the usual symbol is a lower case sigma, σ , and a formula is:

 $\sigma_{x} = \sqrt{\frac{1}{N-1}} \sum_{j=1}^{N} (x_{j} - \overline{x})^{2}$ (1.

This means that N measurements, each an x_j , are averaged to find \overline{x} , then σ is computed. This was applied to characterize frequency sources until it was found that some of the non-white noise processes commonly present caused σ to vary depending on the choice of N. This is even worse because, for larger N, σ can increase instead of converging. Further detail is in NBS Technical Note 669, p. 7, (4).

For these reasons, in the measurement of frequency sources, a special definition of σ , which avoids the divergence problems, is in universal use. This measure is called the Allan variance after its developer. It may be recalled that a variance is the square of a standard deviation. This measure is defined by the formula:

$$\sigma_y^2(\tau) \sim \frac{1}{2(M-1)} \sum_{k=1}^{M-1} (y_{k+1} - y_k)^2$$
 (2.

where M measurements are made of $\Delta f/f$, each of which is a y_k . On sigma, the subscript y means that sigma is a measure of the scatter in fractional frequency difference, $y = \Delta f/f$. The "approximates" symbol, \sim , is used instead of "equals", =, because this is a measure of a random phenomemon by a finite number of samples, M. This means that some scatter must be expected in measurements of $\sigma_y(\tau)$, amounting to several percent for M=100. (15) The time duration of each measurement is τ , also called averaging time or sample time. The significance of the parameter τ appears when we measure $\sigma_y(\tau)$ for different averaging times, in effect varying τ stepwise, then plot the results. This is the familiar frequency standard specification plot of $\sigma_y(\tau)$ versus τ . Since τ is the independent variable, these are called TIME DOMAIN measurements and specifications, and also SHORT TERM STABILITY.

In order to measure the $\sigma_{\gamma}(\tau)$ of all higher quality sources. which includes quartz oscillators well below \$1000, some special arrangement is required beyond a simple frequency counter to attain sufficient resolution. The basic method which has seen the widest use is the heterodyne or beat frequency method. This is diagrammed in Figure 1 and requires that the two oscillators to be compared be offset by the desired difference frequency, f_D , usually between 1.0 and 10 hertz. Proper choice of f_D will make the counter read directly in $\Delta f/f$ scaled by a convenient power of 10. The relationship is:

 $\frac{\Delta f}{f} = \frac{f_D^2 \Delta \tau}{f_D} \tag{3.}$

where $\Delta f/f$ is the fractional frequency difference indicated by an increment in the period count of $\Delta \tau$. The nominal

carrier frequency is f_0 and the beat frequency f_D . For example, if f_0 = 10^7 Hz, f_D = 10 Hz, and the least digit of the period count is $\Delta \tau = 10^{-7}$ second, then the resolution of each measurement is 10^{-12} . This gives the scale of the counter readings so that they may be entered into equation (2. above directly as the y_k measurements. The averaging time of the measurement is the period which is counted, at the minimum, $\tau = 1/f_D$, and multiple periods can be counted for longer τ .

In Figure 1, the block labeled "Mixer, Low Pass Filter, Amplifier" must be designed with some care to achieve a low noise interface between the mixer and the counter, and to set the noise bandwidth of the system to the desired value, conventionally 100 kHz. When measuring in a region of τ where $\sigma_y(\tau)$ shows white noise phase modulation, the measurement result will be proportional to the square root of the system bandwidth. There is a commercial product which serves these needs, the HP 10830A mixer/amplifier shown in the 5390 System (5), Figure 2.

Another parameter which can affect the measurement is the reset interval of the counter, also called dead time. In this arrangement the counter must ignore one period between the completion of one measurement and the start of another, while it outputs data and resets. This dead time biases the measurement result, requiring corrections which are called bias functions. These are tabulated in NBS Monograph 140, pages 190 - 204 (6) and HP Application Note 174-7 (7). An abbreviated table is included in Appendix D.

In order to choose the proper bias function to apply to a data point, the slope of the data at that point must be known. This means that $\sigma_y(\tau)$ must be measured at least two different values of averaging time τ . If only a few values of τ are used, they should be separated by ratios of about two or three. Measurement uncertainty would lead to a large slope uncertainty for a pair of closely spaced points. If a pair of data points were spaced a decade apart in τ , the slope could be changing significantly. The best policy is to plan to take as many data points as circumstances allow. More detailed discussion of which slopes may be expected is located in the section headed "Conversion of Data Between Time and Frequency Domains."

If a 10 Hz offset between the unit under test and the reference can be achieved, then this heterodyne method can be used to measure $\sigma_y(\tau)$ conveniently for τ from at

least 1000 seconds down to 1/10 second. Efforts to increase the offset frequency, to measure at shorter times, must be applied with care, because such conversion techniques as synthesizing and mixing can easily add more noise than that which was to be measured.

If a signal from a third oscillator of similar or better quality to the unit under test is available, then two more sets of data can be taken, pairwise among the three. These three measurements then can be combined to find the performance of each individual unit (8).

$$\sigma_a = \sqrt{\frac{1}{2} (\sigma_{ab}^2 + \sigma_{ac}^2 - \sigma_{bc}^2)}$$
 (4.

The subscripts refer to units a, b, and c. Once the reference unit is calibrated, then future measurements of unknowns can be computed more simply:

$$\sigma_a = \sqrt{\sigma_{ab}^2 - \sigma_b^2}$$
 (5.

Clearly, all measurements combined must be at the same τ .

For nearly all stable sources, their short term stability in the region of approximately one millisecond to one second shows white noise of phase as the dominant process. Direct measurement of this performance requires an additional level of complexity beyond the basic methods of this paper.

Fortunately there is a basic method which, though indirect, gives a more detailed characterization of performance. This method is the phase noise, $\pounds(f)$, measurement in the frequency domain. Most stable sources exhibit a flattening-out of their phase noise spectrum in the 100 Hz to 10 kHz region. The asymptote of this measurement can be converted using the white phase equation for $\sigma_{\mathbf{Y}}(\tau)$ in Table 1 to give the corresponding Allan variance in the time domain.

The improved detail comes from the fact that the phase noise measurement will show the frequency and amplitude of any discrete spurious sidebands. The peak effect of these on $\sigma_V(\tau)$ is calculated by:

$$\sigma_{y}(\tau) = \frac{\sqrt{8}}{\pi f_{o}} \sqrt{\text{antilog} (\mathcal{L}_{PM} dB/10)} \tau^{-1}$$
 (6.

where f_{O} is the nominal carrier frequency and \mathcal{L}_{PM} is the single sideband to carrier ratio in decibels of the spur. A derivation of this formula appears in Appendix A. Note that this result is not a function of the sideband frequency.

The above points are illustrated by actual data plots in Figure 3. The $\sigma_{\mathbf{y}}(\tau)$ data was taken with an HP 5390A Frequency Stability Analyzer and the $\boldsymbol{\mathcal{L}}(f)$ data was taken with the arrangement in Figure 4, using an HP 10534A Mixer, 3581 Wave Analyzer and 7035B X-Y Recorder.

Incidentally for τ less than one millisecond, the frequency domain measurement is still the better choice for the same reasons. In some sources, a bandpass filter is included which causes the phase noise or $\mathcal{L}(f)$, curve to break downward at a slope of f^{-2} starting at some frequency above 10 kHz. This is random walk of phase or white FM and has a time domain slope of $\tau^{-1/2}$. Whenever this performance is encountered in a frequency domain measurement, its asymptotic slope can be converted to $\sigma_{\mathbf{y}}(\tau)$ by using the white frequency equation in Table 1.

Turning to the region of τ =1 second and greater, the situation reverses, and direct measurements of $\sigma_y(\tau)$ become simpler. The following section gives details on phase noise measurement.

FREQUENCY DOMAIN, PHASE NOISE MEASUREMENT

To minimize confusion, this paper deals with frequency domain measurements in terms of only one of the measures available. The choice of single sideband phase noise to carrier ratio, $\mathcal{L}(f)$, was made because this measure is currently in almost universal use on oscillator data sheets, when frequency domain specifications are offered. This situation may change due to strong efforts to standardize on $S_{\varphi}(f)$ to replace $\mathcal{L}(f)$. If this occurs it will proceed slowly and apace with the desires of the user community. Accordingly it is the reader's prerogative to make his preferences known to his vendors in order to cast his vote in the matter. In the comments and equations to follow, $\mathcal{L}(f)$ may be replaced with any of the other measures by including the scaling coefficients tabulated in Appendix B. Some discussion of the uses of the symbol f is in Appendix C.

The basic method of measuring phase noise on signals makes use of the doubly balanced mixer as a phase detector as shown in Figure 4. Two recent publications describe extensions of this approach; NBS Technical Note 679 by David Howe (9), and HP Application Note 207 (10).

This system operates with both the reference and the unit under test at the same frequency. When the two signals into the mixer are in phase quadrature, the mixer's average dc output voltage will be zero and phase fluctuations will be translated to voltage fluctuations about zero. In order to keep the input phases near quadrature where the mixer's phase sensitivity is greatest and linear, and where its amplitude sensitivity is very small, there is a feedback path to the EFC (electronic frequency control) input of the reference oscillator. This constitutes a phase locked loop and functions as a convenience to the operator by helping maintain quadrature. Its operation is not part of the measurement of phase noise; in fact, care should be taken that the time constant of this loop is at least a tenth of a second if phase noise is to be measured as low as 5 Hz, so that the loop will not track and reduce the phase variations to be measured.

The network following the mixer/phase detector in Figure 4 is a low pass filter. The output of the mixer will contain both the sum and difference of the two frequencies at its inputs. Since the two frequencies are the same, f_0 , then the mixer output is dc with phase information plus a 2 f_0 component of amplitude about 6 dB below the smaller of the

two inputs. The low pass attenuates the 2 $\rm f_0$ signal to avoid overload or dynamic range problems with the input stage of the analyzer which follows. The purpose of the $\rm 51\Omega$ resistor is to provice a matched load for the 2 $\rm f_0$ signal from the mixer.

This is desirable because it helps the R and L ports of the mixer perform as specified. The 3900 pf capacitor allows the 2 $\rm f_0$ signal to pass, above 0.5 MHz, while blocking the thermal noise of the resistor to keep it from adding to the signal to be measured. Without the capacitor, if the signal were 6 dB above the resistor noise, the measured value would be made 1 dB worse by the resistor noise. This capacitor also blocks the signal frequencies to be measured and prevents the resistor from loading the mixer at these lower frequencies. This, with the high imput impedance of the analyzer yields 6 dB more signal level than if the mixer were terminated at low frequencies.

The $82\mu H$ inductor and $0.039~\mu F$ capacitor form a two pole low pass section which is flat within 0.1 dB to 50 kHz, is 3 dB down at 100 kHz and has skirts more than 40 dB per decade down above 100 kHz. When constructed of an inexpensive choke coil and mylar capacitor this circuit has reached -60 dB at 2.0 MHz and stayed below -60 dB will past 10 MHz.

The 100 kΩ resistor and 0.1 μF capacitor form a 10 millisecond time constant low pass to assure the slowness of the phase lock loop and help isolate the signal path from the EFC path where an oscilloscope or chopper stabilized sensitive dc voltmeter might be connected.

Calibration Factors Using Double-Balanced-Mixer Phase Detector

For small deviation phase modulation, the total signal instantaneous voltage is given by (11):

$$V(t) = \underbrace{\frac{A_c \cos \omega_c t}{\text{carrier}} - \frac{\frac{1}{2}A_c \beta \cos (\omega_c - \omega_m)t + \frac{1}{2}A_c \beta \cos (\omega_c + \omega_m)t}_{\text{sidebands}}}$$

where A_C is the peak amplitude in volts of the carrier component sine wave alone, ω_C is the carrier frequency and ω_m the modulation frequency both in radians per second, t is time, the independent variable, in seconds, and $\beta \equiv \Delta \phi$, the peak phase excursion in radians, also defined as $\Delta \omega/\omega_m$ or $\Delta f/f_m$, the peak frequency excursion divided by the modulating frequency.

By using the appropriate terms from (1., the ratio of single sideband-to-carrier power can be expressed as:

$$\mathcal{L}(f) = \left(\frac{\frac{1}{2}A_{C}\beta}{A_{C}}\right)^{2} = \frac{\beta^{2}}{4}$$
 (8.

(7.

When a phase noise measurement system, as shown in Figure 4, is calibrated by offsetting the frequency of one of the inputs to the double-balanced mixer phase detector, the voltage, $V_{\rm cal}$, of the sine wave out of the mixer at the difference frequency is usually measured by an rms indicating instrument. This gives the desired mixer transfer coefficient if scaled as follows:

$$\frac{\partial V}{\partial \Delta \phi} \frac{\text{volts peak}}{\text{radians peak}} = \left(V_{\text{cal}} \text{ volts rms} \right) \left(\sqrt{2} \frac{\text{volts peak}}{\text{volts rms}} \right)$$
 (9.

This is because the sinusoidal waveform of the mixer output has a slope, as it crosses the zero axis, expressed in volts per radian, equal to the peak amplitude of the wave in volts. Recall that the sine function has a peak value of one and also a slope at the origin of one.

Then, when a phase noise reading is taken, the indication will represent the actual phase excursions and again will be rms, that is $V_{\rm DSB}$ volts rms and:

$$V_{DSB}$$
 volts peak = V_{DSB} volts rms $(\sqrt{2} \text{ volts peak/volts rms})^{(10)}$.

and the phase modulation is related to the mixer output by its transfer coefficient:

β radians peak =
$$\frac{V_{DSB} \text{ volts peak}}{\frac{\partial V}{\partial \Delta \phi} \frac{\text{volts peak}}{\text{radian peak}}}$$
 (11.

Substituting (9. and (10. into (11.:

β radians peak =
$$\frac{\sqrt{2} \text{ V}_{\text{DSB}} \text{ volts rms}}{\sqrt{2} \text{ V}_{\text{cal}} \text{ volts rms}}$$
 (12.

Then substituting (12. into (8.:

$$\mathcal{L}(f) = \left(\frac{V_{DSB}}{V_{Ca1}}\right)^2 \frac{1}{4}$$

$$\mathcal{L}(f) dB = 20 \log \frac{V_{DSB}}{V_{Ca1}} - 6 dB \qquad (13.$$

Changes in attenuator or gain control settings between calibration and measurement phase must also be taken into account. The signal level applied to the L port of the mixer should be as large as possible, within the mixer specification and should not be changed for either calibration or measurement phases. If it is planned to change the R port signal level between calibration and measurement, then during the calibration phase the R level should be run up to the highest level to be used, while monitoring the changes in $V_{\rm Cal}$ to verify that the mixer is in a linear range. On the other hand the operator may choose to operate the mixer at high levels, where several dB of compression are occurring, to get the best system noise performance. This is valid provided that no signal level changes occur between calibration and measurement at the L and R ports of the mixer.

After offsetting the two oscillators to calibrate the system, they must be returned to the same frequency and the EFC loop locked. The mixer dc average output voltage should be checked to make sure it is near zero, preferably within a few millivolts, before and after making the phase noise measurement.

Thus far all the points discussed apply equally to a discrete spectral component (bright line) as well as to the random noise phase modulation contained in a specified noise bandwidth. Since most of the measuring instruments which might be used for these tests are designed to measure and are calibrated for discrete spectral components, equation (13. applies directly for them. Examples of these instruments are wave analyzers, spectrum analyzers, and tuned voltmeters.

In the case of random phase modulation, if the bandpass filtering function of the measuring instrument were followed by a true rms detector, followed by linear low-pass smoothing or averaging, then equation (13. would still apply. However, in order to give a reading linear in decibels, many analyzers utilize logarithmic IF amplifiers followed by an average-responding amplitude detector.

If the measurement system has a logarithmic conversion followed by an average detector before the final averaging or smoothing (which may be by visual estimate), then a factor of ± 2.5 dB must be applied to (13. above when measuring random noise (10, 12, 13, 14). Also the resolution bandwidth control setting is narrower than the actual noise bandwidth effective in the measurement so that a factor of ± 0.8 dB must also be applied to (13. above when measuring random noise (13). For ultimate accuracy, this factor should be checked, because many IF bandwidths are specified as $\pm 10\%$. The resulting formula for random noise is then:

$$L(f) dB = 20 log \frac{V_{DSB}}{V_{Cal}} - 4.3 dB$$
 (14.

In the HP 3580A (and 3581A) Spectrum Analyzer, following the ac log amp and average-responding detector, there is a dc output to the rear panel for an external recorder. Equation (14. applies for this output because it is proportional to the detector output. However this signal is also fed into an analog-to-digital converter for internal display and storage. This converter operates in a time window during which its conversion algorithm increments the digital word whenever an excursion of the analog input exceeds the converted value. This has the effect of "peak grabbing" and seems to give a displayed result which is about one to two sigma of the detected signal above its long-term mean, a source of error from 2 dB for Gaussian to about 6 dB for non-Gaussian noise in the HP 3580A, when measuring random noise. The only defense against this is the use of maximum

smoothing to minimize the variability of the signal being converted, during the conversion time window.

Under many desirable sweep and bandwidth conditions, the use of maximum smoothing will cause the "ADJUST" lamp to light. For the measurement of random noise having a gently sloping spectrum this is of no consequence. The meaning of the lamp is that the instrument will be sweeping past any discrete signals more rapidly than the smoothing circuit can respond so that their indicated amplitude will be depreciated and uncalibrated. A reasonable set-up procedure seems to be the adjustment of the bandwidth, sweep width and rate with the smoothing set at minimum, so that the most expeditious settings are obtained while keeping the adjust lamp off; then switching to maximum smoothing, which brings the adjust lamp on. Should bright lines be present, they will be almost as noticeable above the noise with maximum smoothing as without. If their presence is detected, then a measurement of their true amplitude can be made using settings which extinguish the adjust lamp. The only subtlety discovered in testing this technique occurs whenever a large number of closely spaced discrete lines can, in a wide sweep, masquerade as random noise. An example of this is 60 Hz and its harmonics viewed in a 10 kHz wide sweep. Harmonics through the 50th, to 3 kHz have been seen. In this example, a 10 Hz bandwidth was little help in resolving the true situation. This trap existed with both minimum and maximum smoothing but maximum smoothing makes such situations even less suspicious in appearance. The tactic for testing against this trap is to narrow the sweep width to no more than 100 times the bandwidth and use a sweep rate and smoothing which extinguish the adjust lamp. If, under these conditions the spectrum appears smooth, then there are no discrete lines separated by more than the bandwidth setting.

When measuring a rapidly sloping spectrum it is important to keep the measurement bandwidth narrow enough so that nearby components at a higher level do not come in through the skirt response of the IF and bias the measurement upward.

A measurement worksheet format, included with the figures, has been found useful in unifying the results of different workers. The one-tenth decade frequency steps facilitate the use of linear scaled graph paper, for later plotting, on which integer slopes are more readily recognized and manipulated. The steps are also 1/3 octave so that octave

steps starting at any point and proceeding in either direction are pre-computed. This is also true of half decade points as well as five-per-decade points. The most important aspect of the worksheet is that it encourages the worker to record "Raw Readout" so that the scaling of the data may be questioned, reconstructed, and either vindicated or modified at a later date without repeating the measurement.

Individual Oscillator Phase Noise Characterization

The single sideband phase noise, $\mathcal{L}(f)$, of an individual oscillator at a particular frequency f can be deduced from pairwise measurements among three. The approach used here is analogous to one for $\sigma_{\gamma}(\tau)$ developed by Gray and Allan (8). For $\mathcal{L}(f)$ expressed in decibels, the measured values will obey the relationship:

Measurement = 10 log
$$\left(\operatorname{antilog} \left(\mathfrak{L}_{1}(f)/10\right)\right)$$
 + (15. antilog $\left(\mathfrak{L}_{2}(f)/10\right)$)

For example: Measurements among three sources would yield the results depicted in the following examples:

	INDIVIDUAL UNIT PERFORMANCE	PAIR-WISE MEASUREMENT RESULT
UNIT 1	-90 dB	
UNIT 2	-100	-89.6 dB
UNIT 3	-100	- 9 7
UNIT 1	-90	-89.6
UNIT 4	- 90	
UNIT 5	-100	-89.6
UNIT 6	-90	-89.6
		-87
UNIT 4	-90	

	INDIVIDUAL UNIT PERFORMANCE	PAIR-WISE MEASUREMENT RESULT		
UNIT 7	-94			
UNIT 8	-97	-92.2		
UNIT 9	-100	-95.2		
UNIT 7	-94	- 93		

Note that in units 1 through 6 the individual unit performance numbers are simple and repetitious. Now consider the measurement results to discern how these results indicate the particular equalities and differences which exist between the individual units. In particular, the fact that \mathcal{L}_{12} equals \mathcal{L}_{13} means that units 2 and 3 are equal. Then each alone must be 3 dB better than the measured result for \mathcal{L}_{23} . Once this is known, equation (15. can be used to find the individual performance of unit 1.

The example with units 4, 5 and 6 is offered to allow the reader to check the understanding gained from the first trio.

The third example with units 7, 8 and 9 is more representative of the range of performance typically encountered. Note that in this last example, the differences from the median measurement of -93 dB are only +0.8 and -2.2 which could have been brushed aside as experimental error or scatter. This would lead to the interpretation that all three sources are substantially equal, and therefore about -93 - 3 = -96 dB. This would be an unfortunate misuse of the data because it ignores significant differences among the three sources of four times the noise power in the sidebands of the -94 dB source relative to the -100 dB source.

Equation (15. and the examples are based on simple addition of the individual power levels of uncorrelated noise. Expressed in units of watts, this can be stated as:

$$P_{12} = P_1 + P_2$$
 (16.

where P_{12} is a measurement of signal 1 versus signal 2. Given three measurements, the individual source performance can be computed. A formula for this is derived as follows:

$$P_{ab} = P_a + P_b \tag{17.}$$

$$P_{bc} = P_b + P_c \tag{18.}$$

$$P_{ac} = P_a + P_c \tag{19.}$$

1. N. 1. N.

then:

$$P_a = -P_c + P_{ac},$$
 $P_c = -P_b + P_{bc},$ $P_b = -P_a + P_{ab}$

and by substitution:

$$P_{a} = + P_{b} - P_{bc} + P_{ac}$$

$$P_{a} = - P_{a} + P_{ab} - P_{bc} + P_{ac}$$

$$2P_{a} = P_{ab} + P_{ac} - P_{bc}$$

$$P_{a} = \frac{P_{ab} + P_{ac} - P_{bc}}{2}$$
(20.

and similarly for P_b and P_c :

$$P_{b} = \frac{P_{bc} + P_{ab} - P_{ac}}{2}$$
 (21.

$$P_{c} = \frac{P_{ac} + P_{bc} - P_{ab}}{2}$$
 (22.

When these noise sideband powers are expressed in dB power ratio relative to the carrier, equation (20. becomes:

$$\mathcal{L}_{a}(f) dB = 10 \log \left\{ \frac{1}{2} \left[\operatorname{antilog}(\mathcal{L}_{ab}/10) + \operatorname{antilog}(\mathcal{L}_{ac}/10) \right] \right\}$$
antilog(\mathbb{L}_{ac}/10) - \text{antilog}(\mathbb{L}_{bc}/10) \]

and again the form is the same for equations (21. and (22. with appropriate subscript changes.

For development work, after an individual oscillator of good performance has been characterized by this procedure, it can serve as a measurement reference for testing oscillators as much as 3 dB better. Only a single measurement is required, the result being interpreted in the light of the known performance of the reference oscillator by the use of equation (15. This relationship is plotted in Figure 5 so that a measurement against a known reference can be converted graphically to the $\mathcal{L}(f)$ of the unknown. The plot also makes it convenient to notice the uncertainty range of the result versus the uncertainty range of the measurement (respectively, 3 to 1 for \mathcal{L}_{DUT} - \mathcal{L}_{REF} = -3 dB).

The function plotted in Figure 5 can be derived as follows. The desired expression has the form:

$$\ell_{\text{DUT}} - \ell_{\text{REF}} = G \left(\ell_{\text{MEAS}} - \ell_{\text{REF}} \right)$$

because ℓ_{DUT} (device under test) is the desired result and ℓ_{REF} (reference) and ℓ_{MEAS} (measurement data) are the known quantities and G represents the function to be derived. Starting with a version of equation (15:

$$\ell_{\text{MEAS}} = 10 \log \left(\text{antilog } (\ell_{\text{REF}}/10) + \text{antilog } (\ell_{\text{DUT}}/10) \right)^{(24)}$$

Rearranging:

$$\ell_{\rm DUT}$$
 = 10 log (antilog ($\ell_{\rm MEAS}/10$) - antilog ($\ell_{\rm REF}/10$) (25. Subtracting $\ell_{\rm REF}$ from both sides:

 $\mathcal{L}_{\text{DUT}} - \mathcal{L}_{\text{REF}} = 10 \log \left(\text{antilog } (\mathcal{L}_{\text{MEAS}}/10 - \text{antilog } (\mathcal{L}_{\text{REF}}/10) \right)$ $-10 \log \left(\text{antilog } (\mathcal{L}_{\text{REF}}/10) \right)$

= 10 log
$$\frac{\text{antilog } (\ell_{\text{MEAS}}/10) - \text{antilog } (\ell_{\text{REF}}/10)}{\text{antilog } (\ell_{\text{REF}}/10)}$$

$$\ell_{\text{DUT}}$$
 - ℓ_{REF} = 10 log $\left((\ell_{\text{MEAS}} - \ell_{\text{REF}}) / 10 \right)$ -1 (26.

It is important to keep in mind that a measurement result represents the combined performance of the two units. The simplest accurate rule to remember is that the noise powers contributed by the two units add. There has been a prevalent

practice of assuming the two devices under test to have equal performance since little if any other information existed. This rationale is used to justify scaling the measurement result down by 3 dB, then ascribing this performance to both units. Since no other facts exist this assumption is usually allowed to stand unquestioned.

Closer examination of the assumption can begin by hypothesizing a population of units whose performances scatter by +2 dB and -2 dB for one-sigma or standard deviation about the mean for all units. For any realistic distribution shape, it should seem highly unlikely that any two units would exhibit equal performance, even within one decibel. If the purpose of the measurement was to determine how good either of the units might be, then the most pessimistic assumption is 3 dB below the measurement. However if a purpose of the measurement was to determine how poorly a unit might perform, then the assumption of 3 dB below the measurement is not only the most optimistic but also the least likely.

If an assumption must be made, it may be much more supportable engineering judgement to assume a "two source correction factor" between one and two decibels below the measurement, as indicated on Figure 6 (a replot of Figure 5). However this is not recommended practice. It is more informative to report the measurement with no correction.

CONVERSION OF DATA BETWEEN TIME & FREQUENCY DOMAINS

The procedure for converting frequency domain data into time domain or vice versa can be approached in a number of different ways, all valid. This is mostly a matter of personal preference just as any two people may go about solving a given algebraic equation with minor differences but both will agree on the result. The object here is to present a sequence which carries a mnemonic thread of logic, possibly at the expense of brevity, by not "skipping steps" or combining them.

Step one is the choosing of a single portion of the data under consideration which can be represented by a straight line on a dB-log frequency or log-log plot. This will be repeated until all portions of interest are covered. The logic or assumption applied to this step is: "If this straight line represented the total (broad range) and only performance characteristic of the oscillator, it can be converted to the other domain to see what it would look like there."

From this logic follows the most fundamentally important point to be considered in interpreting the results: As each portion of an actual performance curve is approximated by a straight line segment, converted and re-plotted, it has been handled by the mathematics as if it were independent of the other segments. This places the burden on the user to combine the segments into a new curve through a reasonable and logical interpretation. Step three will expand on this later.

Next comes the detailed technique of matching a straight line segment to a smoothly curving and/or randomly scattered plot: A basic constraint is the fact that conversion formulas only exist for particular slopes, and for only five different slopes. In the frequency domain for $\mathcal{L}(f)$ in decibels, these range from flat, white noise of phase or fo, to f-4, random walk of frequency, or -40 dB per decade of frequency, with the intervening slopes occuring with integer steps of the exponent on f, which correspond to 10 dB steps per decade. A "map" of the slopes is shown in Figure 7. It is only reasonable to arbitrarily choose a "convertible" slope. Align parallel rules, or the edge of a triangle opposite a reference straight edge, versus the graduations on the axes of the plot, to the chosen slope, then slide it into the region of the data while maintaining the slope constant. If a region of the data can be found which seems asymptotic to the trial slope, that is within three decibels over a decade of frequency, then an accurately representative straight line segment has probably been found.

Visual averaging of measured data exhibiting scatter or randomness which has been plotted on a logarithmic scale must be done with special consideration of the illusionary effect of the log scale. For example, imagine a linear plot of data points scattered symmetrically about their true mean, that is no skew in their distribution. In this case the mean and the median would very likely coincide quite closely and could be discerned visually with an accuracy of a tiny fraction of a standard deviation. Now imagine this same ensemble of data being replotted on a log scale. The scatter of the values larger than the mean will be compressed by the logarithmic action. Correspondingly, the scatter of the values less than the mean will be expanded. The net effect is to impart a visual skew to the distribution so that if a mean is visually estimated on the log plot, it will be low by a major fraction of a standard deviation.

A defense against this misinterpretation is found in the coincidence of the true mean and the median. This is accomplished by disciplining the eye to estimate a line through the data points such that half the points lie on each side without regard to how far away they may be. The importance of this technique becomes very apparent whenever the total scatter of the data approaches one-half decade where interpretation errors of 30% can occur.

Any straight line is completely specified by its slope and an intercept. The most convenient intercepts to use in frequency stability analysis are one hertz and one second. (Please do not infer any general correspondence between one hertz and one second performances. Experience shows this to be coincidental at best.)

The completion of the first step is writing down the slope and intercept of the line through the data.

The second step is the choosing of the conversion formula, from Table 1, corresponding to the data domain (frequency or time) and slope, then plugging in the intercept and "turning the crank" to calculate the result. Each of the conversion formulas contains both f and τ variables raised to powers appropriate to both cancel the slope of the incoming slope-intercept data as well as establish the slope of the result. The presence of these terms gives rise to the convenience of choosing them equal to unity, then converting only the intercept point, while the slope conversion becomes obvious by inspection of the exponents on f and τ .

The second step is completed by writing down the computed intercept value and slope of the converted line. This result can be assumed to specify a straight line on a log-log plot in the new domain. In the time domain, the slopes change in steps of τ^2 , and range from τ^{-1} for white noise of phase to τ^{+2} for random walk of frequency, with one exception and an additional case.

The exception appears when converting from $\mathcal{L}(f)$ of slope f^{-1} , flicker of phase, to $\sigma_y(\tau)$, which will yield a plot having a slope very near -0.95. This one case is less obvious from the form of the equation, but being unique, is easily remembered and recognized. Also in this case, the simple slope-intercept interpretation of the conversion result sacrifices some accuracy and should be avoided until the user has enough familiarity with the results versus his application to determine whether the error may

be negligible. The preferred method is the computation of three values for $\sigma_{\mathbf{y}}(\tau)$, widely separated in τ , over the range of interest, using the conversion formula.

The additional case is $\sigma_y(\tau)$ data having τ^{+1} slope. This does not appear in conversions from $\mathcal{L}(f)$, frequency domain, but may be seen in actual $\sigma_y(\tau)$ data for $\tau \geq 100$ seconds for quartz oscillators. It can be shown that constant-rate aging drift of frequency results in τ^{+1} slope of $\sigma_y(\tau)$. Slowly changing ambient thermal effects can be responsible for τ^{+1} slope below 100 seconds.

The third step in the conversion process is the plotting of the converted straight lines on log-log axes of the new domain. This begins with locating the intercept points, then drawing a line through each point with the corresponding slope. This slope is indicated by the exponent in the conversion formula for the independent variable, the horizontal axis, frequency or time.

Interpretation of the straight lines in order to combine them into a single smooth curve is quite similar to Bode plot work. The final curve is, at each point, the sum of the component straight lines. From this follows the fact that where two lines intersect, the smooth curve is 3 dB higher for $\boldsymbol{\mathcal{L}}(f)$ or 1.414 for $\sigma_{\boldsymbol{\mathcal{Y}}}(\tau)$. This is because noise powers add, and variances, $\sigma_{\boldsymbol{\mathcal{Y}}}^{2}(\tau)$, also add.

Since the equations of each of the straight lines are the results of step two above, these equations can be programmed into a desk calculator with a plotter and the final result curve (and a tabulation of numerical results) can be obtained directly. The relationships to be computed are:

$$\mathcal{L}(f) = \mathcal{L}_1 + \mathcal{L}_2 + \cdots$$
 (27.

For $\mathcal{L}(f)$ expressed as a power ratio. To convert from decibels:

$$\mathcal{L}(f)$$
 power ratio = antilog $\left(\frac{\mathcal{L}(f) - dB}{10}\right)$ (28.

And for $\sigma_{y}(\tau)$:

$$\sigma_{\mathbf{y}}(\tau) = \sqrt{\sigma_1^2 + \sigma_2^2 + \cdots}$$
 (29.

Since the slope of a group of data points is of similar importance to their magnitude, it is helpful to standardize the choice of scales for plotting data. This fosters visual familiarity which increases with experience. The alternative is to use a variety of scales for plotting, which presents the eye/brain with an assortment of optical illusions.

The recommended standards are:

- 1. Plot σ_y vs. τ on log log scales chosen so that a decade of each variable is the same length. Further, that on both axes linear subdivisions within decades be used and labeled with their logarithmic values.
- 2. Plot $\mathcal L$ vs. f on scales linear in dB for $\mathcal L$ and log for f such that the length of 20 dB of $\mathcal L$ equals the length of one decade of f. Further, that linear subdivisions be used for both $\mathcal L$ and f, and that the subdivisions within the decades of f be labeled with their logarithmic values.

ACKNOWLEDGEMENTS

The author is grateful for the contributions of Bill English and Dave Ricci, the support of Ian Band, and the diligent manuscript preparation by Liz Cypert.

REFERENCES

- (1) Hewlett-Packard staff, "Timekeeping and Frequency Calibration," Application Note 52-2, (Hewlett-Packard, Palo Alto, CA 94304, November 1975).
- (2) Allan, David W., "Report on NBS Dual Mixer Time Difference System (DMTD) Built for Time-Domain Measurements Associated with Phase 1 of GPS," NBSIR 750827, National Bureau of Standards (U.S.), (NTIS, Springfield, VA 22151, January 1976)
- (3) Hewlett-Packard staff, "Measuring Warmup Characteristics and Aging Rates of Crystal Oscillators," Application Note 174-11, (Hewlett-Packard, Palo Alto, CA 94394, November 1974).
- (4) Allan, David W., "The Measurement of Frequency and Frequency Stability of Precision Oscillators," NBS Technical Note 669, National Bureau of Standards (U.S.), (SD Catalog No. C13.46:669, USGPO, Washington, D. C. 20402, May 1975).
- (5) Peregrino, Luiz and Ricci, David W., "Phase Noise Measurement using a High Resolution Counter with On-Line Data Processing," Proc. 30th Ann. Symp. on Frequency Control, US Army Electronics Command, Fort Monmouth, N.J. (1976). Copies available form Electronic Industries Association, 2001 Eye Street, NW, Washington, D. C. 20006.
- (6) Blair, Byron E. (Editor) Time and Frequency: Theory and Fundamentals, NBS Monograph 140, National Bureau of Standards (U.S.), (SD Catalog No, C13.44:140, USGPO, Washington, D. C. 20402, 470 pages, May 1974).
- (7) Hewlett-Packard staff, "Measuring Fractional Frequency Standard Deviation (sigma) Versus Averaging Time (tau)," Application Note 174-7, (Hewlett-Packard, Palo Alto, CA 94304, November 1974).

- (8) Gray, James E., and Allan, David W., "A Method for Estimating the Frequency Stability of an Individual Oscillator," Proc. 28th Ann. Symp on Frequency Control, US Army Electronics Command, Fort Monmouth, N.J. pp 243-246, (1974). Copies available from Electronic Industries Association, 2001 Eye Street, NW. Washington, D. C. 20006.
- (9) Howe, David A., "Frequency Domain Stability Measurements: A Tutorial Introduction," NBS Technical Note 679, National Bureau of Standards (U.S.), (SD Catalog No. C13.46:679, USGPO, Washington, D. C. 20402, March 1976).
- (10) Hewlett-Packard staff, "Understanding and Measuring Phase Noise in the Frequency Domain," Application Note 207, (Hewlett-Packard, Palo Alto, CA 94304, October 1976).
- (11) Reference Data for Radio Engineers, 5th ed. (New York; Howard W. Sams, 1968), p. 21-7.
- (12) Hewlett-Packard staff, "Spectrum Analysis: Noise Measurements," Application Note 150 4, (Hewlett-Packard, Palo Alto, CA 94304, January 1973).
- (13) Hewlett-Packard staff, "Spectrum Analysis: Signal Enhancement," Application Note 150-7, (June 1975). "Spectrum Analysis: Accuracy Improvement," Application Note 150-8, (Hewlett-Packard, Palo Alto, CA 94304, March 1976).
- (14) Hewlett-Packard staff, "Spectrum Analysis: Noise Figure Measurement," Application Note 150-9, (Hewlett-Packard, Palo Alto, CA 94304, April 1976).
- (15) Lesage, Patrick, and Audoin, Claude, "Characterization of Frequency Stability: Uncertainty due to the Finite Number of Measurements," IEEE Trans. on Instrumentation and Measurement, Vol. IM-22, No. 2, June 1973, pp. 157-161.

APPENDIX A

Effect of Sinusoidal Phase Modulation on $\sigma_{_{\mathbf{V}}}(\tau)$

Short term stability of frequency sources is usually characterized by the square root of Allan variance, $\sigma_{\mathbf{y}}(\tau)$, where y is fractional frequency deviation, and τ is the averaging time or measurement interval. To measure an estimate of $\sigma_{\mathbf{y}}(\tau)$, a series of M measurements of $\overline{\mathbf{y}}$ are made and entered into:

$$\sigma_{y}^{2}(\tau) \sim \frac{1}{2(M-1)} \sum_{k=1}^{M-1} \left(\overline{y}_{k+1} - \overline{y}_{k} \right)^{2}$$
 (A1.)

where \overline{y} is the average y over an interval τ long.

The worst case effect of sine wave frequency modulation of modulating frequency f_m will occur when τ is equal to τ_p , the period of one half-cycle of f_m , and the measurement intervals are phased relative to f_m to catch the maximal excursions.

The fractional frequency deviation y can be stated:

$$y = \frac{\Delta f_0}{f_0}$$
 (A2.

where f_0 is the carrier frequency.

For one half-cycle of $f_{m}\text{,}$ the average to peak ratio of a sinusoid is $2/\pi$ and :

$$\overline{y} = \frac{2}{\pi} \frac{\Delta f_0 \text{ peak}}{f_0}$$
 (A3.

and the next half-cycle \overline{y} result would have the same magnitude and opposite sign.

Substituting into (A1, simplifying and letting M=2 because the result is independent of the number of measurements:

$$\sigma_{y}^{2}(\tau_{p}) \sim \frac{1}{2} \left(\left(\frac{2}{\pi} - \frac{\Delta f_{o} \text{ peak}}{f_{o}} \right) - \left(-\frac{2}{\pi} - \frac{\Delta f_{o} \text{ peak}}{f_{o}} \right) \right)^{2}$$

$$\sigma_{y}^{2}(\tau_{p}) = \frac{8}{\pi^{2}} - \left(\frac{\Delta f_{o} \text{ peak}}{f_{o}} \right)^{2}$$
(A4.)

$$\sigma_{y}(\tau_{p}) = \frac{\sqrt{8}}{\pi} - \frac{\Delta f_{o} \text{ peak}}{f_{o}}$$
 (A5.)

From modulation theory, the peak phase deviation or modulation index β is:

$$\beta = \frac{\Delta^{f} o \text{ peak}}{f_{m}}$$
 (A6.

rearranging:

$$\Delta f_{o peak} = \beta f_{m}$$
 (A7.

A bright line of phase modulation whose level is specified as the ratio between a single sideband and the carrier as \mathcal{L}_{PM} (in the same way as random noise) is indistinguishable from FM and:

$$\mathcal{L}_{\text{PM}} = \frac{\beta^2}{4} \tag{A8.}$$

Solving for β with $\boldsymbol{\mathcal{L}}_{pM}$ expressed in decibels:

$$\beta = \sqrt{4 \text{ antilog } (\mathcal{L}_{PM} \text{ dB/10})}$$
 (A9.

Substituting into (A7:

$$\Delta f_{\text{o peak}} = f_{\text{m}} \sqrt{4 \text{ antilog } (\mathcal{L}_{\text{PM}} \text{ dB/10})}$$
 (A10.

Substituting into (A5:

$$\sigma_{y}(\tau_{p}) = \frac{2\sqrt{8}}{\pi} \frac{f_{m}}{f_{o}} \sqrt{\text{antilog } (\mathcal{L}_{PM} \text{ dB/10})}$$
 (A11.

And as was stated earlier:

$$\tau_{p} = \frac{1}{2f_{m}} \tag{A12.}$$

A more rigorous derivation of (All. shows that the general case includes a term of the form ($\sin \pi \tau$)/($\pi \tau$). This causes the function to have lobes whose peaks fall off as τ^{-1} . Incorporating a τ^{-1} term and adjusting coefficients to agree with (All. gives:

to agree with (A11. gives:

$$\sigma_{y}(\tau_{p}) = \frac{\sqrt{8}}{\pi f_{0}} \sqrt{\text{antilog } (\mathcal{L}_{PM} \text{ dB/10})} \quad \tau^{-1} \quad (A13.$$

which, given \mathcal{L}_{PM} , is a worst case predictor of $\sigma_{y}(\tau)$. Conversely, given $\sigma_{y}(\tau)$, equation (A13. yields a minimum value for \mathcal{L}_{PM} . Solving for \mathcal{L}_{PM} :

$$\mathcal{L}_{PM} dB = 10 \log \left(\frac{\tau \pi f_0 \sigma_y(\tau)}{\sqrt{8}} \right)^2$$
 (A14.)

In the case where a frequency source output is displayed on a spectrum analyzer so that the upper and lower sidebands can be examined separately, if they are found to be asymmetrical, that is different amplitudes above versus below the carrier, then this indicates that both am and pm exist, of comparable modulation index, and correlated.

APPENDIX B

Interrelationships of Various Frequency Domain Stability Measures

$$S_{\phi}(f)$$
 rad²/Hz

- = spectral density of variance of phase fluctuations per hertz of bandwidth at sideband frequency f in $V(\tau)$ = cos $(2\pi f_0 \tau^+ \phi)$
- = $S_{\delta\phi}(f)$ (used in some publications 1971-1974)
- $= 2 \mathcal{L}(f)$

power in both upper and lower phase modulation sidebands
= per hertz of bandwidth at sideband frequency f
carrier power

(Some definitions of $S_{\varphi}(f)$ are, in effect, the above ratio by virtue of their use of a mixer as a phase detector. This definition holds only for broadband $^{\Delta\varphi}peak$ $^{<0.1}$ radian.)

$$= \frac{\mathbf{f}_0^2}{\mathbf{f}^2} S_y(\mathbf{f})$$

$$= \frac{\beta^2}{2} = \left(\frac{\Delta f_{rms}}{f_m}\right)^2 = \left(\frac{\Delta \omega_{rms}}{\omega_m}\right)^2$$

= mean square modulation index

$$S_{\phi}(f)$$
 dB (re I rad²/Hz)

- = $10 \log S_{\bullet}(f)$
- $= \mathcal{L}(f) dB + 3$

$\mathcal{L}(f)$ dimensionless power ratio

power in phase modulation single sideband

per hertz of bandwidth at sideband frequency f
carrier power

(defined only for $\Delta \phi_{peak}$ <0.1 radian)

$$= \frac{1}{2} S_{\phi}(f)$$

$$= \frac{\mathbf{c}_{0}^{2}}{2f^{2}} S_{y}(f)$$

$$= \frac{\beta^{2}}{4}$$

 $\mathcal{L}(f)$ dB, dBc (re carrier)

=
$$S_{\phi}(f) dB - 3$$

APPENDIX C

Comments on Symbology

There has been some effort to restrict the use of the symbol f to mean only Fourier frequency (in the context of oscillator stability, at least). It is the author's view that the symbol f is well established as a quite general symbol for frequency (with units of hertz strongly implicit due to convention). Accordingly, any specialization or limitation of meaning will only be accomplished by the use of a subscript or a different symbol entirely. Any attempt to the contrary flies in the face of a universe of deeply ingrained convention.

One specific problem with the restriction of f to mean sideband frequency is that f_0 could no longer be used for carrier frequency without confusion. The next alternative for a carrier frequency symbol would, by usage, be ν . This is very familiar and not confusing to physicists. However, the major number of people who will be trying to decipher the things we are writing today are not physicists, and the confusion between ν and ν make its choice questionable.

The signals whose phase instabilities we are treating may be modeled in voltage versus time as:

$$V(t) = \cos \left(\omega_{O}t + \phi(t)\right)$$
 (C1.

The analysis of the \$\phi\$ term versus frequency is often discussed as Fourier frequency. These become the sideband frequencies when the total spectrum of an actual signal is discussed. It seems much preferable to use the specific term "sideband frequency" when that is specifically what is being discussed, and reserve the use of the term "Fourier frequency" for occasions when its implicit generality is intended to be part of the concept being communicated.

The use of the term Fourier frequency could call to the reader's mind two or three pictures (definitions), only one of which is correct and intended by the author if he actually means sideband frequency. These are shown in Figure C1.

APPENDIX D

Time Domain Measurement Bias Functions

Definition: $\sigma_y(\tau)$ implies N=2 and T= τ , no dead time.

$$\mathbf{r} = \mathbf{T}/\tau$$

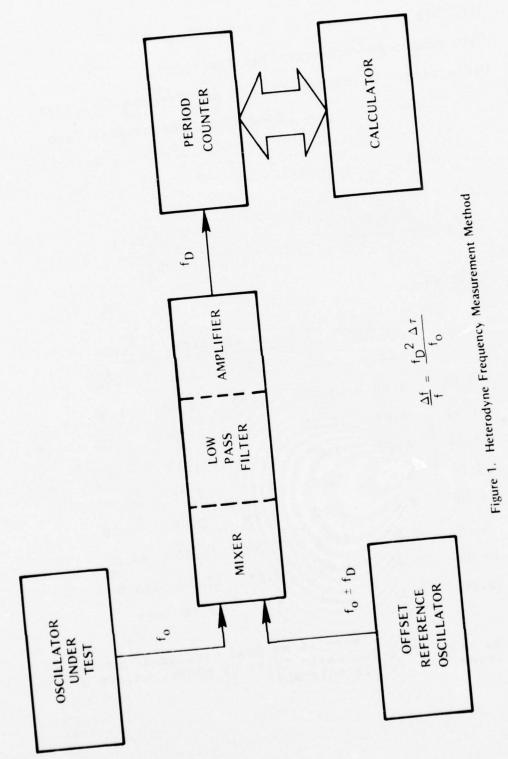
$$\mathbf{B}_{2} = \frac{\sigma_{y}^{2}(2, \mathbf{T}, \tau)}{\sigma_{y}^{2}(\tau)}$$

$$\sigma_{y}(\tau) = \frac{\sigma_{y}(2, \mathbf{T}, \tau)}{\sqrt{\mathbf{B}_{2}}}$$

 $B_2(r,\mu)$

		μ, Slope of Allan Variance, $\sigma_y^2(\tau) \propto \tau^{\mu}$					
		- 2	-1_	0	_1	2	
	1.00	1.00	1.00	1.00	1.00	1.00	
	1.01	0.67	1.00	1.01	1.015	1.02	
r	1.10	0.67	1.00	1.09	1.15	1.21	
	2.00	0.67	1.00	1.57	2.50	4.00	
	4.00	0.67	1.00	2.08	5.50	16.00	
	8,00	0.67	1.00	2.58	11.50	64.00	
	16.00	0.67	1.00	3.08	23.50	256.0	
	32.00	0.67	1.00	3.58	47.50	1024.	
		~~					

NOTE: There is no dead time small enough to be negligible for white noise of phase, unless a 15% error in $\sigma_y(\tau)$ is tolerable.



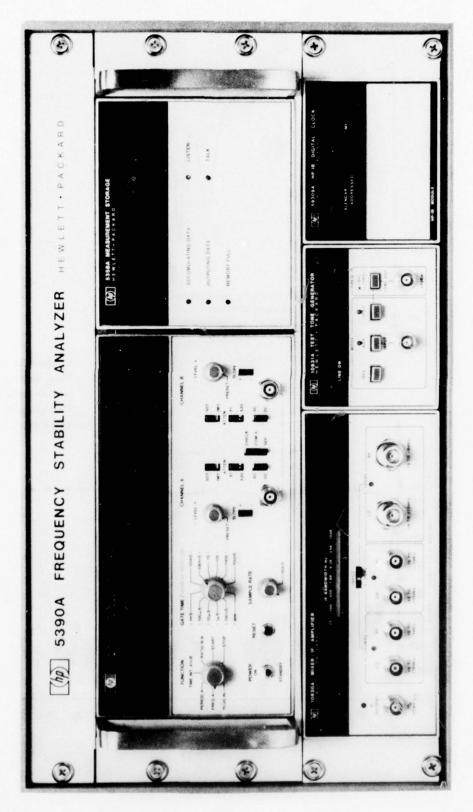
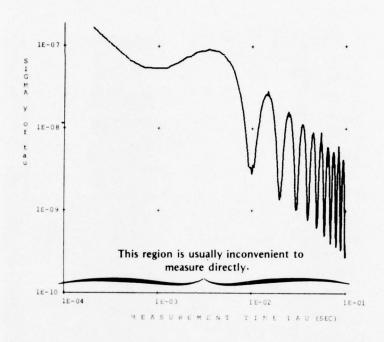


Figure 2. 5390A FREQUENCY STABILITY ANALYZER



10 MHz Carrier, Phase Modulated by 100 Hz Sine Wave, PM Sidebands 46 dB Below Carrier

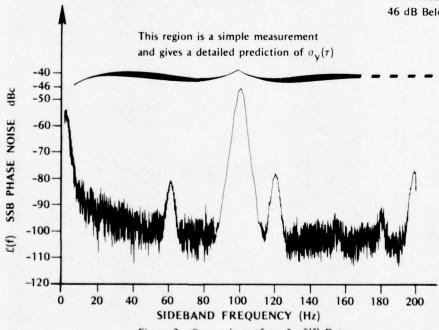


Figure 3. Comparison of $\sigma_{\mathbf{y}}$ & $\mathcal{L}(\mathbf{f})$ Data

TABLE 1

	=	$o_{\mathbf{y}}(\tau) =$	$\mathcal{L}(\mathfrak{t}) =$	β =
WHITE PHASE	-2	-2 $\sqrt{L(f) 6 f_h}/2\pi f_0 \tau$	$(a_{\mathbf{y}}(\tau)\tau \ 2\pi \ \mathbf{f_o})^2/6 \ \mathbf{f_h}$	0
FLICKER PHASE	-1.9	-1.9 $\sqrt{L(f) f (1.269 + \ln (2\pi f_h \tau))/6.58} / f_0 \tau$	$6.58(o_{y}(\tau)\tau f_{o})^{2}/(1.269 + L_{n}(2\pi f_{h} \tau))^{2}$	7
WHITE FREQ.	7	$\sqrt{\mathcal{L}(f)} f^2 / f_0 \tau^{1/2}$	$(a_{y}(\tau)\tau^{1/2} f_{0})^{2} / f^{2}$	-5
FLICKER FREQ.	0	$2\sqrt{\mathcal{L}(f)} f^3 \ln 2 / f_0$	$(a_{y}(\tau) f_{o})^{2}/4 (\ln 2) f^{3}$	٣
RANDOM WALK FREQ.	Ŧ	$\sqrt{\mathcal{L}(f)} f^4 2\pi \tau^{1/2} / \sqrt{6} f_0$	0.75 $(\sigma_{\rm V}(\tau) \ \tau^{-1/2} \ {\rm f_0/\pi})^2/{\rm f^4}$	4

 τ = measurement time, $y = \Delta f_0/f_0$, f_0 = carrier, f = sideband frequency, f_h = measurement system bandwidth

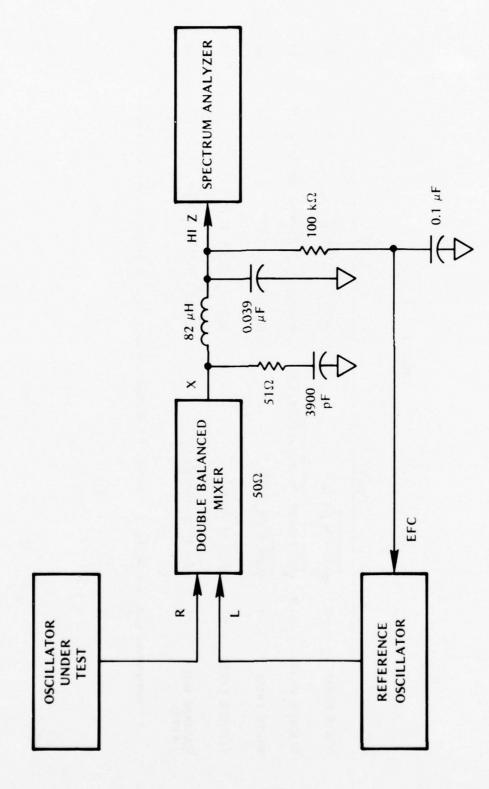


Figure 4. Phase Noise Measurement Method

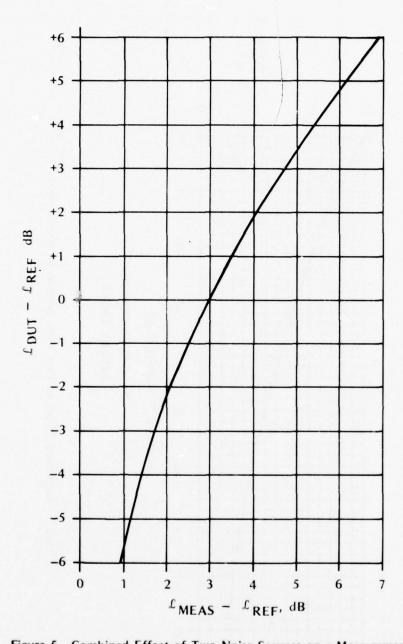


Figure 5. Combined Effect of Two Noise Sources on a Measurement

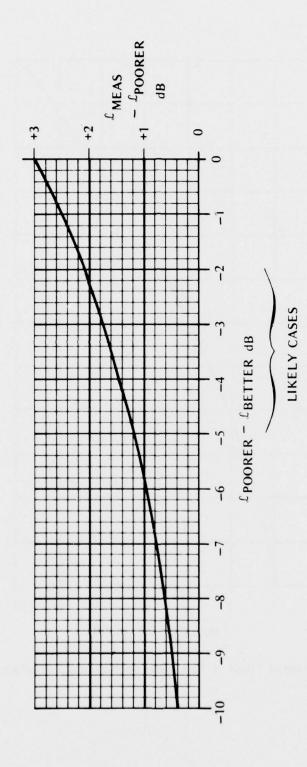


Figure 6. Combined Effect of Two Noise Sources on Measurement

Single Sideband Phase Noise Measurement Worksheet Using a Double-Balanced Mixer and HP 3580A or 3581A

R port signal level must be varied before calibration to verify mixer linearity.

-	RdW	-(Syst.) +	(Scale)	(Meds.)	TEST CONDITIONS AND	
Freq.					SCALE FACTOR COMPUTATIO	11
Hz	dB	dB	dB	dB		
1.0					Calibrate Freq () Hz
1.3						
1.6					-(-) dB RAW READOUT	
2.0					SYST RESP	
2.5					+(-) dB SYST. RESP.	
3.2					e one. They.	
4.0					+(-) dB R PORT ATTEN	
5.0						
6.3					-(-) dB INPUT SENSIT	IV 8
8.0						
10					-(-) dB R PORT ATTEN	
13						
16					+(-) dB INPUT SENSIT	IV 2
20						1
25		-			-6 dB RADIANS TO S	SB
32						
40			-		dB BRIGHT LINE	
50					SCALE FACTOR	
63					' "ADJUST" LAMP? (
80					1	,
100					-() dB=10 log(Hz RW)
130					, () as 10 109(IIZ ON
160					+1.7 dB +2.5 loggin	n
200	-	-	-		-0.8 Gauss	RDF
250		-			0.0 00033	DI I
320						
400					dB RANDOM NOISE	
500					SCALE FACTOR	
		-			SMOOTHING? ()
630 800					Shooming: (,
1.0k						
1.3k						-
1.6k		-			UNIT UNDER TEST:	
2.0k					OATT ORDER TEST !	
2.5k			-			
3.2k						
4.0k					REFERENCE SIGNAL SOURCE	. 1
5.0k					NETERENCE STORKE	
6.3k						
8.0k						-
					MIXÉR:	
10k					MINEN.	
13k			-		AC AMP:	
16k					AC AMP:	
20k					DC AMP:	-
25k					DC AMP:	
32k						
40k			-			
50k		-			NAME	
63k					NAME	
80k						
100k					DATE	

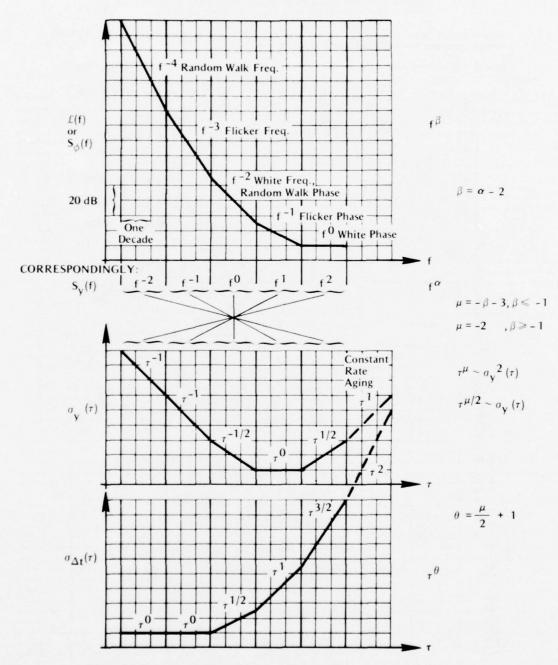


Figure 7. Interrelationships of Various Random Frequency Instabilities

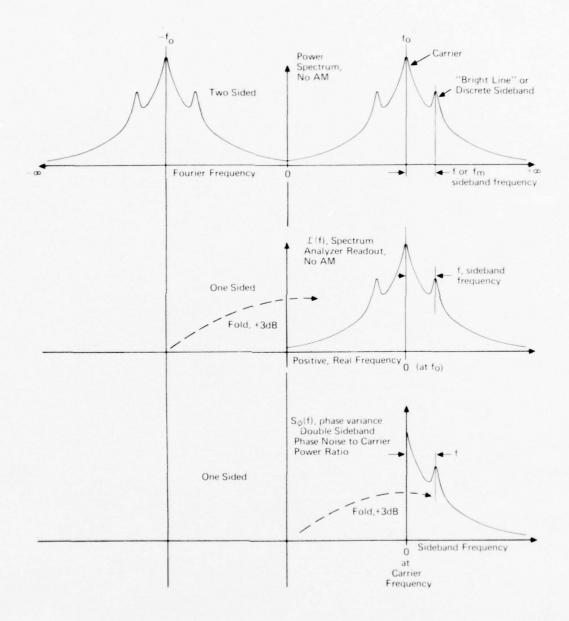


Figure C1. Graphic Comparison of Some Frequency Domain Measures, Definitions and Symbols.

PANEL C

Frequency Stability and Its Interpretation to the Users

Panel Members

Goddard Space Flight Center Andrew Chi National Bureau of Standards David Allen University of Southern California William Lindsey Smithsonian Astrophysical Observatory Robert Vessot Leonard Cutler Hewlett-Packard Company U.S. Naval Observatory Gernot Winkler Ratheon Co. James Mullen Bell Telephone Labs Warren Smith



PANEL C DISCUSSION

MR. CHI: I am delighted to have a special panel discussion on frequency stability in this PTTI meeting. The reason for me to consider this special session is the fact that you probably will know many of the faces, especially those who participated about 12 years ago when we had a special symposium on short-term frequency stability in 1964 at Goddard Space Flight Center.

It was organized on the basis that users generally need stable frequency sources, and do not know how to communicate with another group of people whose specialties were either to make the stable frequency sources or to maintain the frequency sources.

The communication was so inadequate that it became obvious that there should be some kind of conference to open up the communication and establish a common language so that the users can communicate with those who actually make the frequency standards. However, after a dozen years or so, the two groups could not provide any kind of feedback. It was just like a phase lock loop. The time constant was extremely long.

It brings to my mind that it was almost as if we were talking Greek to each other except no one really understood what we were talking about and very few really understood Greek.

Then after some time, we thought we made some progress; enough for us to communicate with the users. It appeared to me that instead of talking in Greek, we were talking in Chinese. Well, I thought that is very good; then I shall be able to understand them. However, it turned out they did not really converse in my dialect.

So what I thought would be appropriate at this time is not to try to impress any particular group of people of how much we know or what kind of theory we can use to improve on the past difficulties but to describe the actual situation. If we try to do this, the panel discussion will be able to establish a link of communication which is the objective of this panel.

However, if you look at the faces, you will notice a few people who are not on the stage — absent, for instance, are Jim Barnes and David Leeson who were not able to attend the meeting. In essence we have essentially the original group of the frequency stability subcommittee of 1964.

Now, I would like further to bring out the fact that in some of the past papers and also in the publications, you will see that the Subcommittee of IEEE on Frequency Stability was comprised to do certain things.

The present chairman of that Committee on Frequency and Time is Dr. Robert Vessot, sitting next to Dr. Winkler, and the Subcommittee chairman on Frequency Stability is Warren Smith, who is to my left.

In the future, should you have any more questions with regard to frequency stability and time, those are the two persons to whom you should address your questions and ask for solutions.

I would like further to make one more statement in regard to frequency stability. The point I would like to say is that when we observe the frequency variations or phase variations, we are looking at the imperfection of a system. What we can measure is the imperfection of the behavior of an oscillator.

What we seek is not the imperfection of the oscillator but ways to improve it. What we need is the best possible performance of the oscillator under the conditions that it encounters. What we want to describe is how good the oscillator is.

It is subject to noise processes. What we require is to understand statistically, how it behaves.

I would like to first allow a few questions to be raised on those papers which were presented this morning. We did not have time to answer any questions.

Are there any questions in regard to the earlier papers? If so please address your question to the author, identify the author and the paper so that author can answer the questions.

MR. CHI: Are there any more questions?

DR. WALL: Fred Wall.

I, too, had at least a comment on Professor Lindsey's paper. I thought he was just a little bit unfair in describing us by saying people who use frequency standards or make them, only describe them in terms of, say, the pair variance.

In fact, is that the IEEE Committees have recommended a number of measures, including a spectral density of frequency or phase fluctuations. And these fully characterize a standard method of characterization. They have all the information there. Further, there is the systematic effects Dr. Winkler described, quite clearly.

The other thing, the reason one uses the pair variance or Allan variance is to condense the data so one has a small number of numbers to talk about rather than 10,000 data points. Furthermore, there are a number of different regions. You might have one that describes, say, the shot noise process or fundamental noise process in the frequency determining element.

Then, as one includes various phase lock or frequency lock loops, one has other regions which are described by perhaps a different power lock. So, typically, in a short-term, one has tau to the minus 1/2 or tau to the minus 1 then a flat region and then some long-term systematic variations.

I don't think any of us have tried to say one describes an oscillator by a single number whether one picks an Allan variance to describe it or something else. I think most of us use the frequency domain notation if he wants to look at the details of an oscillator. If one wants to know what the phase spectrum is one looks at frequency domain, not the time domain.

DR. LINDSEY: I would like to comment on that. I apologize if I was not fair in my comments with respect to the utility of the power spectral density of the frequency process.

I well recognize that in the Abstract of the 1971 or '66 special issue on frequency stability this comment was made. It was stated either can be used as a measure of frequency stability.

However, in the circles that I travel and in the papers that I read, no one surprises me with that data. And in particular, I can quote a couple or three jobs in which I have been concerned where we had to specifically measure the power spectral density of the process in order to make an assessment of performance of the system.

What I would like to say is that I should like to see more emphasis on supplying the user with the power spectral density of the frequency.

If you give him only the Allan variance measurement, say between the interval .1 second up to 1000 seconds or whatever, he is given a curve. How does he use this in a certain particular application?

If he needs the power spectral density of the instability, then he has to make a transformation based upon the measurement and he only has a finite number of points so that

means extrapolation of the Allan variance into regions where the measurements aren't made and which subject the model to error.

Consequently, in that transformation, in fact, for the most part, it has not been recognized how to transform from the Allan variance to the frequency domain. However, in cases where you have to select a performance measure, which contains a dead zone on the order of some minutes, an hour in certain cases, you need power spectral density in order to get to the zero point. The Allan variance does not provide you with that capability.

So I assert that, given the power spectral density of the frequency fluctuations, it contains all the information in accordance with the two sets of structure functions that I described. These two sets of structure functions contain generally the information that the user needs. These represent the performance measures for various systems.

MR. CHI: Dr. Reinhardt.

DR. REINHARDT: I would like to disagree with you strongly. The problem with spectral density measures is that the integrals are not doable.

DR. LINDSEY: Why aren't they doable?

DR. REINHARDT: They are doable numerically, but in many cases very difficult. The spectral density measurements frequently are very difficult in the zero to thousandths Hertz range. From the Allan variance charts from the spectral power law behavior you can usually refer to charts. And the National Bureau of Standards and others have published chart after chart to convert from one measure to another.

Now, I think that most of us will agree that some form of the Allan variance, whether the two, three or four sample variance, can be obtained in real time. You can write them in that form and use the variance weighting functions that are calculated and published to go from the two sample variance with zero dead time to sample variances with finite dead time if you know the spectral process.

DR. LINDSEY: I guess may comment to that would be, I disagree with you the integrals are impossible. If you look in tables of integrals, frequently, you will not find them. For instance, the flicker frequency effect produces a divergent interval if you extend it over all regions.

But in my opinion, integrations which are not found in tables shouldn't frighten the engineer these days. There are well known tabulations of numerical techniques which are available such as Gaussian quadrature techniques. These are quite sophisticated.

However, for experimental data generally engineers are not familiar with them. But we do have computers these days of tremendous power; there is no reason to be frightened by the fact you have an integral you cannot invert or do in closed form.

You go right to the machine and use sophisticated forms if need be. I have used these to get the inversion and get the number.

MR. CHI: I would like to exercise the prerogative of being the moderator. And what I would like to do is to set a time limit on the discussion of this paper to 12:00 o'clock by the clock on the back of the wall. So that we will keep that in mind so that we will be able to move in the discussion of other areas.

MR. CHI: I would like to recognize Bob Vessot.

DR. VESSOT: I would just like to remind people that, in fact, values of both the Allan variance and the power spectral density either of the phase or frequency are now being given almost as a matter of course by most manufacturers of equipment and that both which are complementary in a real sense give the information that I think is required.

The Allan variance, in fact, does not tell it all. We have many ambiguities at the tau to the minus 1 slopes which we can resolve either by tinkering with the bandwidth or

adjusting the number of samples.

I think what Professor Lindsey has said is overstated. These transformations, in fact, are done. There is a way of going from the time to the frequency domain as Cutler and

Searle, I think, have elegantly pointed out.

And at the risk of perhaps exposing my ignorance, there may have been transforms of this form in existence even before that time, but under another name. And I think this fact has since been identified. So I don't think we are that badly off. I think we are somewhat enlightened, but I think we could stand a lot more.

DR. LINDSEY: I hope I haven't been misinterpreted, maybe I have, but I don't think that I have claimed that anybody is off. I represent the user. And as a user and in the circles that I travel over the past two years, in the work that I have done and the applications of selecting an oscillator, the power spectral density has not been supplied to me. It has been something we have had to fight for.

I can give you a couple of examples and how I got involved in the subject, as a matter of fact. It was at TRW, I was doing a consulting job where we needed to specify an oscil-

lator.

One of the problems that we had was that we had, of course, the Allan variance. They were able to make measurements of the variance. However, it was not the Allan variance I needed at that point in time. I was not able to transform it into the frequency domain.

It turns out that this spurred TRW to look into the problem of measuring in the frequency domain. As a matter of fact, I believe over the last two years, they have developed this technique to a certain extent in terms of measuring the phase noise power spectral density of the frequency which we have used. How accurate is it? I can't make a statement with respect to that.

But I am also aware of work in which other areas that I travel having to do with communication systems performance in these cases the performance of a system was not adequately achieved because of the fact the phase noise degraded the system performance and in an unknown way, not in accordance with the Allan variance.

In that context, the engineers required the power spectral density to evaluate performance. And it was not a function explicitly of the Allan variance.

DR. MULLEN: At some times, it is quite hard to find one thing and much easier to find the other. As a matter of fact, as Bob Vessot pointed out, there are some ambiguities with some dependences on the Allan variance. And now that we have got your formula for getting back to the other domain, we can get the inverse of the table that goes from the frequency domain to the time domain, allowing for the cutoffs and get the table that goes back the other way with cutoffs on the Allan variances. So that will be very handy when we have it.

Then, that may save all of us the experimental measurement problem if, in fact, we have found it easy to get the one measurement and find it difficult to get the other. But

what usually happens, is that in the first three to six months after you get the job, you budget everything. And if you made a mistake, you find out about it a couple of years later. And then it is several years before the system, any other system, comes around again. And then provided nobody has been promoted, then they remember what they did the first time. But there is definitely a problem in keeping everyone aware of the best or of standard ways to use things.

I think there has been an ongoing creeping tendency to use Allan variances and spectral densities of frequency. And we have more commonality and more understanding of the problem than we had before. But there is no doubt that we have got a problem in getting the user community tied together with the oscillator-producing community.

MR. CHI: Well, are there any questions from the audience on other papers? I do not see any hands. Therefore, I would like to start the panel discussion.

I would like to start by viewing from the user's point of view rather than by trying to use the viewpoint of the people who actually work in the frequency stability or frequency generation field. Let us start from the more fundamental level that, when you want to use a stable oscillator, what are the questions one should raise.

I would like to list perhaps three questions out of which I would like to ask each member who may wish to comment to provide an answer to any particular question he wishes.

The first one is, what is frequency stability and how is it characterized.

The second one, what is time domain measurement and frequency domain measurement. And under what condition is each selected to meet the user's need?

The third one, how should a user select oscillators from the specifications provided by the manufacturers?

These are the general type questions which a user would have to answer before he can select what particular oscillators he should buy and also a certain amount of trade-offs

I would like to obtain answers or comments and clarifications addressed to these three questions and I would like to start from Len Cutler on my right and then we proceed around the table.

DR. CUTLER: These are pretty general questions, Andy, and they have been asked many times before. We have come a long ways, I think, in getting answers to these questions. I think there is probably a great deal more distance for us to go before we will be able to answer them completely. In a way, that is completely satisfactory both from the standpoint of scientists understanding the fundamental processes that are going on, the design of equipment and the utilization of some of the basic models to improve the designs of equipment. We need to be able to specify the equipment in the terms of users and to understand the specifications of the equipment and how to optimize systems to make use of the equipment that is being produced at a particular given time.

The first question that you gave is "what is frequency stability," and how is it characterized. Well, presently, I think that I would tend to agree with Dr. Mullen that a great deal of the characterization is given in terms of the Allan variance.

This is a characteristic which tends to deal with the very long times or the very low frequencies, because it is very easy to make such measurements in that domain. And indeed, you can transform between the domains as has been pointed out many times and as has been very elegantly presented by Professor Lindsey.

If one has a complete characterization of spectral density in terms of frequency or in terms of phase (by the usual relationship, which may have some mathematical problems) nevertheless it can be used in all practical cases, and one can get measures of stability in the time domain from the spectral density and vice versa.

Generally, but maybe not necessarily, the best way, most characterization is done for long times and very low frequencies in terms of the Allan variance. I don't think very many

people would disagree with that.

For short times, frequency stability is generally characterized by the phase spectral density or L(f) been commonly used in the last few years, which is the single sideband noise spectral density using the carrier power in a one Hertz band width.

This is a characterization many people have found useful for very short-term stability measurements and also measurements or equipment which involve noise powers out in the sidebands. That is my answer to your question number one.

Question number two is on time domain and how they relate to the user.

I think that is pretty well covered in my answer to question number one so I won't dwell any further on it.

The third question is how does the user select an oscillator from the manufacturer's specification.

That is a good question. And if the specification of an oscillator were absolutely complete and all users were well educated, the answer to that question would be they just do it. They go through the necessary exercises to assure that an oscillator specification in a particular domain of interest meets their system requirements.

If not, they look for a better oscillator or they bend their system requirements. I think that is about all I have to say on those three questions.

MR. CHI: Thank you. David Allen.

DR. ALLEN: I would like to respond to the first question of what is frequency stability and how is it characterized by saying that I think that we have seen a very interesting thing historically in the way it was developed.

In '64, as Andy mentioned, the IEEE and NASA Goddard sponsored this Committee on Frequency Stability. And it was obvious at that time there was a critical need in the community to be able to communicate what is stability. And there were many interesting papers given at that symposium.

The IEEE Subcommittee was formed. And out of it came some recommendations. And these have been, I think, quite readily adopted by most of the community.

The interesting thing that has happened, as Dr. Mullen has indicated, that it has provided a high level of communication between laboratories, manufacturers, and users. I enjoyed very much the paper of Professor Lindsey and found it very insightful.

I think, there is still a need in the field of communications that is not being covered, and we need to address that need. And I think this is insightful and helpful.

The thing that has happened in developing time domain and frequency domain measures is that I think there have been some errors committed that have caused problems.

Let me talk about a few of these when I talk about the second question. The first question, I think, has been already addressed by the subcommittee of which you were chairman at one time.

Later with Dr. Barnes as chairman, the committee put together a paper, actually two papers. One is a NBS technical note, and later a publication. I think that the committee many of the members of which are here, did an excellent job.

In regard to the precautions one needs to take, the time domain measure that is typically used, the sigma tau diagram is very powerful if you have power law equal densities. You can then readily translate from the time domain to the frequency domain and vice versa. This happens to be the happy situation of many precision oscillators.

Because it is the happy situation, the reality that models fit in practice, tends to make it a very powerful tool. This is true, I think, for three basic reasons. It is very simple to apply; it is insightful in how you use it; and you can understand in what you are doing in the process of measuring frequency stability in the time domain.

It has a sound theoretical basis for the power law spectra that are applicable. And, in fact, the subcommittee with Dr. Cutler really taking the lead, worked out the transla-

tions very neatly from the frequency domain to time domain.

So I think I would echo Fred Wall's concern that your presentation maybe was a little unfair in saying we didn't try to cover that ground in both the frequency domain and time domain.

Let me echo some concerns. If there is sideband structure in a spectral density, the time domain will lead you to problems. And this has been shown nicely by Mike Fischer

in the previous presentation.

You get this funny looking sigma tau curve, and it is much more difficult to interpret that than if you do the analysis in the frequency domain. So really going to your third question and the difficulty that the user encounters, I think if one is looking basically (and this is a generalization that may have lots of flaws, generalizations always do) for sample times longer than one second, time domain measurements usually give you the information needed.

If you look for times shorter than one second or for Fourier frequencies greater than one Hertz the frequency domain is typically the best characterization.

MR. CHI: Would you repeat that just to make sure it got across?

DR. ALLEN: Okay. This is a generalization applying to precision oscillators and has some definite flaws in it, but typically for sample times longer than one second or for Fourier frequencies less than one Hertz, time domain measurements give you the necessary information. That is typically because usually there is no sideband structure there.

If you go higher than one Hertz in Fourier frequency or shorter than one second in sample time, very often you find structure in the spectra, and the time domain will be

very misleading or hard to interpret.

And you will learn a lot more from the frequency domain analysis of the system whether it is phase of frequency spectral densities. I fully agree with Dr. Cutler, either

one gives you the necessary information.

Another concern that I have is a point that Bob Vessot brought up earlier. And that is that we look at low frequency phenomena and try to classify them statistically. I think we can get into troubles there. If we can find the causal relationships, maybe it isn't the statistical phenomena we think it is. However, given such causal relationships it is much better to go and cure them, than to try to classify them and do predictions based on them.

So in the user sense, of course, if he sees a flicker flattening on the sigma tau curve, he has to live with it, assuming it has some environmental disturbances which causes that type of behavior. But for the manufacturer, that ought to be a real insight looking further

into the heart of the problem. I think I have said enough.

MR. CHI: Bob Vessot. Thank you, David.

DR. VESSOT: With reference to how the user should select an oscillator, I am reminded of a joke about porcupines' lovemaking and the answer is "very carefully" because one has to be, I think, not only wary of the manufacturer's intentions but really aware of our own requirements.

And I think too few people relate their requirements to the property of the oscillator and then go and get the proper oscillator. What they do is look at their requirements and then find somebody who is going to sell them an oscillator.

Naturally, the urge to conduct a transaction sometimes becomes more prominent than the urge to satisfy a need. I suggest that the buyer is really the man who has to do his homework. He has to understand what the properties of the oscillator are that he needs in order to accomplish the job he is doing or wants to do.

I suggest in order to do this, he makes models of how his system will work and that he applies measurements in the time domain if that is the way he wants to use it, if it is in the sense of a timing effort or in the frequency domain if it is in the sense of a spectrally purity as is so often required, for instance, in long baseline interferometry.

Then if he understands what he wants, he can go to the vendor and say, "I need an oscillator with an Allan variance like this and spectral behavior like that." And they better look decently relatable through the Cutler-Searle relationship.

And I think that is when the process of communication will have begun so that he will get what he wants. Personally, I would like to see a more complete representation in the frequency domain of the way data are taken in the frequency domain.

You realize the remarkable completeness of the way in which the time domain things were worked out. The papers that began in 1964 and even much earlier by Barnes, Allan and others, were the result of a very important requirement to understand what clocks were doing at the Bureau of Standards.

And naturally, I think they were led to making their analysis in the time domain. It led us to have this realization that what we saw depended on things like the number of samples, the dead time, the band width (although that came a bit later) and the averaging time; all these parameters have their analog in the case of a spectral analyzer.

What comes to mind to me is that if you run a spectral analyzer and are out to give a spectrum, I think you ought to say what the rate of the sweep, what is the band width of the sweep. After all, that tells you the resolution of what is going to happen, and the duration of the time segment that you actually performed this operation on.

These are exactly analogous to the behavior of the time domain analysis we have grown to understand as the sigma tau plots of all these parameters. I think the spectral domain is likely to be more and more important as the frequencies go higher and higher because, as Dave Allen says, one has a hard time doing a time domain representation of a laser signal.

I also would like to point out that the measurements that we are considering in terms of time and frequency domain are going to be replicated in our discussion of length measurements some day and that I can see a whole new committee coming up with the same problems of definition of length in view of the fact that they would like to relate it to something that is physically available.

In my opinion, the greatest precision now is available in the field of atomic standards. So, somewhere along the line, there is going to be an Allan variance with the determination of an object's length or distance.

MR. CHI: Thank you. Dr. Winkler.

DR. WINKLER: I would like to read for the first question the definition of frequency stability from NBS Technical Note 679 by Dave Allen.

Frequency stability is the degree to which an oscillator signal produces the same value of frequency for any interval throughout a specified period of time.

That is the definition — degree out of which the same frequencies are produced. How is it characterized?

You characterize the deviations from a process by the same way as you characterize any random process. We define randomness.

What is randomness?

Randomness, you have a random process or random signal. If there is no correlation between the disturbance at one moment and the next one, this would be pure randomness.

As you leave that area, there is a completely continuous transition to complete determinus where you have no randomness at all.

In between, then, you have noise steps which are increasingly more internally correlated. That is the whole secret. And we do not have to reinvent the wheel.

I think statistics, the science of how to describe such a random process, has been in the forefront of modern science and technology. But what we are debating here is, insofar as time series are concerned, an attempt to reinvent the wheel. And I don't think it is necessary.

A correlation function, and a spectral density function, are essential characteristics for not completely random processes. In a completely random process, all you have to do is give the mean and the variance.

In view of that, I can only reprat that the only problem which we have here is how to place that cut between random description and deterministic description. That has to be somewhere in the middle. And we can debate that.

And I can only repeat what the other experts have already said. What is time domain and what is frequency domain measurement?

Time domain measurements are obtained through sample time. You sample a quantity, you generate a time series that you do by phase sampling, or you sample frequencies by measuring frequencies over a time interval. But that is only a distinction in the measurement process.

You measure in the frequency domain when you directly determine the side band power in respect to the carrier frequency power either of the variations of phase, where you establish a variance of the phase fluctuations, and you investigate its behavior versus frequency, you can do the same thing in frequency variations. But that is a distinction which is based upon the measurement process. And it is not identical to the distinction which is based on the language in which one states what one has measured.

And here, I must most emphatically remember one should use the same language in which one has the requirements. It would make no sense to insist, for instance, on a spectral density specification if your requirements are purely in longterm timekeeping.

You don't learn very much from that and vice versa. There is no point in using the Allan variance if your requirements are in applications of coherent Doppler radar, for instance.

So the language specification ought to be the same in which your requirement exist. And so I come to the last thing, how does a user select equipment.

Amplifying what you just said, Bob, I think for an important project, for an expensive project, to select anything just on the basis of a piece of paper is sheer madness. The larger the project, the more important it is to set up a little pilot thing yourself. Get a test bench somewhere, spend a few hours, get a little cheap thing, and play around with it. Then you will understand what you need.

And we have seen in most cases the greatest problem is to bring the user really to define what he needs. I begin to use the term "user" in the same way as Congress uses the "taxpayer."

This is not accidental, incidentally, because that is where the money comes from. But I cannot emphasize enough, that for systems design and for specifications and for putting everything together, if you try to save investment for a little initial experimental effort, the study effort (and now I am talking about bench work) you will pay dearly later on.

MR. CHI: Thank you, Dr. Winkler. Jim Mullen.

DR. MULLEN: I would like to speak to the question of how to select oscillators, too. Certainly, the first thing is to decide what the system needs. And in that respect, some of the consolidated results that Professor Lindsey has shown to us will be very useful.

The fact of the matter is there are lots of oscillators that are needed and in many systems these turn out not to be critical. Often, the budget isn't big enough to do very much really to solve the problem of how to do the experiment, which would be much the safer thing to do.

And so somebody of junior level in the program goes out and buys the oscillator. And if anything is wrong, the money is already spent. So it is really important to be able to try to estimate what quality you have to have oscillator with some kind of consolidated or overall estimate of how much effect the oscillator performance will have on the system and then to be able to interpret specifications of available oscillators. The question is which standard descriptions are useful.

It often turns out to be the case that you can find the oscillator that meets all the environmental requirements. But unfortunately, often the measurements that have already been made, are made in the wrong domain, and you have to go back and forth. Either you can call up the oscillator manufacturer and tell him you want one, but want him to measure the whole thing all over again in some other way (in which case he doesn't have that much interest) or else you have got to be able to convert it yourself.

If the oscillator is critical to the whole system, then you generally get the opportunity to do a decent job. But otherwise, there is a fair amount of hard work that has to be done without completely fundamental digging at the problem.

I think the standardizations that we make are not quite capable yet; but not too far from complete and what we have is going to make the problem a lot easier in the future than it has in the past.

MR. CHI: Thank you. Warren.

DR. SMITH: Well, in the interest of time and also due reference to the fact that almost everything that can be said in answer to your questions has been said, I will keep my comments very brief.

It has been very gratifying over the past 10 years or so to see a great increase in the ability to communicate about clocks and about oscillators and frequency standards. I think things are infinitely better than they were in 1964. And in that respect, I think we have accomplished something. It has been very interesting to see the presentation of data here today.

I was particularly interested in some of the slides shown by Dr. Winkler. I would like to make a brief comment.

If one takes the pathological data presented for the cesium standard this morning by merely changing the time scale and, of course, the frequency deviation scale, one sees a perfect picture of a pathological quartz crystal oscillator with which I am much more familiar, having worked in that area a great deal.

But the point of interest that I would like to make here and I think will be of general interest, is that we find in quartz crystals on almost continuous variation in the magnitude of this kind of pathological behavior, which is usually characterized in a plot of raw data as frequency deviations with time that are quasi cyclic.

If you look for any given day, it looks almost like it is sinusoidal perturbation. And it has been possible to take those very bad offenders, open them up, and physically see defects usually in the form of badly adhering plating or small contaminants, semiattached to the surface of the quartz. This kind of behavior is pathological. The point is well taken, that when you see this kind of behavior you should be aware you're not really dealing with statistics, you're dealing with something that is out of the ordinary and abnormal, you should really back off and think.

I might say one word about your last question, the selection of an oscillator, the particular specification. I have been in the unique position of being bitten on this subject many times, and I would only caution that it has been my experience that most catastrophies in this area arise from a lack of knowledge at the beginning of a project as to what the specifications and requirements really are.

And you usually find out what you really need in a system when it is just too late to do anything about it. And it has little to do with the problem of communications between user and manufacturer. The great difficulty, particularly in sophisticated systems, is of assessing the whole question of requirements of your signal source in clocks at the beginning.

MR. CHI: Yes, please.

MR. TURLINGTON: Tom Turlington, Westinghouse Electric in Baltimore.

I have heard a lot about Allan variance and spectral density measurements this morning. There is also another, Hadamard variance, I used in the past for getting in very close to the carrier, less than 20, 30 cycles (all the way into tenths of a cycle) on oscillators that have clean spectral densities. That is, no discrete sidebands.

I find that to be a very useful technique. I haven't heard much about it here today. Do you care to comment?

MR. CHI: Anyone who would like to comment. Dr. Winkler.

DR. WINKLER: You're absolutely correct. But it is particularly useful if you operate at a time constants for integration time where you have a high power spectral density. If that happens, you must use filtering. The transfer function of the Allan

variance is very broad. So you have more dangers in that aspect than if you use the Allan variance.

I consider these may be variations of one and the same thing. Your point is absolutely correct.

Also, I think the so-called curvature variance may find some useful applications because it is insensitive to frequency drifts. And it is not more difficult to compute than the standard version.

For a calculator today, this is not a problem. You're absolutely right, but, of course, we cannot go into every detail here.

I think the least we could do, and I hope we have accomplished that, is to give some idea of the complexity of the subject. And I can only remind you that in order to really go into details, you have to get into details. There is no king's way to success.

Of course, there is an enviable way how to go round if you have no knowledge — simply buy the most expensive. And that's being done very effectively. But I don't think it is engineering.

MR. CHI: I would like to hear some questions from the users' viewpoint rather than trying to go into the theory of modeling or frequency stability. Question, please.

MR. KAHAN: Kahan, IDC.

This will be semi-user point of view. I am still worried about of characterizing oscillators. Assuming I have a transient, for example, a "Burster" variation and gather transient recovery and frequency as a function of real time, is there any way to present this data aside from reams and reams of data as a function of time in terms of a few parameters in a time domain or frequency domain? Or does it make any sense to characterize a transient response by Allan variance or whatever you want to call it in that sense?

MR. CHI: David.

DR. ALLEN: As a part of the work of CCIR, right now, they are trying to talk about questions of that nature. And I think that a point Harry Peters made and has been alluded to by Dr. Winkler at this conference is an exceedingly important one here.

That is, when you have nonstatistical phenomena, you should characterize that as a coefficient function. So much frequency change with certain radiations. So much frequency change per degree C in a certain range, that you should establish these coefficients that you might model these deterministic phenomena rather than trying to do it statistically.

I think it would be a mistake to use the Allan variance in such situations.

DR. CUTLER: I would certainly agree with that. What I would think would best do for that sort of thing would be to try and model it. In other words, you would assume that you have a ideal oscillator and this ideal oscillator under the burst of radiation undergoes a rapid frequency change.

Then it may decay with an exponential or some other law to some other new frequency. And if these things were completely characterized in a deterministic sense, then you would put back the other things, the random variations and so forth. And indeed, some of those random variations may be modulated by this transient effect.

Those modulations can again be a deterministic things that are applied to the random characteristics that are associated with the oscillator under normal conditions.

MR. CHI: Dr. Winkler.

DR. WINKLER: I have not gone into the details, but you will find them in my paper. There are three classes of functions which one can just empirically apply to modeling. And, according to which one you select, they behave differently.

The three classes are, number one, polynomials of degree N that we discussed this morning. Number two, Fourier series. If you have any periodic phenomena, the Fourier series, of course, is the thing to use. Number three, exponential functions. Dr. Cutler mentioned that. In general, it would be a sum of exponentials. If you have several different phenomena interacting over time contents, you could end up with a sum of exponentials. All these transform into another function of the same kind under a transformation when you shift the time axis, but only the first one, the polynomials, have the additional property that they will remain polynomials if you transform time with a different scale.

So these are details which are completely covered in books like Digital Analysis. There is an excellent book by Hamming, 1962, which has an excellent discussion on that.

But here, again, you have two things to consider. You consider the black box approach where you just phenomenologically describe what you see, but you must remember that many of these are parameter-dependent. So one really has to consider whatever function one uses as a function of the excitation, radiation, temperature variations, and what have you. Then you end up in the simplest situation with coefficients which you have determined previously — temperature coefficients or magnetic field coefficient.

MR. **CHI**: One more question from the audience. Tom Healy.

MR. HEALY: There is I think a larger number of semi precision oscillators in the world rather than clocks. And there is a big market for them.

Usually, the user, when he is faced with an Allan variance or so forth, it can't really transform these into its system. He knows what his system requirements are. Usually, in many systems, communications and radar and so forth, the script L of F is a much more suitable description of an oscillator for the user.

And the other fact, is tied in with his environment. Usually, when there are thousands of oscillators we are talking about systems where the environment isn't as nice and benign as in the Naval Observatory Laboratory. Temperature, vibration, shock, all these causal phenomena, are very important. So his linear coefficient should be specified. And there should be some specification of the spectral density of frequency for offsets greater than one Hertz. And the thing is whether it should be $S\phi$, $S\phi$ or L(f), that is a question.

Most people I have dealt with, are system designers who can more easily determine the script L of F because they have to convert all these other things in order to be able to incorporate the data into their system.

Another thing I would like to point out is the Hadamard variance isn't a cure-all of evils anyway because the function does have side lobes. And it can land right in a bright line and louse up the observation. So you have to be very careful.

MR. CHI: In the remaining few minutes which we have, I propose to assume that the user now has his oscillator. While he has it, presumably, he can separate all the systematic

errors out and find the performance of the specification or whatever information he obtained.

The question that should be raised, in my view, is how much confidence he should have in the oscillator performance. Now, if he wishes to make tests, should be completely redo the specification test or should he make nominal tests.

And then, once he has established a certain amount of confidence in the oscillator which he owns, the problem is that when he uses it, it will be in the real world of systematic variations which consists of transient for voltages, temperature.

Can he actually predict the performance such that he can make sure that the frequency which he obtains will fall within the band which he is allowed to stay? In most activities, this is a real world situation.

I will not go through every panel member to answer all these questions, but whoever wishes to answer any or all or one question, please raise your hand. And we will use some of the lunch hour, if we may, for about 10 minutes or so. We will terminate the panel discussion at 1:00 o'clock.

Dr. Winkler.

DR. WINKLER: Confidence in your data. That is the reason why one must give the number of measurements or one must give the confidence interval. Remember the slide I showed on the probability distribution function?

There were two lines. These were the 95 percent confidence. That is a phenomenological side. When it comes how much confidence can you place in an actual application, you must derive that from the range of environmental conditions and environmental sensitivities which you expect. That's all.

MR. CHI: Warren.

DR. SMITH: Just a short statement. It seems to me that we have spent most of our time here talking about the difficulties in assessing the random behavior of signal sources. In the real world, I agree with Mr. Healy, that the problems are primarily those of the causal or deterministic effects.

Temperature coefficients, voltage coefficients, shock and vibration, all the rest of it, are the things that make real world specifications extremely difficult and which all of you and all users need to keep well in mind. These are the things that one really has to be careful in tying down for any particular application.

The discussion of random variables is much more interesting and can be treated in much greater depth. And in particular, as it applies to precision sources and clocks and timekeeping it is probably the fundamental one.

But in the field of communications, and the things that go in the field, I would caution you that the toughest thing to do is meet your deterministic and causal specification.

MR. CHI: Len.

DR. CUTLER: I agree. Yes, I agree. And I would like to add one other note of caution.

Very often, one must be concerned with rates of change of temperature, durations of shock, and things like this. Very often, these things are extremely difficult to specify or put limits on.

I caution the users of such situations; that in many cases, they may have to make their own very specific teats or request the manufacturers to make very specific tests involving rates of change of things.

MR. CHI: Anyone else? Anybody in the audience who may want to make any comment?

DR. KLEPCZYNSKI: I would like to ask any member of the panel if they feel that development of crystal oscillators is far behind in terms of its ability to function in a deterministic way, i.e., in an environment that is somewhat hostile. And compare that with the development of the oscillator in terms of low noise levels.

In other words, has the crystal oscillator been developed to a degree that is much, much better in terms of its noise floors and various other noise properties in proportion to its performance in an environment?

MR. CHI: Warren Smith.

DR. SMITH: I will make a brief statement on that point. Crystal oscillators have been around a long time. A lot of work has been done to achieve low noise floors. The name of that game as in any other game that we talk about is power.

The higher the power that you can dissipate in the crystal unit, the better the signal to noise that I can come up with. Unfortunately, quartz crystals are still the same. The other performance factors degrade as you increase the power level in the crystal. So you're back to the same trade-offs.

I would say there has probably been some improvement over the years. I don't know of any, I personally have not been in contact with any great breakthroughs. However, the crystal oscillators are still very widely used, especially in the communications of radartype of application.

MR. CHI: David.

DR. ALLEN: I would like to add to those comments. We have one of our people from NBS here who is involved with crystal studies that we are doing. I see this as an extremely exciting field right now even though crystals have been around for a long time.

We see already some breakthroughs that have occurred with some commercial products. And in fact, some of the work we are doing is directed toward some significant breakthroughs, both as to environmental insensitivity and low noise.

Just to throw out some numbers, we have hope that even in long term, one might have a crystal oscillator that would exceed in performance the stability of rubidium in atomic devices. Whether that is true in a harsh environment is another thing. Those are separate problems.

MR. CHI: Lauren Rueger.

MR. RUEGER: I would like to come a little to the defense of the system engineers who overdesign their oscillators in systems. Part of that is because we find these beautiful characteristics you get when you deliver the oscillator, but what do you have one, three, five, 10 years later if you put it in a place where you can't get to it like in orbit?

A little extra margin is a pretty important factor in the system. It has been our practice in general to try to design or ask for specifications far enough over the margins needed so that as time goes on and you get radiation from the natural effects, for example, reduce the gain of the transistors or it may cause some other drift or other aging characteristics, you're still in business.

So I would like to defend in the design initially, you would like to overdesign so that

you will retain all these margins.

MR. CHI: Dr. Winkler.

DR. WINKLER: I cannot agree more with you. My comment should not be misunderstood. I think there is a very important difference between specifying something out of ignorance versus application of a conservative safety margin.

I would be on the side of the conservative approach.

MR. CHI: You have a question?

MR. BRESHON: John Breshon, University of Maryland.

I was concerned about your statement about crystals. And are there some other types of crystals? Are quartz crystals considered for these clocks?

DR. ALLEN: I think some of the very fine work that is being done in new crystals is being done outside of this country even, and it is still quartz crystal as far as I know.

DR. VESSOT: I am not in the quartz crystal game, but I have heard of sapphire crystals of considerable size that have enormously high Q from the mechanical point of view, far, far higher than we would expect from quartz. They have the difficulty that they require a somewhat more eloquent approach in order to communicate with some electrical circuit.

However, I, too, wonder whether or not there isn't some opportunity to look for better mechanical oscillators. The sapphire crystals I know of are made in Salem, Mass. Dr. Fred Schmidt of Crystal Systems, Inc., makes single crystals that are of the size of a basketball. It is really extraordinary. These crystals are being used by Prof. D. Douglass of Rochester University for gravity wave detectors. I expect we will be hearing more about these in the future.

MR. CHI: Dr. Winkler.

DR. WINKLER: I believe (and I am really speaking with very little definite knowledge about this) that other than quartz is a very unique material. And it is my feeling that it will be hard to find something much better to make further improvements in the quartz crystals which are under development right now. This will likely have to do with improvements in the circuitry, and so on. There are, however, two further aspects. One. Either one could put the quartz back into the cryogenic environment (which was done at NBS 20 or 25 years ago the first time) and immediately one get much better mechanical performance, or we could consider the super conductive cavity again (which is also an oscillator which is not based on the quartz resonator, but nevertheless based on mechanical stability), or one could refer to the NBS development of ammonia; a relatively inexpensive ammonia-controlled oscillator which I think is a very interesting development.

So there are a variety of things cooking at the moment. And I think what one bets on will depend to a great degree on what one has available. If one can tolerate a cryogenic complication, I think that may be something to look forward to.

MR. CHI: Unless you really want to look at some earlier activities in this area, there is a book by Warren Mason who was formerly with Bell Telephone Lab, presently at Columbia University, I think called Sonics and Ultrasonics. You will see a whole list of materials which were examined as possible material in this field.

I would like to use the remaining minute to express, in behalf of the Executive Committee, my thanks to all the authors for this session who have given such excellent papers and the members of the panel.

NTS-2 CESIUM BEAM FREQUENCY STANDARD FOR GPS

J. White, F. Danzy, S. Falvey, A. Frank, J. Marshall U. S. Naval Research Laboratory, Washington, D.C. 20375

ABSTRACT

NTS-2 is being built by the Naval Research Laboratory. It is scheduled for launch in mid 1977 and will be a part of the demonstration phase of the NAVSTAR Global Positioning Program (GPS). NTS-2 and Air Force Navigational Development Satellites will form a six satellite demonstration system which will permit a thorough evaluation of GPS.

NTS-2 will have two cesium beam frequency standards and will be the first satellite application for this type of atomic standard. Utilizing experience gained from the successful launch of rubidium frequency standards on NTS-1 in 1974 NRL has defined operating specifications for atomic standards in the space environment.

Flight standards are being delivered to NRL for testing. Each unit was subjected to environmental and stability testing at NRL. The temperature qualification range is -10°C to $+50^{\circ}\text{C}$ in vacuum. The standards are required to pass random vibration. Phase noise and short term stability tests have also been performed.

Additional equipment has been designed and constructed to synthesize the 10.23 MHz signal required to drive the GPS navigation system electronics. In order to compensate for the relativistic effects a device was developed to offset the frequency of the cesium standard.

INTRODUCTION

NTS-2 (Navigation Technology Satellite 2), Figure 1 is being prepared for launch by the Naval Research Lab for the Navstar Global Positioning System (GPS). NTS-2 and the Navigational Development Satellites (NDS) which are being

constructed for the Air Force will form a six satellite constellation for the demonstration Phase of GPS ⁽¹⁾. NTS-2 builds upon the technology developed with NTS-1 which contained two rubidium frequency standards^{2,3,4}. Two cesium beam frequency standards were designed and constructed under contract for NRL by Frequency and Time Systems, Inc. These standards are designed to deliver reliable performance in the satellite environment and survive the rigors of launch. NRL has performed extensive testing in both the laboratory environment and the varied environments which could possibly be encountered in launch and on orbit.

In addition to the frequency standard it was necessary to develop additional hardware to interface it to the satellite telemetry control system, the Orbit Determination and Tracking System (ODATS) and the GPS navigation system.

These devices include a direct synthesizer to generate 10.23 MHz for the GPS system, the relativistic synthesizer which creates frequency offsets to compensate for the effects predicted by general relativity and a command interface which translates signals from the satellite telemetry systems into usable control signals for the frequency standards and synthesizers.

CESIUM BEAM FREQUENCY STANDARD DEVELOPMENT

The NTS-2 cesium standards were specified to provide the long term frequency accuracy and stability of existing commercial clocks and to survive and operate in the environment of an orbiting spacecraft. At the time the idea of using a cesium standard in space was first under serious consideration there was considerable speculation in the time and frequency community about whether or not a beam tube with it's precision mechanical alignments could be made sturdy enough to withstand a launch environment in the 20 to 30 grms range. Accordingly, the earliest efforts in the program were directed primarily towards the goal of vibration qualification. Under NRL contract Frequency and Time Systems embarked upon a program to produce a vibration qualified version of their FTS-1 beam tube. During 1974 tubes were built by FTS and tested at NRL to identify and correct vibration sensitive areas of the tube. On March 1, 1975, a tube passed 23 grms random vibration in three axes with no significant failures observable in limited performance testing at NRL. That tube was returned to FTS for analysis and was found to be operating nominally. Figure 2 lists the pre and post vibration performance. Work on the

electronics which was under way at FTS continued toward the goal of clock operation with the qualified beam tube with interface for remote monitoring and command control through the satellite telemetry. A brassboard model of the proposed flight frequency standard was constructed at FTS and delivered to NRL for testing in the spring of 1975. While the brassboard was not mechanically designed for flight vibration tests it was in all other respects designed to meet flight specifications. It was tested at NRL to measure it's short term stability, phase noise, electrical characteristics, and environmental performance. The period of testing ran through the summer of 1975 and resulted in several improvements in the basic design. summary of the brassboard's performance is shown in Figure As reflected in the data the stability of the standard appeared to have a flicker floor of about 5x10-13. this was above the contract specification of 2x10-13 the matter was investigated by FTS and improvements resulted which have ultimately reduced the flicker floor for the brassboard to about 1x10⁻¹³. Long term frequency drift over a period of seventy days was curve fit by computer to be less than $2x10^{-15}/day$. The changes made to the brassboard design were incorporated into the units built for NTS-2. These units are designated as prototypes. units have been built and delivered. Of these, one unit (serial number 4) was used as a qualification unit and was subjected to qualification levels of environmental testing. Units numbered 3 & 5 have been designated as flight units for NTS-2 and the remaining standard (Number 2) is the backup unit. Figures 4 and 5 show one of the prototypes.

THEORY OF OPERATION

The basic operating principle of the cesium standard is similar to most other cesium clocks⁶. The user's output signal (5.000 MHz) is obtained from a high-quality voltage-controlled quartz crystal oscillator, and the frequency of this oscillator is regulated by comparison with the cesium hyperfine transition. The accuracy and long-term stability of the output frequency are determined by the cesium tube, while the short-term stability (outside the bandwidth of the frequency-control servo loop) is obtained from the quartz "flywheel" oscillator (figure 6).

The cesium beam tube utilized is a standard FTS-1 tube modified to survive the mechanical shock and vibration environment of the satellite launch. The width of the cesium resonance in this tube is approximately 500 Hz at a

center frequency of 9192 MHz. In the servo system, squarewave phase modulation is used. The modulation frequency is chosen approximately equal to the resonance line width, where the second harmonic signal is theoretically zero, and the amplifier gain and filtering requirements are therefore set only by noise considerations. All of the usual tuned, narrow-band, audio filter circuits have been eliminated or replaced by commutating filters. Thus, the servo system has been made relatively insensitive to drift and gain variations; all essential circuit functions are synchronous. Another important and unusual feature of the servo loop is the integrator in the error signal path. The time constant of this integrator helps determine the overall bandwidth of the servo system, and hence the crossover between shortterm crystal stability and long-term cesium control. Both the long time constant and low leakage requirements are satisfied in the system through the use of a hybrid analog/ digital integrator circuit. The principle of this hybrid approach is shown in Figure 7. The analog integrator has a relatively short time constant (0.033 sec. in the unit) so that leakage effects are unimportant. The effective integration time constant of the hybrid circuit, however, is this value multiplied by the maximum digital count (4096) or 140 seconds. The overall servo loop time constant under these conditions is 10 sec. The hybrid integrator circuit also offers a convenient interface for direct digital control of the quartz oscillator, when the cesium loop is inactivated.

The 5 MHz crystal oscillator used in the standard is a special ruggedized version of the Oscilloquartz B-5400 commercial oscillator. This modified design has met all the shock, vibration, temperature and other environmental requirements of the satellite specification while at the same time exhibiting electrical performance and stability equal to or better than that of the B5400. A special output amplifier design permits multiple, highly buffered, independent outputs with considerable reduced primary power consumption.

The internal functions of the standard may be monitored remotely by means of the satellite telemetry system. The monitors on these parameters are scaled to a 0 to +5 VDC output and are brought to a connector for interfacing to the satellite. The functions available are:

control voltage
c-field
Cs beam current

ionizer current
C_S oven temperature
ion pump current
electron multiplier voltage
lock indicator
power on indicator
synthesizer lock indicator
quartz oven temperature

These monitors are continuously available.

TESTING

Upon arrival at NRL each standard went through a rigorous testing sequence. Unit number 4 (designated as qualification standard) was subjected to full qualification level vibration and the full qualification temperature range. The remaining units were required to meet acceptance levels. All units were tested to see that stability, noise, power, weight and interfacing specifications were met. test sequence was intended to give earliest possible indication of failure in those areas where least was known about its performance or durability. Four separate vibration tests comprising about 16 minutes of time on the shake table were done on the qual unit. The NTS-2 random vibration specification calls for an overall level of 18.5 grms (13.1 grms for acceptance) with a maximum input of .170 g /Hz (.085 g /Hz for acceptance) in the frequency range of 100 to 2000 Hz in power spectral density. Because the NTS-2 mission does not require that the cesium standard be operational during the launch phase the testing is done with only the quartz oscillator and ion pump portions of the standard operating. All four prototypes have passed vibration. The two flight units will be subjected to acceptance level vibration in the acoustic test of the assembled spacecraft.

Similarly the thermal vacuum test qualification was done before any flight unit was tested in the vacuum chamber. The NTS-2 specifications require that the frequency standard operate in vacuum over the temperature range of -10 degrees centrigrade to +45 degrees centigrade (0 to +40 for acceptance). The required long term stability should be met even when the baseplate temperature varies by up to 4 degrees/day at a rate no greater than 5 degrees/hour. Other functions of the standard such as warm up under hot and cold conditions, function of commands, and input and output power levels were checked in vacuum. As an example figure 8 shows DC power versus temperature

for the brassboard. Figure 9 is a summary of thermal vacuum test data. Because brassboard testing in vacuum had been completed and design corrections incorporated into the prototype design there were no major problems encountered in this phase of testing. However, because the mechanical structure was somewhat changed from the brassboard a serious study was made of the thermal design. The results of that work will be presented at a later date (7). Short term stability was measured on all units for averaging times ranging from about one second to as long as 100,000 seconds as test times permitted. The qual unit has been sent to the National Bureau of Standards for long term testing. At both NBS and NRL quality quartz oscillators were used for the shorter averaging times and option 004 cesium standards as references for the longer terms. A graph summarizing the data is included as figure 10.

Single sideband phase noise was measured at NRL on all four units using an Oscilloquartz B-5400 as reference. As expected for this type of clock the spectral density was essentially that of the quartz oscillator. Figure 11 shows the results for the designated flight units.

All standards were tested in the Laboratory and thermal vacuum environment to insure that the power consumption, remote tuning capabilities, and command functions operated properly. This included c-field tuning curve measurements, quartz oscillator tuning measurements, spectrum analysis of harmonic and spurious outputs. As an example figure 12 shows quartz oscillator tuning curves for units three and five.

COMMAND INTERFACE UNIT

The command interface unit was designed to address and control the frequency standards from the ground control station via the telemetry system. This unit was designed to have full redundancy including power crossover.

The interface takes the commands that have a magnitude of 27 volts, pulse width of 50 milliseconds, and rise and fall times of one millisecond and converts them to transistor-transistor-logic (T²L) which is compatible to the frequency standard system. Tuning for the frequency standards is accomplished by taking serial command bits and converting them to parallel tuning words. A monitor is provided to look at the tuning words and at the state of other discrete points in the system.

The command interface unit, diagrammed in figure 13, takes the commands from the Integrated Command and Telemetry System (ICATS) and shapes the commands, not used for relay operations, through a Schmitt limiter circuit into $\mathbf{T}^2\mathbf{L}$ compatible pulses. The commands used for switching latching relays are direct coupled to the relay selenoid with diodes mounted across the relay solenoid for reverse voltage suppression.

The initial preset command should always be the first command after power is supplied to the command interface unit to initialize the unit to nominal operation mode. The control commands operate latch circuits for the specific requirement with the output of the latch circuit output remaining at "O" or "l" until the complimentary command is transmitted which toggles the latch.

The interface points are listed in the NTS-2 connector identification list under box A404 (Frequency Standard Command Interface).

REGISTERS

The unit has seven redundant registers which are identified as follows:

Load registers
Relativistic offset generator register

FS #1 C field transfer register

FS #1 Quartz transfer register FS #2 C field transfer register

FS #2 Quartz transfer register monitor status register.

The load register is a serial register containing 16 bits. A tuning enable command must precede a desired combination of 16 tuning load "1" or tuning load "0" commands. The first tuning load bit is the lowest significant bit (LSB) with each succeeding bit increasing in power until the 16th bit which is the most significant bit (MSB). Bit positions 1 through 12 contain the desired tuning word, bit positions 13 through 15 contain the identification address (ID) bits and bit position 16 is the tuning enable (1) or disable (0). The tuning enable command switches the monitor gate circuitry to monitor the load register for verification of the loaded data word.

The data word is then parallel loaded into the addressed transfer register with the transfer execute command. The

transfer execute command switches the monitor gate circuitry to look at the addressed transfer register for verification of the loaded data word. The data word is next shifted into the frequency standard addressed storage register with the storage register execute command and remains in the transfer register for later recall.

The monitor status register and any of the transfer registers may be monitored at any time by sending a register monitor select enable command, four tuning load "1" or tuning load "0" to make up the required ID address, and a register monitor select execute.

RELATIVISTIC OFFSET PULSE GENERATOR

The input 0.5 MHz frequency from the Relativistic Synthesizer unit is divided by 2 and then divided by 2 producing the input frequency plus eight divided frequencies. These nine frequencies are then pulse subtracted and gated with the desired offset setting in an eight bit relativistic offset generator register to produce 256 discrete number of pulses per unit time. This output is then divided by 2 producing 1.907 pulses per second to 488.28 pulses per second in incremental steps of 1,907 pulses.

The output of this pulse generator is harnessed to the relativistic synthesizer unit on two lines where either line may be active by selection of the relativistic offset select positive or negative command. The positive or negative refers to the relativistic synthesizer output frequency. The pulse generator may be inhibited with the relativistic offset off command or-turned on with the relativistic offset on command.

POWER

DC power for the command interface unit is provided by the 5.5 VDC regulators with crossover redundance accomplished by switching.

RELATIVISTIC SYNTHESIZER

The NTS-2 program office at NRL was tasked by GPS NAVSTAR program office to generate a 10.23 MHz frequency for use with the Pseudo Random Noise System (PRNSA) onboard the NTS-2 Satellite. Frequency requirements for the NTS-2 Orbit Determination and Tracking System (ODATS) was 5 MHz with a tunable ΔF offset of approximately +1 x 10^{-9} with a

resolution of approximately 3 x 10^{-12} . The ΔF offset was to compensate for relativistic effects and could not be accomplished by offsetting the cesium standard which has a tuning range of \pm 1 x 10^{-11} . The relativistic offset was later added to the 10.23 MHz requirement.

RF inputs are the two 5 MHz signals from the two cesium frequency standards which are selectable, by a relay to use either of the two standards and still have the other standard in a powered mode. The positive and negative offset pulses to control the ΔF are redundant and go through exclusive rf gates to allow for crossover redundancy.

RF outputs are redundant 5 MHz \pm Δ F for ODATS, redundant 10.23 MHz \pm Δ F to the 10.23 MHz VCXO unit, redundant 0.5 MHz to the command interface unit for deviation of the positive and negative offset pulses, 42.82 KHz zeeman frequency for the frequency standards, and 5 MHz to the ICAT system.

Primary DC power is 27 VDC on either one of the two power lines but not both simultaneously. An output 5.5 VDC is provided for the command Interface Unit on one of two lines but not both simultaneously being consistent with the 27 VDC input.

The basic operating principle of the relativistic offset synthesizer may be compared to rotating a phase vector by means of a coherent motor driven resolver. Figure 14 shows a block diagram. Pulses are coherently added to or subtracted from the input 5 MHz pulse chain at a settable number of pulses per unit time for the desired offset.

The input 5 MHz signal is shaped into approximately a 50 percent waveform with the negative edge triggering a pulse generator and the positive edge controlling the insertion of pulses. The output of the pulse generator and the inserted pulses are gated to produce the nominal 5 MPPS plus the inserted pulses, if desired, in a pulse chain. This pulse chain is gated with an omission pulse, if desired, to omit pulses from the pulse chain. This pulse chain is divided and heterodyned with the input signal in a series of steps to obtain the desired integration or phase shift per insertion or omission of pulses. The division ratios in the NTS-2 unit is 131,220 to 1 in six stages of division and heterodyning. The output frequency is 5 MHz \pm ΔF range and resolution is 7.44 x 10 and 2.91 \overline{x} 10-12 respectively.

The 5 MHz to 10.23 MHz synthesizer is a direct frequency synthesis technique incorporating digital and linear logic. This technique of frequency synthesis assures the output frequency stability is directly related to the reference or input frequency. The synthesis derivation is

$$[(5\div5x3\div4+5)\div5+5]\div5+5\div5x9 = 1.23+9.0 = 10.23.$$

Circuitry used in the synthesis is a hybrid of digital and linear logic, see figure 15.

The Zeeman frequency generator is non redundant in the NTS-2 unit. The purpose of the Zeeman frequency is an attempt to make a measurement of the relativistic effects of the satellite clock. Using the Zeeman to set the cesium standard to atomic time should be > 2 orders of magnitude better resolution than the calculated relativistic offset for the NTS-2 satellite orbit.

The Zeeman generator is a direct digital frequency synthesis with an op-amp filtered output. The reference frequency is 1 MHz which is derived from the input 5 MHz. The synthesis derivation is

$$\{1 + [1 \div 4 + (1 \div 1 \div 5) \div 25] \div 4\} \div 25.$$

The Zeeman frequency is switchable on-off, and between the two frequency standards by relays which are commanded through the telemetry command system.

The 10.23 MHz VCXO was added to the system to meet the GPS phase noise specification when the relativistic offset was on. The circuitry is a basic phase lock loop (PLL) controlling a voltage control crystal oscillator (VCXO). The reference frequency to the PLL is the direct synthesized 10.23 MHz which is derived from the cesium standard plus or minus the direct synthesized relativistic offset frequency. The unit is fully redundant by selecting the appropriate power on command.

The PLL incorporates a balanced mixer used as a phase detector. The synthesized 10.23 MHz plus or minus the relativistic offset, with the stability of the cesium frequency standard, is phase compared with the VCXO RF output. The proportional DC voltage output of the phase detector is fed into an analog integrator. The analog integration is an operational amplifier where the bias voltage is set to the nominal VCXO control voltage. The gain of the amplifier is 30 and has an integrator response

time of 3 seconds. The output of the analog integrator is the control voltage for the VCXO unit. Figure 16 shows the circuit.

The VCXO unit was designed by Frequency Electronics Incorporated for satellite system use. The unit meets all frequency stability, phase noise, electrical and environmental characteristics requirements for use in NTS-2.

RF AMPLIFIERS

The RF amplifier takes the + 3dBm 10.23 MHz signal from the VCXO unit and amplifies this signal by 15 dB to + 18 dBm output.

POWER

This unit is powered from the same secondary switched points as unit A403. Unit A is powered when RSCI A is selected and Unit B is powered when RSCI B is selected.

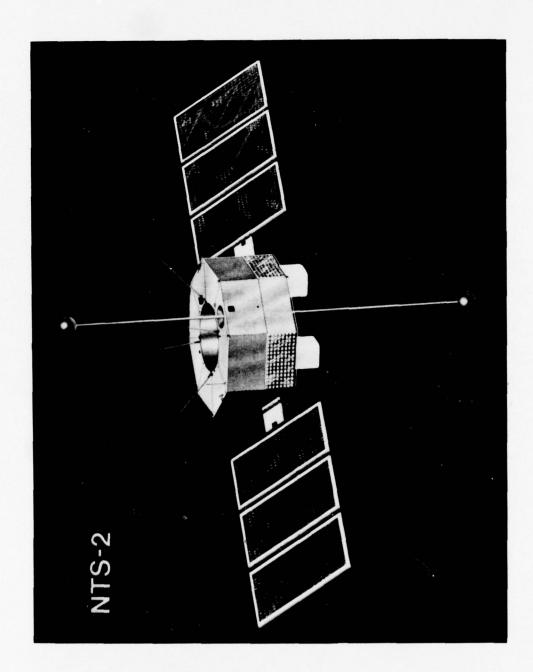
ACKNOWLEDGEMENTS

The authors wish to thank the following people for their many contributions to this work: Robert Kern and Tom Gregory of Frequency and Time Systems and C A. Bartholomew, Robert Hersh, Wayne Lloyd, Robert Moore and Stephen Nichols of the U. S. Naval Research Laboratory.

REFERENCES

- 1. GPS NAVSTAR Global Positioning System, Astronautics and Aeronautics, Volume 14, Number 4, April, 1976.
- 2. Performance of a Rubidium Standard For Space Environment, Nichols, et al, National Telemetry Conference, 1973.
- 3. Satellite Application of a Rubidium Frequency Standard, Nichols, et al, 28th Annual Symposium On Frequency Control, 1974.
- 4. Design and Ground Test of the NTS-1 Frequency Standard System, Nichols et al, NRL Report Number 7904, 1975.
- 5. A New Compact Cesium Beam Frequency Standard, Graf, Johnson, and Kern, Symposium on Frequency Control, 1975.
- 6. Final Prototype Report, Navy Contract, N00014-74-C-0061, 29 April, 1976.
- 7. Thermal Vacuum Testing Techniques for Spacecraft, S. A. Nichols, to be presented at the 9th Space Simulation Conference, Los Angeles, CA, April 1977.

NATIONAL AERONAUTICS AND SPACE ADMINISTRATION GREENB--ETC F/G 14/2 PROCEEDINGS OF THE ANNUAL PRECISE TIME AND TIME INTERVAL (PTTI)--ETC(U) AD-A043 856 1977 UNCLASSIFIED NASA-6SFC-X-814-77-149 NL 8 OF 8 AD 43856 END DATE 9 -77 DDC



FTS TUBE ANALYSIS

PARAMETER	PRE SHAKE	POST SHAKE
ACCURACY $\left(\frac{\Delta f}{f}\right)$	< 1 x 10 ⁻¹¹	< 1 × 10 ⁻¹¹
FLOP/BACKGROUND RATIO	12:1	12:1
SIGNAL TO NOISE RATIO	1900*	1850*
LINE WIDTH	447*	454*
FIGURE OF MERIT	4.3*	4.0*
I SIGNAL	2.5×10^{-8}	2.2×10^{-8}
I DARK CURRENT	10-12	10-12
I ION PUMP	1 ua	1 ua**
FULL RESONANCE SPECTRUM		NO CHANGE

^{*}DIFFERENCES IN THESE VALUES ARE WITHIN THE RESOLUTION OF OUR PARTICULAR TEST APPARATUS.

Figure 2.

^{**}AFTER SHAKE, A VACUUM LEAK IN A MICROWAVE WINDOW METAL TO METAL BRAZE CAUSED A RATE OF RISE IN INTERVAL TUBE PRESSURE. ALTHOUGH UNDESIRABLE, THE MAGNITUDE OF THE LEAK WOULD NOT INHIBIT NORMAL OPERATION IN EARTHS ATMOSPHERE. LEAK STOPPED AT NRL — ADDITIONAL QC STEPS NOW IN FORCE TO AVOID ANY POSSIBLE REPETITION IN FUTURE TUBES.

BRASSBOARD TEST DATA

$\frac{\sigma(2, \tau) \star 10^{12}}{}$	
3.2	
1.8	
3.1	
1.5	
.6	
.55	
1 Hz BW	
<u>L (f)</u>	
- 117	
- 139	
- 137	
- 141	
- 142	

THERMAL COEFFICIENT
7.5 * 10⁻¹⁵/°C OVER +5°C TO +25°C

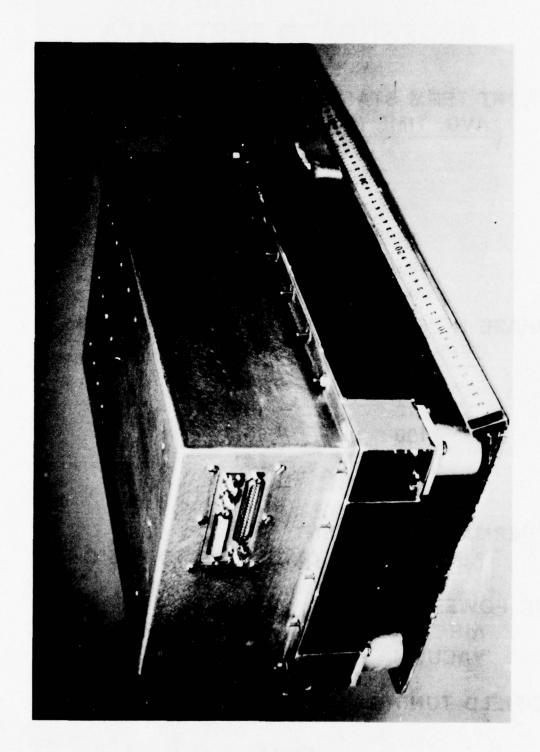
DC POWER

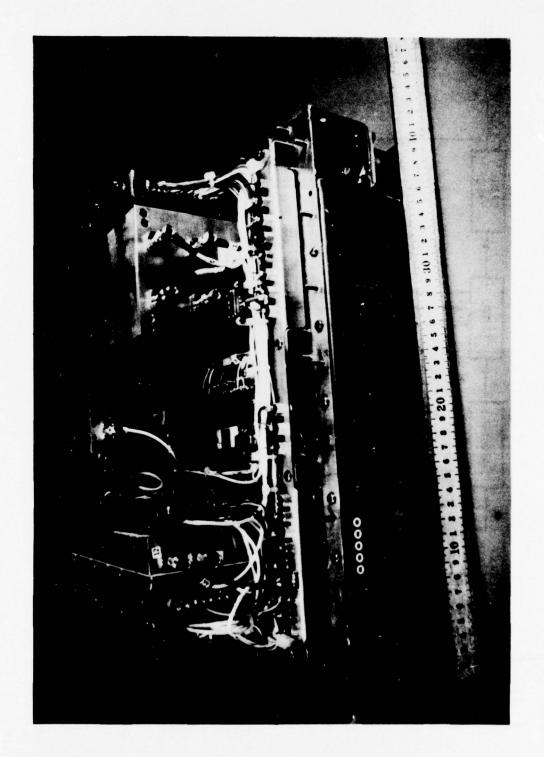
22.4 AMBIENT TEMP ~ 25°C

VACUUM 19.4 WATTS AT 25°C

C-FIELD TUNING 1.4×10^{-13} /TUNING BIT

Figure 3





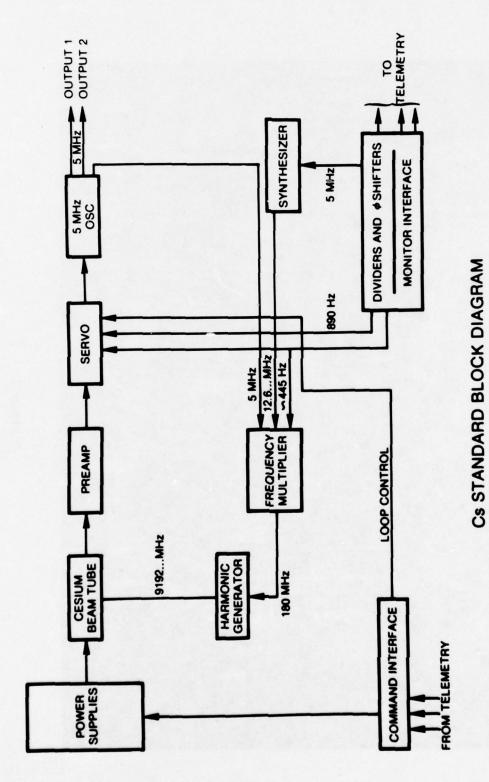
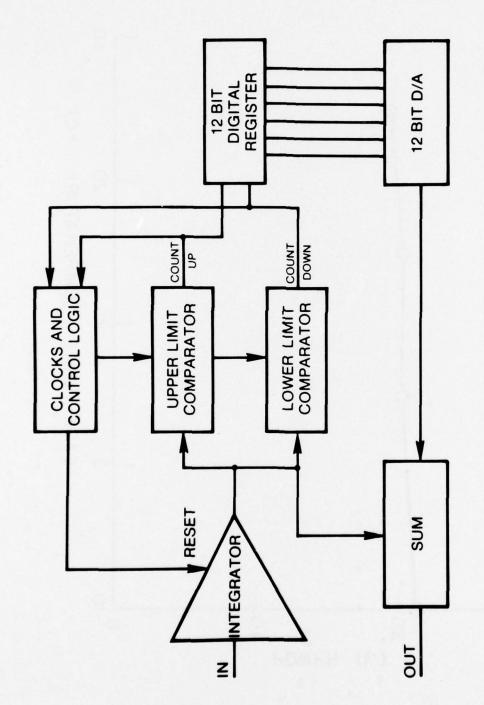


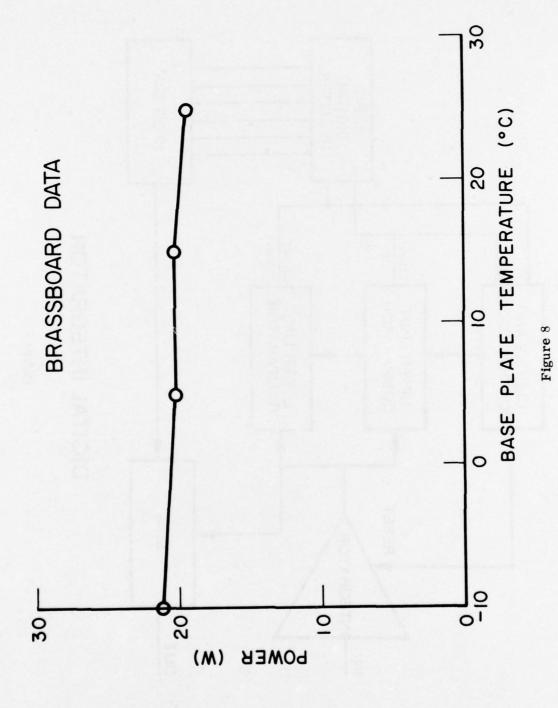
Figure 6

654



DIGITAL INTEGRATOR

Figure 7



PROTOTYPE PERFORMANCE DATA

PRO-5	1.3×10^{-13} /BIT
PRO-3	$1.5 \times 10^{-13}/BIT$
PRO-2	,
	C-FIELD TUNING

_	3.7 × 10 ⁻¹⁴ /°C 1.2 × 10 ⁻¹³ /°C 6.0 × 10 ⁻¹⁴ /°C	
TEM IN	TEMP COEFFICIENT 3.7 × 1	DC POWER

22.0 W	21.6 W	
22.0 W	20.8 W	
20.7 W	20.3 W	
AIR	VACUUM	

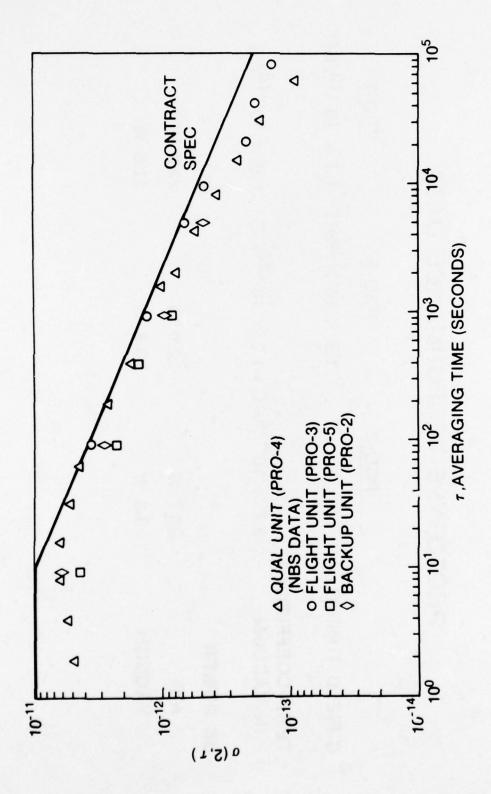


Figure 10

PHASE NOISE MEASUREMNENT OF FLIGHT CANDIDATE

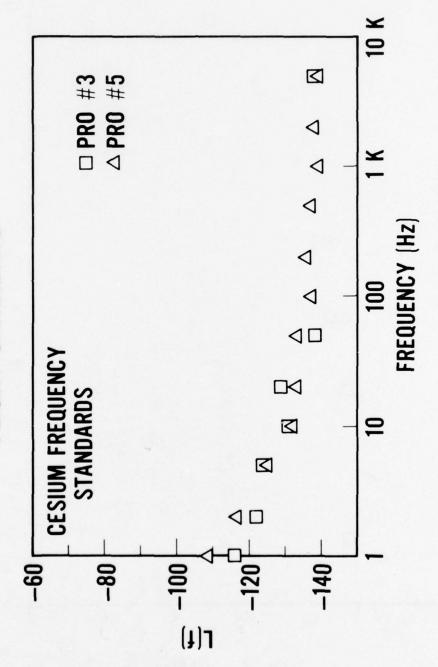
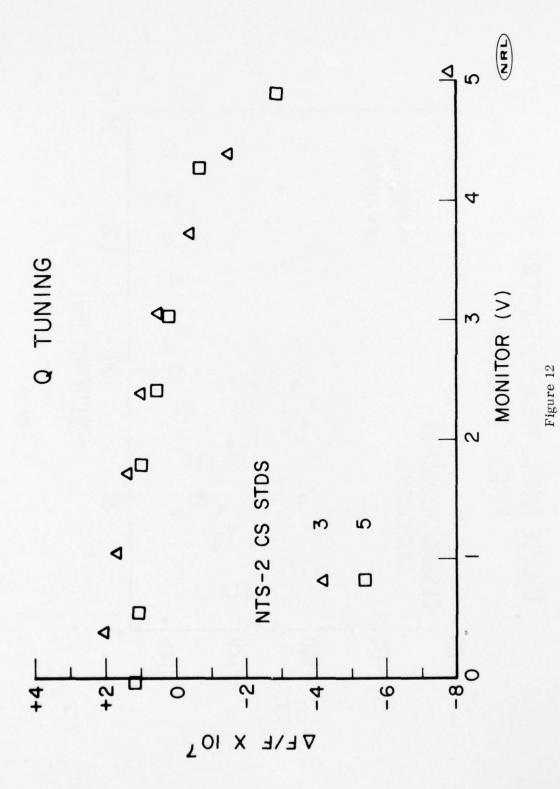


Figure 11



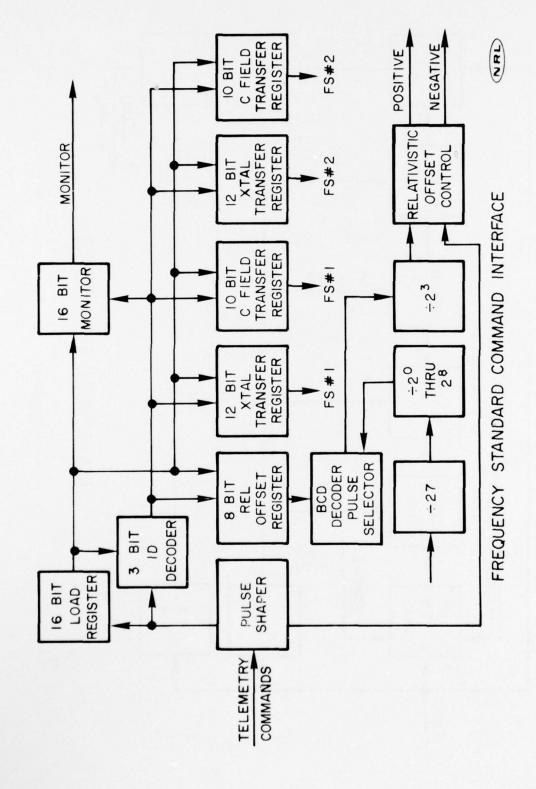


Figure 13

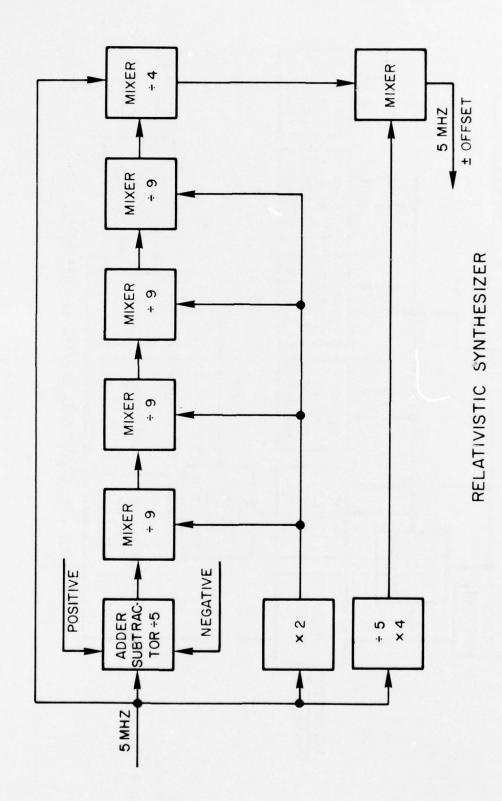


Figure 14

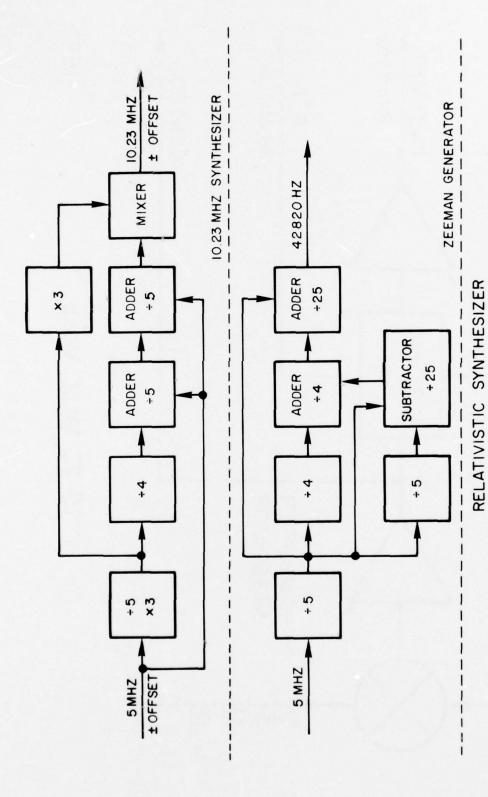
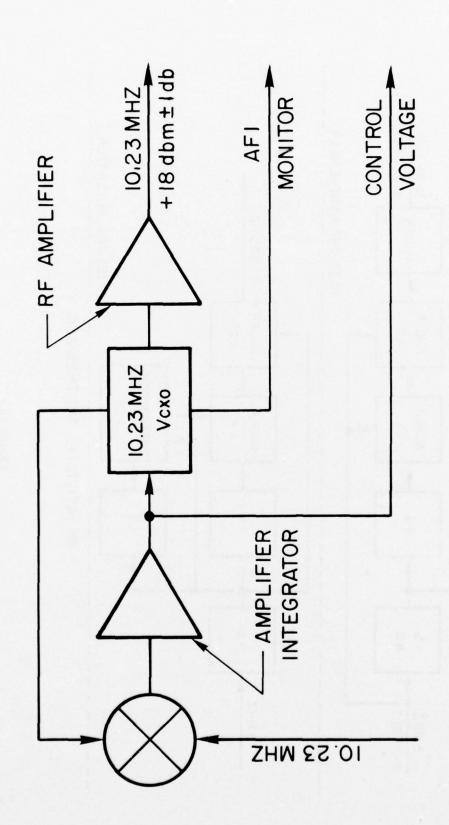


Figure 15



10.23 MHZ Vcxo



Figure 16

A NEW RUGGED LOW NOISE HIGH PRECISION OSCILLATOR

D. A. Emmons
Frequency and Time Systems, Inc.
Danvers, Massachusetts

ABSTRACT

This paper describes the performance characteristics of a new, rugged 5 MHz quartz crystal oscillator having good short and long term stability. It exhibits high spectral purity at frequencies close to the carrier, with phase noise typically -120 db at 1 Hz. Short term stability is characterized by σ (τ) less than 1 x 10⁻¹² for sample times of 1 second to 100 seconds.

The oscillator provides a precision low-noise source suitable for high order frequency multiplication in navigation or communications systems which must survive physical abuse as well as hostile radiation environments. It meets the demanding environmental specifications of the satellite portion of the NAVSTAR GPS system. Power consumption of less than two watts is compatible with the requirements of a satellite-borne cesium frequency standard. Linear voltage controlled tuning permits operation over a 5-year satellite mission duration.

Frequency stability against ambient temperature changes is an important consideration in the design. The oscillator exhibits stability of better than 5 x 10^{-10} over the ambient range of -55°C to +61°C. Thermal stability data and results of shock and vibration testing will be presented.

INTRODUCTION

A rugged high precision 5 MHz oscillator has been developed for applications requiring a frequency source which has good spectral purity and frequency stability, and which is able to withstand severe shock and vibration. The oscillator exhibits very low phase noise close to the carrier, typically -120 db in a 1 Hz bandwidth at 1 Hz. Short term frequency stability is characterized by an Allan variance σ (τ) of less than 1 x 10⁻¹² for sample times of 1 to 100 seconds. (Fig. 1)

The oscillator thus provides a precision low-noise source suitable for high order frequency multiplication in navigational or communications systems which must survive physical abuse, extremes of temperature, or severe radiation environments. In spite of the overriding design requirements of physical survivability, it has been possible to achieve the kind of low-noise performance described by Brandenberger et al (1), and we have been fortunate in being able to draw on that experience.

The 5th overtone AT cut quartz crystal and associated electronics are held at the frequency turnover point in a proportionally controlled oven whose temperature is maintained constant to better than $0.1^{\rm OC}$ over an ambient temperature range of $-55^{\rm OC}$ to $+61^{\rm OC}$.

At present we produce the oscillator in two configurations; one designed specifically for GPS application, and one in a slightly modified package for more general applications in severe environments.

To emphasize the survivability aspect of this design, I will first describe the 5.115 MHz variation being produced for satellite cesium frequency standards in the NAVSTAR GPS system. Then I will discuss detailed specifications and performance of this new oscillator design, the FTS Model 1000.

SATELLITE OSCILLATOR REQUIREMENTS AND PERFORMANCE

One of the tasks of FTS in the NAVSTAR GPS program was to provide prototype model cesium standards, with a low aging

rate quartz oscillator which would demonstrate the required survivability for rocket launch and a long term space mission. The first units were delivered to NRL early in 1976 for evaluation and use in the NTS-2 satellite. Quartz resonators were fabricated from premium Q grade swept quartz and then subjected to extensive testing, selection and processing before use.

The next generation Engineering Development Model oscillator contains selected, screened parts, the requisite radiation resistant circuitry, and appropriate shielding for the GPS-NDS satellite missions.

In the satellite cesium standard back-up mode, the oscillator may operate independently of the cesium control loop as a prime frequency source with low drift rate and good frequency stability. The 5.115 MHz output is frequency doubled outside the oscillator, and additional circuitry provides the desired radiation-immune user signal at the 10.23 MHz GPS frequency.

Figure 2 shows the GPS environmental specifications as well as typical performance. The oscillator has undergone repeated random vibration testing at the (previous) 23.2 g (rms) qualification level both separately, hard mounted to the test fixture, and as part of the EDM cesium standard chassis. Oscillators have also been successfully tested at higher levels up to 29 g (rms).

During 10 g (rms) random vibration tests on an operating oscillator, frequency excursions are well within the electronic control tuning range, with recovery to original frequency in less than 1 hour. The transient excursion is double valued, so the accumulated phase error in a time-keeping system tends to average to zero.

The specified pyrotechnic shock, 2300 g peak at 1850 Hz, is a non-operating survival test, but we have monitored frequency during test of an operating oscillator and find $\Delta f/f$ shifts of a few parts in 10^{10} per pulse. A sequence of 12 pulses produced a final offset of the order of 5 x 10-11 in one instance.

Frequency offset for various ambient operating temperatures is an important consideration. The upper temperature limit of operation becomes especially important in vacuum. It has been our goal to permit stable operation over as wide

a range of temperature as might be expected in diverse non-laboratory applications. Especially important in the prime frequency source back-up mode is frequency stability during temperature changes, since the frequency deviation response to time gradients is in general much larger than for steady operation. In addition to the requirement of operation to +50°C in vacuum, the GPS NTS-2 mission required that all operating specifications be met when the temperature of the mounting surface is controlled to within 4°C at any given operating temperature. From knowledge of the oven control gain and thermal time constants, verified by experimental results, we know that an ambient temperature slew rate of a few degrees per hour will produce less than 10-10 offset and no degradation of short term frequency stability.

The decision not to vacuum-seal the oscillator unit has several consequences for vacuum operation. First is the transient frequency shift associated with changing the stress environment of the resonator, coupled with the thermal perturbations of rapid air removal from the oscillator. The transient frequency offset is typically 10-8 for rapid pump-down, with recovery to the initial frequency in about one hour. Secondly, the thermal resistance between oven and ambient increases so that oven consumption decreases. Internal heat sources then produce a larger temperature differential than normal, and this has been taken into account when setting the upper limit for frequency stable operation.

The low power consumption in vacuum environment is an additional asset for satellite applications. The GPS oscillator typically requires less than 2 w in vacuum even though three buffered signal outputs are provided.

Figure 3 shows the GPS short term frequency stability requirement for the back-up mode (oscillator as prime frequency source). The Allan variance is σ (N=2, T= τ , τ). Also shown are typical data for τ between 1 sec and 100 sec.

The observed short term stability is typically 5 x 10^{-13} , consistent with the measured phase noise in the f⁻³ region of L(f). For τ less than 1 second, one expects a region of τ^{-1} behavior, with τ x σ (τ) = 1.4 x 10^{-13} based on the measured -145 db white phase noise floor and a 1 kHz measuring system bandwidth.

Figure 4 shows the measured phase noise spectrum for an oscillator after undergoing random vibration to 20.8 g (rms) six minutes on each axis. There was no measurable degradation. The GPS specification for phase noise at the 10.23 MHz user frequency is also shown.

FTS MODEL 1000 OSCILLATOR

Detailed specifications for the FTS Model 1000 oscillator are shown in Figure 5. The weight of 1.9 lbs (0.86 kg) and 62 cubic inch size make it compact for an oscillator exhibiting this state-of-the-art performance. The oscillator requires less than 2 w normal operating power at room temperature, and typically 3.2 w at -55°C. Warm-up requires 14 w for less than 15 minutes, and frequency is within 10⁻⁹ of the final value one hour after turn-on. At this time the rate of change of frequency is less than 10^{-12} per second.

The model 1000 has two independent well buffered outputs at 1 v rms into 50 ohms, short circuit proof. An additional two buffered outputs can be provided. The harmonic distortion is at least 40 db below the rated output, and spurious output is better than 100 db down. Sensitivity of frequency change to output loading is < 5 x 10^{-11} for a 10% change from 50 ohm load.

Both mechanical and electrical frequency adjustments are provided, with the important feature that they are linear. A 25-turn screwdriver adjustment gives a minimum of 4×10^{-7} tuning range, and external dc voltage control (-10 V to +10 V) provides $\Delta f/f = 2 \times 10^{-7}$. These tuning ranges are additive and linearity is good over the whole range. Fig.6 shows the typical frequency shift with control voltage. The integral linearity is better than 5% for voltage control at either end of the mechanical adjustment range. This feature is of particular utility in phase locked loop applications where it is desired that the loop gain not vary with frequency offset.

The phase noise performance specification is shown in Fig.7 along with data taken using a noise measuring system such as described by Allan, et al (2). This is the single sideband phase noise per oscillator in a 1 Hz bandwidth at the fourier frequency f. A low noise mixer is followed by a very low noise amplifier system and loose phase lock to maintain the signals in quadrature. The noise voltage is then measured with a spectrum analyzer.

The behaviour of frequency offset as a function of ambient temperature is shown in Figure 8 for several oscillators. Our specification is shown by the total excursion of $5x10^{-10}$ over the range, and representative data from several units are shown. This performance is the result of careful attention to the control of thermal gradients, since the actual stability of a single proportional oven is not simply dictated by the loop gain. The demonstrated stability of frequency versus changing ambient is an important point when one expects high quality low noise performance in less than ideal physical conditions.

Finally, we see the usual static g sensitivity of about a part in 10⁹ per g, as is typical for the high Q thickness shear mode AT cut crystals. Because the reduction of g sensitivity is a topic of great interest, we have experimented with a scheme to compensate for static g changes along the most sensitive crystal orientation, and indeed very preliminary results show that the sensitivity can be reduced to that of the other axes. However, considerable effort will need to be expended to solve the real problem of dynamic sensitivity.

Acknowledgement

The author wishes to acknowledge the contributions of James Burkhardt and Alain Jendly of FTS to this work. We gratefully acknowledge the support of the Naval Research Laboratory under contract no. N00014-74-C-0061.

References

- (1) H. Brandenberger et al, Proc. 25th Ann. Symp. Frequency Control, 1971, pp. 226-230
- (2) D. W. Allan et al, 1974, NBS Monograph 140 pp 151-204

FREQUENCY & TIME SYSTEMS, INC.

PRECISION 5 MHZ OSCILLATOR

S م 9 z œ APPLICATIO V NAVST • L SATELLITE HARDENAB RADIATION 1 RUGGED

STABLE OVER WIDE AMBIENT TEMPERA

ANGE

œ

TURE

ш

NOIS

w

HAS

م

Z .

CLOSE

LOW

ERY

+

+

MODEST POWER CONSUMPTION

F16. 1

ENYI	RANDOM VIBRATION
	RANDOM

SURVIVES SHOCK TEST AND SHOWS
$$\triangle$$
F OF $\overset{+}{-}$ A FEW PARTS IN 10^{10} PER PULSE

ACCELERATION

672

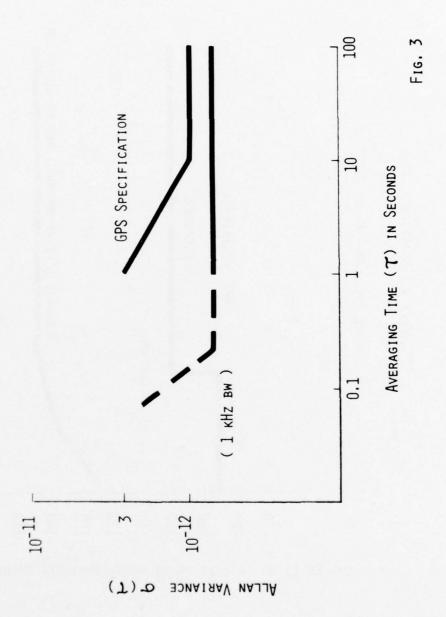
10G(RMS) TESTS ON OPERATING OSCILLATOR SHOW
$$\Delta$$
F DURING 5 MIN WELL WITHIN ELECTRONIC TUNING RANGE

Must operate after being subjected to
$$-10^{\rm o}$$
, $+50^{\rm o}$ C

$$\frac{\Delta E}{F}$$
 <5 X 10^{-10} over the range -50°C to +61°C

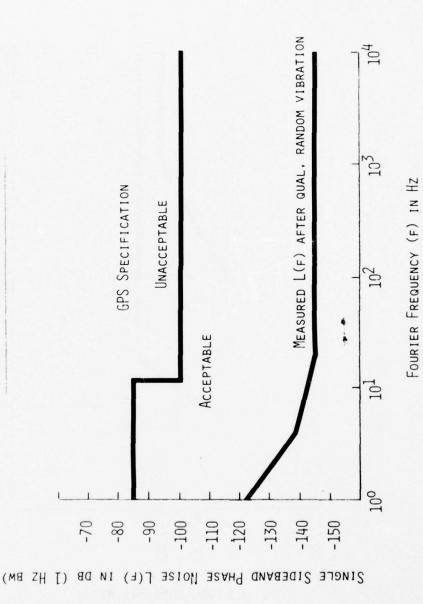
FREQUENCY & TIME SYSTEMS, INC.

OSCILLATOR SHORT TERM FREQUENCY STABILITY





5,115 MHZ OSCILLATOR PHASE NOISE



F16.

FREQUENCY & TIME SYSTEMS, INC.

SPECIFICATIONS MODEL 1000 OSCILLATOR

OPERATING CONDITIONS

SUPPLY VOLTAGE +24 VDC NOMINAL (+22 TO +30 VOLTS)

<2 WATTS OPERATING (25°C) POWER REQUIREMENT

14 WATTS WARM-UP

-55°С то +61°С OPERATING TEMP. RANGE

ENVIRONMENTAL NON-OPERATING

 -60° C to $+80^{\circ}$ C STORAGE TEMP. RANGE

VIBRATION 23 g (RMS) RANDOM, 20,2000 Hz

Pyrotechnic spectrum, 2300 g peak at SHOCK 1850 Hz (5% DAMPING)

MECHANICAL DATA

CONNECTORS

3.00 x 3.00 x 6.88 INCHES DIMENSIONS

WEIGHT 1.9 LBS

M24308/3-1, POWER/CONTROL

SMA JACK OUTPUT

Fig. 5

FREQUENCY & TIME SYSTEMS, INC.

Specifications Model 1000 Oscillator

OUTPUTS 2 INDEPENDENT BUFFERED OUTPUTS

FREQUENCY 5 MHz

FREQUENCY ADJUSTMENT

Mechanical 4×10^{-7} by 25-turn screwdriver adjustment Electrical 2×10^{-7} by external DC voltage (-10 to +10v)

LEVEL 1 V RMS/50 OHMS

HARMONIC DISTORTION AT LEAST 40 DB BELOW RATED OUTPUT
NON-HARMONIC COMPONENTS AT LEAST 100 DB BELOW RATED OUTPUT

FREQUENCY STABILITY

Long Term (aging) <1x10⁻¹⁰/day after 30 days of continuous operation

SHORT TERM ALLAN VARIANCE 10-12 FOR 1-100 SEC.

WARM-UP WITHIN 10⁻⁹ IN 1 HOUR

TEMPERATURE EFFECT <5x10⁻¹⁰ OVER -55°C TO +61°C RANGE OF AMBIENT

LOAD SENSITIVITY <5x10⁻¹¹ FOR 10% CHANGE FROM 50 OHMS

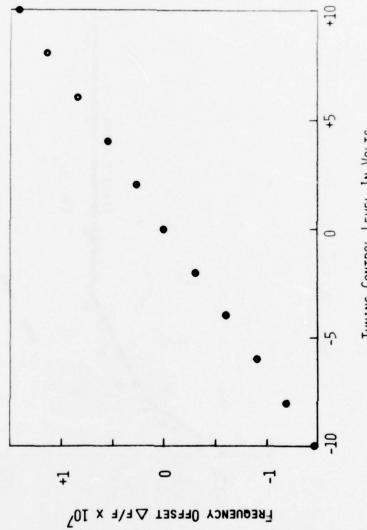
SUPPLY VOLTAGE EFFECT <5x10⁻¹¹ FOR 24 VOLTS ± 10%

STATIC ACCELERATION 1x10-9/G TYPICAL

Fig. 5 (CONT'D.)

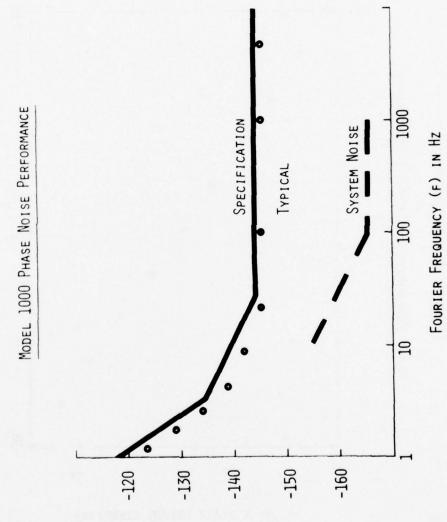
FREQUENCY & TIME SYSTEMS, INC.

Model 1000 QUARTZ OSCILLATOR LINEAR TUNING



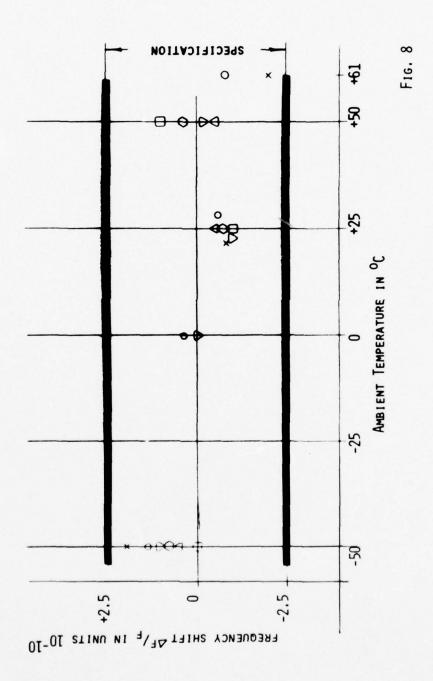
TUNING CONTROL LEVEL IN VOLTS

FREQUENCY & TIME SYSTEMS, INC.



PHASE NOISE SPECTRAL DENSITY L(F) IN DB

FREQUENCY & TIME SYSTEMS, INC. OSCILLATOR FREQUENCY STABILITY VS AMBIENT JEMPERATURE



PERFORMANCE OF A DUAL BEAM HIGH PERFORMANCE CESIUM BEAM TUBE *

Gary A. Seavey Hewlett-Packard Company Santa Clara, California

ABSTRACT

The dual beam high performance cesium beam tube general design and operation is discussed. Computer generated theoretical performance predictions are compared to typical performance measurements on a large sample of tubes. Improvement in cesium oven design and a configuration change of the tube's cesium detector is presented. A few tubes were subjected to adverse environments and the beam tube performane after these tests is discussed. Also, a slightly modified dual beam high performance cesium beam tube was subjected to high level random vibration and its performance before and after the vibration is presented. The possibility of achieving greater than typical performance for relatively short periods of time, for special applications, is discussed. Measurements of accuracy, stability for various time periods and stability in dc magnetic fields carried out on HP 5061A primary frequency standards equipped with dual beam high performance cesium beam tubes is presented. The frequency stability of various types of atomic frequency standards is compared to the typical frequency stability of a HP 5061A primary frequency standard equipped with a dual beam high performance cesium beam tube.

INTRODUCTION

The dual beam high performance cesium beam tube was developed by Hewlett-Packard Company in 1971. During the past three years Hewlett-Packard has been producing the tube to be sold as an option (designated option 004) with the HP 5061A primary frequency standard. Figure 1 shows the high performance tube and an HP 5061A. Utilization of the option

* This paper was presented in part at the 30th Annual Frequency Control Symposium

with the HP 5061A allows one to realize improved short-term stability, reproducibility, settability, and decreased sensitivity to dc magnetic fields.

General Design and Operation

The dual beam high performance cesium beam tube is a passive atomic resonator whose internal components are shown in Figure 2 and are: a cesium oven, which forms and aims the two cesium beams; the state selector magnets, which by means of a magnetic field gradient, spatially separate the atoms of each beam into two energy groups; the microwave cavity, in which an energy state change of the atoms is induced; the hot-wire ionizer, which ionizes the atoms that have undergone an energy state change; the mass spectrometer, which separates the cesium ions from unwanted noise contributing ions; the electron multiplier, which converts the ions to electrons and amplifies the electron current to a level compatible with subsequent electronics; the ion pump, which maintains a high vacuum within the tube; magnetic shielding, which minimize effects of external magnetic fields; solenoid type windings, which produce the homogeneous magnetic field "C-field" over the region of the microwave cavity and for degaussing the beam tube magnetic shields. Also the tube contains gettering material which collects and traps the unwanted expended cesium atoms.

The primary life limiting elements in cesium beam tubes are the cesium supply and the gettering system. The cesium supply and gettering system in the dual beam high performance cesium beam tube have been designed for a five year operating life, as has the standard tube.

The cesium oven or cesium source forms and aims the two cesium beams by means of a multi-tube collimator. We use dual beams primarily to double the output signal to the ionizer which gives a $\sqrt{2}$ increase in the Signal-to-Noise ratio at the input to the electronics. A second advantage of the dual beam, which has been designed in, is relative immunity to acceleration effects. The cesium beam intensity is controlled by the temperature to which the cesium is heated by the oven. Additionally there are intentional conductance limitations in the oven and collimator which reduce the beam intensity. These conductances within the oven are designed to prevent liquid cesium from escaping the oven.

The state selection magnets produce an inhomogeneous, 10⁴ gauss peak, magnetic flux density. The beam comprised of cesium atoms in two energy level groups, as depicted in Figure 3, passes through this large magnetic field gradient. Since:

- 1. an atom's energy is dependent on magnetic field intensity;
- 2. the magnetic field intensity is dependent on position in the state selector magnet gap;
- 3. physical systems tend to the lowest potential energy possible;

then the atoms experience a force in the direction of the magnetic field gradient. The atoms in the levels of F=3 and F=4, $m_F=-4$ group are deflected towards stronger magnetic fields. The atoms in the remaining F=4 levels are deflected towards weaker magnetic fields. Hence the atoms of each of the two beams are spatially separated into two energy level groups.

The first state selector magnet separates the atoms into two energy level groups such that the F=3 levels and F=4, $m_F=-4$ level are directed through the microwave cavity while the remaining group of the F=4 levels is prevented from passing through the microwave cavity.

The second state selector magnet separates the cesium beam which has traveled through the microwave cavity into two groups, the atoms that have not undergone a transition to the F=4 group are directed away from the hot-wire ionizer and the atoms that have undergone a transition to the F=4 group are deflected onto a path toward the hot-wire ionizer. Thus the majority of atoms that are ionized by the hot-wire ionizer are atoms that have experienced an energy transition while traveling through the microwave cavity.

The microwave structure first proposed by Professor Ramsey is a center feed, U-shaped microwave cavity which is machined to close tolerances from oxygen-free copper. The outside configuration of the microwave cavity is fabricated in such a way that it positions the C-field windings and the C-field magnetic shield.

The hot-wire ionizer is a flat tantalum ribbon running at approximately 1000° Celsius. The cesium atoms which have undergone an energy transition in the microwave cavity are

directed toward the ionizer by the second state selector magnet. The atoms intercepted by the ionizer first stick, then are ionized, and finally evaporated and accelerated into the mass spectrometer.

The mass spectrometer spatially separates the cesium ions from any other unwanted noise producing ions, such as potassium, and focuses the cesium ions into the electron multiplier.

The electron multiplier, which is of the box and grid design, converts the 1×10^{-11} ampere ion current to an electron current and then amplifies the electron current to approximately 10^{-7} amperes which becomes the input for the signal processing electronics of the HP 5061A.

Figure 2 depicts the paths of the cesium atoms through the beam tube. The solid lines indicate the path of the atoms that contribute to the signal and the dashed lines indicate the path of the atoms that do not contribute to the signal.

Comparison Theoretical Vs. Actual Performance

A computer program was developed to model the dual beam high performance cesium beam tube and the theoretical performance was calculated based on this model.² The pertinent parameters obtained from the computations are as follows:

- 1. Total beam intensity arriving at the hot-wire ionizer, 7.2 x 10^7 atoms/sec. (1.15 x $10^{-11}a$)
- 2. Linewidth of the field independent transition (F=3, m_F=0 to F=4, m_F=0) is 327 Hz.
- 3. Figure of merit, 31

An initial production group of approximately 30 tubes was produced that exhibited performance somewhat less than predicted. An investigation was carried out to determine the cause of this disagreement. A cesium source problem was discovered as was an improvement in the detector configuration.

The cesium source or "oven problem" which caused erratic beam intensity performance and some very early failure, due to decreased signal level, required a redesign of the cesium oven. This has long since been completed, and since we have

seen no recurrences we feel confident that the problem is cured.

In Figure 4 the shaded area depicts the figure of merit of the initial group, and the outlined area, the figure of merit of the most recent 150 units. The figure of merit increased 44% to a mean value of 24.

Typical performance after the modifications as measured on over 150 tubes:

- 1. Total beam intensity, 1 x 10^{-11} a
- 2. Linewidth, 358 Hz
- 3. Figure of merit, 24.

The most important of these parameters in characterizing overall tube performance is the figure of merit. The figure of merit is defined to be the beam tube output signal to noise ratio as measured in a ¼ Hz bandwidth, divided by the linewidth of the field independent transition. Figure 5 depicts the pertinent measurements and their relation to the figure of merit.³

Typical Performance in an HP 5061A

Figure 6 is a frequency offset histogram of HP 5061A option 004 based on final test data for over 100 instruments.

The frequency stability specification for the 5061A option 004 is based on a realized figure of merit of 10. The high performance tube figure of merit mean of 24, if realized in the environmental and instrument conditions prevailing, would give a 100 second stability of 3.5 x 10^{-13} . Published data of NBS shows a realized stability of 5 x 10^{-13} at 100 seconds. The specification sheet calls for less than 8.5 x 10^{-13} . These NBS data also indicated that the $\tau^{-\frac{1}{2}}$ relation holds past 10^4 seconds, giving 5 x 10^{-14} at 10^4 seconds.

The specification limit for sensitivity to magnetic fields is $\pm 2 \times 10^{-13}$ for a 2 gauss field in any direction. A typical measurement yields:

side to side $\pm 1 \times 10^{-13}$ top to bottom $\pm 5 \times 10^{-14}$ front to rear $\pm 5 \times 10^{-15}$ The reproducibility specification of 3 x 10^{-12} is obtainable when the HP 10638A Degausser is used with the HP 5061A Option 004. This reproducibility is shown by the accuracy histrogram Figure 6. The function of the degausser is to relax the magnetic domains of the inner shield to an equilibrium magnetization after a change in the "C-field" current. The degausser accomplishes in 20 minutes the relaxation that might otherwise proceed for weeks causing a shift in frequency as the "C-field" changes. A high level degaussing is recommended at turn on, and can be performed as the oven is heating. Low level degaussing can be performed without causing the instrument to unlock, and is recommended after changes in "C-field", or magnetic environment changes are made. Reproducibility is defined as the independently set up instrument frequency comparison to the NBS frequency standard.

The settability specification of $\pm 1 \times 10^{-13}$ requires the use of the degausser. Settability or calibration refers to the ability to make relatively small, predictable changes to the output frequency of the standard. One minor division on the "C-field" control corresponds to a nominal change of 5×10^{-14} in output frequency and 2 in the logging numbers on the "C-field" dial which reads from 0 to 1000.

Typical performance with regard to settability is 1×10^{-14} which includes control linearity, operator, beam tube and degausser effects.

Operating life data are still scarce, but recently two early tubes were returned at end of life after more than 4 years in service. These tubes were of the old oven design.

Frequency Stabilities of Various Types of Atomic Frequency Standards

Before the development of the high performance cesium standards, the commercial rubidium standards exhibited superior short-term stability by an order of magnitude when compared to commercial cesium standards. The high performance cesium standard exhibits typical short-term stability approximately equal to the short term stability of commercial rubidium standards.

Figure 7 is a graphic representation of the measured frequency stability of various types of atomic frequency standards.⁵ The shaded area labeled High Performance Commercial Cesium represents the realizable frequency stability range

for $\pm 1\sigma$ of the measured figure of merit for a sample of over 150 dual beam high performance cesium beam tubes. The mean of this range corresponds to a figure of merit of 24.

High Level Vibration

A dual beam high performance cesium beam tube was modified for the Global Positioning System evaluation program. ⁶ The modifications were to strengthen it structurally and change the internal wiring so that the tube could be subjected to high level random vibration and not experience mechanical or electrical failure.

The random vibration characteristics were: acceleration spectral density of 0.35 $\rm G^2/Hz$ from 125 Hz to 1200 Hz, below 125 Hz and above 1200 Hz the vibration spectral density decreases by 6 dB/octave until a total frequency band of 20 Hz to 2000 Hz is reached. Figure 8 is the plot of acceleration spectral density vs. frequency for the above mentioned vibration. This vibration characteristic integrates to approximately 25 g rms.

The tube was measured in an HP 5061A frequency standard prior to the vibration, then subjected to the vibration while non operating and then remeasured in the same HP 5061A frequency standard. A comparison of this electrical performance before and after the vibration is tabulated below:

	Accuracy	Short Term (10 second	
before vibration	4.5×10^{-14}	1.33 x	10-12
after vibration	11.1×10^{-14}	1.68 x	10-12
specification	$300. \times 10^{-14}$	2.70 x	10-12

Modified Performance for Special Applications

The figure of merit (stability) of a cesium beam tube is determined, as mentioned previously, by the signal-to-noise ratio, the linewidth and curve shape factor. In any given beam tube the linewidth and curve shape are relatively constant, but the signal-to-noise ratio can be changed within limits by changing the beam intensity, i.e. oven temperature. Since the vapor pressure of cesium doubles

for approximately a 10° Celsius increase in oven temperature one expects such a change to give a doubling of cesium beam intensity, a $\sqrt{2}$ improvement in figure of merit and a doubling of consumption of cesium, or halving of operating life.

Cesium beam tubes have been operated with oven temperatures increased 12° Celsius from nominal for periods of hundreds of hours. If the cesium vapor pressure is made too great scattering occurs in the beam which adversely affects the curve shape and linewidth which shorten the operating life and yield no benefits.

Similarly a reduction in cesium oven temperature will give reduced beam intensity, cesium consumption, and figure of merit with expected longer life. The initial limitation here would be the need for a detectable signal level which would set a low temperature limit.

Adverse Environments

Randomly chosen tubes have been subjected to adverse environments. One such test was to subject a tube to high level shock. The test called the "hammer blow" is carried out by mounting the tube to a large steel carrier and then striking the carrier with a 400 lb. hammer. The hammer swings through 1, 3, and 5 foot drops in each of three axes for a total of nine blows. The 5 foot drop generates shocks on the order of 1500 g at the table. The tube successfully passed this shock test without mechanical or electrical damage, or measurable change.

Acknowledgements

The author wishes to express his appreciation to L. F. Mueller, R. C. Hyatt, R. F. Lacey, D. W. Allan for discussions invaluable in the preparation of this paper and to Sal Blas and Liz Cypert for their efforts in preparing the illustrations and manuscript.

References

1. R. C. Hyatt, L. F. Mueller, T. N. Osterdock "A High Performance Beam Tube for Cesium Beam Frequency Standards," Hewlett Packard Journal, September 1973, p. 14.

- 2. Unpublished work, L. S. Cutler, R. F. Lacey
- 3. R. F. Lacey, A. L. Helgesson, J. H. Holloway "Short Term Stability of Passive Atomic Frequency Standards," Proc. IEEE, 54, 2, p. 170, February 1966.
- 4. H. Hellwig, D. W. Allan, F. L. Walls "Time and Frequency," Proc. Fifth International Conference on Atomic Masses and Fundamental Constants (AMCO-5) June 1975.
- 5. Helmet W. Hellwig "Atomic Frequency Standards: A Survey," Proc. IEEE, 63, 2, p. 214, February 1975.
- 6. Contract No. N00173-75-C-0471 (NRL).

- Figure 1. a.) HP 5061A, b.) Dual Beam High Performance Cesium Beam Tube
- Figure 2. Pictorial Representation of Dual Beam High Performance Cesium Beam Tube
- Figure 3. Energy Level Diagram of Cesium 133.
- Figure 4. Figure of Merit Histogram
- Figure 5. Figure of Merit
- Figure 6. HP 5061A Opt. 004 Frequency Accuracy Histogram
- Figure 7. Frequency Stability for Various Types of Atomic Frequency Standards
- Figure 8. Acceleration Spectral Density

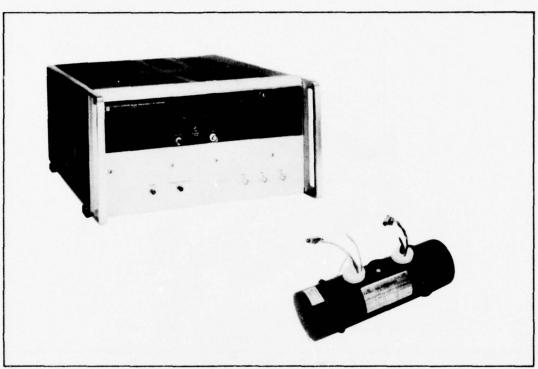


Figure 1. HP 5061A and High Performance tube

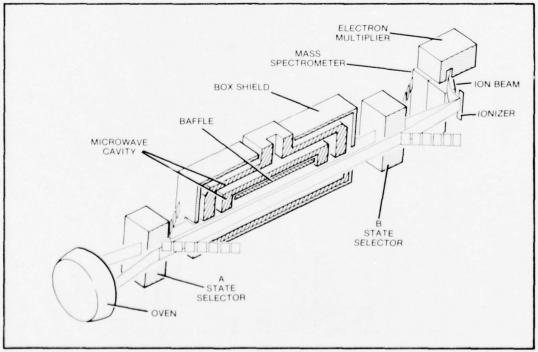


Figure 2. Pictorial representation of Dual Beam High Performance

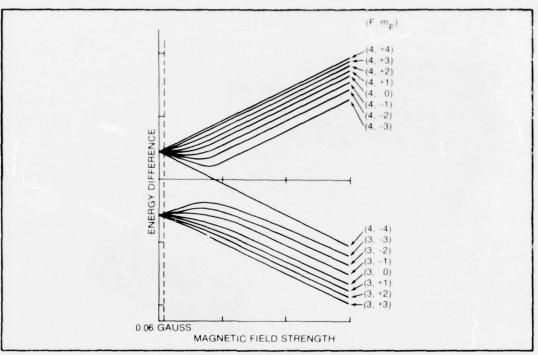


Figure 3. Energy Level Diagram of Cesium 133

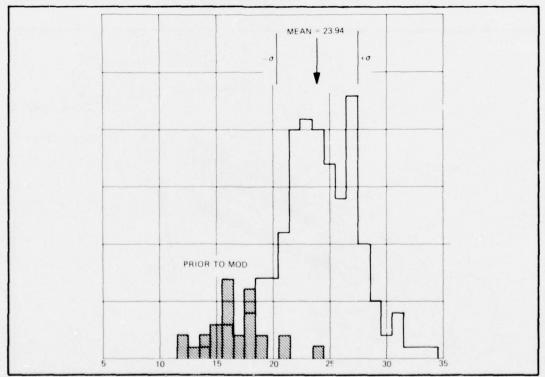


Figure 4. Figure of merit Histogram

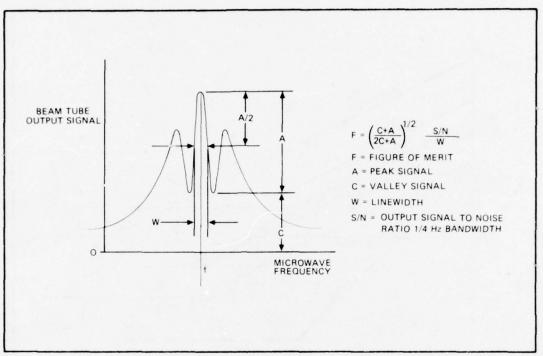


Figure 5. Figure of Merit

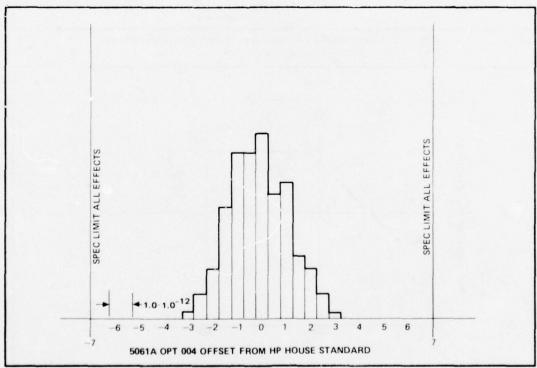


Figure 6.

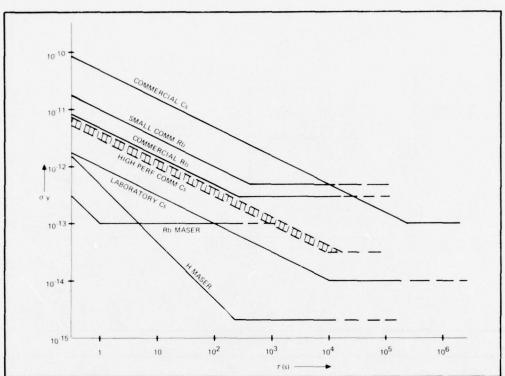


Figure 7. Frequency stabilities of various types of atomic frequency standards

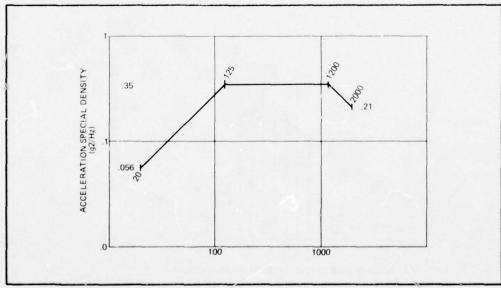


Figure 8. Acceleration spectral density

APPLICATION OF HIGH PERFORMANCE CESIUM BEAM FREQUENCY STANDARDS TO VLBI

W. J. Klepczynski U. S. Naval Observatory Washington, D. C.

K. J. Johnston, J. H. Spencer, and W. B. Waltman E. O. Hulburt Center for Space Research Naval Research Laboratory Washington, D. C. 20375

I. INTRODUCTION

Inherent to any VLBI experiment or observation is the use of independent frequency standards at both elements of the interferometer. These standards generate the signal for the local oscillator (LO) used to convert the observed RF frequencies to a video signal which is then recorded on magnetic tape. They also furnish the reference time recorded along with the observations made by each station. These tapes are then brought together at a later time for crosscorrelation in order to determine the interferometric observables.

The stability requirements of the frequency standards used for VLBI experiments are very demanding. Figure 1 illustrates the relative frequency stability required to insure 90° radio phase stability as a function of time interval for several representative observing frequencies. Until this time, only rubidium frequency standards and hydrogen masers have been used for most VLBI experiments. Usually rubidium standards are used when hydrogen masers are unavailable. MacDoran et. al. (1975) have reported the successful use of a HP 5065A rubidium standard at S-band (2.3 GHz) for the ARIES project. They also make the conjecture that sufficient stability might be obtained for X-band (8.4 GHz) by slaving a rubidium to a cesium frequency standard with a phase-lock loop.

As this last statement implies, the typical commercially available cesium standard does not have sufficient intermediate term frequency stability, i.e., for periods of time less than or equal to 1000 secs, to be of use as a VLBI reference oscillator. Because improved cesium standards, such as the HP 5061A with option 004, High Performance Cesium Beam Tube (HPCBT), approach the short and intermediate term stability of a typical rubidium standard, it appeared that

they might be successfully applied in some VLBI experiments. In addition, the availability of several HPCBT cesium standards which had been specially modified and which appeared to have better short and intermediate term stabilities than rubidium standards (Alley, 1975) led the Naval Research Laboratory and the Naval Observatory to undertake a joint program to test and evaluate their use for VLBI applications.

The program consisted of evaluating the laboratory behavior of the specially modified HPCBT frequency standard and then utilizing it and an "off-the-shelf" HPCBT HP5061A (004) in a VLBI experiment. Participation in the VLBI experiment was to be on a standby basis so as not to interfere with the major goal of the experiment. After sufficient observations had been made using a hydrogen maser as the principal reference standard, the test oscillators were switched into the system.

II. STABILITY MEASUREMENTS

CS 1025, an HPCBT cesium beam frequency standard which had been specially modified was selected for this experiment. The modifications consisted of:

- 1) increased oven temperature in order to obtain a larger beam flux;
- 2) a second order control loop; and
- 3) a special HP proprietary modification.

A system consisting of:

- Dual Mixer Time Difference System, Model 106, manufactured by Boulder Scientific R&D Laboratory, Inc. (as described by Allan, 1976);
- 2) HP 5360A Computing Counter;
- 3) HP 5376A Programmer;
- 4) HP K01-5360B Serial-to-Parallel Converter; and
- 5) HP 5050B Digital Recorder

was used to measure phase differences between CS 1025 and a hydrogen maser and to calculate the Allan variance (Allan, 1966). A beat frequency of 1 Hz was obtained using an HP 106 crystal oscillator. System measurement noise is plotted

in Figure 2 along with the results obtained for the Allan variance of CS 1025 versus the hydrogen maser and typical stability curves (Walcek, 1976) for a rubidium frequency standard (HP 5065A), a HP 5061A and a HP 5061A (option 004) cesium frequency standard.

It was not possible to independently determine the Allan variance for the hydrogen maser used in this experiment. Therefore, the contribution of the hydrogen maser to the "CS 1025 versus hydrogen maser" data could not be removed. Consequently, this curve can be looked upon as an upper limit for the Allan variance of CS 1025. It is important to note that, at this time, it would be erroneous to consider this curve as typical. It is very good and represents a selected clock. More such clocks will have to be evaluated in order to determine the reproducibility of this curve.

Inspection of Figure 2 shows the improvement of this specially modified HPCBT cesium standard over a rubidium standard (HP 5065A), especially in the 1000s region. This strongly indicates that these devices should be of value in VLBI experiments where rubidium frequency standards were applicable and possibly of use in additional areas.

III. VLBI MEASUREMENTS

In March 1976, observations were made *at 22.235 GHz of the strong water vapor maser associated with W3(OH)*. The interferometer elements were the 85 foot antenna at NRL's Maryland Point Observatory located at Maryland Point, Maryland, and the 130 foot antenna of Owens Valley Radio Observatory at Big Pine, California. This baseline has a length of 3547 kilometers, corresponding to a minimum fringe spacing of 0.0008. The data were recorded using the Mark II VLBI system of the National Radio Astronomy Observatory at a bandwidth of 2 MHz. The local oscillator was successively derived from a hydrogen maser frequency standard, a rubidium frequency standard (HP 5065A, Serial #161), and a cesium frequency standard (HP 5061A(004), Serial #871) for two successive periods of 15 minutes each to generate the local oscillator at Maryland Point Observatory. At Owens Valley the local oscillator was always derived from a hydrogen maser frequency standard.

The data were reduced on the NRAO Mark II processor in Charlottesville, Virginia (Clark 1973). The output from the processor was a series of 96 point cross-correlation functions at intervals of 0.2 seconds. These were fourier

^{*}a known water source associated with an HII region.

transformed with uniform weighting on a general purpose computer to give a series of cross power spectra having a spectral resolution of 50 kHz or 0.7 km s⁻¹. The cross power spectra were coherently averaged for one second. A fringe rate was removed from the strongest cross power spectral feature in W3(OH) in order to rotate the fringe phase to zero. The complex fringe phase and amplitude, for the one second averages over a time interval of sixty seconds, were fourier transformed to evaluate the frequency stability of the local oscillators. The phases are displayed in Figure Figures 4-6 show the frequency stability of the hydrogen maser, rubidium and cesium derived local oscillators, respectively. The frequency stability ($\frac{\Delta s}{s}$ respectively. The frequency stability $(\frac{\Delta T}{7})$ of the local oscillators can be estimated as $\leq 8.1 \times 10^{-13}$ for the hydrogen maser, $\sim 1.6 \times 10^{-12}$ for the rubidium standard and 9×10^{-12} for the cesium standard. This is simply the frequency width of signal in the frequency domain divided by the observing frequency (22235 MHz). The integration time is 60 seconds. These frequency stabilities correspond to the 5061A cesium and 5065A rubidium standards displayed in Figure 2. The cesium standard used was a 5061A(004), and the main peak in the frequency display for this oscillator is quite narrow but has many harmonics. The observing procedure was again repeated in September 1976, comparing the frequency stability of the hydrogen maser frequency standard with another HP 5061A(004). The results were the same as those reported for March 1976.

An experiment using the specially modified HPCBT 5061A-(004) at a frequency of 1.670 GHz was attempted between Maryland Point Observatory, the National Radio Astronomy Observatory in Green Bank, West Virginia, and Vermillion River Observatory in Danbury, Illinois. The station at Green Bank, West Virginia failed due to an unstable second local oscillator. The data between Maryland Point Observatory and V.R.O. has not yet yielded successful fringes. However, during the experiment the 5 MHz signal from the hydrogen maser, rubidium standard (HP 5065A, Serial #161) and the specially modified cesium standard (5061A(004), Serial #1025) were compared at Maryland Point Observatory. This was done by mixing the signals from two of the oscillators and studying the resulting signal. The frequency stability of the HP 5065A (Serial #161) and HP 5061A (Serial #1025) duplicated those displayed in Figure 2.

IV. CONCLUSIONS

The typical performance curves for the rubidium standard 5065A) and the HPCBT (5061A(004)) show close agreement, with the rubidium standard exceeding the HPCBT in performance

between 1 and 100 seconds. These curves are so close together that a specially selected HPCBT may exceed the typical performance of the rubidium standard, as does the curve for the specially modified 5061A(004). Similarly, a specially selected rubidium standard may exceed this curve. However, at integration times exceeding 300 seconds, the performance of the rubidium standard, as shown in the typical curve, is limited by flicker noise. For integrations exceeding 300 seconds, therefore, a specially selected HPCBT should prove to be superior to the rubidium standard. ever, from the VLBI observations discussed in this paper, at 22 GHz, this does not prove to be the case. These observations were made at a very high radio frequency that necessitates very good performance, i.e. $\frac{\Delta f}{f} = \frac{10^{-12}}{10^{-12}}$ on a 10 second time scale (integration) to avoid loss of coherence (i.e., a phase rotation of 90°). The frequency stability of the two HPCBT (5061A(004)) used in these observations may be typical, as is shown in Figure 1. At radio frequencies that are ten times below this, i.e. 2.2 GHz (S band), the frequency stability $(\frac{\Delta \mathbf{f}}{\mathbf{f}})$ required to prevent loss of coherence on short time scale is $\sim 10^{-11}$. At integrations exceeding 300 seconds or more, the frequency stability of the HPCBT should prove to be superior to the rubidium standard, as is shown in Figure 2. Therefore, it is our conclusion that at low frequencies, i.e. < 2.5 GHz, for integrations greater than 300 seconds, the HPCBT should yield superior performance in VLBI phase stability to a rubidium standard. However, neither the rubidium nor cesium standards yield, within an order of magnitude, the phase stability offered by a hydrogen maser. More tests of the stability of the HP 5061A(004) need to be made under VLBI conditions to verify the curve shown in Figure 2.

V. ACKNOWLEDGEMENTS

The authors would like to thank Dr. L. Reuger of the JHU/APL for allowing the use of his facilities in performing the measurements between the cesium standard and hydrogen maser, and Mr. Al Bates of the JHU/APL for his valuable assistance.

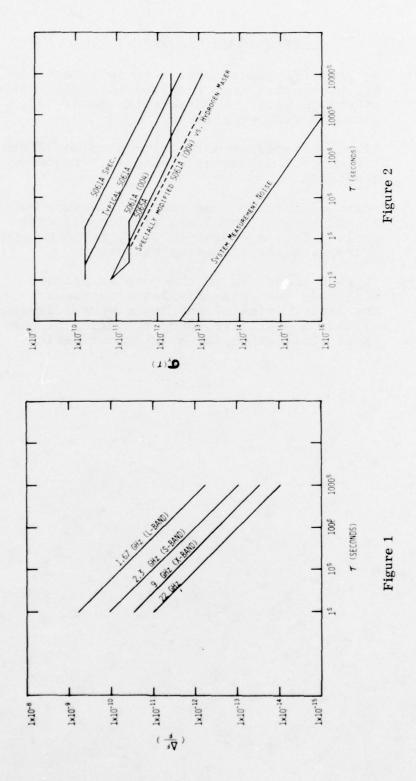
VI. REFERENCES

- 1. Allan, D. W.1966, Proceedings of the IEEE, Vol. 54, pg. 221, "Statistics of Atomic Frequency Standards".
- 2. Allan, D. W. 1976, Report on NGS Dual Mixer Time Difference System (DMTO) Built for Time-Domain Measurements

- Associated with Phase I of GPS, NGSIR 75-827, National Bureau of Standards, Institute for Basic Standards, Boulder, Colorado.
- 3. Alley, C. 1975, Proceedings of the 7th Annual PTTI
 Application and Planning Meeting, pg. 393, "Subnanosec
 -- Laser-pulse Time Transfer to an Airctaft to Measure
 the General Relativity Altitude Effects on Atomic Clock
 Rates".
- 4. Clark, B. G. 1973, <u>Proceedings of the IEEE</u>, Vol. 61, pg. 1242, "The NRAO Tape-Recorder Interferometer System".
- 5. MacDoran, P. F., Thomas, J. B., Ong, K. M., Fleigel, H. F., and Morabito, D. D. 1976, Proceedings of the 7th Annual PTTI Applications and Planning Meeting, pg. 419, "Radio Interferometric Geodesy Using a Rubidium Frequency System".
- 6. Walcek, A. 1976, Private Communication.

CAPTIONS FOR FIGURES

- Figure 1 Relative frequency stability as a function of integration time required to avoid loss of coherence, i.e., a phase rotation of 90°, during a VLBI experiment.
- Figure 2 Allan variance as a function of time interval for several different classes of frequency standards.
- Figure 3 Phase of most intense spectral feature in W3(OH) versus time for a local oscillator derived from a cesium (HPCBT), rubidium and hydrogen maser frequency standard.
- Figure 4-6 Fourier transform of the complex fringe Amplitude and phase displayed in Figure 3. The distribution of amplitude versus frequency illustrates the frequency stability of the local oscillators for a 60-second period.



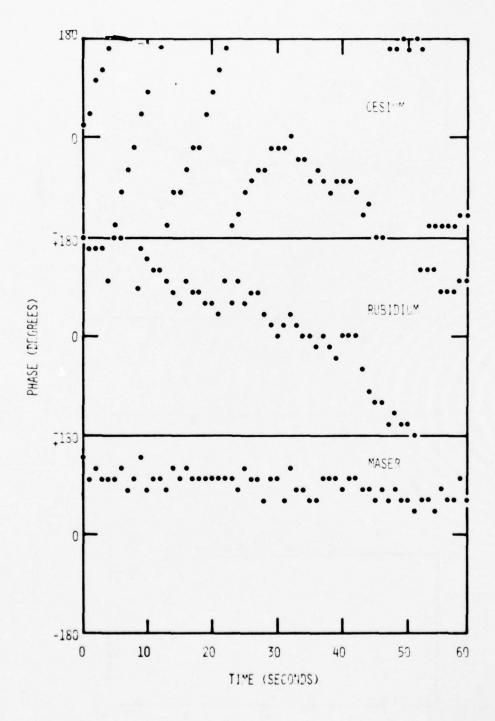
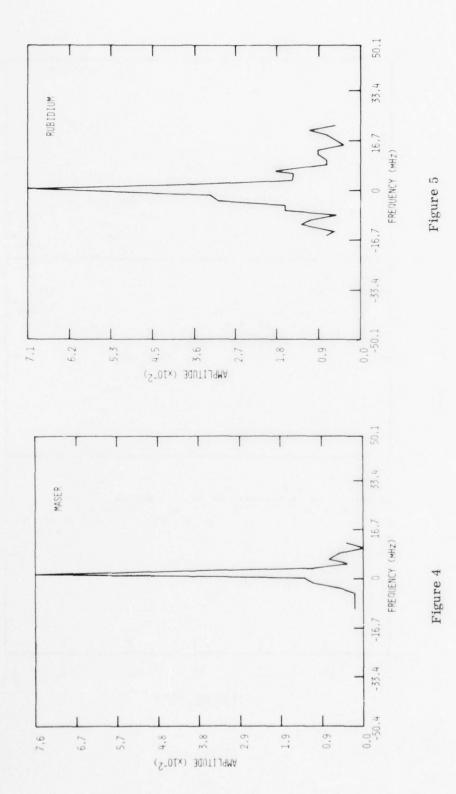


Figure 3



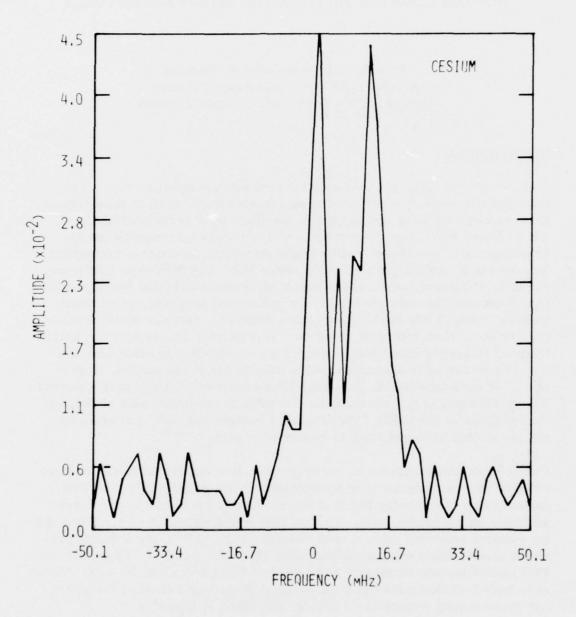


Figure 6

NEW HOROLOGE FOR AIR FORCE METROLOGY LABORATORIES

by

Arnold Alpert and James F. Barnaba Aerospace Guidance & Metrology Center Newark Air Force Station, Newark OH 43055

INTRODUCTION

Because of increasing requirements for precise time and time interval to establish the times of occurrence of significant events, such as time-tagging data, geodetic mapping and passage of satellites over earth locations, the United States Air Force has rapidly moved to improve its capabilities for providing world-wide precise time synchronization. In order to accomplish this the Air Force designated the Air Force Metrology Standards Laboratory (AFMSL) at Newark, Ohio, as the single Air Force focal point for dissemination of precise time and frequency. An operational program was established with the United States Naval Observatory (USNO) for periodic certification of the Air Force time reference standard. This certification is provided periodically by USNO personnel who handcarry a portable Cesium clock from the Naval Observatory in Washington DC to Newark Air Force Station, Newark, Ohio. At each calibration, Universal Time Coordinated (UTC) is transferred with an accuracy of 0.1 microsecond traceable to the Department of Defense Master Clock at the USNO. The frequency between the UNSO portable clock and the AFMSL standard clock is compared to parts in 10¹³.

Current calibration support for many precise time requirements is being provided by two-man precise time synchronization teams (PTSTs). The PTSTs handcarry portable configured Cesium beam precision clocks to Air Force activities on a periodic basis. Precise time synchronization of Air Force timing systems requiring support is performed by the AFMSL and selected precision measurement equipment laboratory (PMEL) personnel. These selected PMELs now include Elmendorf AFB, Thule AFB and Vandenberg AFB. These sites have been designated as Precise Time Reference Stations and support Air Force timing requirements in their geographical locations.

REQUIREMENTS

Within the last several years, a significant increase in precise time requirements has been identified. As an example, AGMC has provided precise time

support, (synchronization, comparisons, or audit evaluations) for approximately 50 sites. Because of the distances involved in carrying precise time to remote sites and the delays encountered in dispatching teams expeditiously to reestablish time when failures occur, coupled with the growing need for new precise time systems support, it was deemed necessary to establish additional precise time measurement facilities within the Air Force PMEL complex.

The Precise Time and Frequency (PT&F) console designed and assembled at AGMC was proposed in early 1974 to support the 616A very low frequency communication system. This system is an update of the present emergency communication system and incorporates both airborne and ground type atomic clocks. The integral parts of the console were also chosen to update existing time and frequency capability in the Air Force precision measurement equipment laboratories (PMELs). The frequency calibration standard available at the PMELs prior to the inception of the PT&F console was a VLF Receiver Model 207-1 manufactured by Fluke Montronics Corporation. The receiver is a phase tracking device that compares VLF signals from 8.0 to 31.9 kHz plus 60 kHz to the local standard. The local standards used to maintain accurate frequencies were low drift quartz crystal oscillators such as the Hewlett-Packard Model 105 or electronic counters with time base stability of 5 x 10^{-10} per day or better. While these receivers were deployed to the field in the early 1960s the time standards were practically nonexistent in the PMELs. Occasionally a rubidium or Cesium clock would be found in the PMEL to support the early Apollo Mission or satellite tracking facilities; therefore, the PT&F console (PTFC) will provide a new measurement capability to over 50 Air Force Laboratories.

EQUIPMENT DETERMINATION

Once the determination was made to develop a time and frequency capability at various PMELs to provide support to activities in certain geographical areas, equipment selection was the next task. In the interest of economy, redundancy, reliability and flexibility, two Austron 1210D portable crystal clocks were selected instead of one Cesium clock. In this way several benefits were realized:

- a. Initial cost was reduced.
- b. In case of clock failure, another one is available.
- c. A precise time or frequency synchronization trip can be accomplished by removing one clock and the PT&F console maintains time and frequency with the second clock.

An Austron Model 2000C Loran C receiver and a Beta Technology Model 209 Line-10 TV timing receiver were selected to keep the two portable clocks calibrated in time and frequency. In order to use either of these items a HF timing receiver was necessary for coarse alignment and pulse determination. A Hewlett-Packard Model 5328A time interval counter with 0.1 microsecond resolution and a Tracor Model 888A phase recorder capable of comparing up to 5 MHz signals were added to compare time ticks and frequency phase differences. Also required was a chart recorder for the LORAN-C timing receiver. An oscilloscope is used with the LORAN-C and the HF receiver but was assumed to be available in the PMEL. A distribution amplifier was added to buffer some of the clock outputs and to provide more standard frequency outputs for various uses in the PMEL or at the base.

Finally, for convenience and ease of operation, a patch-panel was designed so that all significant outputs from the equipment in the console would be available in one area on the front of the console. A switch was also included so that several time interval measurements can be made easily without connecting cables each time. The following time interval measurements can be accomplished at various positions of this switch, Clock No 1 one PPS Vs:

- a. External clock 1 PPS
- b. Clock No 2 one PPS
- c. TV Line-10
- d. LORAN-C

PROCUREMENT, ACCEPTANCE, ASSEMBLY, AND CHECKOUT

After the precise time and frequency console configuration had been determined, the next phase was to acquire and assemble the required items. Specifications were written for those items not on the GSA schedule, and all items were placed on procurement including a rack cabinet, equipment support brackets, power outlet strips and interconnecting coaxial cables. Contracts were accomplished and delivery dates were established. When the equipment began arriving, it was acceptance tested and then assembled into the appropriate rack cabinet configuration.

Each PTFC was then functionally tested for proper operation as a system. The console was put on time and the frequency adjusted using the items in the console with the various timekeeping methods and appropriate frequency adjustment

techniques. The results were then verified using the Air Force Measurement and Standards Laboratory (AFMSL) master time and frequency console.

TRAINING

Training of Air Force PMEL technicians who would operate the PT&F console was outlined in the Air Force Metrology Engineering Support Plan written in February 1975. These plans are required by the Air Force Metrology Directorate to provide guidance in establishing new capabilities at selected Air Force laboratories. The plan required a minimum of two technicians from each laboratory to attend the Lowry Training Center at Lowry AFB, Denver, Colorado. To initiate the plan, a two week course was taught at AGMC in April 1976. The attendees included two Lowry instructors, a technician from the Air Force Satellite Control Facility at Mahe Island and two procedure writers from Metrology Directorate at Newark. The Lowry Training Center has now established its first course and will begin class in November 1976. The Lowry Course will last for two weeks and will provide training for four technicians on two PT&F consoles. This course will be a permanent part of the advanced precision measurement equipment school. The class has also been proposed as a DOD Training Center for all DOD agencies who are involved in precise time efforts.

IMPLEMENTATION

As each PTFC is completed and checked out, a decision is made (or has been made) as to its deployment. The console is prepared for shipment and sent to the selected lab. Upon receipt of the time console, the lab installs the PTFC in the desired location, applies power, connects appropriate antennae, and operationally checks all items in the console. After all checks have been completed and all the equipment appears to be operating correctly, and the crystal clock oscillators have stabilized, the console is then set on time with WWV or some other HF standard time station using the calculated propagation delay numbers. The PTFC should now be within a millisecond or so of the correct precise time. Next, the console is set using the LORAN-C receiver and the associated propagation delay number. Synchronization by TV Line-10 data can also be accomplished if appropriate signals are available.

Daily HF timing, LORAN-C and TV Line-10 data will be sent to AGMC for evaluation. When confidence is established that proper timekeeping techniques are being used, a clock trip from the PMEL to AGMC will be accomplished using one of the crystal clocks from the PTFC.

Upon arrival at AGMC, the PMEL technician and the AGMC lab technician will compare the precise time of the PTFC with that of the Air Force measurement and standards lab precise time console. If the time difference is less than ± 40 microseconds the PT&F console initial time synchronization is considered satisfactory, the crystal clock is set on time, and the PMEL technician returns to his PTFC to refine his reference delay numbers. If the time difference is greater than ± 40 microseconds, a decision is made whether or not to initiate a precise time synchronization trip (PTST) from AGMC to the particular PMEL to resolve the discrepancy and assist in the PTFC implementation.

After the comparison between the new PT&F console and the AFMSL has been accomplished, data shall be submitted to AGMC from the PMEL on a periodic basis to assure proper timekeeping methods are being adhered to.

In the future, it is planned to implement an audit program and check each PTFC on a random basis to make sure that the PTFCs at the selected PMELs are within specification with regard to precise timekeeping.

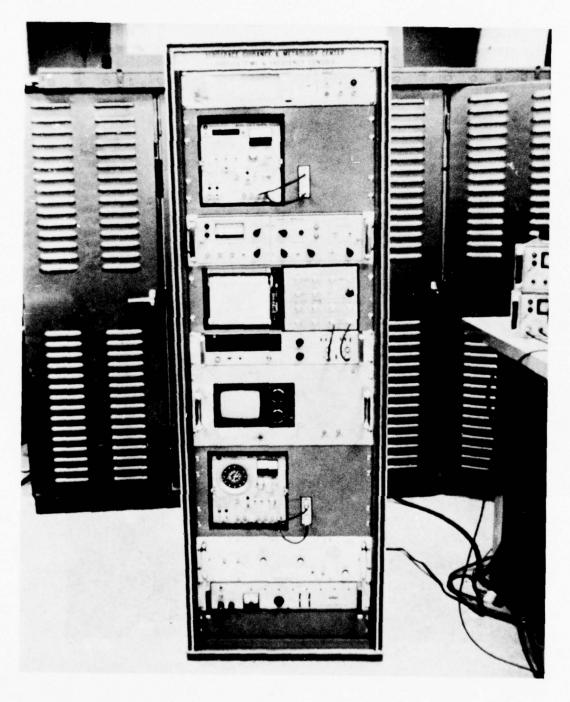


Figure 1. Aerospace Guidance and Metrology Center Precise Time and Frequency Console

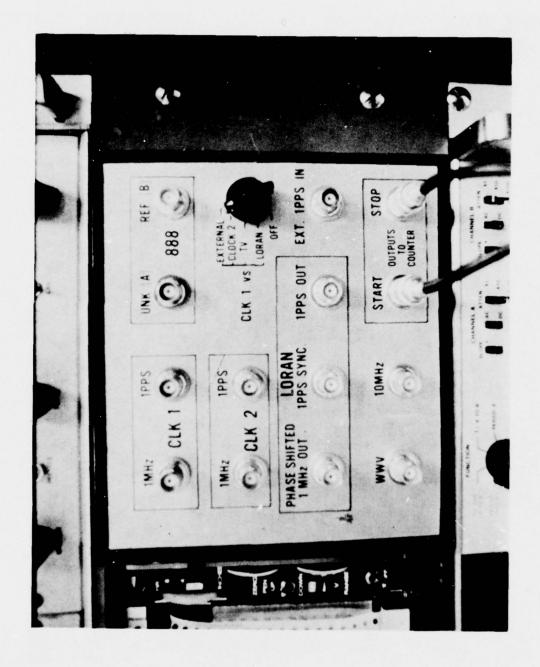


Figure 2. Precise Time and Frequency Signal Distribution Panel

CONSOLE CONFIGURATION

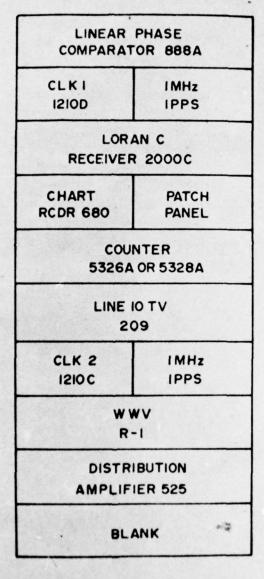


Figure 3. Console Configuration

QUESTIONS AND ANSWERS

Paper 5: "The Role of the International Radio Consultative Committee – Its Functions and Influence" was presented by Hugh S. Fosque, NASA Headquarters, Washington, D.C.

QUESTION: I notice on your draft that you didn't show the 60 kilohertz authorization. Is it a true, guarded frequency?

MR. FOSQUE: This is an experimental frequency, I believe. I will be glad to stand corrected by anybody here, but I don't believe that is an allocation. It is an experimental use of a particular frequency.

QUESTION: Could you say a few words about the methods by which you hope to get down to a one nanosecond time reference distribution?

MR. FOSQUE: With great difficult. I can't say too much about it, except that there is obviously a need, or at least there seems to be a need within the next 20 years for synchronizations of that sort. And especially so among users, but also among the principal laboratories involved in keeping time and frequency. The hope is that one will be able to go to a very broad band satellite and achieve this.

Now, the details of that technique are being looked at at the moment, and were the concern of a study group meeting that we held yesterday. I just don't think they are far enough along for me to provide you with the kind of assurance that you are looking for from the nature of your question. I don't know if we will be able to do that or not, but we will try.

QUESTION: Peter Gorham, JPL, with a comment on an implementation.

In very long baseline interferometry right now we solve for a term, which is related to clock synchronization, and I qualify that by saying related to, because we have some instrumental factors to pull out. But we are getting consistency in our solutions, now, operating independent stations with hydrogen masers. But the offset terms that we get out are good to 10 to the minus 10 seconds, 1/10 of a nanosecond.

Recently we have incorporated a phase and cable calibration system that has been put together by Goddard and Haystack Observatory; and we expect to be able to take out the instrumental terms so that, via the technique of very long baseline interferometry, I think, it is going to be a possibility to come up with nanosecond synchronization at intercontinental distances, and one could operate it in near real time via a satellite communication implementation, if you wanted to go that route.

MR. FOSQUE: Thank you.

I am somewhat of a coward in speaking to this group because we have had some meetings, and there are certain requirements that people think are emerging that would require one to take an even broader look than we have talked about here. In fact, there are a fair number of individuals who think we should strive for a 50 picosecond capability. But as I say, I am somewhat of a coward quoting those numbers to this group.

Paper 7: "Definition, Requirement, and the Determination of UT1 by the U.S. Naval Observatory" was presented by Dennis D. McCarthy, U.S. Naval Observatory, Washington, D.C.

OUESTION: My name is D. Antonio with the Navy Department.

Are there any efforts underway to do any predictive work on the variation of UT1 with UTC?

As I understand it, UT1 is for most people at the moment not very predictable and you have to keep relatively current with the work you do to find out what the current correction factors are.

Are there efforts underway to see if this can be predicted better than it is now?

MR. MC CARTHY: There are always efforts being made to predict time. However, when we are talking about accuracy. We can probably predict UT1 minus UTC to 1/10 of a second with some degree of accuracy for maybe a year. But that doesn't do anyone very much good; to a millisecond accuracy, it just is an impossible thing.

Paper 8: "The Determination of UT1 by the BIH," was presented by Ms. Marine Feissel, Bureau International de l'Heure, Paris, France.

QUESTION: George Milburn, Army, West.

In your prediction technique you mentioned that you had a tectonic factor in there, prediction for smoothing of individual stations. I am wondering if you have a, more or less, regular continental drift term that goes into that for any particular stations.

MS. FEISSEL: No. We have a variation of the drift between Europe and Asia. We found a result which is of the same size as the errors are. So, as the present continental drift is not very well known, we do not use continental drift material in our prediction. This lack of knowledge is one of the reasons why we take only four years of the past to predict.

QUESTION: Rueger, Johns Hopkins.

Did I understand you to say you are using Doppler tracking of transfer satellites as part of your data?

MS. FEISSEL: Yes, we received the final results of the DMA and we used the X and Y results.

QUESTION: Is there any plan in the near future about making comparisons, using satellites exclusively for the UT1 measurement?

MS. FEISSEL: Our methods are devised so that they can include any new method, as long as this method gives regular results, and as long as there has been a longer period of time in the past when systematic deviations from the present system of UT1 can be known and predicted.

QUESTION: Would you be in a position to say whether the errors by the satellite methods are lower or greater than you are realizing by the star observations then?

MS. FEISSEL: For the pole coordinates, the Doppler system has precision which is about the same as the astronomical system and, of course, it is increasing faster as time goes on.

QUESTION: To be able to fall back on?

MS. FEISSEL: Yes, and there is a project to set Doppler net of stations observing the satellites but these stations will be international. It will be, it is expected to give its first results in 1978.

Paper 9: "Precise Worldwide Station Synchronization Via the NAVSTAR GPS, Navigation Technology Satellite (NTS-1)," was presented by Thomas McCaskill, Naval Research Laboratory, Washington, D.C.

QUESTION: Samuel Ward, Jet Propulsion Lab. How long will that receiver remain in Australia?

MR. MC CASKILL: The site in Australia is now considered a permanent tracking station, part of the navigation and technology satellite tracking network. So, it will remain there for an indefinite amount of time.

Paper 28: "Special Purpose Atomic (Molecular) Standard," was presented by Mr. David J. Wineland.

QUESTION: Tom English.

The real question I wanted to ask, where your stability turns up at the end, is there any possibility that might be due to the changes in pressure, pressure fluctuations over a period of a couple minutes or so?

MR. WINELAND: No, in fact, that was not. I could correctly monitor the pressure and rule out that. I am sure to a high degree that was due to our drifts, for example, in the servo offsets. There was a direct correlation with that. As of yet, we haven't implemented the digital servos, which we hope to do. So I am confident we can beat that down.

QUESTION: Mr. Rueger, Johns Hopkins. What is the size of the cavity and what is the shape of it?

MR. WINELAND: We haven't at all finalized it yet. I should have pointed out on the last graph, that was for just a piece of K band wave guide, 50 centimeters long. Essentially, terminated at both ends.

That was also at a fairly higher pressure than we would want to work at. In other words, we would like to reduce the pressure, reduce the temperature sensitivity. So we envisage going to a cell of maybe about a liter volume, but the configuration yet is undecided. It may either be a box, or maybe loops of wave guide, sort of folded up on itself. But that remains to be seen.

Paper 31: "OMEGA Synchronization: Current Operations and Future Plans," was presented by Mr. Howard J. Santamore.

VOICE: I notice your data there. Could these unmodeled forces be due to atmospheric tides?

MR. SANTAMORE: I really don't know. I think Dr. Reder has considerable experience with that. I don't know of any atmospheric tide effects in OMEGA propagation.

DR. REDER: Actually, I am quite glad because I notice some of the variations against our cesium standards, and as a good citizen, a good neighbor, let's say, I blamed our cesium standard for it. But apparently it was not.

MR. SANTAMORE: Thank you.

VOICE: Perhaps I could explain to you why the atmosphere, the tides should affect this, because since the mode of propagation is from the E or D layer, underside, and the surface of the earth, the bulges caused by the atmosphere cause the radiating sources, the sun, would be up closer and the angle of incidence will change, for instance, at new moon when the solar forces and lunar tides are lining up, if you look at those periods, for instance, the diurnal effect, you find that the jump is much bigger during those times.

And in timing when this effect occurs, I have noticed that it occurs approximately 6-1/2 hours after moon passing over head, or even - the effect doesn't quite line up with the instantaneous position of the moon and sun. There is a delay.

MR. SANTAMORE: How large an effect are you talking about?

VOICE: Distances from Fort Collins to Canberra, Australia, the effect was something like as much as 7 to 10 microseconds. And in comparing the same sort of data with the Fort Collins to South Africa, the effect was nearly the same, but of the opposite phase.

MR. SANTAMORE: Thank you.

Paper 32: "A Brief Review of Frequency Stability Measures," was presented by Dr. Knowles.

DR. WINKLER: You have only a one-way transfer, not a two-way?

DR. KNOWLES: Yes, at the moment it is only a one-way transfer. This is essentially because of the combination of the economics of how many link transmitters we could afford and the satellite characteristics.

A possible future extension is a two-way transfer. In order to make that technically worthwhile, one would want to have a fully coherent satellite link whereby you could transmit the phase of your local oscillator from one station to the other as well as simply a time reference signal.

This wouldn't be possible with CTS because it doesn't have coherent oscillators, a future satellite which was equipped for a coherent slave mode, that would be worthwhile.

Paper 38: "NTS-2 Cesium Beam Frequency Standard for GPS," was presented by J. White.

MR. RUEGER: Are there any questions?

Al Bates.

MR. BATES: Bates, APL.

I am curious why all that isn't done within the loop, the relativistic synthesizer.

MR. WHITE: As you know, it could all have been, but the time sequence of things was not such that we could do it that way. We found out the offset was a hard and fast requirement.

The design of the cesium was such we could no longer go back and make the changes within the loop, and it was too late to do it.

MR. BATES: You paid a terrible price.

MR. WHITE: Yes, we did. There is a plug for what is coming up. We hope to report in Atlantic City this spring on the next family of these standards which are now under construction for the Air Force satellites. They will have all of this built in.

The output is 10.23 and it will be offset as it comes out of the standard.

MR. RUEGER: They have the relativistic synthesizer involved.

MR. WHITE: It is all programmed into the synthesizer of the cesium standard.

MR. BATES: You said the resolution synthesizer was 7 parts, 10^{10} .

MR. WHITE: That is the range. The resolution is 3 in 10^{12} . The tuning resolution on the cesium is 1-1/2 in 10^{13} . We have a range of about plus or minus 1 and 10^{11} .

MR. ENGLISH: Tom English.

I would like to point out with regard to the rubidium standards that were used, they were basically modified conversion.

MR. WHITE: At the time we originally prepared, there was a great deal of trouble, but you're quite right, they were commercial units, not designed for space flight. We did modify them to the extent necessary for our purposes.

Paper 39: "A New Rugged Low Noise High Precision Oscillator," was presented by D. A. Emmons.

MR. RUEGER: Are there any questions to this paper?

I have one, you mentioned you have designed this with hardening in mind. Would you care to say what characteristics you were trying to preserve with the hardening, transient performance or survivability or continuous service or what?

MR. EMMONS: I believe that I would prefer not to go into details, but we are using swept quartz and treating the quartz to attempt to get the radiation induced component of aging, if you will, down to acceptable limits.

MR. RUEGER: Thank you.

Are there any other questions? Back there at the microphone.

MR. BARGER: Chuck Barger, Hewlett-Packard.

I have sort of a two-fold question. Number one, you said you had a two and three part 10^{10} shift on the pyrotechnic shock. Was that a permanent shift or did the unit return after shock?

Number two, you made a point of also saying that that particular test was done operationally. Did you also by chance do the vibration tests operationally? And if so, would you be willing to say anything about the sideband performance there?

MR. EMMONS: I am afraid I did not look at sidebands during operational random vibration tests. We did random vibration tests to 10 GRMS and watched the frequency excursions and transients and so on, and watched the oscillator operate during the test, but did not have spectral analyzer equipment there.

The other part of your question could be amplified a little bit by saying that in a sequence of 12 shock pulses, we saw a final frequency offset of about five parts in 10¹¹. So that what happens is that the frequency jumps back and forth. But I don't think that that is very predictable and certainly couldn't be predicted by me.

But it was an interesting result that those shock pulses tended to give an average frequency shift which was not as large as some of the individual shifts.

QUESTION: What kind of thermal insulation system did you use in the oscillator?

MR. EMMONS: It is a dewar single proportional oven.

OUESTION: Glass?

MR. EMMONS: Yes, glass.

MR. RUEGER: You remind me of another question. How did you meet the shock requirement?

MR. EMMONS: Well, by careful attention to details.

Paper 40: "Performance of a Dual Beam High Performance Cesium Beam Tube," was presented by Gary Seavey.

MR. RUEGER: This paper is now open for questions.

QUESTION: Would you care to comment at all on the amount that that package weighs?

MR. SEAVEY: That the package weighs or the tube?

OUESTION: No, the entire electronics, the 5061A.

MR. SEAVEY: I really don't know. Maybe Mike Fischer would have an answer to that.

MR. RUEGER: I have another question. You mentioned that you worked to close tolerance on these tubes. Would you care to say what kind of a tolerance you were talking about? A few mils or something a lot better?

MR. SEAVEY: We are usually talking thousands of an inch on this tube.

MR. RUEGER: Thank you.

Are there any other questions? Here is one.

MR. WARD: Sam Ward, JPL.

After calibrating one of those cesiums with the 004 option and then turning it off and turning it on again, how close will it turn to the calibrated frequency?

MR. SEAVEY: Well, if you go through the correct procedure, you will be well within specification which usually means that it also should be de gaussed anytime the instrument has had a power interruption.

VOICE: How close are the oven temperatures controlled from unit to unit, the temperature setting of the oven controller?

MR. SEAVEY: Within about plus or minus 3 degrees Celsius.

DR. WINKLER: How well do you stabilize the oven temperature to evaluate wherever you set it in the first place?

MR. SEAVEY: I don't think I can very well answer that question right off the top of my head. It is pretty much determined by the electronics in the instrument.

DR. WINKLER: It appears to us some of the pathological behavior of clocks similar to 877, at least in part may have been caused by oven temperature changes.

Such a change of oven temperature will affect the velocity distribution in your tube. And any phase error will produce a frequency shift. That is in conjunction with magnetic field variations and with microwave power level which is another very critical thing.

These are, by far, the most important sources for systematic changes of frequency as we have seen them today. Therefore, I really wonder how well the electronics control is keeping that oven temperature constant.

MR. SEAVEY: I agree with you. I am not sure that I know exactly how well the electronics is doing as far as controlling the oven temperature.

DR. **CUTLER**: I can probably give a little answer on this. Under ordinary ambient conditions or laboratory conditions it is probably better than a few tenths of a degree centigrade.

The source of variations that were seen during this problem with the oven were not caused by temperature variations. They acted like temperature variations, but it was really a cesium vapor pressurization caused either by a chemical contamination or obstructions within the oven. It was not a true temperature variation.

MR. RUEGER: Thank you, Dr. Cutler.

MR. GARGYI: Gyula Gargyi, Tel Line System.

Are the tubes that failed the test for 004 options the tubes being used for 5061 standard oscillators?

MR. SEAVEY: I am not sure I understand.

MR. GARGYI: I understand your figure of merit was an average of 24 and some tubes don't meet that test apparently. Are those tubes the ones that are being used for standard 5061 oscillators?

MR. SEAVEY: No, the typical realized figure was 24. Our specification is 10.

DR. KERN: Bob Kern, F.T.S., Inc., Danvers, Mass.

Gary, you mentioned two tubes came back after four years of service. Were these the modified ones with the higher figure of merit or the initial ones?

MR. SEAVEY: These were the high performance tubes of the old oven design. They were unmodified.

Paper 41: "Application of High Performance Cesium Beam Frequency Standards to VLBI," was presented by W. J. Klepczynski and K. J. Johnston.

MR. RUEGER: I feel compelled to defend the working of these standards. I am sure he must have been referring to the way they operate and are moved around. The ones we had to look at were rarely in place very long at a time.

Mr. Winkler.

DR. WINKLER: First, I must say I am amazed. We can see a new phenomenon, and that is a strong dipole moment in a pair of speakers. They must have been exposed to field gradients of considerable proportion.

Seriously, I think what you have seen on the cesium standard is, of course, what one would expect if you just take in the numbers of an 004 standard and see the random walk in phase. That is typically a random walk in phase.

And you cannot hope to improve things by putting a straight line through as long as you are in it. You're in a walk in phase and not random noise limited.

Now, on the other hand, in regard to your questions, it is my feeling that these standards unless you come and put them down for an extended period, will have a degraded performance.

Dr. Cutler mentioned before the problem of temperature gradients or initial differences. If you expose such a clock to a temperature difference of 10 degrees and along with banging around in a car; they simply do not perform as well as if they can rest in a place for a couple of weeks. One has to consider it as a system which is excited into some kind of an excited state. And that it will relax afterwards at an unpredictable rate. I think I mentioned in the Observatory that we have never been able to take any one of our normal clocks as a standard into the system. They seem to suffer. The very same standards 1025 which you have in vain tried to use for radio experiment performed exceedingly well in our experiment.

MR. JOHNSTON: Let me say there, I guess I wasn't perfectly clear. We didn't really get VLBI proceedings on the 1025 that were very successful. What I did say was that when I took the 1025 down to Maryland Point, it matched the specs. We did check and see that it matched the specs, and have matched specs on that experiment. Unfortunately, we didn't get fringes on that experiment.

The main point was we used three of these cesiums, one very good, probably as good as rubidium. The other two weren't as good. It makes one wonder when one buys one off the shelf what you are going to get.

DR. WINKLER: What is the difference when you go to higher oven temperature?

MR. JOHNSTON: The higher oven does give you about a square root of two better performance. We beat the signal against the maser signal at Maryland Point and looked at them in a strip chart.

When you turn the oven on, you see the nosing down by a square root of two. It is a very graphical demonstration. I could have showed that on a slide, but the actual calibration didn't come out. There was a mistake made in the calibration.

So absolutely, I can't tell you exactly what the number was. But I can see clearly that it was much better.

MR. RUEGER: I believe Bill Lindsey made a measure of that directly against the hydrogen maser and it was the square root of two.

MR. WARD: How much of the phase drift was due to frequency offset between the two standards? And it seems to me when you move one of them, the short-term noise will limit your ability even to measure frequency. It could until it settles down.

MR. JOHNSTON: That is possible. The frequency offset between the different standards, the hydrogen maser and cesium and rubidium, is taken out of these observations. We assumed frequency offsets between the different oscillators, and we do take those out as an experiment frequency offset.

What I am really concerned with from my observation is spectral purity. The frequency could be almost anywhere, but it is the purity of the signal I am concerned with because that indicates how much noise I am going to get on my fringe phase and it limits my integration time.

But I do think, from the observations that we have made, that for low frequencies, I think this cesium standard can be used. And if I was provided with cesium standards by the Naval Observatory and going into the VLBI business, I would not run out and buy rubidium standards because I could select one of the cesium standards they have.

And I think that would prove perfectly adequate under almost every application they would have.

8th PTTI Registration List

Mr. Saeyoung Ahn Naval Research Laboratory 4555 Overlook Avenue Washington, D. C. 20375

Mr. David W. Allan National Bureau of Standards Boulder, Colorado 80302

Mr. Ralph T. Allen, Code 51023 NAVELEX Washington, D. C. 20360

Mr. Charles R. Anderson Hughes Aircraft 625 Norfolk Way Aurora, Co. 80011

Mr. Marvin Austin U.S. Coast Guard 7323 Telegraph Road Alexandria, Virginia 22310

Mr. Jacques Azoubib B. I. H. 67 Av. de L'Observatoire Paris, FRANCE 15074

Mr. Howard S. Babbitt MIT Lincoln Labs. 244 Wood Street Lexington, Mass. 02173

Mr. Heinz Badura Efratom 345 University Drive Costa Mesa, California 92627

Mr. John L. Barrett Williams College Williamstown, Mass. 01267 Mr. A. Barszczewski National Research Council NAE Bldg. U61 Ottawa Ontario, CANADA K1A0R6

Mr. C. A. Bartholomew, Code 7962 Naval Research Laboratory Washington, D. C. 20375

Mr. Alvin Bates
The Johns Hopkins Univ.,
Applied Phy. Lab.
Johns Hopkins Road
Laurel, Md. 20810

Mr. Earl Bayne Defense Mapping Agency 6500 Brookes Lane Washington, D. C.

Mr. Loren S. Bearce Naval Research Laboratory Washington, D. C. 20375

Mr. Ronald Beard, Code 7969 Naval Research Laboratory Washington, D. C. 20375

Dr. Roger E. Beehler National Bureau of Standards 325 Broadway Section 27706 Boulder, Colo. 80302

Dr. Alan Berman, Dir. of Research Naval Research Laboratory Washington, D. C. 20375

Mr. Martin B. Bloch Frequency Electronics 3 Delaware Dr. New Hyde Park, New York 11040 Mr. Eric L. Blomberg Smithsonian Observatory 60 Garden Street Cambridge, Mass. 02138

Dr. Jacques A. Bonanomi Director Observatoire Cantonal 2000 Nauchatel, Switzerland

Mr. John A. Bowman Naval Research Laboratory Code 5424 Washington, D. C. 20375

Mr. Jack C. Bowmerman NAVELEX Code 46014 Washington, D. C. 20360

Mr. W. E. Bradbury Electronic Marketing Kensington, Maryland

Mr. David W. Bradley Harris Corporation P. O. Box 37 Melbourne, Florida 32901

Dr. Robert F. Brammer TASC 6 Jacob Way Reading, Mass. 01867

Mr. Emanuel L. Brancato Naval Research Lab. 4559 Overlook Avenue Washington, D. C. 20375

Mr. Dan H. Briganti Elect. Mktg. Assoc. 11716 Parklawn Drive Rockville, Maryland 20852 Mr. R. Grover Brown Iowa State University Ames, Iowa 50010

Mr. Jim Bruce Harris Corporation P.O. Box 37 Melbourne, Florida 32901

Mr. Keith R. Bruhl Beukers Labs., Inc. 3110 Faber Drive Falls Church, Va. 22044

Mr. Ellis H. Bryant, Jr. The Weatherenron Company 4881 Powers Ferry Road Atlanta, Georgia 30327

Dr. Wolfgang Budich Goddard Space Flight Center Greenbelt, Maryland 20770

Mr. James Buisson Naval Research Laboratory Washington, D.C. 20375

Mr. Rob Burgoon Hewlett Packard 5301 Stevens Creek Santa Clara, California

Mr. Guy W. Burke NAVELEX Jefferson Davis Hwy. Arlington, Va. 22030

Mr. M. R. Burridge Naval Attache Embassy Australia 1601 Mass. Ave., N.W. Washington, D. C. 20036 Mr. Michael K. Busch Embassy of Australia 1601 Mass. Ave., N.W. Washington, D.C. 20036

Mr. Robert F. Butler Naval Surface Weapons Center DF 34 Dahlgren, Va. 22448

Mr. Roy Cashion Satellite Navigation 2141 Industrial Pkwy Silver Spring, Maryland 20904

Dr. Peter O. Cervenka NASA/Goddard/Phoenix P.O. Box 2797 Laurel, Maryland 20811

Mr. Jeng-Fu Chen Republic of China RM S5325 Dept. Labor Washington, D. C. 20210

Mr. Andrew R. Chi Goddard Space Flight Center Code 810 Greenbelt, Md. 20771

Dr. Chak-Ming Chie University of S. California 532 PHE L. A., Calif. 90007

Dr. Thomas A. Clark NASA/Goddard Space Flight Center Code 603 Greenbelt, Md. 20771

Mr. Randolph T. Clarke USNO Time Service Division Washington, D. C. 20390 Mr. John Coffman Goddard/NASA 11004 Hunt Club Drive Potomac, Md. 20854

Ms. Holly Cole Hewlett Packard 5301 Stevens Creek Santa Clara, Calif. 95050

Dr. Robert Cooper Director Goddard Space Flight Center Greenbelt, Maryland 20771

Dr. C. C. Costain National Research Council Physics Division, NRC Ottawa, CANADA K1A0R6

Dr. Duncan B. Cox, Jr. Draper Lab. MS-92 555 Technology Square Cambridge, Mass. 02139

Dr. Stuart Crampton Williams College Williamstown, Mass. 01267

Mr. John Currie Internav Inc. 8 Preston Street Bedford, Mass. 01730

Dr. Leonard S. Cutler Hewlett Packard Company 3500 Deer Creek Road Palo Alto, California 9430

Mr. William B. Dabney USNO 34th & Mass. Washington, D. C. Mr. Peter R. Dachel Jet Propulsion Laboratory 4800 Oak Grove Drive Pasadena, Calif. 91001

Mr. Richard G. Dantonio Navy Strategic Systems Proj. Office Code SSPO 23111 Washington, D. C. 20376

Mr. D. D. Davis National Bureau of Standards 325 Broadway 277.06 Boulder, Colo. 80302

Mr. George W. Davis U.S. Air Force Alaskan PMEL Elmendorf, Ak. 99510

Mr. Rudolf Decher NASA MSFC Huntsville, Ala. ES21 35812

Mr. B. Louis Decker DMA Aero Space Center Second and Arsenal Streets St. Louis AFS, Mo. 63118

Mr. William T. Demmerle Frequency & Time Systems 182 Conant Street Danvers, Mass. 01923

Dr. Desaintfuscien De L'Horloge Atomique Universite Paris - SUD Orsay FRANCE 91405

Mr. Peter Detwiler High Stoy Tech. Corp. Larger Cross Road Gladstone, N. J. 07934 Mr. Ralph E. Dickerson Naval Surface Weapons System Dahlgren, Va. 22448

Mr. Lawrence Doepke DMAAC GDDT St. Louis AFS Missouri 63118

Mr. Paul T. Dolci NSWC/DL DF-15 Dahlgren, Va. 22448

Ms. Theresa M. Donahoe NASA/Goddard Space Flight Center 317 Hillside Avenue Jenkintown, Pa. 19046

Mr. R. W. Donaldson, Jr. Westinghouse P. O. Box 1897 MS679 Baltimore, Md. 21203

Mr. Stephen F. Donnelly Analytic Sciences 6 Jacob Way Reading, Mass. 01867

Mr. R. J. Doubt DMA-HC Code NVE2 Suitland, Md.

Mr. Roger Easton Naval Research Laboratory Code 7960 Washington, D.C. 20375

Mr. Robert F. Ellis Austron, Inc. 1915 Kramer Lane Austin, Texas 78758 Mr. Donald A. Emmons Frequency & Time Systems 182 Conant Street Danvers, Mass. 01923

Mr. William Enck Sperry Systems Mgt. Great Neck, New York 11020

Mr. Thomas C. English Efratom California 3303 Harbor Blvd. Costa Mesa, Calif. 92626

Mr. Anthony J. Falzone U.S. Naval Observatory 34th & Mass. Aves. Washington, D.C. 20008

Mr. William H. Ferwalt W. H. Ferwalt, Inc. Hwy 95 & Webb Road Lapwai, Idaho 83540

Mr. Mike Fischer Hewlett Packard 5301 Stevens Creek Santa Clara, Calif. 95050

Mrs. Laura C. Fisher U. S. Naval Observatory 34th & Mass. Ave., N. W. Washington, D. C. 20390

Mr. Vincent J. Folen, Code 6452 Naval Research Laboratory Washington, D. C. 20375

Mr. H. S. Fosque NASA Headquarters 600 Independence Avenue Washington, D. C. Mr. James W. Foster USN PM1 Washington, D. C. 20376

Dr. William F. Foster Electrospace Systems, Inc. 2001 Jefferson Davis Hwy; Suite 803 Arlington, Virginia 22202

Mr. Victorio Souza Frade Observatorio-Naval Espana 2099 Buenos-Aires

Mr. Warren J. Frederick Megapulse, Inc. 5105 Karen Anne Ct. Camp Springs, Md. 20031

Mr. Charles W. Friend AFAL-DHM Wright Patterson Air Force Base, Ohio

Mr. Theo Frensch Hewlett Packard 5301 Stevens Creek Santa Clara, Calif. 95050

Mr. Richard Fulper, Jr. Naval Research Laboratory 8006 Carey Branch Drive Oxon Hill, Maryland 20022

Mr. Mike Galitzen Jet Propulsion Laboratory Mail Station 238-601 4800 Oak Grove Drive Pasadena, Calif.

Mr. Belton H. Gardner Electrospace Systems Box 2668 Arlington, Va. 22202 Mr. L. M. Gardner Sperry Systems Mgmt. M3 Great Neck, New York 11020

Mr. Gyula Gargyi Teledyne Systems Company 19601 Nordhoff Street Northridge, Calif. 91324

Mr. Thomas H. Gattis Naval Research Lab. Code 5424 Washington, D. C. 20375

Mr. Edwin A. Goldberg RCA 1 Cherry Brook Drive Princeton, New Jersey 08540

Dr. R. Glenn Hall U.S. Naval Observatory Washington, D.C. 20390

Mr. John E. Hanna, Jr. DMA Hydro Center Code NVE Washington, D. C. 20390

Mr. D. Wayne Hanson, 277.06 National Bureau of Commerce 325 Broadway Room 4035 Boulder, Colo. 80302

Mr. Michael D. Harkins Naval Surface Weapons Center Dahlgren, Va. 22401

Mr. Samuel N. Harmatuk 1575 Odell Street Bronx, New York 10462 Mr. N. A. Harmel, D7455 Western Electric Company 2400 Reynolda Road Winston-Salem, N. C. 27106

Mr. Daniel J. Healey III Westinghouse P.O. Box 746 Baltimore, Md. 21203

Mr. Charles E. Heger Hewlett-Packard 5301 Stevens Creek Santa Clara, Calif. 95050

Mr. Thomas D. Henry Western Electric Company 310 W. 4th Street Winston-Salem, N.C. 27106

Mr. Bruce R. Herman Naval Surface Weapons Center Dahlgren, Virginia 22448

Dr. Jan Hers National Physics Research Lab. P.O. Box 395 Pretoria, SOUTH AFRICA 0001

Mr. Dane Hiraiwa NCC Phnsyd P.O. Box 22024 Honolulu, Hawaii 96822

Mr. John C. Hoen Dept. of Defense 9800 Savage Rd. Fort Meade, Md. 20755

Mr. Edward A. Imbier Smithsonian A. O. 60 Garden Street Cambridge, Mass. 02138 Mr. James L. Jespersen National Bureau of Standards 325 Broadway 277.06 Boulder, Colorado 80302

Mr. Andrew C. Johnson U. S. Naval Observatory Washington, D. C. 20390

Mr. Graeme J. Johnson N.A.S.A. 21 Pandanus Street FISHE R.A.C.T. AUSTRALIA 2611

Mr. Alfred Kahan USAF/RADC Hanscom AFB Mass. 01731

Dr. P. Kartaschoff Swiss Post Office Rud Division 3000 Bern 29 SWITZERLAND

Mr. William W. Kellogg Lockheed Missiles & Space Co. 1280 N. Matiloa Avenue Sunnyvale, Calif. 94088

Dr. Robert H. Kern Frequency & Time 182 Conant Street Danvers, Mass. 01923

Mr. J. Morgan Kiker Bell Telephone Labs 1600 Osgood Street N. Andover, Mass. 01845

Dr. W. J. Klepczynski U. S. Naval Observatory Washington, D. C. 20390 Dr. Stephen H. Knowles Naval Research Lab. Code 7132 Washington, D. C. 20375

Mr. Robert M. Kovacs Kentron Hawaii LTD. P.O. Box 1207 APO San Francisco, Calif. 96555

Mr. Bernard A. Kriegsman C.S. Draper Lab. 75 Cambridge Parkway Cambridge, Mass. 02142

Mr. Ralph A. Kriss Bendix Field Eng. Corp. Columbia, Md.

Mr. Paul F. Kuhnle Jet Propulsion Lab. 4800 Oak Grove Drive Pasadena, Calif. 91103

Dr. Ryszard Kunski Inst. of Fundamental Research Polish Academy of Sciences 00049 Warszawa Swietokrsyskaa 21 POLAND

Mr. A. L. Lance TRW - DSSG One Space Park Redondo Beach Los Angeles, Calif. 90278

Mr. Graybill P. Lanois Naval Research Laboratory Washington, D. C. 20375 Mr. J. L. Lanphear GENRAD P.O. Box 842 Gaithersburg, Md. 20760

Mr. Lewis Larmore Office of Naval Res. 800 N. Quincy Street Arlington, Va. 22217

Mr. Eric Lasley 8635 Hydra Lane San Diego, Calif. 92126

Mr. Leonard Lathrem Bendix Corporation 9250 Rt. 108 Columbia, Md. 21045

Mr. Lavanceau U.S. Naval Observatory 34th St. & Mass. Ave., N.W. Washington, D.C. 20390

Dr. R. E. Lawrence VITRO Labs. 14000 Georgia Avenue Silver Spring, Md. 20910

Mr. Lee R. Lawson U.S. Air Force 12085 E. Canal Drive Aurora, Co. 80011

Dr. Felix Lazarus Hewlett-Packard 7 Rue Bois Du Lan 1217 Meyrin 2 Geneva, SWITZERLAND

Mr. Roland E. Leadon IRT Corp. P. O. Box 80817 San Diego, Calif. 92138 Dr. Irwin Lebow Chief Scientist Defense Communications Agency Washington, D. C. 20305

Capt. T. Lechner
Code 05
Deputy Commander
Naval Electronics Systems Command
Washington, D. C. 20360

Mr. D. L. Lerner 350 Bleecker Street New York, New York 10014

Dr. Sigfrido Leschiutta IEN Diazealio 42 Torino ITALY 10125

Mr. Vestal R. Lester Hughes Aircraft Co. 19631 Strathern Street Reseda, Calif. 91335

Mr. Theodore Lieberman 5001 Treetop Lane Alexandria, Va. 22310

Dr. William C. Lindsey Univ. of Southern Calif. 524 Phe Usc La. California 90007

Mr. George H. Luther USNO 34th & Mass. Washington, D. C.

Mr. Donald W. Lynch Naval Research Lab. Washington, D. C. Mr. Peter F. Macdoran Jet Propulsion Lab. 4800 Oak Grove Drive Pasadena, Calif. 91103

Mr. James Marshall Hewlett-Packard 5301 Stevens Creek Santa Clara, Calif. 95050

Ms. Martine Feissel Bureau Int. De L'Meure 61 Ave De L'Observatoire Paris, FRANCE 75014

Dr. Naoyuki Matsunami Tokyo Astronomical Observatory Mitaka, Tokyo, JAPAN 181

Dr. E. Mattison Smithsonian Observatory 60 Garden Street Cambridge, Mass. 62138

Dr. Charles May
The Johns Hopkins Univ.,
Applied Physics Lab.
Johns Hopkins Road
Laurel, Md. 20810

Mr. Cornell H. Mayer Naval Research Laboratory Washington, D. C. 20375

Mr. Robert F. McCann RCA Astro-Electronics P.O. Box 800 Princeton, N. J. 08540

Dr. Dennis D. McCarthy U.S. Naval Observatory Washington, D.C. 20390 Mr. Thomas B. McCaskill U.S. Naval Research Lab. Code 7965 Washington, D.C. 20375

Mr. Raullo J. McConahy The Johns Hopkins Univ., Applied Physics Lab. Johns Hopkins Road Laurel, Md. 20810

Mr. Thomas E. McGunigal NASA/Goddard Space Flight Center Code 723 Greenbelt, Md. 20770

Mr. John W. McIntyre JHU/Applied Physics Laboratory Johns Hopkins Road Laurel, Md. 20810

Mr. Edwin E. Mengel The Johns Hopkins Univ., Applied Physics Lab. Johns Hopkins Road Laurel, Maryland 20810

Mr. Arthur B. Merron DMAHC Washington, D. C. 20390

Mr. John Metcalf Tracur/Nested 101 Guenther Drive Great Mills, Md. 20634

Mr. Wendell D. Metcalf NESTED Patuxent River, Md. 20670

Mr. George E. Milburn U. S. Army Rt. 2 Box 735A Tucson, Arizona 85715 Mr. Tom Mingle Hewlett-Packard 5301 Stevens Creek Santa Clara, Calif. 95050

Mr. D. H. Mitchell Kentron Hawaii LTD. Box 1207 APO San Francisco, Calif. 96555

Mr. B. B. Moon U.S. Air Force 6408 E. Mississippi Denver, Colorado 80224

Mr. Robert B. Moore Naval Research Laboratory Washington, D. C. 20375

Mr. H. J. Morrison Westinghouse P.O. Box 1897 MS 709 Baltimore, Md. 21146

Mr. Ivan I. Mueller Ohio State Univ., Dept. of Geodetic Sc 1958 Neil Avenue Columbus, Ohio 43210

Mr. James A. Mullen Raytheon Co.; Research Division 28 Seyon Street Waltham, Mass. 02154

Mr. James A. Murray, Jr. Naval Research Laboratory Code 5461 Washington, D.C. 20375

Mr. C. J. Neumann Datum, Inc. 1363 State College Anaheim, Calif. 92806 Dr. Stephen Nichols, Code 5483 Naval Research Laboratory Washington, D. C. 20375

Capt. Lionel M. Noel Commanding Officer Naval Research Laboratory Washington, D. C. 20375

Mr. J. R. Norton The Johns Hopkins Univ., Applied Physics Lab. Johns Hopkins Road Laurel, Md. 20810

Dr. Klemens J. Nottarp Inst. Ang. Geodesie 8491 Wettzell Germany Sat Beob Stat

Mr. Michael J. Nugent NSA Ft. George G. Meade Maryland 20755

Mr. O. Jay Oaks, Jr. Naval Surface Weapons Center Dahlgren Lab Dahlgren, Virginia 22448

Mr. Joseph O'Neill NRL 4555 Overlook Avenue Washington, D. C. 20375

Mr. William S. Orr Lowrance Electronics 12000 E. Skelly Drive Tulsa, Oklahoma 74128

Mr. Terry N. Osterdock Hewlett-Packard Company 5301 Stevens Creek Santa Clara, Calif. 95050 Mr. Joseph J. Ostrowski USAF PTF AGMC/MLTE Newark AFS, Ohio 43055

Mr. Doran W. Padgett OWR Arlington, Virginia

Mr. Paul Pellegrin USAF/RADC ETSP Hanscom AFB, Mass.

Mr. Donald Percival Naval Observatory 34th & Mass. Ave., Washington, D.C. 20007

Mr. Henry A. Perfetto Booz Allen Research 4733 Bethesda Avenue Bethesda, Md. 20832

Mr. Harry E. Peters 9803 Good Luck Road Apt. 3 Seabrook, Maryland 20801

Mr. Edward A. Pettit Range Measurements Lab Patrick AFB, Florida 32925

Mr. David H. Phillips NRL Code 5424C Washington, D.C. 20375

Mrs. Ruth Phillips Naval Research Lab. Code 5424C Washington, D. C. 20375 Mr. Paul Phipps Sand A Labs Box 5800 Division 1245 Albuquerque, New Mexico 87115

Dr. John D. H. Pilkington Royal Greenwich Observatory Herstmonceux Castle Hailsham, East Sussex, ENGLAND

Mr. David Pinkowitz ILC Data Device Airport International Plaza Bohemia, New York 11716

Mr. John W. Pitsenberger U.S. Navy Department SSPO CNM 2701 Washington, D.C. 20376

Mr. Adrian E. Popa Hughes Research Labs. 3011 Malibu Cyn. Rd. Malibu, California 80265

Mr. Robert E. Powers Bell Tel Labs 1600 Osgood Street North Andover, Mass. 01845

Mr. R. Pregler Hughes Aircraft P.O. Box N Aurora, Colorado 80011

Mr. Dewey L. Pritt Naval Research Lab. Code 5422 Washington, D. C. 20390

Mr. S. E. Probst Office Telecom Policy Executive Office Washington, D. C. 20504 Mr. Joseph M. Przyjemski C. S. Draper Labs Technology Square Cambridge, Mass. 02139

Mr. Gerard L. Punt Interstate Elect. 707 E. Vermont Anaheim, Calif. 92803

Mr. Ken Putkovich U.S. Naval Observatory 34th & Mass. Ave. Washington, D.C. 20390

Mr. George T. Rado NRL Code 6450 Washington, D. C. 20390

Ms. Marilyn Raines Naval Observatory Mass. Ave. & 34th St., N.W. Washington, D.C. 20390

Dr. Norman Ramsey Harvard University Cambridge, Mass.

Mr. Larry Raymond NSWC DL Dahlgren, Virginia 22448

Dr. Fritz H. Reder USA Electronics Command Ft. Monmouth, New Jersey DRSEL-NL-RH 07703

Mr. Elza K. Redman, Jr. National Security Agency 9800 Savage Road Ft. Meade, Maryland 20755 Dr. Victor S. Reinhardt NASA/Goddard Space Flight Center Code 814 Greenbelt, Maryland 20771

Mr. Eugene A. Rheingans Rockwell International 3370 Miraloma, MS/FB10 Anaheim, California 92803

Mr. J. D. Richard University of Maryland Physics & Astron. College Park, Maryland 20742

Mr. William D. Ringle U.S. Naval Weapon Eng. Sup. Washington Navy Yard ESA5312 Washington, D.C. 20390

Dr. Alan E. Rogers Hays Tack Observatory Westford, Mass. 01886

Dr. Bernt Olof Ronnang Chalmers University Techn. Onsala Space Observatory S-43034 Onsala, SWEDEN

Mr. L. J. Rueger JHU/Applied Physics Laboratory Johns Hopkins Road Laurel, Maryland 20810

Mr. Gustaf Rydbeck Onsala Space Observatory 5430 34, SWEDEN

Mr. Edward Sabisky RCA Laboratories Princeton, New Jersey 08548 Mr. Theodore Saffos Naval Surface Weapons Center Dahlgren, Virginia 22448

Mr. Frank C. Sakran, Jr. U. S. Naval Air Test (AT-41) Center Patuxent River, Maryland 20670

Mr. Edward J. Samario Lockheed 183 Belwood Gateway Los Gatos, California 95030

Mr. Howard J. Santamore U.S. Coast Guard ONSO HQUSCG G-ONSOD/43 Washington, D. C. 20590

Mr. Roger N. Schane TASC 6 Jacob Way Reading, Mass. 01867

Mr. Carl Schellenberg USCG Onsod 2100 2nd Street, S. W. Washington, D. C. 20590

Mr. Bernard R. Schlueter TFI-Oscilloquartz SA Brevards 16 CH NEUCHATEL 2002

Mr. John G. Schmid USAF Samtec Rods Vandenberg AFB, Calif. 83437

Mr. David C. Scull U. S. Coast Guard HQRS Washington, D. C. 20590 Mr. Gary A. Seavey Hewlett-Packard 5301 Stevens Creek Blvd. Santa Clara, California 95050

Mr. Richard D. Shaffer NRL-Bendix Blossom Point Box 578 Laplata 20646

Mr. Richard Sheklin USNAVAIRDEVCEN Code 6013 Warminster, Pa. 18974

Mr. Leonard F. Shepard ILC Data Device 856 School House La. Dover, Delaware 19901

Mr. Arthur E. Smith Pacific Missiletest Center Pt. Mugu, California 93042

Dr. Humphrey Smith Royal Greenwich Observatory Herstmonceux Castle Hailsham Sussex, ENGLAND

Mr. Joseph Collins Smith Superintendent, U.S. Naval Observatory Washington, D.C.

Mr. Warren Smith Bell Telephone Labs 555 Union Blvd. Allentown, Pa. 18103

Ms. Marina Medina Solis Secretaria Comunicaciones Y Transporte Nino Perdido Y Cum-Bres Acultzingo MEXICO 12, DF C. A. Sorensen Singer Instr. Division Los Angeles Operation The Singer Company, 5340 Alla Rd. Los Angeles, Calif. 90066

Mr. Mark L. Spano University of Maryland 6864 Riverdale Road Lanham, Maryland 20801

Mr. John J. Speight Dmahc Washington, D. C. 20390

Mr. Marc I. Spellman Harris E. S. D. P.O. Box 37 Melbourne, Florida 32901

Mr. Peter Staecker Mit Lincoln LAB Box 73 Lexington, Mass. 02173

Mr. Robert R. Stone, Jr. Naval Research Lab. Washington, D. C.

Dr. Harris A. Stover Defense Comm. Agency 1860 Wiehle Avenue Reston, Virginia 22090

Mr. John Strain Frequency Electronics 651 Lofstrand Lane Rockville, Md. 20850

Mr. Peter P. Strucker Navy Metrology 1675 W Mission Blvd. Pomona, Calif. 91776 Mr. Robert V. Suttle, III U.S. Naval Observatory 34th and Mass. Avenue Washington, D. C. 20390

Dr. Richard L. Sydnor Jet Propulsion Lab 4800 Oak Grove Pasadena, Ca. 91103

Mr. Arthur Taber San Fran State 560 Rockdale Drive San Francisco, Ca. 94127

Mr. George T. Tennis DMA TOPO Center 6500 Brookes Lane Washington, D. C. 20315

Mr. Eugene H. Thom Jet Propulsion Lab 4800 Oak Grove Dr. Pasadena, Ca. 91103

Mr. Daryl Thornburg General Dynamics Electronic 4024 Risa Court San Diego, Ca. 92124

Mr. Jimmie L. Toms T. E. Corporation 701 E. Gude Dr. Rockville, Md. 20850

Mr. J. E. Trimm Dynalectron Corp. Drawer R Hafb, New Mexico 88330

Mr. Thomas R. Turlington Westinghouse Electric Co. P. O. Box 746 Baltimore, Md. 21203 Mr. C. A. Sorensen Singer Instr. Division Los Angeles Operation The Singer Company, 5340 Alla Rd. Los Angeles, Calif. 90066

Mr. Mark L. Spano University of Maryland 6864 Riverdale Road Lanham, Maryland 20801

Mr. John J. Speight Dmahc Washington, D. C. 20390

Mr. Marc I. Spellman Harris E. S. D. P.O. Box 37 Melbourne, Florida 32901

Mr. Peter Staecker Mit Lincoln LAB Box 73 Lexington, Mass. 02173

Mr. Robert R. Stone, Jr. Naval Research Lab. Washington, D. C.

Dr. Harris A. Stover Defense Comm. Agency 1860 Wiehle Avenue Reston, Virginia 22090

Mr. John Strain Frequency Electronics 651 Lofstrand Lane Rockville, Md. 20850

Mr. Peter P. Strucker Navy Metrology 1675 W Mission Blvd. Pomona, Calif. 91776 Mr. Robert V. Suttle, III U.S. Naval Observatory 34th and Mass. Avenue Washington, D. C. 20390

Dr. Richard L. Sydnor Jet Propulsion Lab 4800 Oak Grove Pasadena, Ca. 91103

Mr. Arthur Taber San Fran State 560 Rockdale Drive San Francisco, Ca. 94127

Mr. George T. Tennis DMA TOPO Center 6500 Brookes Lane Washington, D. C. 20315

Mr. Eugene H. Thom Jet Propulsion Lab 4800 Oak Grove Dr. Pasadena, Ca. 91103

Mr. Daryl Thornburg General Dynamics Electronic 4024 Risa Court San Diego, Ca. 92124

Mr. Jimmie L. Toms T. E. Corporation 701 E. Gude Dr. Rockville, Md. 20850

Mr. J. E. Trimm Dynalectron Corp. Drawer R Hafb, New Mexico 88330

Mr. Thomas R. Turlington Westinghouse Electric Co. P. O. Box 746 Baltimore, Md. 21203 Mr. Pierre H. Venne Canadian Broadcasting Corp. 1400 East Dorchester Montreal, Pr Quebec

Dr. Robert F. C. Vessot Smithsonian Astrophysical Obs. 601 Garden Street Cambridge, Mass. 02138

Mr. J. R. Vetter JHU/Applied Physics Lab. Johns Hopkins Road Laurel, Md. 20810

Mr. Belisario Vicente Observatorio Naval Espana 2099 Buenos Aires

Mr. Alfred Vulcan Frequency Electronics 3 Delaware Dr. NGW Hyde Park, N.Y. 11040

Mr. Alan Waiss Electrospace System, Inc. Suite 803, 2001 Jeff. Davis Highway Arlington, Va. 22202

Mr. E. S. (Bill) Walker Hughes Aircraft Co. P. O. Box N Aurora, Co. 80011

Mr. W. C. Walker Pan Am World Airways Building 989 Mail Unit 840 Patrick AFB, Fla. 32925

Dr. Fred L. Walls National Bureau of Standards 325 Broadway Boulder, Co. 80303 Mr. Harry Wang Hughes Res. Labs. 3011 Malibu Canyon Malibu, Ca. 90265

Mr. Samuel C. Ward Jet Propulsion Lab 4800 Oak Grove Dr. Pasadena, Ca. 91103

Mr. S. C. Wardrip NASA/GSFC Code 814 Greenbelt, Md. 20771

Mr. Hugh Warren Bendix Corp. 3132 Brinkley Rd. Oxon Hill, Md. 20031

Mr. William D. Wathen Jr. NESTED Patuxent River, Maryland 20670

Mr. Andre Wavre Oscilloquartz SA Brevards 16 Neuchatel, SWITZERLAND 2002

Mr. Herbert Weakliem RCA Labs Princeton, N. J. 08540

Mr. Paul J. Wheeler U.S. Naval Observatory Washington, D.C. 20390

Mr. Joe White NRL 4555 Overlook, 7962 Washington, D. C. 20375 Mr. Gary G. Whitworth Applied Physics Lab Johns Hopkins Road Laurel, Maryland 20810

Mr. Randall E. Wiley NAVELEXSYSCOM 9517 Vandola Court Burke, Va. 22015

Mr. Lindsey W. Williams Quest Research Corp. 6845 Elm St., Suite 407 McLean, Va. 22101

Mr. Warren L. Wilson Fairchild Systems 707 Spindrift Drive San Jose, Ca. 95134

Dr. David J. Wineland National Bureau of Standards Boulder, Colorado 80302

Dr. Gernot Winkler U. S. Naval Observatory Washington, D. C. 20390 Mr. Sing F. Wong NARF NAS Code 62210 Alameda, Ca. 94501

Mr. Nick Yannoni USAF/RADC Hanscom AFB, Mass. 01731

Mr. Phil Young Naval Surface Weapons Center Attn: DK 13 Dahlgren, Va. 22401

Mr. Harry D. Zink Applied Physics Laboratory Johns Hopkins Road Laurel, Maryland 20810

Mr. Rudolph Robert Zirm NRL 7911 Indian Head Highway Oxon Hill, Maryland 20021

Mr. Thomas G. Zogakis Harris ESD P.O. Box 37 Melbourne, Fla. 32901